

# Catalytic Strain Release of Photoproducts and its Application in Organic Chemistry



**Dissertation zur Erlangung des Grades „Doktor der Naturwissenschaften“  
im Promotionsfach Chemie  
am Fachbereich Chemie, Pharmazie und Geowissenschaften der  
Johannes Gutenberg-Universität in Mainz**

von

**Adriana Lisseth Luque Diaz**  
geboren in Bucaramanga, Kolumbien

Mainz, 2022



Die vorliegende Arbeit wurde im Zeitraum von Juni 2018 bis April 2022 im Arbeitskreis von Herrn Prof. Dr. Till Opatz am Department Chemie der Johannes Gutenberg-Universität Mainz angefertigt

Dekanin: [REDACTED]

1. Berichterstatter: Prof. Dr. Till Opatz

2. Berichterstatter: [REDACTED]

Tag der mündlichen Prüfung: 14.06.22





*To my beloved parents*



## **Erklärung**

Hiermit erkläre ich, dass ich die vorliegende Arbeit selbstständig angefertigt habe. Es wurden dabei nur die genannten Quellen sowie Hilfsmittel verwendet. Wörtlich oder sinngemäß übernommenes Gedankengut wurde eindeutig als solches kenntlich gemacht.

*Adriana Luque D.*

---

Adriana Lisseth Luque Diaz



# Kurzzusammenfassung

Verschiedene photochemische Prozesse, wie Isomerisierungen und Cycloadditionen, haben sich als besonders nützlich beim Aufbau hochgespannter Photoprodukte erwiesen. Der Effekt dieser Ringspannung in Bezug auf chemische Reaktivität und Grundzustandsenergie stellt einen großen Vorteil auf dem Gebiet der organischen Chemie dar, da die Freisetzung der Ringspannung als treibende Kraft für Folgereaktionen dienen kann. Die Kombination der Erzeugung eines photogenerierten, gespannten Addukts mit einer spannungsfreisetzenden Folgetransformation erleichtert die Herstellung komplexer Produkte unter sehr milden, und potenziell umweltfreundlichen, Reaktionsbedingungen. Daher wurden in der vorliegenden Arbeit Reaktionsequenzen entwickelt, die literaturbekannte photochemische Isomerisierungen, die zu hochenergetisch gespannten Intermediaten führen, mit einer neuen katalytischen Folgereaktion kombinieren. Im ersten Teil wurden meta-Photocycloaddukte aus Alkylbenzylallylaminen unter photoinduzierten Reaktionsbedingungen synthetisiert und anschließend die Möglichkeit einer Vinylcyclopropan-Ringöffnung, mit verschiedenen Reaktionspartnern unter Metallkatalyse und katalysiert durch sichtbares Licht, untersucht. Versuche einer formalen [3+2]-Cycloaddition mit verschiedenen Alkenen und Alkinen führten zu einer neuartigen, durch sichtbares Licht vermittelten Reaktion, mit Ir(III)-Komplexen in Kombination mit acetylenischen Sulfonen. DFT-Rechnungen und zeitaufgelöste optische Spektroskopiestudien belegen einen Triplett-Energietransfermechanismus für diese Umwandlung. Im zweiten Teil dieser Arbeit wurde die Ringöffnung eines, aus 2-Propionylpyridins photochemisch synthetisierten, Cyclopropanols hinsichtlich metallsowie photoredoxkatalysierter Folgereaktionen mit verschiedenen Reaktionspartnern untersucht. Als effizienteste Reaktion wurde eine literaturbekannte Pd-katalysierte Kreuzkupplungsreaktion mit Benzylchloriden identifiziert. Die Optimierung dieser Reaktionsbedingungen für die Verwendung des photogenerierten Cyclopropanols ermöglichte die Herstellung einer Reihe von neuen 2-Pyridylketonen



# Abstract

Different photochemical processes such as isomerizations and cycloadditions have shown to be particularly useful in the construction of highly strained photoproducts. The effect of that ring strain in terms of chemical reactivity and ground state energy represents a big advantage in the field of organic chemistry since the relief of ring strain energy can serve as the driving force for subsequent reactions. The combination of the generation of a photogenerated strained adduct with a strain-releasing follow-up transformation eases the preparation of complex products under very mild and potentially eco-friendly reaction conditions. Therefore, in the present work sequences that combine literature-known photochemical isomerizations that lead to high-energy strained intermediates with a new subsequent catalytic downstream reaction were developed. In the first part, *meta* photocycloadducts were synthesized from alkyl benzyl allylamines under photoinduced reaction conditions and afterwards, the possibility of a vinylcyclopropane ring-opening was evaluated with different reaction partners under metal-base and visible light catalysis. Attempts for a formal [3+2] cycloaddition with different alkenes and alkynes led to a novel visible light-mediated reaction with Ir (III) complexes in combination with acetylenic sulfones. DFT-calculations and time-resolved optical spectroscopy studies substantiated a triplet energy transfer mechanism for this transformation. In the second part of this work, the ring-opening of a cyclopropanol photochemically synthesized from 2-propionylpyridine was investigated in terms of metal as well as photoredox catalyzed downstream reactions with different reaction partners. A literature-known Pd-catalyzed cross-coupling reaction with benzyl chlorides was identified as the most efficient reaction. The optimization of these reaction conditions for the use of the photogenerated cyclopropanol allowed the preparation of a new series of 2-pyridylketones.

# Table of Contents

Publications .....	XIV
List of Abbreviations.....	XV
<b>1. Introduction.....</b>	<b>1</b>
1.1. Photochemistry .....	1
1.1.1. Fundamentals and concepts.....	2
1.1.2. UV Photoreactions .....	10
1.1.3. Visible Light Photocatalysis .....	17
1.2. Metal-catalyzed activation of strained molecules .....	17
1.2.1. Strain energy .....	30
1.2.2. Transition metal-catalyzed carbon-carbon bond activation .....	32
<b>2. Catalytic activation of skeletal bonds in strained photoproducts .....</b>	<b>43</b>
2.1. Introduction .....	43
2.2. Aim of the research.....	44
2.3. Results and discussion .....	48
2.3.1. <i>meta</i> photocycloaddition products .....	48
2.3.2. Photogenerated cyclopropanols.....	73
2.4. Summary and outlook.....	86
2.4.1. <i>meta</i> photocycloadducts .....	86
2.4.1. Photogenerated cyclopropanols.....	87
<b>3. Three-component arylation and sulfonylation of styrene derivatives .....</b>	<b>89</b>
3.2. Introduction .....	89
3.3. Aim of the research.....	90
3.4. Results and discussion .....	92
3.4.1. Optimization of reaction conditions .....	92



3.4.2. Mechanistic Considerations.....	96
3.5. Summary and outlook.....	106
<b>4. Experimental section.....</b>	<b>107</b>
4.1. General methods .....	107
4.2. Reaction Procedures .....	116
4.2.1. Section 2.3.1 .....	116
4.2.2. Section 2.3.2 .....	158
4.2.3. Section 3.4.1 .....	171
<b>5. References .....</b>	<b>182</b>
<b>6. Appendix .....</b>	<b>191</b>
6.1. Crystal structure analysis .....	191
6.2. NMR Spectra .....	203
6.2.1. Spectra section 2.3.1 .....	203
6.2.2. Spectra section 2.3.2 .....	247
6.2.3. Spectra section 3.4.1 .....	264
Acknowledgments .....	<b>Fehler! Textmarke nicht definiert.</b>

# Publications

- [A. Luque](#), J. Groß, T. J. B. Zähringer, C. Kerzig, T. Opatz. Vinylcyclopropane [3+2] cycloaddition with acetylenic sulfones based on visible light photocatalysis, *Chem. Eur. J.*, **2022**, 28, e2021043.
- [A. Luque](#), J. Paternoga, T. Opatz. Strain Release Chemistry of Photogenerated Small-Ring-Intermediates, *Chem. Eur. J.* **2020**, 27, 4500–4516.
- B. Lipp, L. M. Kammer, M. Küçükdisli, [A. Luque](#), J. Kühlborn, S. Pusch, G. Matulevičiūtė, D. Schollmeyer, A. Šačkus, T. Opatz. Visible Light-Induced Sulfonylation/Arylation of Styrenes in a Double Radical Three-Component Photoredox Reaction, *Chem. Eur. J.* **2019**, 8965–8969.

# List of Abbreviations

Å	Ångström
Ac	Acetyl
AIBN	Azobis(isobutyronitril)
ATR	Attenuated total reflection
Bn	Benzyl
bpy	2,2'-Bipyridine
Bz	Benzene
CFL	Compact Fluorecent Lamp
CyH	Cyclohexane
COSY	Correlation spectroscopy
DCM	Dichloromethane
DFT	Density Functional Theory
DMF	<i>N,N</i> -Dimethylformamide
DMSO	Dimethylsulfoxide
dtbpy	4,4'-Di-tert-butyl-2,2'-biyridine
ESI	Electrospray ionization
Et	Ethyl
EnT	Energy Transfer
<i>et al.</i>	<i>et alii</i>
EWG	Electron-withdrawing groups
GC	Gas chromatography
HOMO	Highest occupied molecular orbital
HMBC	Heteronuclear multibond coherence

HPLC	High performance liquid chromatography
HRMS	High resolution mass spectrometry
HSQC	Heteronuclear single quantum coherence
Hz	Hertz
IR	Infrared
ISC	Intersystem Crossing
LDA	Lithium diisopropylamide
LED	Light-emitting diode
Me	Methyl
MS	Mass spectrometry
NBS	<i>N</i> -Bromosuccinimide
NMR	Nuclear magnetic resonance
NOESY	Nuclear Overhauser effect spectroscopy
PC	Photocatalyst
Ph	Phenyl
ppm	Parts per million
Py	Pyridine
quant.	Quantitative
$R_f$	Retardation factor
rt	Room temperature
SET	Single electron transfer
TEA	Triethylamine
TEMPO	(2,2,6,6-Tetramethylpiperidin-1-yl)oxyl
THF	Tetrahydrofuran
TLC	Thin layer chromatography

TMS	Trimethylsilyl
TOF	Time-of-flight
Ts	Tosyl
UV	Ultraviolet
Vis	Visible



# 1. Introduction

## 1.1. Photochemistry

Photochemical reactions are abundant in nature and play an important role in numerous processes on earth. The energy that starts these reactions comes from the sun in the form of electromagnetic radiation of ultraviolet, visible, or infrared wavelengths.<sup>[1]</sup> The visible radiation is responsible for initiating vital processes such as photosynthesis which is the most important process for providing energy and food as well as for maintaining the climate and the ecosystem.<sup>[2]</sup> The sun's ultraviolet radiation also plays an important role in our environment, maintaining a balance in the amount of ozone in the upper atmosphere preventing most of the more harmful short wavelength radiation reach the earth's surface.<sup>[3]</sup>

The field of photochemistry deals with chemical reactions and other physicochemical phenomena induced by the absorption of light within a part of the substrate, that is its chromophore.<sup>[4]</sup> Once the substrate is promoted from its ground state to a higher-energy state, it can undergo various physical and chemical mechanisms by which energy is redistributed.<sup>[5]</sup> These multiple pathways are typically summarized in a Jablonski diagram (Figure 1).<sup>[6]</sup> By the physical processes of fluorescence, phosphorescence, and internal conversion, the excited substrate loses its excess energy and subsequently returns to the ground state. The excited-state energy can alternatively initiate a chemical reaction, such as elimination, cleavage, rearrangement, isomerization, cyclization, addition, or electron transfer. Photochemical reactions include direct excitation, photosensitization, photocatalysis, and photoinduced electron transfer (PET).

Excited-state photocatalytic reactions employ light as an eco-friendly tool to promote the reaction while the photocatalysts are not consumed. During this process, light is adsorbed, which generates electronically excited states of molecules, species often more reactive than those formed by interaction with the aggressive chemicals otherwise used for promoting chemical reactions. As a result, a clean reaction often arises, which satisfies the postulate of atom economy and occurs under unparalleled mild conditions.<sup>[7]</sup> Thus, photochemistry is generally quoted as one of the most promising and innovative methods and considered one of the key approaches to green synthesis. The relevance of photochemistry also lies in its application in the industry. In recent years there have been various advanced photochemical

reactor technologies that show great promise to conduct photochemical processes ranging from laboratory to production scale.<sup>[8]</sup> Hence, a lot of effort has been put into the development of more sustainable and energy-efficient processes focusing on commercializing standardized equipment to carry out photocatalytic transformations on different scales with reduced waste generation and minimal environmental impact.<sup>[9]</sup>

### 1.1.1. Fundamentals and concepts

Energy quantization is of primary importance for photochemistry because it implies that only photons, which bring a definite quantity of energy corresponding to a difference between two allowed energy values, can be absorbed. A key to this theory was Planck-Einstein's suggestion (Equation 1.1)<sup>[10]</sup> that the energy of light is quantized, whereby the energy of the light quanta (photons) can be related to the wavelength (or the frequency) of the light:

$$E = h\nu = h\frac{c}{\lambda} \quad (1.1)$$

A mole of photons (corresponding to  $6.022 \times 10^{23}$  photons) is called an Einstein. where  $E$  is the energy of a single photon [J],  $h$  is Planck's constant [ $6.63 \times 10^{-34}$ J·s],  $\nu$  is the frequency of light [Hz or  $s^{-1}$ ],  $\lambda$  is the wavelength of light [nm], and  $c$  is the speed of light in vacuum [ $3.0 \times 10^8$  m·s<sup>-1</sup>]. Hence, the energy of photons may be calculated from their respective wavelength or frequency (Table 1).<sup>[11]</sup>

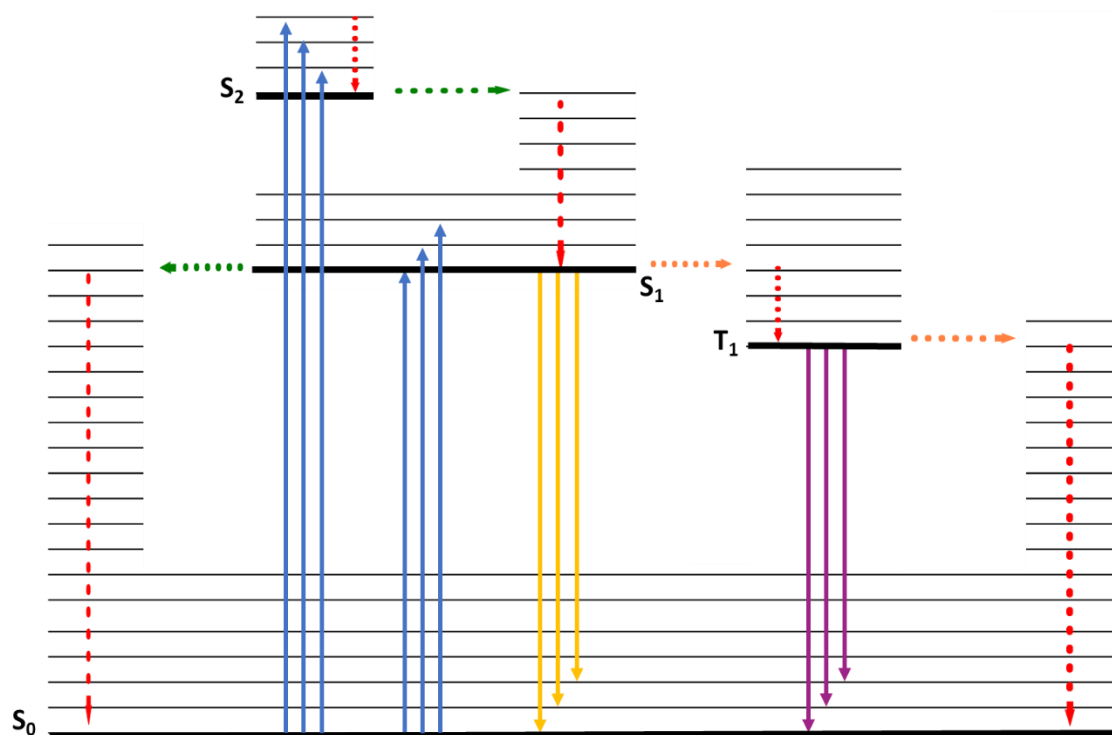
Due to the wave-particle dualism, a photon or light quantum can also be viewed as a massless interaction particle.<sup>[12]</sup> This particle can interact with another molecule (mostly in electronic ground state  $S_0$ ) and thereby enable electronic excitation. If this molecule is supplied with a sufficiently large amount of energy from the outside, an outer electron can absorb the energy and move to a higher orbital without changing the spin of the electron as it was in the ground state (paired). In this higher-energy state, the electron usually cannot stay longer than a few nanoseconds, after which it falls back into its original orbital while the absorbed energy is released again. The absorbed energy is emitted as a photon. The two orbitals, the highest occupied molecular orbital HOMO ( $S_0$ ) and the lowest unoccupied molecular orbital LUMO ( $S_1$ ) are also called frontier orbitals.<sup>[13]</sup> They play a decisive role in all luminescence



processes but also in photochemical reactions. The fundamental connected processes can be illustrated and described using a Jablonski diagram (Figure 1).

Table 1. Relationship between wavelength and energy.

Type of radiation	Wavelength ( $\lambda$ =nm)	Energy (kcal·mol <sup>-1</sup> )
UV-C	100–280	286–102
UV-B	280–315	102–90.8
UV-A	315–400	90.8–71.5
Blue	~450	63.6
Green	~500	57.2
Red	~650	44



**Figure 1.** Simplified Jablonski diagram. <sup>[10, 14]</sup> Thick horizontal lines symbolize the electronic states ( $S_0$ ,  $S_1$ ,  $S_2$ ,  $T_1$ ). Thin horizontal lines symbolize the oscillation states (ascending:  $v = 0, 1, 2, \dots$ ) within an electronic state; dashed arrows: Nonradiative processes; solid arrows: radiative processes. Blue: Absorption; Yellow: Fluorescence; Purple: Phosphorescence; Green: Internal conversion; Red: Vibrational relaxation; Orange: Intersystem crossing.

The most favorable relaxation process depends on the type of molecule and the nature of the excited states. The energy absorbed by a molecule can be released mainly via two pathways: radiative (transitions to lower-energy states with emission of light) or nonradiative (vibrational relaxation).

One of the most interesting properties of electronically excited molecules is their tendency to emit radiation in order to return to the ground state. Two types of radiative transitions can be distinguished: fluorescence and phosphorescence. The phenomenon of fluorescence involves radiative emission from an excited state of the same multiplicity as the lower state of the transition. Generally, in organic molecules, this transition occurs from the lowest energy singlet excited state,  $S_1$ , to the ground state  $S_0$ . Since there is no change in the multiplicity of the state, this transition is spin-permitted and usually occurs rapidly, in the range from picoseconds to nanoseconds.<sup>[14]</sup> On the contrary, phosphorescence occurs if the spin multiplicity of the emitting state is different from that of the lower state. Thus, if the triplet state of lower energy is populated, often due to the intersystem crossing process from the  $S_1$  state, the subsequent transition  $T_1 \rightarrow S_0$  can be observed, giving rise to phosphorescence. This transition is spin-forbidden, which results in a much longer lifetime for the  $T_1$  state ( $\mu\text{s}$  to  $\text{ms}$  range) than for the  $S_1$  state ( $\text{ns}$  range).<sup>[15]</sup>

Nonradiative transitions involve the conversion of one molecular quantum state into another without emission of radiation. These processes occur between quantum states of an individual molecule without the need for external disturbances such as collisions with other particles. According to the Jablonski diagram, the radiative transitions are vertical while the nonradiative transitions are horizontal since the latter occur between degenerate electronic states. As with radiative relaxations, it is possible to identify two different types of nonradiative deexcitations depending on the spin multiplicities of the states involved. Internal conversion (IC) involves population transfer between electronic states of equal spin multiplicity, while intersystem crossing (ISC) population transfer occurs between electronic states of different spin multiplicity.<sup>[10]</sup> As in the case of fluorescence and phosphorescence, the first process is permitted while the second is forbidden.

### 1.1.1.1. Electronic Energy Transfers

Apart from intramolecular relaxation processes, the deactivation of an excited state can also occur by interaction with another component of the same system. In fluid solution, an excited molecule  $D^*$  may have a chance to encounter and interact with a molecule of another solute  $A$ , if the excited state lifetime of the molecule is sufficiently long, meaning the intramolecular deactivation processes are not too fast. In this case, the deactivation of the excited state can occur via two specific processes: electron and energy transfer, which can be expressed in the following equations:



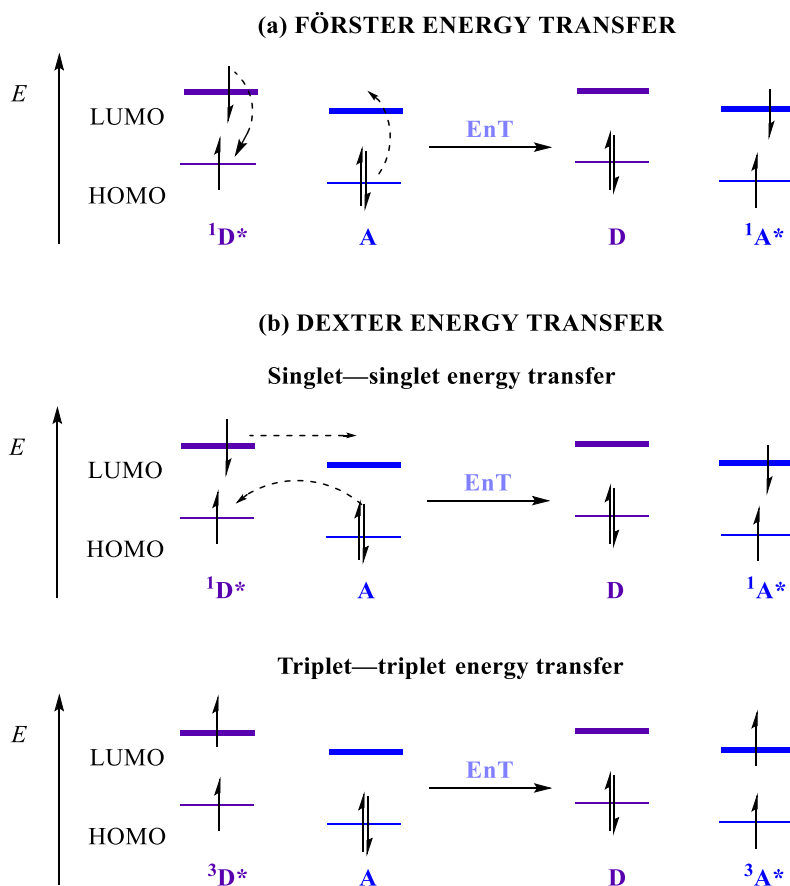
These processes quench the excited state  $D^*$  which prevents its luminescence and/or intramolecular reactivity, but instead sensitizes other species, for example, to induce a chemical change of species,<sup>[14]</sup> which otherwise could not absorb light. While electron transfer involves oxidation (Equation 1.2) or reduction (Equation 1.3) of the excited species, energy transfer (Equation 1.4) however, leads to the formation of an excited state ( $A^*$ ) of the quencher, which will then undergo its deactivation processes, including luminescence (sensitized luminescence) and reaction (sensitized reaction). In both cases, as in other nonadiabatic processes, part of the initially available energy is converted into vibrational, rotational, and translational energy shared by the two partners and eventually lost to the medium.

#### ***Energy transfer***

An electronically-excited molecule (donor) may relax to a lower-lying electronic state by transferring its excess energy to another molecule (acceptor), which is simultaneously promoted to a higher electronic state *via* a non-radiative process of energy transfer. At the end of this process, the donor molecule is in the ground state and the acceptor molecule in the excited state. The two mechanisms, known to be effective in the singlet-singlet energy

transfers between a donor (D) and an acceptor (A), are the Förster energy transfer<sup>[16]</sup> and the Dexter energy transfer<sup>[17]</sup> mechanisms.

The principle of Förster resonance energy transfer (FRET) is associated with the radiationless energy transfer of an energetically excited fluorophore (donor) to another molecule (acceptor) through dipole-dipole coupling (through space).<sup>[18]</sup> Moreover, the excited acceptor molecule returns to the ground state by losing its energy via fluorescence (in case, the acceptor is a fluorophore). Here, energy transfer is a two-step process that involves the excitation of electrons from the ground to the excited state of the donor and the energy transfer process from excited donor to acceptor molecule through the dipolar coupling between donor emission and acceptor excitation dipole moments (Scheme 1a).<sup>[19]</sup> FRET efficiency depends on the intermolecular distance of the donor-acceptor pair which typically lies between 2 and 10 nm.<sup>[20]</sup>

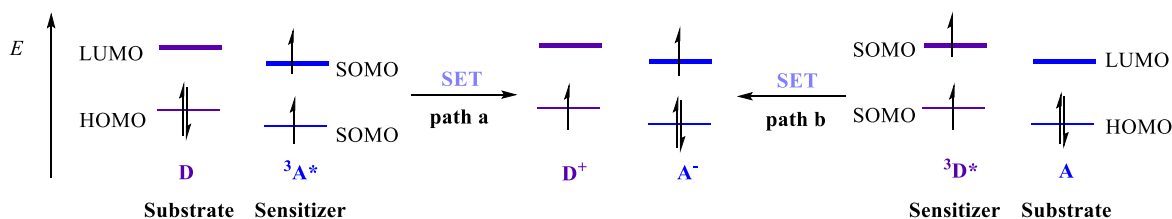


**Scheme 1.** Schematic illustrations of (a) Förster energy transfer (through-space). (b) Dexter energy transfer (through-bond) that can occur between donor and acceptor pairs.

During the Dexter energy transfer, there is an actual electron exchange between the donor and acceptor. In this type of energy transfer, the reaction rate decays exponentially with the distance between the donor and acceptor, hence this process is only important at short intermolecular distances (normally within 1 nm)<sup>[21]</sup> when there is a significant overlap of molecular orbitals (MO). Both singlet and triplet excitons may be transferred by this mechanism.<sup>[22]</sup> FRET usually outperforms the efficiency of the Dexter energy transfer for singlet excitons, while triplets may be transferred between non-phosphorescent molecules mostly by the Dexter mechanism (Scheme 1c). The main reason is that in the triplet state, the electron spins exhibit three degrees of freedom, and to achieve such a lower energy spin state, the electron density is distributed in a manner to minimize the spin-spin interactions.<sup>[23]</sup>

### ***Photoinduced electron transfer***

In a photoinduced electron transfer (PET), an electron migrates between a photoexcited and ground-state species. In order to achieve exothermic electron transfer in the ground state, the energy of the HOMO of the reductant (electron donor) must lie higher, compared to the LUMO of the oxidant (electron acceptor).<sup>[24]</sup> In most cases, the corresponding frontier orbitals for organic molecules in the ground state are energetically close to each other so exothermic electron transfer is unlikely to occur. In the excited state, however, the LUMO (with respect to the ground state) gets populated by one electron, changing both frontier orbitals (HOMO and LUMO) to singly occupied molecular orbitals (SOMO). Electron transfer processes that are endothermic at ground state configurations are thus made possible (Scheme 2) since the excited molecule becomes both, a stronger oxidant and reductant. One of these processes can occur from the energetically higher HOMO of the donor molecule into the lower-lying SOMO of the excited acceptor. The substrate molecule will then be oxidized by the electronically excited sensitizer (path **a**). Electron transfer can also take place from the higher-lying SOMO of the excited donor to the lower LUMO of the acceptor molecule in its ground state, rendering this process a reduction of the substrate molecule by an electronically excited sensitizer (path **b**).<sup>[25]</sup>



**Scheme 2.** Energy scheme of orbitals that are involved in photochemical electron transfer processes.

The kinetics of photoinduced electron transfer is described by the Marcus theory.<sup>[26]</sup> Within this framework, the electron transfer kinetics depend on the thermodynamic driving force of the electron transfer reaction, the associated reorganization energy, and the electronic coupling between the excited fluorophore and the successor radical ion pair

$$\Delta G_{SET} = E^{\text{Red}}(D^{\bullet+}/D) - E^{\text{Oxd}}(A/A^{\bullet-}) - \Delta E_{00} + w_p \quad (1.5)$$

The energy balance  $\Delta G_{PET}$  of a photoinduced electron transfer reaction is given by the Rehm-Weller equation (Equation 1.5),<sup>[27]</sup> where  $E(D^+/D)$  and  $E(A/A^-)$  correspond to the donor (oxidation) and acceptor (reduction) ground state reduction potentials, respectively,  $\Delta E_{00}$  is the transition energy between the vibrationally relaxed ground and excited states of the fluorophore, and  $w_p$  is the Coulomb stabilization energy associated with the intermediate radical ion pair.

Electron transfer occurs spontaneously when the reaction possesses sufficient driving force,  $-\Delta G_{PET}$ . In the photoinduced electron transfer, the positive free enthalpy of the corresponding process in the ground state is compensated by the excitation energy. Analyzing Equation 1.5, it is possible to conclude that electron transfer strongly depends on the redox properties of the donor and acceptor and the excited-state energy. Additionally, it can be observed that the solvent polarity and the distance between the donor and acceptor will affect the driving force.

$$\Delta G_{SET} = -F \left[ E_{1/2}(A/A^{\bullet-}) - E_{1/2}(D^{\bullet+}/D) - \frac{Z_D Z_A e^2}{4\pi\epsilon_0\epsilon_r\alpha} \right] - E_{0.0}^* \quad (1.6)$$

To calculate the thermodynamic feasibility of the single-electron transfer (SET) in solution, solvent effects, the formation of charge transfer intermediates, and Coulomb interactions must be taken into account. For this purpose, the calculation of the Gibbs energy for photo-induced electron transfer processes can be done by using a variation of the Rehm-Weller equation (Equation 1.6) where  $F$  is the Faraday constant ( $23.06 \text{ kcal V}^{-1}\text{mol}^{-1}$ )<sup>[15b]</sup> and  $E_{1/2}(A/A^{\bullet-})$  and  $E_{1/2}(D^{\bullet+}/D)$  are ground state redox potentials obtained experimentally through cyclic voltammetry for each species A and D undergoing reduction and oxidation, respectively.  $E_{0,0}^*$  is the energy difference between the oscillation states  $S_0$  and the involved excited state ( $S_1, T_1$ ), which can be determined by spectroscopic methods.<sup>[28]</sup> The fraction in this equation is called the Coulomb term and describes the Coulomb interactions, which depend on the solvent used.<sup>[29]</sup> Here,  $z$  is the charge of the reactants involved, which is usually not present because the acceptor and donor are predominantly uncharged. The term also includes the elementary charge  $e$  ( $1.60217653 \times 10^{-19} \text{ C}$ ), the electric field constant  $\epsilon_0$  ( $8.854187817 \times 10^{-12} \text{ C}^2\text{J}^{-1}\text{m}^{-1}$ ), the relative permittivity of the reaction medium  $\epsilon_r$  and the distance between the reactants in question  $\alpha$ .<sup>[30]</sup> Since most PET reactions take place in polar solvents such as acetonitrile and there the effect of the electrostatic Coulomb term on the free enthalpy is quite small (in MeCN  $\sim 1.3 \text{ kcal/mol}$  ( $0.06 \text{ eV}$ ))<sup>[15a, 31]</sup> this can be neglected and the free enthalpy of photo-induced electron transfer processes can be calculated using Equation 1.7 for oxidative quenching of an excited donor or 1.8 for reductive quenching of an excited acceptor. The redox potentials of the excited species can be calculated from  $E_{0,0}^*$  and the redox potentials from the respective ground states (1.9, 1.10).

$$\Delta G_{SET} = -F[E_{1/2}(A/A^{\bullet-}) - E_{1/2}(D^{\bullet+}/D^*)] \quad (1.7)$$

$$\Delta G_{SET} = -F[E_{1/2}(A^*/A^{\bullet-}) - E_{1/2}^*(D^{\bullet+}/D)] \quad (1.8)$$

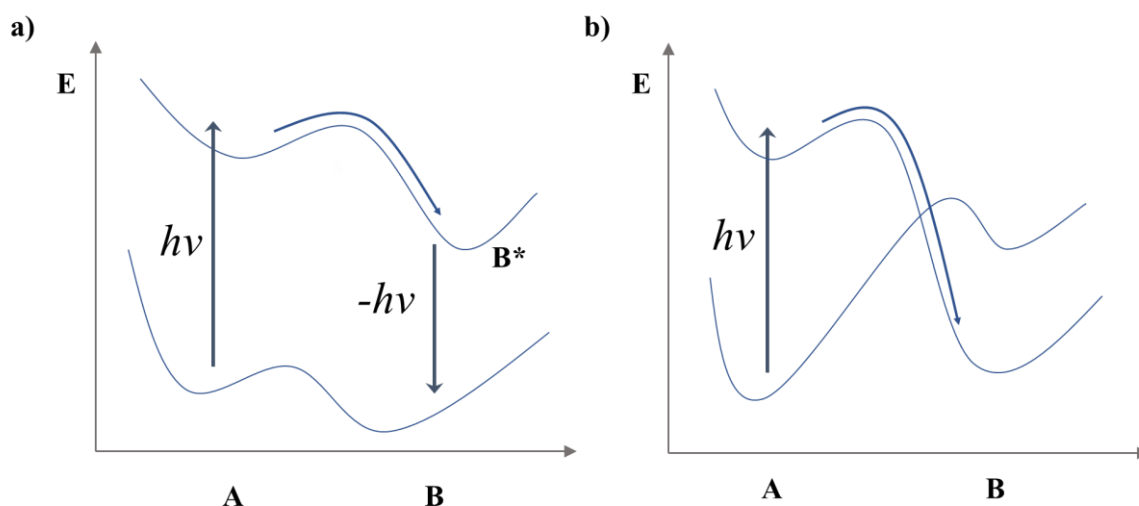
$$E_{1/2}(D^{\bullet+}/D^*) = E_{1/2}(D^{\bullet+}/D) - E_{0,0}^* \quad (1.9)$$

$$E_{1/2}(A^*/A^{\bullet-}) = E_{1/2}(A/A^{\bullet-}) - E_{0,0}^* \quad (1.10)$$

## 1.1.2. UV Photoreactions

### 1.1.2.1. Physical basics

UV Photochemical reaction pathways can be described by applying the concept of potential energy surfaces (PES). Within the Born-Oppenheimer approximation, potential energy surfaces govern nuclear motion and, therefore, chemical reactivity. A comprehensive picture of nuclear dynamics can be obtained by solving the time-independent electronic Schrödinger equation with quantum chemistry (electronic structure) methods. The result is a potential energy surface parameterized by the  $3N - 6$  internal nuclear coordinates ( $3N - 5$  for linear molecules) that define the molecular geometry of an  $N$ -atom system. The lowest electronic energy plotted against all internal variables forms a multidimensional hypersurface corresponding to the ground state. The energy released when the molecule starts moving through the excited-state surface is irreversibly dissipated to the surrounding medium. The molecule is likely to follow the path of steepest descent and once it arrives at a local minimum, the possibility of various photophysical processes appears, e.g. fluorescence, internal conversion, or intersystem crossing. In principle, this choice is always available, but thermal relaxation is fastest on a slope of the PES.<sup>[10]</sup>



**Figure 2.** Types of photochemical reactions: Potential energy surfaces of a) adiabatic and b) diabatic photoreactions.<sup>[10]</sup>

According to Förster, photochemical reactions can be generally classified as adiabatic or as diabatic whether the chemical change occurs on the same potential energy surface or not. In

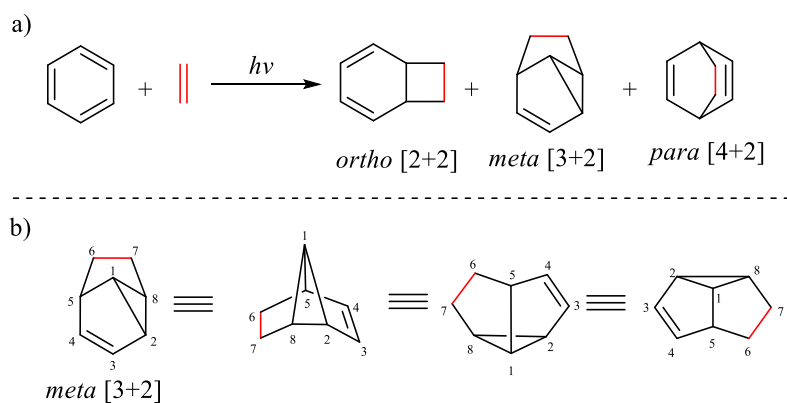


the adiabatic cases, relaxation occurs either in the reactant (A) or in the product (B) while in the diabatic case it occurs in between them.<sup>[32]</sup> Figure 2. shows two-dimensional cross-sections of an excited- and a ground-state PES along a reaction coordinate leading from reactant A to product B. The adiabatic photoreaction involves the absorption of light by the reactant to generate the excited state electron configuration and then, by the normal thermal motions that are imparted to that excited state molecule, it travels along to the excited state of the product, which eventually will emit a photon and generate the final product (Figure 2a). In contrast, during a diabatic reaction, both the excited state potential energy surface and the ground state potential energy surface are involved. The reactant absorbs a photon of light and changes into the excited state electron configuration and at some point, crosses back to the ground state without emitting light and generates the product in its ground state (Figure 2b).

In the following, some typical classes of reactions occurring in organic photochemistry are given to be introduced.

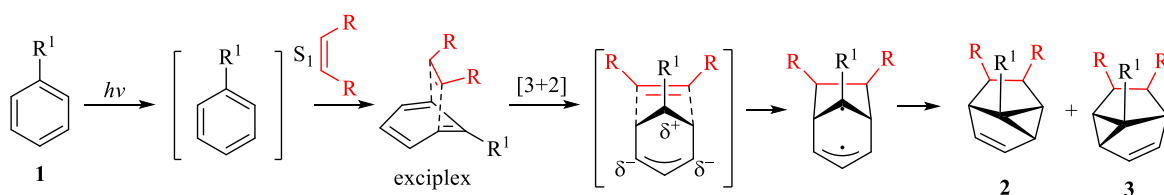
#### 1.1.2.2. The *meta* photocycloaddition of arenes to alkenes

The photochemical cycloaddition reactions of aromatic rings with olefins have been of great interest to chemists for the last 60 years.<sup>[33]</sup> Upon irradiation with UV-C light, the aromatic ring is electronically excited to the first singlet excited state and undergoes a cycloaddition with a double bond, breaking the aromaticity and leading to the formation of three possible cycloadducts: *ortho* [2+2], *meta* [3+2] and *para* [4+2] (Scheme 3a). The latter is rarely observed, but the *ortho* and *meta* photoproducts are more frequently encountered and much work has been reported regarding a predictive model to delineate which one is favored when conducting a specific reaction.<sup>[34]</sup> Studies based on the valence bond (VB) theory suggest that a common non-polar biradical intermediate exists and the distinction between the [2+2] and the [3+2] cycloaddition occurs by dynamic effects mainly influenced by the placement of groups on the aromatic ring.<sup>[35]</sup> For the purposes of this chapter, this section will be focused exclusively on the *meta* photocycloaddition.



**Scheme 3.** A) Three possible photoproducts of the cycloaddition of an alkene to benzene. b) Different ways of representing the central core structure of the adduct derived from *meta* photoaddition.

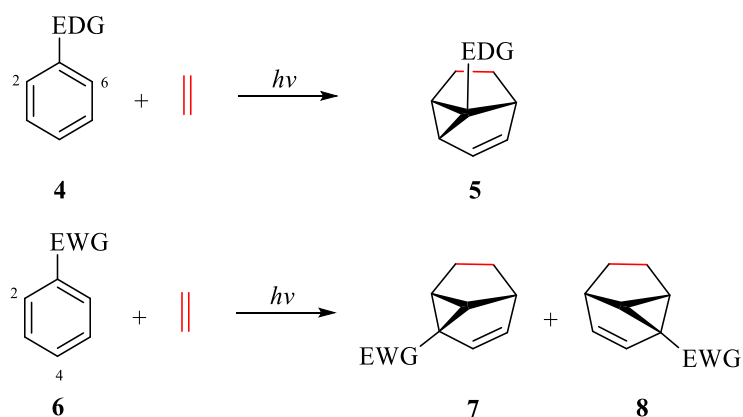
The *meta* [3+2] form stands apart from the other modes. First, it results in the formation of three new carbon-carbon  $\sigma$ -bonds in one step, which is a considerable increase in molecular complexity in a single reaction step. Second, this transformation in its intramolecular version can generate tetracyclic sesquiterpenes bearing six new stereocenters using simple planar achiral starting materials, and third, it has great synthetic value since there is no direct equivalent in thermal chemistry. Even though the mechanism of the *meta* photocycloaddition and its stereo- and regiochemical aspects have been widely studied and discussed, the details are still a matter of contention.<sup>[33a]</sup> The [3+2] photocycloaddition mechanism is represented as a multistep reaction in Scheme 4. Although there have been extensive mechanistic and theoretical studies on the *meta*-photocycloaddition reaction, the pathway followed is still the subject of debate.<sup>[35]</sup>



**Scheme 4.** A possible mechanism for the *meta*-photocycloaddition.

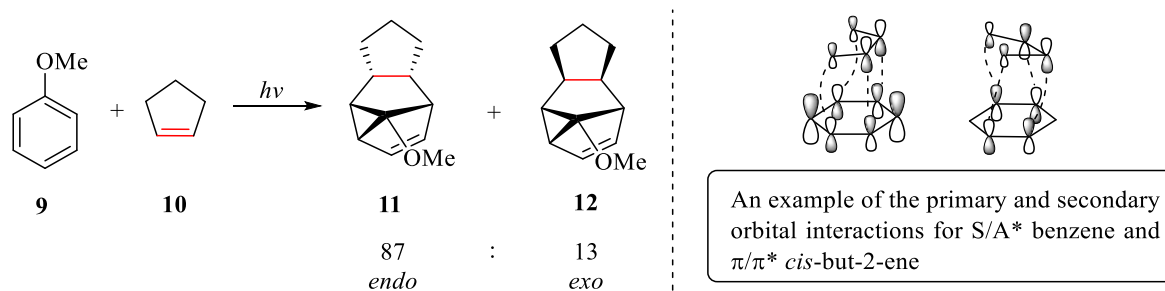
The first step is the excitation of the substituted benzene to its excited state  $S_1$  by using UV-C light. The HOMO and the LUMO of the excited arene interact with the HOMO ( $\pi$ ) and LUMO ( $\pi^*$ ) of the alkene generating two new sigma C–C bonds from the exciplex, a step that is believed to proceed through a slightly polarized intermediate. The two final products

are formed from the intermediate which still has singlet multiplicity and therefore possesses zwitterionic mesomeric or a biradical<sup>[36]</sup> structure. The ratio of these two observed regioisomeric cyclopropane products depends on the electronic nature of the substituents in the aromatic ring. In general, it is observed that electron-donating groups (EDG) can stabilize the 2,6-addition whilst electron-withdrawing groups (EWG) favor the 2,4-addition (Scheme 5).



**Scheme 5.** Regiochemical preferences in the *meta*-photocycloaddition with substituted benzenes.

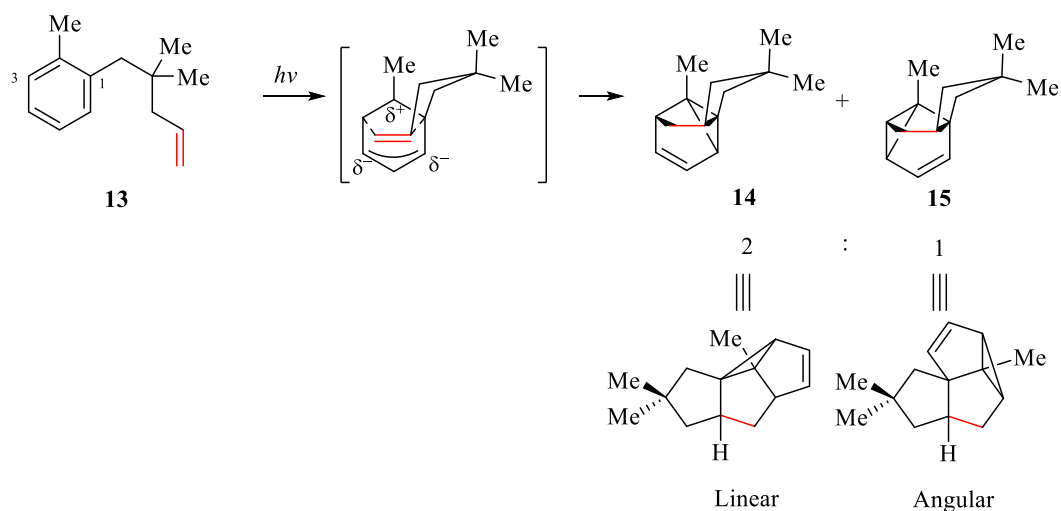
Aside from regioisomers, stereoisomers are formed when using substituted olefin derivatives. The addition can either occur from the *exo* or *endo* exciplex to the aromatic moiety. The *endo/exo* ratio can be explained by analyzing the secondary orbital interactions on the formation of the exciplex and by considering steric effects. In the case of intermolecular cycloadditions, different studies with cyclic alkenes have shown that *endo*-isomers are generally predominant.<sup>[37]</sup> A good example of such selectivity is the case of anisole and cyclopentene reaction represented in the scheme 6 where the observed *endo*-selectivity can be explained in the same way as the *exo/endo*-selectivity in a Diels-Alder reaction, secondary orbital interactions stabilize the *endo* complex and destabilize the *exo* complex (Scheme 6).



**Scheme 6.** Stereoselectivity in the intermolecular *meta*-cycloaddition reaction.

Contrary to the intermolecular *meta* photocycloaddition, during the intramolecular version, the *endo* approach induces significant strain resulting in the formation of *exo* rather than *endo* adducts.<sup>[38]</sup> Additionally, if the olefin contains *cis* substituents, the *exo* addition exhibits repulsion between these substituents and the hydrogens in the tether leading to a preference in the 1,3-addition over the 2,6-addition especially when electron-donating groups are *ortho* to the tether in the aromatic ring.<sup>[39]</sup>

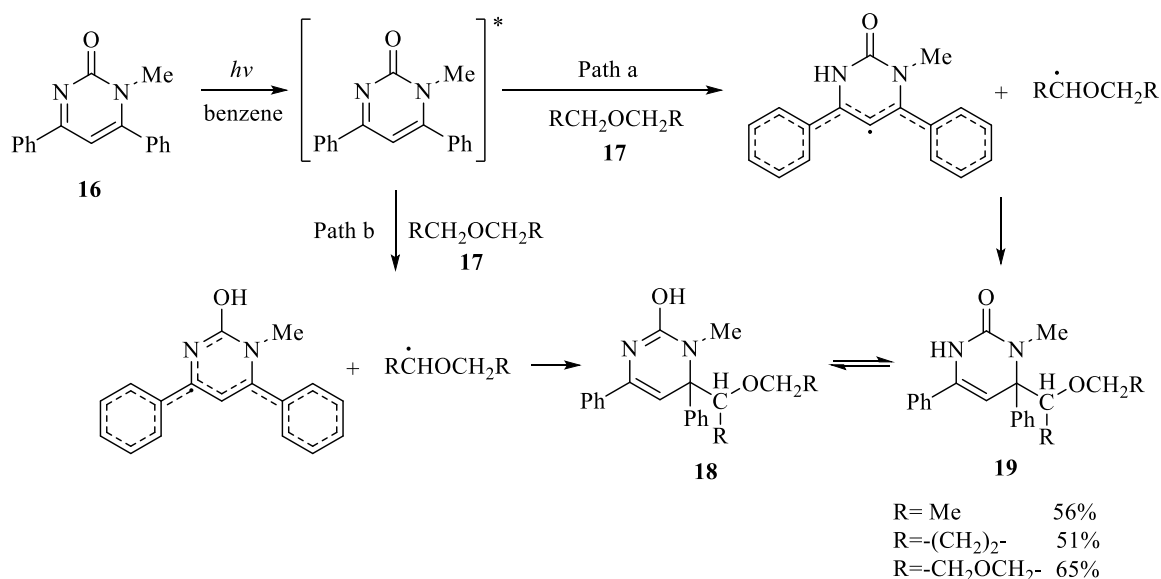
The example in Scheme 7 highlights other important aspects of the intramolecular 1,3-addition reaction: firstly, it may give either a linear or an angular isomer. In general, the intramolecular *meta* photocycloaddition that occurs within chromophores containing on the aromatic ring an *ortho* group to the side-chain substituent is prone in favor of the linear adduct.<sup>[40]</sup> The second aspect is, that the tether between arene and alkene should contain the optimal length of three atoms, more than that could represent a significant reduction in the yield of the *meta* photocycloaddition reaction presumably due to the increased degrees of freedom.



**Scheme 7.** Regio and stereoselectivity outcome in the intramolecular *meta* photocycloaddition of **13**.

### 1.1.2.3. Photochemical Abstraction of Hydrogen by singlet and triplet $n\pi^*$ states of Aromatic nitrogen

Despite the relevance of the photochemical abstraction of hydrogen by aromatic nitrogen and the importance of nitrogen-containing substances in biological systems,<sup>[41]</sup> this process has attracted much less attention than the related abstraction by aromatic carbonyl oxygen. However, processes involving  $(n,\pi^*)$  excitations of the lone-pair electrons associated with hydrogen bonding have gained increasing interest. Excited-state studies of these systems are especially useful as excitation changes the tautomer's relative energies, promoting photochemical reactions. Functionalized nitrogen heteroaromatics can display such chemistry and have a large number of electronically excited states. For instance, pyridines have one  $\pi\pi^*$  and two  $n\pi^*$  triplets in the range of 75-85 kcal/mol<sup>[42]</sup>, and asymmetrically substituted pyrimidines are expected to possess an even more extensive arrange of triplets.<sup>[43]</sup>

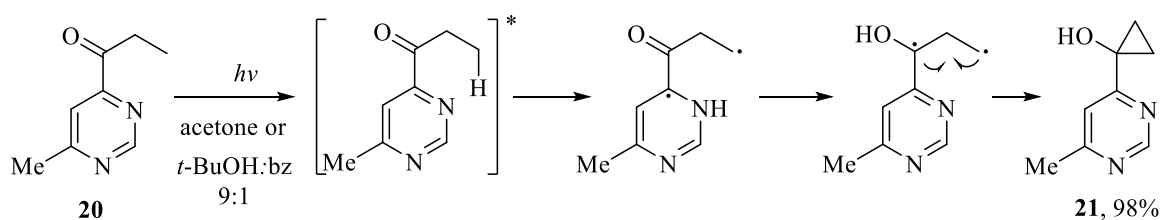


**Scheme 8.** Intermolecular photochemical  $\alpha$ -hydrogen abstraction by imino nitrogen or by carbonyl oxygen.

The excited states of imines are known to have a low tendency to carry out a hydrogen abstraction process due to the low reactivity of the carbon–nitrogen double bond. However, different reactions analogous to the hydrogen abstraction by carbonyl oxygen have been described. For example, the study of the photochemical behaviors of pyrimidin-2(1*H*)-ones (**16**), a structure present in the nucleoside cytosine, showed such reactivity. Upon irradiation in the presence of, cyclic or acyclic aliphatic ethers, they can undergo a photochemical

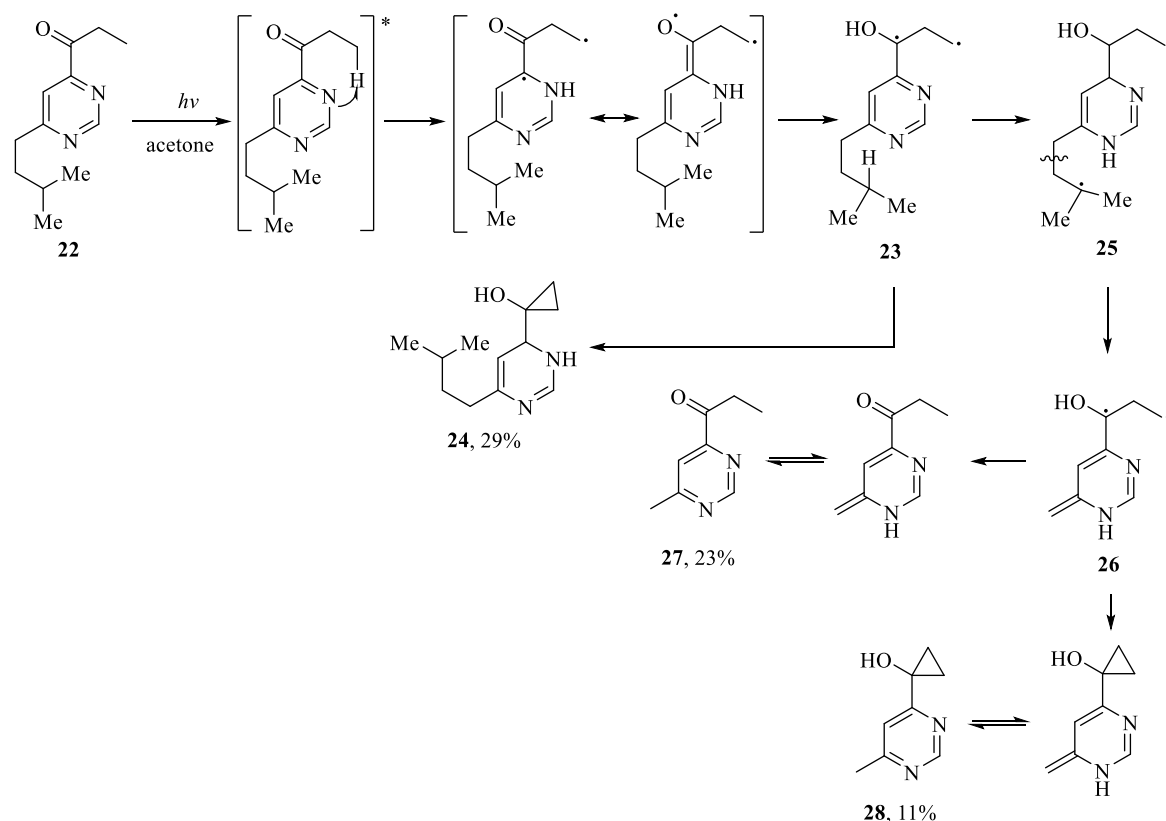
addition reaction through an intermolecular  $\alpha$ -hydrogen abstraction of the ether by the excited imino nitrogen (path a) or by the carbonyl oxygen (path b), to give **19** in moderate to good yields (Scheme 8).<sup>[44]</sup>

Photochemistry studies of 4-acylpyrimidines proved that its direct irradiation ( $\lambda > 340$  nm) or acetone-sensitized irradiation leads to intramolecular hydrogen abstraction by the N-3 from the C-4 of the side chain following isomerization to cyclopropanol **21** (Scheme 9). However, it seems likely that the unperturbed triplets of the heteroaromatic ring and the carbonyl group mix to produce one or more low-lying  $n\pi^*$  triplets and one of these states has electron deficiency on both carbonyl oxygen and the adjacent heteroaromatic ring making it thus capable of mediating hydrogen abstraction by either the nitrogen N-3 or the carbonyl oxygen.<sup>[45]</sup>



**Scheme 9.** Intramolecular photochemical hydrogen abstraction by nitrogen and ring-closing transformation.

Irradiation of **22** proceeds through a different mechanism which is not possible for **20**. Direct or acetone-sensitized irradiation gives the formation of three different photoproducts. The reaction starts with the abstraction of the hydrogen by N-3, analog to Scheme 9, and can either follow isomerization to form **24** or also undergo another abstraction by N-1, but without excited state activation of N-1. Then, **25** fragments to **26**, can either give the cyclopropanol **28** or transfer the hydrogen of the OH group, to restore the carbonyl group in **27** (Scheme 10).<sup>[46]</sup>



**Scheme 10.** Acetone-sensitized hydrogen abstraction and fragmentation mechanism.

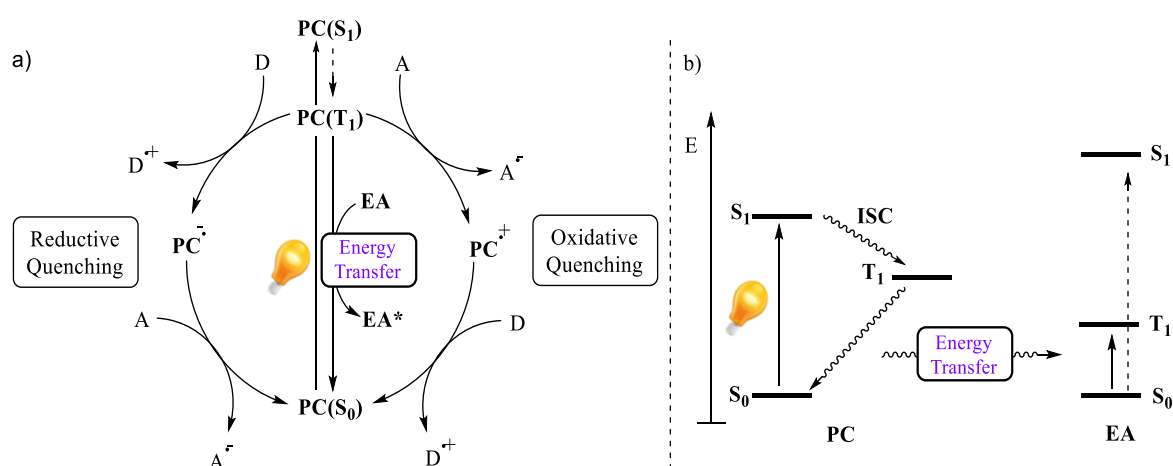
Stern-Volmer quenching plots of these types of reactions describe identical  $k_q\tau$  values for products of abstraction by both nitrogen and oxygen, showing that these processes are competitive and can occur through either a single triplet with electron deficiency on both nitrogen and oxygen or by two triplets that interconvert rapidly.<sup>[47]</sup>

### 1.1.3. Visible Light Photocatalysis

Direct excitation of organic compounds using ultraviolet light is a relevant field of chemistry with a historical background that spans more than a century. Nevertheless, its use has decreased over the last years as organic chemists consider this technique not easy to apply due to its negative impact on selectivity and functional group tolerance.<sup>[48]</sup> The development and use of visible light photocatalysis has changed this perception as it evolved as an alternative strategy that employs milder conditions to access excited (triplet) states. Moreover, since photons from visible light are less energetic than UV photons, more selective, predictable, and easy to control reactions can be achieved.

The general principles of photochemistry are still valid to explain visible-light photocatalysis processes that only differ in the use of irradiation with a longer wavelength. Visible-light-induced photochemical reactions can be explained by two possible mechanisms: single-electron transfer (SET) or energy transfer (EnT). In the first case the photocatalyst (PC) is excited ( $PC^*$ ) by irradiation, and then can either accept or donate a single electron enabling oxidative or reductive quenching cycles depending on the substrate. In the case of the oxidative quenching cycle,  $PC^*$  reduces an electron-deficient substrate or acceptor (A) by donating an electron which results in the formation of a strong oxidant ( $PC^{+}$ ). To close the catalytic cycle, this oxidized form of the catalyst accepts another electron from an electron-rich substrate or a donor (D). Additionally,  $PC^*$  also can undergo a reductive quenching oxidizing a donor (D) by accepting an electron. This interaction generates the reduced form of the catalyst ( $PC^{-}$ ) which can then donate an electron to an acceptor (A), reestablishing the ground state photocatalyst (PC) and completing the catalytic cycle (Figure 3a).<sup>[15a, 49]</sup>

The main factor governing the process of photoredox catalysis is the redox properties of the photoexcited catalyst as well as the substrates and reagents that are present in the reaction mixture. When a combination of substrates and an excited photocatalyst has incompatible oxidation or reduction potentials they cannot undergo a SET process. However, when the energy of the triplet state of the excited photocatalyst is higher than the triplet energy of the substrate, an EnT process can take place.



**Figure 3.** Photocatalysis modes: a) Electron transfer. b) Energy transfer.



As described in Figure 3b the EnT photocatalysis process starts with the excitation of the PC from its ground single state ( $S_0$ ) to the low-lying  $S_1$  state. Next, an intersystem crossing (ISC) process could lead the PC to its triplet state ( $T_1$ ) allowing the intermolecular energy transfer to the substrate or energy acceptor (EA), which is not able to absorb light at the given wavelength and has an accessible low energy triplet state (comparable to the photo-excited triplet state energy). In this interaction, triplet-triplet energy transfer results in a photo-excited triplet state of the EA while the ground state of the photocatalyst is reestablished. Once the substrate gets excited to its triple-state ( $T_1$ ), the substrate can take part in a later chemical reaction. On a molecular level, EnT in the context of organic synthesis and catalysis can be categorized as Dexter-type energy transfer.<sup>[50]</sup>

The efficiency of an EnT process is determined by three factors: i) the energy donor (photocatalyst) must have triplet energy higher than that of the EA (substrate/reagent), ii) the photocatalyst should have a high ISC rate, as this will increase the quantum yield of  $T_1$ , and iii) the process of EnT from the photocatalyst to the energy acceptor must be exergonic. If the EnT event itself is thermodynamically and kinetically possible, the observable EnT rate in solution is then limited by the diffusion-mediated formation of the encounter complex.

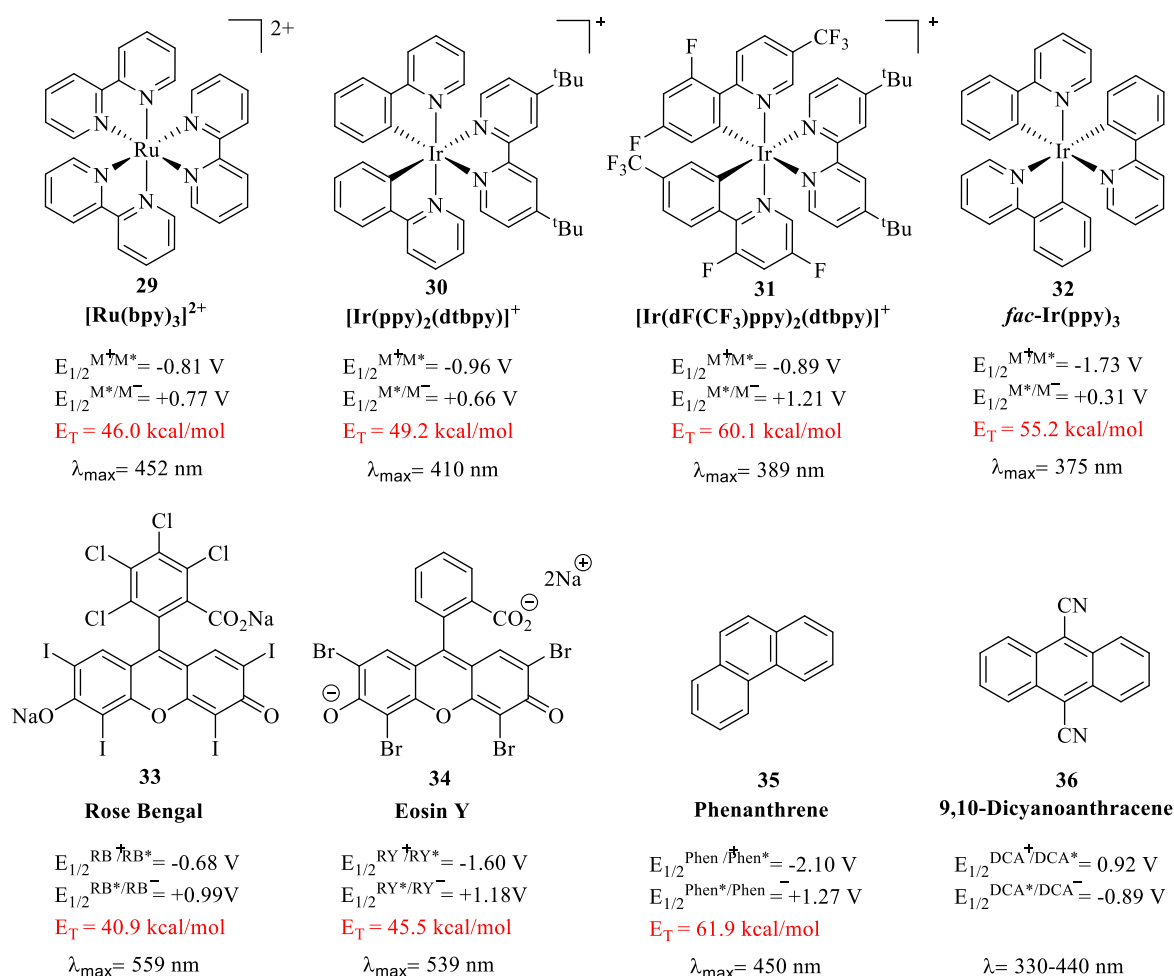
For synthetic applications, the EnT process has commonly been simplified to evaluate and compare the triplet excited-state energy (or triplet energy,  $E_T$ ) of donor and acceptor, i.e., the energy difference between the singlet ground state ( $S_0$ ) and the lowest triplet state ( $T_1$ ). Such values can be determined from low-temperature emission spectroscopy, sensitization experiments, or computational studies.<sup>[50b]</sup> Moreover, Stern-Volmer luminescence quenching experiments are generally carried out to address the effective quencher(s) from a set of reagents present in the reaction mixture.<sup>[15a]</sup>

### ***Photocatalysts***

Most photocatalytic reactions use different visible light-absorbing chromophores/photocatalysts that can be activated with low-energy photons. Recent literature has focused on the use of coordinatively saturated organometallic photocatalysts, predominantly ruthenium or iridium complexes, which are chemically and conformationally stable under standard reaction conditions and do not generally bind to the substrates.<sup>[15a, 51]</sup> Even though organic chromophores have proved to have the ability to take part in visible

light SET and EnT processes, their use in organic synthesis as photocatalysts is less common.<sup>[15b]</sup>

A photocatalyst (sensitizer) for visible light photocatalysis should have a suitable redox potential window or higher triplet excited-state energy than the targeted substrate and triplet states with long lifetimes, to provide effective interactions with the substrates in their proximity. Figure 4 shows some representative photocatalysts used in photochemical reactions with their redox potentials, and photophysical properties.<sup>[52]</sup>

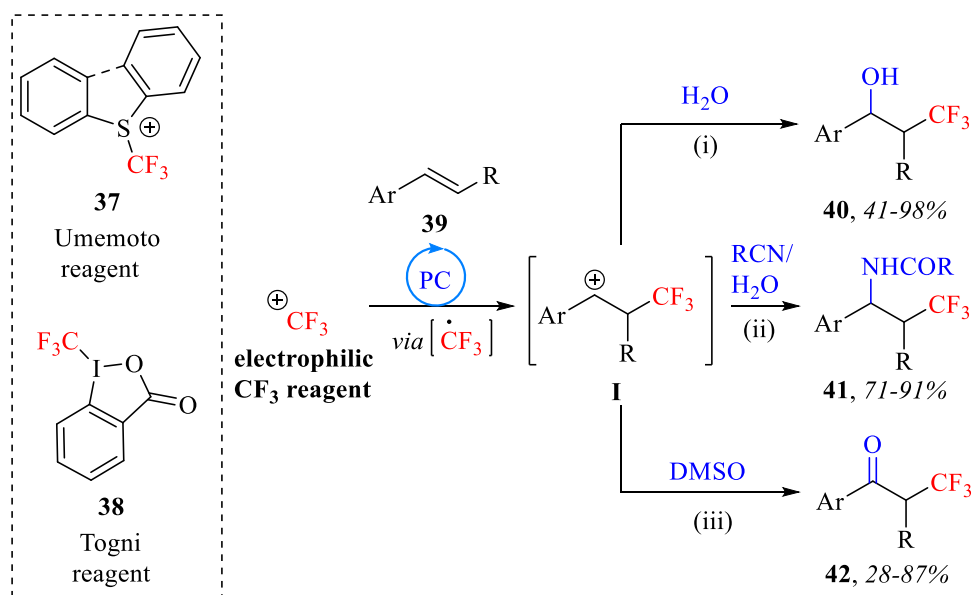


**Figure 4.** Photocatalysts and their redox potentials in MeCN [V vs. SCE].

### 1.1.3.1. Relevant examples of photoredox catalysis

#### *Functionalization of Alkenes by Photoredox Catalysis*

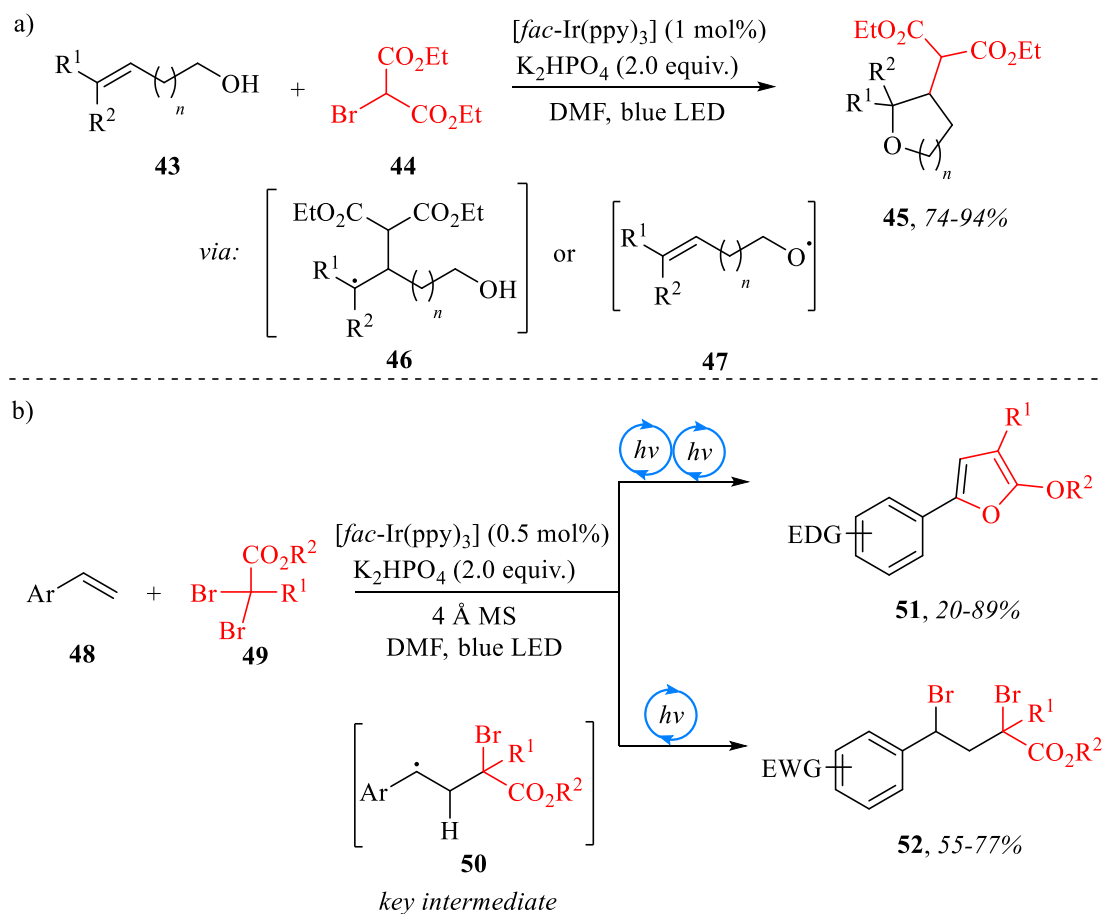
Difunctionalization of double bonds is common in organic synthesis to create structural frameworks with molecular diversity and to build up molecular complexity.<sup>[53]</sup> Among other things, photoredox catalysis enables the introduction of two different functional groups regio-specifically across double bonds. The first step in a difunctionalization is always the addition of the radicals generated by the PC to the side of the double bond-forming a more stable radical intermediate.



**Scheme 11.** Fluoromethylation of aromatic alkenes.

$\alpha$ -Trifluoromethylation of alkenes has become a vital subject in organic chemistry due to the relevance of trifluoromethyl ( $\text{CF}_3$ ) groups in the fields of agrochemicals, pharmaceuticals, and material science. Thus, the development of new methodologies to introduce this functional group has emerged as a subject of growing interest. One example of this is the methodology developed by Koike, and Akita which uses electrophilic  $\text{CF}_3$  reagents such as the Umemoto reagent (**37**)<sup>[54]</sup> or Togni reagent (**38**)<sup>[55]</sup>. In addition to being stable and easy to use, they possess redox potentials low enough to undergo SET from the photoexcited  $[\text{Ru}(\text{bpy})_3]^{2+}$  and *fac*- $[\text{Ir}(\text{ppy})_3]$  catalysts serving as electron acceptors. After the addition of the  $\text{CF}_3$  radical to the aromatic alkenes (**39**) and subsequent oxidation of the resulting benzylic radical, the intermediate **I** can then (i) react with nucleophiles like water, alcohols,

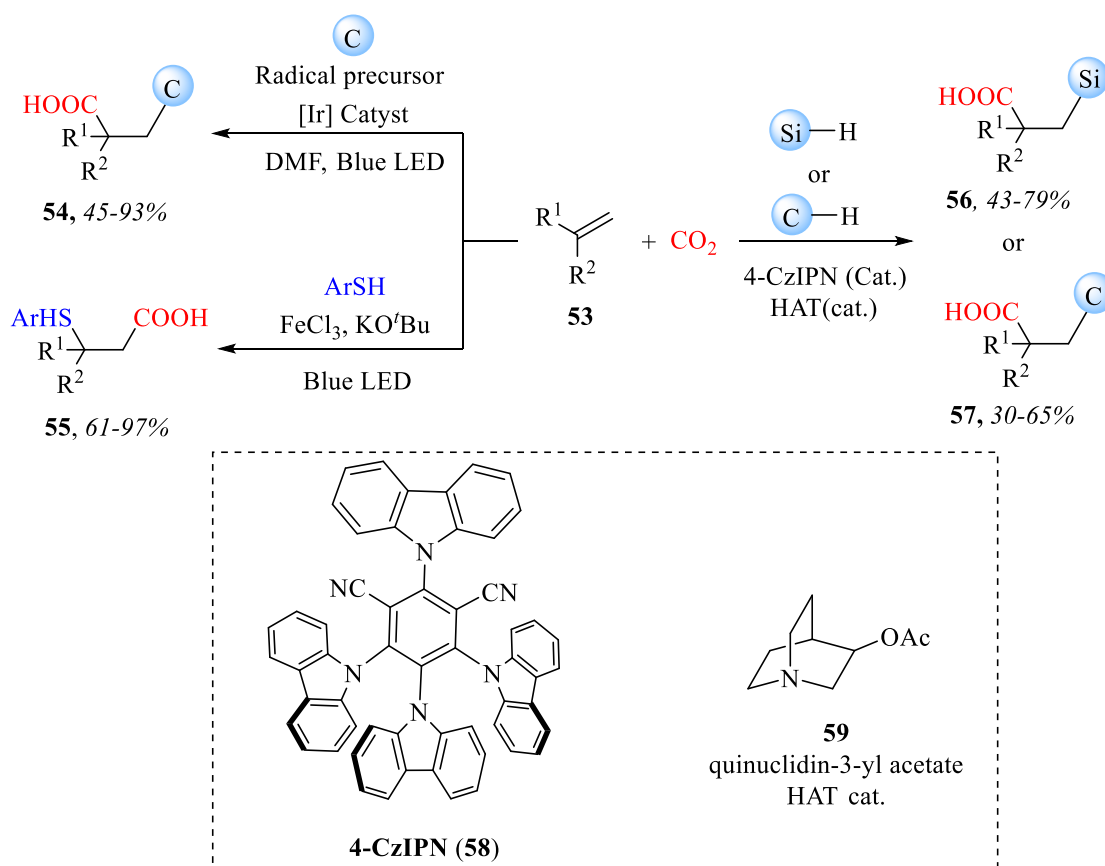
carboxylic acids, and amides; (ii) undergo Ritter-type amination and (iii) Kornblum-type oxidation (Scheme 11).<sup>[56]</sup>



**Scheme 12.** a) Synthesis of tetrahydrofurans and tetrahydropyrans. b) 1,2-Difunctionalization of alkenes with *gem*-dibromides.

A visible light-induced intramolecular difunctionalization of electron-rich styrenes using  $[\text{fac-Ir(ppy)}_3]$  as a photoredox catalyst and  $\text{K}_2\text{HPO}_4$  as an additive was developed by Yang, Xie, et al. This approach led to the synthesis of various substituted tetrahydrofurans and tetrahydropyrans (**45**) through highly efficient and regioselective cycloaddition of styrenes. After the alkyl radical  $\cdot\text{CH}(\text{CO}_2\text{Et})_2$  is generated by oxidative quenching of the visible light-induced excited state  $\text{Ir}^{3+*}$ , two possible reaction pathways can take place, its addition to the double bond of **43** forming intermediate **46** or hydrogen atom transfer (HAT) from  $\cdot\text{CH}(\text{CO}_2\text{Et})_2$  to the oxygen in **43** leading to the intermediate **47** (Scheme 12a).<sup>[57]</sup> In both cases, further oxidation of these intermediates by  $\text{Ir}^{4+}$  and rearrangement of the generated carbocations lead to the formation of **45**. A related intermolecular version described by Zhu

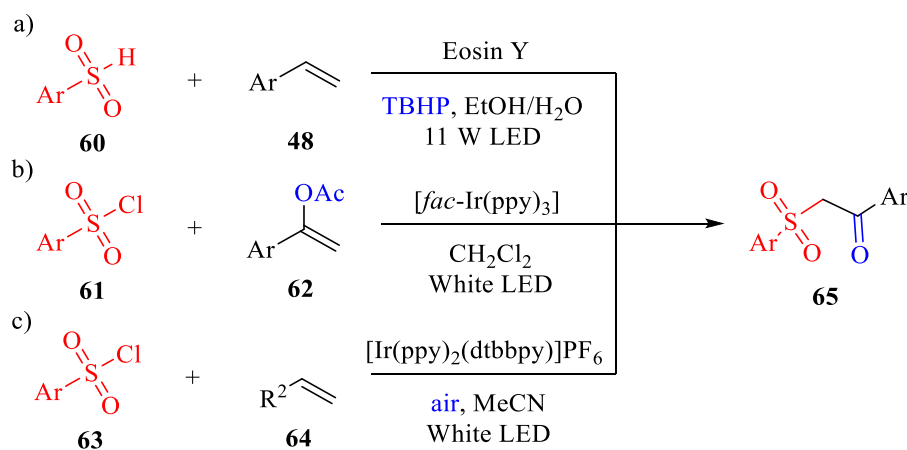
et al. serves as a platform to construct biologically important heterocyclic skeletons (**51**) and versatile 1,3-dibromide building blocks (**52**) using a diverse array of styrenes (**48**) and *gem*-dibromides (**49**). Depending on the electronic effect of alkenes **48** this 1,2-difunctionalization can achieve 1,2-carboxylation and 1,2-carbohalogenation (Scheme 12b).<sup>[58]</sup> Benzylic radical reduction potential indicates that electron-donating groups on styrene arenes would facilitate single-electron oxidation of benzylic radical to its cation species easing the formation of furans **51**.



**Scheme 13.** Difunctionalization of simple alkenes through C–H or Si–H activation.

The activation of C(sp<sup>3</sup>)–H or Si–H bonds is an effective process for alkene difunctionalization allowing the simultaneous introduction of a carbon or silicon group and a second functional group across the double bond. The photocatalyzed activation of C(sp<sup>3</sup>)–H and Si–H bonds, such as in hydrosilylations and hydroalkylations of alkenes, often involve HAT processes. In 2018 Wu et al. reported a convenient visible-light-driven metal-free difunctionalization of simple alkenes using CO<sub>2</sub> and readily available Si–H and

C(sp<sup>3</sup>)-H reagents combining photoredox and HAT catalysis. This strategy represents an uncommon example of difunctionalization of alkenes via Si-H or C-H activation using an organic photocatalyst (**58**).<sup>[59]</sup> Although in the previous year Martin et al. reported a dicarbofunctionalization of styrenes with CO<sub>2</sub> and carbon radicals generated from Ir-catalyzed photoredox processes and in the same year Yu et al. reported an iron-catalyzed thiocarboxylation of styrenes and acrylates with CO<sub>2</sub> by using visible light as driving force, these two methodologies require strong bases, transition metals or pre-functionalized radical precursors (Scheme 13).<sup>[60]</sup>



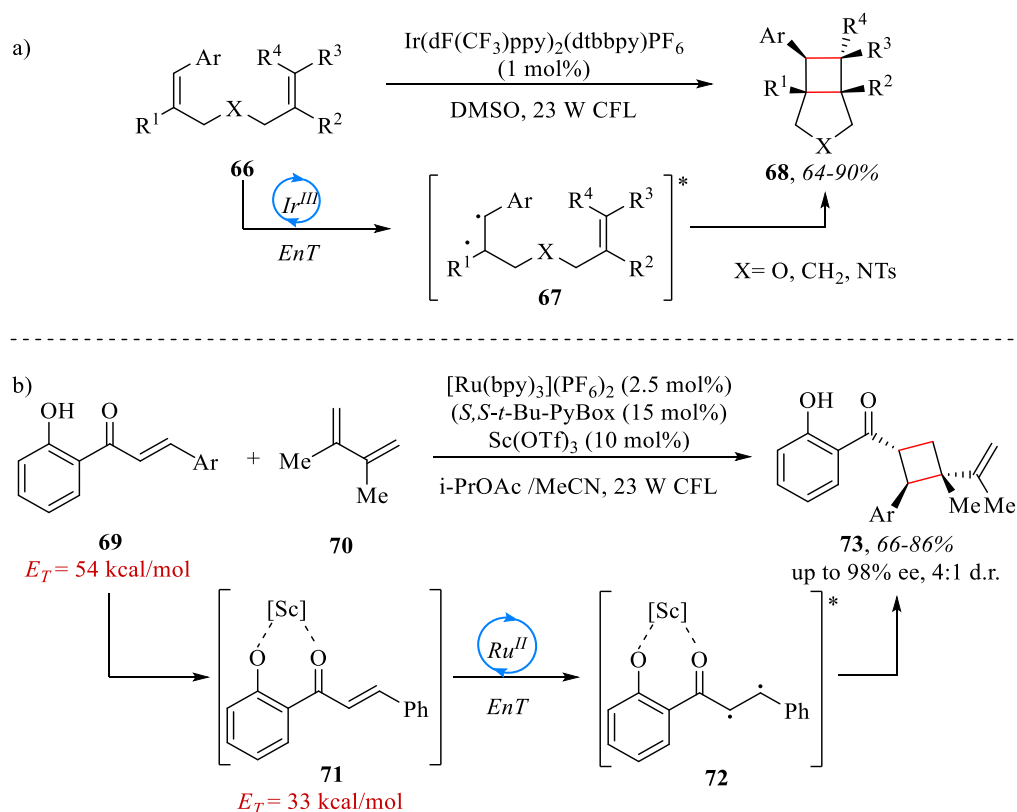
**Scheme 14.** Synthesis of  $\beta$ -keto sulfones by visible-light photocatalysis.

The synthesis of difunctional ketone derivatives (**65**) through visible light promoted oxidative difunctionalization of alkenes has made great progress in the formation of C-S and C-O bonds. For example, Yang and co-workers described a direct difunctionalization of alkenes through an efficient eosin Y-catalyzed, visible light-initiated direct oxysulfonylation with arylsulfinic acids to access  $\beta$ -ketosulfones using *tert*-butyl hydroperoxide TBHP as oxidant (Scheme 14a).<sup>[61]</sup> Additionally, it is possible to find related works in the synthesis of  $\beta$ -keto sulfones including the report of Yu and Zhang which describes a visible-light-promoted directed sulfonylation with enol acetates and sulfonyl chlorides (Scheme 14b)<sup>[62]</sup> and the contribution of Niu et al. which developed an Ir-catalyzed visible-light-induced oxidative difunctionalization of alkenes with sulfonyl chlorides in the presence of air (Scheme 14c).<sup>[63]</sup>

### 1.1.3.2. Relevant examples of visible light-induced energy-transfer (EnT) reactions

#### [2+2] photocycloadditions

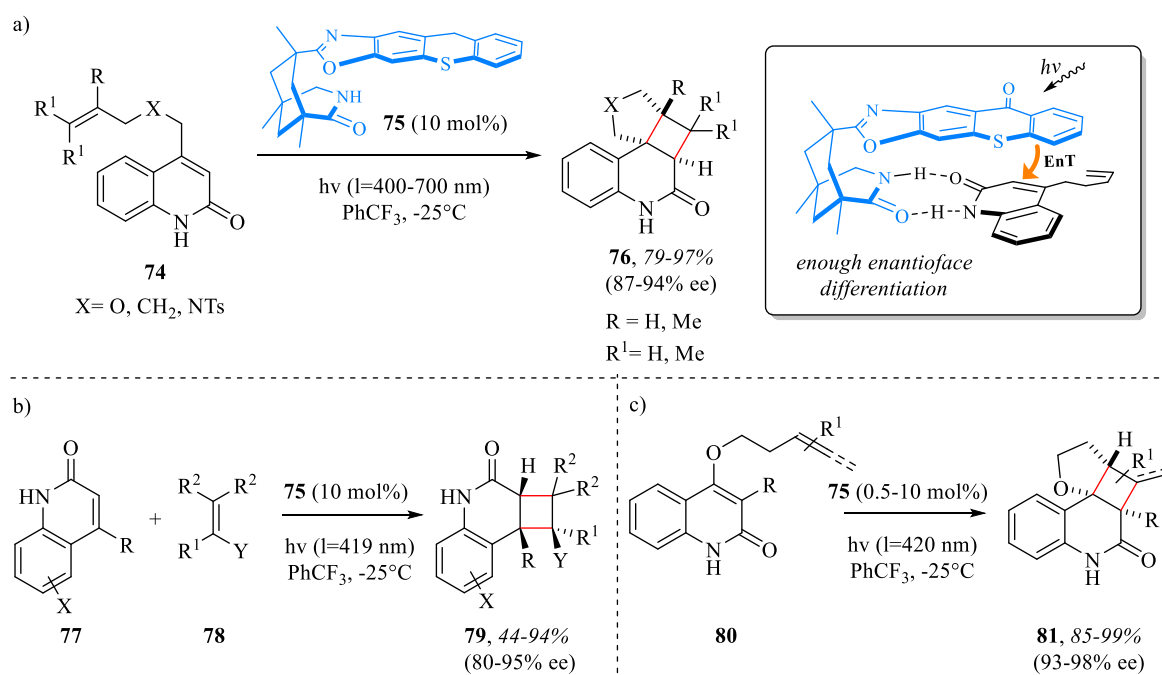
Direct excitation of alkenes to their triplet state by UV irradiation is a classic strategy for [2+2] photocycloaddition reactions. However, the latest advances in visible light photoredox catalysis have contributed to the development of new modes of alkene activation, where olefins can undergo cycloaddition through SET or EnT pathways. Although SET processes have been investigated more widely, many transformations of these compounds through visible light-induced EnT processes have recently been reported.



**Scheme 15.** a) Photosensitized [2+2] cycloaddition of styrenes. b) Enantioselective catalytic [2+2] cycloaddition of 2'-hydroxychalcones.

One of the first examples in modern visible light-mediated EnT catalysis is the work of Yoon and co-workers, who described the intramolecular [2+2] photocycloaddition of alkene tethered styrenes **66**. In this work a variety of substituted cyclobutanes was prepared in good yields by using  $\text{Ir}(\text{dF}(\text{CF}_3)\text{ppy})_2(\text{dtbbpy})\text{PF}_6$  ( $E_T = 61.8$  kcal/mol) as a triplet sensitizer. This

iridium catalyst could access the triplet styrenes **67\*** ( $E_T = \sim 55-60$  kcal/mol), which then react in an intramolecular fashion to afford the cyclobutanes **68** (Scheme 15a).<sup>[64]</sup> Later the same group contributed a significant advancement with an enantioselective variant using chiral Lewis acid catalysis to promote enantioselective [2+2] photocycloadditions. The 2'-hydroxychalcone **69** has triplet energy of 54.0 kcal/mol outside of the range of  $[\text{Ru}(\text{bpy})_3]^{2+}$  as a triplet sensitizer ( $E_T = 46.0$  kcal/mol) preventing a possible sensitization. When the reaction was conducted in the presence of a chiral scandium complex a dramatic reduction of the triplet energy was observed allowing the photocatalyst to selectively sensitize the coordinated complexes **71** in a fast exergonic EnT event. In this way, the chiral triplet intermediates **72\*** could undergo [2+2] photocycloadditions with dienes to afford the vinyl cyclobutane products **73** with high enantio- and diastereoselectivity (Scheme 15b).<sup>[65]</sup>



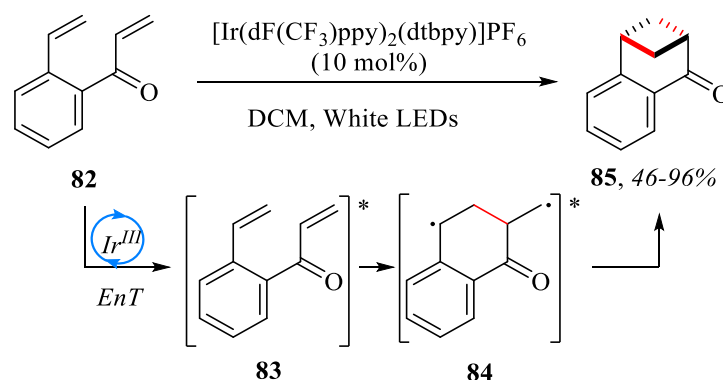
**Scheme 16.** Introduction of thioxanthone **75** as chiral photocatalyst in the [2+2] cycloaddition.

The Bach group also made a significant contribution to the synthesis of highly substituted chiral cyclobutanes by applying a metal-free photocatalysis strategy, that involves the use of the chiral thioxanthone motif **75** which is capable to absorb visible light showing a classic photocatalyst performance through triplet energy sensitization.<sup>[66]</sup> After studying the spectral properties of **75**, the authors were able to prepare the cyclobutanes **76** using the starting



quinolones **74** under 400-700 nm wavelength irradiation through presumably EnT. The authors attributed the recorded high levels of enantioselectivity to the planar thioxanthone so the attack at the quinolone double bond occurs with high selectivity (Scheme 16a).

Following the above studies, the same group continued using the mentioned strategy in the enantioselective intermolecular [2+2] cycloaddition of several quinolones **77** and electron-deficient olefins **78** (Scheme 16b).<sup>[67]</sup> For the success of this reaction, the association between the catalyst and the substrate by hydrogen bonding was essential. Dissociation of the photoexcited substrate from the catalyst could lead to a loss in enantioselectivity. Additionally, a recent study showed the enantioselective intramolecular [2+2] photocycloaddition of 3-alkylquinolones **80** with 4-O-tethered alkenes and allenes in the C4 carbon. The reaction proceeds with high enantioselectivity under visible light and in the presence of the chiral sensitizer **75** (Scheme 16c).<sup>[68]</sup>

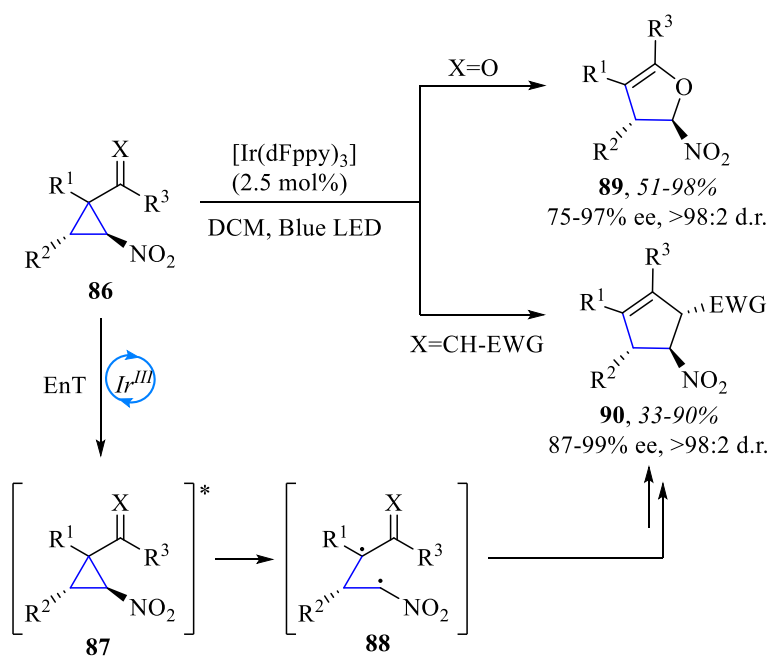


**Scheme 17.** Intramolecular [2+2] photocycloadditions of dienones.

Kwon and co-workers reported the synthesis of bridged benzobicyclo[3.1.1]heptanones (**83**) with excellent regioselectivity through [2+2] photocycloadditions under irradiation with visible light. Mechanistically, the crossed [2+2] cycloaddition proceeds via EnT from the triplet sensitizer  $[\text{Ir}(\text{dF}(\text{CF}_3)\text{ppy})_2(\text{dtbbpy})]\text{PF}_6$  to the *o*-styrenyl enones **82**, the constrained substrate structure was proposed to force the triplet intermediates **83\*** to cyclize and then form the bridged cyclobutane ring system following radical-radical recombination (Scheme 17).<sup>[69]</sup>

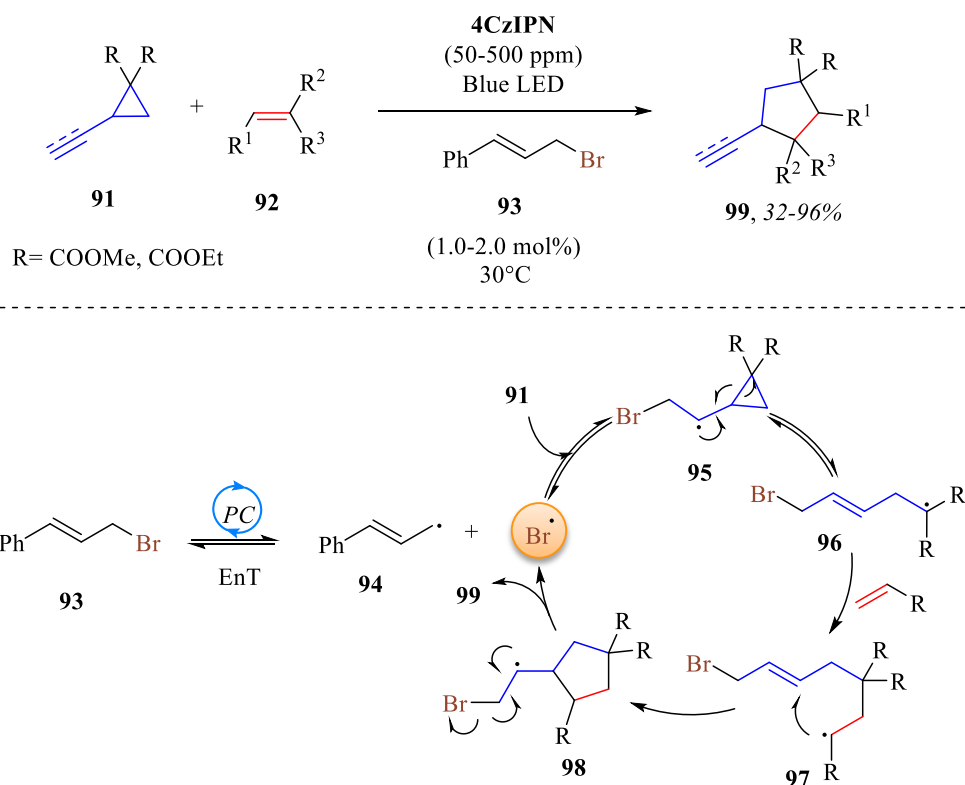
**[3+2] photocycloadditions**

Most [3+2] cycloadditions of cyclopropanes reported to date have utilized “donor–acceptor” cyclopropanes (DACs), methylene cyclopropanes, or similar highly activated cyclopropanes that bear substituents that predispose them toward ring-opening.<sup>[70]</sup> Although visible light photocatalysis has attracted increasing attention in recent years and advances have been made in understanding the process, there are not many examples of intermolecular cyclopropane ring expansion using photocatalysis and in most cases, photoredox processes are involved.<sup>[71]</sup>



**Scheme 18.** Visible-Light Photocatalytic Intramolecular Cyclopropane Ring Expansion.

Among the few [3+2] cycloadditions of cyclopropanes involving energy transfer catalysis mediated by visible light is the method reported by Alemán et al. for the synthesis of enantioenriched dihydrofurans **89** and cyclopentenenes **90** by an intramolecular nitro cyclopropane ring expansion reaction (Scheme 18).<sup>[72]</sup> This methodology works under mild reaction conditions, achieving good yields with excellent enantioselectivities in the final products. Moreover, DFT calculations demonstrated the ring-expansion proceeded through an EnT pathway and how the nitro group plays an important role in the photocatalytic activation of the cyclopropane being essential for the ring-expansion process. Selective C–C bond cleavage of the excited-state cyclopropanes leads to key biradical intermediate **88**.

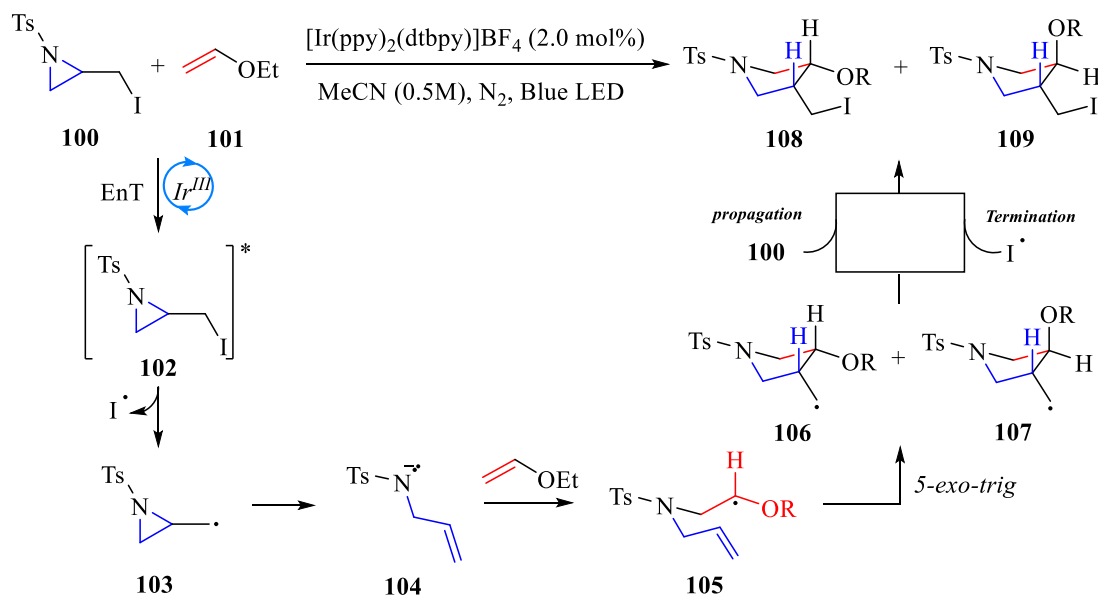


**Scheme 19.** [3 + 2] cycloaddition of substituted vinyl- and ethynylcyclopropanes with substituted alkenes.

The Miyake group reported a bromine radical catalysis system, which enables efficient [3+2] cycloaddition of diversely substituted vinyl- and ethynylcyclopropanes (**91**) with different substituted alkenes (**92**) through photosensitization. In this strategy, the authors use cinnamyl bromide as a precatalyst due to its photosensitizing triplet-state and ability to undergo  $\beta$ -fragmentation to generate bromine radicals in a controlled manner after irradiation in presence of the catalyst 4CzIPN (Scheme 19). The key to success for this transformation is, that bromine radicals can reversibly add to carbon-carbon  $\pi$ -bonds (via addition and elimination).<sup>[73]</sup> The relevance of the bromine radical in this reaction was proved by using NBS or through direct photolysis of  $\text{Br}_2$  and similar catalytic reactivity was observed but in much lower yields.

Atom transfer radical addition (ATRA), cyclization (ATRC), and polymerization (ATRP) are valuable synthetic methods for the functionalization of olefins.<sup>[74]</sup> Although energy transfer-based ATRA hasn't received much attention as electron-transfer ATRA did, the Wallentin group could develop a protocol that enables easy access to functionalized

pyrrolidines. The methodology employs visible light-mediated ATRA [3+2] cyclization with aziridinylmethyl iodides (**100**) and electron-rich olefins (**101**) as substrates (Scheme 20).<sup>[75]</sup> The authors proposed that the reaction is initiated by an energy-transfer process and mainly propagated by iodine transfer.

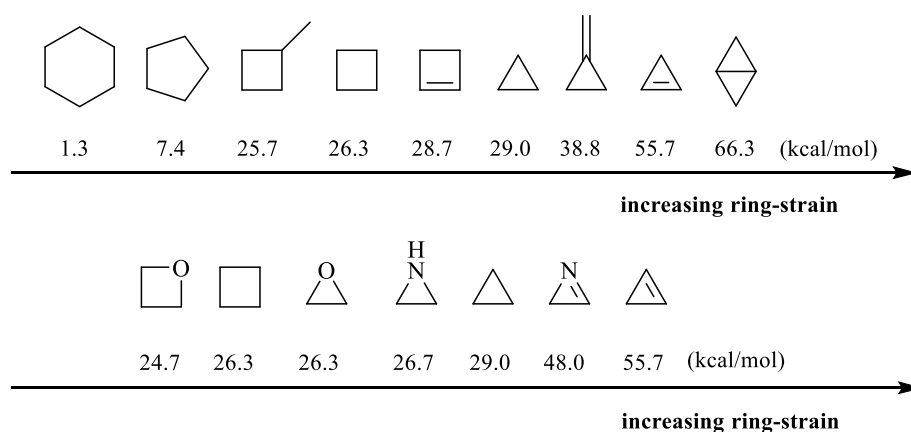


**Scheme 20.** Visible light mediated [3+2]-cycloaddition for the synthesis of functionalized pyrrolidines.

## 1.2. Metal-catalyzed activation of strained molecules

### 1.2.1. Strain energy

In 1885, Adolf von Baeyer described for the first time the concept of ring strain,<sup>[76]</sup> which has been widely applied in organic chemistry, biochemistry, and photochemistry. Baeyer strain theory explains the specific behavior of chemical compounds in terms of bond angle distortion away from the ideal. Some other governing factors of ring strain are conformational strain or Pitzer strain (torsional eclipsing interactions), which comes from conformational eclipsic arrangements of CH<sub>2</sub> groups, as well as the Prelog strain, which is based on transannular interactions. The difference between the sum of these effects and the acyclic system is described by the concept of ring strain.<sup>[77]</sup> In the context of this work, small cycloalkanes were used and their ring strain is dominated by the Baeyer and Pitzer strains.



**Figure 5.** Ring strain energies of different small carbocycles and their heteroanalogs.<sup>[78]</sup>

As can be seen in Figure 5, by reducing the ring size, the inherent strain energy is increased. However, the difference between the cyclobutanes and cyclopropanes is relatively small and therefore they often show comparable reactivities. This characteristic could be attributed to the fact that C–H bonds in the cyclopropane ring are stronger than those of cyclobutane or larger ring carbocycles such as cyclohexane<sup>[79]</sup> and they can compensate somehow the increment in the strain energy caused by the weaker C–C bonds in the cyclopropane.<sup>[80]</sup> The incorporation of  $sp^2$  carbons, on the other hand, induces an increased ring strain, so that alkylidenecyclopropanes and cyclopropenes are significantly more reactive toward ring-opening reactions. The highest ring stress is observed with condensed bicyclic substrates, whereby even higher ring stresses are often observed via torsional stresses than via the pure addition of the individual components. Ring strain energy can be described as a balance of stabilization and destabilization effects present in cyclic molecules. One important variable that should remain constant, determining the strain energy of three-membered rings, is angle strain. In general, a three-membered ring has bond angles of approximately  $60^\circ$ , nevertheless, the strain energy of a wide variety of carbocyclic and heterocyclic three-membered rings can vary over a wide range up to 40 kcal/mol.<sup>[81]</sup> Compared to their unsubstituted relatives, hetero-substituted cycloalkanes are slightly stabilized due to the space requirements of the lone pairs of electrons and their more diffuse orbitals.

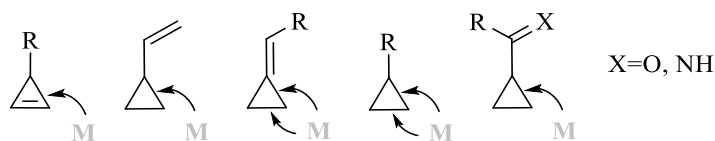
## 1.2.2. Transition metal-catalyzed carbon-carbon bond activation

### 1.2.2.1. Fundamentals

Activation of C–C bonds is a highly attractive and challenging subject in organometallic chemistry as it can serve in the construction of complex organic molecules from simple and readily available precursors. Although processes involving the formation of C–C bonds have been widely studied and many related organic transformations are known to date, the use of the activation (cleavage) process of C–C bonds remains relatively unexplored. This can mainly be attributed to two obstacles that have to be addressed for successful C–C activations: 1) the small orbital overlap of the metals with the C–C- $\sigma$  bonds sterically shielded by their substituents 2) an oxidative addition into an unactivated C–C bond corresponds to a strongly endothermic reaction, considering that a stable bond has an energy of about 81–84 kcal/mol and leads to the formation of a new significantly weaker bond with energies in the range of about 29–36 kcal/mol.<sup>[82]</sup> Accordingly, indirect activations via  $\beta$ -carbon elimination or retroallylation are often chosen, in which the formation of low-molecular-weight by-products such as carbon monoxide serves as a driving force.<sup>[82]</sup> In addition, it is well known that regarding C–C bond activation small strained rings occupy a privileged position because their use can compensate the thermodynamic disadvantage of the C–C bond activation by forming more stable ring expanded metallacyclic complexes through metal insertion into the strained C–C bond and lead to energy release by strain reduction during ring-opening reactions. Although the implementation of this concept is still a challenge, relevant advances have been made over the last years, mainly using metal complexes based on palladium, rhodium, iridium, and nickel.<sup>[83]</sup>

### 1.2.2.2. C–C Activation in Cyclopropanes by transition metal catalysts

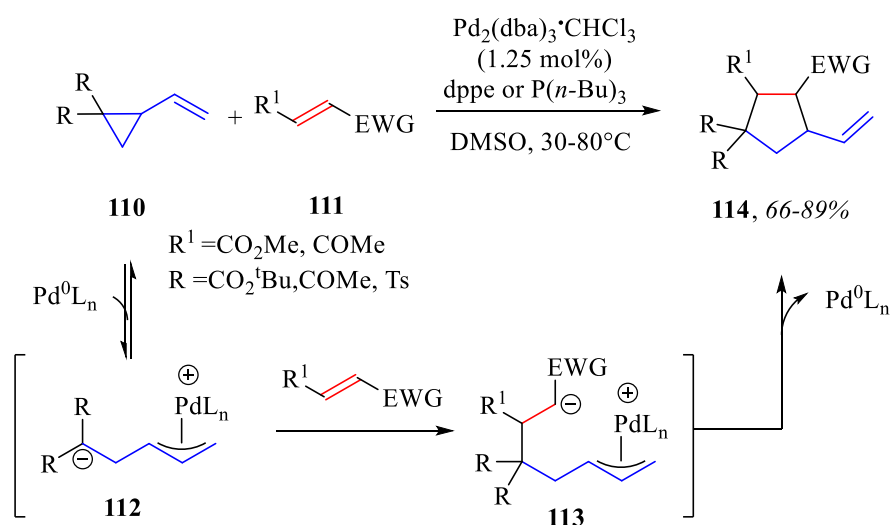
In the context of this work, only three-membered ring systems such as cyclopropanols and vinylcyclopropanes were used. The introduction of trigonal centers onto cyclopropanes has long been known to result in a significant increase in ring strain.<sup>[84]</sup> This type of system has preferred sites for metal insertion and selective oxidative addition always takes place in the single bonds (Figure 6). Despite the energetically favorable release of ring strain, directing groups such as unsaturated tethers, ketones, esters, or imines ease the activation of the cyclopropane ring and direct the metal toward the cleavable C–C bond. Processes involving nonactivated cyclopropanes are much rarer but have started to emerge.<sup>[82]</sup>



**Figure 6.** Common sites for metal insertion in single bonds of cyclopropanes derivatives.

## Vinylcyclopropanes

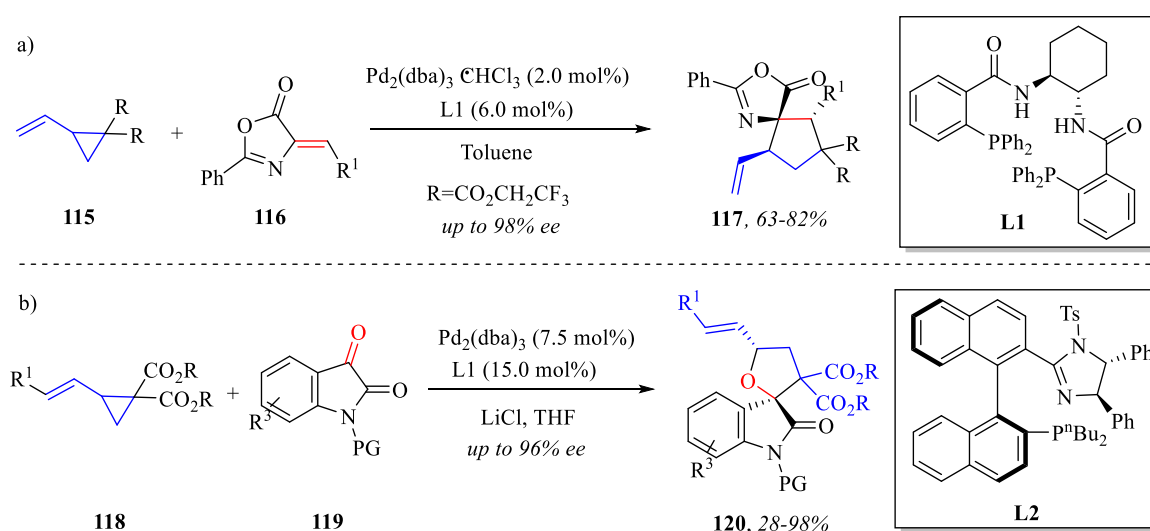
In the case of vinylcyclopropanes (VCPs) the vinyl substituent is usually necessary for activation of the cyclopropane opening, but it does not have to take part in all possible cycloaddition modes, acting as either a five-carbon synthon or a three-carbon synthon. The following section will focus on the VCPs as three-carbon synthon and the use of different transition metals for their activation.



**Scheme 21.** Tsuji-Type [3+2] Cycloaddition of VCPs and substituted alkenes.

For the first time, Tsuji and co-workers reported VCP derivatives acting as three carbon synthons in the palladium-catalyzed intermolecular formal [3+2] cycloaddition with  $\alpha,\beta$ -unsaturated esters, and ketones in 1985, resulting in the preparation of vinyl-substituted cyclopentane derivatives in good yields. The reaction is believed to proceed through the formation of the acyclic zwitterionic  $\pi$ -allylpalladium complexes **112** and **113** after an  $S_N2$ -like oxidative addition (Scheme 21).

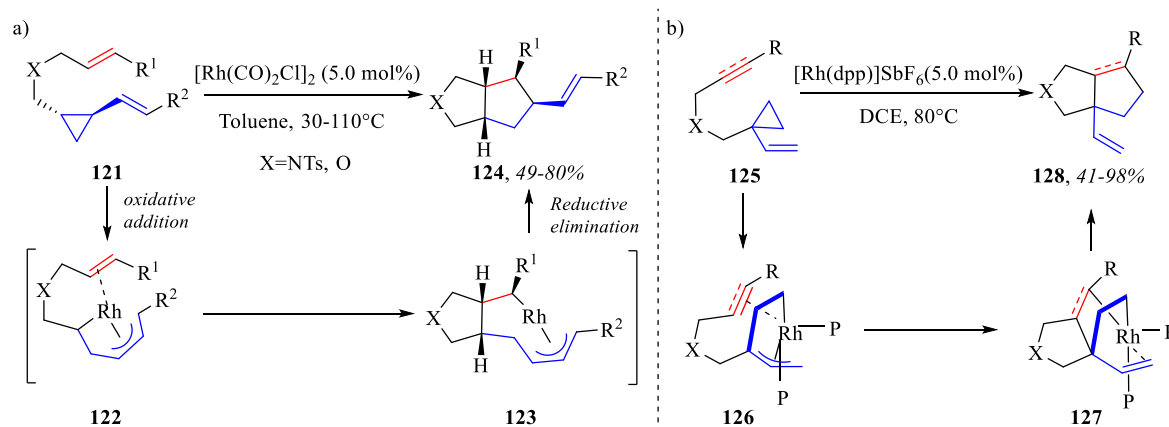
Since the discovery of the Tsuji's [3+2] cycloaddition, different asymmetric variants of this method have appeared. For instance, Trost et al. developed a palladium-catalyzed enantioselective formal [3+2] cycloaddition between VCPs and prochiral Michael acceptors using the chiral ligand **L1** (Scheme 22a).<sup>[85]</sup> The Shi group also reported a highly efficient Pd-catalyzed asymmetric formal [3+2] cycloaddition of VCPs with isatins, affording functionalized spirotetrahydrofuran oxindoles **120** using the chiral imidazoline-phosphine ligand **L2** (Scheme 22b).<sup>[86]</sup>



**Scheme 22.** Asymmetric Pd-catalyzed [3+2] cycloadditions.

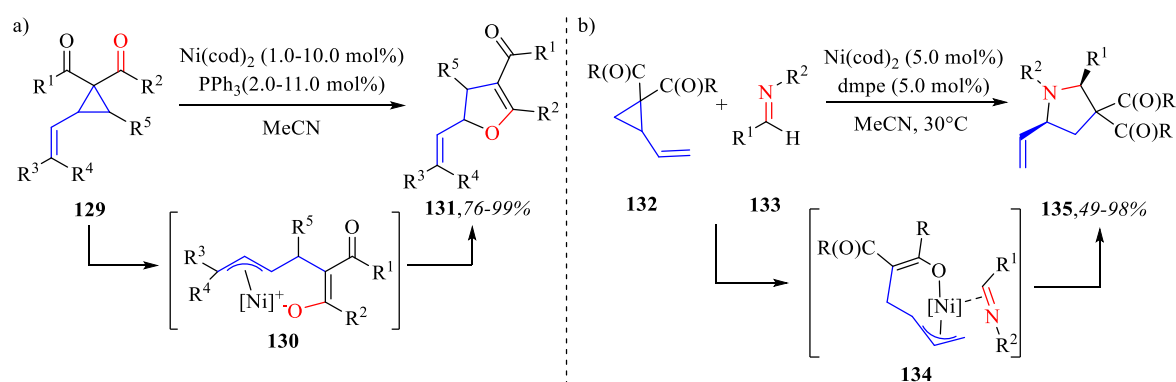
Unactivated VCPs acting as three-carbon synthon appear for the first time when Yu's group developed an Rh-catalyzed intramolecular [3+2] cycloaddition of ene-vinylcyclopropane (ene-VCP, **121**) bearing an alkene tethered to the cyclopropane ring of VCP. In this case, the VCP moiety serves as a three-carbon synthon leading to the formation of a symmetric bicyclic 5,5-ring compound **124** (Scheme 23a).<sup>[87]</sup> Further studies using 1-ene-, and 1-yne-VCP substrates (**125**) were also evaluated to undergo Rh-catalyzed [3+2] cycloaddition (Scheme 23b).<sup>[88]</sup> These methodologies provide an efficient and diastereoselective approach to synthesizing five-membered-ring-embedded polycyclic structures.





**Scheme 23.** Rh(I)-catalyzed intramolecular [3 + 2] cycloaddition reactions.

Examples describing the use of Ni-catalyzed processes to trigger the C–C bond cleavage of activated VCPs include the strategy applied by Johnson et al. to access dihydrofuran derivatives which proceeds via rearrangements of 1-acyl-2-vinyl cyclopropanes **129** (Scheme 24a).<sup>[89]</sup> The method is noteworthy for low catalyst loadings and is tolerant of both functional and structural changes made to the cyclopropane ring. Another example is the nickel-catalyzed [3+2] cycloaddition of VCPs to imines to obtain polysubstituted pyrrolidines developed by the Matsubara group (Scheme 24b). The mechanism of the reaction is believed to take place through the coordination of an imine to an oxanickelacycle forming the cyclic intermediate **134** followed by a nucleophilic attack of the VCP towards the imine to eventually undergo the diastereoselective cycloaddition. The pyrrolidines are obtained in high yields with good regio- and diastereoselectivity.<sup>[90]</sup>



**Scheme 24.** Nickel-catalyzed cycloaddition of VCPs.

## Cyclopropanols

Due to their high ring strain, distinct bonding properties, and relative ease of ring-opening, cyclopropanols have been used in an increasing number of transition metal-catalyzed ring-expansion and ring-opening functionalization processes.<sup>[91]</sup> Cleavage of the ring normally occurs under mild conditions, and the regioselectivity of the reaction can be controlled by choosing a proper reagent or catalyst. In general, cyclopropanol ring-opening cross-coupling reactions promoted by transition metal catalysts go through either a metal-homoenolate (**137**) or a  $\beta$ -alkyl radical intermediate (**138**) (Figure 7).

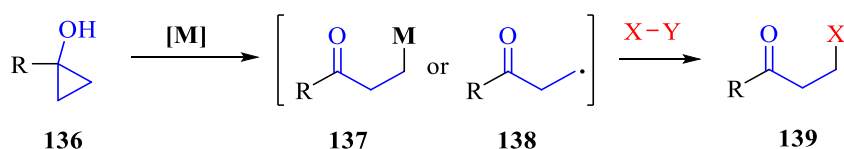
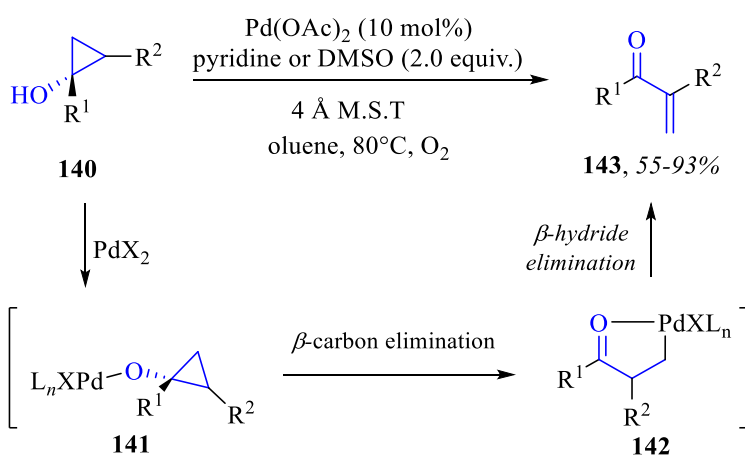


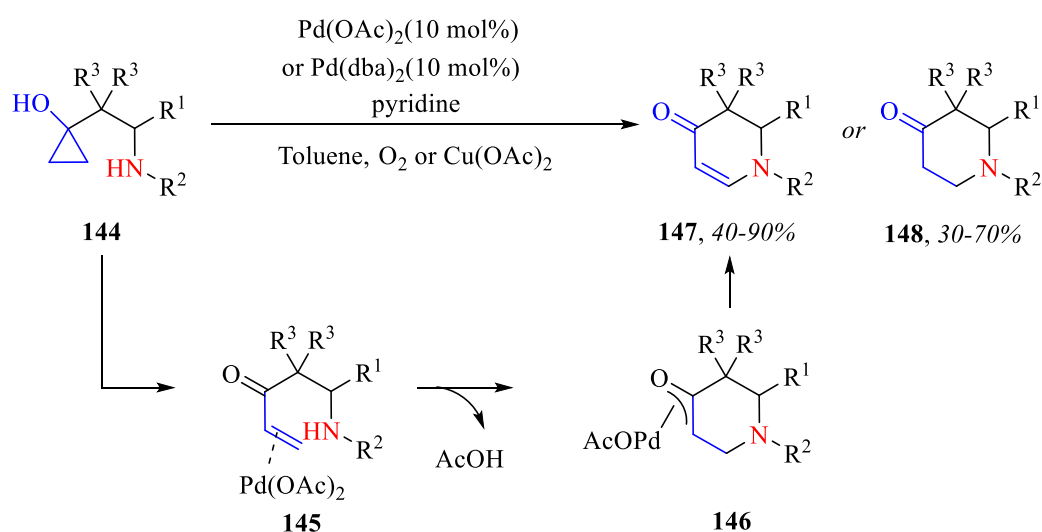
Figure 7. General cyclopropanol ring-opening cross-couplings.

The use of cyclopropanols as homoenolate precursors was first evaluated by Cha and co-workers to prepare enones (**143**) through a ring-opening isomerization catalyzed by a Pd (II) catalyst.<sup>[92]</sup> This transformation has as a key step the  $\beta$ -carbon elimination to form the Pd homoenolate **142** and the subsequent  $\beta$ -hydride elimination (Scheme 25).



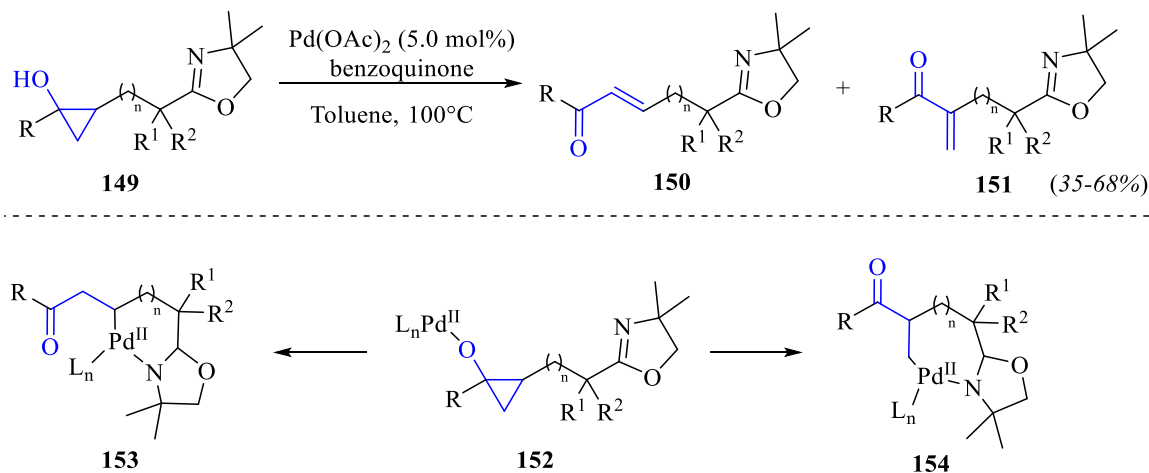
Scheme 25. Pd-catalyzed ring-opening of cyclopropyl alcohols to form enones.

Pd(II) catalyzed domino reactions of  $\beta$ -aminocyclopropanols leading to 2,3-dihydro-1*H*-pyridin-4-ones were reported by Brandi and co-workers.<sup>[93]</sup> The observed process appears to resemble the Wacker oxidation of  $\alpha,\beta$ -unsaturated esters. After the formation of the enone (**145**), the amine undergoes Pd-catalyzed 6-*endo-trig* cyclization followed by oxidation to afford **147** (Scheme 26). Conversely, the use of a Pd(0) derivative, Pd(dba)<sub>2</sub>, afforded the corresponding tetrahydropyrid-4-ones **148**. Moreover, the use of Cu(OAc)<sub>2</sub> instead of oxygen to regenerate the catalyst favored the formation of the saturated heterocycle.



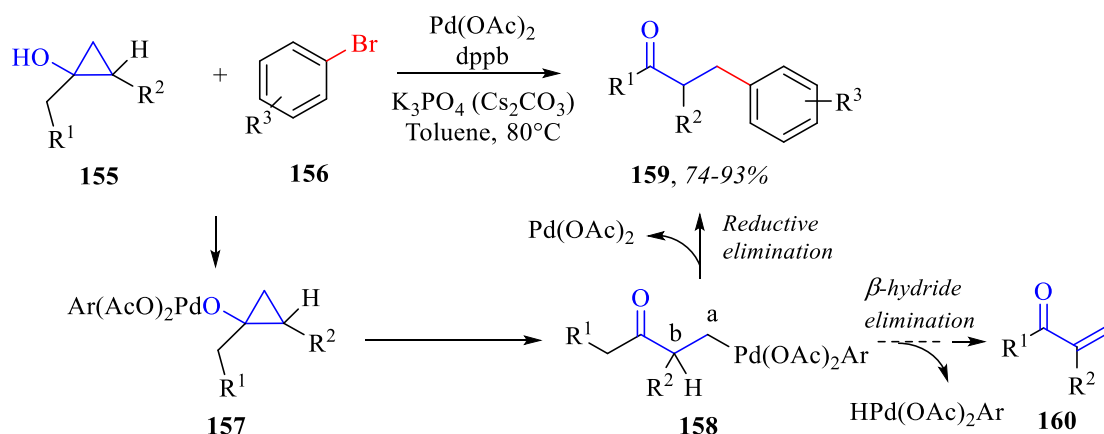
**Scheme 26.** Synthesis of 2,3-dihydro-1*H*-pyridin-4-ones and tetrahydropyrid-4-ones.

A related domino-type process described by Hurski showed that cyclopropanols bearing oxazoline directing group can undergo oxidative ring-opening with uncommon regioselectivity leading to linear and branched enones as products.<sup>[94]</sup> Preferential formation of the linear isomer could be explained by considering two possible intermediates **153** and **154** in which Pd(II) center is coordinated by the nitrogen in the oxazoline group.  $\beta$ -Hydride elimination from **153** would lead to major linear enones **150**, while intermediate **154** would lead to the minor product **151** (Scheme 27).



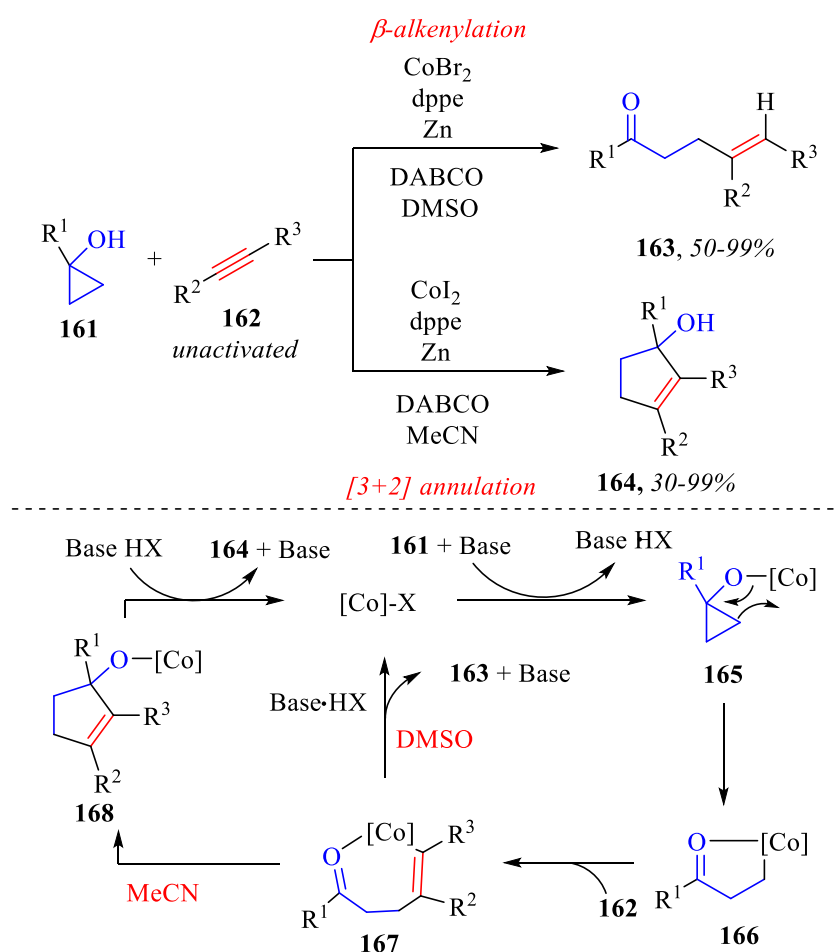
**Scheme 27.** Oxazoline-directed palladium-catalyzed synthesis of enones from cyclopropanols.

A palladium-catalyzed cross-coupling reaction of cyclopropanol-derived homoenolates with aryl and hetaryl bromides was reported for the first time by Orellana et al. This strategy generates a palladium homoenolate **158** bearing  $\beta$ -hydrogen atoms (relative to palladium) upon ring-opening, promoting a reductive elimination to give the coupled product **159** rather than the competing  $\beta$ -hydride elimination, which would give the corresponding unsaturated ketone **160** (Scheme 28).<sup>[95]</sup>



**Scheme 28.** Cross-coupling of aryl bromides with ketone homoenolates and competing for side reactions.

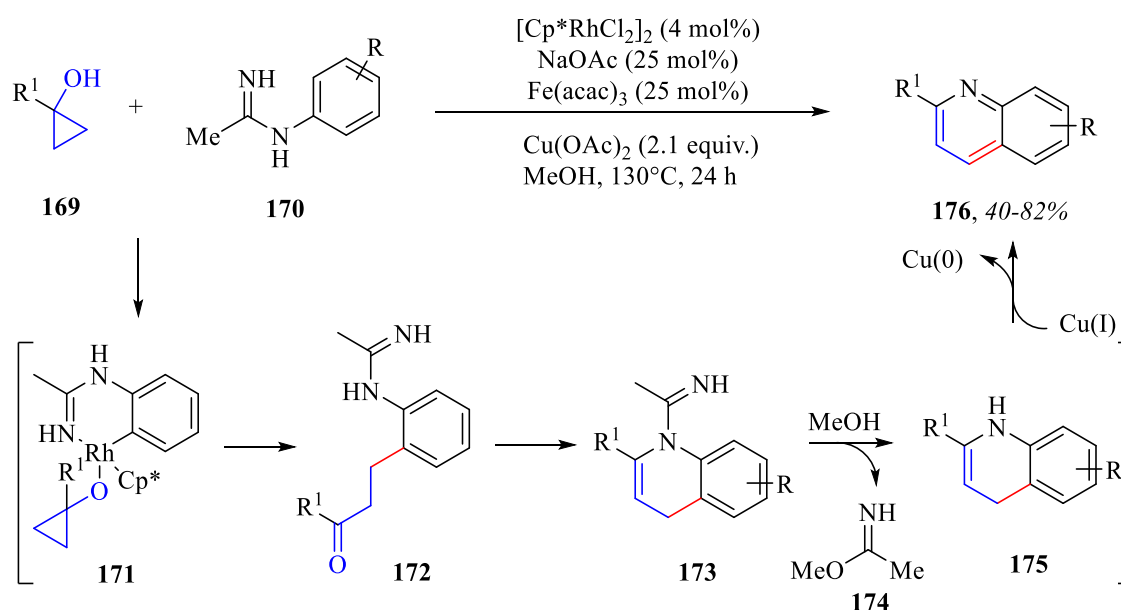
Yoshikai and co-workers described cobalt-catalyzed divergent coupling reactions between cyclopropanols and internal alkynes that afford either  $\beta$ -alkenyl ketones or multisubstituted cyclopentenol derivatives.<sup>[96]</sup> The chemoselectivity between this  $\beta$ -alkenylation and [3 + 2] annulation reactions mainly depends on the type of solvent. After the ring-opening formation of a cobalt homoenolate **166** and subsequent alkyne insertion to form an alkenylcobalt intermediate **167**, the alkenyl product is obtained when using DMSO while the use of MeCN directs the reaction to the cyclic product formation (Scheme 29).



**Scheme 29.**  $\beta$ -alkenylation and [3 + 2] annulation reactions under cobalt catalysis.

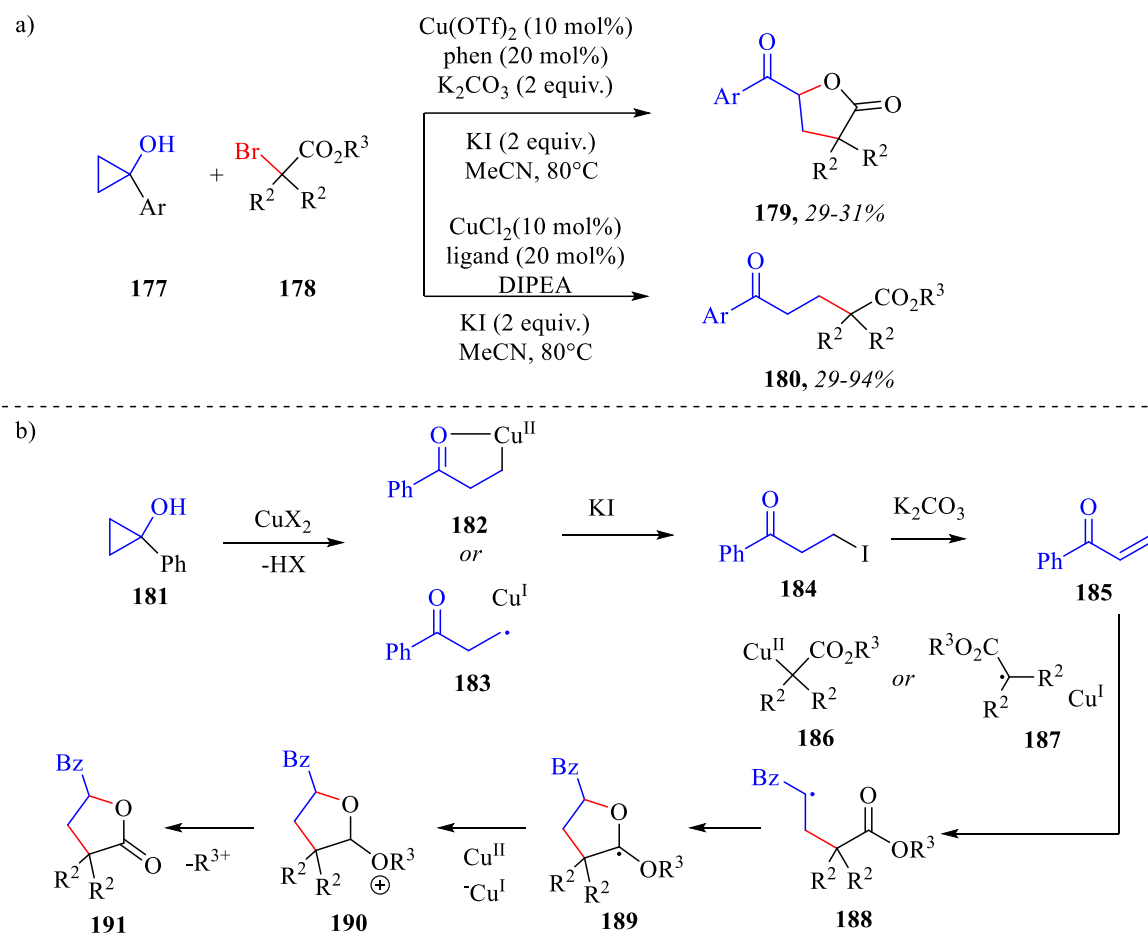
Efficient rhodium(III)-catalyzed coupling between cyclopropanols and aryl amidines for the synthesis of 2-substituted quinolines was reported by Li and co-workers (Scheme 30).<sup>[97]</sup> Mechanistic studies led to propose that the reaction starts with the C–H functionalization of

the amidine which acts as a directing group forming the intermediate **171**. After the  $\beta$ -arylketone (**172**) is generated, it can condense to form the enamine **173**. The nucleophilic deprotection with methanol releases acetimidate to give the dihydroquinoline **175**, which is readily oxidized by a Cu(I) species to eventually furnish the product **176**.



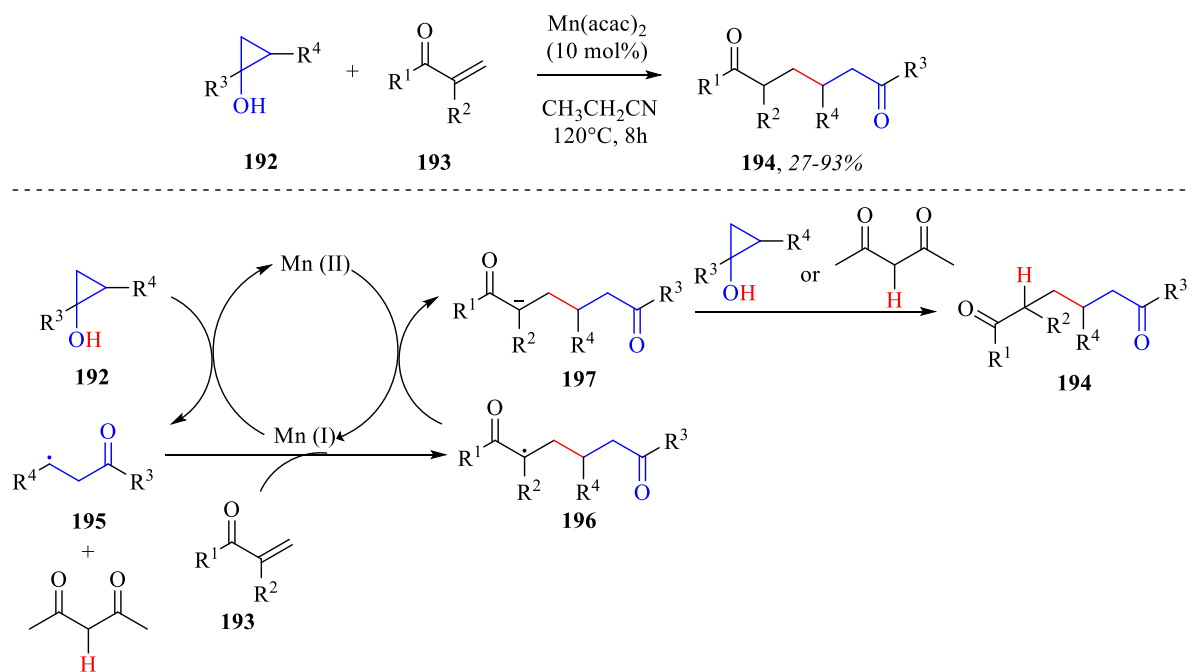
**Scheme 30.** Synthesis of quinolines via Rhodium(III)-Catalyzed C–H Activation of Imidamides.

Dai and co-workers established a methodology to prepare  $\gamma$ -butyrolactones and  $\delta$ -ketoesters in which cyclopropyl alcohols (**177**) can be treated with  $\alpha$ -haloesters (**178**) under Cu catalysis (Scheme 31a).<sup>[98]</sup> The  $\gamma$ -butyrolactones synthesis is believed to start with the formation of either the Cu(II) homoenolate **182** or the  $\beta$ -keto radical **183** from the cyclopropyl alcohol **181** in presence of  $Cu(OTf)_2$ . The following reaction with KI generates a  $\beta$ -iodoketone **184**, which in presence of  $K_2CO_3$  undergoes elimination to give the enone **185**. Meanwhile, the Cu(II) enolate **186** or the  $\alpha$ -radical **187** generated via oxidative addition or reduction of alkyl bromide **178** perform a Michael addition to the enone **185** giving the formation of the radical **188**. After the *endo-trig* cyclization of this intermediate, the oxidation by Cu(II) generates the carbocation **190** that finally proceeds to product **191** after the loss of an alkyl group (Scheme 31b). The change of base and catalyst in the coupling of substrates **177** and **178** yields the uncyclized  $\delta$ -ketoester **180** (Scheme 31a).



**Scheme 31.** Catalytic cyclopropanol ring-opening for divergent syntheses of  $\gamma$ -butyrolactones and  $\delta$ -ketoesters.

Zhao and Loh developed an efficient manganese-catalyzed ring-opening coupling reaction of cyclopropanols with enones to generate unsymmetrical 1,6-dicarbonyl compounds **194**.<sup>[99]</sup> Preliminary mechanistic studies support a radical-mediated pathway in which no external hydrogen atom donor is required since the cyclopropyl alcohol presumably goes through proton-coupled electron transfer (PCET), wherein the proton transfers to the acetylacetonate anion to form acetylacetonate. Once the enolate **197** is generated via the addition of oxidized **195** to **193** followed by reduction of the resulting radical by Mn(I), its protonation occurs either by the generated acetylacetonate or another equivalent of the cyclopropyl alcohol **192** (Scheme 32). This transformation exhibits broad substrate scopes and excellent tolerance to diverse functional groups in both the cyclopropanols as well as the enones.



**Scheme 32.** Mn-catalyzed ring-opening coupling reaction of cyclopropanols with enones.



## 2. Catalytic activation of skeletal bonds in strained photoproducts

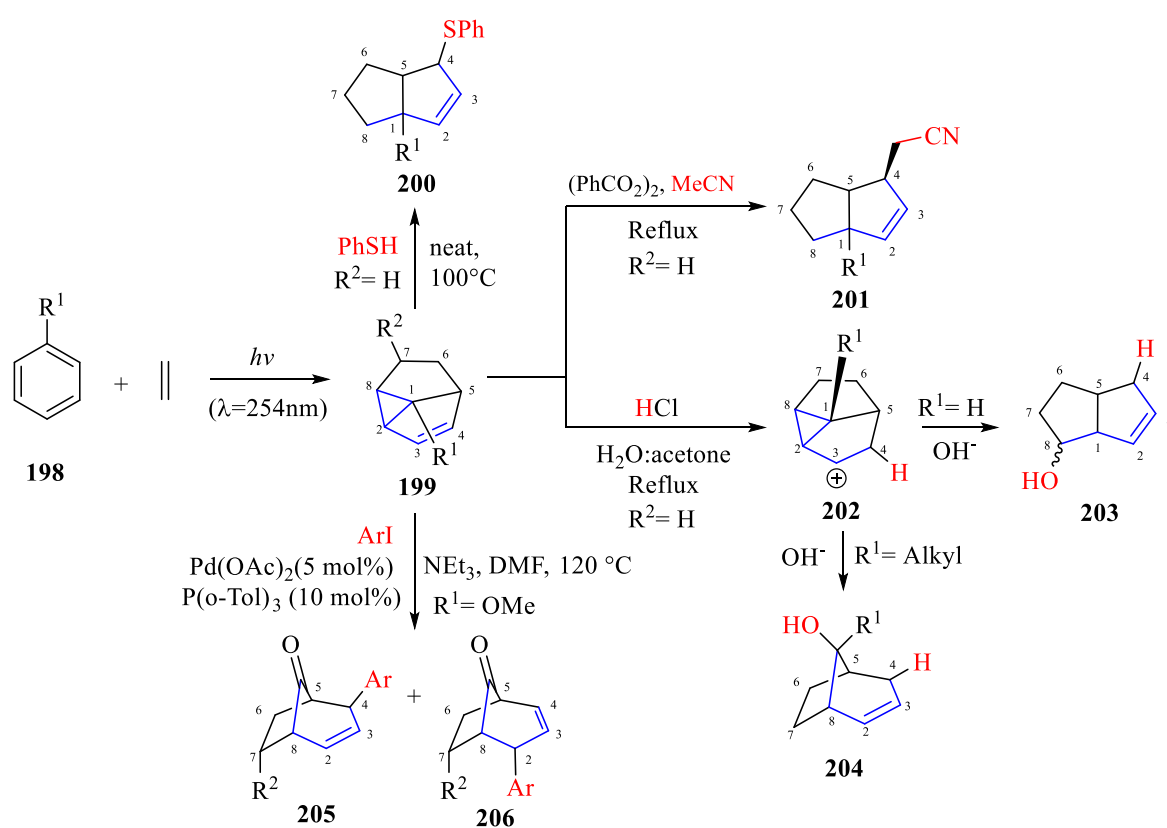
### 2.1. Introduction

Preparative organic photochemistry in view of the concept of green chemistry is a favorable process since it uses light as the sole energy source and can avoid the generation of undesirable side products such as metal salts. The energy of a photon with a wavelength of  $\lambda \approx 300$  nm injects about  $95 \text{ kcal mol}^{-1}$  into a molecule making it able to induce the formation of high-energy structures that are difficult to obtain by other means and are located energetically uphill of the starting materials. This light energy often is converted into a certain ring strain of the photoproducts, which can undergo catalyzed follow-up reactions. Although the use of visible light has recently received a lot of attention, the amount of energy that can be transferred to the substrate during these processes is lower than in the case of UV transformations that can excite even small  $\pi$ -systems. As a potential disadvantage, strained high-energy photogenerated intermediates are commonly susceptible to undergoing thermal or photochemical secondary reactions, making it often necessary to transform them directly into thermodynamically stable products to achieve high yields.

Photochemistry enables the generation of highly reactive intermediates and depending on their reactivity and the characteristics of the reaction partner the planned follow-up reactions can be carried out without any added catalyst like acid, base, or metals.<sup>[100]</sup> Recently, different transition metal and visible light catalysis in follow-up transformations of strained photoproducts have been reported, and in all of the cases, the inherent strain of these small systems serves as the activation energy for the subsequent ring transformation. In contrast to the fast-growing number of reported transition metals <sup>[82, 101]</sup> as well as photoredox-catalyzed<sup>[15, 102]</sup> ring-opening transformations of small ring systems via C–H and C–C bond activations, only a few of these examples involve the use of strained photogenerated substrates. The application of this strategy represents an advantageous general concept because the photochemical generation of the high-energy intermediates allows formally endergonic reactions that are compensated by the release of strain in the ring in the subsequent reaction.

## 2.2. Aim of the research

Among the examples of photoinduced ring strain as a driving force for metal-catalyzed subsequent reactions, some studies show the utilization of the cyclopropyl ring-opening in *meta* photoproducts like **199** to give a variety of common structures found in natural products (Scheme 33). Some of these reports involve a radical addition to the double bond and it has been described as an effective way to induce the cyclopropane ring-opening; for example, thiophenol can be very efficient in such transformation by going through a free-radical S<sub>N</sub>2' displacement reaction to form **200**.<sup>[39-40]</sup> Another type of radical ring-opening reaction is the addition of acetonitrile radicals to the double bond to yield hexahydropentalene derivatives (**201**).<sup>[103]</sup>

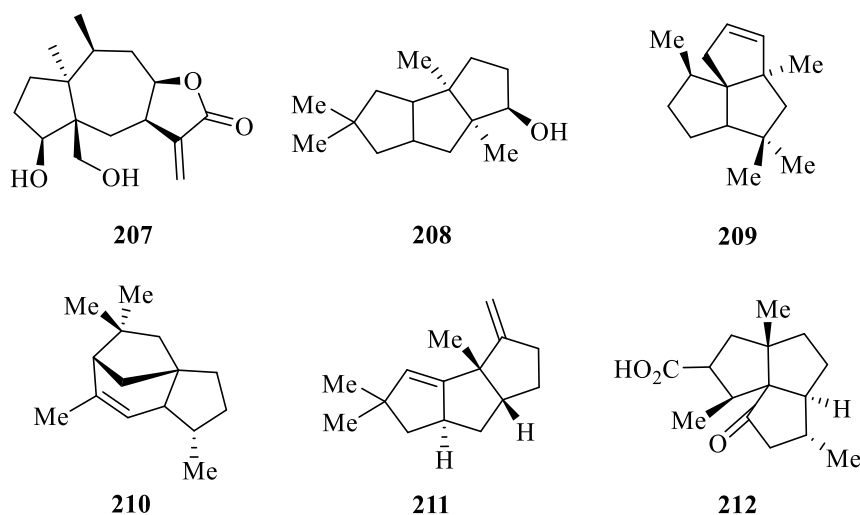


**Scheme 33.** Diversification possibilities of the *meta* photocycloaddition product.

The *meta* photocycloadduct can also undergo ring-opening upon protonation of the double bond. If the *meta* photocycloaddition product contains a substituent at position 1, the ring-opening gives the bicyclo[3.2.1]octane derivative **204**, but if there is no substituent at this position, the product of the ring-opening is a hexahydropentalene (**203**).<sup>[104]</sup> Other

electrophiles also tend to add to the alkene, Penkett demonstrated that the cyclopropane ring opening can occur via Heck-type reaction if the substituent at position 1 is a methoxy group. The intermediate palladium  $\sigma$ -complex opens the cyclopropane ring to afford a mixture of bridged bicyclic ketone isomers **205** and **206** when there is a substituent in C-7.<sup>[105]</sup> The latter strategy was used in an attempt toward the construction of the core skeleton of the alkaloid gelsemine.<sup>[106]</sup>

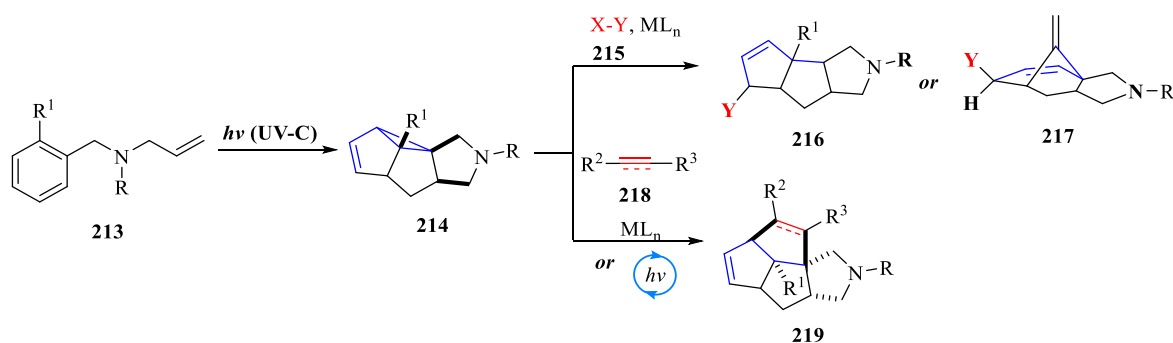
To illustrate the power of this strategy some natural products that have been synthesized based on the *meta* photocycloaddition reaction<sup>[107]</sup> are shown in Figure 8.<sup>[108]</sup> Most of these compounds have similar structural motifs. Rudmollin (**207**)<sup>[109]</sup>, as well as  $\alpha$ -cedrene (**210**),<sup>[110]</sup> can be prepared from a *meta* adduct holding an oxygen functionality at the bridgehead position that eventually is fragmented, but in the case of Rudmollin, the bridge is reductively cleaved. Ceratopicanol (**208**)<sup>[39]</sup> and Hirsutene (**211**)<sup>[111]</sup> are synthesized based on the radically cleaved triquinane core of an intramolecular linear *meta* photocycloadduct. Alternatively, triquinanes that have been synthesized by using angular *meta* photocycloadducts include the ( $\pm$ )-silphinene (**209**)<sup>[112]</sup> and ( $\pm$ )-subergorgic acid (**212**)<sup>[103]</sup>.



**Figure 8.** Examples of natural products synthesized using *meta* photocycloaddition products.

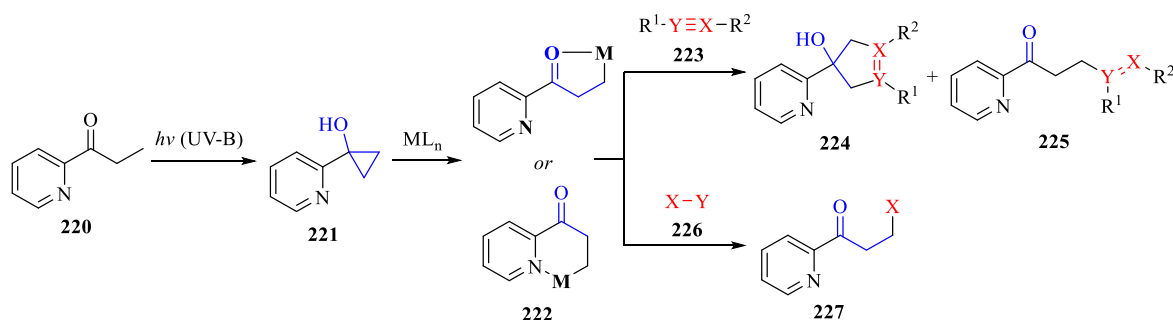
Based on the scope of this strategy and the reports described above, in the first part of this work, the ring-opening process of the VCP unit in a *meta* photoproduct (**214**) was evaluated with different reaction partners using metal-based or visible light catalysis. This transformation was expected to take place via either an  $S_N2'$  ( $S_E2'$ ) displacement reaction or

a [3+2] cycloaddition with the VCP moiety acting like a three-carbon synthon (Scheme 34). Since there are many examples of cycloadditions and opening reactions involving VCPs,<sup>[113]</sup> these served as a starting point for the present work.



**Scheme 34.** Subsequent reactions for the photogenerated *meta* photocycloaddition products are considered in this work.

Another important group of biologically active compounds are pyridine-based ring systems which could be recognized as some of the most extensively employed heterocycles in the field of drug design, primarily because they can be used to threaten a broad range of indications like lung cancer,<sup>[114]</sup> HIV<sup>[115]</sup> and arthritis,<sup>[116]</sup> amongst many others. Substituted pyridine rings are also of importance as ligands in metal-catalyzed cross-coupling reactions.<sup>[117]</sup> Given the importance of the pyridine motif and the increased interest in cross-coupling chemistry the second part of this work applied the same UV-driven strain-promoted/metal-catalyzed strain-releasing strategy in the preparation of pyridine derivatives starting with the photogenerated cyclopropanol **221** expected to undergo either a ring-expansion or ring-opening functionalization reaction (Scheme 35).



**Scheme 35.** Metal-catalyzed subsequent reactions of the photogenerated cyclopropanol **221**.

As described in section 1.2.2 there are many reports for cyclopropyl alcohol ring-opening transformations and the first step for this approach was to set up the ring-opening of the photogenerated cyclopropanol testing different reagents and catalysts employed in such protocols. The application of the designed strategy to get access to new pyridine derivatives using a photogenerated cyclopropanol bearing a heterocyclic functionality would represent an alternative to methodologies that usually have as starting point common preparations of cyclopropanols like the Kulinkovich<sup>[118]</sup> or Simmons–Smith<sup>[119]</sup> reactions.

## 2.3. Results and discussion

### 2.3.1. *meta* photocycloaddition products

#### 2.3.1.1. Preparation of the *meta* photocycloadducts

The first stage of the synthetic plan corresponds to the preparation of the *meta* photocycloadduct that served as the universal precursor. For this purpose, the substrate for the *meta* photocycloaddition reaction was prepared in two steps starting with the reductive amination of the benzaldehydes **228**, followed by the reaction with an amine-protecting agent to afford the substituted benzylallylamines **213** (Table 2).

**Table 2.** Preparation of substituted benzylallylamines **213**.

Entry	Substrate	R	Amine-protecting agent	Yield (%) <sup>a</sup>
1	<b>229a</b>	CH <sub>3</sub>	Cl <sub>3</sub> CCOCl	91
2	<b>229a</b>	CH <sub>3</sub>	ClCOOCH <sub>3</sub>	71
3	<b>229a</b>	CH <sub>3</sub>	Boc <sub>2</sub> O <sup>b</sup>	72
4	<b>229a</b>	CH <sub>3</sub>	TsCl <sup>b</sup>	90
5	<b>229a</b>	CH <sub>3</sub>	(CF <sub>3</sub> SO <sub>2</sub> ) <sub>2</sub> O	85
6	<b>229b</b>	OCH <sub>3</sub>	(CF <sub>3</sub> SO <sub>2</sub> ) <sub>2</sub> O	88

<sup>a</sup> isolated yield. <sup>b</sup> 5 mol% of DMAP was added.

Photochemical reactions with substrates **213** were performed with low-pressure mercury lamps (UV-C) in quartz vessels at ambient temperature (Table 3). A mixture of tetracyclic products, **214** described as linear adducts and **230**, described as angular, were deduced as having arisen from *meta* addition across the methyl position as expected (entries 2-3 and 5). Despite registering better yields while using precursors with Boc and acetoxy protecting groups, the precursor with the triflyl group showed a better ratio of the linear and angular regioisomers. In the case of entries 1 and 4, there was no product formation. The yields given

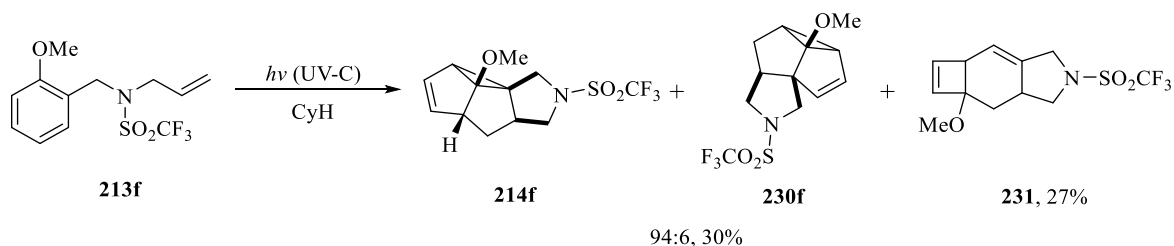
in Table 3 refer, however, to the mixture of the two isomers. Their ratio remained unchanged after purification as compared to the ratio in the crude product mixture and it was determined through NMR analysis.

**Table 3.** Linear and angular *meta* photocycloaddition products depending on the amine-protecting group.

Entry	Substrate	R	R <sup>1</sup>	Time (h)	Yield (%) <sup>a</sup>	Ratio <sup>b</sup>
1	<b>213a</b>	CH <sub>3</sub>	COCCl <sub>3</sub>	12	0	-
2	<b>213b</b>	CH <sub>3</sub>	COOCH <sub>3</sub>	2	79	88:12
3	<b>213c</b>	CH <sub>3</sub>	Boc	2	78	86:14
4	<b>213d</b>	CH <sub>3</sub>	Ts	12	0	-
5	<b>213e</b>	CH <sub>3</sub>	SO <sub>2</sub> CF <sub>3</sub>	3.5	72	92:8
6	<b>213f</b>	OCH <sub>3</sub>	SO <sub>2</sub> CF <sub>3</sub>	3.0	30	94:6

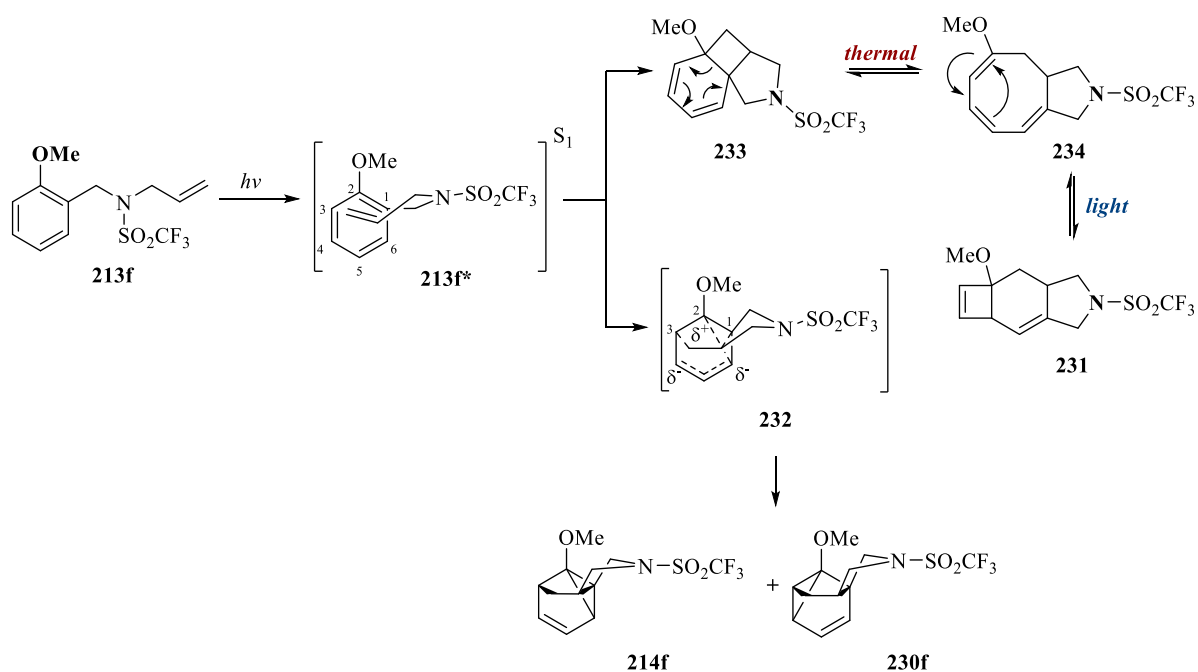
<sup>a</sup> isolated yield. Irradiation at room temperature using Rayonet reactor equipped with ~254 nm light tubes (16 tubes × 14 W). <sup>b</sup> The ratio of regioisomers (r.r.) was determined in the crude product mixture by <sup>1</sup>H NMR which remained unchanged after purification.

The regioselectivity of the *meta* photocycloaddition changed upon replacing the methyl group in **213e** for a methoxy substituent in the entry 6 also generating the *ortho*-derived photocycloadduct **231** (Scheme 36). In this case, a separation of the *meta* photocycloadducts and the *ortho* photoproduct was possible, but the yields were considerably low.



**Scheme 36.** *meta* and *ortho* photocycloaddition products upon irradiation of **213g**.

In earlier works,<sup>[119]</sup> it was discussed that the length and flexibility of the three-atom tether could determine the regioselectivity of the intramolecular *meta* photocycloaddition reaction. In this case, the photocycloaddition of the short allylmethylamine substituent to the  $S_1$  benzene ring could be an asynchronous process. Thus the change to  $sp^3$ -hybridization at carbon atom C-1 may occur before C-3 favoring the cyclopropane ring formation between C-2 and C-6 in **232**.<sup>[120]</sup> This conformation and ring closure results in the preferred form of the linear product **214f** over the angular one **230f**. Alternatively, an electrostatic repulsion of the lone pairs in the methoxy group at C-2, and the olefinic  $\pi$  system<sup>[121]</sup> could alter this conformation, positioning the terminal end of the double bond across the arene ring occurring an *ortho* cyclization, then a thermally induced six-electron electrocyclic disrotatory ring-opening, and finally a photochemically induced four-electron electrocyclic disrotatory ring-closure forming **231** (Scheme 37).



**Scheme 37.** Proposed mechanism for the formation of *ortho* and *meta* cycloadducts from **213g**.

### 2.3.1.2. Reactions using *meta* photocycloadducts

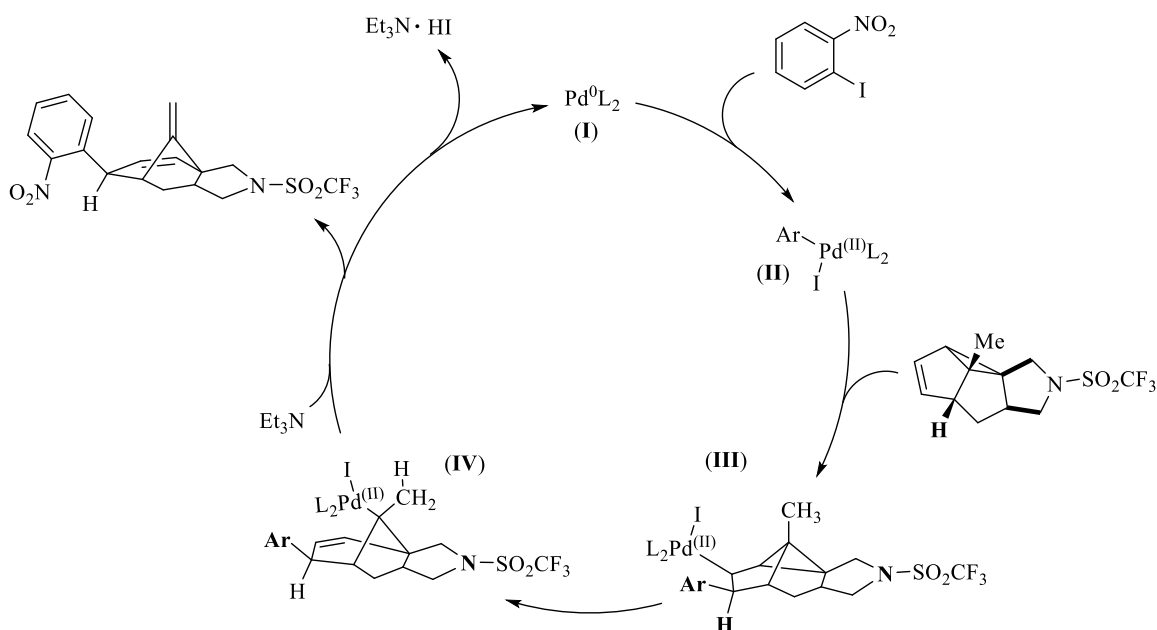
During the study of the *meta* photocycloaddition using the benzylallyl amines **213a-f**, the use of **213e** gave the best regioisomeric ratio and a good yield, making its *meta* photocycloadduct the proper precursor in the planned follow-up reactions. Thus, based on the methods



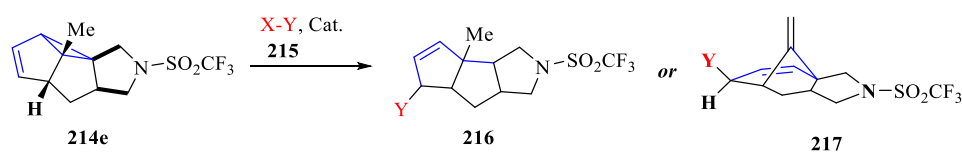
described in the sections 1.2.2 and 2.2, **214e** was tested in a catalyst screening with a variety of nucleophiles or electrophiles producing in some cases the S<sub>N</sub>2' or S<sub>E</sub>2' displacement that generates through the vinyl cyclopropane ring opening either a linear tricycle **216** or a bridged bicyclic with an alkene at the bridgehead position **217**.

As can be seen in Table 4, after applying the method developed by Penkett<sup>[105-106]</sup> and co-workers a bridged bicyclic **217c** was obtained (entries 3-4, Figure 9). This Heck-like arylation reaction performed on the *meta* photocycloadduct **214e** showed the versatility of the implemented strategy. However, compared with Penkett's work there was no substantial difference in how the reported products are obtained and the yields were even lower.

A plausible catalytic cycle that could explain the modified Heck reaction is depicted in Scheme 38. The first transformations involve oxidative addition of a palladium(0) species with 1-iodo-2-nitrobenzene (II) and the carbopalladation of the alkene in the *meta* photocycloadduct that results in the formation of the intermediate III. The latter cannot undergo the usual β-hydride elimination that takes place in the classic mechanism due to its rigid structure. This feature does not allow the carbon–palladium σ-bond to align *syn* with a β hydrogen atom and as consequence, a cyclopropane ring-opening occurs.<sup>[106]</sup> The final stages of the catalytic cycle involve the formation of the arylated bicyclic product and the regeneration of the palladium(0) catalyst with the assistance of the base.

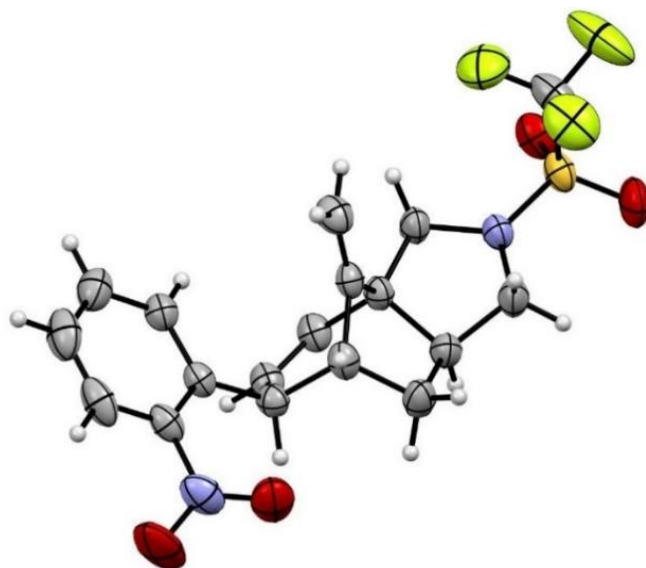


**Scheme 38.** Proposed mechanism for the modified Heck reaction.

**Table 4.** Catalyst screening in the ring-opening reaction of the *meta* photocycloadduct **214e** using different nucleophiles and electrophiles.

Entry	Reaction partner	Catalyst	Yield % <sup>a</sup>		Entry	Reaction partner	Catalyst	Yield % <sup>a</sup>	
			216	217				216	217
1	4-Nitro-iodobenzene	Pd(dba) <sub>2</sub> , dppe	-	-	14	(PhS) <sub>2</sub>	I <sub>2</sub>	-	-
2	4-Nitro-iodobenzene	PdCl <sub>2</sub> , dppe	-	-	15	(PhS) <sub>2</sub>	AIBN	-	-
3	4-Nitro-iodobenzene	Pd(OAc) <sub>2</sub> , P(o-Tol) <sub>3</sub>	-	10	16	(PhS) <sub>2</sub>	PdCl <sub>2</sub>	-	-
4	4-Nitro-iodobenzene	Pd(OAc) <sub>2</sub> , dppe	-	16	17	(PhSe) <sub>2</sub>	PhI(OAc) <sub>2</sub>	-	-
5	TsNHCH <sub>3</sub>	AuPPh <sub>3</sub> OTf	-	-	18	(PhSe) <sub>2</sub>	CuI	-	-
6	TsNHCH <sub>3</sub>	AuCl <sub>3</sub>	-	-	19	(PhSe) <sub>2</sub>	AIBN	-	-
7	4-Methoxyphenol	(Ph <sub>3</sub> P)AuCl, AgOTf	-	-	20	(PhSe) <sub>2</sub>	Cu(OAc) <sub>2</sub> ·H <sub>2</sub> O	-	-
8	PhCH <sub>2</sub> NH <sub>2</sub>	AuCl <sub>3</sub>	-	-	21	PhMgBr	Ni(PPh <sub>3</sub> ) <sub>2</sub> Cl <sub>2</sub>	-	-
9	PhCH <sub>2</sub> NH <sub>2</sub>	Ir(COD)Cl <sub>2</sub>	-	-	22	PhMgBr	CuBrSMe <sub>2</sub>	-	-
10	PhNHCH <sub>3</sub>	Ir(COD)Cl <sub>2</sub>	-	-	23	PhSH	--	50	-
11	(PhS) <sub>2</sub>	CuI, bpy	-	7	24	PhSH	PdCl <sub>2</sub> (PhCN) <sub>2</sub>	39	-
12	(PhS) <sub>2</sub>	Cu(OTf) <sub>2</sub> , I <sub>2</sub>	-	11	25	PhSH	AIBN	35	-
13	(PhS) <sub>2</sub>	FeCl <sub>3</sub>	-	-	26	BrCF <sub>2</sub> COOEt	Ir(PPy) <sub>2</sub> (dtbbpy)PF <sub>6</sub> <sup>b</sup>	-	-

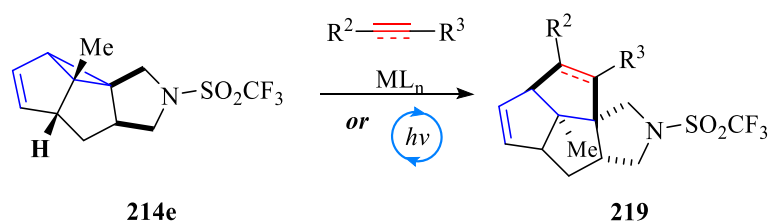
<sup>a</sup> isolated yield. <sup>b</sup> Visible light catalysis using Blue LED



**Figure 9.** Crystal structure of the bridged bicyclic **217c** (ORTEP, thermal ellipsoids at 50% probability. C: black, H: gray, N: blue, O: red, S: yellow, F: green).

The copper catalyzed sulfenylation<sup>[123]</sup> of **214e** using diphenyl disulfide also led to the formation of the bridged bicyclic with an alkene at the bridgehead position in low yields (entries 11-12). There was no product formation or improvement in yield when using other catalysts or changing the diphenyl disulfide to diphenyl diselenide<sup>[124]</sup> (entries 13-20). In contrast, as mentioned in section 2.2 the metal-free sulfenylation employing thiophenol generated a tricycle like **216** with moderate yield (entry 23). For this transformation, the use of the radical initiator AIBN or the Pd catalyst PdCl<sub>2</sub>(PhCN)<sub>2</sub> even decreased the yield (entries 24-25).

Given that the implementation of the described methodologies could not afford the expected products in a considerable good yield and the other strategies using Au, Ni, Cu, Ir-based catalysts did not show product formation, the possibility of the [3+2] cycloaddition of the *meta* photocycloadduct **214e** with different alkenes and alkynes was evaluated using metal-based or visible light catalysis (Table 5). The use of different rhodium<sup>[125]</sup> and iridium<sup>[126]</sup> salts as described in section 1.2.2 in the designed [3+2] cycloaddition reaction showed no product formation (entries 1-9). However, the visible light-mediated [3+2] cycloaddition of **214e** with 1-methyl-4-(phenylethynyl)sulfonyl)benzene led to the formation of tetracycle **219a** in 53% yield (entry 10). The development and standardization of this reaction are discussed in the next section.

**Table 5.** Metal screening for the [3+2] cycloaddition of the *meta* photocycloadduct **214e** with different alkenes and alkynes.

Entry	Alkyne/alkene	Catalyst	Yield %	Entry	Alkyne/alkene	Catalyst	Yield %
1	CH <sub>2</sub> =CHCOOMe	[Rh(CO) <sub>2</sub> Cl] <sub>2</sub> , AgOTf	-	6	PhC≡CPh	[Rh(CO) <sub>2</sub> Cl] <sub>2</sub> , AgOTf	-
2	CH <sub>2</sub> =CHPh	[Rh(CO) <sub>2</sub> Cl] <sub>2</sub> , AgOTf	-	7	MeOOC≡COOMe	Ir(COD)Cl <sub>2</sub> , AgPF <sub>6</sub>	-
3	CH <sub>2</sub> =CHPh	[Rh(dpp)]SbF <sub>6</sub>	-	8	PhC≡CPh	Ir(COD)Cl <sub>2</sub> , AgPF <sub>6</sub>	-
4	CH <sub>2</sub> =CHCOOMe	[Rh(dpp)]SbF <sub>6</sub>	-	9	H <sub>7</sub> C <sub>3</sub> C≡CC <sub>3</sub> H <sub>7</sub>	Ir(COD)Cl <sub>2</sub> , AgPF <sub>6</sub>	-
5	MeOOC≡COOMe	[Rh(CO) <sub>2</sub> Cl] <sub>2</sub> , AgOTf	-	10	PhC≡CTs	Ir(PPy) <sub>2</sub> (dtbbpy)PF <sub>6</sub> <sup>a</sup>	53

All yields are those of isolated products. <sup>a</sup> Visible light catalysis using Blue LED

### 2.3.1.3. Visible light-induced vinylcyclopropane [3+2] cycloaddition with acetylenic sulfones

Since the above-described attempts to perform a [3+2] cycloaddition reaction using the *meta* photocycloadduct **214e** and simple alkenes or alkynes with different catalytic systems were unsuccessful, the use of acetylenic sulfones as reaction partners under visible light catalysis stood for an attractive alternative. The intrinsic strain of the three-membered ring in the *meta* photocycloadduct served as the driving force for the ring expansion with an alkynyl sulfone **218a** resulting in the formation of a new complex tetracycle (Scheme 39, Figure 10).<sup>[127]</sup> In this case, the reactivity of the  $\pi$ -bond in the acetylenic sulfone is increased through the lowering of the LUMO energy by the adjacent sulfonyl group while offering means for controlling a predominant regiochemical pathway.<sup>[128]</sup> Additionally, the sulfonyl group can be easily removed via desulfonylation or reductive elimination giving important value to acetylenic sulfones as reagents in a variety of cycloadditions.<sup>[129]</sup>



The acetylenic sulfones **218a-k** as reaction partners were prepared in a two-step synthesis. The first step involved two different methods to prepare the intermediates  $\beta$ -iodovinyl sulfones, one method is the cerium(IV) ammonium nitrate (CAN) mediated addition of aryl sulfinate and sodium iodide to terminal alkynes<sup>[130]</sup> and the other one is the iodine-promoted reaction of the same type of alkynes, in aqueous solution.<sup>[131]</sup> The second step was the dehydroiodination of the generated intermediates with potassium carbonate under reflux to obtain the expected acetylenic sulfones in moderate to high yields (Scheme 40).<sup>[130]</sup>

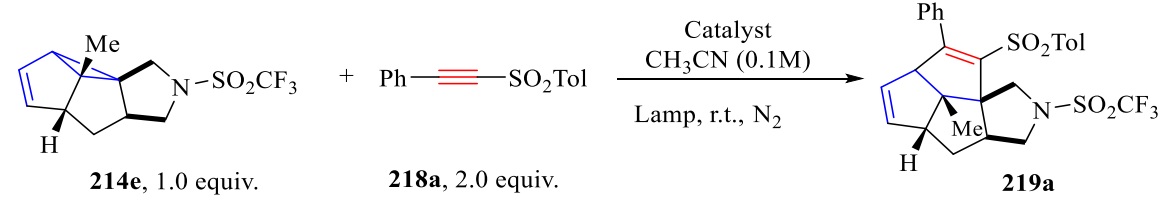
### Reaction optimization

The screening of various photocatalysts for the visible light-induced [3+2] cycloaddition was performed on *meta* photocycloadduct **214e** and the acetylenic sulfone **218a** as the coupling reaction partners. As can be seen in Table 6, the highest yields of the desired tetracycle **219a** were obtained when employing  $[\text{Ir}(\text{ppy})_2(\text{dtbbpy})]\text{PF}_6$  and phenanthrene (entries 1-2). Further optimization studies with these two catalysts (Table 7) revealed that decreasing the iridium loading to 2 mol% increases the yield while variations in the phenanthrene loading did not lead to a higher yield (entries 3 and 6).

**Table 6.** Catalyst screening for the [3+2] cycloaddition of the *meta* photocycloadduct **214e** with the acetylenic sulfone **218a**.

Entry	Catalyst <sup>a</sup>	Yield (%) <sup>c</sup>
1	$[\text{Ir}(\text{ppy})_2(\text{dtbbpy})]\text{PF}_6$	53
2	phenanthrene (100 mol%) <sup>b</sup>	63
3	$\text{Ir}(\text{ppy})_3$	49
4	$[\text{Ru}(\text{bpy})_3]\text{Cl}_2$	traces <sup>d</sup>
5	$[\text{Ir}(\text{dFCF}_3\text{ppy})_2(\text{bpy})]\text{PF}_6$	51
6	$[\text{Ir}(\text{dF}(\text{CF}_3)\text{ppy})_2(\text{dtbbpy})]\text{PF}_6$	49

<sup>a</sup> A 40 W blue LED 456 nm module was used for irradiation. <sup>b</sup> A UV/vis CFL bulb was used for irradiation. <sup>c</sup> All yields are those of isolated products. <sup>d</sup> No isolated.

**Table 7.** Catalyst loading of the iridium and phenanthrene catalyst.


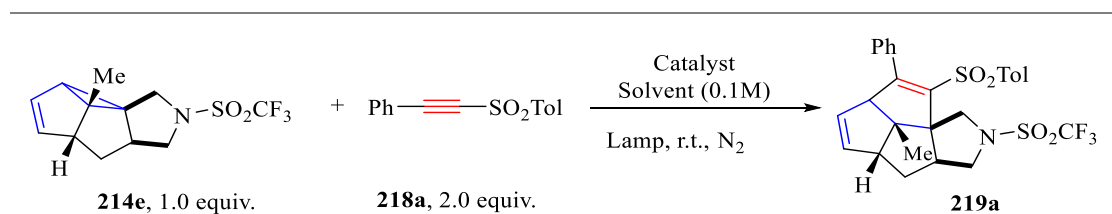
Entry	Catalyst	Loading (mol %)	Yield (%) <sup>c</sup>
1	[Ir(ppy) <sub>2</sub> (dtbbpy)]PF <sub>6</sub> <sup>a</sup>	1.0	55
2	[Ir(ppy) <sub>2</sub> (dtbbpy)]PF <sub>6</sub> <sup>a</sup>	1.5	56
3	[Ir(ppy) <sub>2</sub> (dtbbpy)]PF <sub>6</sub> <sup>a</sup>	2.0	58
4	[Ir(ppy) <sub>2</sub> (dtbbpy)]PF <sub>6</sub> <sup>a</sup>	2.5	53
5	phenanthrene <sup>b</sup>	50	55
6	phenanthrene <sup>b</sup>	100	63
7	phenanthrene <sup>b</sup>	150	63

<sup>a</sup> A 40 W blue LED 456 nm module was used for irradiation. <sup>b</sup> A UV/vis CFL bulb was used for irradiation. <sup>c</sup> All yields are those of isolated products.

The screening of different organic solvents (Table 8) showed how increasing the polarity of the solvent also increased the yield when using the iridium catalyst, having the best result with methanol (entry 6). In contrast, parallel variations of the solvent using phenanthrene were not efficient (entries 7-9) and further optimization of the reaction conditions was conducted using only the iridium catalyst.

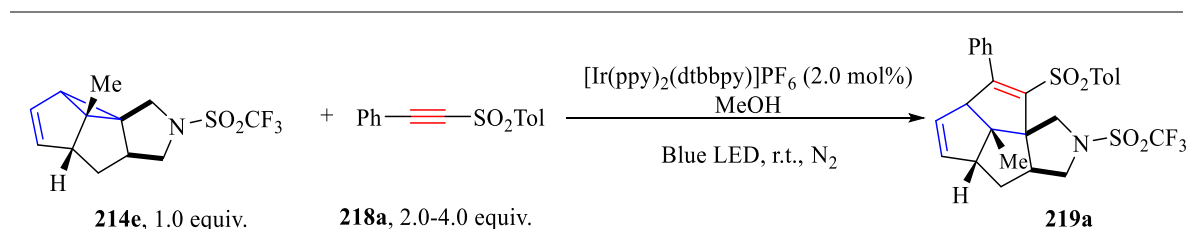
The best conditions to prepare the tetracycle **219a** were found after making additional variations in the stoichiometry of the acetylenic sulfone **218a** and the concentration of the *meta* photocycloadduct **214e** in the reaction mixture (Table 9). The highest yield was obtained when using 2 equivalents of **218a** and employing the *meta* photocycloadduct **214e** in a concentration of 0.15 M (entry 4).

After improving the reaction conditions for the preparation of **219a**, the scope of the synthesized acetylenic sulfones **218a-k** was evaluated next (Scheme 41). Alkynyl sulfones bearing electron-neutral, electron-rich, and electron-withdrawing aromatic rings were found to be suitable substrates. The desired product was also prepared in moderate to good yields when the substrate was bearing alkyl groups on the sulfone moiety (**219i** and **219j**). However, **218k** featuring a butyl-substituted alkynyl sulfone gave no reaction, indicating the need for aromatic groups at the triple bond for the reaction to proceed successfully.

**Table 8.** Catalyst screening for the [3+2] cycloaddition of the *meta* photocycloadduct **214e** with the acetylenic sulfone **218a**.

Entry	Catalyst	Solvent	Yield (%) <sup>c</sup>
1	[Ir(ppy) <sub>2</sub> (dtbbpy)]PF <sub>6</sub> <sup>a</sup>	DCM	49
2	[Ir(ppy) <sub>2</sub> (dtbbpy)]PF <sub>6</sub> <sup>a</sup>	DMF	60
3	[Ir(ppy) <sub>2</sub> (dtbbpy)]PF <sub>6</sub> <sup>a</sup>	DMSO	53
4	[Ir(ppy) <sub>2</sub> (dtbbpy)]PF <sub>6</sub> <sup>a</sup>	CH <sub>3</sub> CN	58
5	[Ir(ppy) <sub>2</sub> (dtbbpy)]PF <sub>6</sub> <sup>a</sup>	CH <sub>3</sub> CN:H <sub>2</sub> O (9:1)	68
6	[Ir(ppy) <sub>2</sub> (dtbbpy)]PF <sub>6</sub> <sup>a</sup>	CH <sub>3</sub> OH	80
7	phenanthrene <sup>b</sup>	CH <sub>3</sub> CN	63
8	phenanthrene <sup>b</sup>	CH <sub>3</sub> CN:H <sub>2</sub> O (9:1)	58
9	phenanthrene <sup>b</sup>	CH <sub>3</sub> CN: CH <sub>3</sub> OH (8:2)	58

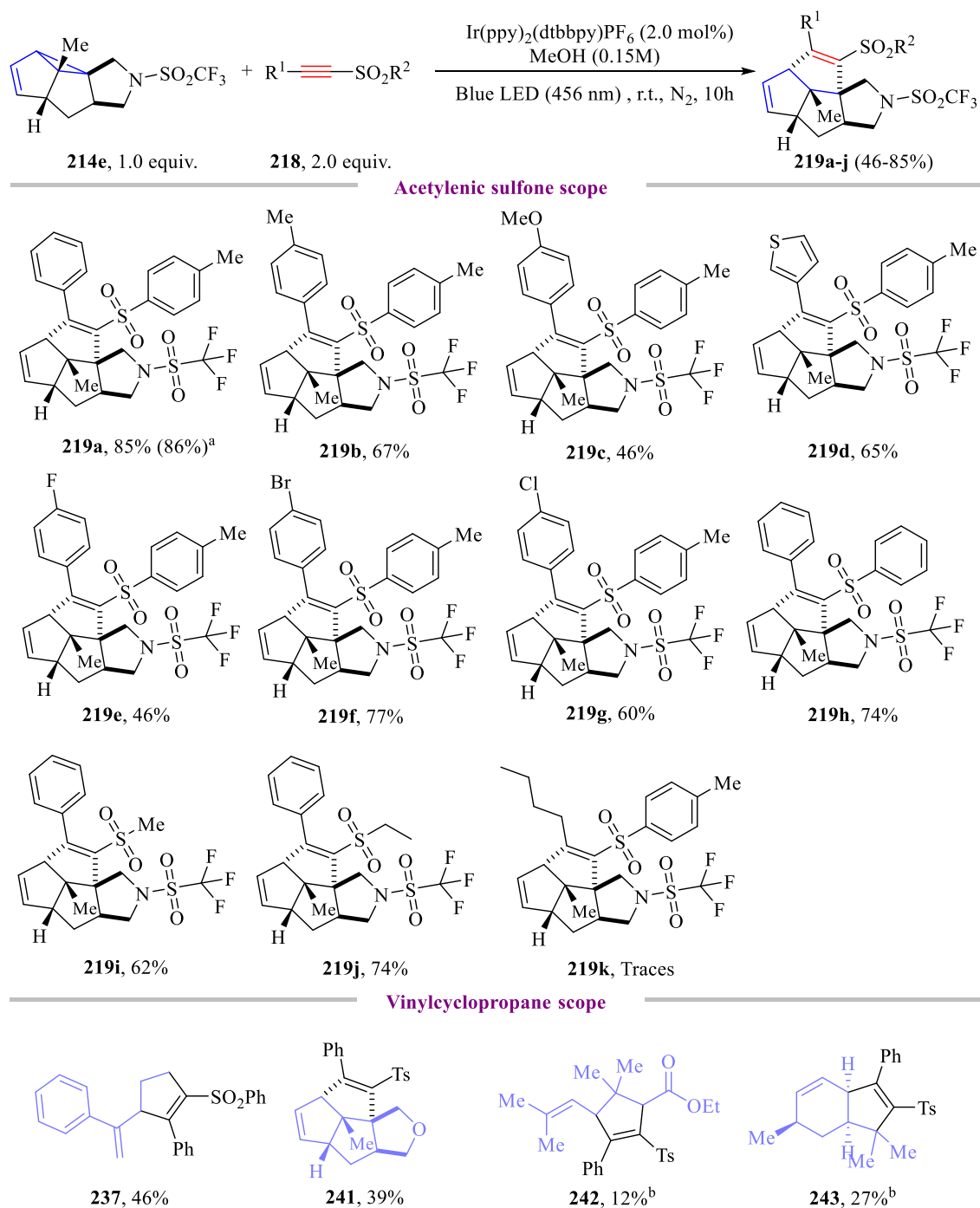
<sup>a</sup> A 40 W blue LED 456 nm module was used for irradiation, catalyst (2.5% mol). <sup>b</sup> A UV/vis CFL bulb was used for irradiation, catalyst (100% mol). <sup>c</sup> All yields are those of isolated products.

**Table 9.** Screening of reaction stoichiometry and concentration.

Entry	Equiv. of 218a	Concentration of 214e (M)	Yield (%) <sup>a</sup>
1	1.0	0.10	63
2	2.0	0.10	80
3	4.0	0.10	85
4	2.0	0.15	85
5	2.0	0.20	78

<sup>a</sup> All yields are those of isolated products.





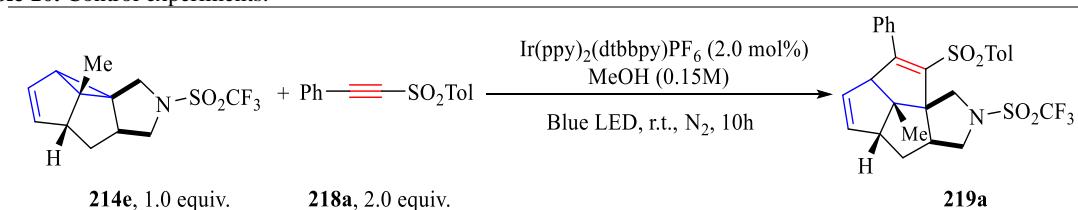
**Scheme 41.** Substrate scope in the formal [3+2] cycloaddition using the optimized conditions. All yields are those of isolated products. <sup>a</sup> [Ir(dF(CF<sub>3</sub>)ppy)<sub>2</sub>(dtbbpy)]PF<sub>6</sub> and Blue LED 440 nm were used. <sup>b</sup> Synthesized by [REDACTED].

### Mechanistic considerations

Initial control experiments (Table 10) proved the reaction to be light and catalyst-dependent (entries 2 and 4). Furthermore, the presence of air suppresses product formation. No desired product was obtained when performing a radical trapping experiment using

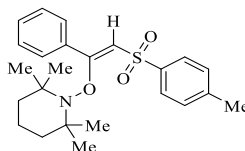
(2,2,6,6-tetramethylpiperidin-1-yl)oxyl (TEMPO). A TEMPO trapping product was isolated instead, and its structure was determined by ESI-HRMS and NMR. Temporal on/off control experiments on the reaction (Figure 11) highlights the light-controlled feature of this [3+2] cycloaddition.

**Table 10.** Control experiments.



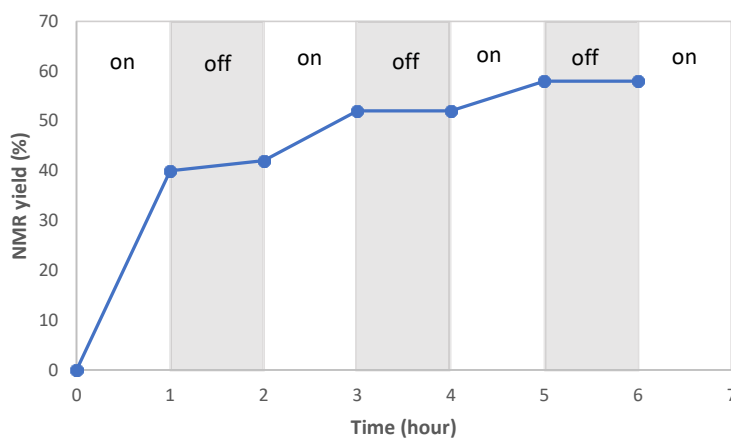
Entry	Deviation from the optimized conditions <sup>a</sup>	Yield (%) <sup>b</sup>
1	No deviation	85
2	no light	0
3	with air	0
4	No $[\text{Ir}(\text{ppy})_2(\text{dtbbpy})]\text{PF}_6$	0

**TEMPO coupling product detected by HRMS and NMR**



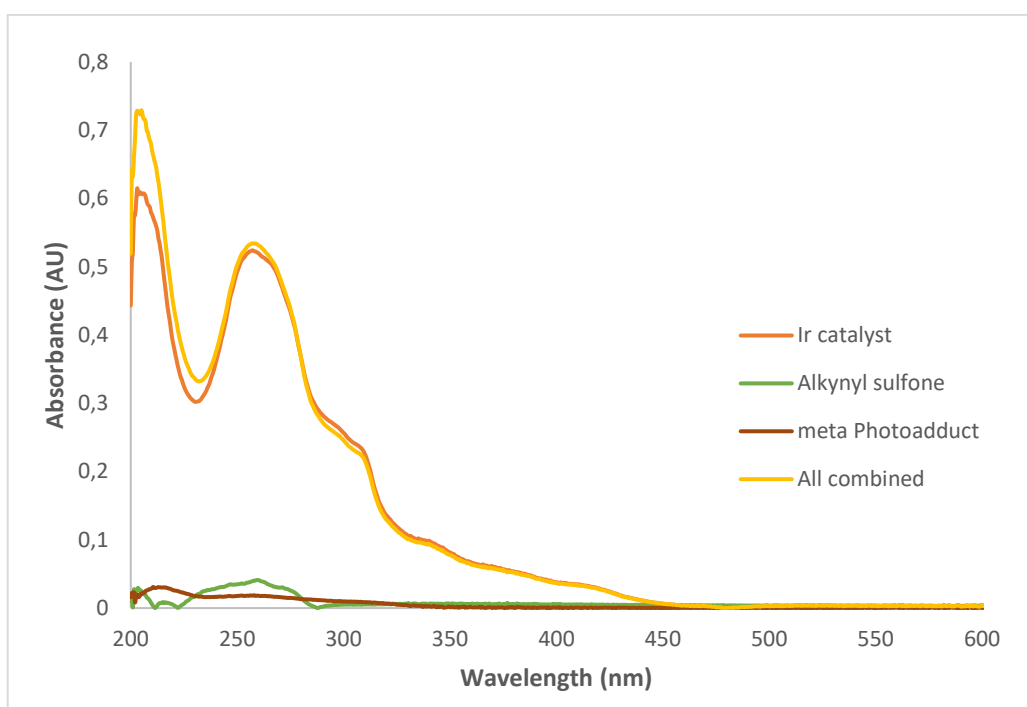
<sup>a</sup> Optimized conditions: *meta* photoadduct (**214e**, 35 mg, 0.12 mmol, 1.00 equiv.), 1-methyl-4-(phenylethynylsulfonyl)benzene (**218a**, 61.2 mg, 0.24 mmol, 2.00 equiv.),  $[\text{Ir}(\text{ppy})_2(\text{dtbbpy})]\text{PF}_6$  (2.2 mg, 2.4  $\mu\text{mol}$ , 0.02 equiv.) and 0.8 mL of degassed solvent (15 mM). A 40 W blue LED 456 nm module was used for irradiation.

<sup>b</sup> All yields are those of isolated products.



**Figure 11.** "On/off" experiment.

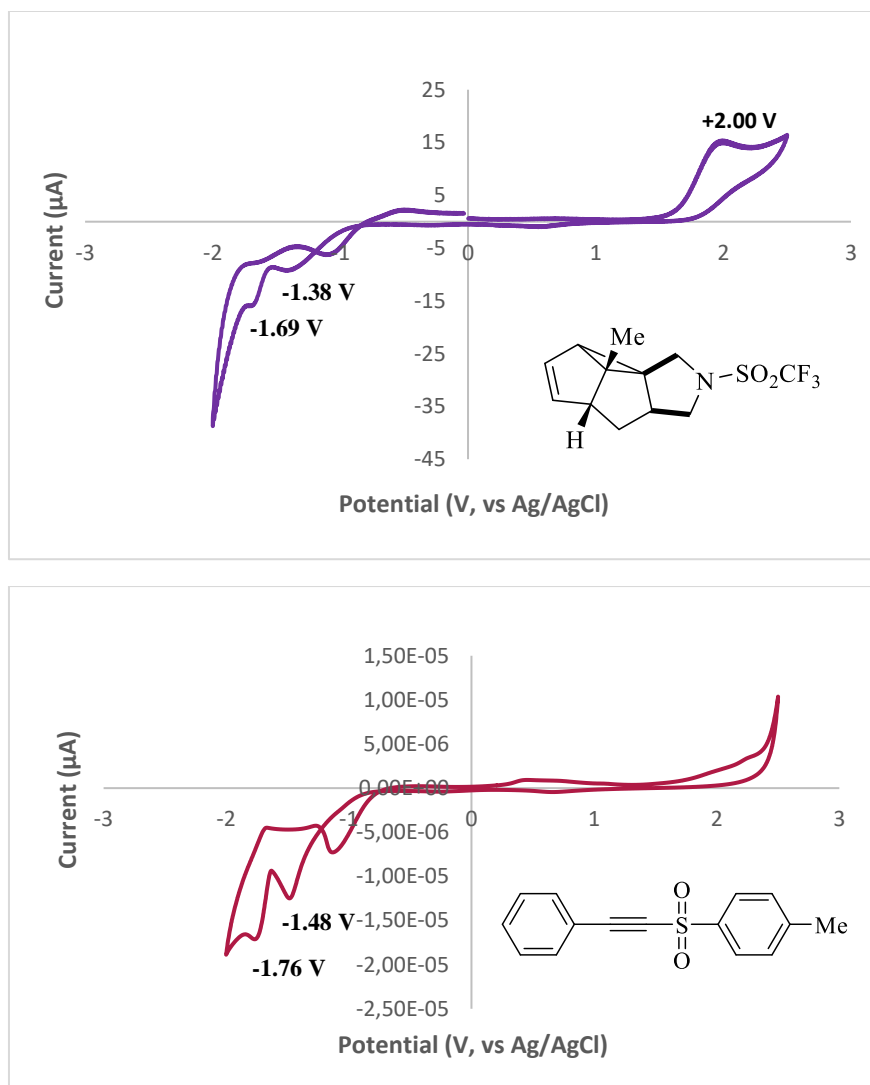
Since the reaction is light-dependent, UV-Vis absorbance measurements were performed to identify the light-absorbing species (Figure 12). For this purpose, the individual components and their mixture were measured. No new absorption maxima can be seen in the spectrum of the mixture so that the formation of charge-transfer complexes as visible light-absorbing species can be ruled out. Given that all the individual components absorb below 350 nm and the emission spectrum of the blue LED Kessil lamp ( $\lambda_{\text{max}} \approx 456$  nm), the absorption spectra indicate that the catalyst is the only compound absorbing light and initiates the difunctionalization through its  $^3\text{MLCT}$  excited state.



**Figure 12.** Absorption UV/vis spectra of all reaction components from the model reaction and their mixture. All spectra were measured in MeOH with a concentration of  $1 \times 10^{-5}$  M for all compounds.

In the cyclic voltammograms of the *meta* photoadduct **214e**, oxidation and reduction features were observed with half-peak potentials of  $E_{\text{red}} = -1.69$  V vs Ag/AgCl =  $-1.65$  V vs SCE;  $E_{\text{red}} = -1.38$  V vs Ag/AgCl =  $-1.34$  V vs SCE  $E_{\text{ox}} = +2.00$  V vs Ag/AgCl =  $+1.96$  V vs SCE. The reduction potentials of the acetylenic sulfone **218a** were determined to be  $E_{\text{red}} = -1.76$  V vs Ag/AgCl =  $-1.72$  V vs SCE;  $E_{\text{red}} = -1.48$  V vs Ag/AgCl =  $-1.44$  V vs SCE (Figure 13). The potentials were expressed against the Ag/AgCl in 3M KCl reference electrode and converted against SCE by subtracting 45 mV. Cyclic voltammograms were recorded at room

temperature with solution of the substrate (5.0 mM) in acetonitrile with  $\text{Bu}_4\text{NBF}_6$  (0.1 M) as electrolyte.



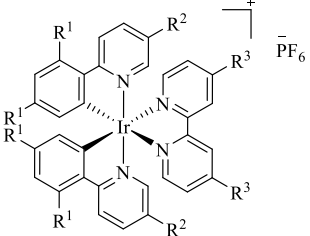
**Figure 13.** Cyclic voltammograms of the tetracycle **214e** and the acetylenic sulfone **218a** at room temperature ( $22\text{ }^\circ\text{C}$ ) using an Autolab PGSTAT 204 potentiostat from Metrohm. Conditions: 5 mM substrate in acetonitrile (10 mL) with 0.1 M  $\text{Bu}_4\text{NBF}_6$ . WE: platinum tip ( $d = 2\text{ mm}$ ); CE: glassy carbon rod; RE: Ag/AgCl in 3 M KCl; Scan rate: 100 mV/s.

To elucidate the mechanism of the reaction and distinguish the two possible general mechanisms, ET or EnT, the redox potentials, and the calculated triplet energy ( $E_T$ ) of the *meta* photoadduct **214e** were compared with those of the catalysts (Tables 11 and 12).

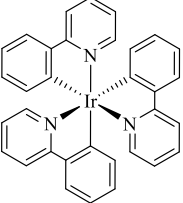
The thermodynamic feasibility of SET steps that can occur during the reaction was evaluated by evaluating the Gibbs free energies of the possible single SET steps. These Gibbs free energies were calculated as described in section 1.1.1 (equations 1.7-1.8) and they are

summarized in Table 11. In this case, the Gibbs free energies provided are rather estimations than true values since the literature redox potentials might fluctuate due to the variations in reaction conditions.

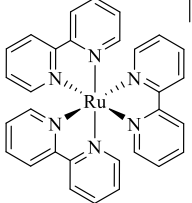
**Table 11.** Relevant redox potentials and Gibbs free energies of possible SET steps.



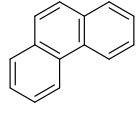
[Ir(ppy)<sub>2</sub>(dtbbpy)]PF<sub>6</sub> (**PC I**): R<sup>1</sup>=R<sup>2</sup>=H, R<sup>3</sup>=<sup>t</sup>Bu



*fac*-Ir(ppy)<sub>3</sub> (**PC IV**)



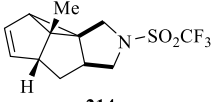
[Ru(bpy)<sub>3</sub>]Cl<sub>2</sub> (**PC V**)



Phenanthrene (**PC VI**)

[Ir(dFCF<sub>3</sub>ppy)<sub>2</sub>(bpy)]PF<sub>6</sub> (**PC II**): R<sup>1</sup>=F, R<sup>2</sup>=CF<sub>3</sub>, R<sup>3</sup>=H

[Ir(dF(CF<sub>3</sub>)ppy)<sub>2</sub>(dtbbpy)]PF<sub>6</sub> (**PC III**): R<sup>1</sup>=F, R<sup>2</sup>=CF<sub>3</sub>, R<sup>3</sup>=<sup>t</sup>Bu



**214e**

**Redox potentials of 214e:**

$E_{1/2}^{\text{red}} = -1.65$  V vs. SCE

$E_{1/2}^{\text{red}} = -1.34$  V vs. SCE

$E_{1/2}^{\text{oxd}} = +1.96$  V vs. SCE

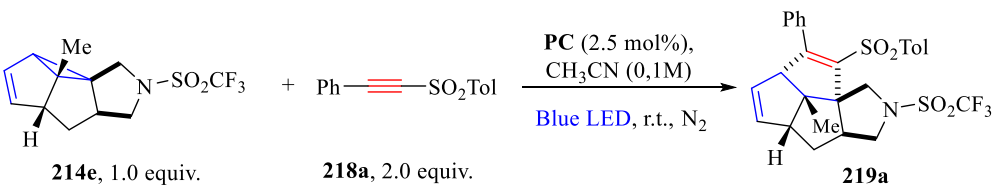
Entry	PC	Catalyst $E_{1/2}^{\text{red}}/E_{1/2}^{\text{oxd}}$ (V vs SCE)	Electron acceptor	Electron donor	Gibbs free energy (kcal/mol)	Comment
1	VI <sup>[132]</sup>	-2.10	<b>214e</b>	[ <b>PC VI</b> ] <sup>*</sup>	-10.38	Oxidative quenching
		+1.27	[ <b>PC VI</b> ] <sup>*</sup>	<b>214e</b>	+15.91	Reductive quenching
2	III <sup>[133]</sup>	-0.89	<b>214e</b>	[ <b>PC III</b> ] <sup>++</sup>	+17.53	Oxidative quenching
		+1.21	[ <b>PC III</b> ] <sup>++</sup>	<b>214e</b>	+17.30	Reductive quenching
3	II <sup>[133]</sup>	-1.00	<b>214e</b>	[ <b>PC II</b> ] <sup>++</sup>	+14.99	Oxidative quenching
		+1.32	[ <b>PC II</b> ] <sup>++</sup>	<b>214e</b>	+14.76	Reductive quenching
4	IV <sup>[134]</sup>	-1.73	<b>214e</b>	[ <b>PC IV</b> ] <sup>*</sup>	-1.85	Oxidative quenching
		+0.31	[ <b>PC IV</b> ] <sup>*</sup>	<b>214e</b>	+38.05	Reductive quenching
5	I <sup>[133]</sup>	-0.96	<b>214e</b>	[ <b>PC I</b> ] <sup>++</sup>	+15.91	Oxidative quenching
		+0.66	[ <b>PC I</b> ] <sup>++</sup>	<b>214e</b>	+29.97	Reductive quenching
6	V <sup>[15a, 135]</sup>	-0.81	<b>214e</b>	[ <b>PC V</b> ] <sup>+2*</sup>	+19.37	Oxidative quenching
		+0.77	[ <b>PC V</b> ] <sup>+2*</sup>	<b>214e</b>	+27.44	Reductive quenching

By analyzing the compiled data in Table 11 can be implied that an oxidative quenching pathway is possible when using **PC VI** (entry 1) or **PC IV** (entry 4), where the electron

transfer from these catalysts to the *meta* photoadduct **214e** is exergonic. However, the possibility of SET steps that enable either oxidative or reduction quenching when using the catalyst **PC V** (entry 6) or the other iridium catalysts (entries 2-3, 5) can be excluded since these processes are likely endergonic and therefore thermodynamically unfavorable.

As the reaction proceeds when using almost all the listed catalysts except for **PC V** (Table 12), it appears less likely that a photo-initiated electron transfer mechanism is involved. Therefore, it is possible to propose that an energy transfer mechanism could be in operation for this cycloaddition reaction. However, from the data in Table 12, it can be inferred that there is no clear correlation between the triplet energies of the catalysts and the reaction yield, making a Dexter energy transfer also difficult.<sup>[50a]</sup>

**Table 12.** Influence of triplet energies on the yield of the [3+2] cycloaddition.

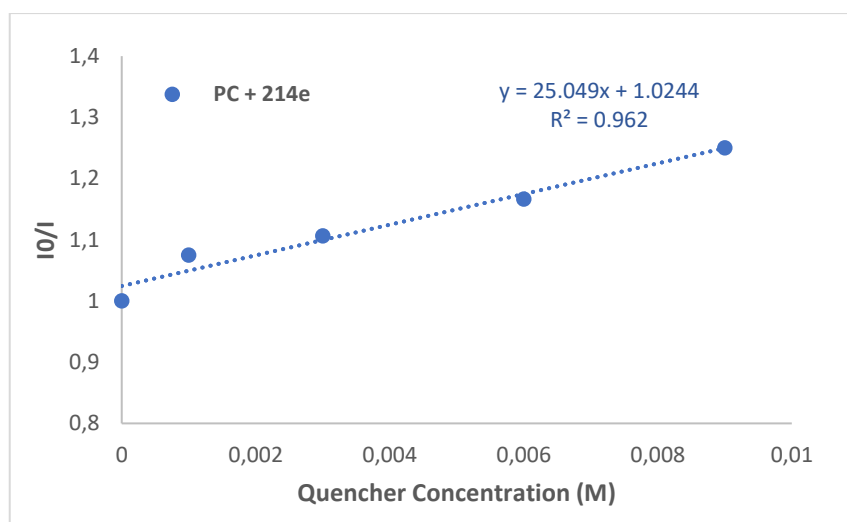


Entry	PC	$E_T$ (kcal/mol)	Yield (%) <sup>a</sup>
1	VI <sup>b</sup>	61.9	63
2	III	60.1	49
3	II	60.0	51
4	IV	55.2	49
5	I	49.2	53
6	V	46.0	traces

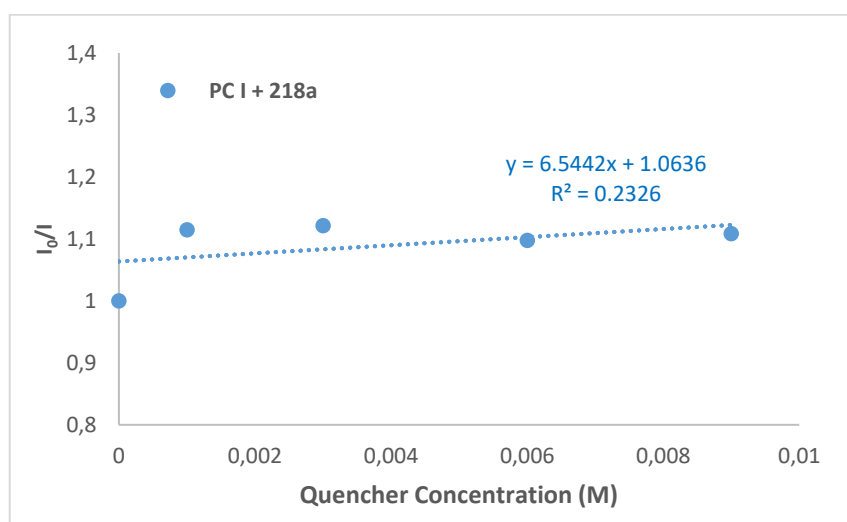
<sup>a</sup> isolated yields. <sup>b</sup> 100 mol% of catalyst loading and UV/vis CFL bulb was used.

Density functional theory calculations (DFT) (performed by [REDACTED]) were performed to predict the Gibbs free energy of each reaction intermediate (Scheme 42).<sup>[65, 69, 136]</sup> All structures were optimized applying the functionals B3LYP,<sup>[137]</sup> CAM-B3LYP<sup>[138]</sup> as well as M062X<sup>[139]</sup> in conjunction with the Pople basis-set 6-311+G(2d,p)<sup>[140]</sup> with the IEFPCM solvation model<sup>[141]</sup> for methanol. The adiabatic  $S_0-T_1$  energy gaps were determined as the difference between the electronically excited states ( $T_1$ ) and the respective ground states ( $S_0$ ).

Although the reaction releases  $48.9 \text{ kcal mol}^{-1}$  of energy and follows an overall exergonic pathway, the computed adiabatic triplet energy of **214e** ( $59.1 \text{ kcal mol}^{-1}$ ) is considerably higher than those of **PC I** and **PC IV** (Table 11, entries 4 and 5) but for the rest of iridium catalysts and **PC VI** is low enough for an EnT process. Even though these results alone cannot lead to the conclusion that the reaction is initiated by an energy transfer process, the direct excitation of the VCP moiety by UV irradiation of **214e** also gives rise to the tetracycle **219a** in 27% yield.<sup>[142]</sup>



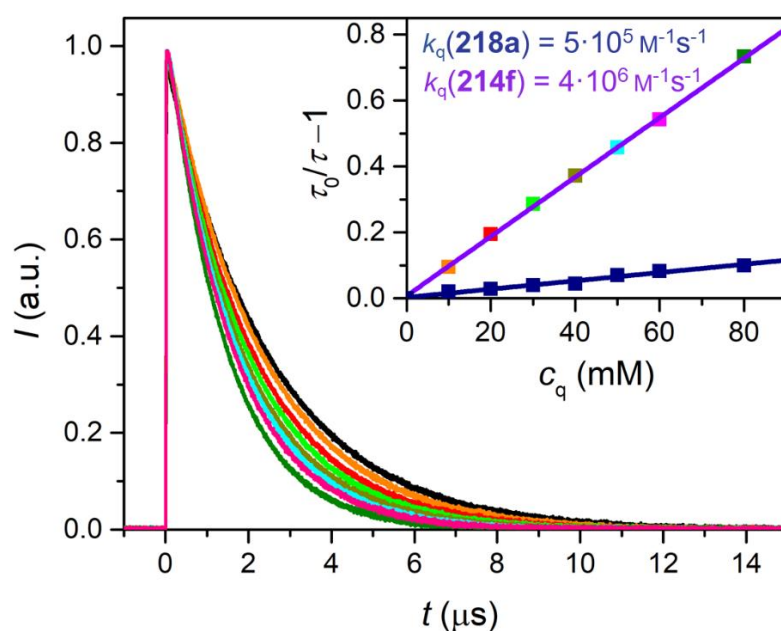
**Figure 14.** Stern-Volmer plot for the fluorescence quenching of the **PC I** ( $1 \times 10^{-5} \text{ M}$  in degassed methanol) with the *meta* photoadduct **214e**.



**Figure 15.** Stern-Volmer plot for the fluorescence quenching of the **PC I** ( $1 \times 10^{-5} \text{ M}$  in degassed methanol) with the acetylenic sulfone **218a**.

Initial intensity-based Stern-Volmer quenching experiments on **PC I** revealed that the phosphorescence of the catalyst could be quenched by **214e**, suggesting the possibility of an electron or energy transfer from the excited triplet state of **PC I** to **214e** (Figures 14 and 15). However, to get more reliable kinetic results, lifetime-based Stern-Volmer laser flash photolysis (LFP) studies were performed.

Lifetime-based quenching experiments (performed by [REDACTED]) with selected photosensitizers **PC IV**, **PC III**, and **PC I** showed that **PC III** is most effectively quenched by the *meta* photoadduct **214e**, consistent with its highest triplet energy. **PC III** could efficiently catalyze the initial test reaction under optimized conditions when using a blue LED 440 nm (86 % yield of **219a**) letting to assume the very same reaction mechanism as with **PC I** might be involved. Additionally, **PC III** is known to possess observable spectroscopic signatures in all states that might occur during photocatalytic cycles making it well-suited for mechanistic investigations by LFP.<sup>[143]</sup> Consequently, all further LFP experiments were conducted with **PC III** as a sensitizer. Lifetime-based Stern-Volmer experiments of **PC III** (32  $\mu\text{M}$ ) with varying concentrations of *meta* photoadduct **214e** and sulfone **218a** yielded quenching rates  $k_q$  of  $4 \cdot 10^6 \text{ M}^{-1} \text{ s}^{-1}$  and  $5 \cdot 10^5 \text{ M}^{-1} \text{ s}^{-1}$ , respectively (Figure 16).

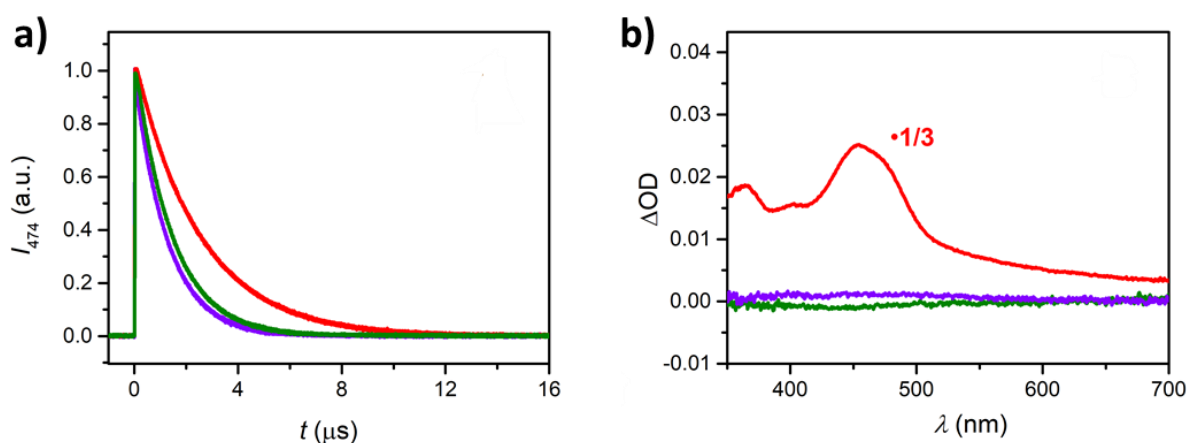


**Figure 16.** Emission decay kinetics of excited **PC III** (32  $\mu\text{M}$ ) in the presence of varying concentrations of **214e** in Ar-saturated MeCN. Enclosure: Stern-Volmer plots of **PC III** and **214e** (purple fit, the colored squares correspond to the same quencher concentration as in the main plot), and **PC III** combined with **218a** (dark blue). Detection occurred at 474 nm.



The linear Stern-Volmer plots show a much faster quenching by the *meta* photocycloadduct **214e** than with the acetylenic sulfone **218a** (Figure 16). Regardless of the high triplet energy of **PC III** (Table 12), the quenching rate constant for the reaction between the excited catalyst and **214e** ( $4 \times 10^6 \text{ M}^{-1} \text{ s}^{-1}$ ) is lower than the diffusion limit by almost 4 orders of magnitude. Nevertheless, quenching can be very effective under typical conditions used for lab-scale photocatalysis with substrate concentrations on the order of 0.1 M.

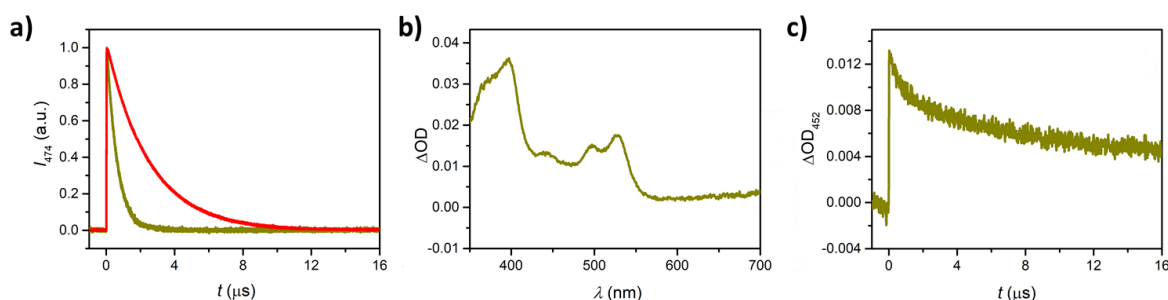
Subsequently, it was explored whether the sensitizer quenching proceeds through EnT or SET. Transient absorption (TA) studies were performed with the LFP setup of the Kerzig group<sup>[144]</sup> upon selective excitation of **PC III** to check the quenching products. Three different solutions having 32  $\mu\text{M}$  of **PC III** in the absence of any substrate, in combination with 80 mM of **214e**, and with 80 mM of both **214e** and **218a**, were prepared in degassed MeCN. After excitation, the iridium photosensitizer efficiently populates the triplet-excited state with a lifetime of 2.5  $\mu\text{s}$  in MeCN (Equation 3.1). The TA spectrum of the triplet-excited state of **PC III** is shown in Figure 17.



**Figure 17.** LFP experiments upon excitation with 355 nm laser pulses of solutions of 32  $\mu\text{M}$  **PC III** and 80 mM **214e** (green), and 80 mM of both **214e** and **218a** (purple) in degassed MeCN. a) Time-resolved emission checked at 474 nm in the absence (red) and presence of quenchers. b) TA spectrum of the triplet-excited  ${}^3\text{PC III}$  (red, delay 10 ns) and spectra recorded right after the initial photosensitizer triplet decay (delay 10  $\mu\text{s}$ ).

Based on reference measurements the transient spectra were expected to have intense photocatalyst-derived bands for both reductive and oxidative quenching pathways. However, as could be seen in Figure 17b, this type of TA signal was not recorded (green and purple spectra) which allows to exclude quenching via ET.<sup>[145]</sup>

To provide further evidence that an electron transfer process is not involved in the described [3+2] cycloaddition reaction between the sensitizer and one of the substrates, TA spectra of the oxidized and reduced catalyst were recorded with other oxidative or reductive quenchers. A 32  $\mu\text{M}$  solution of **PC III** with 5 mM of the well-known reductive quencher triethanolamine (TEOA), the radical cation of which is transparent in the resulting TA spectra, was prepared to evaluate a possible reductive quenching of the excited catalyst (Figure 18). Time-resolved emission spectroscopy showed that the lifetime of the sensitizer emission is strongly reduced by the addition of TEOA (Figure 18a). A transient absorption spectrum was recorded once the excited sensitizer was fully quenched, 6  $\mu\text{s}$  after excitation (Figure 18b). Comparing with the TA spectra recorded for **PC III** in combination with **214e** and **218a**, a new absorbing species can be observed. This novel species decays on a much longer timescale as time-resolved transient spectroscopy at a detection wavelength of 452 nm revealed (Figure 18c).



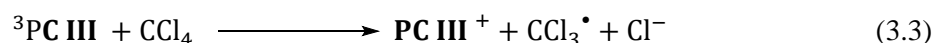
**Figure 18.** Detection of the reduced **PC III** species by LFP experiments upon excitation with 355 nm laser pulses of a solution containing 32  $\mu\text{M}$  **PC III** and 5 mM TEOA in degassed MeCN. a) Time-resolved emission monitored at 474 nm in the absence (red) and presence of TEOA (green). b) TA spectrum of the quenching product (delay 6  $\mu\text{s}$ , integration over 100 ns). c) Transient absorption traces were monitored at 452 nm.

TEOA is a commonly used reductive quencher with an oxidation potential of 0.57-0.82 V vs SCE (aqueous solution),<sup>[146]</sup> which is low enough to be oxidized by  $^3\text{PC III}$  ( $E_{1/2}^{\text{oxd}} = +1.21$  V vs SCE) (Equation 3.2). The reaction generates the reduced species, **PC III** $^-$ , and the radical cation,  $\text{N}(\text{C}_2\text{H}_4\text{OH})_3^+$ . In general, radical cations of aliphatic amines are

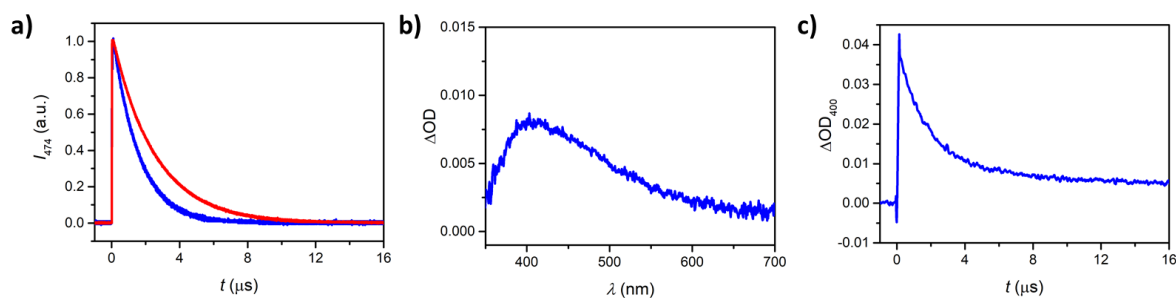
essentially transparent in the used detection range;<sup>[147]</sup> thus is possible to assign the TA spectrum in Figure 18 to the reduced catalyst (**PC III**<sup>-</sup>). Similar absorption spectra of the reduced form of the catalyst can be found in the literature.<sup>[143b]</sup>



To evaluate the oxidative quenching of the excited catalyst, a solution of 32  $\mu\text{M}$  **PC III** and 2 M tetrachloromethane was prepared. The tetrachloromethane as the quencher with a reduction potential of -0.78 V vs SCE<sup>[148]</sup> was expected to reduce the excited state of **PC III** ( $E_{1/2}^{\text{red}} = -0.89$  V vs SCE) while generating fragments  $\text{CCl}_3$  and  $\text{Cl}^-$  which are not supposed to absorb in the selected detection range (350-700 nm) (Equation 3.3).<sup>[149]</sup> The related lab-scale reaction with the very same iridium complex has also been reported in the literature.<sup>[150]</sup> The use of methyl viologen dihexafluorophosphate as an alternative oxidative quencher was unsuccessful due to its strong absorption in the visible region once it is reduced, making it difficult to get a clean spectrum of the oxidized sensitizer.



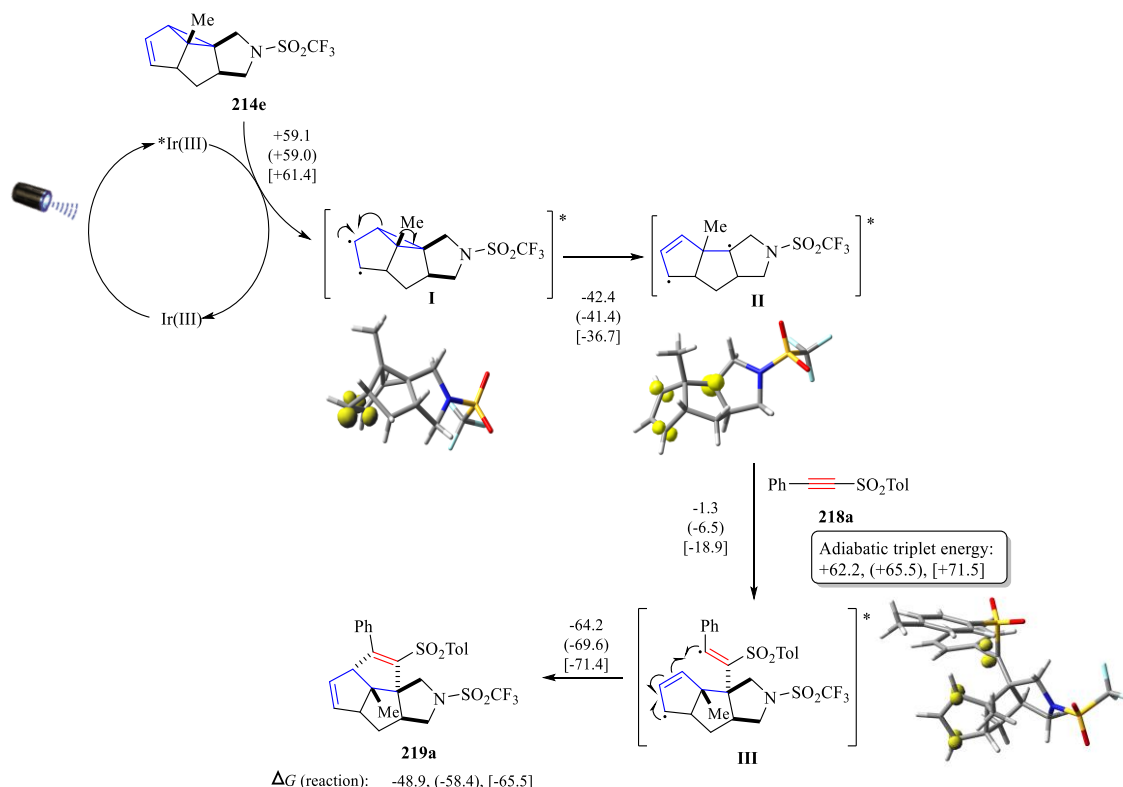
Time-resolved emission spectroscopy showed that the lifetime of the sensitizer emission is reduced by the addition of tetrachloromethane (Figure 19a). A transient absorption spectrum was recorded once the luminescence fully returned to baseline, 10.5  $\mu\text{s}$  after excitation (Figure 19b). The maximum at 410 nm shows the formation of a new absorbing species which decays on a longer timescale (detection wavelength of 400 nm) compared to the sensitizer emission (Figures 19a and 19c). No other compound apart from the oxidized sensitizer is expected to absorb in the established range, allowing to assign the absorbing species to **PC III**<sup>+</sup>.



**Figure 19.** Detection of the oxidized **PC III**<sup>+</sup> species by LFP experiments upon excitation with 355 nm laser pulses of a solution containing 32  $\mu\text{M}$  **PC III** and 2 M  $\text{CCl}_4$  in degassed MeCN. a) Time-resolved emission monitored at 474 nm in the absence (red) and presence of  $\text{CCl}_4$  (blue). b) TA spectrum of the quenching product (delay 10.5  $\mu\text{s}$ ). c) Transient absorption traces were monitored at 400 nm.

Based on the above observations, a plausible mechanistic pathway for the current transformation is depicted in Scheme 42. Upon visible light irradiation, **PC I** (or **PC III**) is capable to photosensitize **214e** by transferring energy from its <sup>3</sup>MLCT state to the VCP moiety giving the transient radical species **I**, which undergoes a fast ring-opening process to give the intermediate **II**. The latter adds to the acetylenic sulfone to generate the intermediate **III**, providing a translocated radical, which undertakes a ring-closure reaction yielding the tetracycle **219**. The existence of the radical intermediate **III** can be supported by the finding that aromatic substituents at  $\text{R}^1$  in the acetylenic sulfone are required for the reaction to proceed. The signals of the excited photosensitizer fully return to the baseline for EnT mechanisms and the intermediates **II** and **III** (compare, Scheme 42) are expected to have very weak absorption (and mainly in the UV region), due to the lack of  $\pi$ -conjugation and adjacent functional groups explaining the absence of new signals in the TA spectra right after significant energy transfer quenching. Time-dependent DFT calculations were used to predict the light-absorbing properties of the triplet diradical intermediates **II** and **III**. For the excitation of these intermediates, the energy of at least 3.67 eV (oscillator strength  $f = 0.0002$ ) and 2.71 eV ( $f = 0.0093$ ) is required for the first excited state. Local absorption maxima were predicted to be at 239 nm and 282 nm, respectively (For technical details, see the publication).<sup>[127]</sup> Additionally, the factors controlling the lifetimes of diradicals are not entirely understood<sup>[151]</sup> and most of these species have short lifetimes making efficient detection difficult. Compared with the alkyl cyclopropane radical clock (ring-opening rate constant,  $1.3 \times 10^8 \text{ s}^{-1}$ ),<sup>[152]</sup> the cyclopropane ring-opening of the intermediate **I** in its triplet state is presumably faster by orders of magnitudes taking into account the accelerating effects of substituents and/or fused rings at the cyclopropane unit.<sup>[153]</sup> Assuming that strain release and the associated significant energy gain could in theory occur on a comparable

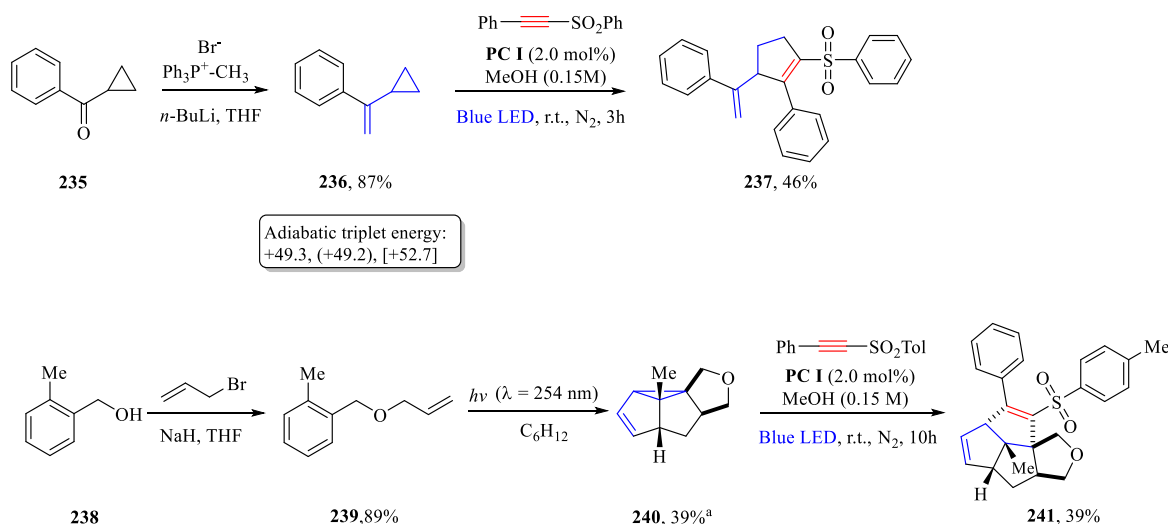
timescale as molecular collision and the actual Dexter energy transfer from the excited catalyst. A concerted reaction mechanism like that (without the presence of intermediate **I**) could justify the observed quenching and energy transfer product when **PC I** is used, in which case the formation of intermediate **I** would be thermodynamically unfavorable by about 10 kcal mol<sup>-1</sup> (9.9 kcal mol<sup>-1</sup>) through conventional mechanisms.<sup>[154]</sup>



**Scheme 42.** Proposed mechanism for the [3+2] photocycloaddition. The reported adiabatic energy differences obtained with different functionals are given in kcal mol<sup>-1</sup> (no bracket): (U)B3LYP, parentheses: (U)CAM-B3LYP, square bracket: (U)M06-2X). The spin densities (yellow, isovalue = 0.04) were plotted for the triplet intermediates **I-III**.

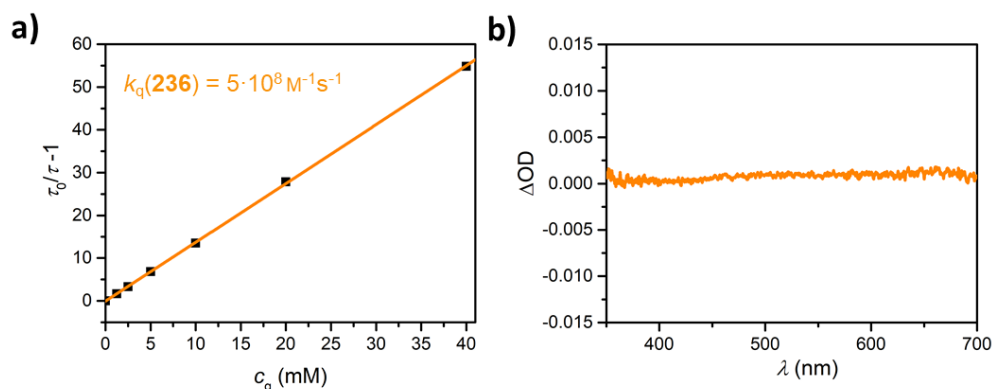
The possibility of an energy transfer process from the catalyst to the acetylenic sulfone can be considered less likely as the calculated triplet energy of the latter (62.2 kcal mol<sup>-1</sup>) is higher than that of **PC I**, no gain from a follow-up reaction such as the ring-opening of the VCP can occur and the reaction of the triplet acetylenic sulfone to the VCP should occur at the distal carbon of the C=C double bond, contradicting the observed regioselectivity. To test the hypothesis that only the vinylcyclopropane moiety in the *meta* photoadduct **214e** participates in the proposed mechanism reaction, different substrates were reacted under the standardized conditions of the developed [3+2] cycloaddition reaction (Scheme 41). The synthesis of **237**, **241-243** demonstrated that the described strategy could be extended to

other VCP-type substrates. The substituted cyclopentene **237** and tetracycle **241** were prepared in 46 and 39% yield in a two-step and three-step synthesis, respectively (Scheme 43) while **242-243**, which were synthesized by [REDACTED] were obtained only in moderate yields by using the commercial and naturally occurring VCPs, ethyl *trans*-chrysanthemate and (1*S*,3*R*)-*cis*-4-carene.



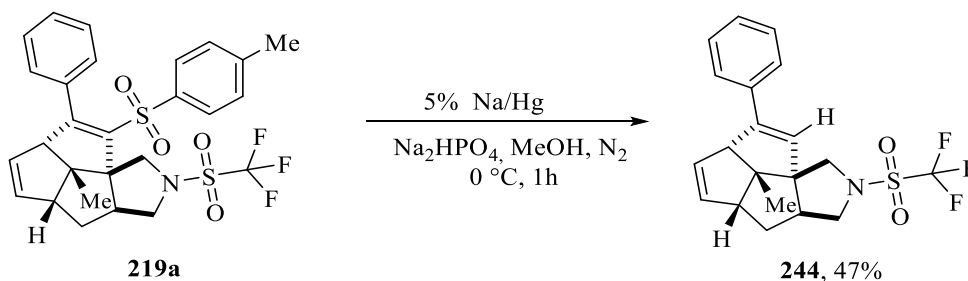
**Scheme 43.** Synthesis and use of alternative substrates in the [3+2] photocycloaddition under standard conditions. The predicted energy differences are given in kcal mol<sup>-1</sup> (no bracket: (U)B3LYP, parentheses: (U)CAM-B3LYP, square bracket: (U)M06-2X). <sup>a</sup> Inseparable mixture.

Additional LFP measurements using a mixture of photocatalyst **PC III** with the (1-cyclopropylvinyl)benzene **236** as quencher led to obtaining from the Stern-Volmer plot (Figure 20a) the quenching rate constant of  $5 \times 10^8 \text{ M}^{-1}\text{s}^{-1}$  that is about two orders of magnitude faster than obtained with substrate **214e**, consistent with the expectations for a Dexter-type energy transfer. This may be due to the extended  $\pi$ -system present in compound **236** which lowers the *in silico* triplet energy (ca. 10 kcal mol<sup>-1</sup>) in comparison with the *meta* photoadduct **214e**. After the photosensitizer's emission was fully quenched and at above 95% quenching efficiencies (40 mM of **236**) no new absorbing species was detected (Figure 20b). If electron transfer quenching pathways were to occur, pronounced spectroscopic signatures of the reduced or oxidized sensitizer would have been observed in the TA spectrum.



**Figure 20.** LFP experiments upon excitation with 355 nm laser pulses of a solution containing 32  $\mu\text{M}$  **PC III** and the presence of varying concentrations of (1-cyclopropylvinyl)benzene (**236**) in degassed MeCN. a) Lifetime-based Stern-Volmer plot with varying concentrations of **236**. b) TA spectrum of the quenching product of 32  $\mu\text{M}$  **PC III** and 40 mM of **236** (delay 0.4  $\mu\text{s}$ ).

To illustrate the synthetic usefulness of the resulting sulfonyl containing cycloadducts, the tetracycle **219a** was subjected to a selective reductive desulfonylation (experiment performed by [REDACTED]), generating a compound bearing a styrene moiety that is difficult to obtain via direct cycloaddition and is suitable for further follow-up reactions (Scheme 44).



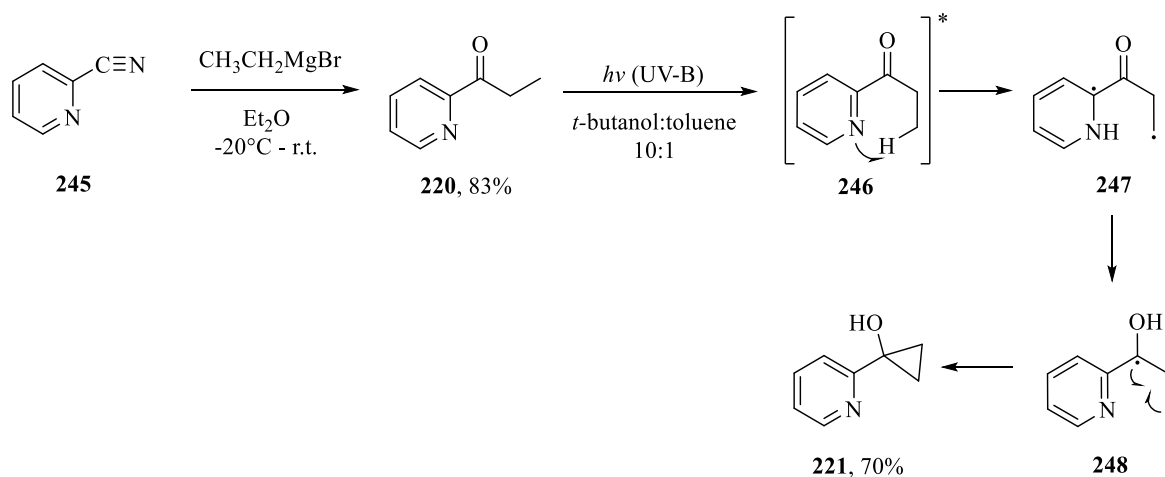
**Scheme 44.** Desulfonation of the tetracycle **219a**.

## 2.3.2. Photogenerated cyclopropanols

### 2.3.2.1. Preparation of the cyclopropanols and their use as substrates in catalyzed follow-up reactions

In the second part of this work, photogenerated cyclopropanols were investigated in addition to the *meta* photocycloadduct regarding their possibility of subsequent reactions mediated by ring strain. Due to their relative ease of ring-cleavage, cyclopropanols have been used in an increasing number of transition metal-catalyzed C–X (X = heteroatom) and C–C

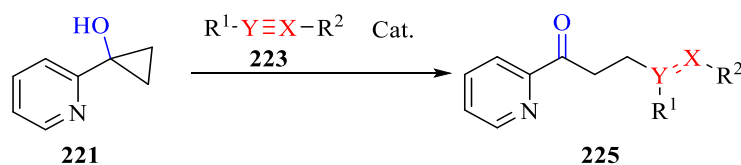
bond-forming reactions as described in the section 1.2.2. These examples were used as the basis to conduct the designed synthetic plan and the first step for this purpose was the preparation of suitable substrates from readily available reagents. To pursue this, the cyclopropanol **221** was synthesized in a two-step synthesis starting with the 2-pyridincarbonitril **245** followed by the photochemical ring-closing transformation based on Agosta's work as mentioned in section 1.1.2 using a Rayonet reactor (Scheme 45).



**Scheme 45.** Synthesis of the photochemically generated cyclopropanol **221**.

As previously discussed, the success of the above ring-closing reaction depends on the nitrogen *ortho* to the acyl group in the substrate molecule, which upon direct irradiation removes the hydrogen of the C-4 of the side chain to generate the intermediate **247** that following isomerization affords the cyclopropanol **221**. In an attempt to prepare its pyrimidine derivative the use of 4-cyanopyrimidine in the first part of this synthetic method did not afford the expected 1-(pyrimidin-4-yl)propan-1-one, therefore only **221** was employed as a precursor in the planned follow-up reactions. Accordingly, based on the methods described in the literature<sup>[155]</sup> including some mentioned in section 1.2.2, **221** was evaluated in a catalyst screening with a different nitrile, alkynes, and alkenes finding that none of these reactions conducted to the expected ring-opening functionalized product **225** (Table 13).



**Table 13.** Catalyst screening in the ring-opening reaction of the cyclopropanol **221** using different alkynes and alkenes.

Entry	Reaction partner	Catalyst	Yield %	Entry	Reaction partner	Catalyst	Yield %
1	4-Octyne	CoI <sub>2</sub> , Zn, dppe	-	6	Styrene	[Rh(CO) <sub>2</sub> Cl] <sub>2</sub>	-
2	Benzonitrile	SnCl <sub>4</sub>	-	7	PhC≡CPh	[Cp(CO) <sub>2</sub> Cl] <sub>2</sub> , Cu(OAc) <sub>2</sub>	-
3	Benzonitrile	(Ph <sub>3</sub> P)AuCl, AgSbF <sub>6</sub>	-	8	PhC≡CPh	[Ir(OMe)(COD)] <sub>2</sub>	-
4	MeOOC≡COOMe	(Ph <sub>3</sub> P)AuCl, AgSbF <sub>6</sub>	-	9	Cinnamaldehyde	Mn(acac) <sub>2</sub>	-
5	MeOOC≡COOMe	[Rh(CO) <sub>2</sub> Cl] <sub>2</sub>	-	10	Cinnamaldehyde	AgNO <sub>3</sub> , Na <sub>2</sub> S <sub>2</sub> O <sub>8</sub>	-

For most of the cases decomposition or no reaction between the employed substrates was observed, except for the reaction between the cyclopropanol **221** and dimethyl acetylenedicarboxylate (DMAD) which gave the dimethyl 2-(1-(pyridin-2-yl)cyclopropoxy)maleate (**251**) in 16% (entry 4), but in absence of the catalyst, the yield was increased to 44%. Earlier reports<sup>[156]</sup> support the possibility that the reaction proceeds through the addition of the *N*-heterocycle to DMAD to form a zwitterionic intermediate (**249**), followed by hydrogen abstraction from the alcohol functionality and subsequent nucleophilic attack of the resulting alkoxy group on the electrophilic center in the fumarate moiety to produce **251**. Thus, a plausible mechanism for this transformation is given in Scheme 46.

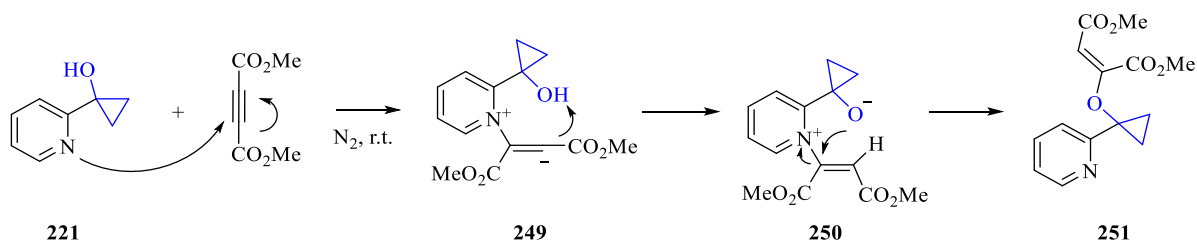
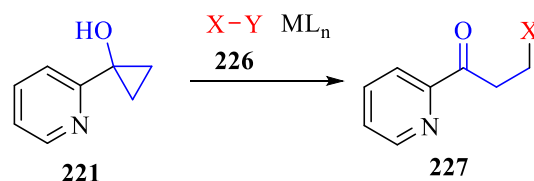
**Scheme 46.** A plausible mechanism for the formation of **251**.

Table 14. Catalyst screening in the ring-opening reaction of the cyclopropanol **221**.

Entry	Reaction partner	Catalyst	Yield % <sup>a</sup>
1	BrCF <sub>2</sub> COOEt	CuI <sub>2</sub> , 1,10-Phen	-
2	Tetrahydroisoquinoline	CuCl <sub>2</sub>	-
3	Sodium benzenesulfinate	Cu(OAc) <sub>2</sub>	traces <sup>c</sup>
4	Benzylsulfonic acid	Pd(OAc) <sub>2</sub> , Cu(OAc) <sub>2</sub>	30
5	Methylamine	Pd(OAc) <sub>2</sub> , Cu(OAc) <sub>2</sub>	-
6	1-Chloro-4-iodobenzene	Pd(OAc), AgOAc	-
7	2-Bromopyridine	Pd(OAc) <sub>2</sub> , dppb	14
8	Benzyl chloride	Pd(OAc) <sub>2</sub> , Xphos	51
9	4-cyanopyridine	Ir(ppy) <sub>2</sub> (dtbbpy)PF <sub>6</sub> , PIDA <sup>b</sup>	-
10	PhC≡CSO <sub>2</sub> Ph	Ir(ppy) <sub>2</sub> (dtbbpy)PF <sub>6</sub> , PIDA <sup>b</sup>	9
11	PhC=CSO <sub>2</sub> Ph	Ir(ppy) <sub>2</sub> (dtbbpy)PF <sub>6</sub> , PIDA <sup>b</sup>	-
12	PhC=CSO <sub>2</sub> Ph	Ir(ppy) <sub>2</sub> (dtbbpy)PF <sub>6</sub> , K <sub>2</sub> S <sub>2</sub> O <sub>8</sub> <sup>b</sup>	-

<sup>a</sup> All yields are those of isolated products. <sup>b</sup> Visible light catalysis using Blue LED. <sup>c</sup> No isolated.

Further studies employing strategies with Pd, Cu, and Ir-based catalysts in some cases led to the selective ring-opening of the cyclopropanol **221** that delivers the β-functionalized ketone **227** (Table 14). Initial experiments to conduct the copper-catalyzed ethoxycarbonyldifluoromethylation<sup>[98, 155c]</sup> and C-H functionalization of the tetrahydroisoquinoline<sup>[157]</sup> did not show product formation (entries 1-2). In contrast to the sulfonylation with sodium benzenesulfinate in presence of copper(II) acetate catalyst that gave only traces of the corresponding γ-keto sulfone (entry 3),<sup>[158]</sup> the same transformation

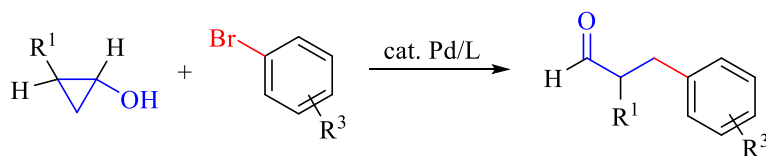
using benzyldisulfonic acid and a combination of the palladium(II) acetate with the same Cu catalyst<sup>[159]</sup> gave the expected functionalized carbonyl compound in 30% yield (entry 4). However, after applying the strategy of Brandi and co-workers using methylamine under the latter catalytic system, no conversion was observed (entry 5).<sup>[93]</sup> Although the attempt for establishing a cross-coupling reaction with Pd(OAc)<sub>2</sub> and the 1-chloro-4-iodobenzene only led to decomposition, the use of this catalyst showed product formation when using 2-bromopyridine<sup>[95]</sup> and benzyl chloride<sup>[160]</sup> in 14 and 51% yield, respectively (entries 7-8). The visible light-induced oxidation of the cyclopropanol **221** is mediated by phenyliodine diacetate (PIDA) (entries 9-11) or potassium persulfate (entry 12) using Ir(ppy)<sub>2</sub>(dtbbpy)PF<sub>6</sub> as photocatalyst and later alkyne/ alkenylation reaction<sup>[161]</sup> proceeded when using the acetylenic sulfone **218h** affording the alkynylative adduct in 9% yield (entry 10).

Although in most of the cases during the above catalyst screening minimal or no product formation was observed, Pd(OAc)<sub>2</sub> was shown to be the most efficient catalyst, and its use to promote the cross-coupling reaction of the cyclopropanol **221** with benzyl chloride provided the corresponding  $\gamma$ -arylated ketone in moderate yields. Therefore, the development and standardization of this reaction were continued, and these results are discussed in the next section.

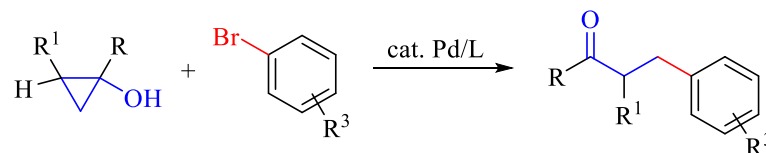
### 2.3.2.2. Pd-catalyzed cross-coupling synthesis of $\gamma$ -arylated ketones

As mentioned in section 1.2.2. cyclopropanols can easily undergo ring-opening processes as a result of their high strain energy (30 kcal·mol<sup>-1</sup>)<sup>[78c]</sup> and they have the ability to coordinate with transition metals while acting as homoenolate equivalents,<sup>[162]</sup> two characteristics that make them good coupling reaction partners. A variety of Pd-catalyzed ring-opening coupling reactions of organic halides, such as benzyl and aryl halides with cyclopropanols which serve as metal homoenolate surrogates, have been reported (Scheme 47).<sup>[95, 160, 163]</sup> After the metal and substrate screening described in the previous section it was found that this strategy could be extended to the use of the photogenerated pyridine cyclopropanol **221** as a nucleophilic coupling partner.

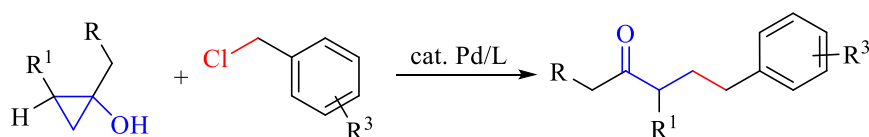
## a) Arylation of Aldehyde Homoenoates (Walsh and Cheng)



## b) Arylation of ketone Homoenoates (Orellana and Rosa)



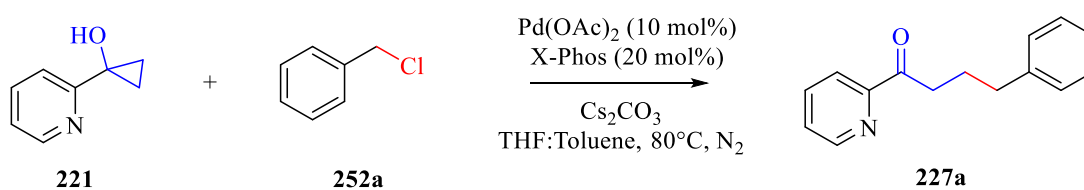
## c) Arylation of ketone Homoenoates (Orellana and Nithiy)



**Scheme 47.** Pd-catalyzed cross-coupling arylation of cyclopropanol derived ketone and aldehyde homoenoates.

### Reaction optimization

The preliminary study of the Pd-catalyzed ring-opening reaction of **221** using benzyl chloride as a reaction partner under the conditions described by Orellana and Nithy gave the corresponding  $\gamma$ -arylated ketone in 51% yield (Scheme 48).



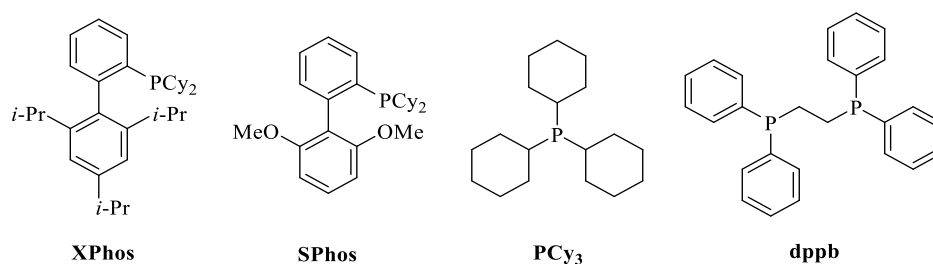
**Scheme 48.** Pd-catalyzed ring-opening reaction of **221** using the benzyl chloride **227a**.

Using the above conditions as the starting point and keeping the Pd source consistent, some catalyst and ligand (Figure 21) screening experiments were carried out in order to improve the reported yield of this reaction (Table 15).

**Table 15.** Pd-catalyst and ligand screening.

Entry	Catalyst	Ligand	Yield (%) <sup>a</sup>
1	Pd(OAc) <sub>2</sub>	X-Phos	51
2	Pd <sub>2</sub> dba <sub>3</sub>	X-Phos	24
3	Pd(PPh <sub>3</sub> ) <sub>4</sub>	-	traces <sup>b</sup>
4	Pd(OAc) <sub>2</sub>	dppb	-
5	Pd(OAc) <sub>2</sub>	Sphos	-
6	Pd(OAc) <sub>2</sub>	PCy <sub>3</sub>	10

<sup>a</sup> All yields are those of isolated products. <sup>b</sup> No isolated.

**Figure 21.** Structures of the phosphine ligands for the Pd-catalyzed ring-opening reaction.

From the results listed in Table 15, it was clear that there was no increment in the yield, on the contrary decrement (entries 2-3, 6) or no product formation was observed (entries 4-5). The same outcome was obtained when the catalyst and ligand loadings were decreased (Table 16), making it necessary to continue applying the first conditions (entry 1).

Orellana and Nithiy concluded after a base screening with a benzylcyclopropanol that Cs<sub>2</sub>CO<sub>3</sub> does not promote base-catalyzed ring-opening of the cyclopropanol to the corresponding ketone.<sup>[160]</sup> Based on these results, other alkali metal carbonates like K<sub>2</sub>CO<sub>3</sub> and Ag<sub>2</sub>CO<sub>3</sub> were compared (Table 17, entries 1-2) to Cs<sub>2</sub>CO<sub>3</sub> (entry 3). The use of Cs<sub>2</sub>CO<sub>3</sub> as the base for this transformation continued giving the best yield of the coupled product probably due to its larger alkali metal cation, which often provides big advantages in terms of obtainable yields or rates.<sup>[164]</sup>

**Table 16.** Variation of the catalyst and ligand loading.

Entry	Catalyst loading (mol %)	Ligand loading (mol %)	Yield (%) <sup>a</sup>
1	10	20	51
2	5	10	47
3	1	2	24

<sup>a</sup> All yields are those of isolated products.**Table 17.** Base variations.

Entry	Base	Yield (%) <sup>a</sup>
1	Ag <sub>2</sub> CO <sub>3</sub>	5
2	K <sub>2</sub> CO <sub>3</sub>	14
3	Cs <sub>2</sub> CO <sub>3</sub>	51

<sup>a</sup> All yields are those of isolated products.

The solvent is very important in this type of Pd-catalyzed cross-couplings, the stability of the catalyst can be affected by coordinating solvents competing with the ligand, plus the function of the base can be suppressed by a complementary functionality of the solvent.<sup>[165]</sup> Since the reaction medium must dissolve quite dissimilar substances including the Cs<sub>2</sub>CO<sub>3</sub> and it can significantly affect basicity via solubility and coordination, the obvious choice of solvent for this transformation is a dipolar aprotic solvent. Thus, solvent screening was carried out using solvents of varying polarities (Table 18). Compared to the first conditions (entry 1) the use of dioxane only increase to 58% yield (entry 2). The solvent mixture of dioxane with trifluoromethylbenzene (BTF) did not show variations (entry 3) while the use of *N*-Methyl-2-pyrrolidone (NMP) and DMF resulted in a decrement in the yield (entries 4-5).

**Table 18.** Influence of the solvent.

Entry	Solvent	Yield (%) <sup>a</sup>
1	Toluene:THF (1:1)	51
2	Dioxane	58
3	Dioxane:BTF (1:1)	58
4	NMP	27
5	DMF	20

<sup>a</sup> All yields are those of isolated products.

At this point, dioxane gave the best result with a 58% yield of coupled product. Lower yields obtained when using NMP and DMF could indicate their amide group coordinates with the catalyst affecting the reaction effectivity.<sup>[166]</sup> Hence, the increment of yield when using dioxane could be attributed to its ability to increase the solubility of the base and not to possible interactions with the catalyst that stabilize the transition state. The solubility of the base and substrates can help to improve the catalytic activity and the polarity of dioxane may be contributing to this.

**Table 19.** Screening of reaction stoichiometry and concentration.

Entry	Equiv. of 221	Equiv. of 252a	Concentration of 252a (M)	Yield (%) <sup>a</sup>
1	1.5	1.0	0.10	86
2	1.0	2.0	0.10 <sup>b</sup>	70
3	1.5	1.0	0.08	65
4	1.5	1.0	0.15	73

<sup>a</sup> All yields are those of isolated products. <sup>b</sup> Concentration of **221**.

Additional variations in the stoichiometry and concentration were conducted to the best conditions for this cross-coupling reaction. Increasing the equivalent of cyclopropanol to 1.5 while keeping the concentration at 0.10 M resulted in an 86% yield of the corresponding  $\gamma$ -arylated ketone (Table 19). Finally, variations in the temperature only led to a decrement in the yield (Table 20).

**Table 20.** Temperature variations.

Entry	Temperature (°C)	Yield (%) <sup>a</sup>
1	80	86
2	100	16
3	60	34

<sup>a</sup> All yields are those of isolated products.

**Table 21.** Evaluation of benzyl derivatives.

Entry	R	Time (h)	Yield (%) <sup>a</sup>
1	Cl	0.5	86
2	Br	2.0	63
3	OTs	2.0	48

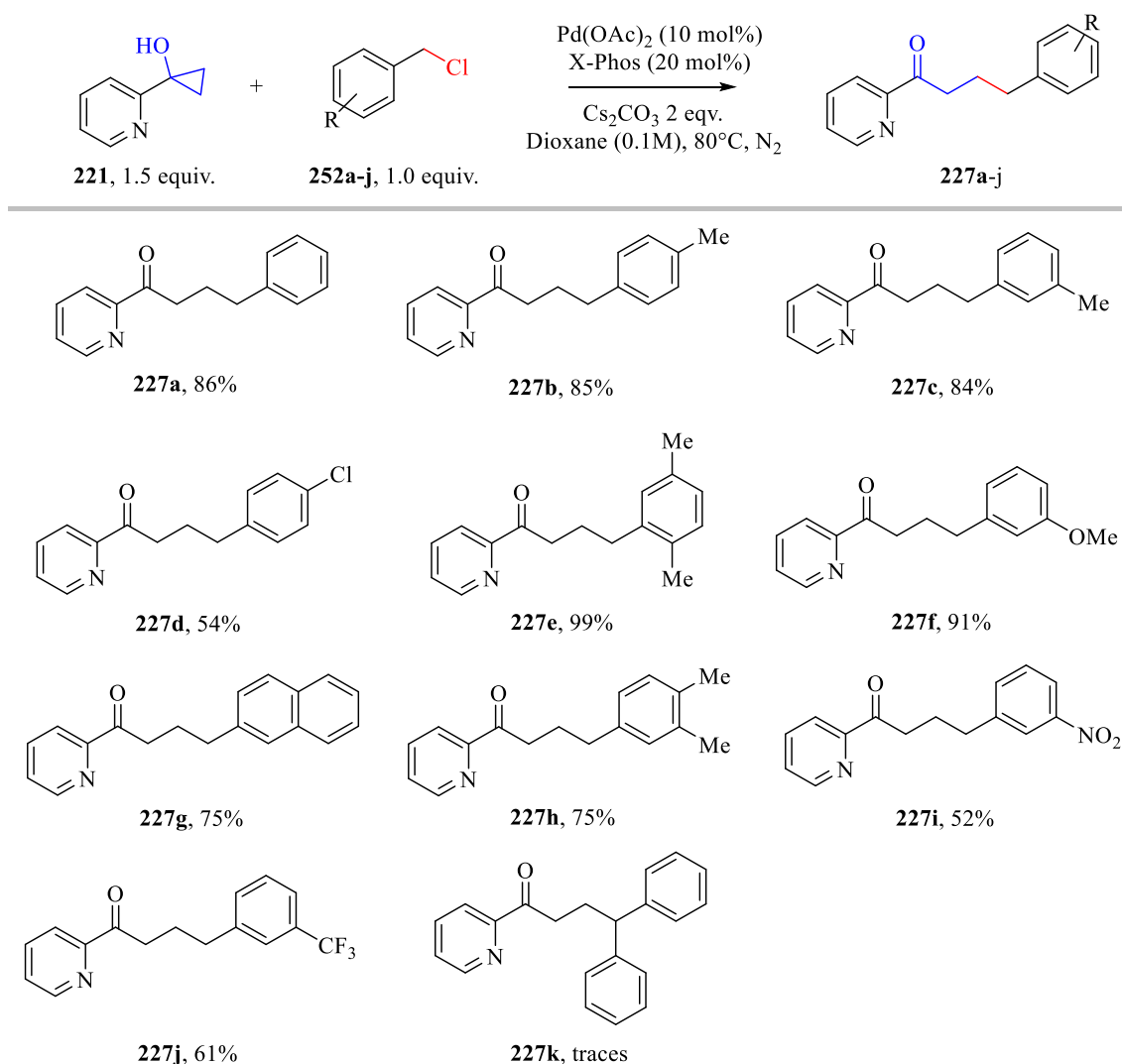
<sup>a</sup> All yields are those of isolated products.

The effect of the halide was evaluated by using benzyl bromide (Table 21, entry 2) instead of benzyl chloride and decomposition of the catalyst was noted since the reaction mixture turned black within 20 min. This color was not observed when using benzyl tosylate (entry



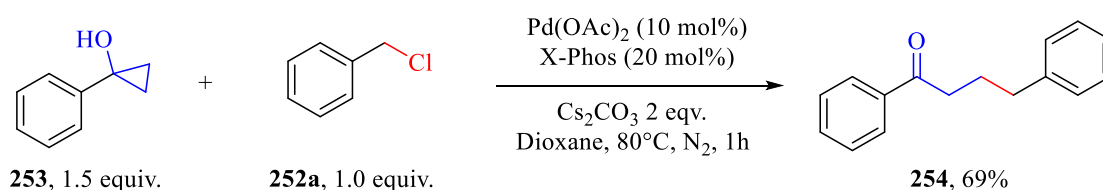
3), but in this case, the cross-coupled product was obtained with a lower yield and in longer times.

Under these optimized conditions, other benzyl chloride derivatives were studied to evaluate the scope of the benzyl component and the results are shown in Scheme 49. The results disclosed that all *ortho*-substituted, *meta* substituted and *para*-substituted benzyl chlorides were suitable substrates and afforded the corresponding products in moderate to good yields. The best yields were observed when using substrates bearing electron-donating groups while moderate yields were obtained when substrates bearing electron-deficient groups were used. Additionally, the  $\alpha$ -substituted benzyl chloride (chloromethylene)dibenzene gave only traces of the corresponding  $\gamma$ -arylated ketone **227j**.

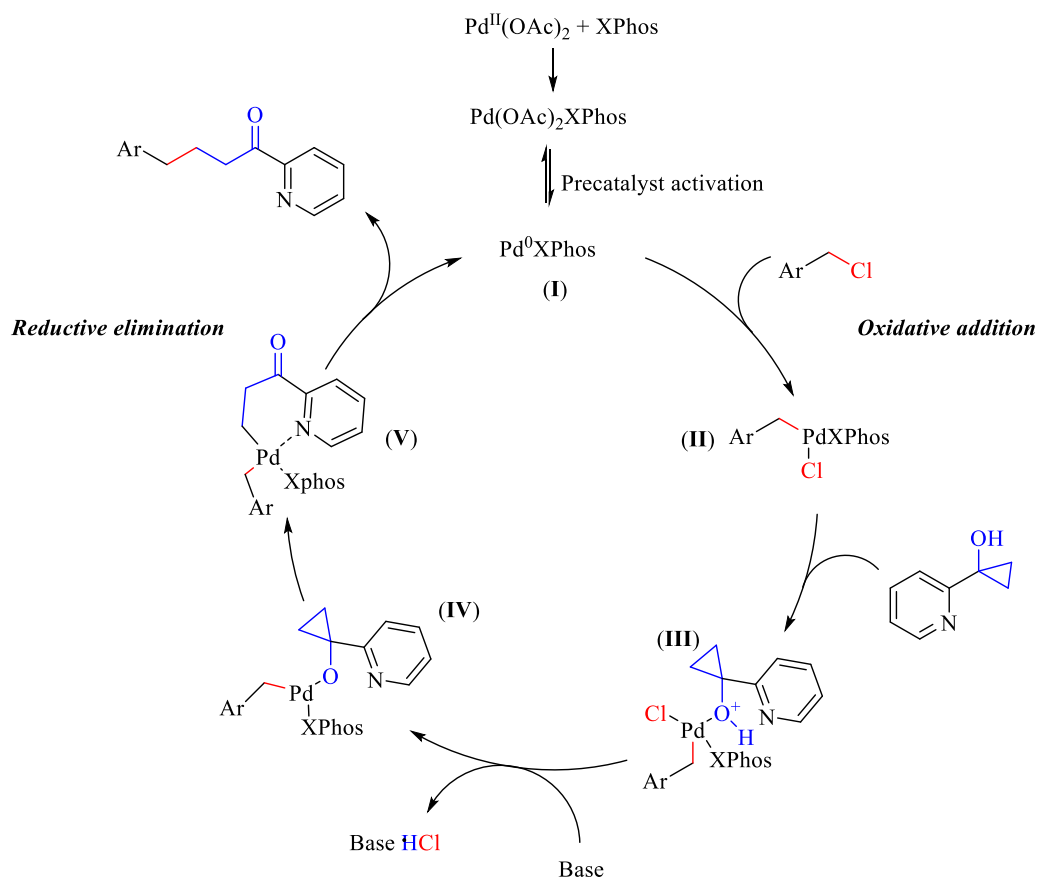


**Scheme 49.** Benzyl chloride scope in the Pd-catalyzed cross-coupling reaction under standardized conditions.

To evaluate the role of the nitrogen atom in the pyridine ring of the photogenerated cyclopropanol **221** on the cross-coupling reaction it was substituted by a carbon atom. For this purpose, cyclopropanol **253** was used under standardized conditions. In Scheme 50 can be seen that the coupled product was isolated with a lower yield (69%) than its counterpart with the nitrogen atom (86%) in a reaction time 30 minutes slower. This result lets to propose the possibility of the pyridine ring acting as a directing group having efficient N/Pd interactions with the catalyst.



**Scheme 50.** Isomorphous replacement for elucidation of the role of the nitrogen.



**Scheme 51.** Plausible catalytic cycle

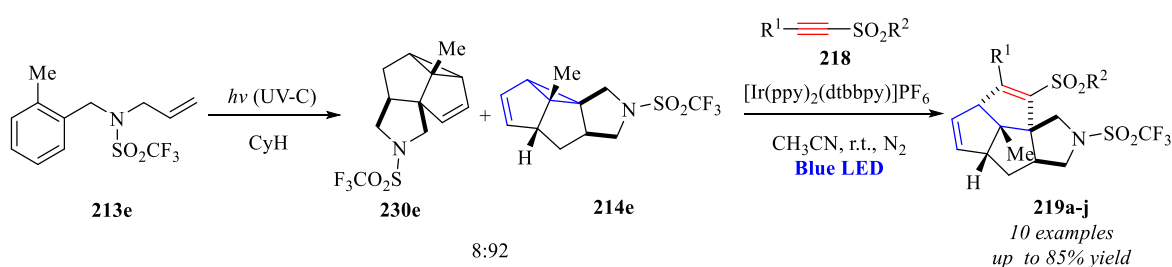
Finally, a proposed reaction pathway is depicted in scheme 51. Initially, the mixture of palladium acetate and the ligand XPhos reacts to form Pd(OAc)<sub>2</sub>XPhos which is then reduced under reaction conditions to a zero-valent Pd species **I**.<sup>[167]</sup> The catalytic cycle starts when this complex undergoes oxidative addition to the benzyl chloride to give a benzyl palladium(II) complex (**II**). Overall, the substitution of the alcohol functionality for the (pseudo) chloride simulates a “transmetalation” event which occurs in a two-step sequence that starts with the hydroxyl group binding followed by deprotonation. In the first step, the Pd(II) center acts as a Lewis acid to bind the alcohol functionality, forming OH-bound complex **III**, thereby acidifying the proton on the oxygen atom. In the second step, base-mediated elimination of HCl forms a Pd- $\pi$ -benzyl intermediate (**IV**), which via  $\beta$ -carbon elimination generates the homoenolate **V** that upon reductive elimination regenerates Pd(0)XPhos with the simultaneous release of the coupled product.

## 2.4. Summary and outlook

During the development of this work, it was possible to exploit the inherent ring strain in photogenerated strained ring systems as the driving force for strain-release subsequent reactions, allowing the facile construction of diversified structural scaffolds via integrating C–C catalytic activation and ring-scission. The methods developed show possibilities for the light-mediated as well as the metal-catalyzed synthesis of complex structures from readily available and stable starting materials and allow the use of mild reaction conditions due to the high ring strain of the intermediates. These developed synthetic sequences are summarized below.

### 2.4.1. *meta* photocycloadducts

In the first part of this dissertation, different *meta* photocycloadducts **214a-f** were prepared under UV irradiation following standardized conditions described in the literature. The use of the triflyl group as a protecting group in the benzylallylamine **213** led to isolating a mixture of linear and angular *meta* photocycloadducts with the best regioisomeric ratio compare with the other synthesized *meta* photocycloaddition products. The use of the *meta* photocycloadduct **214e** in a metal catalyst screening with different reaction partners showed in some of the cases the two usual possible vinylcyclopropane ring-opening pathways in this type of system, but when reacting with acetylenic sulfones under visible light catalysis a ring expansion through a [3+2] cycloaddition reaction was observed. Herein the vinylcyclopropane ring unit in the *meta* photocycloadduct **214e** acts as three-carbon synthon generating a new cyclopentene ring within the complex tetracycle **219** (Scheme 52).



**Scheme 52.** Consecutive UV/visible light activation sequence in the synthesis of the tetracycles **219a-j**.

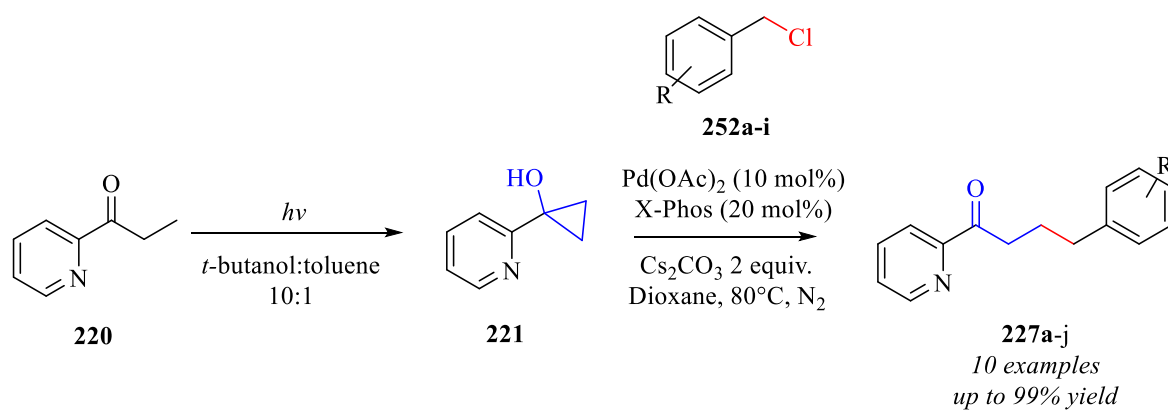
DFT calculations and time-resolved optical spectroscopy proved this reaction to proceed through an energy transfer pathway with the iridium complex acting as a triplet sensitizer. Additional experiments demonstrated that this strategy could be applicable to other VCP-type products showing the power of the consecutive UV/visible light activation sequence based on the generation of a strained intermediate and successive catalytic strain release. Thus, the focus of further research should be placed back on the extension of the substrate scope and evaluate the possibility of converting the resulting sulfonyl-containing cycloadducts into cycloadducts that are difficult to obtain via direct cycloaddition which was already proven to be possible in the present work through the selective reductive desulfonylation of the tetracycle **219a**. Processes based on C–C activation of unactivated vinylcyclopropanes are still rare and the development of this new visible light-induced transformation represents an important contribution to the field of photochemistry.

### 2.4.1. Photogenerated cyclopropanols

The second part of this work involved the preparation of the photogenerated cyclopropanol **221** following the standardized conditions in Agosta's work. Upon irradiation (UV-B) the 2-acylpyridine **220** through an intramolecular hydrogen abstraction that occurs from the C-4 of the side chain by the <sup>3</sup>N in the aromatic ring followed by the photochemical ring-closing transformation generates the cyclopropanol **221**. The subsequent metal catalyst screening of this cyclopropanol with different reaction partners revealed that the most efficient catalyst was Pd(OAc)<sub>2</sub> showing effective cross-coupling reactions with different substrates. The best result was observed when using the benzyl chloride under the standardized conditions in Orellana and Nithiy's work leading to the corresponding  $\gamma$ -arylated ketone **227** in moderate yields and therefore the reaction conditions were optimized (Scheme 53).

The isomorphous replacement of the nitrogen atom at the aromatic ring in the cyclopropanol for a carbon atom showed that the coupled product is generated in lower yield, suggesting that the pyridine ring could have some involvement as directing group via N/Pd interactions with the catalyst. The development and application of this consecutive UV/Pd-catalyzed activation sequence to acquire new pyridine derivatives using as substrate a photogenerated cyclopropanol represent an alternative to methodologies that commonly employ cyclopropanol derivatives prepared through the Kulinkovich cyclopropanation reaction. Therefore, further studies exploring new acylpyridine derivatives that upon direct irradiation

could get access to their corresponding photogenerated cyclopropanols would serve as a starting point in the identification of new catalyst systems and control strategies that exploit the aromatic ring containing the nitrogen atom as a directing group.



**Scheme 53.** Consecutive UV/Pd-catalyzed activation sequence in the synthesis of the  $\gamma$ -arylated ketone **227a-j**.

# 3. Three-component arylation and sulfonylation of styrene derivatives

## 3.2. Introduction

The radical difunctionalization of double bonds plays an important role in organic synthesis for the regioselective introduction of two different functional groups while generating new C–C or C–X bonds.<sup>[53]</sup> The initial carbon radicals are usually generated by metal-containing SET agents, under photoredox conditions or by employing peroxides. Among the alkenes used in this type of transformation, styrene derivatives have received a lot of attention because after a regioselective addition of initial radicals they can form stabilized benzylic radicals which can be readily oxidized to benzylic cations that can easily undergo nucleophilic additions. This method allows functionalizing olefins with a wide variety of reagents in a selective manner since radicals and nucleophiles generally react complementarily.

As described in section 1.1.3, photoredox catalysis has emerged as a strong synthetic tool to develop many elusive radical-mediated chemical transformations and this activation mode in many cases can provide a promising approach for the development of radical multicomponent reactions. Merging the concept and features of multicomponent reactions and photoredox catalysis represent a useful strategy for difunctionalization of carbon-carbon multiple bonds. Moreover, the appropriate design of the electrophilic radical precursor and choice of the nucleophile has been proved to enable a regiocontrolled three-component reaction.<sup>[168]</sup> Photocatalyzed multicomponent reactions are commonly initiated by the oxidative or reductive formation of radicals which can add to an olefin. The resulting radical can be oxidized to a cation in a radical-polar crossover (RPC) or reduced to an anion, and the latter can be trapped in different ways.<sup>[169]</sup> Apart from that, the reaction can be finished at the radical level by HAT,<sup>[15, 170]</sup> addition to a heteroarene,<sup>[171]</sup> or elimination of a leaving group.<sup>[172]</sup> A less common variant, specifically for scavenging benzylic radicals, is a radical-radical heterocoupling with a second radical species.<sup>[173]</sup> This scavenging method permanently competes with the oxidation or reduction of the radical. Dimerization and polymerization can also occur, making this strategy much more complex than that of RPC.

### 3.3. Aim of the research

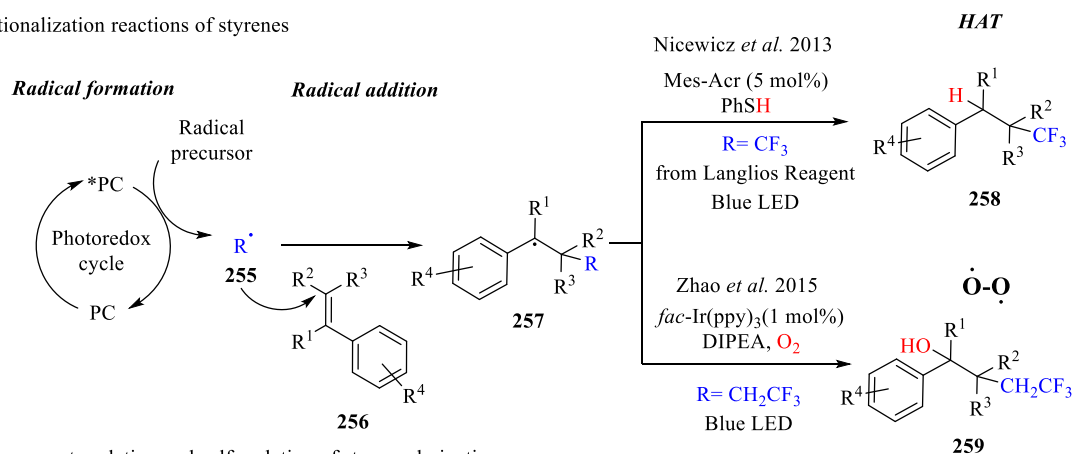
At the beginning of the development of the designed method, there were only known examples of visible light-induced photoredox difunctionalization reactions of styrenes involving radical trapping via a HAT,<sup>[174]</sup> and the addition of oxygen to benzylic radicals<sup>[175]</sup> (scheme 54a). These reports started the idea to expand the repertoire of difunctionalizations of styrene derivatives through radical-radical coupling, using the stabilization of benzylic radicals to trap them with another persistent radical like those generated by 4-cyanopyridine (4-CP) after reduction,<sup>[176]</sup> which does not dimerize due to its electrostatic repulsion<sup>[177]</sup> (Scheme 54b). Atom efficiency of the individual reactions was also the focus of method development. For this purpose, the strategy of multicomponent reactions<sup>[178]</sup> to build up complex structures in a one-pot process is used. This enables the rapid construction of highly functionalized products, with a reduced number of work-up steps as well as solvent and reagent waste compared to multistep syntheses, enabling in most cases a more resource-efficient process.<sup>[179]</sup>

Shortly before the publication of the present work,<sup>[180]</sup> the group of Lingling Chu reported a branch-selective pyridylation of alkenes via a sulfinate assisted photoredox catalysis. Chu used *fac*-Ir(ppy)<sub>3</sub> to oxidize sodium methanesulfinate forming a sulfonyl radical that undergoes radical addition to the alkene to generate the nucleophilic benzylic radical. The subsequent radical-radical anion coupling with the persistent pyridyl radical anion generated after a single-electron reduction of the 4-cyanopyridine **261** furnishes an alkyl sulfone intermediate (**264**) that undergoes sulfinic acid elimination assisted by the base, furnishing the final branched alkenylpyridine product **265** (Scheme 54c).<sup>[181]</sup> A more recent publication from the same group disclosed a similar transformation to the reported in this dissertation by implementing the photoinduced 9,10-diphenylanthracene (DPA)-mediated sulfonylative pyridylation of styrene derivatives with sulfonates and cyanopyridines (Scheme 54d).<sup>[182]</sup> This metal-free photoinduced method was reported as a complementary protocol to the conditions described in Scheme 54b.

The project described in this chapter was worked in a large team. Contributions by others are marked in the relevant places and, as usual, are not listed in the experimental section (Section 4.2.3).

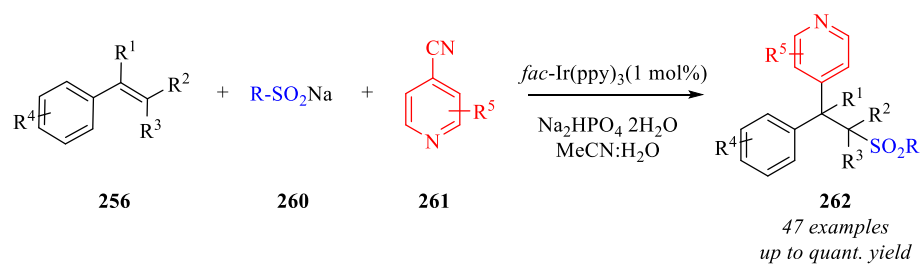
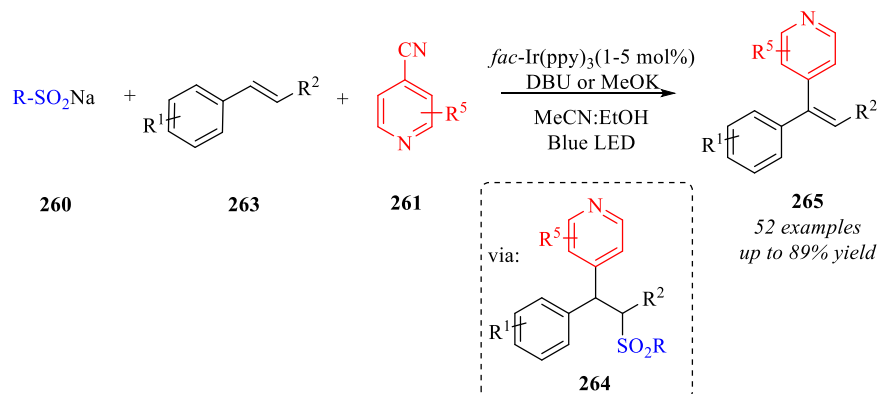
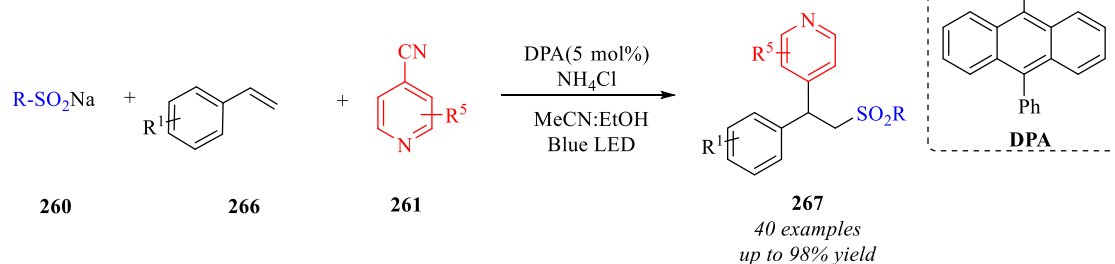


a) Difunctionalization reactions of styrenes



Three-component arylation and sulfonylation of styrene derivatives

b) This work, 2019

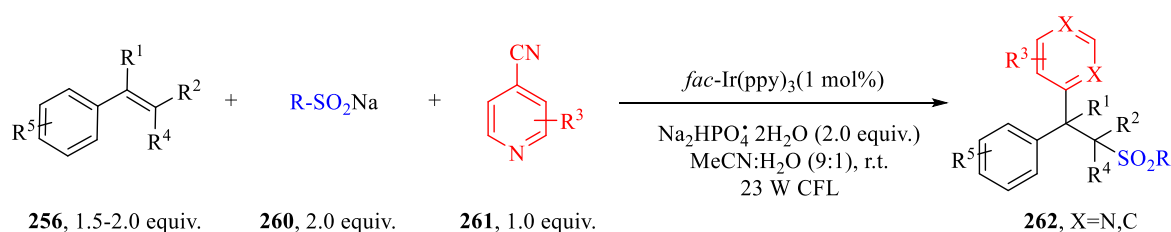

 d) Chu *et al.* 2019

 c) Chu *et al.* 2021


**Scheme 54.** a) Methodologies for the photoredox-catalyzed difunctionalization of styrene derivatives. b) Three-component arylation and sulfonylation of styrene derivatives. c) Radical-radical anion coupling that was reported shortly before the publication of the present work. d) Recent publication that is complementary to the present work.

## 3.4. Results and discussion

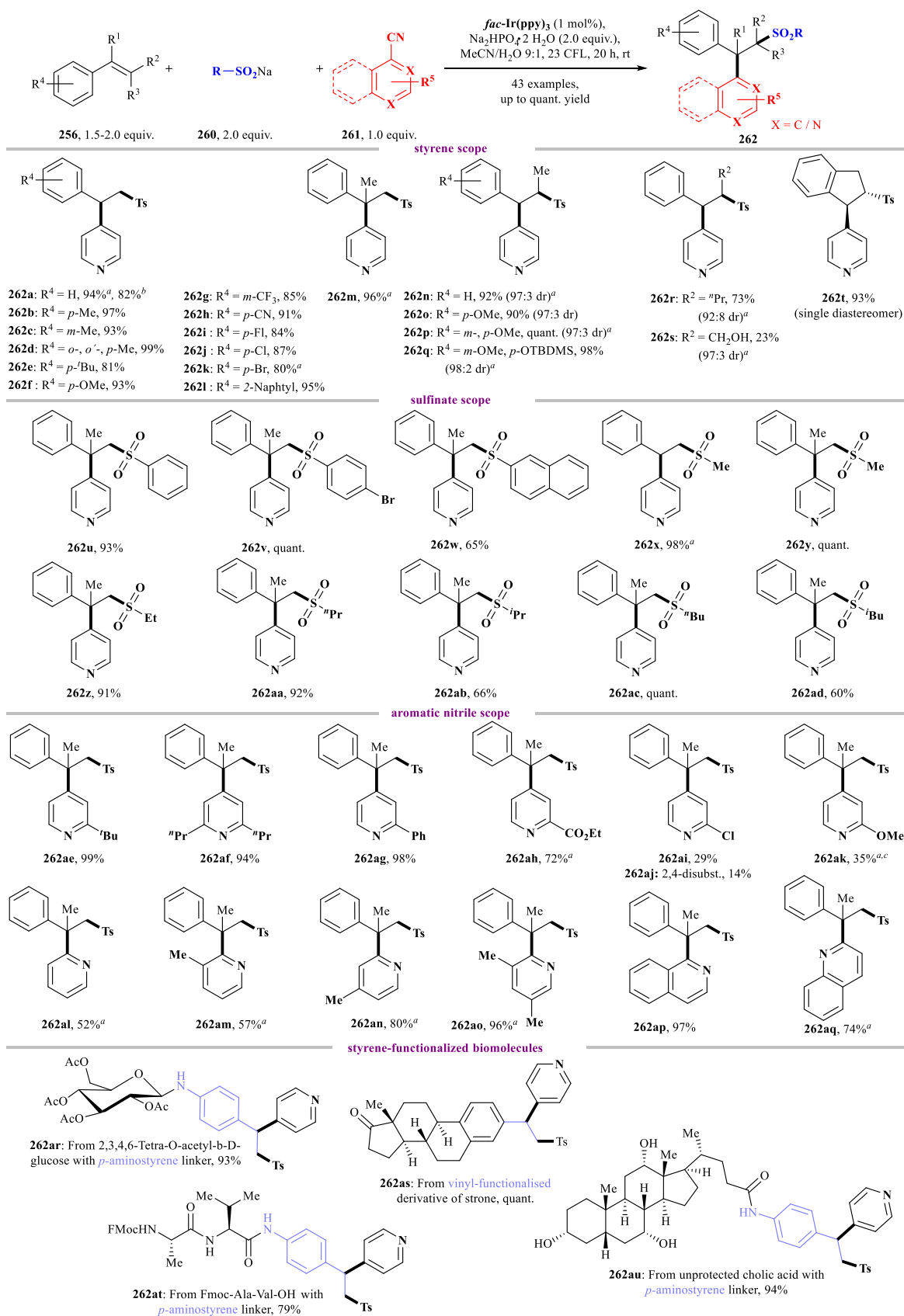
### 3.4.1. Optimization of reaction conditions

The development and optimization of the reaction conditions were performed by [REDACTED] [REDACTED]. The initial conditions of the target three-component reaction consisting of either phenanthrene (Phen, 50 mol%) or *fac*-Ir(ppy)<sub>3</sub> (2 mol%), sodium *p*-toluenesulfinate, styrene, 4-cyanopyridine led to the desired product in appreciable yields (61% and 63%, respectively). During the reaction optimization using these catalysts, better yields were obtained when using *fac*-Ir(ppy)<sub>3</sub> with the addition of sodium dihydrogen phosphate in an acetonitrile/water mixture than with phenanthrene. The reduction of the catalyst loading to 1 mol% increased the yield of the desired product to 94%. The optimized reaction conditions are summarized in Scheme 55.



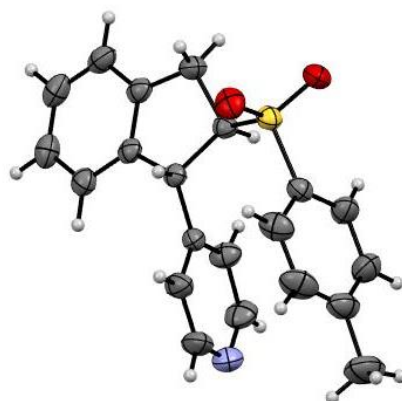
**Scheme 55.** Optimized conditions of the visible light-induced sulfonylation/arylation of styrenes.

After improving the reaction conditions for the preparation of **262**, the study of the substrate spectrum was carried out in cooperation with [REDACTED] (variation of the styrene component), [REDACTED] (variation of the styrene component), [REDACTED] (Variation of the nitrile component), and [REDACTED] (variation of the styrene component). The own contribution included the variation of the sulfinate component. For reasons of clarity, the entire substrate spectrum (Scheme 56) is shown and discussed. However, only the experiments carried out in this doctorate are listed in the experimental part.



**Scheme 56.** Substrate spectrum of the developed three-component arylation and sulfonylation of styrene derivatives. All yields are those of isolated products. <sup>a</sup> 2.0 equiv. styrene derivative, <sup>b</sup> starting from 1.5 g 4-CP, <sup>c</sup> Purification with prep. HPLC.

The reaction using styrene derivatives with electron-donating (**262b-f**) as well as electron-withdrawing groups (**262g-k**) could be functionalized in very high yields (80-99%) and be scaled up to gram scale (4.8 g of product **262a** from 1.5 g of 4-CP, 82% yield). The reaction also worked well using 2-vinylnaphthalene (**262l**, 95% yield), as well as with  $\alpha$ -methylstyrene,  $\beta$ -substituted styrene derivatives, and indene providing the desired products **262m-r** and **262t** in very high yields (73%-quant.). Only a hydroxymethyl group in the  $\beta$ -position had a negative effect (**262s**, 23% yield) which could be attributed to intramolecular hydrogen atom abstraction in the intermediate benzylic radical. Surprisingly, the products **262n-t** were formed with exceptional diastereoselectivity (dr  $\geq$  92:8). All diastereomeric ratios were determined from the crude products after extractive work-up and based on integrals of characteristic  $^1\text{H}$  NMR signals. To understand better the nature of this diastereoselectivity, DFT calculations and comparison with the experimental NMR data (DP4+probability) were performed to determine the relative configurations of the major diastereomers of products **262n-p** and **262r-t**. (For technical details refer to the publication).<sup>[180]</sup> This data agrees with the relative configuration of the diastereomer **262t** which was determined as (*S*)-(*S*)/(*R*)-(*R*) based on X-ray crystallography (Figure 22). A possible explanation for the observed diastereoselectivity is discussed in the next section.



**Figure 22.** Molecular structure of compound **262t** in the solid-state (ORTEP, thermal ellipsoids at 50% probability, C: black, H: gray, N: blue, O: red, S: yellow). CCDC Number:1891336.

The developed styrene functionalization reaction also allows significant variations regarding the sulfinate. Various aryl and alkyl sulfonates gave the products **262u-ad** in good yields (60%-quant.). While a bromide substituent gave a very good yield (**262v**, quant.), expanding

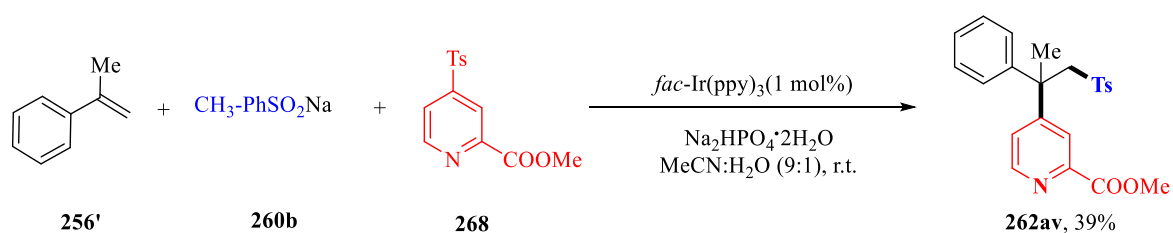
the aromatic system of the sulfinate had a negative impact on the reaction outcome (**262w**, 65%), possibly due to increased steric hindrance or electronic stabilization of the sulfonyl radical generated during the photocatalytic cycle. Alkyl sulfonates are also amenable to standardized conditions and the corresponding products (**262x-ad**) could be obtained in good to excellent yields (60%–quant.). However, linear alkyl sulfonates (**262x-y**) proved far better than their branched isomers (**262aa-ad**).

Next, the substrate spectrum of cyanopyridines was examined. Common alkyl and phenyl substituents in the heteroaromatic ring are tolerated without any problems (**262ae-ag**, 94-99%), as well as an electron-withdrawing ester group in the 2-position (**265ah**, 72%). The high yields are due to the *ipso* substitution of the nitriles performing particularly well when the spin density at the ipso carbon of the 4-CP radical anion (or its protonated form, since the work is carried out in an aqueous solution) is higher than other positions.<sup>[183]</sup> Dr. Stefan Pusch performed DFT calculations that showed that this applies to 4-cyanopyridine.<sup>[180]</sup> At the same time, Dr. Pusch shows that the radical anion of 2-cyanopyridine has high spin densities at the *ipso*-carbon as well as at positions 4 (protonated form) and 5 (radical anion), which explains the comparatively low yield of **262al** (52%). Blocking these also activated positions 4 and 5 with methyl groups (**262an-ao**) increased the yield to 80% and 96%, respectively. Electron-donating substituents such as methoxy on cyanopyridine can only be converted with low yields (**262ak**, 35%). This could be attributed to the more difficult reduction of the radical anion due to the increased electron density on the aromatic ring and the resulting lower stability of this species. In the case of 2-chloro-4-cyanopyridine, the disubstituted product **262aj** was isolated in a 14% yield. Since the reduction potential of the excited iridium catalyst ( $E_{1/2}(\text{Ir}^{\text{IV}}/\text{Ir}^{\text{III}*}) = -1.73 \text{ V vs. SCE}$ )<sup>[15a]</sup> is not sufficient to donate an electron to 2-chloropyridine ( $-2.38 \text{ V vs. SCE in DMF}$ )<sup>[184]</sup>, therefore it can be assumed that the double alkylation was initiated by another *ipso* substitution. The introduction of a benzyl group in the  $\alpha$ -position to the nitrogen in heteroaromatics is usually problematic in classic Minisci reactions.<sup>[185]</sup> The use of the developed multicomponent protocol proved to solve this matter when using 1-cyanoisoquinoline and 2-cyanoquinoline furnishing Minisci-like products **262ap** and **262aq** in 97% and 74% yields, respectively. Based on these results, the designed reaction probably will be useful to access papaverine-like structures containing a sulfone moiety.

The developed method was also applied to modify styrene-functionalized biomolecules. A corresponding peptide **262at** and carbohydrate **262ar** as well as the two steroid derivatives

**262as** and **262au** were obtained in very high yields (79%–quant.). This demonstrates the broad applicability of the reported multicomponent strategy to functionalize even very complex targets under particularly mild conditions.

A variation of the nitrile group for a tosyl group in the substrate **268** led to the corresponding product **262av** under the standardized conditions, but the yield (39%) was not as good as its equivalent **262ah** (72%) (Scheme 57). This shows that the best reaction partner for this type of photoredox transformation is the 4-CP.



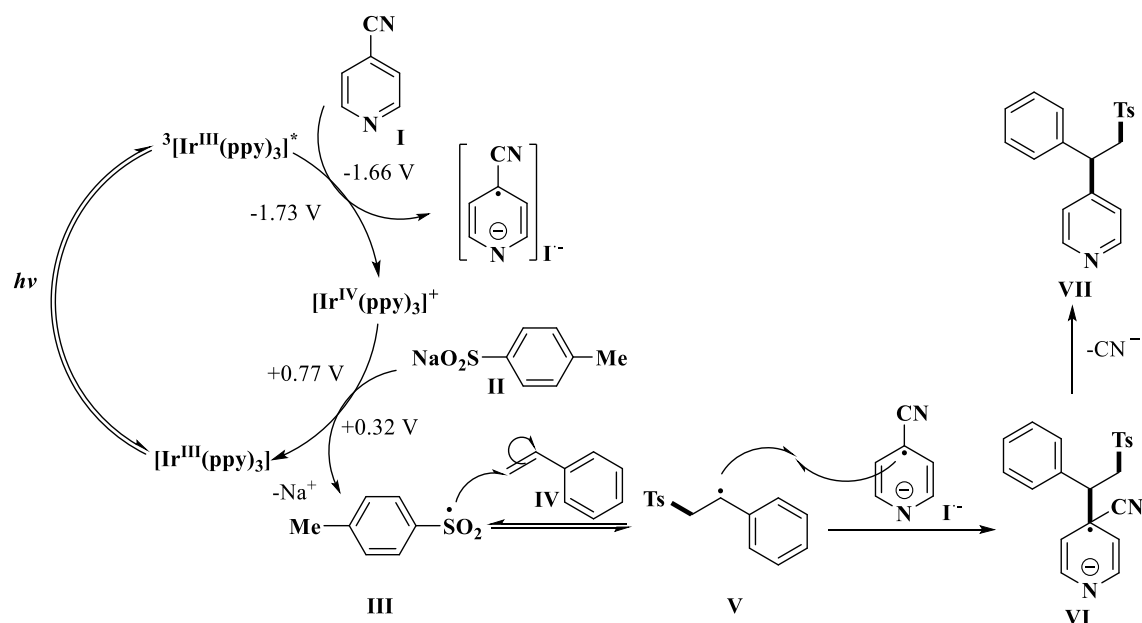
**Scheme 57.** Variation of the leaving group in the heteroaromatic ring of the substrate in the multicomponent protocol.

### 3.4.2. Mechanistic Considerations

The mechanistic investigations described in this subchapter were carried out in cooperation with [REDACTED] and [REDACTED].

#### *Postulated mechanism:*

A plausible mechanism for the developed multicomponent protocol is summarized in Scheme 58. Upon absorption of visible light,  $\text{fac-Ir(ppy)}_3$  is electronically excited and reaches a long-lived (ca. 1.9  $\mu\text{s}$ , degassed acetonitrile, room temperature)  $^3\text{MLCT}$  state.<sup>[186]</sup> It is oxidatively quenched by the aromatic nitrile **I** and, during its regeneration, mediates the oxidation of the sulfinate **II**. The resulting sulfonyl radical **III** attacks the styrenic double bond to form the benzylic radical **V**. The latter combined with the radical anion of the nitrile formed during the quenching process  $\text{I}^{\cdot-}$  to afford the intermediate **VI**.<sup>[176a, 188]</sup> Rearomatization by cyanide elimination affords the desired product **VII**.<sup>[176a]</sup> The SET steps for generating the radical species  $\text{I}^{\cdot-}$  and **III** and subsequent mechanistic steps are discussed separately.



**Scheme 58.** Plausible mechanism pathway for the developed styrene-difunctionalization.

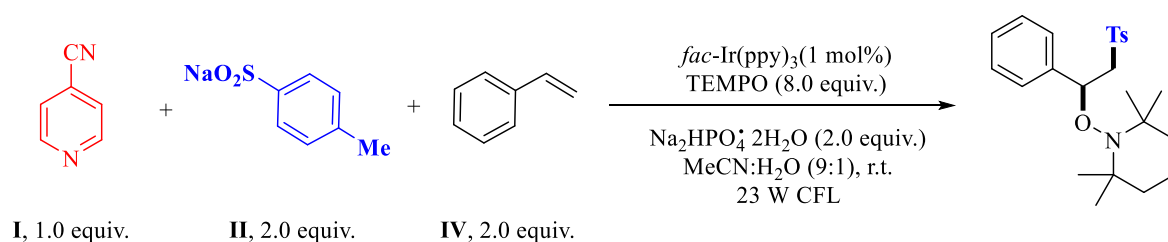
Table 22 summarizes control experiments relating to the reaction shown in Scheme 58, which are referred to as appropriate points in the mechanistic discussion.

**Table 22.** Control experiments.

entry	conditions	yield (%) <sup>a</sup>
1	optimized	94
2	in the dark	0
3	no <i>fac</i> -Ir(ppy) <sub>3</sub>	0
4	no water, no Na <sub>2</sub> HPO <sub>4</sub> <sup>b</sup>	0
5	no Na <sub>2</sub> HPO <sub>4</sub>	63

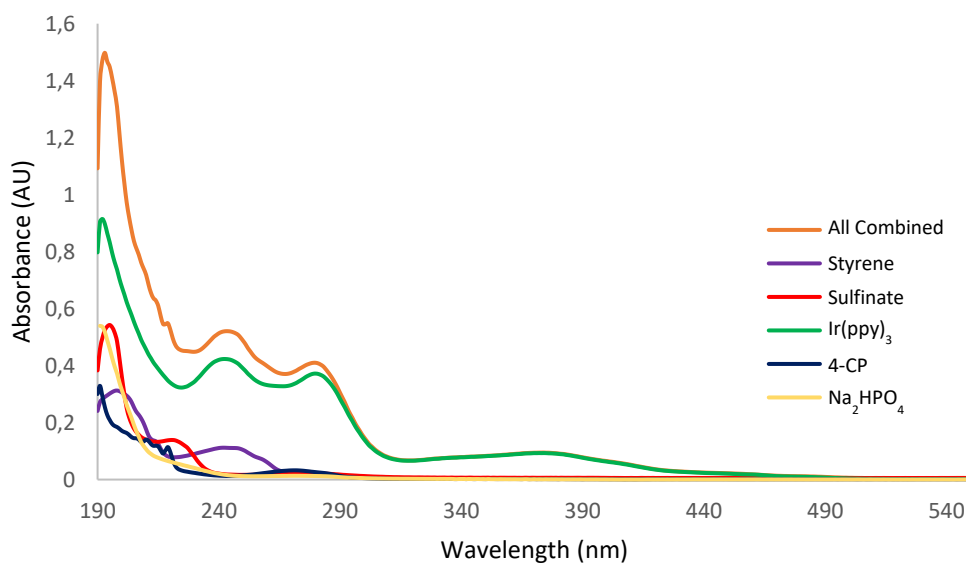
The reactions were performed according to the general procedure for screening reactions using 4-cyanopyridine (**I**, 15.6 mg, 0.15 mmol, 1.00 equiv.), sodium *p*-toluenesulfonate (**II**, 53.5 mg, 0.30 mmol, 2.00 equiv.), styrene (**IV**, 34.3  $\mu$ L, 31.2 mg, 0.30 mmol, 2.00 equiv.), *fac*-Ir(ppy)<sub>3</sub> (982  $\mu$ g, 1.5  $\mu$ mol, 0.01 equiv.) and 8 mL of solvent (20 mM). <sup>a</sup> All yields are those of isolated products. <sup>b</sup> The reaction in pure acetonitrile was performed in the absence of Na<sub>2</sub>HPO<sub>4</sub> to ensure that the result is independent of the then reduced solubility of this additive.

The control experiments confirm that the difunctionalization of the styrene discussed here is completely light-induced and catalyst-dependent (entries 2 and 3 in Table 22). The addition of TEMPO completely inhibited the three-component reaction (Scheme 59). No product was formed, instead, the intermediate benzylic radicals were trapped by TEMPO and the corresponding adduct was detected by HRMS. This control experiment is an indication that a radical mechanism is present.



**Scheme 59.** Three-component reaction under standardized conditions in presence of TEMPO.

Absorption spectra of all reaction components and a combination of them in a 9:1 mixture of acetonitrile and water are shown in Figure 23. The absence of new absorption maxima or wavelength-shift suggests that no charge-transfer complexes occur as absorbing species.

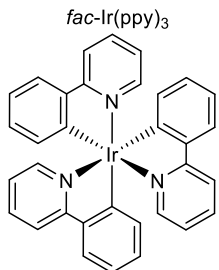
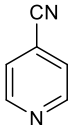
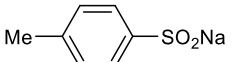
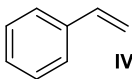
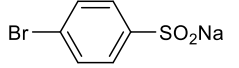
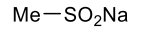


**Figure 23.** Absorption spectra of all substrates from the model reaction and their mixture. Measurements were taken in a MeCN/water mixture (9:1) at a concentration of  $1 \times 10^{-5}$  M.



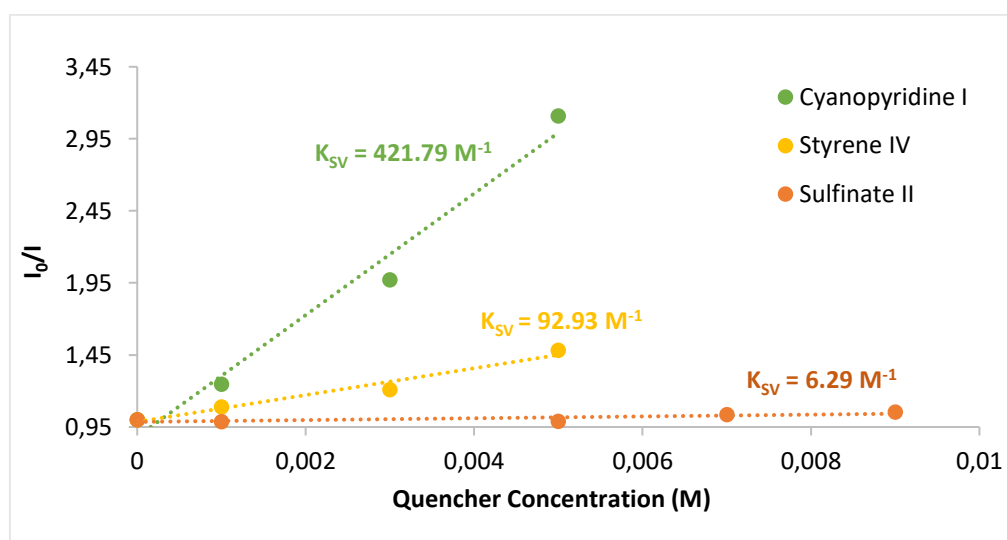
The emission spectrum of the household lamp used for all exposures in this chapter is given in Figure 29 (Experimental section). From this, it can be inferred that the reaction solutions are exposed to intense radiation with wavelengths longer than about 400 nm. As shown in Figure 23, this light can only be absorbed by the iridium catalyst which initiates the difunctionalization reaction through its <sup>3</sup>MLCT excited state.<sup>[187]</sup>

**Table 23.** Redox potentials<sup>[189]</sup> and Gibbs free energies for relevant SET steps between the reaction components.

<div style="display: flex; justify-content: space-around; align-items: flex-start;"> <div style="text-align: center;">  <p><i>fac</i>-Ir(ppy)<sub>3</sub></p> <p><math>E_{1/2}([\text{Ir}^{\text{IV}}(\text{ppy})_3]^+ / ^3[\text{Ir}^{\text{III}}(\text{ppy})_3]^*) = -1.73 \text{ V vs SCE}</math>  <math>E_{1/2}([\text{Ir}^{\text{IV}}(\text{ppy})_3]^+ / [\text{Ir}^{\text{III}}(\text{ppy})_3]) = +0.77 \text{ V vs SCE}</math>  <math>E_{1/2}(^3[\text{Ir}^{\text{III}}(\text{ppy})_3]^* / [\text{Ir}^{\text{II}}(\text{ppy})_3]) = +0.31 \text{ V vs SCE}</math>  <math>E_{1/2}([\text{Ir}^{\text{III}}(\text{ppy})_3] / [\text{Ir}^{\text{I}}(\text{ppy})_3]) = -2.19 \text{ V vs SCE}</math></p> </div> <div style="text-align: center;">  <p><b>I</b></p> <p><math>E_{1/2}(\text{II}^{\bullet-} / \text{I}) = -1.66 \text{ V vs SCE}</math></p> </div> <div style="text-align: center;">  <p><b>II</b></p> <p><math>E_{1/2}(\text{II}^{\bullet+} / \text{II}) = +0.32 \text{ V vs SCE}</math></p> </div> </div> <div style="display: flex; justify-content: space-around; align-items: flex-start; margin-top: 10px;"> <div style="text-align: center;">  <p><b>IV</b></p> <p><math>E_{1/2}(\text{IV}^{\bullet+} / \text{IV}) = +1.97 \text{ V vs SCE}</math>  <math>E_{1/2}(\text{IV} / \text{IV}^{\bullet-}) = -2.64 \text{ V vs SCE}</math></p> </div> <div style="text-align: center;">  <p><b>VIII</b></p> <p><math>E_{1/2}(\text{VIII}^{\bullet+} / \text{VIII}) = +0.54 \text{ V vs SCE}</math></p> </div> <div style="text-align: center;">  <p><b>IX</b></p> <p><math>E_{1/2}(\text{IX}^{\bullet+} / \text{IX}) = +0.46 \text{ V vs SCE}</math></p> </div> </div>				
entry	electron acceptor	electron donor	Gibbs free energy (kcal/mol)	comment
1	<b>I</b>	<sup>3</sup> [ <i>fac</i> -Ir <sup>III</sup> (ppy) <sub>3</sub> ] <sup>*</sup>	-1.61	oxidative quenching
2	<b>IV</b>	<sup>3</sup> [ <i>fac</i> -Ir <sup>III</sup> (ppy) <sub>3</sub> ] <sup>*</sup>	+20.99	oxidative quenching
3	<sup>3</sup> [ <i>fac</i> -Ir <sup>III</sup> (ppy) <sub>3</sub> ] <sup>*</sup>	<b>II</b> <sup>-</sup>	+0.23	
4	<sup>3</sup> [ <i>fac</i> -Ir <sup>III</sup> (ppy) <sub>3</sub> ] <sup>*</sup>	<b>VIII</b> <sup>-</sup>	+5.30	reductive quenching
5	<sup>3</sup> [ <i>fac</i> -Ir <sup>III</sup> (ppy) <sub>3</sub> ] <sup>*</sup>	<b>IX</b> <sup>-</sup>	+3.46	reductive quenching
6	<sup>3</sup> [ <i>fac</i> -Ir <sup>III</sup> (ppy) <sub>3</sub> ] <sup>*</sup>	<b>IV</b>	+38.28	
7	[ <i>fac</i> -Ir <sup>IV</sup> (ppy) <sub>3</sub> ] <sup>+</sup>	<b>II</b> <sup>-</sup>	-10.38	
8	[ <i>fac</i> -Ir <sup>IV</sup> (ppy) <sub>3</sub> ] <sup>+</sup>	<b>VIII</b> <sup>-</sup>	-5.30	SET steps following oxid. quenching
9	[ <i>fac</i> -Ir <sup>IV</sup> (ppy) <sub>3</sub> ] <sup>+</sup>	<b>IX</b> <sup>-</sup>	-7.15	
10	[ <i>fac</i> -Ir <sup>IV</sup> (ppy) <sub>3</sub> ] <sup>+</sup>	<b>IV</b>	+27.67	
11	<b>I</b>	[ <i>fac</i> -Ir <sup>II</sup> (ppy) <sub>3</sub> ] <sup>-</sup>	-12.22	SET steps following red. quenching
12	<b>IV</b>	[ <i>fac</i> -Ir <sup>II</sup> (ppy) <sub>3</sub> ] <sup>-</sup>	+10.38	

In the proposed mechanism, an oxidative quenching cycle was suggested (Scheme 58). However, there could also be the possibility of reductive quenching by the sulfinate.<sup>[187]</sup> To

further investigate the events leading to radical formation, the thermodynamic feasibility of all reasonable SET events was evaluated by calculating the Gibbs free energies of the possible single SET steps. For this purpose, the redox potentials of the iridium catalyst, 4-CP, and styrene, as well as exemplary sodium sulfinates **II**, **VIII**, and **IX** are listed in Table 23. Additionally, the Gibbs free energies that were calculated as described in section 1.1.1 (equations 1.7-1.8) are also listed. From them, it can be inferred that the oxidative quenching of the  $^3\text{MLCT}$  state of the catalyst by 4-CP should be exergonic (entry 1). All other realistic quenching processes are likely to be thermodynamically unfavorable (entries 2–6). In the case of styrene **IV**, the approximate free energies are sufficiently large to rule out the quenching of this olefin with a high degree of probability (entries 2 and 6), which does not apply to sulfinates **II**, **VIII**, and **IX** (entries 3–5). Furthermore, it has been repeatedly confirmed in practice that even such weakly endergonic SET steps can proceed and be directly involved in product formation.<sup>[190]</sup> Based on this thermodynamic consideration, it cannot be ruled out that the sulfinates are involved in product formation as reductive quenchers.



**Figure 24.** Stern–Volmer plots for luminescence quenching of *fac*-Ir(ppy)<sub>3</sub> ( $1 \cdot 10^{-6}$  M) by 4-cyanopyridine (**I**), styrene (**IV**), and sodium *p*-toluenesulfinate (**II**). Measurements were taken in a degassed MeCN/water mixture (9:1). Excitation wavelength: 372 nm, emission wavelength (536 nm). The respective Stern-Volmer constants ( $K_{SV}$ ) are given.

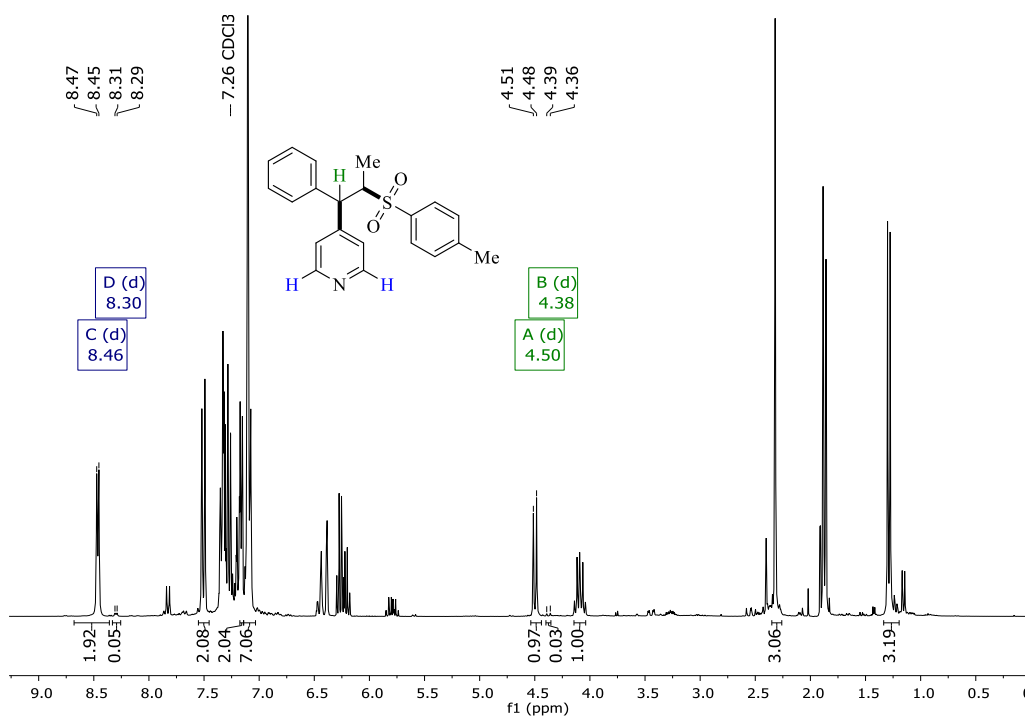
To confirm the above, luminescence quenching studies were performed with *fac*-Ir(ppy)<sub>3</sub>, 4-CP, styrene, and sodium *p*-toluenesulfinate. The Stern-Volmer plots (Figure 24) show that the luminescence of the iridium catalyst is very efficiently quenched by the aromatic nitrile

(I). Therefore, an oxidatively quenched catalytic cycle can be assumed in agreement with the results from Table 23 (entry 1). Reductive quenching by the sulfinate (II), if it occurs at all, is much less efficient and therefore not significantly involved in product formation. In terms of amount, sodium *p*-toluenesulfinate shows the lowest oxidation potential of the sulfonates, so it seems unlikely that other sulfonates are more efficient quenchers.<sup>[189b]</sup>

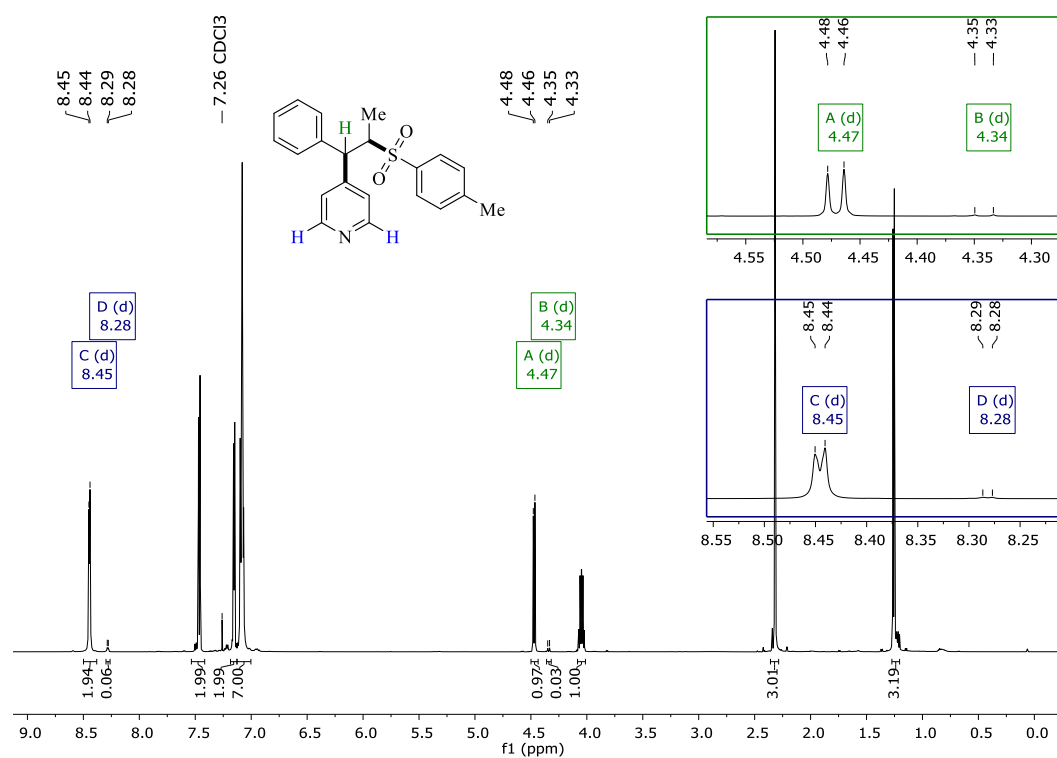
From Figure 24 it can be seen that styrene also quenches the excited catalyst, but less efficiently than 4-CP. In view of the redox potentials from Table 23 (entries 2 and 6), reductive or oxidative quenching by styrene is not possible. This type of quenching, therefore, is not via electron transfer, but much more likely triplet through energy transfer.<sup>[50a]</sup>

### Epimerization studies

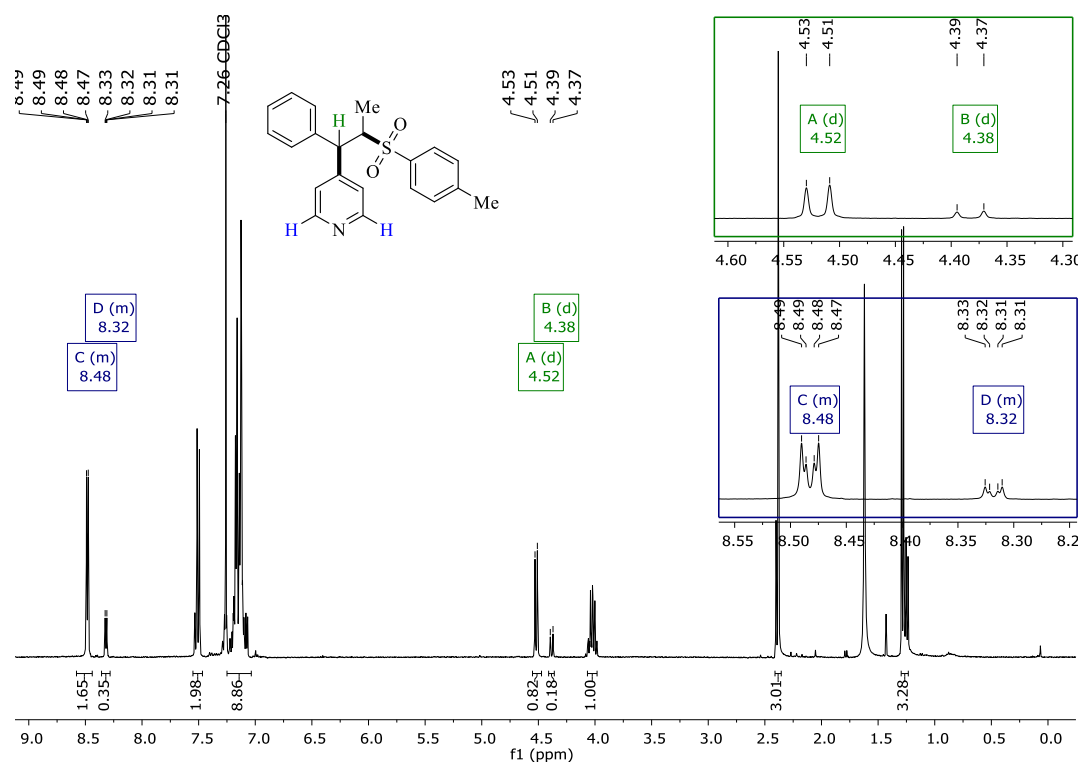
As previously mentioned, the developed three-component reaction simultaneously constructs two neighboring stereocenters when performed with  $\beta$ -substituted styrene derivatives. The difunctionalized products **262n-t** were obtained with high diastereoselectivity ( $dr \geq 92:8$  in all cases). Exemplarily, figure 25 displays the <sup>1</sup>H NMR spectrum obtained from the crude of the product **262n** prior to chromatographic purification.



**Figure 25.** <sup>1</sup>H NMR-spectrum (300 MHz, CDCl<sub>3</sub>) of crude **262n**. The diastereomeric ratio ( $dr$  97:3) was determined based on the integrals of the signals in squares.

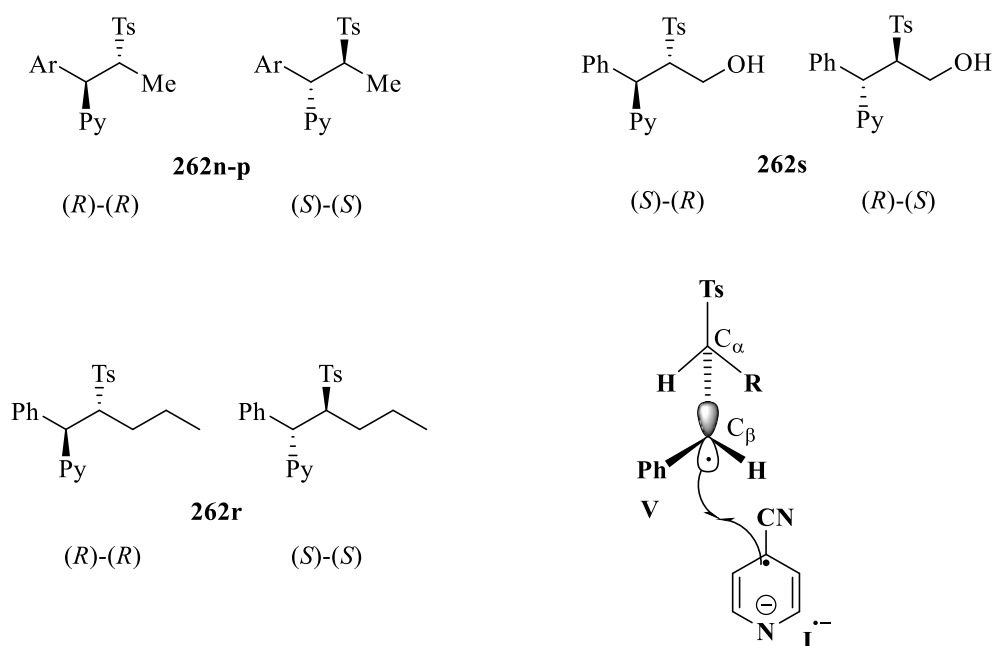


**Figure 26.**  $^1\text{H}$  NMR-spectrum (600 MHz,  $\text{CDCl}_3$ ) of **262** after chromatographic purification. The diastereomeric ratio (dr 97:3) was determined based on the integrals of the signals highlighted in green and blue.



**Figure 27.**  $^1\text{H}$  NMR-spectrum (400 MHz,  $\text{CDCl}_3$ ) of **262n** after treatment with LDA. The diastereomeric ratio (dr 82:18) was determined based on the integrals of the signals highlighted in green and blue.

To confirm that the small  $^1\text{H}$  NMR signals can be really attributed to the minor diastereomer, the compound **262n** was treated with LDA (2.0 equiv.) in dry THF at  $-78\text{ }^\circ\text{C}$ . After 20 min the reaction mixture was quenched with methanol followed by extractive work-up. Figure 27 shows the  $^1\text{H}$  NMR spectrum of **262n** after LDA treatment and extraction. The epimerization is observed when comparing the  $^1\text{H}$  NMR spectra before and after LDA treatment showing that the small signals used for integration are indeed derived from the minor diastereomer (Figures 26 and 27).

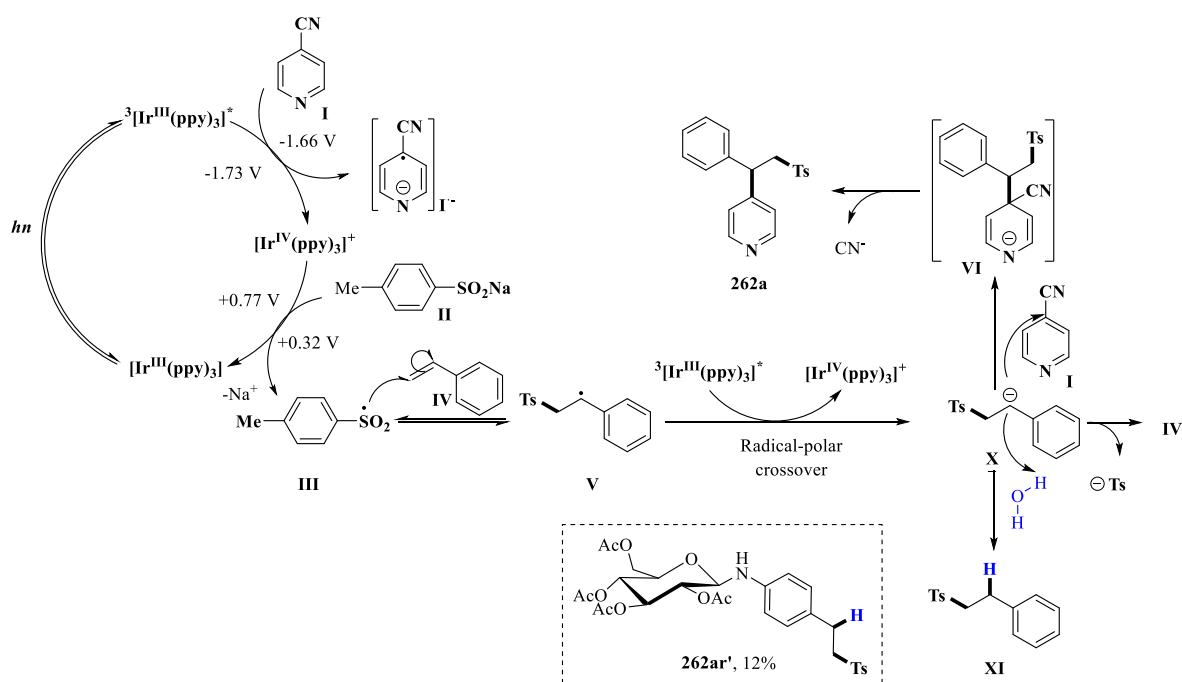


**Scheme 60.** Determination of the relative configuration of compounds **262n-s** by DFT calculations and comparison with the experimentally obtained NMR data (DP4+ probabilities). Dr. Stefan Pusch and Dr. Jonas Kuehlborn made these calculations. For technical details see the publication.

DFT calculations were performed by Dr. Stefan Pusch and Dr. Jonas Kuehlborn for compounds **262n-p**, **262r**, and **262s**, which revealed that the pyridine and tosyl rings are always on opposite sides in the main diastereomer (Scheme 60). The radical combination between the benzylic radical **V** and 4-cyanopyridine radical anion **I<sup>-</sup>** leads to the formation of the diastereomeric excess. According to Hammond's postulate, it can be assumed that the transition state for this step is similar to that of the free radicals and it is determined by the preferred conformation of the benzylic radical **V**.<sup>[191]</sup> It can be assumed that the rotation around the central  $\text{C}_\alpha$ - $\text{C}_\beta$  bond is slower than the radical combination, for which very small activation energy is expected, Curtin-Hammett kinetics will not be obeyed and the

conformation of the low energy rotamer will be reflected in the major product.<sup>[192]</sup> The approach of the radical anion  $\mathbf{I}^{\bullet-}$  probably occurred from the opposite side to the tosyl group. The relative configurations predicted for the acyclic products **262n-p**, **262r**, and **262s** based on this putative explanation and the molecular structure of compound **262t** (Figure 22) agree well with the results obtained from the DFT calculations.

### *A closer look at radical combination and product formation*



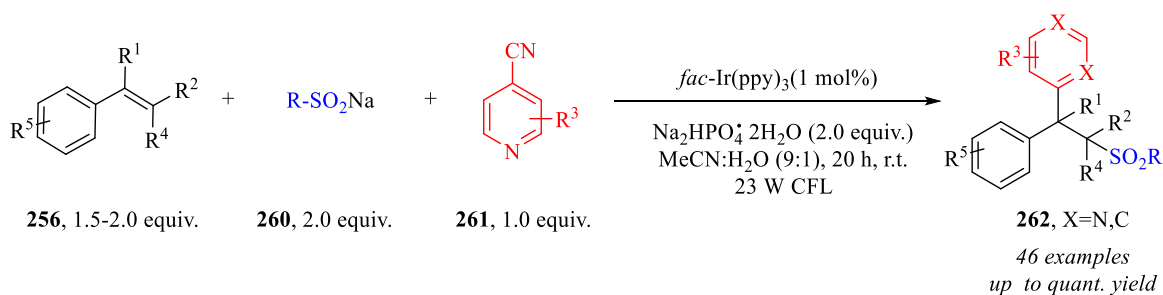
**Scheme 61.** Competition of the styrene-difunctionalization in a hypothetical radical-polar crossover mechanism with protonation of the intermediate carbanions **X** and with the elimination of tosylate.

Although the oxidative quenching cycle is the most plausible catalytic pathway, different competing reactions can occur like styrene polymerization, which occurs to a small extent, and it is the reason why an excess of the olefin is always used in these reactions. Because of the electrostatic repulsion, the persistent radical anions  $\mathbf{I}^{\bullet-}$  are less likely to undergo homodimerization (persistent radical effect)<sup>[177]</sup> and accumulate in the course of the reaction so that there is a sufficiently high concentration for coupling with benzyl radicals such as **V**, which is favored over styrene polymerization. The reaction between **V** and  $\mathbf{I}^{\bullet-}$  seems to be more favorable than the attack of **V** on another styrene molecule **IV**. As already discussed, the yield correlates with the spin density at the *ipso* carbon of the cyanopyridine radical anion, which is indicative that a radical-radical anion combination can be seen. Moreover, a

radical-polar crossover (RPC) would also be conceivable as shown in Scheme 61. The resulting benzyl radical **V** could be reduced to the anion by the excited catalyst ( $E_{1/2}(\mathbf{V}^{\bullet}/\mathbf{V}^{-}) \approx -1.14$  to  $-1.82$  V vs. SCE). In this case, the 4-CP would function as a redox mediator and could undergo nucleophilic substitution with the anion  $\mathbf{V}^{-}$  to give the desired product **262a** after cyanide elimination. However, since the reaction developed takes place in an aqueous solution, it can be assumed that the anion is protonated faster than it can undergo a substitution reaction. In fact, **262ar'** could be isolated in 12% as a by-product that probably has evolved from the protonation of the corresponding anion. This type of by-product could only be isolated for this example. Additionally, elimination of the sulfinate in the anion  $\mathbf{V}^{-}$  is also conceivable (Scheme 61).

### 3.5. Summary and outlook

The third part of this dissertation involved the development of a photoredox catalyzed difunctionalization of styrene derivatives with sodium sulfinates and heteroaromatic nitriles reaction (Scheme 62), which key step is a rather atypical radical-radical-anion coupling, whereas classic difunctionalization methods tend to proceed via a radical-polar crossover reaction. The reaction allows significant variation within each of the three components in its substitution pattern. The use of  $\beta$ -substituted styrenes led to products with high diastereoselectivity ( $dr \geq 92:8$ ). Additionally, the reaction can also be performed on a gram scale, and structurally more complex biomolecules are tolerated and obtained in high yields. Mechanistic studies proved that the reaction proceeds in a redox-neutral, oxidatively quenched catalytic cycle in which the heteroaromatic nitrile acts as a quencher.



**Scheme 62.** Developed photoredox catalyzed difunctionalization of styrene derivatives with sodium sulfinates and heteroaromatic nitriles (collaborative project, see text).

This radical-radical anion coupling strategy for the photoredox-catalyzed difunctionalization of styrene derivatives was implemented in its metal-free version by the group of Lingling Chu.<sup>[182]</sup> It is very likely that the heteroaromatic nitriles can be exchanged for other sources of persistent radical anions, such as di-electron-withdrawing substituted olefins or imines.<sup>[193]</sup> The latter perhaps could be generated in situ to realize a four-component reaction. The use of alternative radical sources such as trimethylsilyl azide is also possible.<sup>[194]</sup>



## 4. Experimental section

### 4.1. General methods

#### Solvents and chemicals

All chemicals and solvents, unless otherwise noted, were purchased from commercial suppliers and used without further purification. Acetonitrile, dichloromethane, acetone, and toluene were treated over calcium hydride under a nitrogen atmosphere, dried, and then distilled. Diethyl ether and tetrahydrofuran (THF) were made absolute over sodium with the presence of benzophenone as an indicator. Since 2019 dry acetonitrile, dichloromethane, diethyl ether, tetrahydrofuran, and toluene were used from a solvent drying system (SPS 5) from MBraun. Anhydrous methanol (99.8%, Acros Seal<sup>®</sup>), *N,N*-dimethylformamide (DMF, 99.8%, Acros Seal<sup>®</sup>), dichloromethane (99.8%, Acros Seal<sup>®</sup>), and dimethyl sulfoxide (DMSO, 99.7%, Acros Seal<sup>®</sup>) were commercially available and obtained from *Acros Organics*. Solvents for photoinduced reactions were degassed immediately before use and, if applicable, after drying by passing a vigorous stream of argon through an ultrasonic bath for at least 20 min. The solvents ethyl acetate and cyclohexane were used as eluent in column chromatography and purchased in technical quality and purified by distillation before use. Deuterated chloroform for NMR spectroscopy was stored over basic alumina.

#### Reactions under inert atmosphere

Reactions, where exclusion of air and moisture was necessary, were performed, unless otherwise indicated, in vessels flooded through three cycles of vacuum and filling with argon or nitrogen. If necessary and highlighted, procedures were carried out with the exclusion of moisture. For this purpose, the set-up was performed in heated Schlenk or Young tubes or flasks and with absolute solvents.

#### Removal of solvents and drying of products

Unless otherwise stated, organic solvents were removed in a membrane pump vacuum on a rotary evaporator at a water bath temperature of 40 °C. Solids or high-boiling, liquid products were additionally dried overnight under a fine vacuum (oil pump) in a 45 °C water bath. Water or mixtures of acetonitrile and water, which were mainly obtained after reverse-phase

chromatographic separations and preparative HPLC, were removed by lyophilization. An Alpha 2-4 LDplus freeze-dryer from *Martin Christ* was used.

## Chromatography

### Thin-layer chromatography

TLC experiments were performed on aluminum sheets coated with silica gel 60 F<sub>254</sub> (Merck). The eluent mixtures are given in volume ratios. Detection was carried out using UV light with a wavelength of  $\lambda = 254$  nm or  $\lambda = 365$  nm. The following staining reagents were also used:

- Dragendorff reagent: 170 mg of bismuth nitrate oxide, 4 g of potassium iodide, 12 mL of conc. acetic acid, 28 mL of water.
- Ninhydrin reagent: 1.5 g of ninhydrin, 15 mL of conc. acetic acid, 485 mL of methanol.
- Potassium permanganate reagent: 2 g of potassium permanganate, 5 g of sodium carbonate, 250 mL of water;
- Seebach reagent: 2.5 g of cerium(IV) sulfate, 6.3 g of phosphomolybdic acid, 235 mL of water, and 15 mL of concentrated sulfuric acid.

### Column chromatography

Flash chromatography was carried out using silica gel from Acros Organics with a particle size of 3570  $\mu\text{m}$ . Column chromatographic purifications were also performed by flash chromatography with a nitrogen overpressure of about 0.2 bar or automated using a Biotage Isolera™ One, a chromatography system with an integrated diode array detector. Biotage SNAP Ultra C<sub>18</sub> cartridges were used in reverse phase chromatographic separations with mixtures of ultrapure water and acetonitrile (HPLC grade) as eluent. The used eluent mixtures are marked at the relevant point and always refer to volume ratios.

### Analytical HPLC

Methods for preparative HPLC were developed using a *1260 Infinity II* HPLC system from *Agilent Technologies* with a built-in binary pump and integrated diode array detector. An *ACE3-C<sub>18</sub>PPF* column (particle size: 3  $\mu\text{m}$ , length: 15 cm, diameter: 4.6 mm) from *Advanced Chromatography Technologies* served as the stationary phase. Mixtures of ultrapure water (taken from an *Omnia-Pure* system from *Stakpure*, sometimes with 0.1% formic acid as an

additive) and acetonitrile (HPLC grade) as the eluent. Separations were always performed at a column temperature of 40 °C with a flow rate of 1 mL·min<sup>-1</sup>.

## Preparative HPLC

Preparative HPLC purifications were carried out using a *Knauer Smartline* system with two *K-1800* pumps and an *S-2600* diode array detector. Unless otherwise indicated, an *ACE5-C<sub>18</sub>PFP* column (particle size 5 µm, length 15 cm, diameter 30 mm, from *Advanced Chromatography Technologies*) was used as the stationary phase. A mixture of acetonitrile (HPLC grade) and ultrapure water (taken from an *Omnia-Pure* system from *Stakpure*) served as eluent at a flow rate of 37.5 mL min<sup>-1</sup>. The sample to be separated was injected manually as a solution in methanol or DMSO via a sample loop with a capacity of 5 mL. Alternatively, a 1290 Infinity II preparative system from *Agilent Technologies* (consisting of 1290 Infinity II pumps, a 1260 Infinity II diode array detector, and a 1290 Infinity II fraction collector) was used. Mixtures of acetonitrile (HPLC grade) and ultrapure water (taken from an *Omnia-Pure* system from *Stakpure*) with 0.1% formic acid (LC-MS grade) at a flow rate of 42.5 mL min<sup>-1</sup>.

## Mass Spectroscopy

### HPLC-ESI-MS

A 1200 Series HPLC from *Agilent Technologies* with a binary pump, integrated UV diode array detector and coupled *LC/MSD Trap XCT*-mass spectrometer from the same manufacturer was used for mass spectrometric analysis of reaction mixtures, crude products, and isolated pure substances. An *Ascentis Express C<sub>18</sub>*-column (particle size: 2.7 µm, length: 3 cm, diameter: 2.1 mm) from *Supelco*, which was heated at 40 °C, served as the stationary phase. Mixtures of acetonitrile, water, and 0.1% of formic acid served as the mobile phase. A gradient of acetonitrile and water (10%–90% acetonitrile in 6 minutes) was chosen as the eluent under a flow rate of 1 mL·min<sup>-1</sup>. All samples were prepared with a concentration of about 1 mg·mL<sup>-1</sup> in neat acetonitrile.

### HR-ESI/APCI/APPI-MS

HR-ESI-MS experiments were mostly performed with a *Waters Micromass q-tof Ultima-3* instrument with *LockSpray* interface. HR-ESI mass spectra were performed on an *Agilent Technologies 6545 QTOF* instrument. In individual cases, HR-APCI and HR-APP.I mass

spectra were recorded on the same instrument. The Department of Mass Spectrometry at the Institute for Organic Chemistry at the Johannes Gutenberg University in Mainz recorded all the high-resolution mass spectra of pure substances.

### GC/EI-MS

Gas chromatographic analyses were conducted using an 8890 GC gas chromatograph from *Agilent Technologies*, coupled to a 5977 GC/MS detector (*Agilent Technologies*). An *Agilent Technologies HP 5MS UI* GC column (30 m x 0.25 mm x 0.25  $\mu\text{m}$ ) having helium as the carrier gas with a flow rate of 1.2 mL $\cdot\text{min}^{-1}$  was used. The column oven temperature was ramped from 40 °C to 320 °C. The samples were prepared as solutions in acetonitrile (LC-MS grade) with a concentration of  $\leq 0.1 \text{ mg mL}^{-1}$ .

## **NMR Spectroscopy**

The samples to be analyzed by NMR spectroscopy were recorded in deuterated solvents and measured on one of the *Bruker* NMR spectrometers listed below:

- Avance-III HD 300:  $^1\text{H}$  NMR (300 MHz),  $^{13}\text{C}$  NMR (75.5 MHz),  $^{19}\text{F}$ -NMR (282.4 MHz).
- Avance-II 400:  $^1\text{H}$  NMR (400 MHz),  $^{13}\text{C}$  NMR (100.6 MHz), (376.5 MHz)  $^{19}\text{F}$ -NMR (376 MHz,  $\text{CDCl}_3$ ).
- Avance-III HD 400:  $^1\text{H}$  NMR (400 MHz),  $^{13}\text{C}$  NMR (100.6 MHz),  $^{19}\text{F}$ -NMR (376 MHz,  $\text{CDCl}_3$ ).
- Avance-III 600:  $^1\text{H}$  NMR (600 MHz),  $^{13}\text{C}$  NMR (150.6 MHz).

COSY, HSQC, and HMBC measurements were performed in all spectrometers. NOESY was recorded in the Avance-III HD 400 and Avance-III 600 apparatus. The signals of the  $^1\text{H}$  and  $^{13}\text{C}$  NMR spectra were referenced to the corresponding deuterated solvent and given in ppm relative to TMS (0 ppm) ( $\text{CDCl}_3$ :  $^1\text{H}$  NMR  $\delta = 7.26$  ppm,  $^{13}\text{C}$  NMR  $\delta = 77.16$  ppm;  $\text{DMSO-d}_6$ :  $^1\text{H}$ -NMR  $\delta=2.50$  ppm,  $^{13}\text{C}$ -NMR  $\delta=39.52$  ppm;  $\text{Methanol-d}_4$ :  $^1\text{H}$ -NMR  $\delta=3.31$  ppm,  $^{13}\text{C}$ -NMR  $\delta=49.00$  ppm;  $\text{D}_2\text{O}$ :  $^1\text{H}$ -NMR  $\delta=4.79$  ppm ).<sup>[195]</sup> The chemical shifts of the  $^{19}\text{F}$  NMR spectra are relative to  $\text{C}(^{35}\text{Cl})_2(^{37}\text{Cl})\text{F}$ . The NMR spectra were evaluated using the MestreNova software from Mestrelab Research.

## **Infrared Spectroscopy**

Infrared spectra were recorded on a *Bruker Tensor 27* IR spectrometer with an integrated diamond ATR unit. The evaluation of the spectra was achieved using the software *Opus 6.5* from *Bruker*.

## **UV-Vis spectroscopy**

UV-Vis absorption spectra were recorded on a *Thermo Fisher Scientific Evolution 201* spectrometer. A 1 cm quartz cuvette was used.

## **Fluorescence Spectroscopy**

Fluorescence spectroscopic investigations were carried out on a *Jasco FP-8300* spectrofluorometer. A *Starna* quartz cuvette with a path length of 1 cm was used, which could be sealed with a septum. To record Stern-Volmer plots, the samples, which had already been prepared under an argon atmosphere and with degassed solvents, were transferred with a syringe into the quartz cuvette, which was also filled with argon. Before the measurement, a weak stream of argon was passed through the respective sample in the cuvette via a cannula for 30 seconds.

## **Transient Absorption Spectroscopy**

An *LP980KS* setup from *Edinburgh Instruments* equipped with an *Nd:YAG* laser from *Litron (Nano LG 300-10)* was employed for laser flash photolysis. The frequency-tripled laser output with a wavelength of 355 nm served as an excitation source. The laser pulse duration was ~5 ns and the pulse frequency 10 Hz. The typical pulse energy used for transient absorption and emission studies was 15 mJ. Detection of transient absorption spectra occurred on an *iCCD* camera from *Andor*. Single-wavelength kinetics were recorded using a photomultiplier tube. The spectroscopic experiments were performed at 293 K using a cuvette holder that allows temperature control. If not stated otherwise the TA spectra were integrated over 100 ns. All samples were prepared in 1 cm quartz cuvettes and degassed by bubbling argon through the analytical sample for 10 minutes.

## Polarimetry

The rotational values of optically active compounds were determined on a Perkin Elmer 241 polarimeter at a wavelength of 589 nm (Na lamp) using a 10 cm quartz.

## Melting Point Determination

Melting point ranges were determined with a *KSPIN* digital melting point apparatus from *Krüss*.

## Crystal Structure Analysis

The crystal structures were recorded on an *STOE IPDS 2T* diffractometer. The evaluation was carried out via the central facility for crystal structure analysis at the Department of Chemistry using the programs *SIR-2004*<sup>[196]</sup> and *SHELXL-2018*<sup>[197]</sup>. For visualization of the structure, the *Mercury* program of the organization CAMBRIDGE CRYSTALLOGRAPHIC DATA CENTER (CCDC) was used.

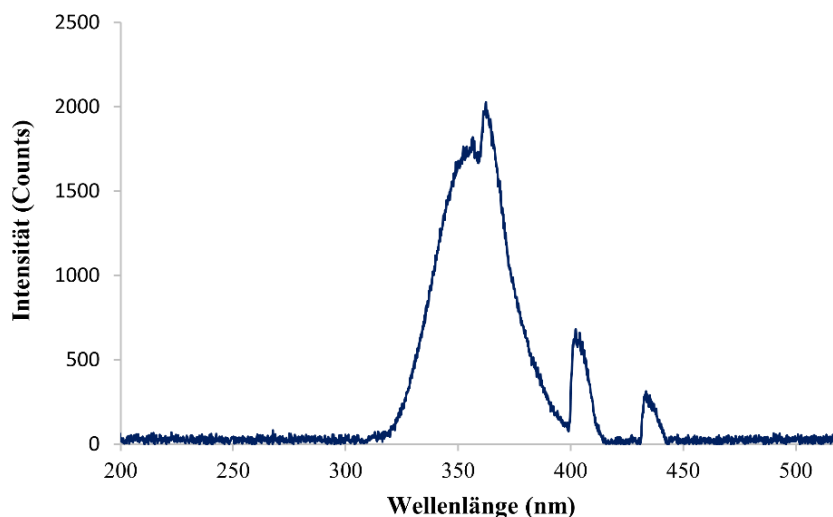
## Light Sources

### Photoreactions using UV light

Photochemical reactions under UV irradiation were performed with a Rayonet photoreactor (*RPR 100*, *Southern New England Ultraviolet Company*). The mixing was done with a retrofitted magnetic stirrer. Cooling was provided by a built-in fan so that the internal temperature of the irradiated solutions (unless otherwise stated) was between 25–30 °C. The equipment has 16 cylindrically arranged lamps of the type Philips TUV-8W (8 W, UV-C,  $\lambda_{\text{max}} = 254$  nm), Ushio G8T5E (7.2 W, UV-B,  $\lambda_{\text{max}} = 306$  nm), and Philips TL 8W BLB (8W, UV-A,  $\lambda_{\text{max}} = 375$  nm).

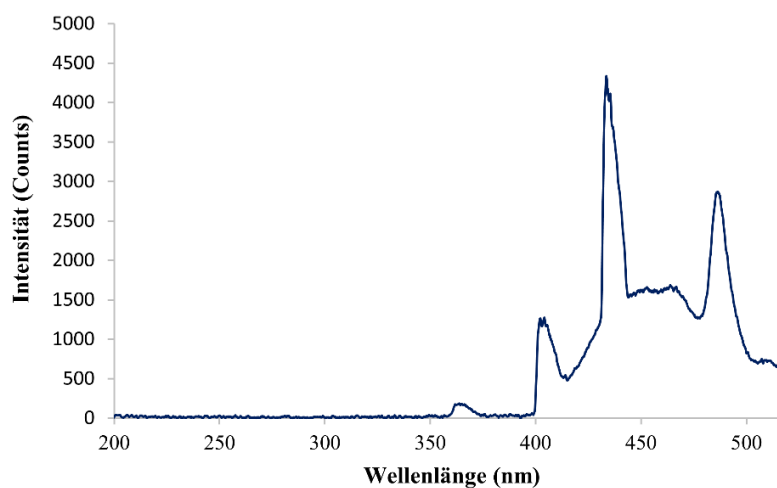
### Photoreactions using visible light

**25W UV-A lamp:** Individual photoreactions in section 3.4.1 using phenanthrene were carried out using a 25 W UV-A energy-saving lamp from *Omnilux* (model number: 89507005). A spotlight from Eurolite served as the housing (model number: 51100700). The emission spectrum ( $\lambda = 200$  nm–520 nm) of this light source is shown in Figure 28.



**Figure 28.** Emission spectrum ( $\lambda = 200 \text{ nm} - 520 \text{ nm}$ ) of a 25 W UV-A energy-saving lamp from *Omnilux*.

**23 W Vis-CFL:** Photoreactions in section 3.4.1 using iridium-based catalysts were exposed with a 23 W *Philips Tornado* household energy-saving lamp (light color: cool daylight, 865; color temperature: 6500 K; product code: 872790092600200). A free-hanging porcelain socket of the type *Pro Socket* (product number: 76105) from *TRIXIE Heimtierbedarf* was used. Figure 29 shows the emission spectrum ( $\lambda = 200\text{--}520 \text{ nm}$ ) of such a tornado compact fluorescent lamp.



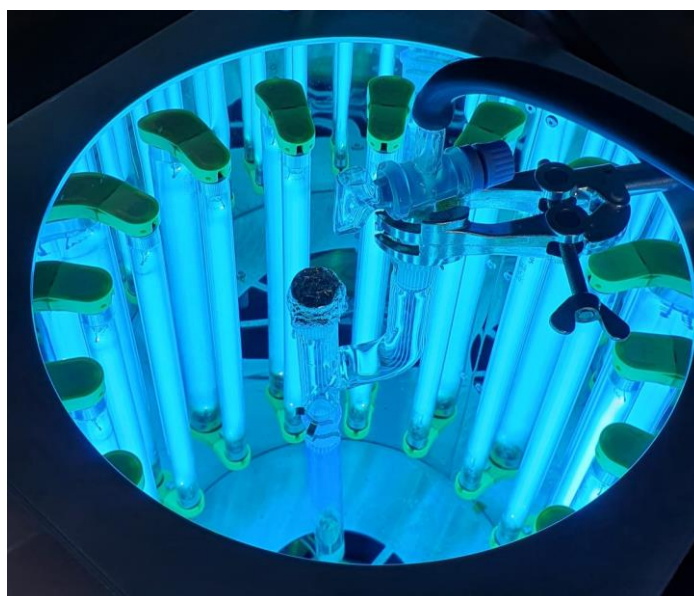
**Figure 29.** Emission spectrum ( $\lambda = 200 \text{ nm} - 520 \text{ nm}$ ) of the 23 W household energy-saving lamp *Tornado* from *Philips*.

**Kessil Lamps:** All photoreactions using blue LEDs were performed with Kessil lamps (KSPR, 50 W, 160L-456 nm) and (KSPR, 45 W, 160L-440 nm). The emission spectra of the lamps can be found on the manufacturer's homepage: <https://www.kessil.com/science/PR160L.php>.

## Set-up of the photochemical reactions

### Exposure to intense UV radiation

For exposure in the previously presented Rayonet photoreactor, the quartz tubes with the reaction solution were placed in the middle of the reactor space. All reactions were conducted under inert atmosphere (Figure 30).



**Figure 30.** Set-up for the irradiation using UV light in a Rayonet photoreactor.

### Exposure with 23-25 W energy-saving lamps

Most of the PET reaction solutions were exposed at a distance of about 5 cm using the 23–25 W energy-saving lamps previously described. Batches on a multigram scale were exposed simultaneously from different sides with three energy-saving lamps. Argon-filled balloons were used to prevent overpressure in multigram batches with gas evolution. All reactions were exposed in a well-ventilated fume hood with a protective screen lined with UV protection film. Figure 31 shows the typical setup of such experiments.





Figure 31. Set-up of preparative photoredox reactions with a 25 W UV/Vis-CFL (left) and with a 23 W Vis-CFL household lamp as a multigram scale approach (right).

### Exposure with blue LEDs

Kessil 45-50 W blue LED spotlights were placed approximately 3-5 cm from the reaction tube under a fan that was used to prevent increment of the reaction temperature. All reactions were exposed in a well-ventilated fume hood, the protective screen of which was completely covered with cardboard. The usual setup of such experiments is shown in Figure 32.

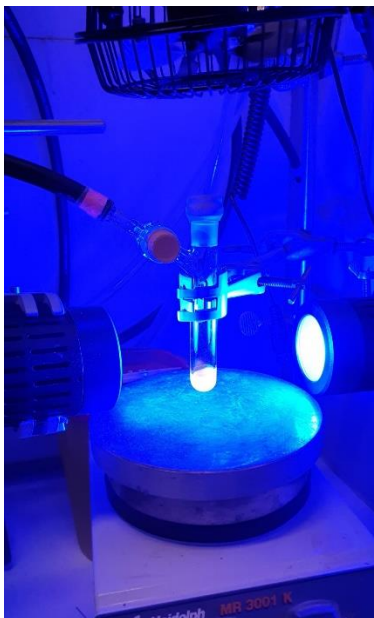


Figure 32. The usual setup for irradiation with blue LED lamps.

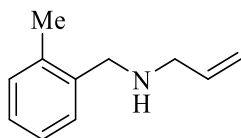
## 4.2. Reaction Procedures

### 4.2.1. Section 2.3.1

#### General procedure of reductive amination (Synthesis of secondary amines)

To a solution of allylamine (1.00 equiv.) in methanol ( $c=0.52$  mmol/mL) at 0 °C, was added the corresponding benzaldehyde (1.00 equiv.). After stirring at 0 °C until full consumption of the amine and formation of the corresponding imine, NaBH<sub>4</sub> (1.20 equiv.) was added portionwise at 0 °C and the reaction mixture was stirred at 0 °C for 30 min. The mixture was concentrated under reduced pressure to remove the methanol then was diluted with ethyl acetate and washed with water. The aqueous layer was extracted three times with ethyl acetate (3 x 50 mL). The residue was purified by flash chromatography (SiO<sub>2</sub>, eluent: cyclohexane/ethyl acetate, 20:0 → 5:1).

#### *N*-(2-Methylbenzyl)prop-2-en-1-amine (229a)



Following the general procedure with allylamine (0.62 mL, 8.32 mmol, 1.00 equiv.) and 2-methylbenzaldehyde (0.96 mL, 8.32 mmol, 1.00 equiv.) the title compound (1.10 g, 6.82 mmol, 82%) was isolated as a colorless oil.

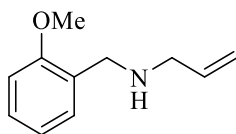
$R_f = 0.23$  (3:1 cyclohexane/ethyl acetate).

**IR** (ATR):  $\tilde{\nu}/\text{cm}^{-1} = 3015, 2976, 2975, 1643, 1492, 1457, 1097, 1049, 993, 916$ .

**<sup>1</sup>H NMR, COSY** (400 MHz, CDCl<sub>3</sub>)  $\delta$  /ppm = 7.33–7.29 (m, 1H, H-6), 7.21–7.15 (m, 3H, H-3, 4, 5), 5.97 (ddt,  $J = 17.2, 10.2, 6.0$  Hz, 1H, -CH=), 5.24 (dq,  $J = 17.2, 1.7$  Hz, 1H, =CH<sub>trans</sub>), 5.14 (dq,  $J = 10.2, 1.4$  Hz, 1H, =CH<sub>cis</sub>), 3.79 (s, 2H, -CH<sub>2</sub>-), 3.34 (dt,  $J = 6.0, 1.4$  Hz, 2H, -CH<sub>2</sub>-CH=), 2.37 (s, 3H, -CH<sub>3</sub>).

**<sup>13</sup>C NMR, HSQC, HMBC** (101 MHz, CDCl<sub>3</sub>)  $\delta$  /ppm =  $\delta$  138.3 (C-1), 137.0 (-CH=), 136.4 (C-2), 130.4 (C<sub>Ar</sub>H), 128.5 (C-6), 127.1 (C<sub>Ar</sub>H), 126.0 (C<sub>Ar</sub>H), 116.2 (=CH<sub>2</sub>), 52.3 (-CH<sub>2</sub>-CH=), 50.9 (-CH<sub>2</sub>-), 19.1 (-CH<sub>3</sub>).

**MS** (EI):  $m/z = 161.1$  [M]<sup>+</sup>.

***N*-(2-Methoxybenzyl)prop-2-en-1-amine (229b)**

Following the general procedure with allylamine (0.96 mL, 12.85 mmol, 1.00 equiv.) and 2-anisaldehyde (1.55 mL, 12.85 mmol, 1.00 equiv.) the title compound (1.27 g, 7.19 mmol, 56%) was isolated as a colorless oil.

$R_f = 0.21$  (3:1 cyclohexane/ethyl acetate).

**IR** (ATR):  $\tilde{\nu}/\text{cm}^{-1} = 3010, 2979, 2969, 1639, 1501, 1453, 1098, 1037, 994, 916$ .

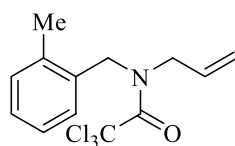
**$^1\text{H}$  NMR, COSY** (400 MHz,  $\text{CDCl}_3$ )  $\delta$  /ppm = 7.30–7.18 (m, 2H, H-4, 6), 6.91 (td,  $J = 7.4, 1.1$  Hz, 1H, H-5), 6.87 (dd,  $J = 8.6, 1.1$  Hz, 1H, H-3), 5.94 (ddt,  $J = 17.1, 10.2, 5.9$  Hz, 1H, -CH=), 5.19 (dq,  $J = 17.1, 1.7$  Hz, 1H, =CH<sub>trans</sub>), 5.10 (dq,  $J = 10.2, 1.4$  Hz, 1H, =CH<sub>cis</sub>), 3.84 (s, 3H, -OCH<sub>3</sub>), 3.79 (s, 2H, -CH<sub>2</sub>-), 3.24 (dt,  $J = 6.0, 1.5$  Hz, 2H, -CH<sub>2</sub>-CH=).

**$^{13}\text{C}$  NMR, HSQC, HMBC** (101 MHz,  $\text{CDCl}_3$ )  $\delta$  /ppm = 157.7 (C-2), 137.0 (-CH=), 130.4 (C<sub>Ar</sub>H), 128.3 (C<sub>Ar</sub>H), 128.1 (C-1), 120.4 (C-5), 116.0 (=CH<sub>2</sub>), 110.3 (C-3), 55.3 (-OCH<sub>3</sub>), 51.7 (-CH<sub>2</sub>-CH=), 48.7 (-CH<sub>2</sub>-).

**MS** (EI):  $m/z = 177.1$  [M]<sup>+</sup>.

**General procedure for the protection of the amine 229**

To a solution of amine **229** (1.00 equiv.) in dry  $\text{CH}_2\text{Cl}_2$  (C= 1.72 mmol/mL) at  $-78$  °C (or  $0$  °C) and under an  $\text{N}_2$  atmosphere was added triethylamine (1.20 equiv.) followed by the addition dropwise of a solution of the corresponding acid anhydride or acyl chloride (1.20 equiv.) in a minimum of  $\text{CH}_2\text{Cl}_2$ . After 1 h the mixture was allowed to warm to room temperature and stirred for around 12 h. The reaction was quenched with brine (30 mL), and the organic layer was separated. The aqueous was extracted twice with  $\text{CH}_2\text{Cl}_2$  (3 x 60 mL). The combined organic phase was dried over  $\text{NaSO}_4$ , filtered, concentrated under reduced pressure, and purified by flash chromatography ( $\text{SiO}_2$ , eluent: cyclohexane/ethyl acetate, 50:1 → 20:1).

**2,2,2-Trichloro-N-[(2-methylphenyl)methyl]-N-(prop-2-en-1-yl)acetamide (213a)**

Following the general procedure with amine **229a** (0.15 g, 0.93 mmol, 1.00 equiv.) and trichloroacetyl chloride (0.10 mL, 0.93 mmol, 1.20 equiv.), the title compound (0.26 g, 0.85 mmol, 91%) was isolated as a slightly yellow oil.

$R_f$  = 0.63 (6:1 cyclohexane/ethyl acetate).

**IR** (ATR):  $\tilde{\nu}/\text{cm}^{-1}$  = 3023, 2254, 1674, 1497, 1414, 1234, 991, 905, 847, 725.

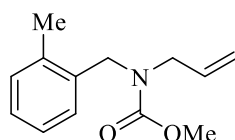
Spectroscopic data of this amide was obtained as a 2:1 mixture of two rotational isomers:

**<sup>1</sup>H NMR, COSY** (400 MHz, CDCl<sub>3</sub>)  $\delta$  /ppm = 7.24–7.03 (m, 4H, minor/major, H-3, 4, 5,6), 5.93–5.73 (m, 1 H, minor/major, -CH=), 5.42–5.07 (m, 2H, minor/major, =CH<sub>2</sub>), 4.91 (s, 2H, minor, -CH<sub>2</sub>-), 4.69 (s, 2H, major, -CH<sub>2</sub>-), 4.28 (bs, 2H, major, -CH<sub>2</sub>-CH=), 4.00 (bs, 2H, minor, -CH<sub>2</sub>-CH=), 2.28 (s, 3H, minor/major, -CH<sub>3</sub>).

**<sup>13</sup>C NMR, HSQC, HMBC** (101 MHz, CDCl<sub>3</sub>)  $\delta$  /ppm = *major isomer*: 160.7 (C=O), 136.6 (C-1), 133.4 (C-2), 132.3 (-CH=), 130.8 (C<sub>Ar</sub>H), 127.8 (C<sub>Ar</sub>H), 127.1 (C<sub>Ar</sub>H), 126.4 (C<sub>Ar</sub>H), 119.7 (=CH<sub>2</sub>), 93.3 (CCl<sub>3</sub>), 51.3(-CH<sub>2</sub>-CH=), 48.2 (-CH<sub>2</sub>-), 19.2(-CH<sub>3</sub>). *minor isomer*: 161.2 (C=O), 135.4 (C-1), 133.4 (C-2), 132.3 (-CH=), 131.0 (C<sub>Ar</sub>H), 127.5 (C<sub>Ar</sub>H), 127.1 (C<sub>Ar</sub>H), 126.1 (C<sub>Ar</sub>H), 118.4 (=CH<sub>2</sub>), 93.1 (CCl<sub>3</sub>), 51.0 (-CH<sub>2</sub>-CH=), 50.0 (-CH<sub>2</sub>-), 19.2(-CH<sub>3</sub>).

**MS** (ESI):  $m/z$  = 328.1 [M + Na]<sup>+</sup>.

**HRMS** (ESI-ToF)  $m/z$  = [M + Na]<sup>+</sup> calcd for C<sub>13</sub>H<sub>14</sub>Cl<sub>3</sub>NONa: 328.0033, found: 308.0193.

**Methyl [(2-methylphenyl)methyl]prop-2-en-1-ylcarbamate (213b)**

Following the general procedure with amine **229a** (0.25 g, 0.42 mol, 1.00 equiv.) and methyl chloroformate (0.14 mL, 1.86 mol, 1.20 equiv.), after TLC showed completion of the reaction, the title compound (0.24 g, 1.09 mmol, 71%) was isolated as a slightly yellow oil.

$R_f = 0.50$  (5:1 cyclohexane/ethyl acetate).

**IR** (ATR):  $\tilde{\nu}/\text{cm}^{-1} = 3068, 2954, 1699, 1461, 1403, 1237, 994, 930, 771, 743$ .

Spectroscopic data of this amide was obtained as a 1:0.9 mixture of two rotational isomers:

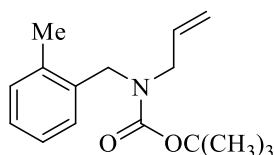
**$^1\text{H}$  NMR, COSY** (400 MHz,  $\text{CDCl}_3$ )  $\delta$  /ppm = 7.20–7.11 (m, 4H, minor/major, H-3, 4, 5, 6), 5.75 (bs, 1 H, minor/major, -CH=), 5.16–5.06 (m, 2H, minor/major, =CH<sub>2</sub>), 4.51 (s, 2H, minor, -CH<sub>2</sub>-), 4.44 (s, 2H, major, -CH<sub>2</sub>-), 3.87 (s, 2H, major, -CH<sub>2</sub>-CH=), 3.75 (s, 2H, minor, -CH<sub>2</sub>-CH=), 3.75 (s, 3H, minor/major, -OCH<sub>3</sub>), 2.27 (s, 3H, minor/major, -CH<sub>3</sub>).

**$^{13}\text{C}$  NMR, HSQC, HMBC** (101 MHz,  $\text{CDCl}_3$ )  $\delta$  /ppm = 157.2 (C=O), 136.6 (C-1), 135.3 (C-2), 133.4 (-CH=), 130.6 (C<sub>Ar</sub>H), 127.8 (C<sub>Ar</sub>H), 127.3 (C<sub>Ar</sub>H), 126.2 (C<sub>Ar</sub>H), 116.9 (=CH<sub>2</sub>), 53.0 (-OCH<sub>3</sub>), 47.9(-CH<sub>2</sub>-CH=), 47.3 (-CH<sub>2</sub>-), 19.0(-CH<sub>3</sub>).

**MS** (ESI):  $m/z = 220.1$  [M + H]<sup>+</sup>.

**HRMS** (ESI-ToF)  $m/z = [\text{M} + \text{H}]^+$  calcd for C<sub>13</sub>H<sub>18</sub>NO<sub>2</sub>: 220,1332, found: 220.1337.

#### ***tert*-Butyl [(2-methylphenyl)methyl]prop-2-en-1-ylcarbamate (**213c**)**



Following the general procedure with amine **229a** (0.32 g, 1.98 mmol, 1.00 equiv.) and ditert-butyl dicarbonate (0.55mL, 2.38 mmol, 1.20 equiv.) the title compound (0.38 g, 1.45 mmol, 72%) was isolated as a slightly yellow oil.

$R_f = 0.62$  (5:1 cyclohexane/ethyl acetate).

**IR** (ATR):  $\tilde{\nu}/\text{cm}^{-1} = 2976, 2930, 1663, 1477, 1455, 1245, 923, 878, 767, 742$ .

Spectroscopic data of this amide was obtained as a 1:0.8 mixture of two rotational isomers:

**$^1\text{H}$  NMR, COSY** (400 MHz,  $\text{CDCl}_3$ )  $\delta$  /ppm = 7.18–7.11 (m, 4H, minor/major, H-3, 4, 5,6), 5.74 (bs, 1 H, minor/major, -CH=), 5.13–5.05 (m, 2H, minor/major, =CH<sub>2</sub>), 4.46 (s, 2H, major, -CH<sub>2</sub>-), 4.41 (s, 2H, minor, -CH<sub>2</sub>-), 3.82 (s, 2H, major, -CH<sub>2</sub>-CH=), 3.70 (s, 2H,

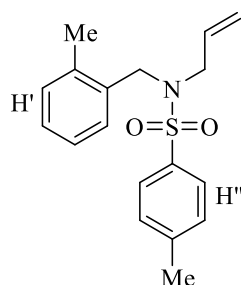
minor, -CH<sub>2</sub>-CH=), 3.73 (s, 3H, minor/major, -OCH<sub>3</sub>), 2.27 (s, 3H, minor/major, -CH<sub>3</sub>), 1.48 (bs, 9H, CCH<sub>3</sub>).

<sup>13</sup>C NMR, HSQC, HMBC (101 MHz, CDCl<sub>3</sub>) δ /ppm = 155.8 (C=O), 136.7 (C-1), 135.8 (C-2), 133.8 (-CH=), 130.5 (C<sub>Ar</sub>H), 128.0 (C<sub>Ar</sub>H), 127.2 (C<sub>Ar</sub>H), 126.1 (C<sub>Ar</sub>H), 116.9 (=CH<sub>2</sub>), 79.9 (-OC(CH<sub>3</sub>)<sub>3</sub>), 48.5(-CH<sub>2</sub>-CH=), 47.3 (-CH<sub>2</sub>-), 28.5 (-OC(CH<sub>3</sub>)<sub>3</sub>), 19.2(-CH<sub>3</sub>).

MS (ESI): *m/z* = 284.1 [M + Na]<sup>+</sup>.

HRMS (APCI) *m/z* = [M + H]<sup>+</sup> calcd for C<sub>16</sub>H<sub>23</sub>NO<sub>2</sub>Na: 284,1621, found: 284.1698.

**4-Methyl-N-[(2-methylphenyl)methyl]-N-(prop-2-en-1-yl)benzene-1-sulfonamide (213 d)**



Following the general procedure with the amine **229a** (0.20 g, 1.24 mmol, 1.00 equiv.) and 4-methylbenzenesulfonyl chloride (0.35 mL g, 1.49 mmol, 1.20 equiv.) the title compound (0.35 g, 1.12 mmol, 90%) was isolated as a slightly yellow oil.

*R<sub>f</sub>* = 0.56 (5:1 cyclohexane/ethyl acetate).

IR (ATR):  $\tilde{\nu}/\text{cm}^{-1}$  = 3023, 2922, 1597, 1494, 1342, 1158, 903, 878, 745, 662.

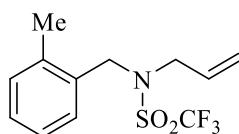
<sup>1</sup>H NMR, COSY (400 MHz, CDCl<sub>3</sub>) δ /ppm = 7.78 (d, *J* = 8.3 Hz, AA' part of AA'-BB' system, 2H, H-2'',6''), 7.35 (d, *J* = 8.3 Hz, BB' part of AA'-BB' system, 2H, H-3'',5''), 7.23-7.20 (m, 1H, 6-H'), 7.19-7.16 (m, 1H, 4-H'), 7.15-7.10 (m, 2H, H-3',5'), 5.43 (ddt, *J* = 17.0, 10.2, 6.5 Hz, 1H, -CH=), 4.99 (dq, *J* = 10.2, 1.2 Hz, 1H, =CH<sub>cis</sub>), 5.07 (dq, *J* = 17.0, 1.4 Hz, 1H, =CH<sub>trans</sub>), 4.34 (s, 2H, -CH<sub>2</sub>-), 3.71 (dt, *J* = 6.5, 1.4 Hz, 2H, -CH<sub>2</sub>-CH=), 2.45 (s, 3H, -CH<sub>3</sub>''), 2.31 (s, 3H, -CH<sub>3</sub>').

<sup>13</sup>C NMR, HSQC, HMBC (101 MHz, CDCl<sub>3</sub>) δ /ppm = 143.5 (C-4''), 137.2 (2C, C-1'', C-1'), 133.6 (C-2'), 132.5 (-CH=), 130.7 (C-3'), 129.9 (C-3'',5''), 129.2 (C-6'), 127.9 (C-4'), 127.5 (C-2'',6''), 126.0 (C-5'), 119.1 (=CH<sub>2</sub>), 49.8 (-CH<sub>2</sub>-CH=), 48.9 (-CH<sub>2</sub>-), 21.7(-CH<sub>3</sub>''), 19.3(-CH<sub>3</sub>').

**MS** (ESI):  $m/z = 318.1$   $[M + Na]^+$ .

**HRMS** (ESI-ToF)  $m/z = [M + Na]^+$  calcd for  $C_{12}H_{14}F_3NO_2SNa$ : 338,1185, found: 338,1194.

***N*-Allyl-1,1,1-trifluoro-*N*-(2-methylbenzyl)methanesulfonamide (213e)**



Following the general procedure with amine **229a** (5.27 g, 32.7 mmol, 1.00 equiv.) and trifluoromethanesulfonic anhydride (10.14 mL, 36.0 mmol, 1.20 equiv.) the title compound (8.15 g, 27.8 mmol, 85%) was isolated as a slightly yellow oil.

$R_f = 0.54$  (10:1 cyclohexane/ethyl acetate).

**IR** (ATR):  $\tilde{\nu}/\text{cm}^{-1} = 3026, 2933, 1494, 1389, 1226, 1187, 1140, 1060, 912, 610$ .

**$^1\text{H}$  NMR, COSY** (400 MHz,  $\text{CDCl}_3$ )  $\delta$  /ppm = 7.31–7.27 (m, 1H, H-6), 7.26–7.22 (m, 2H, H-4, 5), 7.20–7.16 (m, 1H, H-3), 5.71 (ddt,  $J = 17.0, 10.2, 6.7$  Hz, 1 H, -CH=), 5.24 (dq,  $J = 10.2, 1.4$  Hz, 1H, =CH<sub>cis</sub>), 5.07 (dq,  $J = 17.0, 1.4$  Hz, 1H, =CH<sub>trans</sub>), 4.57 (s, 2H, -CH<sub>2</sub>-), 3.89 (s, 2H, -CH<sub>2</sub>-CH=), 2.32 (s, 3H, -CH<sub>3</sub>).

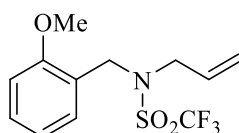
**$^{13}\text{C}$  NMR, HSQC, HMBC** (101 MHz,  $\text{CDCl}_3$ )  $\delta$  /ppm = 136.8 (C-1), 131.7 (C-2), 131.1 (-CH=), 131.0 (C-3), 128.5 (C-6), 128.4 (C-4), 126.4 (C-5), 122.0 (=CH<sub>2</sub>), 120.1 (q, CF<sub>3</sub>,  $J = 323.2$  Hz), 50.2 (-CH<sub>2</sub>-CH=), 48.9 (-CH<sub>2</sub>-), 19.3(-CH<sub>3</sub>).

**$^{19}\text{F}$  NMR** (376 MHz,  $\text{CDCl}_3$ )  $\delta$  /ppm = -76.8 (s, CF<sub>3</sub>).

**MS** (ESI):  $m/z = 316.1$   $[M + Na]^+$ .

**HRMS** (ESI-ToF)  $m/z = [M + Na]^+$  calcd for  $C_{12}H_{14}F_3NO_2SNa$ : 316.0589, found: 316.0596.

***N*-allyl-1,1,1-trifluoro-*N*-(2-methoxybenzyl)methanesulfonamide (213f)**



Following the general procedure with the amine **229b** (1.60 g, 9.03 mmol, 1.00 equiv.) and trifluoromethanesulfonic anhydride (1.80 mL, 10.83 mmol, 1.20 equiv.) the title compound (2.47 g, 7.99 mmol, 88%) was isolated as a slightly yellow oil.

$R_f = 0.41$  (20:1 cyclohexane/ethyl acetate).

**IR** (ATR):  $\tilde{\nu}/\text{cm}^{-1} = 3021, 2945, 1490, 1401, 1236, 1190, 1137, 1064, 912, 611$ .

**$^1\text{H}$  NMR, COSY** (400 MHz,  $\text{CDCl}_3$ )  $\delta$  /ppm = 7.37–7.29 (m, 2H, H-4, 6), 6.98 (td,  $J = 7.5, 1.1$  Hz, 1H, H-5), 6.89 (dd,  $J = 8.3, 1.3$  Hz, 1H, H-3), 5.75 (ddt,  $J = 17.0, 10.1, 6.7$  Hz, 1H, =CH=), 5.24 (dq,  $J = 10.1, 1.4$  Hz, 1H, =CH<sub>cis</sub>), 5.16 (dq,  $J = 17.0, 1.4$  Hz, 1H, =CH<sub>trans</sub>), 4.58 (s, 2H, -CH<sub>2</sub>-), 3.91 (bs, 2H, -CH<sub>2</sub>-CH=), 3.84 (s, 3H, -OCH<sub>3</sub>).

**$^{13}\text{C}$  NMR, HSQC, HMBC** (101 MHz,  $\text{CDCl}_3$ )  $\delta$  /ppm = 157.7 (C-2), 131.5 (-CH=), 130.2 (C<sub>Ar</sub>H), 129.9 (C<sub>Ar</sub>H), 122.6 (C-1), 120.9 (C-5), 120.4 (=CH<sub>2</sub>), 120.2 (q, CF<sub>3</sub>,  $J = 323.9$  Hz), 110.6 (C-3), 55.3 (-OCH<sub>3</sub>), 50.7 (-CH<sub>2</sub>-CH=), 46.0 (-CH<sub>2</sub>-).

**$^{19}\text{F}$  NMR** (376 MHz,  $\text{CDCl}_3$ )  $\delta$  /ppm = -76.9 (s, CF<sub>3</sub>).

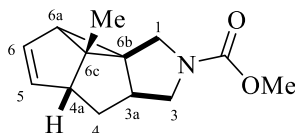
**MS** (ESI):  $m/z = 332.1$  [M + Na]<sup>+</sup>.

**HRMS** (ESI-ToF)  $m/z =$  [M + Na]<sup>+</sup> calcd for C<sub>12</sub>H<sub>14</sub>F<sub>3</sub>NO<sub>3</sub>S Na: 332.0538, found: 332.0545.

## Synthesis of *meta* photocycloadducts

In an oven-dried quartz tube under a nitrogen atmosphere were charged 100.0 mg of the protected amine and 10 mL of anhydrous cyclohexane. The solution was degassed for 15 min and placed in a Rayonet photoreactor. The vessel was irradiated ( $\lambda_{\text{max}} = 254$  nm, 16 × 8 W) at room temperature for 2.0–4.0 h. After removal of the solvent under reduced pressure, the crude material was separated by flash chromatography.

### (3*aS*,4*aR*,6*cR*)-methyl 6*c*-methyl-3,3*a*,4,4*a*,6*a*,6*c*-hexahydrocyclopropa[1,6]pentaleno[1,2-*c*]pyrrole-2(1*H*)-carboxylate (**214b**)



Following the general procedure, a mixture of allyl benzylamine **213b** (100.0 mg, 0.45 mmol) and 10 mL of anhydrous cyclohexane was irradiated for 2.0 h. After column chromatography (SiO<sub>2</sub>, eluent: cyclohexane/ethyl acetate, 100:0 → 98:1) an 88:12 colorless



oil mixture of two isomeric *meta*-photocycloadducts were isolated (79.0 mg, 0.36 mmol, 79%).

$R_f = 0.19$  [KMnO<sub>4</sub>] (6:1 cyclohexane/ethyl acetate).

**IR** (ATR):  $\tilde{\nu}/\text{cm}^{-1} = 3051, 2926, 1702, 1449, 1384, 1388, 1192, 1123, 1106, 968$ .

Spectroscopic data are those of the major isomer:

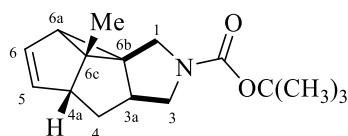
**<sup>1</sup>H NMR, COSY NOESY** (400 MHz, CDCl<sub>3</sub>)  $\delta$  /ppm = 5.62 (dd,  $J = 5.5, 2.1$  Hz, 1H, H-6), 5.45 (ddd,  $J = 5.5, 2.4, 0.8$  Hz, 1H, H-5), 3.69 (s, 3H, CO<sub>2</sub>Me), 3.53–3.14 (m, 4H, H-1<sub>a,b</sub>, H-3<sub>ab</sub>), 2.96 (dd,  $J = 5.3, 2.4$  Hz, 1H, H-4<sub>a</sub>), 2.48–2.42 (m, 1H, H-3<sub>a</sub>), 1.88 (dd,  $J = 11.7, 6.3$  Hz, 1H, H-4<sub>b</sub>), 1.79–1.72 (m, 1H, H-4<sub>a</sub>), 1.62–1.59 (m, 1H, H-6<sub>a</sub>), 1.29 (s, 3H, CH<sub>3</sub>--C-4<sub>a</sub><sup>1</sup>).

**<sup>13</sup>C NMR, HSQC, HMBC** (101 MHz, CDCl<sub>3</sub>)  $\delta$  /ppm = 155.6 (C=O), 133.2 (C-5), 128.1 (C-6), 57.7 (C-4<sub>a</sub>), 52.5 (OMe), 52.1 (C-3), 46.7 (C-4), 46.2 (C-1), 40.2 (C-3<sub>a</sub>), 39.8 (C-6<sub>a</sub>), 37.7(C-6<sub>b</sub>), 35.8 (C-4<sub>a</sub><sup>1</sup>), 14.0 (CH<sub>3</sub>--C-4<sub>a</sub><sup>1</sup>).

**MS** (ESI):  $m/z = 220.1$  [M + H]<sup>+</sup>.

**HRMS** (ESI-ToF)  $m/z = [M + H]^+$  calcd. for C<sub>13</sub>H<sub>18</sub>NO<sub>2</sub>: 220.1332, found: 220.1341.

**(3*aS*,4*aR*,6*cR*)-*tert*-Butyl-6*c*-methyl-3,3*a*,4,4*a*,6*a*,6*c*-hexahydrocyclopropa[1,6]pentale no[1,2-*c*]pyrrole-2(1*H*)-carboxylate (214*c*)**



Following the general procedure, a mixture of allyl benzylamine **213c** (100.0 mg, 0.38 mmol) and 10 mL of anhydrous cyclohexane was irradiated for 2.0 h. After column chromatography (SiO<sub>2</sub>, eluent: cyclohexane/ethyl acetate, 100:0 → 98:1) an 86:14 colorless oil mixture of two isomeric *meta*-photocycloadducts were isolated (78.0 mg, 0.30 mmol, 78%).

$R_f = 0.43$  [KMnO<sub>4</sub>] (6:1 cyclohexane/ethyl acetate).

**IR** (ATR):  $\tilde{\nu}/\text{cm}^{-1} = 2974, 2926, 1696, 1478, 1393, 1365, 1247, 1169, 1121, 879$ .

Spectroscopic data are those of the major isomer:

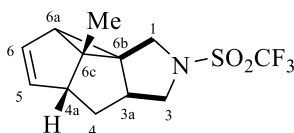
**<sup>1</sup>H NMR, COSY NOESY** (400 MHz, CDCl<sub>3</sub>)  $\delta$  /ppm = 5.62 (dd,  $J$  = 5.4, 2.4 Hz, 1H, H-6), 5.44 (ddd,  $J$  = 5.4, 2.4, 0.8 Hz, 1H, H-5), 3.64 (dd,  $J$  = 11.2, 9.3 Hz, 2H, H-1<sub>a,b</sub>, H-3<sub>ab</sub>), 3.28 (d,  $J$  = 11.5, 9.3 Hz, 2H, H-1<sub>a,b</sub>), 2.95 (dd,  $J$  = 5.3, 2.4 Hz, 1H, H-4<sub>a</sub>), 2.43 (ddd,  $J$  = 15.0, 9.5, 5.5 Hz, 1H, H-3<sub>a</sub>), 1.85 (d,  $J$  = 6.4 Hz, 1H, H-4<sub>b</sub>), 1.78–1.75 (m, 1H, H-4<sub>a</sub>), 1.63–1.62 (m, 1H, H-6<sub>a</sub>), 1.46 (s, 9H, CO<sub>2</sub>C(CH<sub>3</sub>)<sub>3</sub>), 1.30 (s, 3H, CH<sub>3</sub>-C-4<sub>a</sub><sup>1</sup>).

**<sup>13</sup>C NMR, HSQC, HMBC** (101 MHz, CDCl<sub>3</sub>)  $\delta$  /ppm = 154.7 (C=O), 133.2 (C-5), 128.2 (C-6), 79.3 (C(CH<sub>3</sub>)<sub>3</sub>), 57.7 (C-4<sub>a</sub>), 52.1 (C-3), 46.6 (C-4), 46.3 (C-1), 39.9 (C-3<sub>a</sub>), 39.6 (C-6<sub>a</sub>), 37.9 (C-6<sub>b</sub>), 35.8 (C-4<sub>a</sub><sup>1</sup>), 28.7 (C(CH<sub>3</sub>)<sub>3</sub>), 14.1 (CH<sub>3</sub>-C-4<sub>a</sub><sup>1</sup>).

**MS** (ESI):  $m/z$  = 284.1 [M + Na]<sup>+</sup>.

**HRMS** (ESI-ToF)  $m/z$  = [M + Na]<sup>+</sup> calcd. for C<sub>16</sub>H<sub>23</sub>NO<sub>2</sub>Na: 284.1621, found: 284.1623.

**(3*aS*,4*aR*,6*cR*)-6*c*-Methyl-2-[(trifluoromethyl)sulfonyl]-1,2,3,3*a*,4,4*a*,6*a*,6*c*-octahydrocyclopropa[1,6]pentaleno[1,2-*c*]pyrrole (214e)**



Following the general procedure, a mixture of allyl benzylamine **213e** (100.0 mg, 0.34 mmol) and 10 mL of anhydrous cyclohexane was irradiated for 3.5 h. After column chromatography (SiO<sub>2</sub>, eluent: cyclohexane/ethyl acetate, 100:0 → 98:1) a 92:8 colorless oil mixture of two isomeric *meta*-photocycloadducts were isolated (72.0 mg, 0.25 mmol, 72%).

$R_f$  = 0.50 [KMnO<sub>4</sub>] (10:1 cyclohexane/ethyl acetate).

**IR** (ATR):  $\tilde{\nu}$ /cm<sup>-1</sup> = 3056, 2931, 1479, 1451, 1388, 1226, 1184, 1152, 1023, 729.

Spectroscopic data are those of the major isomer:

**<sup>1</sup>H NMR, COSY, NOESY** (400 MHz, CDCl<sub>3</sub>)  $\delta$  /ppm = 5.64 (dd,  $J$  = 5.5, 2.2 Hz, 1H, H-6), 5.49 (ddd,  $J$  = 5.5, 2.3, 0.8 Hz, 1H, H-5), 3.73 (t,  $J$  = 9.5 Hz, 1H, H-3<sub>a</sub>), 3.51 (d,  $J$  = 4.1 Hz, 2H, H-1<sub>a,b</sub>), 3.42 (dd,  $J$  = 10.6, 3.6 Hz, 1H, H-3<sub>b</sub>), 3.01 (dd,  $J$  = 5.3, 2.3 Hz, 1H, H-4<sub>a</sub>), 2.52 (dtd,  $J$  = 9.5, 6.2, 3.2 Hz, 1H, H-3<sub>a</sub>), 1.92 (dt,  $J$  = 6.2, 1.0 Hz, 1H, H-4<sub>b</sub>), 1.83 (dd,  $J$  = 5.1, 2.2 Hz, 1H, H-4<sub>a</sub>), 1.75–1.72 (m, 1H, H-6<sub>a</sub>), 1.32 (s, 3H, CH<sub>3</sub>-C-6<sub>b</sub>).

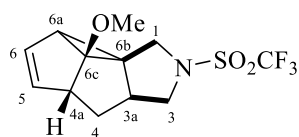
**$^{13}\text{C}$  NMR, HSQC, HMBC** (101 MHz,  $\text{CDCl}_3$ )  $\delta$  /ppm = 133.6 (C-5), 128.2 (C-6), 120.4 (q,  $\text{CF}_3$ ,  $J = 323.8$  Hz), 57.2 (C-4a), 54.2 (C-3), 48.9 (C-1), 48.1 (C-6b), 47.3 (C-6b), 46.0 (C-4), 41.3 (C-3a), 39.4 (C-6a), 13.7 ( $\text{CH}_3$ -C-6b).

**$^{19}\text{F}$  NMR** (376 MHz,  $\text{CDCl}_3$ )  $\delta$  /ppm = -76.2 (s,  $\text{CF}_3$ ).

**MS** (EI):  $m/z = 293.1$  [ $\text{M}$ ] $^+$ .

**HRMS** (API)  $m/z = [\text{M}]^+$  calcd. for  $\text{C}_{12}\text{H}_{14}\text{F}_3\text{NO}_2\text{S}$ : 293.0697, found: 293.0696.

**(3a*S*,4a*R*,6c*R*)-6c-Methoxy-2-[(trifluoromethyl)sulfonyl]-1,2,3,3a,4,4a,6a,6c-octahydro cyclopropa[1,6]pentaleno[1,2-*c*]pyrrole (214f)**



Following the general procedure, a mixture of allyl benzylamine **213f** (100.0 mg, 0.32 mmol) and 10 mL of anhydrous cyclohexane was irradiated for 3.0 h. After column chromatography ( $\text{SiO}_2$ , eluent: cyclohexane/ethyl acetate, 100:0  $\rightarrow$  98:1) a 94:6 colorless oil mixture of two isomeric *meta*-photocycloadducts were isolated (30.0 mg, 0.10 mmol, 30%).

$R_f = 0.56$  [ $\text{KMnO}_4$ ] (6:1 cyclohexane/ethyl acetate).

**IR** (ATR):  $\tilde{\nu}/\text{cm}^{-1} = 2943, 1452, 1385, 1297, 1225, 1181, 1149, 1091, 1055, 742$ .

Spectroscopic data are those of the major isomer:

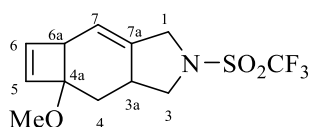
**$^1\text{H}$  NMR, COSY NOESY** (400 MHz,  $\text{CDCl}_3$ )  $\delta$  /ppm = 5.67 (dd,  $J = 5.7, 2.4$  Hz, 1H, H-6), 5.49 (ddd,  $J = 5.7, 2.7, 1.2$  Hz, 1H, H-5), 3.80 (d,  $J = 10.4$  Hz, 2H, H-1<sub>a</sub>), 3.76 (d,  $J = 9.4$  Hz, 1H, H-3<sub>a</sub>), 3.56 (d,  $J = 10.4$  Hz, 2H, H-1<sub>b</sub>), 3.42 (dd,  $J = 10.4, 3.6$  Hz, 1H, H-3<sub>b</sub>), 3.41--3.39 (m, 1H, H-4a), 3.41 (s, 3H,  $\text{OCH}_3$ ), 2.45--2.40 (m, 1H, H-3a), 2.23--2.21 (m, 1H, H-6a), 2.01--1.96 (m, 2H, H-4<sub>a,b</sub>).

**$^{13}\text{C}$  NMR, HSQC, HMBC** (101 MHz,  $\text{CDCl}_3$ )  $\delta$  /ppm = 133.4 (C-5), 127.5 (C-6), 124.1 (q,  $J = 401.6$  Hz,  $\text{CF}_3$ ), 89.3 (C-4a<sup>1</sup>), 57.2 ( $\text{OCH}_3$ ), 54.2 (C-3), 52.7 (C-4a), 49.8 (C-6b), 47.5 (C-1), 45.3 (C-4), 40.9 (C-3a), 38.1 (C-6a).

**MS** (EI):  $m/z = 309.1$  [ $\text{M}$ ] $^+$ .

**HRMS** (API)  $m/z = [\text{M}]^+$  calcd. for  $\text{C}_{12}\text{H}_{14}\text{F}_3\text{NO}_3\text{S}$ : 309.0641, found: 309.0640.

### 4a-Methoxy-2-[(trifluoromethyl)sulfonyl]-2,3,3a,4,4a,6a-hexahydro-1H-cyclobuta[f]is oindole (231)



Following the general procedure, a mixture of allyl benzylamine **213f** (100.0 mg, 0.32 mmol) and 10 mL of anhydrous cyclohexane was irradiated for 3.0 h. After column chromatography (SiO<sub>2</sub>, eluent: cyclohexane/ethyl acetate, 100:0 → 98:1) the title compound (27.0 mg, 0.10 mmol, 27%) was isolated as a colorless oil.

$R_f = 0.45$  [KMnO<sub>4</sub>] (3:1 cyclohexane/ethyl acetate).

IR (ATR):  $\tilde{\nu}/\text{cm}^{-1} = 2978, 1695, 1583, 4354, 1224, 991, 757$ .

<sup>1</sup>H NMR, COSY (400 MHz, CDCl<sub>3</sub>)  $\delta$  /ppm = 5.18 (dt,  $J = 2.8, 0.8$  Hz, 1H, H-6), 6.08 (dd,  $J = 2.8, 0.9$  Hz, 1H, H-5), 5:77 (dq,  $J = 5.3, 2.5$  Hz, 1H, H-7), 4.26 (d,  $J = 14.4$  Hz, 1H, H-1<sub>a</sub>), 4.16 (d,  $J = 14.4$  Hz, 1H, H-1<sub>b</sub>), 4.07–3.99 (m, 1H, H-3<sub>a</sub>), 3.39 (dq,  $J = 6.1, 0.8$  Hz, 1H, H-6<sub>a</sub>), 3.33 (s, 3H, OCH<sub>3</sub>), 3.20 (ddt,  $J = 11.4, 10.0, 1.4$  Hz, 1H, H-3<sub>b</sub>), 2.75–2.62 (m, 1H, H-3<sub>a</sub>), 2.18 (dd,  $J = 12.5, 5.2$  Hz, 1H, H-4<sub>a</sub>), 1.32 (t,  $J = 12.4$  Hz, 1H, H-4<sub>b</sub>).

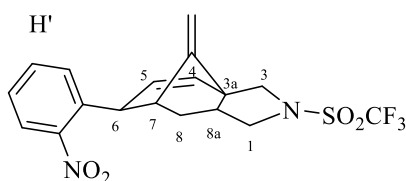
<sup>13</sup>C NMR, HSQC, HMBC (101 MHz, CDCl<sub>3</sub>)  $\delta$  /ppm = 139.8 (C-7<sub>a</sub>), 138.8 (C-5), 136.7 (C-6), 120.4 (q,  $J = 324.5$  Hz, CF<sub>3</sub>), 119.9 (C-7), 84.1 (C-4<sub>a</sub>), 54.5 (C-3), 52.0 (C-1), 51.9 (OCH<sub>3</sub>), 46.3 (C-6<sub>a</sub>), 36.2 (C-3<sub>a</sub>), 34.4 (C-4).

MS (ED):  $m/z = 309.1$  [M]<sup>+</sup>.

HRMS (API)  $m/z = [M]^+$  calcd. for C<sub>12</sub>H<sub>14</sub>F<sub>3</sub>NO<sub>3</sub>S: 309.0641, found: 309.0630.

### Reactions using *meta* photocycloadducts

#### Synthesis of the 9-methylidene-6-(2-nitrophenyl)-2-[(trifluoromethyl)sulfonyl]-2,3,6,7,8,8a-hexahydro-1H-3a,7-methanocyclohepta[c]pyrrole (217c)



A mixture of *meta* photoadduct **214e** (100 mg, 0.34 mmol, 1.00 equiv.), 1-iodo-2-nitrobenzene (91.7 mg, 0.37 mmol, 1.08 equiv.), palladium(II) acetate (4.2 mg, 0.02 mmol, 0.05 equiv.), 1,2-bis(diphenylphosphino)ethane (6.8 mg, 0.02 mmol, 0.05 equiv.), triethylamine (0.051 mL, 0.36 mmol, 1.08 equiv.), and 2.0 mL of dry DMF was added to a sealed reaction tube which was flushed with nitrogen and heated while stirring at 120 °C. After 2 h, the reaction was poured into a solution of HCl 2.0 M. The resulting solution was extracted with diethyl ether (3x20 mL), washed with water (3x20 mL), and dried over Na<sub>2</sub>SO<sub>4</sub> and concentrated under vacuum. The product was obtained after being purified by flash chromatography (SiO<sub>2</sub>, eluent: cyclohexane/ethyl acetate, 70:1 → 30:1) as a colorless solid (22.0 mg, 0.05 mmol, 16 % yield).

**R<sub>f</sub>** = 0.23 (10:1 cyclohexane/ethyl acetate).

**Mp** = 128–130 °C (cyclohexane-ethyl acetate)

**IR** (ATR):  $\tilde{\nu}/\text{cm}^{-1}$  = 2958, 1522, 1385, 1347, 1225, 1181, 1049, 1037, 898, 740.

**<sup>1</sup>H NMR, COSY NOESY** (400 MHz, CDCl<sub>3</sub>)  $\delta$  /ppm = 7.92 (dd, *J* = 8.1, 1.4 Hz, 1H, H-3'), 7.51 (td, *J* = 7.6, 1.5 Hz, 1H, H-5'), 7.42–7.37 (m, 1H, H-4'), 7.23 (dd, *J* = 7.8, 1.5 Hz, 1H, H-6'), 6.04 (dd, *J* = 9.3, 1.8 Hz, 1H, H-4), 5.51 (ddd, *J* = 9.3, 3.5, 1.5 Hz, 1H, H-5), 4.84 (s, 1H, -C=CH<sub>2</sub>), 4.52 (s, 1H, -C=CH<sub>2</sub>), 4.10 (dt, *J* = 3.5, 1.7 Hz, 1H, H-6), 4.06 (d, *J* = 10.5 Hz, 1H, H-3<sub>a</sub>), 3.85–3.76 (m, 1H, H-1<sub>a</sub>), 3.57 (d, *J* = 10.4 Hz, 1H, H-3<sub>b</sub>), 3.01–2.91 (m, 3H, H-1<sub>b</sub>, H-7, H-8<sub>a</sub>), 2.02 (ddd, *J* = 14.1, 7.6, 1.4 Hz, 1H, H-8<sub>a</sub>), 1.93 (ddd, *J* = 14.1, 7.2, 2.0 Hz, 1H, H-8<sub>b</sub>).

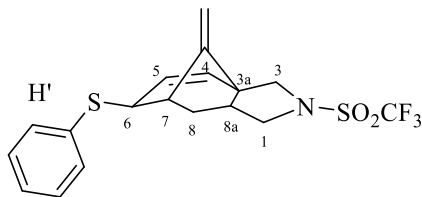
**<sup>13</sup>C NMR, HSQC, HMBC** (101 MHz, CDCl<sub>3</sub>)  $\delta$  /ppm = 148.8 (C-2'), 146.9 (-C=CH<sub>2</sub>), 135.8 (C-1'), 134.2 (C-4), 132.5 (C-5'), 131.5 (C-6'), 129.0 (C-5), 127.9 (C-4'), 124.7 (C-3'), 120.4 (q, *J* = 323.5 Hz, CF<sub>3</sub>), 104.1 (-C=CH<sub>2</sub>), 54.8 (C-3<sub>a</sub>), 54.3 (C-1), 51.9 (C-3), 51.3 (C-7), 49.6 (C-6), 49.4 (C-8<sub>a</sub>), 33.1 (C-8).

**<sup>19</sup>F NMR** (376 MHz, CDCl<sub>3</sub>)  $\delta$  /ppm = -76.3 (s, CF<sub>3</sub>).

**MS** (ESI): *m/z* = 415.1 [M + H]<sup>+</sup>.

**HRMS** (ESI-ToF) *m/z* = [M + H]<sup>+</sup> calcd for C<sub>18</sub>H<sub>18</sub>F<sub>3</sub>N<sub>2</sub>O<sub>4</sub>S: 415.0934, found: 415.0932.

**Synthesis of the 9-methylidene-6-(phenylsulfanyl)-2-[(trifluoromethyl)sulfonyl]-2,3,6,7,8,8a-hexahydro-1H-3a,7-methanocyclohepta[c]pyrrole (217k)**



To a sealed reaction tube with a magnetic stirring bar was added *meta* photoadduct **214e** (50 mg, 0.15 mmol, 1.00 equiv.), Cu(OTf)<sub>2</sub> (6.17 mg, 0.02 mmol, 0.10 equiv.), and I<sub>2</sub> (43.3 mg, 0.02 mmol, 1.00 equiv.) in DMSO (1.5 mL) under air atmosphere. The reaction was stirred at 110 °C for 24 h. After the complete consumption of the starting material, the mixture was poured into ethyl acetate, which was washed with saturated Na<sub>2</sub>S<sub>2</sub>O<sub>3</sub> (2 x 5 mL) and then brine (1 x 5 mL). After the aqueous layer was extracted with ethyl acetate (3x 15 mL), the combined organic layers were dried over anhydrous Na<sub>2</sub>SO<sub>4</sub> and evaporated under vacuum. The product was obtained after being purified by flash chromatography (SiO<sub>2</sub>, eluent: cyclohexane/ethyl acetate, 50:1 → 20:1) as a yellowish oil (8.0 mg, 0.02 mmol, 11 % yield).

*R<sub>f</sub>* = 0.19 (20:1 cyclohexane/ethyl acetate).

**<sup>1</sup>H NMR, COSY NOESY** (400 MHz, CDCl<sub>3</sub>) δ /ppm = 7.46–7.41 (m, 2H, H-2',6'), 7.36–7.29 (m, 2H, H-3',5'), 7.28–7.24 (m, 1H, H-4'), 5.86 (dd, *J* = 9.2, 1.3 Hz, 1H, H-4), 5.68 (ddd, *J* = 9.3, 3.8, 1.5 Hz, 1H, H-5), 5.13 (s, 1H, -C=CH<sub>2</sub>), 4.98 (s, 1H, -C=CH<sub>2</sub>), 4.03 (d, *J* = 10.0 Hz, 1H, H-3<sub>a</sub>), 3.88 (dt, *J* = 3.7, 2.0 Hz, 1H, H-6), 3.75 (t, *J* = 9.0 Hz, 1H, H-1<sub>a</sub>), 3.49 (d, *J* = 11.1 Hz, 1H, H-3<sub>b</sub>), 3.01 (d, *J* = 4.3 Hz, 1H, H-7), 2.95 (t, *J* = 9.8 Hz, 1H, H-1<sub>b</sub>), 2.86–2.77 (m, 1H, H-8<sub>a</sub>), 1.81–1.74 (m, 2H, H-8<sub>a</sub>,8<sub>b</sub>).

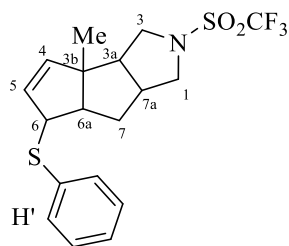
**<sup>13</sup>C NMR, HSQC, HMBC** (101 MHz, CDCl<sub>3</sub>) δ /ppm = 146.8 (-C=CH<sub>2</sub>), 135.4 (C-1'), 134.1 (C-4), 131.9 (C-2'',6''), 129.3 (C-3'',5''), 127.4 (C-4'), 127.3 (C-5), 120.4 (q, *J* = 323.9 Hz, CF<sub>3</sub>), 104.7 (-C=CH<sub>2</sub>), 56.7 (C-6), 54.8 (C-3<sub>a</sub>), 54.0 (C-1), 51.8 (C-3), 51.0 (C-8<sub>a</sub>), 47.5 (C-7), 31.8 (C-8).

**<sup>19</sup>F NMR** (376 MHz, CDCl<sub>3</sub>) δ/ppm = -76.3 (s, CF<sub>3</sub>).

**MS** (ESI): *m/z* = 402.1 [M + H]<sup>+</sup>.

**HRMS** (ESI-ToF) *m/z* = [M + H]<sup>+</sup> calcd for C<sub>18</sub>H<sub>19</sub>F<sub>3</sub>NO<sub>2</sub>S<sub>2</sub>: 402,0804, found: 402.0806.

**3b-Methyl-6-(phenylsulfanyl)-2-[(trifluoromethyl)sulfonyl]-2,3,3a,3b,6,6a,7,7a-octahydro-1H-pentaleno[1,2-c]pyrrole (216w)**



To a sealed reaction tube with a magnetic stirring bar was added *meta* photoadduct **214e** (60 mg, 0.20 mmol, 1.00 equiv.), and thiophenol (20.8  $\mu$ L, 0.20 mmol, 1.00 equiv.) in toluene (0.5 mL) under argon atmosphere. After stirring the reaction mixture for 24 h at 100  $^{\circ}$ C, the crude reaction mixture was concentrated to dryness. The product was obtained after being purified by flash chromatography (SiO<sub>2</sub>, eluent: cyclohexane/ethyl acetate, 40:0  $\rightarrow$  10:1) as a colorless solid (41.3 mg, 0.1 mmol, 50%).

$R_f$  = 0.25 (20:1 cyclohexane/ethyl acetate).

**<sup>1</sup>H NMR, COSY NOESY** (400 MHz, CDCl<sub>3</sub>)  $\delta$  /ppm = 7.39–7.30 (m, 2H, H-2',6'), 7.35–7.26 (m, 2H, H-3',5'), 7.28–7.19 (m, 1H, H-4'), 5.72 (dd,  $J$  = 5.5, 2.4 Hz, 1H, H-5), 5.57 (dd,  $J$  = 5.5, 1.5 Hz, 1H, H-4), 3.99 (dt,  $J$  = 2.7, 1.5 Hz, 1H, H-6), 3.67–3.63 (m, 1H, H-3a), 3.63–3.58 (m, 1H, H-1a), 3.42 (d,  $J$  = 10.0 Hz, 1H, H-1b), 3.35 (t,  $J$  = 9.5 Hz, 1H, H-3b), 2.69 (ddt,  $J$  = 10.0, 6.0, 1.7 Hz, 1H, H-7a), 2.62–2.49 (m, 2H, H-3a,6a), 2.04–1.90 (m, 1H, H-7a), 1.88–1.77 (m, 1H, H-7b), 1.12 (s, 3H, CH<sub>3</sub>).

**<sup>13</sup>C NMR, HSQC, HMBC** (101 MHz, CDCl<sub>3</sub>)  $\delta$  /ppm = 142.0 (C-4), 135.9 (C-1'), 131.0 (C-2'',6''), 129.3 (C-5), 129.1 (C-3'',5''), 126.9 (C-4'), 120.5 (q,  $J$  = 323.9 Hz, CF<sub>3</sub>), 61.4 (C-6), 59.6 (C-3b), 54.9 (C-3a), 53.5 (C-1), 52.7 (C-6a), 49.8 (C-3), 43.2 (C-7a), 38.3 (C-7), 22.8 (CH<sub>3</sub>).

**<sup>19</sup>F NMR** (376 MHz, CDCl<sub>3</sub>)  $\delta$ /ppm = -76.2 (s, CF<sub>3</sub>).

**MS** (ESI):  $m/z$  = 404.1 [M + H]<sup>+</sup>.

**HRMS** (APCI)  $m/z$  = [M]<sup>+</sup> calcd for C<sub>18</sub>H<sub>20</sub>F<sub>3</sub>NO<sub>2</sub>S<sub>2</sub>: 403.0883, found: 403.0878.

## General procedure for the synthesis of alkynyl sulfones (218)

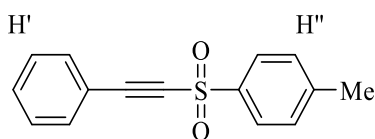
### Method A

A solution of ceric ammonium nitrate (2.50 equiv.) in CH<sub>3</sub>CN (c = 0.25 mmol/mL) was added dropwise to a stirred mixture of the corresponding alkyne (1.00 equiv.), the sodium sulfinate (1.20 equiv.) and sodium iodide (1.20 equiv.) in the same solvent (c=0.20 mmol/mL) under nitrogen atmosphere. After approximately 1 h, the solvent was removed, and the residue was re-dissolved in ethyl acetate and washed with Na<sub>2</sub>S<sub>2</sub>O<sub>3</sub>(aq) (3×50 mL) followed by brine (50 mL) and dried over Na<sub>2</sub>SO<sub>4</sub>. The solvent was removed, and the crude product was refluxed with K<sub>2</sub>CO<sub>3</sub> (2.00 equiv.) in anhydrous acetone (c= 0.4 mmol/mL) until TLC or HPLC/ESI-MS indicated full consumption of the starting material. The reaction mixture was washed with H<sub>2</sub>O (50 mL) and extracted with CH<sub>2</sub>Cl<sub>2</sub> (3×20 mL). The combined organic extracts were washed with brine and dried over anhydrous Na<sub>2</sub>SO<sub>4</sub>. The solvent was removed *in vacuo* and the residue was purified by flash column chromatography (SiO<sub>2</sub>, eluent: cyclohexane/ethyl acetate, 97:3) to afford the expected acetylenic sulfone.

### Method B

A mixture of the corresponding sodium sulfinate (2.00 equiv.), alkyne (1.00 equiv.), and iodine (1.50 equiv.) in water (c=0.15 mmol/mL) was stirred at room temperature for 2h. After the reaction was completed, the mixture was quenched with Na<sub>2</sub>S<sub>2</sub>O<sub>3</sub>(aq) (10 mL). Further stirring was followed by extraction with ethyl acetate (3 × 30 mL). The organic layer was dried with anhydrous Na<sub>2</sub>SO<sub>4</sub> and concentrated *in vacuo*. The residue was refluxed with K<sub>2</sub>CO<sub>3</sub> (2.00 equiv.) in anhydrous acetone (c= 0.4 mmol/mL) until TLC or HPLC/ESI-MS indicated full consumption of the starting material. the reaction mixture was washed with H<sub>2</sub>O (50 mL) and extracted with CH<sub>2</sub>Cl<sub>2</sub> (3×20 mL). The combined organic extracts were washed with brine and dried over anhydrous Na<sub>2</sub>SO<sub>4</sub>. The solvent was removed *in vacuo* and the residue was purified by flash column chromatography (SiO<sub>2</sub>, eluent: cyclohexane/ethyl acetate, 97:3) to afford the expected acetylenic sulfone.

### 1-Methyl-4-(phenylethynyl)sulfone (218a)





Following the general procedure A with phenylacetylene (1.00 g, 9.8 mmol, 1.00 equiv.) and sodium *p*-toluenesulfinate (2.10 g, 11.8 mmol, 1.20 equiv.) the title compound (1.70 g, 6.63 mmol, 68%) was isolated as a colorless solid.

$R_f$  = 0.52 (3:1 cyclohexane/ethyl acetate).

**Mp** = 77–78 °C (cyclohexane-ethyl acetate) Lit.:<sup>[198]</sup> 78–79 °C.

**IR** (ATR):  $\tilde{\nu}/\text{cm}^{-1}$  = 2988, 2179, 1593, 1486, 1443, 1322, 1291, 1180, 1080, 679.

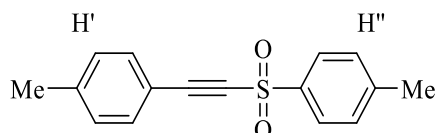
**<sup>1</sup>H NMR, COSY** (400 MHz, CDCl<sub>3</sub>)  $\delta$  /ppm = 7.96 (d,  $J$  = 8.4 Hz, AA' part of AA'BB' system, 2H, H-2'',6''), 7.54–7.50 (m, 2H, H-2',6'), 7.49–7.44 (m, 1H, H-4'), 7.41–7.33 (m, 4H, H-3',5'/H-3'',5''), 2.47 (s, 3H, –CH<sub>3</sub>).

**<sup>13</sup>C NMR, HSQC, HMBC** (101 MHz, CDCl<sub>3</sub>)  $\delta$  /ppm = 145.5 (C-4''), 139.1 (C-1''), 132.9 (C-2',6'), 131.6 (C-4'), 130.2 (C-3'',5''), 128.8 (C-3',5'), 127.8 (C-2'',6''), 118.2 (C-1'), 93.1 (–C≡C–SO<sub>2</sub>), 85.8 (–C≡C–SO<sub>2</sub>), 21.9 (–CH<sub>3</sub>).

**MS** (ESI):  $m/z$  = 257.0 [M + H]<sup>+</sup>.

The spectroscopic data are in accordance with the literature.<sup>[198-199]</sup>

### 1-Methyl-4-[(4-methylbenzene-1-sulfonyl)ethynyl]benzene (218b)



Following the general procedure A with 4-ethynyltoluene (0.50 g, 4.30 mmol, 1.00 equiv.) and sodium *p*-toluenesulfinate (2.10 g, 5.17 mmol, 1.20 equiv.) the title compound (0.81 g, 3.00 mmol, 70%) was isolated as a colorless solid.

$R_f$  = 0.52 (3:1 cyclohexane/ethyl acetate).

**Mp** = 103 – 104 °C (cyclohexane-ethyl acetate) Lit.:<sup>[198]</sup> 103–105 °C.

**IR** (ATR):  $\tilde{\nu}/\text{cm}^{-1}$  = 2988, 2177, 1594, 1486, 1441, 1328, 1155, 1085, 859, 606.

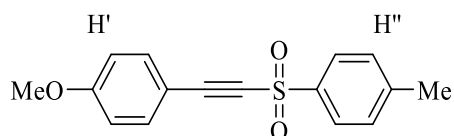
**<sup>1</sup>H NMR, COSY** (400 MHz, CDCl<sub>3</sub>)  $\delta$  /ppm = 7.95 (d,  $J$  = 8.3 Hz, AA' part of AA'BB' system, 2H, H-2'',6''), 7.41 (d,  $J$  = 8.2 Hz, AA' part of AA'BB' system, 2H, H-2',6'), 7.38 (d,  $J$  = 8.3 Hz, BB' part of AA'BB' system, 2H, H-3'',5''), 7.17 (d,  $J$  = 8.2 Hz, BB' part of AA'BB' system, 2H, H-3',5'), 2.47 (s, 3H, –CH<sub>3</sub>''), 2.37 (s, 3H, –CH<sub>3</sub>').

**<sup>13</sup>C NMR, HSQC, HMBC** (101 MHz, CDCl<sub>3</sub>)  $\delta$  /ppm = 145.4 (C-4''), 142.4 (C-4'), 139.2 (C-1''), 132.8 (C-2',6'), 130.1 (C-3'',5''), 129.6 (C-3',5'), 127,8 (C-2'',6''), 115.0 (C-1'), 93.8 (–C≡C–SO<sub>2</sub>), 85.3 (–C≡C–SO<sub>2</sub>), 21.9 (–CH<sub>3</sub>'), 21.8 (–CH<sub>3</sub>'').

**MS (ESI):**  $m/z = 271.0$  [M + H]<sup>+</sup>.

The spectroscopic data are in accordance with the literature.<sup>[198-199]</sup>

### 1-Methoxy-4-[(4-methylbenzene-1-sulfonyl)ethynyl]benzene (218c)



Following general procedure A with 1-ethynyl-4-methoxybenzene (0.60 g, 4.54 mmol, 1.00 equiv.) and sodium *p*-toluenesulfinate (0.97 g, 5.45 mmol, 1.20 equiv.) the title compound (0.65 g, 6.63 mmol, 50%) was isolated as a yellow solid.

**R<sub>f</sub>** = 0.34 (3:1 cyclohexane/ethyl acetate).

**Mp** = 123–124 °C (cyclohexane-ethyl acetate) Lit.:<sup>[198]</sup> 123–124 °C.

**IR** (ATR):  $\tilde{\nu}/\text{cm}^{-1} = 2173, 1602, 1509, 1442, 1328, 1258, 1173, 1085, 861, 670$ .

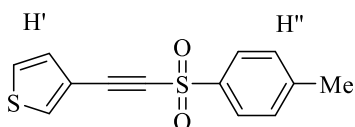
**<sup>1</sup>H NMR, COSY** (400 MHz, CDCl<sub>3</sub>)  $\delta$  /ppm = 7.95 (d,  $J = 8.4$  Hz, AA' part of AA'BB' system, 2H, H-2'',6''), 7.46 (d,  $J = 8.9$  Hz, AA' part of AA'BB' system, 2H, H-2',6'), 7.38 (d,  $J = 8.4$  Hz, BB' part of AA'BB' system, 2H, H-3'',5''), 6.86 (d,  $J = 8.9$  Hz, BB' part of AA'BB' system, 2H, H-3',5'), 3.82 (s, 3H, –OCH<sub>3</sub>), 2.46 (s, 3H, –CH<sub>3</sub>).

**<sup>13</sup>C NMR, HSQC, HMBC** (101 MHz, CDCl<sub>3</sub>)  $\delta$  /ppm = 162.2 (C-4'), 145.3 (C-4''), 139.4 (C-1''), 134.8 (C-2',6'), 130.1 (C-3'',5''), 127,5 (C-2'',6''), 114.5 (C-3',5'), 109.8 (C-1'), 94.2 (–C≡C–SO<sub>2</sub>), 85.0 (–C≡C–SO<sub>2</sub>), 25.6 (–OCH<sub>3</sub>), 21.9 (–CH<sub>3</sub>).

**MS (ESI):**  $m/z = 287.0$  [M + H]<sup>+</sup>.

The spectroscopic data are in accordance with the literature.<sup>[198]</sup>

### 3-[(4-Methylbenzene-1-sulfonyl)ethynyl]thiophene (218d)



Following general procedure A with 3-ethynylthiophene (0.30 g, 2.77 mmol, 1.00 equiv.) and sodium *p*-toluenesulfinate (0.59 g, 3.33 mmol, 1.20 equiv.) the title compound (0.44 g, 1.67 mmol, 60%) was isolated as a colorless solid.

$R_f$  = 0.34 (3:1 cyclohexane/ethyl acetate).

$Mp$  = 98–99 °C (cyclohexane-ethyl acetate) Lit.:<sup>[199]</sup> 74.2–75.3 °C.

**IR** (ATR):  $\tilde{\nu}/\text{cm}^{-1}$  = 2171, 2166, 1593, 1359, 1152, 1083, 950, 875, 838, 741.

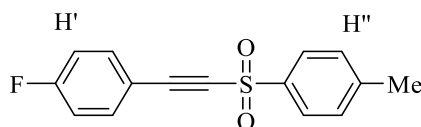
**$^1\text{H}$  NMR, COSY** (400 MHz,  $\text{CDCl}_3$ )  $\delta$  /ppm = 7.95 (d,  $J$  = 8.4 Hz, AA' part of AA'BB' system, 2H, H-2'',6''), 7.74 (dd,  $J$  = 3.0, 1.2 Hz, 1H, H-5'), 7.39 (d,  $J$  = 8.4 Hz, BB' part of AA'BB' system, 2H, H-3'',5''), 7.32 (dd,  $J$  = 5.0, 1.3 Hz, 1H, H-4'), 7.03 (d,  $J$  = 8.3 Hz, BB' part of AA'BB' system, 2H, H-3'',5''), 7.17 (dd,  $J$  = 5.0, 1.2 Hz, 1H, H-2'), 2.47 (s, 3H, -CH<sub>3</sub>).

**$^{13}\text{C}$  NMR, HSQC, HMBC** (101 MHz,  $\text{CDCl}_3$ )  $\delta$  /ppm = 145.5 (C-4''), 139.1 (C-1''), 134.7 (C-5'), 130.1 (C-3'',5''), 130.0 (C-2'), 127.7 (C-2'',6''), 126.6 (C-4'), 117.4 (C-3'), 88.7 (-C $\equiv$ C-SO<sub>2</sub>), 85.7 (-C $\equiv$ C-SO<sub>2</sub>), 21.9 (-CH<sub>3</sub>).

**MS** (ESI):  $m/z$  = 263.0 [M + H]<sup>+</sup>.

The spectroscopic data are in accordance with the literature.<sup>[199]</sup>

### 1-Fluoro-4-[(4-methylbenzene-1-sulfonyl)ethynyl]benzene (218e)



Following general procedure A with 1-ethynyl-4-fluorobenzene (0.50 g, 4.16 mmol, 1.00 equiv.) and sodium *p*-toluenesulfinate (0.89 g, 5.00 mmol, 1.20 equiv.) the title compound (0.46 g, 1.68 mmol, 40%) was isolated as a colorless solid.

$R_f$  = 0.43 (3:1 cyclohexane/ethyl acetate).

$Mp$  = 85–87 °C (cyclohexane-ethyl acetate) Lit.:<sup>[200]</sup> 86.0–87.0 °C.

**IR** (ATR):  $\tilde{\nu}/\text{cm}^{-1}$  = 2183, 1598, 1506, 1402, 1332, 1239, 1158, 1087, 863, 669.

**$^1\text{H}$  NMR, COSY** (400 MHz,  $\text{CDCl}_3$ )  $\delta$  /ppm = 7.95 (d,  $J$  = 8.4 Hz, AA' part of AA'BB' system, 2H, H-2'',6''), 7.56–7.50 (m, AA' part of AA'BB' system, 2H, H-2',6'), 7.39 (d,

$J = 8.4$  Hz, BB' part of AA'BB' system, 2H, H-3'',5''), 7.11–7.02 (m, BB' part of AA'BB' system, 2H, H-3',5'), 2.47 (s, 3H, –CH<sub>3</sub>).

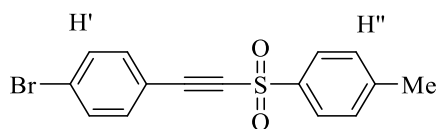
**<sup>13</sup>C NMR, HSQC, HMBC** (101 MHz, CDCl<sub>3</sub>)  $\delta$  /ppm = 162.5 (d,  $J_{CF} = 255.2$  Hz, C-4'), 145.6 (C-4''), 138.9 (C-1''), 135.3 (d,  $J_{CF} = 9.0$  Hz, C-2',6'), 130.2 (C-3'',5''), 127,7 (C-2'',6''), 116.5 (d,  $J_{CF} = 22.4$  Hz, C-3',5'), 114.3 (C-1'), 92.0 (–C≡C–SO<sub>2</sub>), 85.7 (–C≡C–SO<sub>2</sub>), 21.9 (–CH<sub>3</sub>).

**<sup>19</sup>F NMR** (376 MHz, CDCl<sub>3</sub>)  $\delta$  /ppm = –105.77 (tt,  $J = 9.2, 5.2$  Hz, 1F, F–C-4').

**MS** (ESI):  $m/z = 275.0$  [M + H]<sup>+</sup>.

The spectroscopic data are in accordance with the literature.<sup>[199-200]</sup>

### 1-Bromo-4-[(4-methylbenzene-1-sulfonyl)ethynyl]benzene (218f)



Following general procedure A with 1-bromo-4-ethynylbenzene (0.50 g, 2.76 mmol, 1.00 equiv.) and sodium *p*-toluenesulfinate (0.59 g, 3.31 mmol, 1.20 equiv.) the title compound (0.73 g, 2.18 mmol, 78%) was isolated as a colorless solid.

$R_f = 0.43$  (3:1 cyclohexane/ethyl acetate).

**Mp** = 105–106 °C (cyclohexane-ethyl acetate) Lit.:<sup>[200]</sup> 106.7–107.7 °C.

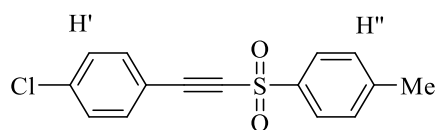
**IR** (ATR):  $\tilde{\nu}/\text{cm}^{-1} = 2183, 1583, 1485, 1395, 1332, 1185, 1159, 1086, 851, 652$ .

**<sup>1</sup>H NMR, COSY** (400 MHz, CDCl<sub>3</sub>)  $\delta$  /ppm = 7.95 (d,  $J = 8.4$  Hz, AA' part of AA'BB' system, 2H, H-2'',6''), 7.52 (d,  $J = 8.6$  Hz, AA' part of AA'BB' system, 2H, H-2',6'), 7.39 (d,  $J = 8.4$  Hz, BB' part of AA'BB' system, 2H, H-3'',5''), 7.36 (d,  $J = 8.6$  Hz, BB' part of AA'BB' system, 2H, H-3',5'), 2.47 (s, 3H, –CH<sub>3</sub>).

**<sup>13</sup>C NMR, HSQC, HMBC** (101 MHz, CDCl<sub>3</sub>)  $\delta$  /ppm = 145.7 (C-4''), 138.8 (C-1''), 134.1 (C-3',5'), 132.3 (C-2',6'), 130.2 (C-3'',5''), 127,7 (C-2'',6''), 126.6 (C-4'), 117.1 (C-1'), 91.7 (–C≡C–SO<sub>2</sub>), 86.7 (–C≡C–SO<sub>2</sub>), 21.9 (–CH<sub>3</sub>).

**MS** (ESI):  $m/z = 335.0$  [M + H]<sup>+</sup>.

The spectroscopic data are in accordance with the literature.<sup>[200]</sup>

**1-Chloro-4-[(4-methylbenzene-1-sulfonyl)ethynyl]benzene (218g)**

Following general procedure A with 1-chloro-4-ethynylbenzene (0.60 g, 4.39 mmol, 1.00 equiv.) and sodium *p*-toluenesulfinate (0.94 g, 5.27 mmol, 1.20 equiv.) the title compound (0.66 g, 2.28 mmol, 52%) was isolated as a colorless solid.

$R_f$  = 0.51 (3:1 cyclohexane/ethyl acetate).

**Mp** = 98–100 °C (cyclohexane-ethyl acetate) Lit.:<sup>[200]</sup> 98.7–99.2 °C.

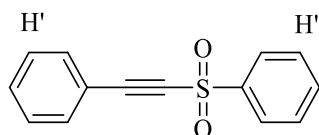
**IR** (ATR):  $\tilde{\nu}/\text{cm}^{-1}$  = 2182, 1592, 1488, 1400, 1331, 1185, 1159, 1087, 852, 659.

**<sup>1</sup>H NMR, COSY** (400 MHz, CDCl<sub>3</sub>)  $\delta$  /ppm = 7.95 (d,  $J$  = 8.4 Hz, AA' part of AA'BB' system, 2H, H-2'',6''), 7.44 (d,  $J$  = 8.6 Hz, AA' part of AA'BB' system, 2H, H-2',6'), 7.39 (d,  $J$  = 8.4 Hz, BB' part of AA'BB' system, 2H, H-3'',5''), 7.35 (d,  $J$  = 8.6 Hz, BB' part of AA'BB' system, 2H, H-3',5'), 2.47 (s, 3H, -CH<sub>3</sub>).

**<sup>13</sup>C NMR, HSQC, HMBC** (101 MHz, CDCl<sub>3</sub>)  $\delta$  /ppm = 145.7 (C-4''), 138.8 (C-1''), 138.1 (C-4'), 134.0 (C-2',6'), 130.2 (C-3'',5''), 129.3 (C-3',5'), 127.7 (C-2'',6''), 116.6 (C-1'), 91.6 (-C≡C-SO<sub>2</sub>), 86.6 (-C≡C-SO<sub>2</sub>), 21.9 (-CH<sub>3</sub>).

**MS** (ESI):  $m/z$  = 291.0 [M + H]<sup>+</sup>.

The spectroscopic data are in accordance with the literature.<sup>[199-200]</sup>

**[(Benzenesulfonyl)ethynyl]benzene (218h)**

Following general procedure A with phenylacetylene (0.80 g, 7.83 mmol, 1.00 equiv.) and sodium benzenesulfinate (1.54 g, 9.40 mmol, 1.20 equiv.) the title compound (1.21 g, 5.01 mmol, 64%) was isolated as a colorless solid.

$R_f$  = 0.41 (3:1 cyclohexane/ethyl acetate).

**Mp** = 67–69 °C (cyclohexane-ethyl acetate) Lit.:<sup>[199]</sup> 55.4–55.1 °C.

**IR** (ATR):  $\tilde{\nu}/\text{cm}^{-1} = 2988, 2179, 1328, 1159, 1086, 850, 756, 727, 685, 657$ .

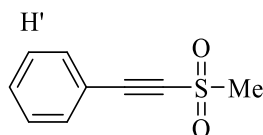
**$^1\text{H}$  NMR, COSY** (400 MHz,  $\text{CDCl}_3$ )  $\delta$  /ppm = 8.11–8.06 (m, 2H, H-2'',6''), 7.72–7.66 (m, 1H, H-4''), 7.63–7.57 (m, 2H, H-3'',5''), 7.54–7.50 (m, 2H, H-2',6'), 7.50–7.44 (m, 1H, H-4'), 7.40–7.33 (m, 2H, H-3',5').

**$^{13}\text{C}$  NMR, HSQC, HMBC** (101 MHz,  $\text{CDCl}_3$ )  $\delta$  /ppm = 141.8 (C-1''), 134.3 (C-4''), 132.9 (C-2',6'), 131.7 (C-4'), 129.5 (C-3'',5''), 128.8 (C-3',5'), 127.5 (C-2'',6''), 117.9 (C-1'), 93.6 ( $-\text{C}\equiv\text{C}-\text{SO}_2$ ), 85.4 ( $-\text{C}\equiv\text{C}-\text{SO}_2$ ).

**MS** (ESI):  $m/z = 243.0$   $[\text{M} + \text{H}]^+$ .

The spectroscopic data are in accordance with the literature.<sup>[199]</sup>

**[(Methanesulfonyl)ethynyl]benzene (218i)**



Following general procedure B with phenylacetylene (0.25 g, 2.45 mmol, 1.00 equiv.) and sodium methanesulfinate (0.50 g, 5.00 mmol, 2.00 equiv.) the title compound (0.28 g, 1.57 mmol, 64%) was isolated as a yellow solid.

$R_f = 0.28$  (3:1 cyclohexane/ethyl acetate).

**Mp** = 58–59 °C (cyclohexane-ethyl acetate) Lit.:<sup>[201]</sup> 57–58 °C.

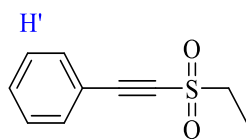
**IR** (ATR):  $\tilde{\nu}/\text{cm}^{-1} = 2988, 2928, 2184, 1489, 1322, 1149, 1066, 965, 847, 765$ .

**$^1\text{H}$  NMR, COSY** (400 MHz,  $\text{CDCl}_3$ )  $\delta$  /ppm = 7.65–7.58 (m, 2H, H-2',6'), 7.58–7.52 (m, 1H, H-4'), 7.48–7.41 (m, 2H, H-3',5'), 3.33 (s, 3H,  $-\text{SO}_2\text{CH}_3$ ).

**$^{13}\text{C}$  NMR, HSQC, HMBC** (101 MHz,  $\text{CDCl}_3$ )  $\delta$  /ppm = 133.0 (C-2',6'), 131.9 (C-4'), 129.0 (C-3',5'), 117.6 (C-1'), 91.7 ( $-\text{C}\equiv\text{C}-\text{SO}_2$ ), 84.5 ( $-\text{C}\equiv\text{C}-\text{SO}_2$ ), 47.0 ( $-\text{SO}_2\text{CH}_3$ ).

**MS** (ESI):  $m/z = 203.0$   $[\text{M} + \text{Na}]^+$ .

The spectroscopic data are in accordance with the literature.<sup>[201]</sup>

**[(Ethanesulfonyl)ethynyl]benzene (218j)**

Following general procedure B with phenylacetylene (0.30 g, 2.94 mmol, 1.00 equiv.) and sodium ethanesulfinate (0.62 g, 5.87 mmol, 2.00 equiv.) the title compound (0.11 g, 0.57 mmol, 20%) was isolated as a yellow oil.

$R_f = 0.35$  (3:1 cyclohexane/ethyl acetate).

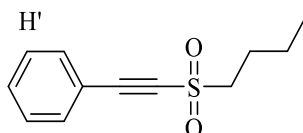
**IR** (ATR):  $\tilde{\nu}/\text{cm}^{-1} = 2984, 2184, 1492, 1324, 1141, 1047, 849, 760, 733, 690$ .

**$^1\text{H NMR}$ , COSY** (400 MHz,  $\text{CDCl}_3$ )  $\delta$  /ppm = 7.63–7.56 (m, 2H, H-2',6'), 7.56–7.48 (m, 1H, H-4'), 7.46–7.37 (m, 2H, H-3',5'), 3.30 (q,  $J = 7.4$  Hz, 2H,  $\text{SO}_2\text{CH}_2-$ ), 1.54 (t,  $J = 7.4$  Hz, 3H,  $-\text{CH}_3$ ).

**$^{13}\text{C NMR}$ , HSQC, HMBC** (101 MHz,  $\text{CDCl}_3$ )  $\delta$  /ppm = 133.0 (C-2',6'), 131.9 (C-4'), 129.0 (C-3',5'), 117.8 (C-1'), 92.7 ( $-\text{C}\equiv\text{C}-\text{SO}_2$ ), 82.8 ( $-\text{C}\equiv\text{C}-\text{SO}_2$ ), 52.9 ( $\text{SO}_2\text{CH}_2-$ ), 7.9 ( $-\text{CH}_3$ ).

**MS** (ESI):  $m/z = 217.0$  [ $\text{M} + \text{Na}$ ] $^+$ .

The spectroscopic data are in accordance with the literature.<sup>[201]</sup>

**[(Butane-1-sulfonyl)ethynyl]benzene (218k)**

Following general procedure B with 1-hexyne (0.60 g, 7.30 mmol, 1.00 equiv.) and sodium *p*-toluenesulfinate (2.60 g, 14.6 mmol, 2.00 equiv.) the title compound (1.04 g, 4.68 mmol, 64%) was isolated as a colorless oil.

$R_f = 0.50$  (3:1 cyclohexane/ethyl acetate).

**IR** (ATR):  $\tilde{\nu}/\text{cm}^{-1} = 2960, 2200, 1596, 1329, 1185, 1090, 814, 706, 678, 620$ .

**$^1\text{H NMR}$ , COSY** (400 MHz,  $\text{CDCl}_3$ )  $\delta$  /ppm = 7.85 (d,  $J = 8.4$  Hz, AA' part of AA'BB' system, 2H, H-2'',6''), 7.34 (d,  $J = 8.4$  Hz, BB' part of AA'BB' system, 2H, H-3'',5''), 2.44

(s, 3H,  $-\text{CH}_3$ ), 2.33 (t,  $J = 7.1$  Hz, 2H, H-1'), 1.55–1.45 (m, 2H, H-2'), 1.40–1.28 (m, 2H, H-3'), 0.86 (t,  $J = 7.3$  Hz, 3H, H-4').

$^{13}\text{C}$  NMR, HSQC, HMBC (101 MHz,  $\text{CDCl}_3$ )  $\delta$  /ppm = 145.2 (C-4''), 139.2 (C-1''), 129.9 (C-3'',5''), 127.3 (C-2'',6''), 97.4 ( $-\text{C}\equiv\text{C}-\text{SO}_2$ ), 78.4 ( $-\text{C}\equiv\text{C}-\text{SO}_2$ ), 133.0 (C-2'), 21.9 (C-3'), 21.8 ( $-\text{CH}_3$ ), 18.7 (C-1'), 13.4 (C-4').

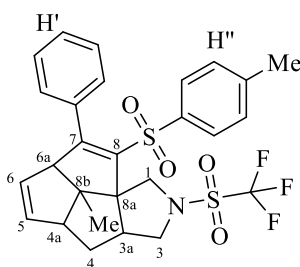
MS (ESI): 275.0  $m/z$  = 237.1  $[\text{M} + \text{H}]^+$ .

The spectroscopic data are in accordance with the literature.<sup>[201]</sup>

## General procedure for the synthesis of the tetracycle 219

The *meta* photoadduct **214e** (35.0 mg, 0.12 mmol, 1.00 equiv.), alkynyl sulfone **218** (0.24 mmol, 2.00 equiv.),  $\text{Ir}(\text{ppy})_2(\text{dtbbpy})\text{PF}_6$  (2.2 mg, 0.002 mmol, 0.02 equiv.) and methanol (0.8 mL,  $c = 0.15$  M) were loaded in an oven-dried Schlenk tube (10 mL) under nitrogen atmosphere, and the mixture was degassed and then placed in front of two blue LEDs 456 nm (see the materials section) at a distance of 5 cm. The vessel was irradiated until TLC or HPLC/ESI-MS indicated full consumption of the starting material (approx. 10-14 h). The resultant solution was concentrated and purified by flash column chromatography on silica gel (cyclohexane/ethyl acetate) or reversed-phase column chromatography ( $\text{SiO}_2\text{-C}_{18}$ , water/acetonitrile) to give the corresponding product **7** as a racemic mixture.

### 8b-Methyl-8-[(4-methylphenyl)sulfonyl]-7-phenyl-2-[(trifluoromethyl)sulfonyl]-1,2,3,3a,4,4a,6a,8b-octahydrocyclopenta[3,4]pentaleno[1,6a-c]pyrrole (219a)



Following the general procedure using 1-methyl-4-(phenylethynesulfonyl)benzene (61.2 mg, 0.24 mmol, 2.00 equiv.) after 10 h, column chromatography ( $\text{SiO}_2$ , eluent: cyclohexane/ethyl acetate, 95:1  $\rightarrow$  20:1) afforded the title compound (54.5 mg, 0.10 mmol, 85%) as a colorless solid.



**Non-catalyzed cycloaddition (sensitization protocol). Preparation of the tetracycle 219a.**

In an oven-dried quartz tube under nitrogen atmosphere was charged *meta* photoadduct **214e** (35.0 mg, 0.12 mmol, 1.00 equiv.), 1-methyl-4-(phenylethynylsulfonyl)benzene (61.2 mg, 0.24 mmol, 2.00 equiv.), and methanol (0.8 mL, *c* = 0.15 M). The solution was degassed for 15 min and placed in a Rayonet photoreactor. The vessel was irradiated ( $\lambda_{\text{max}} = 254 \text{ nm}$ ,  $16 \times 8 \text{ W}$ ) at room temperature for 14 h. After removal of the solvent under reduced pressure, column chromatography (SiO<sub>2</sub>, eluent: cyclohexane/ethyl acetate, 95:1 → 20:1) afforded the title compound (17.7 mg, 0.03 mmol, 27%) as a colorless solid.

**Synthesis of the tetracycle 219a using [Ir(dF(CF<sub>3</sub>)ppy)<sub>2</sub>(dtbbpy)]PF<sub>6</sub>**

The *meta* photoadduct **214e** (35.0 mg, 0.12 mmol, 1.00 equiv.), alkynyl sulfone **218a** (61.2 mg, 0.24 mmol, 2.00 equiv.), [Ir(dF(CF<sub>3</sub>)ppy)<sub>2</sub>(dtbbpy)]PF<sub>6</sub> (2.7 mg, 0.002 mmol, 0.02 equiv.) and methanol (0.8 mL, *c* = 0.15 M) were loaded in an oven-dried Schlenk tube (10 mL) under nitrogen atmosphere, and the mixture was degassed and then placed in front of two blue LEDs 440 nm (see the materials section) at a distance of 5 cm. After 10 h, the resultant solution was concentrated and purified by flash column chromatography (SiO<sub>2</sub>, eluent: cyclohexane/ethyl acetate, 95:1 → 20:1) to afford **7a** (56.5 mg, 0.10 mmol, 86%) as a colorless solid.

**R<sub>f</sub>** = 0.52 (3:1 cyclohexane/ethyl acetate).

**Mp** = 140–142 °C (ethanol).

**IR** (ATR):  $\tilde{\nu}/\text{cm}^{-1} = 3056, 2956, 2871, 1595, 1259, 1225, 1189, 1144, 720, 619$ .

**<sup>1</sup>H NMR, COSY, NOESY** (400 MHz, CDCl<sub>3</sub>)  $\delta$  /ppm = 7.26–7.23 (m, 1H, H-4'), 7.16 (t, *J* = 7.5 Hz, 2H, H-3', 5'), 7.05 (d, *J* = 8.4 Hz, AA' part of AA'BB' system, 2H, H-2'', 6''), 6.95 (d, *J* = 8.4 Hz, BB' part of AA'BB' system, 2H, H-3'', 5''), 6.85–6.73 (m, 2H, H-2', 6'), 5.81 (dt, *J* = 5.6, 2.2 Hz, 1H, H-5), 5.29 (ddd, *J* = 5.6, 2.7, 1.4 Hz, 1H, H-6), 4.59 (d, *J* = 10.2 Hz, 1H, H-1<sub>a</sub>), 4.03 (t, *J* = 9.4 Hz, 1H, H-3<sub>a</sub>), 3.98 (d, *J* = 10.2 Hz, 1H, H-1<sub>b</sub>), 3.79 (tdd, *J* = 8.6, 5.9, 2.4 Hz, 1H, H-3<sub>a</sub>), 3.38 (t, *J* = 9.4 Hz, 1H, H-3<sub>b</sub>), 3.35 (dd, *J* = 2.7, 1.9 Hz, 1H, H-6<sub>a</sub>), 2.98 (t, *J* = 8.4 Hz, 1H, H-4<sub>a</sub>), 2.31 (s, 3H, CH<sub>3</sub>-C4''), 2.06 (ddd, *J* = 13.6, 8.1, 2.5 Hz, 1H, H-4<sub>b</sub>), 1.68 (ddd, *J* = 13.6, 8.7, 2.5 Hz, 1H, H-4<sub>a</sub>), 1.36 (s, 3H, CH<sub>3</sub>-C-8b).

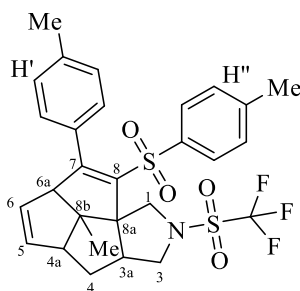
**$^{13}\text{C}$  NMR, HSQC, HMBC** (101 MHz,  $\text{CDCl}_3$ )  $\delta$  /ppm = 159.6 (C-8), 143.8 (C-4''), 138.3 (C-1''), 137.7 (C-7), 136.1 (C-5), 133.9 (C-1'), 129.1 (C-3'',5''), 128.2 (C-6), 128.1 (C-4'), 127.9 (C-3',5'), 127.7 (C-2',6'), 127.5 (C-2'',6''), 120.4 (q,  $J = 323.4$  Hz,  $\text{CF}_3$ ), 71.0 (C-6a), 70.4 (C-8a), 61.3 (C-8b), 58.7 (C-4a), 52.7 (C-3a), 52.4 (C-3), 52.2 (C-1), 34.4 (C-4), 23.8 ( $\text{CH}_3\text{-C-8b}$ ), 21.6 ( $\text{CH}_3\text{-C4''}$ ).

**$^{19}\text{F}$  NMR** (376 MHz,  $\text{CDCl}_3$ )  $\delta$  /ppm = -76.3 (s,  $\text{CF}_3$ ).

**MS** (ESI):  $m/z = 550.1$  [ $\text{M} + \text{H}$ ] $^+$ .

**HRMS** (ESI-ToF)  $m/z = [\text{M} + \text{Na}]^+$  calcd for  $\text{C}_{27}\text{H}_{26}\text{F}_3\text{NO}_4\text{S}_2\text{Na}$ : 572.1147, found: 572.1161.

**8b-Methyl-7-(4-methylphenyl)-8-[(4-methylphenyl)sulfonyl]-2-[(trifluoromethyl)sulfonyl]-1,2,3,3a,4,4a,6a,8b-octahydrocyclopenta[3,4]pentaleno[1,6a-c]pyrrole (219b)**



Following the general procedure using 1-methyl-4-[(4-methylbenzene-1-sulfonyl)ethynyl]benzene (64.5 mg, 0.24 mmol, 2.00 equiv.) after 10 h, column chromatography ( $\text{SiO}_2$ , eluent: cyclohexane/ethyl acetate, 95:1  $\rightarrow$  20:1) afforded the title compound (45 mg, 0.08 mmol, 67%) as a colorless solid.

$R_f = 0.53$  (3:1 cyclohexane/ethyl acetate).

**Mp** = 143–145  $^\circ\text{C}$  (ethanol).

**IR** (ATR):  $\tilde{\nu}/\text{cm}^{-1} = 3051, 2927, 2871, 1597, 1259, 1225, 1189, 1144, 813, 616$ .

**$^1\text{H}$  NMR, COSY, NOESY** (400 MHz,  $\text{CDCl}_3$ )  $\delta$  /ppm = 7.07 (d,  $J = 8.1$  Hz, AA' part of AA'BB' system, 2H, H-2'',6''), 6.98 (d,  $J = 8.1$  Hz, BB' part of AA'BB' system, 2H, H-3',5'), 6.96 (d,  $J = 8.1$  Hz, BB' part of AA'BB' system, 2H, H-3'',5''), 6.71 (d,  $J = 8.1$  Hz, AA' part of AA'BB' system, 2H, H-2',6'), 5.80 (dt,  $J = 5.6, 2.2$  Hz, 1H, H-5), 5.30 (ddd,  $J = 5.7, 2.7, 1.4$  Hz, 1H, H-6), 4.57 (d,  $J = 10.3$  Hz, 1H, H-1<sub>a</sub>), 4.02 (t,  $J = 9.4$  Hz, 1H, H-3<sub>a</sub>), 3.95 (d,  $J = 10.3$  Hz, 1H, H-1<sub>b</sub>), 3.77 (tdd,  $J = 8.6, 5.9, 2.5$  Hz, 1H, H-3<sub>a</sub>), 3.36 (t,

$J = 9.4$  Hz, 1H, H-3<sub>b</sub>), 3.33 (dd,  $J = 2.7, 1.9$  Hz, 1H, H-6<sub>a</sub>), 2.96 (t,  $J = 8.5$  Hz, 1H, H-4<sub>a</sub>), 2.34 (s, 3H, CH<sub>3</sub>-C4'), 2.32 (s, 3H, CH<sub>3</sub>-C4''), 2.04 (ddd,  $J = 13.6, 8.1, 2.5$  Hz, 1H, H-4<sub>b</sub>), 1.66 (ddd,  $J = 13.6, 8.7, 6.0$  Hz, 1H, H-4<sub>a</sub>), 1.35 (s, 3H, CH<sub>3</sub>-C-8b).

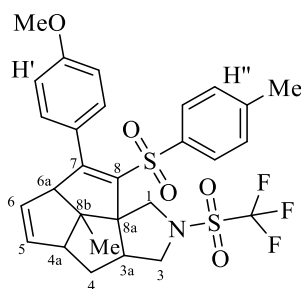
**<sup>13</sup>C NMR, HSQC, HMBC** (101 MHz, CDCl<sub>3</sub>)  $\delta$  /ppm = 159.9 (C-8), 143.8 (C-4''), 138.5 (C-4'), 138.2 (C-1''), 137.5 (C-7), 136.0 (C-5), 131.0 (C-1'), 129.0 (C-3'',5''), 128.6 (C-3',5'), 128.4 (C-6), 127.7 (C-2',6'), 127.6 (C-2'',6''), 120.4 (q,  $J = 323.9$  Hz, CF<sub>3</sub>), 71.2 (C-6a), 70.3 (C-8a), 61.2 (C-8b), 58.8 (C-4a), 52.7 (C-3a), 52.4 (C-3), 52.2 (C-1), 34.4 (C-4), 23.8 (CH<sub>3</sub>-C-8b), 21.7 (CH<sub>3</sub>-C4''), 21.4 (CH<sub>3</sub>-C4').

**<sup>19</sup>F NMR** (376 MHz, CDCl<sub>3</sub>)  $\delta$  /ppm = -76.3 (s, CF<sub>3</sub>).

**MS** (ESI):  $m/z = 564.2$  [M + H]<sup>+</sup>.

**HRMS** (APCI-ToF)  $m/z = [M]^+$  calcd for C<sub>28</sub>H<sub>28</sub>F<sub>3</sub>NO<sub>4</sub>S<sub>2</sub>: 563.1412, found: 563.1407.

**7-(4-Methoxyphenyl)-8b-methyl-8-[(4-methylphenyl)sulfonyl]-2-[(trifluoromethyl)sulfonyl]-1,2,3,3a,4,4a,6a,8b-octahydrocyclopenta[3,4]pentaleno[1,6a-c]pyrrole (219c)**



Following the general procedure using 1-methoxy-4-[(4-methylbenzene-1-sulfonyl)ethynyl]benzene (68.3 mg, 0.24 mmol, 2.00 equiv.) after 10 h, column chromatography (SiO<sub>2</sub>, eluent: cyclohexane/ethyl acetate, 95:1 → 20:1) afforded the title compound (32 mg, 0.05 mmol, 46%) as a colorless solid.

$R_f = 0.37$  (3:1 cyclohexane/ethyl acetate).

**Mp** = 145–146 °C (ethanol).

**IR** (ATR):  $\tilde{\nu}$  /cm<sup>-1</sup> = 2957, 2902, 2840, 1602, 1387, 1226, 1183, 1144, 813, 615.

**<sup>1</sup>H NMR, COSY, NOESY** (400 MHz, CDCl<sub>3</sub>)  $\delta$  /ppm = 7.08 (d,  $J = 8.1$  Hz, AA' part of AA'BB' system, 2H, H-2'',6''), 6.98 (d,  $J = 8.1$  Hz, BB' part of AA'BB' system, 2H, H-3'',5''), 6.78 (d,  $J = 8.8$  Hz, AA' part of AA'BB' system, 2H, H-2',6'), 6.71 (d,  $J = 8.8$

Hz, BB' part of AA'BB' system, 2H, H-3',5'), 5.80 (dt,  $J = 5.7, 2.2$  Hz, 1H, H-5), 5.29 (ddd,  $J = 5.7, 2.7, 1.5$  Hz, 1H, H-6), 4.57 (d,  $J = 10.3$  Hz, 1H, H-1<sub>a</sub>), 4.02 (t,  $J = 9.4$  Hz, 1H, H-3<sub>a</sub>), 3.95 (d,  $J = 10.3$  Hz, 1H, H-1<sub>b</sub>), 3.81 (s, 3H, CH<sub>3</sub>O-C4'), 3.78 (m, 1H, H-3<sub>a</sub>), 3.36 (t,  $J = 9.4$  Hz, 1H, H-3<sub>b</sub>), 3.33 (dd,  $J = 2.6, 1.9$  Hz, 1H, H-6<sub>a</sub>), 2.96 (t,  $J = 8.3$  Hz, 1H, H-4<sub>a</sub>), 2.32 (s, 3H, CH<sub>3</sub>-C4''), 2.05 (ddd,  $J = 13.6, 8.0, 2.5$  Hz, 1H, H-4<sub>b</sub>), 1.66 (ddd,  $J = 13.6, 8.7, 6.0$  Hz, 1H, H-4<sub>a</sub>), 1.35 (s, 3H, CH<sub>3</sub>-C-8b).

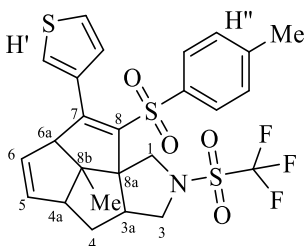
<sup>13</sup>C NMR, HSQC, HMBC (101 MHz, CDCl<sub>3</sub>)  $\delta$  /ppm = 159.8 (C4'), 159.7 (C-8), 143.7 (C-4''), 138.5 (C-1''), 137.5 (C-7), 136.1 (C-5), 129.2 (C-2',6'), 129.1 (C-3'',5''), 128.4 (C-6), 127.5 (C-2'',6''), 126.1 (C-1'), 113.4 (C-3',5'), 120.4 (q,  $J = 323.6$  Hz, CF<sub>3</sub>), 71.1 (C-6<sub>a</sub>), 70.3 (C-8<sub>a</sub>), 61.1 (C-8<sub>b</sub>), 58.8 (C-4<sub>a</sub>), 55.5 (CH<sub>3</sub>O-C4'), 52.8 (C-3<sub>a</sub>), 52.4 (C-3), 52.2 (C-1), 34.4 (C-4), 23.8 (CH<sub>3</sub>-C-8b), 21.7 (CH<sub>3</sub>-C4'').

<sup>19</sup>F NMR (376 MHz, CDCl<sub>3</sub>)  $\delta$  /ppm = -76.3 (s, CF<sub>3</sub>).

MS (ESI):  $m/z = 580.2$  [M + H]<sup>+</sup>.

HRMS (APCI-ToF)  $m/z = [M]^+$  calcd for C<sub>28</sub>H<sub>28</sub>F<sub>3</sub>NO<sub>5</sub>S<sub>2</sub>: 579.1361, found: 579.1362.

**8b-Methyl-8-[(4-methylphenyl)sulfonyl]-7-(thiophen-3-yl)-2-[(trifluoromethyl)sulfonyl]-1,2,3,3a,4,4a,6a,8b-octahydrocyclopenta[3,4]pentaleno[1,6a-c]pyrrole (219d)**



Following the general procedure using 3-[(4-methylbenzene-1-sulfonyl)ethynyl]thiophene (62.6 mg, 0.24 mmol, 2.00 equiv.) after 13 h, column chromatography (SiO<sub>2</sub>, eluent: cyclohexane/ethyl acetate, 95:1 → 20:1) afforded the title compound (43.0 mg, 0.08 mmol, 65%) as a colorless solid.

$R_f = 0.50$  (3:1 cyclohexane/ethyl acetate).

$Mp = 150-152$  °C (ethanol).

IR (ATR):  $\tilde{\nu}/\text{cm}^{-1} = 3058, 2954, 2871, 1597, 1387, 1226, 1188, 1144, 706, 621$ .

**<sup>1</sup>H NMR, COSY, NOESY** (400 MHz, CDCl<sub>3</sub>)  $\delta$ /ppm = 7.19 (dd,  $J$  = 3.0, 1.3 Hz, 1H, H-2'), 7.16 (d,  $J$  = 8.3 Hz, AA' part of AA'BB' system, 2H, H-2'',6''), 7.15–7.13 (m, 1H, H-5'), 7.03 (d,  $J$  = 8.3 Hz, BB' part of AA'BB' system, 2H, H-3'',5''), 6.66 (dd,  $J$  = 5.0, 1.3 Hz, 1H, H-4'), 5.80 (ddd,  $J$  = 5.7, 2.7, 1.9 Hz, 1H, H-5), 5.33 (ddd,  $J$  = 5.7, 2.7, 1.4 Hz, 1H, H-6), 4.57 (d,  $J$  = 10.3 Hz, 1H, H-1<sub>a</sub>), 4.02 (t,  $J$  = 9.4 Hz, 1H, H-3<sub>a</sub>), 3.96 (d,  $J$  = 10.3 Hz, 1H, H-1<sub>b</sub>), 3.78 (tdd,  $J$  = 8.7, 5.9, 2.5 Hz, 1H, H-3<sub>a</sub>), 3.37 (dd,  $J$  = 2.7, 1.9 Hz, 1H, H-6<sub>a</sub>), 3.36 (t,  $J$  = 9.4 Hz, 1H, H-3<sub>b</sub>), 2.97 (t,  $J$  = 8.3 Hz, 1H, H-4<sub>a</sub>), 2.33 (s, 3H, CH<sub>3</sub>-C4''), 2.04 (ddd,  $J$  = 13.6, 8.1, 2.5 Hz, 1H, H-4<sub>b</sub>), 1.65 (ddd,  $J$  = 13.6, 8.6, 5.9 Hz, 1H, H-4<sub>a</sub>), 1.36 (s, 3H, CH<sub>3</sub>-C-8b).

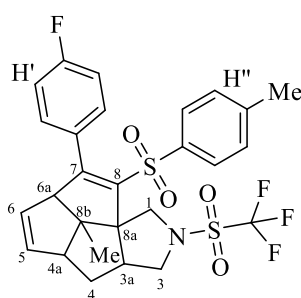
**<sup>13</sup>C NMR, HSQC, HMBC** (101 MHz, CDCl<sub>3</sub>)  $\delta$ /ppm = 155.1 (C-8), 143.9 (C-4''), 138.3 (C-1''), 137.9 (C-7), 136.3 (C-5), 133.3 (C-3'), 129.2 (C-3'',5''), 128.5 (C-6), 127.4 (C-4'), 127.2 (C-2'',6''), 126.0 (C-2'), 125.4 (C-5'), 120.42 (q,  $J$  = 323.1 Hz, CF<sub>3</sub>), 70.5 (C-6<sub>a</sub>), 70.4 (C-8<sub>a</sub>), 61.1 (C-8<sub>b</sub>), 58.8 (C-4<sub>a</sub>), 52.8 (C-3<sub>a</sub>), 52.5 (C-3), 52.2 (C-1), 34.5 (C-4), 23.9 (CH<sub>3</sub>-C-8b), 21.7 (CH<sub>3</sub>-C4'').

**<sup>19</sup>F NMR** (376 MHz, CDCl<sub>3</sub>)  $\delta$ /ppm = -76.1 (s, CF<sub>3</sub>).

**MS** (ESI):  $m/z$  = 556.1 [M + H]<sup>+</sup>.

**HRMS** (APCI-ToF)  $m/z$  = [M]<sup>+</sup> calcd for C<sub>25</sub>H<sub>24</sub>F<sub>3</sub>NO<sub>4</sub>S<sub>3</sub>: 555.082, found: 555.0817.

**7-(4-Fluorophenyl)-8b-methyl-8-[(4-methylphenyl)sulfonyl]-2-[(trifluoromethyl)sulfonyl]-1,2,3,3a,4,4a,6a,8b-octahydrocyclopenta[3,4]pentaleno[1,6a-c]pyrrole (219e)**



Following the general procedure using 1-fluoro-4-[(4-methylbenzene-1-sulfonyl)ethynyl]benzene (65.5 mg, 0.24 mmol, 2.00 equiv.) after 12 h, column chromatography (SiO<sub>2</sub>, eluent: cyclohexane/ethyl acetate, 95:1 → 20:1) afforded the title compound (31.0 mg, 0.05 mmol, 65%) as a colorless solid.

$R_f$  = 0.53 (3:1 cyclohexane/ethyl acetate).

**Mp**= 141–142 °C (ethanol).

**IR** (ATR):  $\tilde{\nu}/\text{cm}^{-1}$  = 3048, 2954, 1598, 1387, 1506, 1225, 1189, 1144, 736, 615.

**<sup>1</sup>H NMR, COSY, NOESY** (400 MHz, CDCl<sub>3</sub>)  $\delta$  /ppm = 7.08 (d,  $J$  = 8.3 Hz, AA' part of AA'BB' system, 2H, H-2'',6''), 7.01 (d,  $J$  = 8.3 Hz, BB' part of AA'BB' system, 2H, H-3'',5''), 6.92–6.82 (m, BB' part of AA'BB' system, 2H, H-3',5'), 6.84–6.74 (m, AA' part of AA'BB' system, 2H, H-2',6'), 5.83 (ddd,  $J$  = 5.7, 2.7, 1.9 Hz, 1H, H-5), 5.27 (ddd,  $J$  = 5.7, 2.7, 1.4 Hz, 1H, H-6), 4.58 (d,  $J$  = 10.4 Hz, 1H, H-1<sub>a</sub>), 4.02 (t,  $J$  = 9.4 Hz, 1H, H-3<sub>a</sub>), 3.97 (d,  $J$  = 10.4 Hz, 1H, H-1<sub>b</sub>), 3.78 (tdd,  $J$  = 8.7, 5.7, 2.1 Hz, 1H, H-3<sub>a</sub>), 3.36 (t,  $J$  = 9.4 Hz, 1H, H-3<sub>b</sub>), 3.32 (dd,  $J$  = 2.7, 1.9 Hz, 1H, H-6<sub>a</sub>), 2.98 (t,  $J$  = 8.3 Hz, 1H, H-4<sub>a</sub>), 2.34 (s, 3H, CH<sub>3</sub>-C4'), 2.07 (ddd,  $J$  = 13.6, 8.3, 2.5 Hz, 1H, H-4<sub>b</sub>), 1.66 (ddd,  $J$  = 13.6, 8.7, 6.0 Hz, 1H, H-4<sub>a</sub>), 1.36 (s, 3H, CH<sub>3</sub>-C-8b).

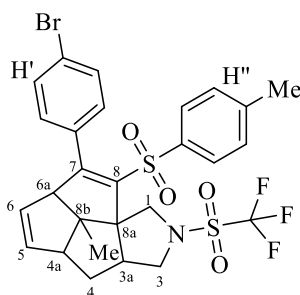
**<sup>13</sup>C NMR, HSQC, HMBC** (101 MHz, CDCl<sub>3</sub>)  $\delta$  /ppm = 162.7 (d,  $J_{CF}$  = 248.5 Hz, C-4'), 158.5 (C-8), 144.1 (C-4''), 138.5 (C-7), 138.3 (C-1''), 136.5 (C-5), 129.8 (d,  $J_{CF}$  = 3.3 Hz, C-1'), 129.7 (d,  $J_{CF}$  = 8.3 Hz, C-2',6'), 129.2 (C-3'',5''), 128.0 (C-6), 127.4 (C-2'',6''), 120.4 (q,  $J$  = 323.6 Hz, CF<sub>3</sub>), 115.1 (d,  $J_{CF}$  = 21.5 Hz, C-3',5'), 71.0 (C-6<sub>a</sub>), 70.4 (C-8<sub>a</sub>), 61.3 (C-8<sub>b</sub>), 58.8 (C-4<sub>a</sub>), 52.8 (C-3<sub>a</sub>), 52.4 (C-3), 52.2 (C-1), 34.4 (C-4), 23.8 (CH<sub>3</sub>-C-8b), 21.7 (CH<sub>3</sub>-C4'').

**<sup>19</sup>F NMR** (376 MHz, CDCl<sub>3</sub>)  $\delta$  /ppm = -76.3 (s, CF<sub>3</sub>), -113.9–(-114.0) (m, F-C-4').

**MS** (ESI):  $m/z$  = 568.2 [M + H]<sup>+</sup>.

**HRMS** (APCI-ToF)  $m/z$ : [M]<sup>+</sup> calcd for C<sub>27</sub>H<sub>25</sub>F<sub>4</sub>NO<sub>4</sub>S<sub>2</sub>: 567.1161, found: 567.1158.

**7-(4-Bromophenyl)-8b-methyl-8-[(4-methylphenyl)sulfonyl]-2-[(trifluoromethyl)sulfonyl]-1,2,3,3a,4,4a,6a,8b-octahydrocyclopenta[3,4]pentaleno[1,6a-c]pyrrole (219f)**



Following the general procedure using 1-bromo-4-[(4-methylbenzene-1-sulfonyl)ethynyl]benzene (80.0 mg, 0.24 mmol, 2.00

equiv.) after 10 h, column chromatography (SiO<sub>2</sub>, eluent: cyclohexane/ethyl acetate, 95:1 → 20:1) afforded the title compound (32 mg, 0.05 mmol, 46%) as a colorless solid.

$R_f$  = 0.55 (3:1 cyclohexane/ethyl acetate).

**Mp** = 150–152 °C (methanol).

**IR** (ATR):  $\tilde{\nu}/\text{cm}^{-1}$  = 3057, 2954, 2871, 1597, 1387, 1301, 1259, 1188, 1144, 813, 615.

**<sup>1</sup>H NMR, COSY, NOESY** (400 MHz, CDCl<sub>3</sub>)  $\delta$  /ppm = 7.29 (d,  $J$  = 8.4 Hz, BB' part of AA'BB' system, 2H, H-3',5'), 7.09 (d,  $J$  = 8.4 Hz, AA' part of AA'BB' system, 2H, H-2'',6''), 7.03 (d,  $J$  = 8.4 Hz, BB' part of AA'BB' system, 2H, H-3'',5''), 6.67 (d,  $J$  = 8.4 Hz, AA' part of AA'BB' system, 2H, H-2',6'), 5.83 (ddd,  $J$  = 5.7, 2.7, 1.9 Hz, 1H, H-5), 5.27 (ddd,  $J$  = 5.7, 2.7, 1.4 Hz, 1H, H-6), 4.57 (d,  $J$  = 10.2 Hz, 1H, H-1<sub>a</sub>), 4.02 (t,  $J$  = 9.4 Hz, 1H, H-3<sub>a</sub>), 3.96 (d,  $J$  = 10.2 Hz, 1H, H-1<sub>b</sub>), 3.78 (tdd,  $J$  = 8.6, 5.9, 2.3 Hz, 1H, H-3<sub>a</sub>), 3.36 (t,  $J$  = 9.4 Hz, 1H, H-3<sub>b</sub>), 3.32 (dd,  $J$  = 2.7, 1.9 Hz, 1H, H-6<sub>a</sub>), 2.98 (t,  $J$  = 8.4 Hz, 1H, H-4<sub>a</sub>), 2.35 (s, 3H, CH<sub>3</sub>-C4''), 2.06 (ddd,  $J$  = 13.6, 8.1, 2.5 Hz, 1H, H-4<sub>b</sub>), 1.65 (ddd,  $J$  = 13.6, 8.7, 6.0 Hz, 1H, H-4<sub>a</sub>), 1.35 (s, 3H, CH<sub>3</sub>-C-8b).

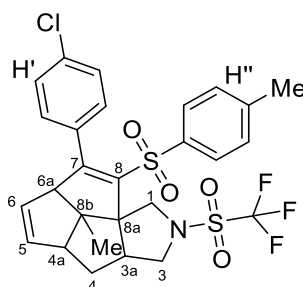
**<sup>13</sup>C NMR, HSQC, HMBC** (101 MHz, CDCl<sub>3</sub>)  $\delta$  /ppm = 158.0 (C-8), 144.3 (C-4''), 138.6 (C-7), 138.1 (C-1''), 136.6 (C-5), 132.9 (C-1'), 131.2 (C-3',5'), 129.4 (C-2',6'), 129.3 (C-3'',5''), 127.9 (C-6), 127.5 (C-2'',6''), 122.6 (C4'), 118.8 (q,  $J$  = 323.2 Hz, CF<sub>3</sub>), 70.8 (C-6<sub>a</sub>), 70.4 (C-8<sub>a</sub>), 61.4 (C-8<sub>b</sub>), 58.8 (C-4<sub>a</sub>), 52.7 (C-3<sub>a</sub>), 52.4 (C-3), 52.1 (C-1), 34.4 (C-4), 23.8 (CH<sub>3</sub>-C-8b), 21.7 (CH<sub>3</sub>-C4'').

**<sup>19</sup>F NMR** (376 MHz, CDCl<sub>3</sub>)  $\delta$  /ppm = -76.3 (s, CF<sub>3</sub>).

**MS** (ESI):  $m/z$  = 628.1 [M + H]<sup>+</sup>.

**HRMS** (APCI-ToF)  $m/z$  = [M]<sup>+</sup> calcd for C<sub>27</sub>H<sub>25</sub>BrF<sub>3</sub>NO<sub>4</sub>S<sub>2</sub>: 627.0360, found: 627.0349.

**7-(4-Chlorophenyl)-8b-methyl-8-[(4-methylphenyl)sulfonyl]-2-[(trifluoromethyl)sulfonyl]-1,2,3,3a,4,4a,6a,8b-octahydrocyclopenta[3,4]pentaleno[1,6a-c]pyrrole (219g)**



Following the general procedure using 1-chloro-4-[(4-methylbenzene-1-sulfonyl)ethynyl]benzene (69.4 mg, 0.24 mmol, 2.00 equiv.) after 10 h, column chromatography (SiO<sub>2</sub>, eluent: cyclohexane/ethyl acetate, 95:1 → 20:1) afforded the title compound (42 mg, 0.07 mmol, 60%) as a colorless solid.

*R<sub>f</sub>* = 0.53 (3:1 cyclohexane/ethyl acetate).

**Mp** = 148–149 °C (ethanol).

**IR** (ATR):  $\tilde{\nu}/\text{cm}^{-1}$  = 3056, 2954, 2872, 1596, 1387, 1302, 1259, 1190, 1144, 813, 615.

**<sup>1</sup>H NMR, COSY, NOESY** (400 MHz, CDCl<sub>3</sub>)  $\delta$  /ppm = 7.14 (d, *J* = 8.5 Hz, BB' part of AA'BB' system, 2H, H-3',5'), 7.10 (d, *J* = 8.3 Hz, AA' part of AA'BB' system, 2H, H-2'',6''), 7.02 (d, *J* = 8.3 Hz, BB' part of AA'BB' system, 2H, H-3'',5''), 6.74 (d, *J* = 8.5 Hz, AA' part of AA'BB' system, 2H, H-2',6'), 5.83 (ddd, *J* = 5.7, 2.7, 1.9 Hz, 1H, H-5), 5.27 (ddd, *J* = 5.7, 2.7, 1.4 Hz, 1H, H-6), 4.57 (d, *J* = 10.3 Hz, 1H, H-1<sub>a</sub>), 4.02 (t, *J* = 9.4 Hz, 1H, H-3<sub>a</sub>), 3.96 (d, *J* = 10.3 Hz, 1H, H-1<sub>b</sub>), 3.78 (tdd, *J* = 8.5, 5.7, 2.3 Hz, 1H, H-3<sub>a</sub>), 3.36 (t, *J* = 9.4 Hz, 1H, H-3<sub>b</sub>), 3.32 (dd, *J* = 2.7, 1.9 Hz, 1H, H-6<sub>a</sub>), 2.98 (t, *J* = 8.4 Hz, 1H, H-4<sub>a</sub>), 2.35 (s, 3H, CH<sub>3</sub>-C4''), 2.06 (ddd, *J* = 13.7, 8.1, 2.5 Hz, 1H, H-4<sub>b</sub>), 1.66 (ddd, *J* = 13.7, 8.7, 6.0 Hz, 1H, H-4<sub>a</sub>), 1.36 (s, 3H, CH<sub>3</sub>-C-8b).

**<sup>13</sup>C NMR, HSQC, HMBC** (101 MHz, CDCl<sub>3</sub>)  $\delta$  /ppm = 158.1 (C-8), 144.2 (C-4''), 138.6 (C-7), 138.2 (C-1''), 136.6 (C-5), 134.5 (C4'), 132.4 (C-1'), 129.2 (C-3'',5''), 129.2 (C-2',6'), 128.2 (C-3',5'), 127.9 (C-6), 127.5 (C-2'',6''), 118.8 (q, *J* = 320.5 Hz, CF<sub>3</sub>), 70.9 (C-6<sub>a</sub>), 70.4 (C-8<sub>a</sub>), 61.4 (C-8<sub>b</sub>), 58.8 (C-4<sub>a</sub>), 52.7 (C-3<sub>a</sub>), 52.4 (C-3), 52.1 (C-1), 34.4 (C-4), 23.8 (CH<sub>3</sub>-C-8b), 21.7 (CH<sub>3</sub>-C4'').

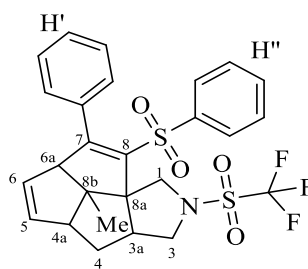
**<sup>19</sup>F NMR** (376 MHz, CDCl<sub>3</sub>)  $\delta$  /ppm = -76.3 (s, CF<sub>3</sub>).

**MS** (ESI): *m/z* = 584.1 [M + H]<sup>+</sup>.

**HRMS** (ESI-ToF) *m/z*: [M]<sup>+</sup> calcd for C<sub>27</sub>H<sub>25</sub>ClF<sub>3</sub>NO<sub>4</sub>S<sub>2</sub>: 583.0866, found: 583.0879.



**8b-Methyl-7-phenyl-8-(phenylsulfonyl)-2-[(trifluoromethyl)sulfonyl]-1,2,3,3a,4,4a,6a, 8b-octahydrocyclopenta[3,4]pentaleno[1,6a-c]pyrrole (219h)**



Following the general procedure using [(benzenesulfonyl)ethynyl]benzene (57.8 mg, 0.24 mmol, 2.00 equiv.) after 10 h, column chromatography (SiO<sub>2</sub>, eluent: cyclohexane/ethyl acetate, 95:1 → 20:1) afforded the title compound (47.0 mg, 0.09 mmol, 74%) as a colorless solid.

$R_f$  = 0.44 (3:1 cyclohexane/ethyl acetate).

$M_p$  = 154–156 °C (methanol).

**IR** (ATR):  $\tilde{\nu}/\text{cm}^{-1}$  = 3059, 2953, 2872, 1593, 1259, 1225, 1190, 1145, 726, 619.

**<sup>1</sup>H NMR, COSY, NOESY** (400 MHz, CDCl<sub>3</sub>)  $\delta$  /ppm = 7.38–7.34 (m, 1H, H-4''), 7.25--7.20 (m, 1H, H<sub>Ar</sub>), 7.19–7.12 (m, 6H, H<sub>Ar</sub>), 6.79–6.76 (m, 2H, H-2',6'), 5.82 (dt,  $J$  = 5.7, 2.3 Hz, 1H, H-5), 5.29 (ddd,  $J$  = 5.7, 2.7, 1.4 Hz, 1H, H-6), 4.61 (d,  $J$  = 10.2 Hz, 1H, H-1<sub>a</sub>), 4.04 (t,  $J$  = 9.3 Hz, 1H, H-3<sub>a</sub>), 4.00 (d,  $J$  = 10.2 Hz, 1H, H-1<sub>b</sub>), 3.80 (tdd,  $J$  = 8.6, 5.9, 2.4 Hz, 1H, H-3<sub>a</sub>), 3.38 (t,  $J$  = 9.4 Hz, 1H, H-3<sub>b</sub>), 3.36 (dd,  $J$  = 2.7, 1.9 Hz, 1H, H-6<sub>a</sub>), 2.99 (td,  $J$  = 8.5, 4.5 Hz, 1H, H-4<sub>a</sub>), 2.08 (ddd,  $J$  = 13.6, 8.1, 2.5 Hz, 1H, H-4<sub>b</sub>), 1.69 (ddd,  $J$  = 13.6, 8.7, 6.0 Hz, 1H, H-4<sub>a</sub>), 1.37 (s, 3H, CH<sub>3</sub>-C-8b).

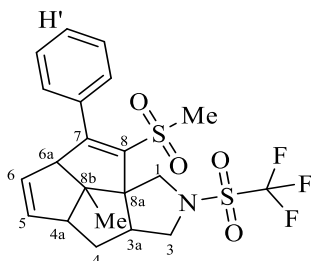
**<sup>13</sup>C NMR, HSQC, HMBC** (101 MHz, CDCl<sub>3</sub>)  $\delta$  /ppm = 160.0 (C-8), 141.1 (C-1''), 137.6 (C-7), 136.2 (C-5), 133.8 (C-1'), 132.8 (C-4''), 128.5 (2C, C<sub>Ar</sub>H), 128.3 (C-4'), 128.2 (C-6), 128.1 (2C, C<sub>Ar</sub>H), 127.7 (C-2',6'), 127.4 (2C, C<sub>Ar</sub>H), 120.4 (q,  $J$  = 324.0 Hz, CF<sub>3</sub>), 71.2 (C-6<sub>a</sub>), 70.4 (C-8<sub>a</sub>), 61.3 (C-8<sub>b</sub>), 58.8 (C-4<sub>a</sub>), 52.7 (C-3<sub>a</sub>), 52.4 (C-3), 52.2 (C-1), 34.4 (C-4), 23.8 (CH<sub>3</sub>-C-8b).

**<sup>19</sup>F NMR** (376 MHz, CDCl<sub>3</sub>)  $\delta$  /ppm = -76.3 (s, CF<sub>3</sub>).

**MS** (ESI):  $m/z$  = 536.1 [M + H]<sup>+</sup>.

**HRMS** (ESI-ToF)  $m/z = [M + Na]^+$  calcd for  $C_{26}H_{24}F_3NO_4S_2Na$ : 535.1099, found: 535.1111.

**8b-Methyl-8-(methylsulfonyl)-7-phenyl-2-[(trifluoromethyl)sulfonyl]-1,2,3,3a,4,4a,6a,8b-octahydrocyclopenta[3,4]pentaleno[1,6a-c]pyrrole (219i)**



Following the general procedure using [(methanesulfonyl)ethynyl]benzene (43.0 mg, 0.24 mmol, 2.00 equiv.) after 10 h, reversed-phase column chromatography ( $SiO_2-C_{18}$ , eluent: water/acetonitrile, 99:1  $\rightarrow$  80:20) afforded the title compound (35.0 mg, 0.07 mmol, 62%) as a colorless solid.

$R_f = 0.34$  (3:1 cyclohexane/ethyl acetate).

$Mp = 182-184$  °C (cyclohexane-chloroform).

**IR** (ATR):  $\tilde{\nu}/cm^{-1} = 3056, 2956, 2873, 1594, 1259, 1225, 1189, 1134, 737, 619$ .

**$^1H$  NMR, COSY, NOESY** (400 MHz,  $CDCl_3$ )  $\delta$  /ppm = 7.47–7.37 (m, 3H, H-3', 4', 5'), 7.31–7.27 (m, 2H, H-2', 6'), 5.84 (ddd,  $J = 5.7, 2.6, 1.9$  Hz, 1H, H-5), 5.37 (ddd,  $J = 5.7, 2.7, 1.5$  Hz, 1H, H-6), 4.43 (d,  $J = 10.2$  Hz, 1H, H-1<sub>a</sub>), 3.95 (t,  $J = 9.4$  Hz, 1H, H-3<sub>a</sub>), 3.93 (d,  $J = 10.2$  Hz, 1H, H-1<sub>b</sub>), 3.58 (ddd,  $J = 5.7, 2.7, 1.5$  Hz, 1H, H-3<sub>a</sub>), 3.56–3.53 (m, 1H, H-6<sub>a</sub>), 3.33 (t,  $J = 9.4$  Hz, 1H, H-3<sub>b</sub>), 3.02–2.96 (m, 1H, H-4<sub>a</sub>), 2.50 (s, 3H,  $SO_2CH_3$ ), 2.03 (ddd,  $J = 13.6, 8.1, 2.7$  Hz, 1H, H-4<sub>b</sub>), 1.67 (ddd,  $J = 13.6, 8.5, 6.1$  Hz, 1H, H-4<sub>a</sub>), 1.39 (s, 3H,  $CH_3-C-8b$ ).

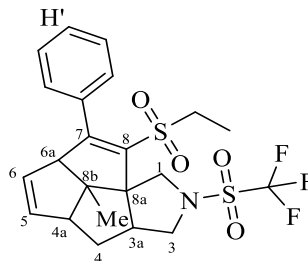
**$^{13}C$  NMR, HSQC, HMBC** (101 MHz,  $CDCl_3$ )  $\delta$  /ppm = 158.7 (C-8), 136.7 (C-7), 136.4 (C-5), 134.0 (C-1'), 129.3 (C-4'), 128.8 (C-3', 5'), 128.2 (C-6), 127.7 (C-2', 6'), 120.4 (q,  $J = 323.5$  Hz,  $CF_3$ ), 71.1 (C-6<sub>a</sub>), 70.4 (C-8<sub>a</sub>), 61.3 (C-8<sub>b</sub>), 58.8 (C-4<sub>a</sub>), 52.8 (C-3<sub>a</sub>), 52.3 (C-3), 52.0 (C-1), 44.9 ( $SO_2CH_3$ ), 34.4 (C-4), 23.8 ( $CH_3-C-8b$ ).

**$^{19}F$  NMR** (376 MHz,  $CDCl_3$ )  $\delta$  /ppm = -76.4 (s,  $CF_3$ ).

**MS** (ESI):  $m/z = 474.1$  [ $M + H$ ] $^+$ .

**HRMS** (ESI-ToF)  $m/z = [M + H]^+$  calcd for  $C_{21}H_{22}F_3NO_4S_2$ : 474.1021, found: 474.1006.

**8-(Ethylsulfonyl)-8b-methyl-7-phenyl-2-[(trifluoromethyl)sulfonyl]-1,2,3,3a,4,4a,6a,8b-octahydrocyclopenta[3,4]pentaleno[1,6a-c]pyrrole (219j)**



Following the general procedure using [(ethanesulfonyl)ethynyl]benzene (46.4 mg, 0.24 mmol, 2.00 equiv.) after 10 h, reversed-phase column chromatography ( $SiO_2-C_{18}$ , eluent: water/acetonitrile, 99:1  $\rightarrow$  80:20) afforded the title compound (43.0 mg, 0.09 mmol, 74%) as a colorless solid.

$R_f = 0.39$  (3:1 cyclohexane/ethyl acetate).

$Mp = 152-153$  °C (cyclohexane-chloroform).

**IR** (ATR):  $\tilde{\nu}/cm^{-1} = 3057, 2945, 2901, 1594, 1260, 1225, 1189, 1047, 728, 619$ .

**$^1H$  NMR, COSY, NOESY** (400 MHz,  $CDCl_3$ )  $\delta$  /ppm = 7.45–7.38 (m, 3H, H-3', 4', 5'), 7.32–7.28 (m, 2H, H-2', 6'), 5.85 (ddd,  $J = 5.7, 2.7, 1.8$  Hz, 1H, H-5), 5.39 (ddd,  $J = 5.7, 2.7, 1.4$  Hz, 1H, H-6), 4.39 (d,  $J = 10.3$  Hz, 1H, H-1<sub>a</sub>), 3.95 (t,  $J = 9.4$  Hz, 1H, H-3<sub>a</sub>), 3.90 (d,  $J = 10.3$  Hz, 1H, H-1<sub>b</sub>), 3.58 (ddt,  $J = 8.8, 5.4, 2.7$  Hz, 1H, H-3<sub>a</sub>), 3.55 (dd,  $J = 2.7, 1.8$  Hz, 1H, H-6<sub>a</sub>), 3.33 (t,  $J = 9.4$  Hz, 1H, H-3<sub>b</sub>), 3.07–2.94 (m, 1H, H-4<sub>a</sub>), 2.41 (qd,  $J = 7.4, 3.5$  Hz, 1H,  $SO_2CH_2CH_3$ ), 2.03 (ddd,  $J = 13.6, 8.1, 2.7$  Hz, 1H, H-4<sub>b</sub>), 1.68 (ddd,  $J = 13.6, 8.5, 6.0$  Hz, 1H, H-4<sub>a</sub>), 1.39 (s, 3H,  $CH_3-C-8b$ ), 2.50 (t,  $J = 7.4$  Hz, 1H,  $SO_2CH_2CH_3$ ).

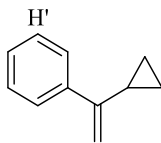
**$^{13}C$  NMR, HSQC, HMBC** (101 MHz,  $CDCl_3$ )  $\delta$  /ppm = 158.5 (C-8), 136.4 (C-5), 134.8 (C-7), 134.0 (C-1'), 129.3 (C-4'), 128.8 (C-3', 5'), 128.2 (C-6), 127.6 (C-2', 6'), 120.4 (q,  $J = 323.7$  Hz,  $CF_3$ ), 71.2 (C-6<sub>a</sub>), 70.3 (C-8<sub>a</sub>), 61.3 (C-8<sub>b</sub>), 58.8 (C-4<sub>a</sub>), 52.7 (C-3<sub>a</sub>), 52.3 (C-3), 52.1 (C-1), 49.6 ( $SO_2CH_2CH_3$ ), 34.4 (C-4), 23.9 ( $CH_3-C-8b$ ), 7.1 ( $SO_2CH_2CH_3$ ).

**$^{19}F$  NMR** (376 MHz,  $CDCl_3$ )  $\delta$  /ppm = -76.3 (s,  $CF_3$ ).

**MS** (ESI):  $m/z = 488.1$  [ $M + H$ ]<sup>+</sup>.

**HRMS** (ESI-ToF)  $m/z = [M]^+$  calcd for  $C_{22}H_{24}F_3NO_4S_2$ : 487.1099, found: 487.1091.

### Synthesis of (1-Cyclopropylvinyl)benzene (236)



To a solution cooled to  $-78\text{ }^{\circ}\text{C}$  of methyltriphenylphosphonium bromide (1.79 g, 5.0 mmol, 2.00 equiv.) in dry THF (15 mL) *n*BuLi (2.0 mL, 2.5M, 5 mmol, 2.00 equiv.) was added dropwise, after which the cooling was removed. To this mixture, cyclopropyl phenyl ketone (0.37 g, 2.5 mmol, 1.00 equiv.) dissolved in dry THF (1.5 mL) was added dropwise and the reaction was left to stir for 3 hours. After this time, brine was added and the phases were separated. The aqueous phase was extracted with pentane (3x 10 mL), and the combined organic phases were dried over  $\text{Na}_2\text{SO}_4$ , filtered onto celite, and concentrated under reduced pressure. The residue was purified by flash chromatography ( $\text{SiO}_2$ , eluent: cyclohexane/ethyl acetate, 100:0  $\rightarrow$  98:1) and **8** was isolated as a colorless liquid (0.30 g, 2.1 mmol, 87%).

$R_f = 0.69$  (50:1 cyclohexane/ethyl acetate).

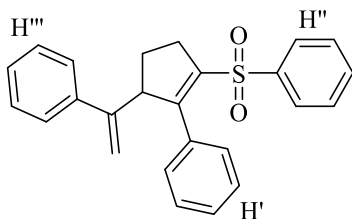
$^1\text{H NMR}$ , COSY, NOESY (400 MHz,  $\text{CDCl}_3$ )  $\delta$  /ppm = 7.61 (d,  $J = 7.3$  Hz, 2H, H-2',6'), 7.39–7.32 (m, 2H, H-3', 5'), 7.32–7.27 (m, 1H, H-4'), 5.29 (s, 1H,  $-\text{C}=\text{CH}_a\text{H}$ ), 4.95 (s, 1H,  $-\text{C}=\text{CH}_b\text{H}$ ), 1.67 (dddd,  $J = 8.3, 6.8, 5.3, 4.0$  Hz, 1H, H-1), 0.91–0.81 (m, 2H, H-2), 0.63–0.59 (m, 2H, H-3).

$^{13}\text{C NMR}$ , HSQC, HMBC (101 MHz,  $\text{CDCl}_3$ )  $\delta$  /ppm = 149.5 ( $-\text{C}=\text{CH}_2$ ), 141.8 (C-1'), 128.3 (C-3',5'), 127.6 (C-4'), 126.3 (C-2',6'), 109.2( $-\text{C}=\text{CH}_2$ ), 15.8 (C-1), 6.8 (C-1,2).

MS (EI):  $m/z = 144.1$   $[\text{M}]^+$ .

These data are consistent with those previously reported.<sup>[202]</sup>

### Synthesis of ((2-Phenyl-3-(1-phenylvinyl)cyclopent-1-en-1-yl)sulfonyl)benzene (237)



Following the general procedure for the preparation of **219** a mixture of (1-cyclopropylvinyl)benzene **8** (35.0 mg, 0.24 mmol, 1.00 equiv.) and

((phenylethynyl)sulfonyl)benzene (117.6 mg, 0.49 mmol, 2.00 equiv.) was irradiated for 2.5 h. After column chromatography (SiO<sub>2</sub>, eluent: cyclohexane/ethyl acetate, 95:1 → 20:1), the title compound (38.0 mg, 0.01 mmol, 41%) was isolated as a colorless oil.

$R_f = 0.55$  (3:1 cyclohexane/ethyl acetate).

**IR** (ATR):  $\tilde{\nu}/\text{cm}^{-1} = 3058, 2965, 2861, 1378, 1445, 1319, 1305, 1149, 1082, 904$ .

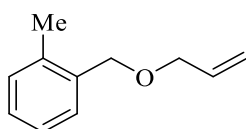
**<sup>1</sup>H NMR, COSY, NOESY** (400 MHz, acetone-d<sub>6</sub>)  $\delta$  /ppm = 7.72–7.68 (m, 2H, H-2'',6''), 7.67–7.64 (m, 1H, H-4''), 7.56–7.51 (m, 2H, H-3'',5''), 7.32–7.22 (m, 10H, H-2',3',4',5',6'/H-2'',3'',4'',5'',6''), 5.28 (s, 1H, -C=CH<sub>a</sub>H), 5.01 (s, 1H, -C=CH<sub>b</sub>H), 4.38 (ddt,  $J = 9.1, 4.4, 2.0$  Hz, 1H, H-3), 2.87–2.83 (m, 2H, H-5<sub>ab</sub>), 2.44 (dtd,  $J = 13.0, 9.1, 7.1$  Hz, 1H, H-4<sub>a</sub>), 1.88 (dtd,  $J = 13.0, 8.4, 4.9$  Hz, 1H).

**<sup>13</sup>C NMR, HSQC, HMBC** (101 MHz, acetone-d<sub>6</sub>)  $\delta$  /ppm = 156.2 (C-1), 149.6 (-C=CH<sub>2</sub>), 142.2 (C-1''), 141.8 (C-1'''), 140.7 (C-2), 135.3 (C-1'), 134.2 (C-4''), 129.9 (C-3'',5''), 129.7 (2C, C<sub>Ar</sub>H), 129.2 (2C, C<sub>Ar</sub>H), 129.0 (1C, C<sub>Ar</sub>H), 128.5 (1C, C<sub>Ar</sub>H), 128.(C-2'',6''), 128.3 (2C, C<sub>Ar</sub>H), 127.2 (2C, C<sub>Ar</sub>H), 115.0 (-C=CH<sub>2</sub>), 58.7 (C-3), 30.6 (C-5), 30.4 (C-4).

**MS** (ESI):  $m/z = 387.1$  [M + H]<sup>+</sup>.

**HRMS** (ESI-ToF)  $m/z = [M]^+$  calcd for C<sub>25</sub>H<sub>22</sub>O<sub>2</sub>S: 386.1341, found: 386.1354.

### Preparation of 1-((Allyloxy)methyl)-2-methylbenzene (**239**)



To a suspension of sodium hydride (0.11 g, 4.50 mmol, 1.10 equiv.) in dry THF (5.31 mL) was added a solution of benzyl alcohol (0.50 g, 4.09 mmol, 1.00 equiv.) in dry THF (0.8 mL). After the reaction was stirred at room temperature for two hours under an inert atmosphere, allyl bromide (0.39 mL, 4.50 mmol, 1.10 equiv.) was added dropwise and the resulting suspension was stirred overnight at room temperature. The solvent was partially removed in vacuo and saturated ammonium chloride solution (5 mL) was added. The aqueous phase was extracted with ethyl acetate (3 x 50 mL) and the combined organic extracts were dried over Na<sub>2</sub>SO<sub>4</sub>, filtered, and concentrated under reduced pressure. The residue was purified by flash chromatography (SiO<sub>2</sub>, eluent: cyclohexane/ethyl acetate, 100:0 → 95:1) to give **239** as a colorless oil (0.59 g, 3.64 mmol, 89%).

$R_f = 0.56$  (10:1 cyclohexane/ethyl acetate).

**IR** (ATR):  $\tilde{\nu}/\text{cm}^{-1} = 3021, 2856, 1460, 1356, 1123, 1080, 989, 923, 764, 743$ .

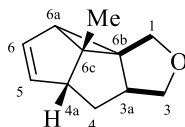
**$^1\text{H}$  NMR, COSY, NOESY** (400 MHz,  $\text{CDCl}_3$ )  $\delta$  /ppm = 7.36–7.34 (m, 1H, H-6), 7.25–7.14 (m, 3H, H-3, 4, 5), 5.99 (ddt,  $J = 17.2, 10.4, 5.6$  Hz, 1H, -CH=), 5.34 (dq,  $J = 17.2, 1.7$  Hz, 1H, =CH<sub>trans</sub>), 5.23 (dq,  $J = 10.4, 1.4$  Hz, 1H, =CH<sub>cis</sub>), 4.54 (s, 2H, -CH<sub>2</sub>-), 4.06 (dt,  $J = 5.6, 1.4$  Hz, 2H, -CH<sub>2</sub>-CH=), 2.32 (s, 3H, -CH<sub>3</sub>).

**$^{13}\text{C}$  NMR, HSQC, HMBC** (101 MHz,  $\text{CDCl}_3$ )  $\delta$  /ppm = 136.8 (C-1), 136.3 (C-2), 135.0 (-CH=), 130.3 (C<sub>Ar</sub>H), 128.7 (C-6), 127.9 (C<sub>Ar</sub>H), 125.9 (C<sub>Ar</sub>H), 117.2 (=CH<sub>2</sub>), 71.4 (-CH<sub>2</sub>-CH=), 70.6 (-CH<sub>2</sub>-), 18.9(-CH<sub>3</sub>).

**MS** (EI):  $m/z = 162.1$  [M]<sup>+</sup>.

These data are consistent with those previously reported.<sup>[203]</sup>

#### Preparation of (3a*S*,4a*R*,6c*R*)-6c-methyl-3,3a,4,4a,6a,6c-hexahydrocyclopropa[1,6]pent-2-eno[1,2-*c*]furan (240)



Following the general procedure for the *meta* photoadduct synthesis, a mixture of 1-((allyloxy)methyl)-2-methylbenzene **239** (100 mg, 0.62 mmol) and 10 mL of anhydrous cyclohexane was irradiated for 4 h. After column chromatography ( $\text{SiO}_2$ , eluent: cyclohexane/ethyl acetate, 100:0  $\rightarrow$  50:1), a 7:1 colorless oil mixture of two isomeric *meta*-photocycloadducts was isolated (38.5 mg, 0.24 mmol, 39%).<sup>[120a]</sup>

$R_f = 0.38$  [ $\text{KMnO}_4$ ] (10:1 cyclohexane/ethyl acetate).

**IR** (ATR):  $\tilde{\nu}/\text{cm}^{-1} = 2922, 2851, 1448, 1378, 1360, 1065, 1016, 914, 795, 735$ .

Spectroscopic data are those of the major isomer:

**$^1\text{H}$  NMR, COSY, NOESY** (400 MHz,  $\text{CDCl}_3$ )  $\delta$  /ppm = 5.67 (dd,  $J = 5.5, 2.3$  Hz, 1H, H-6), 5.45 (ddd,  $J = 5.5, 2.4, 0.8$  Hz, 1H, H-5), 3.88 (t,  $J = 9.0$  Hz, 1H, H-3<sub>a</sub>), 3.67–3.65 (m, 1H, H-3<sub>b</sub>), 3.64–3.62 (m, 2H, H-1<sub>a,b</sub>), 2.98 (dd,  $J = 4.1, 1.9$  Hz, 1H, H-4<sub>a</sub>), 2.40–2.32 (m, 1H, H-3<sub>a</sub>), 1.86–1.79 (m, 2H, H-4<sub>ab</sub>), 1.70–1.63 (m, 1H, H-6a), 1.29 (s, 3H, CH<sub>3</sub>-C-6b).

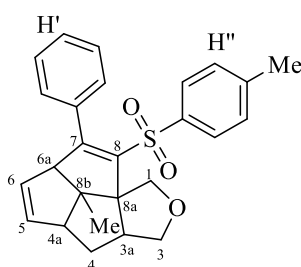
**$^{13}\text{C}$  NMR, HSQC, HMBC** (101 MHz,  $\text{CDCl}_3$ )  $\delta$ /ppm = 133.3 (C-5), 129.1 (C-6), 73.7 (C-3), 67.5 (C-1), 57.9 (C-4a), 51.1 (C-6b), 46.0 (C-6b), 45.5 (C-4), 42.9 (C-3a), 38.2 (C-6a), 13.8 ( $\text{CH}_3$ -C-6b).

**MS** (EI):  $m/z$  = 162.1  $[\text{M}]^+$ .

**HRMS** (API)  $m/z$  =  $[\text{M}]^+$  calcd. for  $\text{C}_{11}\text{H}_{14}\text{O}$ : 162.1045, found: 162.1041.

These data are consistent with those previously reported.<sup>[120a]</sup>

**8b-methyl-8-[(4-methylphenyl)sulfonyl]-7-phenyl-3,3a,4,4a,6a,8b-hexahydrocyclopenta[3,4]pentaleno[1,6a-c]furan (241)**



Following the general procedure for the preparation of **219**, a mixture of the *meta* photoadduct **240** (25.0 mg, 0.15 mmol, 1.00 equiv.) and 1-methyl-4-(phenylethynylsulfonyl)benzene (79.0 mg, 0.31 mmol, 2.00 equiv.) was irradiated for 10 h. After column chromatography ( $\text{SiO}_2$ , eluent: cyclohexane/ethyl acetate, 99:1  $\rightarrow$  93:1), the title compound (22.3 mg, 0.05 mmol, 39%) was isolated as a colorless solid.

**$R_f$**  = 0.40 (3:1 cyclohexane/ethyl acetate).

**Mp** = 180–182 °C (cyclohexane-ethyl acetate).

**IR** (ATR):  $\tilde{\nu}/\text{cm}^{-1}$  = 3056, 2924, 2867, 1594, 1311, 1144, 1086, 920, 720, 581.

**$^1\text{H}$  NMR, COSY, NOESY** (400 MHz,  $\text{CDCl}_3$ )  $\delta$ /ppm = 7.25–7.20 (m, 1H, H-4'), 7.18–7.12 (m,  $J$  = 7.5 Hz, 2H, H-3', 5'), 7.09 (d,  $J$  = 8.4 Hz, AA' part of AA'BB' system, 2H, H-2'', 6''), 6.96 (d,  $J$  = 8.4 Hz, BB' part of AA'BB' system, 2H, H-3'', 5''), 6.85–6.77 (m, 2H, H-2', 6'), 5.79 (dt,  $J$  = 5.7, 2.3 Hz, 1H, H-5), 5.32 (ddd,  $J$  = 5.7, 2.7, 1.5 Hz, 1H, H-6), 4.65 (d,  $J$  = 8.9 Hz, 1H, H-1<sub>a</sub>), 4.26 (t,  $J$  = 8.1 Hz, 1H, H-3<sub>a</sub>), 4.16 (d,  $J$  = 8.9 Hz, 1H, H-1<sub>b</sub>), 3.68 (tdd,  $J$  = 7.8, 7.3, 2.4 Hz, 1H, H-3<sub>a</sub>), 3.62 (t,  $J$  = 8.1 Hz, 1H, H-3<sub>b</sub>), 3.30 (t,  $J$  = 2.3 Hz, 1H, H-6<sub>a</sub>),

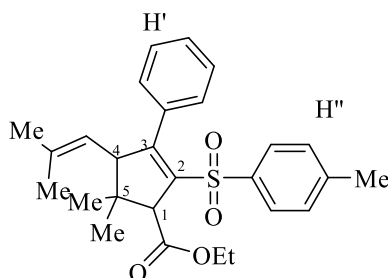
2.93 (m, 1H, H-4a), 2.31 (s, 3H, CH<sub>3</sub>-C4''), 2.03 (ddd,  $J= 13.5, 8.4, 2.5$  Hz, 1H, H-4b), 1.67 (ddd,  $J= 13.5, 8.2, 6.5$  Hz, 1H, H-4a), 1.33 (s, 3H, CH<sub>3</sub>-C-8b).

<sup>13</sup>C NMR, HSQC, HMBC (101 MHz, CDCl<sub>3</sub>)  $\delta$  /ppm = 159.6 (C-8), 143.3 (C-4''), 139.0 (C-1''), 138.5 (C-7), 136.8(C-5), 134.8 (C-1'), 129.0 (C-3'',5''), 128.0 (C-6), 127.8 (C-3',4',5'), 127.8 (C-2',6'), 127,5 (C-2'',6''), 73.0 (C-3), 72.3 (C-8a), 71.5 (C-6a), 71.3 (C-1), 61.3 (C-8b), 59.5 (C-4a), 54.1 (C-3a), 35.2 (C-4), 23.8 (CH<sub>3</sub>-C-8b), 21.6 (CH<sub>3</sub>-C4'').

MS (ESI):  $m/z = 419.1$  [M + H]<sup>+</sup>.

HRMS (ESI-ToF)  $m/z = [M]^+$  calcd for C<sub>26</sub>H<sub>26</sub>O<sub>3</sub>S: 418.1603, found: 418.1600.

### Preparation of ethyl 5,5-dimethyl-2-[(4-methylphenyl)sulfonyl]-4-(2-methylprop-1-en-1-yl)-3-phenylcyclopent-2-ene-1-carboxylate (**242**)



Following the general procedure for the preparation of **219**, a mixture of ethyl 2,2-dimethyl-3-(2-methyl-1-propenyl)cyclopropane-1-carboxylate (120.0 mg, 0.611 mmol, 1.0 equiv.), 1-methyl-4-(phenylethynylsulfonyl)benzene (313.2 mg, 1.222 mmol, 2.0 equiv.) and [Ir(ppy)<sub>2</sub>(dtbbpy)]PF<sub>6</sub> (11.0 mg, 0.01 mmol, 0.02 equiv.) in methanol (4.1 mL,  $c = 0.15$  M) was irradiated overnight. The full consumption of the starting material was confirmed via TLC and HPLC/ESI-MS. The crude product was dissolved in 1 mL of acetonitrile and 0.2 mL of this solution purified via preparative HPLC (Macherey-Nagel NUCLEODUR C18 HTec, oven temperature: 40 °C, eluent: water (+0.1% formic acid)/acetonitrile, 30:70) yielding the title compound (6.7 mg, 0.015 mmol, 12%) as a mixture of diastereomers (*cis/trans*, 2:3, based on <sup>1</sup>H NMR) as a colorless oil.<sup>1</sup>

$R_f = 0.36$  (10:1 cyclohexane/ethyl acetate).

IR (ATR):  $\tilde{\nu}/\text{cm}^{-1} = 2969, 2930, 1729, 1444, 1313, 1302, 1146, 768, 700, 583$ .

<sup>1</sup> This compound was synthesized by Jonathan Groß.



**<sup>1</sup>H NMR, COSY, NOESY** (600 MHz, CDCl<sub>3</sub>, *trans*-**14**)  $\delta$  /ppm = 7.19–7.16 (m, 2H, H-2''), 6.93 (d,  $J$  = 8.0 Hz, 2H, H-3'',5''), 6.80 (d,  $J$  = 7.0 Hz, 2H, H-2',6'), 4.62–4.60 (m, 1H, (CH<sub>3</sub>)<sub>2</sub>C=CH), 4.27–4.23 (m, 1H, H-4), 4.22–4.12 (m, 2H, O-CH<sub>2</sub>), 2.72 (d,  $J$  = 9.4 Hz, 1H, H-1), 2.29 (s, 3H, C4''-CH<sub>3</sub>), 1.78 (s, 3H, C5-C<sub>a</sub>H<sub>3</sub>), 1.46 (s, 3H, C5-C<sub>b</sub>H<sub>3</sub>), 1.42 (d,  $J$  = 1.4 Hz, 3H, C=C(C<sub>a</sub>H<sub>3</sub>C<sub>b</sub>H<sub>3</sub>)), 1.38 (d,  $J$  = 1.4 Hz, 3H, C=C(C<sub>a</sub>H<sub>3</sub>C<sub>b</sub>H<sub>3</sub>)), 1.34–1.29 (m, 3H, OCH<sub>2</sub>-CH<sub>3</sub>).

**<sup>13</sup>C NMR, HSQC, HMBC** (151 MHz, CDCl<sub>3</sub>, *trans*-**14**)  $\delta$  /ppm = 171.9 (CO<sub>2</sub>CH<sub>2</sub>CH<sub>3</sub>), 155.3 (C-2), 144.8 (C-3), 143.1 (C-4''), 139.0 (C-1''), 136.3 ((CH<sub>3</sub>)<sub>2</sub>C=CH), 128.8 (C-3'',5''), 128.1 (C-2',5'), 127.5 (C-2'',6''), 127.4 (C-3',4',5'), 123.3 (C4-CH), 61.9 (C-1), 61.0 (CO<sub>2</sub>-CH<sub>2</sub>), 51.1 (C-5), 49.9 (C-4), 28.2 (C5-C<sub>a</sub>H<sub>3</sub>), 25.8 (C=C(C<sub>a</sub>H<sub>3</sub>C<sub>b</sub>H<sub>3</sub>)), 22.6 (C5-C<sub>b</sub>H<sub>3</sub>), 21.6 (C4''-CH<sub>3</sub>), 18.1 (C=C(C<sub>a</sub>H<sub>3</sub>C<sub>b</sub>H<sub>3</sub>)), 14.5 (OCH<sub>2</sub>-CH<sub>3</sub>).

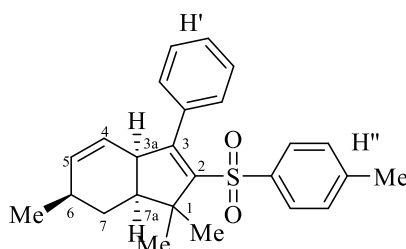
**<sup>1</sup>H NMR, COSY, NOESY** (600 MHz, CDCl<sub>3</sub>, *cis*-**14**)  $\delta$  /ppm = 7.38–7.36 (m, 2H, H-2'',6''), 7.15–7.12 (m, 3H, H-3',4',5'), 6.97–6.96 (m, 2H, H-2',6'), 6.96 (d,  $J$  = 9.1 Hz, 2H, H-3'',5''), 4.71 (dp,  $J$  = 10.8, 1.4 Hz, 1H, (CH<sub>3</sub>)<sub>2</sub>C=CH), 4.22–4.12 (m, 2H, O-CH<sub>2</sub>), 3.97 (dd,  $J$  = 10.8, 1.7 Hz, 1H, H-4), 3.75 (d,  $J$  = 1.7 Hz, 1H, H-1), 2.28 (s, 3H, C4''-CH<sub>3</sub>), 1.52 (d,  $J$  = 1.4 Hz, 3H, C=C(C<sub>a</sub>H<sub>3</sub>C<sub>b</sub>H<sub>3</sub>)), 1.50 (d,  $J$  = 1.4 Hz, 3H, C=C(C<sub>a</sub>H<sub>3</sub>C<sub>b</sub>H<sub>3</sub>)), 1.34–1.29 (m, 3H, OCH<sub>2</sub>-CH<sub>3</sub>), 1.11 (s, 3H, C5-C<sub>a</sub>H<sub>3</sub>), 1.07 (s, 3H, C5-C<sub>b</sub>H<sub>3</sub>).

**<sup>13</sup>C NMR, HSQC, HMBC** (151 MHz, CDCl<sub>3</sub>, *cis*-**14**)  $\delta$  /ppm = 171.9 (CO<sub>2</sub>CH<sub>2</sub>CH<sub>3</sub>), 159.3 (C-2), 143.5 (C-3), 143.1 (C-4''), 137.8 (C-2), 137.4 (C-1''), 137.4 ((CH<sub>3</sub>)<sub>2</sub>C=CH), 128.8 (C-3'',5''), 128.2 (C-2'',5''), 128.1 (C-2'',6''), 127.5 (C-3',4',5'), 61.0 (CO<sub>2</sub>-CH<sub>2</sub>), 62.3 (C-1), 57.9 (C-4), 46.6 (C-5), 26.1 (C=C(C<sub>a</sub>H<sub>3</sub>C<sub>b</sub>H<sub>3</sub>)), 25.2 (C5-C<sub>a</sub>H<sub>3</sub>), 23.4 (C5-C<sub>b</sub>H<sub>3</sub>), 18.0 (C=C(C<sub>a</sub>H<sub>3</sub>C<sub>b</sub>H<sub>3</sub>)), 14.5 (OCH<sub>2</sub>-CH<sub>3</sub>).

**MS** (ESI):  $m/z$  = 453.2 [M + H]<sup>+</sup>.

**HRMS** (ESI)  $m/z$ : [M+Na]<sup>+</sup> calcd for C<sub>27</sub>H<sub>32</sub>NaO<sub>4</sub>S: 475.1913, found: 475.1908.

**Preparation of (3*aR*,6*R*,7*aS*)-1,1,6-trimethyl-3-phenyl-2-tosyl-3*a*,6,7,7*a*-tetrahydro-1*H*-indene (243)**



Following the general procedure for the preparation of **7** a mixture of (1*S*,3*R*)-*cis*-4-carene (120.0 mg, 0.881 mmol, 1.0 equiv.), 1-methyl-4-(phenylethynylsulfonyl)benzene (451.6 mg, 1.762 mmol, 2.0 equiv.) and [Ir(ppy)<sub>2</sub>(dtbbpy)]PF<sub>6</sub> (16.5 mg, 0.018 mmol, 0.02 equiv.) in methanol (5.8 mL, *c* = 0.15 M) was irradiated overnight. The full consumption of the starting material was confirmed via TLC and HPLC/ESI-MS. The crude product was dissolved in 1 mL of acetonitrile and 0.2 mL of this solution was purified via preparative HPLC (ACE C18-PFP, oven temperature: 40 °C, eluent: water (+0.1% formic acid)/acetonitrile, 35:65) yielding the title compound (18.4 mg, 0.047 mmol, 27%) as a colorless solid.<sup>2</sup>

*R<sub>f</sub>* = 0.43 (10:1 cyclohexane/ethyl acetate).

*Mp* = 116 – 117 °C (chloroform).

**IR** (ATR):  $\tilde{\nu}/\text{cm}^{-1}$  = 3022, 2955, 1311, 1300, 1142, 1087, 812, 698, 665, 591.

**<sup>1</sup>H NMR, COSY, NOESY** (600 MHz, CDCl<sub>3</sub>)  $\delta$  /ppm = 7.29–7.28 (m, 2H, H-2'',6''), 7.25–7.23 (m, 1H, H-4'), 7.20–7.18 (m, 2H, H-3',5'), 7.16–7.14 (t, *J* = 7.4 Hz, 2H, H-2',6'), 6.98 (d, *J* = 8.1 Hz, 2H, H-3'',5''), 5.52–5.50 (m, 1H, H-5), 5.09 (ddd, *J* = 10.0, 4.7, 2.7 Hz, 1H, H-4), 3.57 (ddt, *J* = 6.9, 4.7, 2.6 Hz, 1H, H-3a), 2.31 (s, 3H, C4''–CH<sub>3</sub>), 2.08–2.04 (m, 1H, H-7a), 2.04–2.00 (m, 1H, H-6), 1.73 (m, 1H, H-7a), 1.50 (s, 3H, C1–C<sub>b</sub>H<sub>3</sub>), 1.45 (s, 3H, C1–C<sub>a</sub>H<sub>3</sub>), 0.96 (d, *J* = 7.1 Hz, 3H, C6–C<sub>a</sub>H<sub>3</sub>), 0.94 (d, *J* = 11.9 Hz, 1H, H-7b).

**<sup>13</sup>C NMR, HSQC, HMBC** (151 MHz, CDCl<sub>3</sub>)  $\delta$  /ppm = 155.2 (C-3), 143.9 (C-2), 143.0 (C-4''), 139.4 (C-1''), 136.5 (C-5), 134.7 (C-1'), 128.9 (C-3'',5''), 127.7 (C-2',4',6'), 127.6 (C-2'',6''), 124.0 (C-4), 50.3 (C-1), 49.3 (C-7a), 48.1 (C-3a), 31.1 (C-7), 30.0 (C-6), 27.2 (C1–C<sub>a</sub>H<sub>3</sub>), 22.1 (C1–C<sub>b</sub>H<sub>3</sub>), 21.8 (C6–CH<sub>3</sub>), 21.3 (C4''–CH<sub>3</sub>).

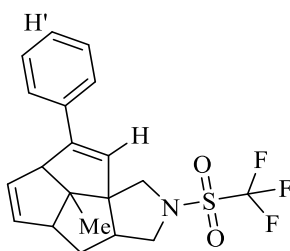
**MS** (ESI): *m/z* = 393.3 [M + H]<sup>+</sup>.

**HRMS** (ESI) *m/z* = [M]<sup>+</sup> calcd for C<sub>25</sub>H<sub>28</sub>O<sub>2</sub>S: 415.1702, found: 415.1695.

**[ $\alpha$ ]<sub>D</sub><sup>20</sup>** = –17.8 (*c* = 1.84, ethyl acetate).

<sup>2</sup> This compound was synthesized by Jonathan Groß.

**Preparation of 8b-methyl-7-phenyl-2-[(trifluoromethyl)sulfonyl]-1,2,3,3a,4,4a,6a,8b-octahydrocyclopenta[3,4]pentaleno[1,6a-c]pyrrole (244)**



Following a procedure published by Tam et al.,<sup>[204]</sup> 5% sodium amalgam (149.5 mg, 0.325 mmol, 9.0 equiv.) was added to a solution of 8b-methyl-8-[(4-methylphenyl)sulfonyl]-7-phenyl-2-[(trifluoromethyl)sulfonyl]-1,2,3,3a,4,4a,6a,8b-octahydrocyclopenta[3,4]pentaleno[1,6a-c]pyrrole (**219a**) (19.9 mg, 0.036 mmol, 1.0 equiv.) and sodium hydrogen phosphate (30.7 mg, 0.216 mmol, 6.0 equiv.) in methanol (4 mL) at 0 °C under nitrogen atmosphere. After 1 h, TLC indicated full consumption of **219a**, and the reaction mixture was filtrated over silica. The solvent was removed under reduced pressure and the residue purified by flash column chromatography (SiO<sub>2</sub>, eluent: cyclohexane/ethyl acetate, 98:2) to afford the desired product (6.9 mg, 0.017 mmol, 47%) as a colorless solid.<sup>3</sup>

**R<sub>f</sub>** = 0.65 (4:1 cyclohexane/ethyl acetate).

**Mp** = 118 – 119 °C (chloroform).

**IR** (ATR):  $\tilde{\nu}/\text{cm}^{-1}$  = 3051, 2952, 2896, 1385, 1226, 1182, 1005, 730, 626, 583.

**<sup>1</sup>H NMR, COSY, NOESY** (600 MHz, CDCl<sub>3</sub>)  $\delta$  /ppm = 7.47–7.45 (m, 2H, H-2', 6'), 7.35 (dd, *J* = 8.5, 7.0 Hz, 2H, H-3', 5'), 7.30–7.27 (m, 1H, H-4'), 5.81 (dt, *J* = 5.8, 2.1 Hz, 1H, H-6), 5.74 (d, *J* = 1.6 Hz, 1H, H-8), 5.63 (dt, *J* = 5.8, 2.2 Hz, 1H, H-5), 3.83 (d, *J* = 10.6 Hz, 1H, H-1<sub>b</sub>), 3.82 (d, *J* = 9.0 Hz, 1H, H-3<sub>a</sub>), 3.72 (d, *J* = 2.1 Hz, 1H, H-6<sub>a</sub>), 3.56 (d, *J* = 10.6 Hz, 1H, H-1<sub>a</sub>), 3.37–3.34 (m, 1H, H-3<sub>b</sub>), 2.91 (ddd, *J* = 8.4, 6.3, 2.2 Hz, 1H, H-4<sub>a</sub>), 2.77 (ddd, *J* = 13.3, 7.7, 5.5 Hz, 1H, H-3<sub>a</sub>), 1.90 (ddd, *J* = 13.0, 7.7, 4.9 Hz, 1H, H-4<sub>b</sub>), 1.60 (dt, *J* = 13.0, 6.3 Hz, 1H, H-4<sub>a</sub>), 1.34 (s, 3H, CH<sub>3</sub>-C-8b).

**<sup>13</sup>C NMR, HSQC, HMBC** (151 MHz, CDCl<sub>3</sub>)  $\delta$  /ppm = 146.2 (C-7), 134.7 (C-1'), 134.0 (C-5), 130.7 (C-6), 128.7 (C-3',5'), 128.1 (C-4'), 126.3 (C-8), 126.2 (C-2',6'), 120.5 (q,

<sup>3</sup> This compound was synthesized by Jonathan Groß.

$J = 323.8$  Hz,  $\text{CF}_3$ ), 68.1 (C-8a), 66.4 (C-6a), 61.4 (C-8b), 58.1 (C-4a), 53.6 (C-1), 52.9 (C-3a), 52.6 (C-3), 35.3 (C-4), 23.6 ( $\text{CH}_3$ -C-8b).

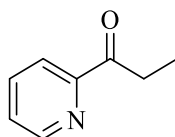
$^{19}\text{F}$  NMR (377 MHz,  $\text{CDCl}_3$ )  $\delta$  /ppm = -76.2 (s,  $\text{CF}_3$ ).

MS (ESI):  $m/z = 396.1$  [ $\text{M} + \text{H}$ ] $^+$ .

HRMS (APCI)  $m/z$ : [ $\text{M}$ ] $^{+}$  calcd for  $\text{C}_{20}\text{H}_{20}\text{F}_3\text{NO}_2\text{S}$ : 395.1162, found: 395.1153.

## 4.2.2. Section 2.3.2

### Synthesis of the 1-(pyridin-2-yl)propan-1-one (220)



To a solution of 2-cyanopyridine (1.39 mL, 14.4 mmol, 1.00 equiv.) in dry  $\text{Et}_2\text{O}$  (22 mL) at  $-20$  °C, a solution of ethyl magnesium bromide (21.6 mL, 1.0 M, 21.6 mmol, 1.50 equiv.) was slowly added. After the addition, the reaction mixture was stirred at that temperature for 1 h and then gradually warmed up to room temperature over 4 h. The reaction was quenched with 3 N HCl (5 mL) and stirred for 15 minutes. The two layers were separated, and the aqueous phase was neutralized to pH = 8 using NaOH 10%. The organic phase was extracted with  $\text{CH}_2\text{Cl}_2$  (3 x 10 mL), washed with water, and brine, dried over  $\text{Na}_2\text{SO}_4$ , and concentrated under vacuum. The pure product was obtained after being purified by flash chromatography ( $\text{SiO}_2$ , eluent: cyclohexane/ethyl acetate, 90:1  $\rightarrow$  50:1) as a yellowish oil (1.62 g, 12.0 mmol, 83 % yield).

$R_f = 0.62$  (2:1 cyclohexane/ethyl acetate).

IR (ATR):  $\tilde{\nu}/\text{cm}^{-1} = 2974, 1695, 1583, 1298, 1250, 1129, 1050, 996, 863, 767$ .

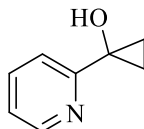
$^1\text{H}$  NMR, COSY (400 MHz,  $\text{CDCl}_3$ )  $\delta$  /ppm = 8.66 (ddd,  $J = 4.8, 1.8, 0.9$  Hz, 1H, H-6'), 8.03 (dt,  $J = 7.9, 1.1$  Hz, H-4'), 7.82 (td,  $J = 7.7, 1.8$  Hz, 1H, H-3'), 7.45 (ddd,  $J = 7.5, 4.8, 1.3$  Hz, 1H, H-5'), 3.23 (q,  $J = 7.3$  Hz, 2H,  $-\text{CH}_2-$ ), 1.21 (t,  $J = 7.3$  Hz, 3H,  $-\text{CH}_3$ ).

$^{13}\text{C}$  NMR, HSQC, HMBC (101 MHz,  $\text{CDCl}_3$ )  $\delta$  /ppm = 202.7 (C=O), 153.6 (C-2''), 149.0 (C-6''), 136.9 (C-4''), 127.1 (C-5''), 121.8 (C-3''), 31.2 ( $-\text{CH}_2-$ ), 8.1 ( $-\text{CH}_3$ ).

**MS** (ESI):  $m/z = 136.1$   $[M+H]^+$

The spectroscopic data are in accordance with those reported in the literature.<sup>[205]</sup>

### Preparation of 1-(pyridin-2-yl)cyclopropanol (221)



In an oven-dried quartz tube under a nitrogen atmosphere was charged 100.0 mg of the protected amine and 10 mL of a 10:1 *t*-butanol: toluene mixture. The solution was degassed for 15 min and placed in a Rayonet photoreactor. The vessel was irradiated ( $\lambda_{\text{max}} = 254$  nm,  $16 \times 8$  W) at room temperature for 3 h. After removal of the solvent under reduced pressure, the crude material was separated by flash chromatography ( $\text{SiO}_2$ , eluent: cyclohexane/ethyl acetate, 50:1  $\rightarrow$  20:1), to isolate the title compound (65.0 mg, 0.5 mmol, 62%) as a colorless solid.

**Mp**: 72–74 °C (cyclohexane-ethyl acetate) Lit.<sup>[206]</sup>: 75–76 °C.

$R_f = 0.38$  (2:1 cyclohexane/ethyl acetate).

**IR** (ATR):  $\tilde{\nu}/\text{cm}^{-1} = 3294, 1592, 1476, 1298, 1250, 1129, 1049, 998, 865, 777$ .

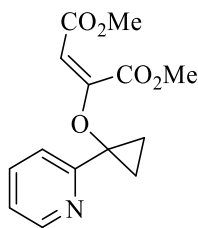
**$^1\text{H}$  NMR, COSY** (400 MHz,  $\text{CDCl}_3$ )  $\delta$  /ppm = 8.49 (dt,  $J = 4.9, 1.3$  Hz, 1H, H-6'), 7.65 (td,  $J = 7.8, 1.8$  Hz, 1H, H-4'), 7.18 (dt,  $J = 8.1, 1.1$  Hz, 1H, H-3'), 7.12 (ddd,  $J = 7.6, 5.0, 1.1$  Hz, 1H, H-5'), 1.40–1.33 (m, 2H, H-2), 1.25–1.18 (m, 2H, H-3).

**$^{13}\text{C}$  NMR, HSQC, HMBC** (101 MHz,  $\text{CDCl}_3$ )  $\delta$  /ppm = 162.9 (C-2'), 148.0 (C-6'), 136.9 (C-4'), 121.1 (C-5'), 117.2 (C-3'), 57.6 (C-1), 18.4 (2C, C-2,3).

**MS** (ESI):  $m/z = 136.1$   $[M+H]^+$ .

**HRMS** (ESI-ToF)  $m/z$ :  $[M + H]^+$  calcd for  $\text{C}_8\text{H}_{10}\text{NO}$ : 136.0757, found: 136.0763.

The spectroscopic data are in accordance with those reported in the literature.<sup>[206]</sup>

**Preparation of the dimethyl 2-(1-(pyridin-2-yl)cyclopropoxy)maleate (251)**

An oven-dried tube under a nitrogen atmosphere was charged with the cyclopropanol **221** (30.0 mg, 0.22 mmol, 1.00 equiv.), dimethyl acetylenedicarboxylate (0.03 mL, 0.26 mmol, 1.20 equiv.), and 1 mL of acetonitrile. The solution was stirred at room temperature until full consumption of the cyclopropanol. After 46 h the solvent was removed under reduced pressure, and the crude material was separated by flash chromatography (SiO<sub>2</sub>, eluent: cyclohexane/ethyl acetate, 50:1 → 10:1) to isolate the title compound (27.0 mg, 0.10 mmol, 44%) as a colorless oil.

$R_f$  = 0.38 (3:1 cyclohexane/ethyl acetate).

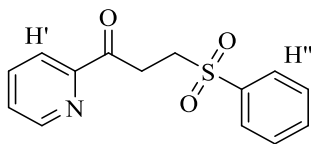
**IR** (ATR):  $\tilde{\nu}/\text{cm}^{-1}$  = 2953, 1752, 1720, 1632, 1438, 1366, 1142, 1036, 836, 762.

**<sup>1</sup>H NMR, COSY** (400 MHz, CDCl<sub>3</sub>)  $\delta$  /ppm = 8.48 (ddd,  $J$  = 4.9, 1.8, 1.0 Hz, 1H, H-6'), 7.66 (td,  $J$  = 7.8, 1.8 Hz, 1H, H-4'), 7.46 (dt,  $J$  = 8.0, 1.1 Hz, 1H, H-3'), 7.12 (ddd,  $J$  = 7.6, 4.8, 1.1 Hz, 1H, H-5'), 5.26 (s, 1H, =CH), 3.93 (s, 3H, -OCH<sub>3</sub>), 3.63 (s, 3H, -OCH<sub>3</sub>), 1.71–1.63 (m, 2H, H-2), 1.48–1.38 (m, 2H, H-3).

**<sup>13</sup>C NMR, HSQC, HMBC** (101 MHz, CDCl<sub>3</sub>)  $\delta$  /ppm = 166.1 (COO-), 164.0 (COO-), 159.8 (C-2'), 157.3 (C=CH), 149.7 (C-6'), 136.4 (C-4'), 121.7 (C-5'), 119.8 (C-3'), 98.1 (C=CH), 64.9 (C-1), 53.2 (CH<sub>3</sub>), 51.7 (CH<sub>3</sub>), 17.6 (2C, C-2,3).

**MS** (ESI):  $m/z$  = 278.1 [M+H]<sup>+</sup>.

**HRMS** (ESI-ToF)  $m/z$  = [M + H]<sup>+</sup> calcd for C<sub>14</sub>H<sub>15</sub>NO<sub>5</sub>: 278.1023, found: 278.1033.

**Synthesis of the 3-(phenylsulfonyl)-1-(pyridin-2-yl)propan-1-one (227d')**

The cyclopropanol **221** (35.0 mg, 0.26 mmol, 1.00 equiv.) was added to a suspension of benzylnsulfonic acid (29.5 mg, 0.21 mmol, 0.80 equiv.), obtained by acidification of the

commercially available sodium benzenesulfinate and recrystallization from water)<sup>[159]</sup> Pd(OAc)<sub>2</sub> (4.7 mg, 0.021 mmol, 0.10 equiv.), and Cu(OAc)<sub>2</sub>·H<sub>2</sub>O (41.4 mg, 0.21 mmol, 0.80 equiv.) in dioxane (1.3 mL). After 1 h at 100 °C, the solvent was removed under reduced pressure and the crude material was separated by flash chromatography (SiO<sub>2</sub>, eluent: cyclohexane/ethyl acetate, 30:1 → 5:1) to isolate the title compound (21.0 mg, 0.008 mmol, 30%) as a colorless oil.

*R<sub>f</sub>* = 0.45 (1:1 cyclohexane/ethyl acetate).

**IR** (ATR):  $\tilde{\nu}/\text{cm}^{-1}$  = 3059, 2930, 1699, 1584, 1447, 1355, 1241, 1149, 1087, 995.

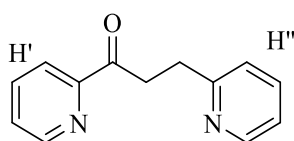
**<sup>1</sup>H NMR, COSY** (400 MHz, CDCl<sub>3</sub>)  $\delta$  /ppm = 8.66 (d, *J* = 4.8 Hz, 1H, H-6'), 7.97–7.95 (m, 3H, H-3',2'',6''), 7.82 (td, *J* = 7.8, 1.9 Hz, 1H, H-4'), 7.65 (t, *J* = 7.4 Hz, 1H, H-4''), 7.57 (d, *J* = 7.5 Hz, 1H, H-3'',5''), 7.48 (dd, *J* = 7.5, 4.9 Hz, 1H, H-5'), 3.77–3.65 (m, 2H, -CH<sub>2</sub>-), 3.63–3.53 (m, 1H, -COCH<sub>2</sub>-)

**<sup>13</sup>C NMR, HSQC, HMBC** (101 MHz, CDCl<sub>3</sub>)  $\delta$  /ppm = 191.6 (C=O), 152.4 (C-1'), 149.3 (C-6'), 139.1 (C-1''), 137.1 (C-4'), 133.9 (C-4''), 129.5 (C-3'',5''), 128.3 (C-2'',6''), 127.8 (C-5'), 122.0 (C-3'), 51.2 (-CH<sub>2</sub>SO<sub>2</sub>-), 31.4 (-COCH<sub>2</sub>-).

**MS** (ESI): *m/z* = 276.1 [M+H]<sup>+</sup>.

**HRMS** (ESI-ToF) *m/z* = [M + H]<sup>+</sup> calcd for C<sub>14</sub>H<sub>13</sub>NO<sub>3</sub>S: 276,0689, found: 276,0691.

### Preparation of the 1,3-di(pyridin-2-yl)propan-1-one (227g')



An oven-dried tube was charged with cyclopropanol **221** (35.0 mg, 0.26 mmol, 1.0 equiv.), palladium (II) diacetate (5.8 mg, 0.025 mmol, 0.10 equiv.), 1,4-bis(diphenylphosphino)butane (dppb) (22.1 mg, 0.052 mmol, 0.20 equiv.) and K<sub>3</sub>PO<sub>4</sub> (109.9 mg, 0.52 mmol, 2.0 equiv.). The reaction vessel was capped with a rubber septum and flushed with argon for 10 minutes at ambient temperature prior to the addition of toluene (2.6 mL). The resulting mixture was stirred at room temperature for 5 minutes. Neat 4-bromoanisole (0.037 mL, 0.39 mmol, 1.5 equiv.) was added via syringe. The resulting mixture was heated to 80 °C. After 8 h the solvent was removed under reduced pressure, and the crude material was separated by flash chromatography (SiO<sub>2</sub>, eluent: cyclohexane/ethyl

acetate, 30:1 → 10:1) to isolate the title compound (8.0 mg, 0.004 mmol, 14%) as a colorless oil.

$R_f$  = 0.19 (1:1 cyclohexane/ethyl acetate).

**IR** (ATR):  $\tilde{\nu}/\text{cm}^{-1}$  = 3055, 2924, 1697, 1592, 1569, 1436, 1365, 1042, 995, 766.

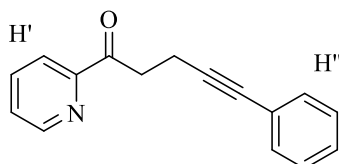
**$^1\text{H}$  NMR, COSY** (400 MHz,  $\text{CDCl}_3$ )  $\delta$  /ppm = 8.69–8.64 (m, 1H, H-6'), 8.51–8.47 (m, 1H, H-6''), 8.03 (dd,  $J$  = 7.8, 1.3 Hz, 1H, H-3'), 7.82 (td,  $J$  = 7.7, 1.8 Hz, 1H, H-4'), 7.59 (td,  $J$  = 7.7, 1.9 Hz, 1H, H-4''), 7.45 (ddd,  $J$  = 7.7, 4.7, 1.3 Hz, 1H, H-5'), 7.29–7.22 (m, 1H, H-3''), 7.09 (dt,  $J$  = 8.7, 3.2 Hz, 1H, H-5''), 3.73 (t,  $J$  = 7.4 Hz, 2H,  $-\text{CH}_2-$ ), 3.25 (t,  $J$  = 7.4 Hz, 2H,  $-\text{COCH}_2-$ ).

**$^{13}\text{C}$  NMR, HSQC, HMBC** (101 MHz,  $\text{CDCl}_3$ )  $\delta$  /ppm = 201.1 (C=O), 161.0 (C-1''), 153.5 (C-1'), 149.3 (C-6''), 149.1 (C-6'), 137.0 (C-4'), 136.5 (C-4''), 127.2 (C-5'), 123.2 (C-3''), 121.9 (C-3'), 121.3 (C-5''), 37.5 ( $-\text{CH}_2-$ ), 32.5 ( $-\text{COCH}_2-$ ).

**MS** (ESI):  $m/z$  = 213.1  $[\text{M}+\text{H}]^+$ .

**HRMS** (ESI-ToF)  $m/z$  =  $[\text{M} + \text{H}]^+$  calcd for  $\text{C}_{13}\text{H}_{12}\text{N}_2\text{O}$ : 213.1023, found: 213.1023.

#### Preparation of the 5-phenyl-1-(pyridin-2-yl)pent-4-yn-1-one (**227j**)



The cyclopropanol **221** (30.0 mg, 0.22 mmol, 1.0 equiv.), the photocatalyst  $[\text{Ir}(\text{ppy})_2(\text{dtbbpy})]\text{PF}_6$  (6.1 mg, 0.007 mmol, 0.03 equiv.), PIDA (143.0 mg, 0.4 mmol, 2.0 equiv.), and the alkynyl sulfone **218h** were loaded in an oven-dried tube which was flushed with  $\text{N}_2$ . The reaction was irradiated with a blue LED and after 1 h, the reaction mixture was extracted with ethyl acetate (3 x 10 mL). The combined organic extracts were washed by brine, dried over  $\text{Na}_2\text{SO}_4$ , filtered, concentrated, and purified by flash column chromatography on silica gel (eluent: cyclohexane/acetone/ $\text{Et}_3\text{N}$ , 9:0.8:0.2) to give the title compound (9.9 mg, 0.004 mmol, 19%) as a colorless oil.

$R_f$  = 0.56 (9:0.8:0.2 cyclohexane/acetone/ $\text{Et}_3\text{N}$ ).

**IR** (ATR):  $\tilde{\nu}/\text{cm}^{-1}$  = 3056, 2922, 1699, 1598, 1491, 1465, 1362, 1210, 995, 755.



**$^1\text{H}$  NMR, COSY** (400 MHz,  $\text{CDCl}_3$ )  $\delta$  /ppm = 8.71 (ddd,  $J$  = 4.8, 1.7, 0.9 Hz, 1H, H-6'), 8.08 (dt,  $J$  = 7.9, 1.1 Hz, 1H, H-3'), 7.87 (td,  $J$  = 7.7, 1.7 Hz, 1H, H-4'), 7.51 (ddd,  $J$  = 7.7, 4.8, 1.3 Hz, 1H, H-5'), 7.40–7.36 (m, 2H, H-2'',6''), 7.29–7.26 (m, 3H, H-3'',4'',5''), 3.60 (t,  $J$  = 7.6 Hz, 2H,  $-\text{CH}_2-$ ), 2.85 (t,  $J$  = 7.6 Hz, 2H,  $-\text{COCH}_2-$ ).

**$^{13}\text{C}$  NMR, HSQC, HMBC** (101 MHz,  $\text{CDCl}_3$ )  $\delta$  /ppm = 199.8 (C=O), 153.1 (C-1'), 149.1 (C-6'), 137.2 (C-4'), 131.7 (C-2'',6''), 128.3 (C-3'',5''), 127.8 (C-4''), 127.5 (C-5''), 123.9 (C-1''), 122.1 (C-3'), 89.1 ( $-\text{CH}_2-\text{C}\equiv\text{C}-$ ), 81.0 ( $-\text{CH}_2-\text{C}\equiv\text{C}-$ ), 37.5 ( $-\text{CH}_2-\text{C}\equiv\text{C}-$ ), 14.3 ( $-\text{COCH}_2-$ ).

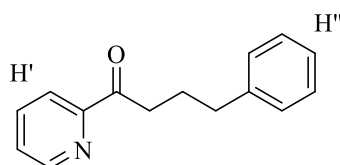
**MS** (ESI):  $m/z$  = 236.1  $[\text{M}+\text{H}]^+$ .

**HRMS** (ESI-ToF)  $m/z$  =  $[\text{M} + \text{H}]^+$  calcd for  $\text{C}_{16}\text{H}_{13}\text{NO}$ : 236.1070, found: 236.1067.

## General procedure for the synthesis of ketones.

An oven-dried Schlenk tube (10 mL) equipped with a stir bar was charged with palladium diacetate (0.10 equiv.), 2-dicyclohexylphosphino-2',4',6'-triisopropylbiphenyl (Xphos) (0.20 equiv.), cesium carbonate (2.00 equiv.) and the corresponding benzyl chloride (1.00 equiv.). The reaction vessel was capped with a rubber septum and flushed with argon for 10 minutes prior to the addition of dioxane (1.34 mL). The resulting reaction mixture was stirred at ambient temperature for 5 min and a solution of cyclopropanol **221** (1.50 equiv.) in 0.43 mL of solvent, was added via syringe. The solution was stirred at 80 °C until TLC or HPLC/ESI-MS showed full consumption of the starting material. After completion of the reaction, the crude reaction mixture was diluted with ethyl acetate, filtered through a plug of celite, and concentrated to dryness. The residue was purified by flash chromatography ( $\text{SiO}_2$ , eluent: cyclohexane/ethyl acetate, 30:0  $\rightarrow$  10:1).

### 4-Phenyl-1-(pyridin-2-yl)butan-1-one (**227a**)



Following the general procedure with the benzyl chloride (0.023 mL, 0.20 mmol) the title compound (38.2 mg, 0.17 mmol, 86%) was isolated as a colorless oil.

$R_f = 0.64$  (2:1 cyclohexane/ethyl acetate).

**IR** (ATR):  $\tilde{\nu}/\text{cm}^{-1} = 2923, 1697, 1583, 1496, 1436, 1369, 1226, 995, 772, 745$ .

**$^1\text{H}$  NMR, COSY** (400 MHz,  $\text{CDCl}_3$ )  $\delta$  /ppm = 8.67 (ddd,  $J = 4.8, 1.7, 1.0$  Hz, 1H, H-6'), 8.03 (dt,  $J = 7.8, 1.1$  Hz, 1H, H-3'), 7.82 (td,  $J = 7.6, 1.7$  Hz, 1H, H-4'), 7.46 (ddd,  $J = 7.6, 4.8, 1.2$  Hz, 1H, H-5'), 7.32–7.24 (m, 2H, H-3'',5''), 7.26–7.19 (m, 2H, H-2'',6''), 7.22–7.13 (m, 1H, H-4''), 3.26 (t,  $J = 7.4$  Hz, 2H, H-2), 2.73 (t,  $J = 7.6$  Hz, 2H, H-4), 2.08 (p,  $J = 7.6$  Hz, 2H, H-3).

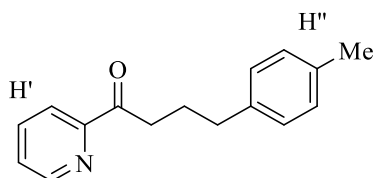
**$^{13}\text{C}$  NMR, HSQC, HMBC** (101 MHz,  $\text{CDCl}_3$ )  $\delta$  /ppm = 202.0 (C=O), 153.6 (C-2'), 149.0 (C-6'), 142.1 (C-1''), 137.0 (C-4'), 128.7 (C-2'',6''), 128.5 (C-3'',5''), 127.2 (C-5'), 126.0 (C-4''), 121.9 (C-3'), 37.3 (C-2), 35.5 (C-4), 25.7 (C-3).

**MS** (ESI):  $m/z = 226.1$   $[\text{M}+\text{H}]^+$ .

**HRMS** (ESI-ToF)  $m/z$ :  $[\text{M}]^+$  calcd for  $\text{C}_{15}\text{H}_{15}\text{NO}$ : 225.1154, found: 225.1153.

The spectroscopic data are in accordance with those reported in the literature.<sup>[207]</sup>

#### 4-(4-Methylphenyl)-1-(pyridin-2-yl)butan-1-one (227b)



Following the general procedure with 4-methylbenzyl chloride (0.026 mL, 0.20 mmol) the title compound (40.2 mg, 0.17 mmol, 85%) was isolated as a yellowish oil.

$R_f = 0.53$  (4:1 cyclohexane/ethyl acetate).

**IR** (ATR):  $\tilde{\nu}/\text{cm}^{-1} = 2923, 1697, 1584, 1515, 1436, 1370, 1226, 995, 804, 773$ .

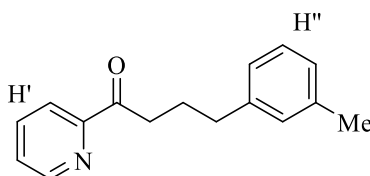
**$^1\text{H}$  NMR, COSY** (400 MHz,  $\text{CDCl}_3$ )  $\delta$  /ppm = 8.67 (ddd,  $J = 4.8, 1.8, 0.9$  Hz, 1H, H-6'), 8.03 (dt,  $J = 7.9, 1.1$  Hz, 1H, H-3'), 7.83 (td,  $J = 7.7, 1.7$  Hz, 1H, H-4'), 7.46 (ddd,  $J = 7.6, 4.8, 1.2$  Hz, 1H, H-5'), 7.12 (d,  $J = 8.2$  Hz, AA' part of AA'BB' system, 2H, H-2'',6''), 7.08 (d,  $J = 8.2$  Hz, 2H, BB' part of AA'BB' system, 2H, H-3'',5''), 3.26 (t,  $J = 7.4$  Hz, 2H, H-2), 2.69 (t,  $J = 7.6$  Hz, 2H, H-4), 2.31 (s, 3H,  $-\text{CH}_3$ ), 2.06 (p,  $J = 7.6$  Hz, 2H, H-3).

**$^{13}\text{C}$  NMR, HSQC, HMBC** (101 MHz,  $\text{CDCl}_3$ )  $\delta$  /ppm = 201.9 (C=O), 153.5 (C-2'), 148.9 (C-6'), 139.0 (C-1''), 137.1 (C-4'), 135.4 (C-4''), 129.1 (C-3'',5''), 128.5 (C-2'',6''), 127.2 (C-5'), 121.9 (C-3'), 37.4 (C-2), 35.0 (C-4), 25.9 (C-3) 21.1(- $\text{CH}_3$ ).

**MS** (ESI):  $m/z$  = 240.1  $[\text{M}+\text{H}]^+$ .

**HRMS** (ESI-ToF)  $m/z$ :  $[\text{M}+\text{H}]^+$  calcd for  $\text{C}_{16}\text{H}_{18}\text{NO}$ : 240.1383, found: 240.1389.

#### 4-(3-Methylphenyl)-1-(pyridin-2-yl)butan-1-one (227c)



Following the general procedure with 3-methylbenzyl chloride (0.023 mL, 0.17 mmol) the title compound (34.8 mg, 0.15 mmol, 84 %) was isolated as a yellowish oil.

$R_f$  = 0.58 (3:1 cyclohexane/ethyl acetate).

**IR** (ATR):  $\tilde{\nu}/\text{cm}^{-1}$  = 2927, 1697, 1584, 1568, 1436, 1369, 1226, 995, 773, 700.

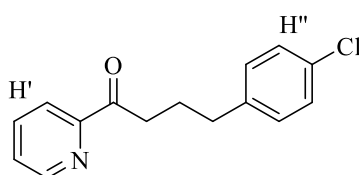
**$^1\text{H}$  NMR, COSY** (400 MHz,  $\text{CDCl}_3$ )  $\delta$  /ppm = 8.67 (ddd,  $J$  = 4.8, 1.7, 1.0 Hz, 1H, H-6'), 8.03 (dt,  $J$  = 7.8, 1.2 Hz, 1H, H-3'), 7.83 (td,  $J$  = 7.6, 1.7 Hz, 1H, H-4'), 7.46 (ddd,  $J$  = 7.6, 4.8, 1.3 Hz, 1H, H-5'), 7.17 (t,  $J$  = 7.5 Hz, 1H, H-5''), 7.05–6.95 (m, 3H, H-2'',4'',6''), 3.26 (t,  $J$  = 7.3 Hz, 2H, H-2), 2.69 (t,  $J$  = 7.6 Hz, 2H, H-4), 2.32 (s, 3H, - $\text{CH}_3$ ), 2.07 (p,  $J$  = 7.6 Hz, 2H, H-3).

**$^{13}\text{C}$  NMR, HSQC, HMBC** (101 MHz,  $\text{CDCl}_3$ )  $\delta$  /ppm = 202.0 (C=O), 153.6 (C-2'), 149.0 (C-6'), 142.0 (C-1''), 138.0 (C-3''), 137.1 (C-4'), 129.5 (C-2''), 128.4 (C-5''), 127.2 (C-5'), 126.7 (C-4''), 125.7 (C-6''), 121.9 (C-3'), 37.3 (C-2), 35.4 (C-4), 25.7 (C-3), 21.5(- $\text{CH}_3$ ).

**MS** (ESI):  $m/z$  = 240.1  $[\text{M}+\text{H}]^+$ .

**HRMS** (ESI-ToF)  $m/z$ :  $[\text{M}]^+$  calcd for  $\text{C}_{16}\text{H}_{17}\text{NO}$ : 239.1305, found: 239.1311.

#### 4-(4-Chlorophenyl)-1-(pyridin-2-yl)butan-1-one (227d)



Following the general procedure with 4-chlorobenzyl chloride (27.8 mg, 0.17 mmol) the title compound (24.0 mg, 0.09 mmol, 54 %) was isolated as a colorless oil.

$R_f$  = 0.52 (3:1 cyclohexane/ethyl acetate).

**IR** (ATR):  $\tilde{\nu}/\text{cm}^{-1}$  = 2936, 1697, 1584, 1492, 1436, 1370, 1226, 1090, 772, 618.

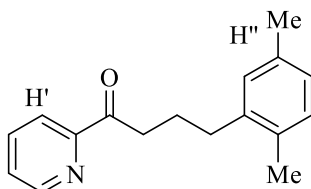
**$^1\text{H}$  NMR, COSY** (400 MHz,  $\text{CDCl}_3$ )  $\delta$  /ppm = 8.66 (dt,  $J$  = 4.8, 1.3 Hz, 1H, H-6'), 8.02 (dt,  $J$  = 7.9, 1.2 Hz, 1H, H-3'), 7.83 (td,  $J$  = 7.7, 1.8 Hz, 1H, H-4'), 7.46 (ddd,  $J$  = 7.7, 4.8, 1.5 Hz, 1H, H-5'), 7.23 (d,  $J$  = 8.4 Hz, AA' part of AA'BB' system, 2H, H-2'',6''), 7.14 (d,  $J$  = 8.4 Hz, 2H, BB' part of AA'BB' system, 2H, H-3'',5''), 3.24 (t,  $J$  = 7.3 Hz, 2H, H-2), 2.69 (t,  $J$  = 7.5 Hz, 2H, H-4), 2.05 (p,  $J$  = 7.5 Hz, 2H, H-3).

**$^{13}\text{C}$  NMR, HSQC, HMBC** (101 MHz,  $\text{CDCl}_3$ )  $\delta$  /ppm = 201.7 (C=O), 153.4 (C-2'), 149.0 (C-6'), 140.5 (C-1''), 137.1 (C-4'), 131.7 (C-4''), 130.0 (C-3'',5''), 128.5 (C-2'',6''), 127.3 (C-5'), 121.9 (C-3'), 37.1 (C-2), 34.8 (C-4), 25.6 (C-3).

**MS** (ESI):  $m/z$  = 260.1  $[\text{M}+\text{H}]^+$ .

**HRMS** (ESI-ToF)  $m/z$ :  $[\text{M}]^+$  calcd for  $\text{C}_{15}\text{H}_{14}\text{ClNO}$ : 259.0764, found: 259.0762.

#### 4-(2,5-Dimethylphenyl)-1-(pyridin-2-yl)butan-1-one (227e)



Following the general procedure with 2,5-dimethylbenzyl chloride (0.026 mL, 0.17 mmol) the title compound (43.2 mg, 0.17 mmol, 99 %) was isolated as a colorless oil.

$R_f$  = 0.56 (3:1 cyclohexane/ethyl acetate).

**IR** (ATR):  $\tilde{\nu}/\text{cm}^{-1}$  = 2943, 1697, 1583, 1461, 1436, 1364, 1227, 994, 809, 618.

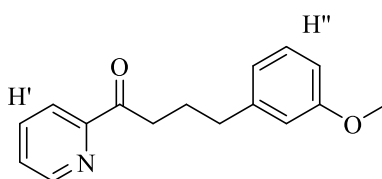
**$^1\text{H}$  NMR, COSY** (400 MHz,  $\text{CDCl}_3$ )  $\delta$  /ppm = 8.72 (ddd,  $J$  = 4.8, 1.7, 0.9 Hz, 1H, H-6'), 8.09–8.05 (m, 1H, H-3'), 7.88 (td,  $J$  = 7.7, 1.7 Hz, 1H, H-4'), 7.51 (ddd,  $J$  = 7.6, 4.8, 1.3 Hz, 1H, H-5'), 7.07–7.01 (m, 2H, H-3'',6''), 6.93 (dd,  $J$  = 7.7, 1.9 Hz, 1H, H-4''), 3.34 (t,  $J$  = 7.2 Hz, 2H, H-2), 2.76–2.64 (m, 2H, H-4), 2.31 (s, 3H, 2- $\text{CH}_3$ ), 2.30 (s, 3H, 5- $\text{CH}_3$ ), 2.11–1.97 (m, 2H, H-3).

**$^{13}\text{C}$  NMR, HSQC, HMBC** (101 MHz,  $\text{CDCl}_3$ )  $\delta$  /ppm = 201.8 (C=O), 153.4 (C-2'), 148.9 (C-6'), 140.3 (C-1''), 137.3 (C-4'), 135.4 (C-5''), 133.0 (C-2''), 130.2 (C-3''), 129.8 (C-6''), 127.2 (C-5'), 126.8 (C-4''), 122.0 (C-3'), 37.7 (C-2), 32.9 (C-4), 24.6 (C-3), 21.1 (5- $\text{CH}_3$ ), 19.0 (2- $\text{CH}_3$ ).

**MS** (ESI):  $m/z$  = 254.1  $[\text{M}+\text{H}]^+$ .

**HRMS** (ESI-ToF)  $m/z$ :  $[\text{M}+\text{H}]^+$  calcd for  $\text{C}_{17}\text{H}_{20}\text{NO}$ : 254.1545, found: 254.1545.

#### 4-(3-methoxyphenyl)-1-(pyridin-2-yl)butan-1-one (227f)



Following the general procedure with 3-methoxybenzyl chloride (0.025 mL, 0.17 mmol) the title compound (40.1 mg, 0.16 mmol, 91 %) was isolated as a yellowish oil.

$R_f$  = 0.45 (3:1 cyclohexane/ethyl acetate).

**IR** (ATR):  $\tilde{\nu}/\text{cm}^{-1}$  = 2935, 1697, 1583, 1569, 1436, 1369, 1226, 995, 774, 695.

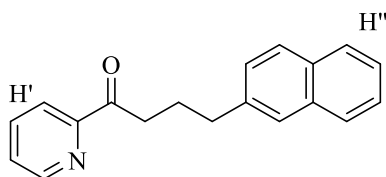
**$^1\text{H}$  NMR, COSY** (400 MHz,  $\text{CDCl}_3$ )  $\delta$  /ppm = 8.67 (ddd,  $J$  = 4.8, 1.8, 0.9 Hz, 1H, H-6'), 8.03 (dt,  $J$  = 7.8, 1.1 Hz, 1H, H-3'), 7.83 (td,  $J$  = 7.7, 1.7 Hz, 1H, H-4'), 7.46 (ddd,  $J$  = 7.6, 4.8, 1.3 Hz, 1H, H-5'), 7.19 (t,  $J$  = 7.8 Hz, 1H, H-5''), 6.82 (dt,  $J$  = 7.6, 1.2 Hz, 1H, H-6''), 6.77 (t,  $J$  = 2.1 Hz, 1H, H-2''), 6.73 (ddd,  $J$  = 8.2, 2.7, 0.9 Hz, 1H, H-4''), 3.79 (s, 3H, - $\text{OCH}_3$ ), 3.26 (t,  $J$  = 7.4 Hz, 2H, H-2), 2.71 (dd,  $J$  = 8.7, 6.8 Hz, 2H, H-4), 2.08 (p,  $J$  = 7.5 Hz, 2H, H-3).

**$^{13}\text{C}$  NMR, HSQC, HMBC** (101 MHz,  $\text{CDCl}_3$ )  $\delta$  /ppm = 201.8 (C=O), 153.5 (C-2'), 159.8 (C-3''), 149.0 (C-6'), 143.7 (C-1''), 137.1 (C-4'), 129.4 (C-5''), 127.2 (C-5'), 121.9 (C-3'), 121.1 (C-6''), 114.3 (C-2''), 111.4 (C-4''), 55.3(- $\text{OCH}_3$ ), 37.3 (C-2), 35.5 (C-4), 25.6 (C-3).

**MS** (ESI):  $m/z$  = 256.1  $[\text{M}+\text{H}]^+$ .

**HRMS** (ESI-ToF)  $m/z$ :  $[\text{M}+\text{H}]^+$  calcd for  $\text{C}_{16}\text{H}_{18}\text{NO}_2$ : 256.1332, found: 256.1337.

**4-(naphthalen-2-yl)-1-(pyridin-2-yl)butan-1-one (227g)**



Following the general procedure with the 2-(chloromethyl)naphthalene (30.5 mg, 0.17 mmol) the title compound (35.8 mg, 0.13 mmol, 75 %) was isolated as a colorless oil.

$R_f = 0.50$  (3:1 cyclohexane/ethyl acetate).

**IR** (ATR):  $\tilde{\nu}/\text{cm}^{-1} = 2930, 1696, 1583, 1569, 1436, 1366, 1227, 995, 770, 746$ .

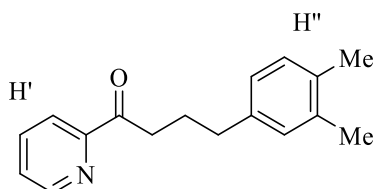
**$^1\text{H NMR}$ , COSY** (400 MHz,  $\text{CDCl}_3$ )  $\delta$  /ppm = 8.68 (d,  $J = 4.6$  Hz, 1H, H-6'), 8.02 (dt,  $J = 7.9, 1.1$  Hz, 1H, H-3'), 7.84 (td,  $J = 7.7, 1.7$  Hz, 1H, H-4'), 7.81–7.74 (m, 3H,  $\text{H}_{\text{Ar}}$ ), 7.66 (s, 1H,  $\text{H}_{\text{Ar}}$ ), 7.51–7.43 (m, 1H, H-5'), 7.46–7.38 (m, 2H,  $\text{H}_{\text{Ar}}$ ), 7.38 (dd,  $J = 8.6, 1.8$  Hz, 1H,  $\text{H}_{\text{Ar}}$ ), 3.31 (t,  $J = 7.3$  Hz, 2H, H-2), 2.91 (t,  $J = 7.6$  Hz, 2H, H-4), 2.19 (p,  $J = 7.4$  Hz, 2H, H-3).

**$^{13}\text{C NMR}$ , HSQC, HMBC** (101 MHz,  $\text{CDCl}_3$ )  $\delta$  /ppm = 202.5 (C=O), 153.1 (C-2'), 148.7 (C-6'), 139.5 (C-1''), 137.5 (C-4'), 133.7 ( $\text{C}_{\text{Ar}}$ ), 132.2 ( $\text{C}_{\text{Ar}}$ ), 128.0 ( $\text{CH}_{\text{Ar}}$ ), 127.7 ( $\text{CH}_{\text{Ar}}$ ), 127.6 ( $\text{CH}_{\text{Ar}}$ ), 127.5 ( $\text{CH}_{\text{Ar}}$ ), 127.3 (C-5'), 126.7 ( $\text{CH}_{\text{Ar}}$ ), 126.0 ( $\text{CH}_{\text{Ar}}$ ), 125.3 ( $\text{CH}_{\text{Ar}}$ ), 122.1 (C-3'), 37.4 (C-2), 35.6 (C-4), 25.6 (C-3).

**MS** (ESI):  $m/z = 276.1$   $[\text{M}+\text{H}]^+$ .

**HRMS** (ESI-ToF)  $m/z$ :  $[\text{M}]^+$  calcd for  $\text{C}_{15}\text{H}_{15}\text{NO}$ : 275.1310, found: 275.1306.

**4-(3,4-dimethylphenyl)-1-(pyridin-2-yl)butan-1-one (227h)**



Following the general procedure with 3,4-dimethylbenzyl chloride (0.036 mL, 0.17 mmol) the title compound (32.9 mg, 0.17 mmol, 75 %) was isolated as a colorless oil.

$R_f = 0.49$  (3:1 cyclohexane/ethyl acetate).

**IR** (ATR):  $\tilde{\nu}/\text{cm}^{-1} = 2934, 1697, 1583, 1452, 1436, 1368, 1226, 995, 809, 618$ .

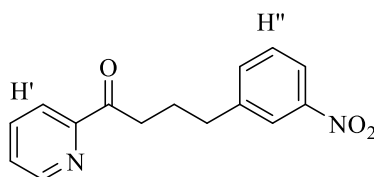
**<sup>1</sup>H NMR, COSY** (400 MHz, CDCl<sub>3</sub>)  $\delta$  /ppm = 8.72–8.64 (m, 1H, H-6'), 8.04 (ddt,  $J$  = 7.9, 4.3, 1.1 Hz, 1H, H-3'), 7.84 (tdd,  $J$  = 7.7, 3.0, 1.7 Hz, 1H, H-4'), 7.47 (dddd,  $J$  = 7.6, 4.8, 3.2, 1.3 Hz, 1H, H-5'), 7.07–6.99 (m, 2H, H-2'',5''), 6.96 (dd,  $J$  = 7.6, 1.9 Hz, 1H, H-6''), 3.26 (t,  $J$  = 7.4 Hz, 1H, H-2), 2.66 (dd,  $J$  = 8.8, 6.8 Hz, 2H, H-4), 2.23 (s, 3H, 2-CH<sub>3</sub>), 2.22 (s, 3H, 3-CH<sub>3</sub>), 2.05 (p,  $J$  = 7.6 Hz, 1H, H-3).

**<sup>13</sup>C NMR, HSQC, HMBC** (101 MHz, CDCl<sub>3</sub>)  $\delta$  /ppm = 201.9 (C=O), 153.4 (C-2'), 148.9 (C-6'), 139.5 (C-1''), 137.2 (C-4'), 136.5 (C-3''), 134.0 (C-4''), 130.0 (C-2''), 129.7 (C-5''), 127.2 (C-5'), 126.0 (C-6''), 122.0 (C-3'), 37.4 (C-2), 35.0 (C-4), 26.0 (C-3), 19.9 (4-CH<sub>3</sub>), 19.5 (3-CH<sub>3</sub>).

**MS** (ESI):  $m/z$  = 254.1 [M+H]<sup>+</sup>.

**HRMS** (ESI-ToF)  $m/z$ : [M]<sup>+</sup> calcd for C<sub>17</sub>H<sub>19</sub>NO: 253.1467, found: 253.1469.

#### 4-(3-nitrophenyl)-1-(pyridin-2-yl)butan-1-one (227i)



Following the general procedure with 3-nitrobenzyl chloride (29.6 mg, 0.17 mmol) the title compound (24.4 mg, 0.09 mmol, 52 %) was isolated as a colorless solid.

**Mp**: 69–71 °C (cyclohexane-ethyl acetate)

**R<sub>f</sub>** = 0.37 (3:1 cyclohexane/ethyl acetate).

**IR** (ATR):  $\tilde{\nu}/\text{cm}^{-1}$  = 2935, 1697, 1583, 1461, 1437, 1351, 1227, 995, 805, 687.

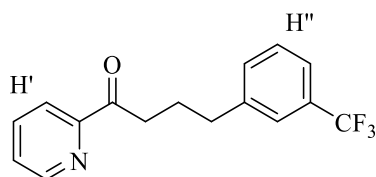
**<sup>1</sup>H NMR, COSY** (400 MHz, CDCl<sub>3</sub>)  $\delta$  /ppm = 8.68 (dt,  $J$  = 4.8, 1.2 Hz, 1H, H-6'), 8.10 (d,  $J$  = 2.0 Hz, 1H, H-2''), 8.08–7.98 (m, 2H, H-3',4''), 7.85 (td,  $J$  = 7.7, 1.8 Hz, 1H, H-4'), 7.59–7.51 (m, 1H, H-6''), 7.51–7.48 (m, 1H, H-5'), 7.48–7.41 (m, 1H, H-5''), 3.28 (t,  $J$  = 7.2 Hz, 2H, H-2), 2.84 (dd,  $J$  = 8.8, 6.8 Hz, 2H, H-4), 2.13 (p,  $J$  = 7.4 Hz, 2H, H-3).

**<sup>13</sup>C NMR, HSQC, HMBC** (101 MHz, CDCl<sub>3</sub>)  $\delta$  /ppm = 201.4 (C=O), 153.3 (C-2'), 149.0 (C-6'), 148.5 (C-3''), 144.1 (C-1''), 137.2 (C-4'), 135.0 (C-6''), 129.4 (C-5''), 127.4 (C-5'), 123.5 (C-2''), 122.0 (C-3'), 121.3 (C-4''), 36.9 (C-2), 35.1 (C-4), 25.4 (C-3).

**MS** (ESI):  $m/z$  = 271.1 [M+H]<sup>+</sup>.

**HRMS** (ESI-ToF)  $m/z$ :  $[M]^+$  calcd for  $C_{15}H_{14}N_2O_3$ : 270.1004, found: 270.1008.

**1-(pyridin-2-yl)-4-[3-(trifluoromethyl)phenyl]butan-1-one (227j)**



Following the general procedure with 3-(Trifluoromethyl)benzyl chloride (0.027 mL, 0.17 mmol) the title compound (31.0 mg, 0.09 mmol, 61 %) was isolated as a yellowish oil.

$R_f$  = 0.42 (3:1 cyclohexane/ethyl acetate).

**IR** (ATR):  $\tilde{\nu}/\text{cm}^{-1}$  = 2985, 1737, 1373, 1235, 1164, 1044, 937, 847, 737, 704, 634.

**$^1\text{H}$  NMR, COSY** (400 MHz,  $\text{CDCl}_3$ )  $\delta$  /ppm = 8.69–8.66 (m, 1H, H-6'), 8.07–8.00 (m, 1H, H-3'), 7.84 (td,  $J$  = 7.8, 1.8 Hz, 1H, H-4'), 7.52–7.35 (m, 5H, H-5', 2'', 4'', 5'', 6''), 3.27 (t,  $J$  = 7.3 Hz, 2H, H-2), 2.79 (t,  $J$  = 7.5 Hz, 2H, H-4), 2.10 (p,  $J$  = 7.5 Hz, 2H, H-3).

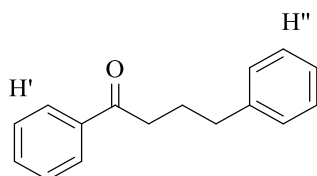
**$^{13}\text{C}$  NMR, HSQC, HMBC** (101 MHz,  $\text{CDCl}_3$ )  $\delta$  /ppm = 201.6 (C=O), 153.4 (C-2'), 149.0 (C-6'), 142.9 (C-1''), 137.2 (C-4'), 132.1 (C-6''), 130.7 (q,  $J$  = 32.0 Hz, C-3''), 128.9 (C-5''), 127.3 (C-5'), 125.3 (q,  $J$  = 4.0 Hz, C-2''), 124.4 (q,  $J$  = 273.6 Hz,  $\text{CF}_3$ ), 122.9 (q,  $J$  = 3.5 Hz, C-4''), 122.0 (C-3'), 37.1 (C-2), 35.2 (C-4), 25.5 (C-3).

**$^{19}\text{F}$  NMR** (376 MHz,  $\text{CDCl}_3$ )  $\delta$  /ppm = -63.7 (s,  $\text{CF}_3$ ).

**MS** (ESI):  $m/z$  = 294.1  $[M+H]^+$ .

**HRMS** (ESI-ToF)  $m/z$ :  $[M]^+$  calcd for  $C_{16}H_{14}F_3NO$ : 293.1027, found: 293.1027.

**1,4-diphenylbutan-1-one (227k)**



Following the general procedure with 1-phenylcyclopropan-1-ol (40 mg, 0.30 mmol) and benzyl chloride (0.023 mL, 0.20 mmol) the title compound (30.7 mg, 0.14 mmol, 69 %) was isolated as a colorless solid.

**Mp**: 55–56 °C (cyclohexane-ethyl acetate). Lit.<sup>[208]</sup>: 54–57 °C.



$R_f = 0.51$  (4:1 cyclohexane/ethyl acetate).

**IR** (ATR):  $\tilde{\nu}/\text{cm}^{-1} = 2935, 1683, 1597, 1496, 1449, 1367, 1265, 1226, 1001, 743, 691$ .

**$^1\text{H}$  NMR, COSY** (400 MHz,  $\text{CDCl}_3$ )  $\delta$  /ppm = 7.97–7.90 (m, 2H, H-2',6'), 7.55 (dd,  $J = 8.6, 6.2$  Hz, 1H, H-4'), 7.45 (t,  $J = 7.7$  Hz, 2H, H-3',5'), 7.34–7.27 (m, 2H, H-3'',5''), 7.24–7.14 (m, 3H, H-2'', 4'',6''), 2.99 (t,  $J = 7.3$  Hz, 2H, H-2), 2.73 (t,  $J = 7.6$  Hz, 2H, H-4), 2.10 (p,  $J = 7.3$  Hz, 2H, H-3).

**$^{13}\text{C}$  NMR, HSQC, HMBC** (101 MHz,  $\text{CDCl}_3$ )  $\delta$  /ppm = 202.3 (C=O), 142.8 (C-1''), 137.1 (C-1'), 133.1 (C-4'), 128.7 (2C,  $\text{CH}_{\text{Ar}}$ ), 128.6 (2C,  $\text{CH}_{\text{Ar}}$ ), 128.5 (2C,  $\text{CH}_{\text{Ar}}$ ), 128.1 (2C,  $\text{CH}_{\text{Ar}}$ ), 37.8 (C-2), 35.3 (C-4), 25.8 (C-3).

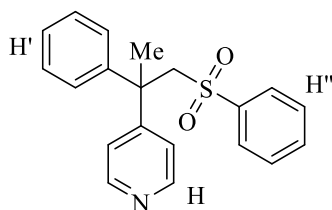
**MS** (ESI):  $m/z = 225.1$   $[\text{M}+\text{H}]^+$ .

The spectroscopic data are in accordance with those reported in the literature.<sup>[209]</sup>

### 4.2.3. Section 3.4.1

#### General procedure for the photoredox-sulfonylation/arylation of styrene derivatives

In a 50 mL, round bottom flask equipped with a stir bar were added the sodium sulfinate (1.00 mmol, 2.00 equiv.), the aromatic nitrile (0.50 mmol, 1.00 equiv.),  $\text{Na}_2\text{HPO}_4 \cdot 2\text{H}_2\text{O}$  (178 mg, 1.00 mmol, 2.00 equiv.),  $\text{fac-Ir}(\text{ppy})_3$  (3.27 mg, 5.00  $\mu\text{mol}$ , 0.01 equiv.) and, if solid, the styrene derivative (0.75–1.00 mmol, 1.50–2.00 equiv.). The flask was sealed with a septum and filled with an atmosphere of argon. A mixture of acetonitrile and deionized water (24.3 mL/2.7 mL, 9:1) was added via syringe. The mixture of solvents had previously been degassed in an ultrasonic bath for 20 min by argon sparging. Liquid styrene derivatives were also added via syringe. The reaction mixture was degassed again by argon sparging for 1 min, followed by irradiation with a 23 W household CFL bulb. After 20 h, 15 mL of a saturated aqueous solution of  $\text{NaHCO}_3$  was added, followed by extraction with EtOAc (3  $\times$  20 mL). The combined organic extracts were dried over  $\text{Na}_2\text{SO}_4$  and filtered. The solvent was removed *in vacuo* and the residue was purified by flash column chromatography ( $\text{SiO}_2$ , 20%  $\rightarrow$  100% ethyl acetate in cyclohexane).

**4-(2-Phenyl-1-(phenylsulfonyl)propan-2-yl)pyridine (262u)**

The title compound was prepared according to the general procedure using 4-cyanopyridine (52.0 mg, 0.50 mmol, 1.00 equiv.),  $\alpha$ -methylstyrene (98.0  $\mu$ L, 0.75 mmol, 1.50 equiv.), and sodium benzenesulfinate (164.0 mg, 1.00 mmol, 2.00 equiv., prepared according to a procedure by König et al.<sup>[188a]</sup>). Purification by flash chromatography afforded the product **262u** (156 mg, 0.46 mmol, 93%) as yellowish oil.

$R_f$  = 0.30 (Ethyl acetate).

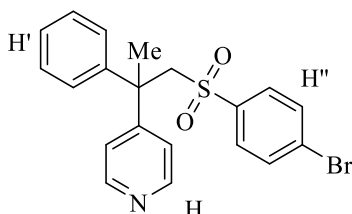
**IR** (ATR):  $\tilde{\nu}/\text{cm}^{-1}$  = 3058, 3026, 2982, 1594, 1495, 1319, 1147, 1083, 822, 699.

**$^1\text{H}$  NMR, COSY** (400 MHz,  $\text{CDCl}_3$ ):  $\delta$  /ppm= 8.41 (dd,  $J$  = 4.8, 1.8 Hz, 2H, H-2,6), 7.58–7.43 (m, 3H, H-2'',4'',6''), 7.36–7.31 (m, 2H, H-3'',5''), 7.23–7.12 (m, 3H, H-3',4',5'), 7.08–6.90 (m, 4H, H-2',6',3,5), 4.06 (s, 2H,  $\text{CH}_2$ ), 2.07 (s, 3H,  $\text{CH}_3$ ).

**$^{13}\text{C}$  NMR, HSQC, HMBC** (101 MHz,  $\text{CDCl}_3$ ):  $\delta$  /ppm= 155.4 (C-4), 149.9 (2C, C-2,6), 145.0 (C-1'), 133.3 (C-4''), 140.8 (C-1''), 129.2 (2C, C-3'',5''), 128.6 (2C, C-3',5'), 127.5 (2C, C-2'',6''), 127.3 (C-4'), 127.1 (2C, C-2',6'), 122.5 (2C, C-3,5), 66.1 ( $\text{CH}_2$ ), 45.8 ( $\text{C}_q$ ), 27.3 ( $\text{CH}_3$ ).

**MS** (ESI):  $m/z$  = 338.1  $[\text{M}+\text{H}]^+$ .

**HRMS** (ESI-ToF)  $m/z$ :  $[\text{M}+\text{H}]^+$  calcd for  $\text{C}_{20}\text{H}_{20}\text{NO}_2\text{S}$ : 338.1209, found 338.1205.

**4-(1-((4-Bromophenyl)sulfonyl)-2-phenylpropan-2-yl)pyridine (262v)**

The title compound was prepared according to the general procedure using 4-cyanopyridine (52.0 mg, 0.50 mmol, 1.00 equiv.),  $\alpha$ -methylstyrene (98.0  $\mu$ L, 0.75 mmol, 1.50 equiv.), and sodium 4-bromobenzenesulfinate (243.0 mg, 1.00 mmol, 2.00 equiv. prepared according to

a procedure by König et al.<sup>[188a]</sup>). Purification by flash chromatography afforded the product **262v** (208.2 mg, 0.5 mmol, 100%) as a colorless solid.

$R_f = 0.30$  (1:2, cyclohexane/ethyl acetate).

$Mp = 122\text{--}123\text{ }^\circ\text{C}$ .

**IR** (ATR):  $\tilde{\nu}/\text{cm}^{-1} = 3058, 3026, 2979, 1593, 1495, 1307, 1144, 1083, 823, 698$ .

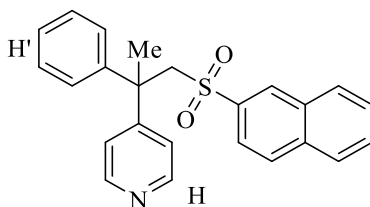
**$^1\text{H NMR}$ , COSY** (400 MHz,  $\text{CDCl}_3$ ):  $\delta/\text{ppm} = 8.45\text{--}8.40$  (m, 2H, H-2,6), 7.46–7.43 (AA' part of AA'–BB' system, 2H, H-3'',5''), 7.33–7.29 (BB' part of AA'–BB' system, 2H, H-2'',6''), 7.19–7.14 (m, 3H, H-3',4',5'), 7.01–6.96 (m, 4H, H-2',6',3,5), 4.08 (d,  $J = 14.6$  Hz, 1H,  $\text{CH}_{2a}$ ), 4.06 (d,  $J = 14.6$  Hz, 1H,  $\text{CH}_{2b}$ ), 2.05 (s, 3H,  $\text{CH}_3$ ).

**$^{13}\text{C NMR}$ , HSQC, HMBC** (101 MHz,  $\text{CDCl}_3$ ):  $\delta/\text{ppm} = 155.8$  (C-4), 150.0 (2C, C-2,6), 144.2 (C-1'), 139.7 (C-1''), 132.4 (2C, C-3'',5''), 129.1 (2C, C-2'',6''), 128.6 (2C, C-3',4',5'), 127.4 (C-4'), 127.3 (2C, C-2',6'), 122.2 (2C, C-3,5), 66.3 ( $\text{CH}_2$ ), 45.8 (CH), 27.3 ( $\text{CH}_3$ ).

**MS** (ESI):  $m/z = 418.0$  [ $\text{M}+3\text{H}$ ]<sup>+</sup>

**HRMS** (ESI-ToF)  $m/z$ : [ $\text{M}+\text{H}$ ]<sup>+</sup> calcd for  $\text{C}_{20}\text{H}_{19}\text{BrNO}_2\text{S}$ : 416.0314, found 416.0310.

#### 4-(1-(Naphthalene-2-ylsulfonyl)-2-phenylpropan-2-yl)pyridine (**262w**)



The title compound was prepared according to the general procedure using 4-cyanopyridine (52.0 mg, 0.50 mmol, 1.00 equiv.),  $\alpha$ -methylstyrene (97.5  $\mu\text{L}$ , 0.75 mmol, 1.50 equiv.), and sodium naphthalene-2-sulfinate (144.0 mg, 1.00 mmol, 2.00 equiv., prepared according to a procedure by König et al.<sup>[188a]</sup>). Purification by flash chromatography afforded the product **262w** (126.0 mg, 0.33 mmol, 65%) as a colorless solid.

$R_f = 0.38$  (1:2, cyclohexane/ethyl acetate).

$Mp = 85\text{--}86\text{ }^\circ\text{C}$ .

**IR** (ATR):  $\tilde{\nu}/\text{cm}^{-1} = 3055, 3024, 2953, 1592, 1410, 1311, 1144, 908, 819, 755$ .

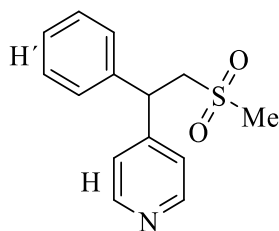
**<sup>1</sup>H NMR, COSY** (400 MHz, CDCl<sub>3</sub>):  $\delta$  /ppm= 8.40 (br s, 2H, H-2,6), 8.00 (d,  $J$  = 1.8 Hz, 1H, H<sub>Naphth</sub>), 7.87 (d,  $J$  = 8.2 Hz, 1H, H<sub>Naphth</sub>), 7.85–7.81 (m, 1H, H<sub>Naphth</sub>), 7.68–7.60 (m, 3H, H<sub>Naphth</sub>), 7.58 (dd,  $J$ =8.7, 1.9 Hz, 1H, H-4'), 7.13–7.11 (m, 2H, H-3,5), 7.08 (dd,  $J$  = 7.2, 1.2 Hz, 2H, H-3',5'), 7.04–7.02 (m, 1H, H<sub>Naphth</sub>), 7.00–6.95 (m, 2H, H-2',6'), 4.12 (s, 2H, CH<sub>2</sub>), 2.11 (s, 3H, CH<sub>3</sub>).

**<sup>13</sup>C NMR, HSQC, HMBC** (101 MHz, CDCl<sub>3</sub>):  $\delta$  /ppm= 157.6 (C-4), 148.2 (2C, C-2,6), 144.3 (C-1'), 137.5 (C<sub>q,Naphth</sub>), 135.1 (C<sub>q,Naphth</sub>), 132.0 (C<sub>q,Naphth</sub>), 129.64 (CH<sub>Naphth</sub>), 129.63 (CH<sub>Naphth</sub>), 129.6 (CH<sub>Naphth</sub>), 129.5 (CH<sub>Naphth</sub>), 128.6 (2C, C-3',5'), 128.0 (CH<sub>Naphth</sub>), 127.8 (CH<sub>Naphth</sub>), 127.5 (C-4'), 127.1 (2C, C-2',6'), 123.0 (2C, C-3,5), 122.0 (CH<sub>Naphth</sub>), 65.8 (CH<sub>2</sub>), 46.1 (C<sub>q</sub>), 27.3 (CH<sub>3</sub>).

**MS** (ESI):  $m/z$  = 388.1 [M+H]<sup>+</sup>

**HRMS** (ESI-ToF)  $m/z$ : [M+H]<sup>+</sup> calcd for C<sub>24</sub>H<sub>22</sub>NO<sub>2</sub>S: 388.1366, found 388.1366.

#### 4-(2-(Methylsulfonyl)-1-phenylethyl)pyridine (**262x**)



The title compound was prepared according to the general procedure using 4-cyanopyridine (52.0 mg, 0.50 mmol, 1.00 equiv.), styrene (115.0  $\mu$ L, 1.00 mmol, 2.00 equiv.), and sodium methanesulfinate (102.0 mg, 1.00 mmol, 2.00 equiv., prepared according to a procedure by König et al.<sup>[188a]</sup>). Purification by flash chromatography afforded the product **262x** (130.0 mg, 0.50 mmol, quant.) as a yellow oil.

$R_f$  = 0.17 (1:10, cyclohexane/ethyl acetate).

**IR** (ATR):  $\tilde{\nu}/\text{cm}^{-1}$  = 3027, 2927, 1595, 1494, 1415, 1125, 918, 864, 747, 701.

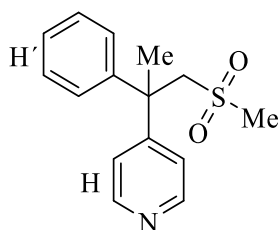
**<sup>1</sup>H NMR, COSY** (300 MHz, CDCl<sub>3</sub>):  $\delta$  /ppm = 8.50–8.49 (m, 2H, H-2,6), 7.33–7.29 (m, 5H, H<sub>Ar</sub>), 7.25–7.19 (m, 2H, H-3,5), 4.61 (dd,  $J$  = 8.1, 6.3 Hz, 1H, CH), 3.83–3.69 (m, 2H, CH<sub>2</sub>), 2.40 (s, 3H, CH<sub>3</sub>).

**$^{13}\text{C}$  NMR, HSQC, HMBC** (75 MHz,  $\text{CDCl}_3$ ):  $\delta$  /ppm = 150.4 ( $\text{C}_{q-4'}$ ), 150.2 ( $\text{C-2}',6'$ ), 139.7 ( $\text{C}_{q-1}$ ), 129.4 (CH), 128.0 (C-4), 127.9 (CH), 122.7 ( $\text{C-3}',5'$ ), 59.5 ( $\text{CH}_2$ ), 45.4 (CH), 42.1 ( $\text{CH}_3$ ).

**MS** (ESI):  $m/z$  = 262.1  $[\text{M}+\text{H}]^+$

**HRMS** (ESI-ToF)  $m/z$ :  $[\text{M}+\text{H}]^+$  calcd for  $\text{C}_{14}\text{H}_{16}\text{NO}_2\text{S}$ : 262.0896, found 262.0893.

#### 4-(1-(Methylsulfonyl)-2-phenylpropan-2-yl)pyridine (262y)



The title compound was prepared according to the general procedure using 4-cyanopyridine (52.0 mg, 0.50 mmol, 1.00 equiv.),  $\alpha$ -methylstyrene (98.0  $\mu\text{L}$ , 0.75 mmol, 1.50 equiv.), and sodium methanesulfinate (102.0 mg, 1.00 mmol, 2.00 equiv., prepared according to a procedure by König et al.<sup>[188a]</sup>). Purification by flash chromatography afforded the product **262y** (135.0 mg, 490  $\mu\text{mol}$ , 98%) as a colorless solid.

$R_f$  = 0.12 (1:2, cyclohexane/ethyl acetate).

$\text{Mp}$  = 167–169  $^\circ\text{C}$ .

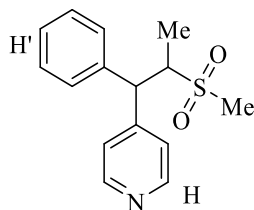
**IR** (ATR):  $\tilde{\nu}/\text{cm}^{-1}$  = 3057, 3027, 2928, 1594, 1411, 1307, 1123, 968, 826, 771, 702.

**$^1\text{H}$  NMR, COSY** (400 MHz,  $\text{CDCl}_3$ ):  $\delta$  /ppm = 8.56 (*pseudo*-d,  $J$  = 5.1 Hz, 2H, H-2,6), 7.39–7.35 (m, 2H, H-3',5'), 7.33–7.29 (m, 1H, H-4'), 7.25–7.22 (m, 2H, H-2',6'), 7.12–7.10 (m, 2H, H-3,5), 3.88 (d,  $J$  = 14.6 Hz, 1H,  $\text{CH}_{2a}$ ), 3.81 (d,  $J$  = 14.6 Hz, 1H,  $\text{CH}_{2b}$ ), 2.10 (s, 3H,  $\text{CH}_3\text{-SO}_2$ ), 2.01 (s, 3H,  $\text{CH}_3\text{-C}_q$ ).

**$^{13}\text{C}$  NMR, HSQC, HMBC** (101 MHz,  $\text{CDCl}_3$ ):  $\delta$  /ppm = 156.7 (C-4), 150.3 (2C, C-2,6), 144.0 (C-1'), 129.0 (2C, C-3',5'), 127.9 (3C, C-2',4',6'), 122.0 (2C, C-3,5), 65.3 ( $\text{CH}_2$ ), 45.7 ( $\text{C}_q$ ), 42.8 ( $\text{CH}_3\text{-SO}_2$ ), 27.1 ( $\text{CH}_3\text{-C}_q$ ).

**MS** (ESI):  $m/z$  = 276.1  $[\text{M}+\text{H}]^+$

**HRMS** (ESI-ToF)  $m/z$ :  $[\text{M}+\text{H}]^+$  calcd for  $\text{C}_{15}\text{H}_{18}\text{NO}_2\text{S}$ : 276.1053, found 276.1056.

**4-(2-(methylsulfonyl)-1-phenylpropyl)pyridine (262y')**

The title compound was prepared according to the general procedure using 4-cyanopyridine (52.0 mg, 0.50 mmol, 1.00 equiv.),  $\beta$ -methylstyrene (97.5  $\mu$ L, 0.75 mmol, 1.50 equiv.), and sodium methanesulfinate (102.0 mg, 1.00 mmol, 2.0 equiv., prepared according to a procedure by König et al.<sup>[188a]</sup>). Purification by flash chromatography afforded the product **262y'** (124 mg, 0.45 mmol, 90%) as a colorless solid.

$R_f$  = 0.19 (1:2, cyclohexane/ethyl acetate).

$M_p$  = 109–110 °C.

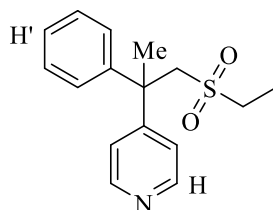
**IR** (ATR):  $\tilde{\nu}/\text{cm}^{-1}$  = 3029, 2931, 1594, 1415, 1293, 1130, 744, 700.

**$^1\text{H}$  NMR, COSY** (400 MHz,  $\text{CDCl}_3$ ):  $\delta$  /ppm = 8.57 (br s, 2H, H-2,6), 7.44–7.33 (m, 4H, H-2',3',5',6'), 7.32–7.22 (m, 3H, H-3,5,4'), 4.38 (d,  $J$  = 10.0 Hz, 1H, CH-C<sub>4</sub>), 3.89 (dq,  $J$  = 10.0 Hz, 7.1 Hz, 1H, CH-SO<sub>2</sub>), 2.23 (s, 3H, SO<sub>2</sub>-CH<sub>3</sub>), 1.38 (d,  $J$  = 7.1 Hz, 3H, CH<sub>3</sub>-CH).

**$^{13}\text{C}$  NMR, HSQC, HMBC** (101 MHz,  $\text{CDCl}_3$ ):  $\delta$  /ppm = 150.5 (2C, C-2,6), 150.0 (C-4), 140.2 (C-1'), 129.7 (2C, C-3',5'), 128.5 (2C, C-2',6'), 128.4 (C-4') 123.7 (2C, C-3,5), 62.7 (CH-C<sub>4</sub>), 52.6 (CH-SO<sub>2</sub>), 42.0 (SO<sub>2</sub>-CH<sub>3</sub>), 12.3 (CH<sub>3</sub>-CH).

**MS** (ESI):  $m/z$  = 276.1 [M+H]<sup>+</sup>

**HRMS** (ESI-ToF)  $m/z$ : [M+H]<sup>+</sup> calcd for C<sub>15</sub>H<sub>18</sub>NO<sub>2</sub>S: 276.1053, found 276.1053.

**4-(1-(Ethylsulfonyl)-2-phenylpropan-2-yl)pyridine (262z)**

The title compound was prepared according to the general procedure using 4-cyanopyridine (52.0 mg, 0.50 mmol, 1.00 equiv.),  $\alpha$ -methylstyrene (98.0  $\mu$ L, 0.75 mmol, 1.50 equiv.), and sodium ethanesulfinate (116.0 mg, 1.00 mmol, 2.00 equiv., prepared according to a procedure by König et al.<sup>[188a]</sup>). Purification by flash chromatography afforded the product **262z** (131.0 mg, 0.45 mmol, 91%) as a yellowish oil.

$R_f$  = 0.14 (1:2, cyclohexane/ethyl acetate).

**IR** (ATR):  $\tilde{\nu}/\text{cm}^{-1}$  = 3057, 3026, 2980, 1594, 1411, 1311, 1122, 825, 701.

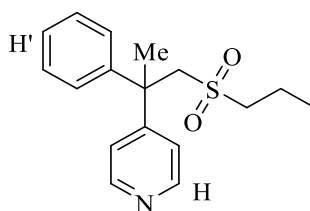
**<sup>1</sup>H NMR, COSY** (400 MHz, CDCl<sub>3</sub>):  $\delta$  /ppm = 8.56 (br s, 2H, H-2,6), 7.39–7.27 (m, 3H, H-3',4',5'), 7.24–7.19 (m, 2H, H-2',6'), 7.17 (d,  $J$  = 5.4 Hz, 2H, H-3,5), 3.83 (d,  $J$  = 14.6 Hz, 1H, CH<sub>2a</sub>), 3.76 (d,  $J$  = 14.6 Hz, 1H, CH<sub>2b</sub>), 2.17 (dq,  $J$  = 8.6, 7.4 Hz, 2H, CH<sub>2</sub>CH<sub>3</sub>), 2.03 (s, 3H, CH<sub>3</sub>-C<sub>q</sub>), 1.14 (t,  $J$  = 7.4 Hz, 3H, CH<sub>3</sub>CH<sub>2</sub>).

**<sup>13</sup>C NMR, HSQC, HMBC** (101 MHz, CDCl<sub>3</sub>):  $\delta$  /ppm = 157.4 (C-4), 149.5 (2C, C-2,6), 144.4 (C-1'), 128.9 (2C, C-3',5'), 127.8 (C-4'), 127.6 (2C, C-2',6'), 122.4 (2C, C-3,5), 62.0 (CH<sub>2</sub>SO<sub>2</sub>), 49.3 (CH<sub>2</sub>CH<sub>3</sub>), 45.8 (C<sub>q</sub>), 27.2 (CH<sub>3</sub>-C<sub>q</sub>), 6.7 (CH<sub>2</sub>CH<sub>3</sub>).

**MS** (ESI):  $m/z$  = 290.1 [M+H]<sup>+</sup>

**HRMS** (ESI-ToF)  $m/z$ : [M+H]<sup>+</sup> calcd for C<sub>16</sub>H<sub>20</sub>NO<sub>2</sub>S: 290.1209, found 290.1207.

#### 4-(2-Phenyl-1-(propylsulfonyl)propan-2-yl)pyridine (**262aa**)



The title compound was prepared according to the general procedure using 4-cyanopyridine (52.0 mg, 0.50 mmol, 1.00 equiv.),  $\alpha$ -methylstyrene (98.0  $\mu$ L, 0.75 mmol, 1.50 equiv.), and sodium propane-1-sulfinate (130.0 mg, 1.00 mmol, 2.00 equiv., prepared according to a procedure by König et al.<sup>[188a]</sup>). Purification by flash chromatography afforded the product **262aa** (139.0 mg, 0.46 mmol, 92%) as a yellowish oil.

$R_f$  = 0.23 (1:2, cyclohexane/ethyl acetate).

**IR** (ATR):  $\tilde{\nu}/\text{cm}^{-1}$  = 3057, 3026, 2970, 1594, 1411, 1312, 1122, 825, 701.

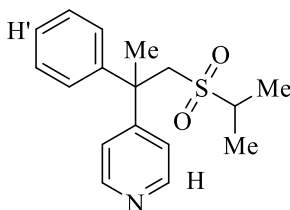
**<sup>1</sup>H NMR, COSY** (400 MHz, CDCl<sub>3</sub>):  $\delta$  /ppm = 8.56 (br s, 2H, H-2,6), 7.40–7.28 (m, 3H, H-3',4',5'), 7.25–7.19 (m, 2H, H-2',6'), 7.15–7.08 (m, 2H, H-3,5), 3.82 (d,  $J$  = 14.6 Hz, 1H, CH<sub>2a</sub>), 3.73 (d,  $J$  = 14.6 Hz, 1H, CH<sub>2b</sub>) 2.11–1.95 (m, 5H, CH<sub>3</sub>-C<sub>q</sub>, H-1''), 1.73– 1.49 (m, 2H, H-2''), 0.80 (t,  $J$  = 7.2 Hz, 3H, H-3'').

**<sup>13</sup>C NMR, HSQC, HMBC** (101 MHz, CDCl<sub>3</sub>):  $\delta$  /ppm = 156.8 (C-4), 150.2 (2C, C-2,6), 144.4 (C-1'), 128.9 (2C, C-3',5'), 127.8 (2C, C-2',6'), 127.7 (C-4'), 122.1 (2C, C-3,5), 62.7 (CH<sub>2</sub>SO<sub>2</sub>), 56.5 (C-1''), 45.7 (C<sub>q</sub>), 27.3 (CH<sub>3</sub>-C<sub>q</sub>), 15.9 (C-2''), 13.0 (C-3'').

**MS** (ESI):  $m/z$  = 304.2 [M+H]<sup>+</sup>

**HRMS** (ESI-ToF)  $m/z$ : [M+H]<sup>+</sup> calcd for C<sub>17</sub>H<sub>22</sub>NO<sub>2</sub>S: 304.1366, found 304.1364.

#### 4-(1-(Isopropylsulfonyl)-2-phenylpropan-2-yl)pyridine (262ab)



The title compound was prepared according to the general procedure using 4-cyanopyridine (52.0 mg, 0.50 mmol, 1.00 equiv.),  $\alpha$ -methylstyrene (98.0  $\mu$ L, 0.75 mmol, 1.50 equiv.), and sodium propane-2-sulfinate (130.0 mg, 1.00 mmol, 2.00 equiv., prepared according to a procedure by König et al.<sup>[188a]</sup>). Purification by flash chromatography afforded the product **262ab** (99.0 mg, 0.33 mmol, 66%) as a yellowish oil.

$R_f$  = 0.13 (1:2, cyclohexane/ethyl acetate).

**IR** (ATR):  $\tilde{\nu}/\text{cm}^{-1}$  = 3057, 3026, 2980, 1594, 1411, 1309, 1120, 825, 700.

**<sup>1</sup>H NMR, COSY** (400 MHz, CDCl<sub>3</sub>):  $\delta$  /ppm = 8.56 (br s, 2H, H-2,6), 7.37– 7.27 (m, 3H, H-3',4',5'), 7.23–7.18 (m, 2H, H-2',6'), 7.17–7.13 (m, 2H, H-3,5), 3.81 (d,  $J$  = 14.3 Hz, 1H, CH<sub>2a</sub>), 3.73 (d,  $J$  = 14.3 Hz, 1H, CH<sub>2b</sub>), 2.23 (sept,  $J$  = 6.8 Hz, 1H, CH), 2.05 (s, 3H, CH<sub>3</sub>-C<sub>q</sub>), 1.21 (t,  $J$  = 6.8 Hz, 6H, CH-(CH<sub>3</sub>)<sub>2</sub>).

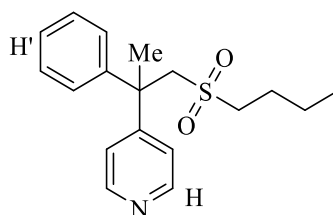
**<sup>13</sup>C NMR, HSQC, HMBC** (101 MHz, CDCl<sub>3</sub>):  $\delta$  /ppm = 156.7 (C-4), 149.8 (2C, C-2,6), 145.0 (C-1'), 128.8 (2C, C-3',5'), 127.6 (C-4'), 127.4 (2C, C-2',6'), 122.4 (2C, C-3,5), 58.8 (CH<sub>2</sub>), 54.8 (CH), 45.8 (C<sub>q</sub>), 27.3 (CH<sub>3</sub>-C<sub>q</sub>), 15.8 (CH-CH<sub>3a</sub>), 15.0 (CH-CH<sub>3b</sub>).

**MS** (ESI):  $m/z$  = 304.1 [M+H]<sup>+</sup>



**HRMS** (ESI-ToF)  $m/z$ :  $[M+H]^+$  calcd for  $C_{17}H_{22}NO_2S$  304.1366, found 304.1361.

**4-(1-(Butylsulfonyl)-2-phenylpropan-2-yl)pyridine (262ac)**



The title compound was prepared according to the general procedure using 4-cyanopyridine (52.0 mg, 0.50 mmol, 1.00 equiv.),  $\alpha$ -methylstyrene (98  $\mu$ L, 0.75 mmol, 1.50 equiv.), and sodium butane-1-sulfinate (144.2 mg, 1.00 mmol, 2.00 equiv., prepared according to a procedure by König et al.<sup>[188a]</sup>). Purification by flash chromatography afforded the product **262ac** (159 mg, 0.5 mmol, 100%) as a yellowish oil.

$R_f$  = 0.22 (1:2, cyclohexane/ethyl acetate).

**IR** (ATR):  $\tilde{\nu}/\text{cm}^{-1}$  = 3058, 3026, 2960, 1594, 1410, 1314, 1120, 823, 700.

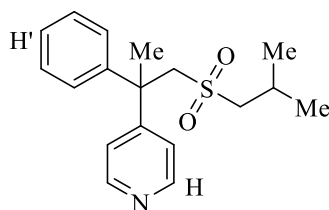
**$^1\text{H}$  NMR, COSY** (400 MHz,  $\text{CDCl}_3$ ):  $\delta$  /ppm = 8.55 (br s, 2H, H-2,6), 7.37–7.27 (m, 3H, H-3',4',5'), 7.23–7.20 (m, 2H, H-2',6'), 7.15–7.13 (m, 2H, H-3,5), 3.82 (d,  $J$  = 14.6 Hz, 1H,  $\text{CH}_{2a}\text{-C}_q$ ), 3.74 (d,  $J$  = 14.6 Hz, 1H,  $\text{CH}_{2b}\text{-C}_q$ ), 2.13–2.05 (m, 2H, H-1''), 2.02 (s, 3H,  $\text{CH}_3\text{-C}_q$ ), 1.64–1.46 (m, 2H, H-2''), 1.17 (sext,  $J$  = 7.4 Hz, 2H, H-3''), 0.78 (t,  $J$  = 7.4 Hz, 3H, H-4'').

**$^{13}\text{C}$  NMR, HSQC, HMBC** (101 MHz,  $\text{CDCl}_3$ ):  $\delta$  /ppm = 157.2 (C-4), 149.8 (2C, C-2,6), 144.3 (C-1'), 128.9 (2C, C-3',5'), 127.8 (3C, C-2',4',6'), 123.1 (2C, C-3,5), 62.7 ( $\text{CH}_2\text{-C}_q$ ), 54.6 (C-1''), 45.8 ( $\text{C}_q$ ), 27.3 ( $\text{CH}_3\text{-C}_q$ ), 23.8 (C-2''), 21.6 (C-3''), 13.5 (C-4'').

**MS** (ESI):  $m/z$  = 318.1  $[M+H]^+$

**HRMS** (ESI-ToF)  $m/z$ :  $[M+H]^+$  calcd for  $C_{18}H_{24}NO_2S$ : 318.1522, found 318.1524.

**4-(1-(Isobutylsulfonyl)-2-phenylpropan-2-yl)pyridine (262ad)**



The title compound was prepared according to the general procedure using 4-cyanopyridine (52.0 mg, 0.50 mmol, 1.00 equiv.),  $\alpha$ -methylstyrene (98  $\mu$ L, 0.75 mmol, 1.50 equiv.), and sodium 2-methylpropane-1-sulfinate (144.2 mg, 1.00 mmol, 2.00 equiv., prepared according to a procedure by König et al.<sup>[188a]</sup>). Purification by flash chromatography afforded the product **262ad** (95.0 mg, 0.30 mmol, 60%) as a yellowish oil.

$R_f$  = 0.25 (1:2, cyclohexane/ethyl acetate).

**IR** (ATR):  $\tilde{\nu}/\text{cm}^{-1}$  = 3058, 3026, 2962, 1594, 1410, 1307, 1124, 826, 701.

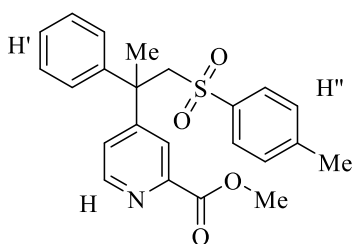
**<sup>1</sup>H NMR, COSY** (400 MHz, CDCl<sub>3</sub>):  $\delta$  /ppm = 8.57 (br s, 2H, H-2,6), 7.40–7.28 (m, 3H, H-3',4',5'), 7.22–7.19 (m, 4H, H-2',6',3,5), 3.82 (d,  $J$  = 14.5 Hz, 1H, CH<sub>2a</sub>-C<sub>q</sub>), 3.76 (d,  $J$  = 14.5 Hz, 1H, CH<sub>2b</sub>-C<sub>q</sub>), 2.19–2.08 (m, 2H, CH<sub>2</sub>CH), 2.04 (s, 3H, CH<sub>3</sub>-C<sub>q</sub>), 2.03–1.95 (m, 1H, CH), 0.91 (d,  $J$  = 6.5 Hz, 3H, CH-CH<sub>3a</sub>), 0.90 (d,  $J$  = 6.5 Hz, 3H, CH-CH<sub>3b</sub>).

**<sup>13</sup>C NMR, HSQC, HMBC** (101 MHz, CDCl<sub>3</sub>):  $\delta$  /ppm = 158.0 (C-4), 149.0 (2C, C-2,6), 144.4 (C-1'), 129.0 (2C, C-3',5'), 127.8 (C-4'), 127.8 (2C, C-2',6'), 122.7 (2C, C-3,5), 64.3 (CH<sub>2</sub>SO<sub>2</sub>), 62.4 (CH<sub>2</sub>CH), 46.0 (C<sub>q</sub>), 27.3 (CH<sub>3</sub>-C<sub>q</sub>), 23.4 (CH), 22.9 (CH-CH<sub>3</sub>), 22.7 (CH-CH<sub>3</sub>).

**MS** (ESI):  $m/z$  = 318.1 [M+H]<sup>+</sup>

**HRMS** (ESI-ToF)  $m/z$ : [M+H]<sup>+</sup> calcd for C<sub>18</sub>H<sub>24</sub>NO<sub>2</sub>S: 318.1522, found 318.1524.

#### Methyl 4-(2-phenyl-1-tosylpropan-2-yl)picolinate (**262av**)



The title compound was prepared according to the general procedure using 4-tosylpyridine (146.0 mg, 0.50 mmol, 1.00 equiv., prepared according to a procedure by Guo et al.<sup>[210]</sup>),  $\alpha$ -methylstyrene (98  $\mu$ L, 0.75 mmol, 1.50 equiv.), and sodium *p*-toluenesulfinate (102.0 mg, 1.00 mmol, 2.00 equiv., prepared according to a procedure by König et al.<sup>[188a]</sup>). Purification by flash chromatography afforded the product **262av** (80.0 mg, 0.20 mmol, 39%) as a colorless solid.

$R_f$  = 0.43 (1:2, cyclohexane/ethyl acetate).

**Mp** = 171–172°C.

**IR** (ATR):  $\tilde{\nu}/\text{cm}^{-1}$  = 3029, 2926, 1595, 1441, 1290, 1143, 730, 701.

**<sup>1</sup>H NMR, COSY** (400 MHz, CDCl<sub>3</sub>):  $\delta$  /ppm = 8.57 (dd,  $J$  = 5.16, 0.8 Hz, 1H, H-2), 7.76 (dd,  $J$  = 2.0, 0.8 Hz, 1H, H-5), 7.40–7.37 (AA' part of AA'–BB' system, 2H, H-3'',5''), 7.27 (dd,  $J$  = 5.16, 2.0 Hz, 1H, H-3), 7.24–7.16 (m, 3H, H-,3',4',5'), 7.00–6.96 (BB' part of AA'–BB' system, 2H, H-2'',6''), 4.11 (d,  $J$  = 14.6 Hz, 1H, CH<sub>2a</sub>), 4.03 (d,  $J$  = 14.6 Hz, 1H, CH<sub>2b</sub>), 3.96 (s, 3H, OCH<sub>3</sub>), 2.36 (s, 3H, CH<sub>3</sub>), 2.09 (s, 3H, C<sub>4</sub>–CH<sub>3</sub>).

**<sup>13</sup>C NMR, HSQC, HMBC** (101 MHz, CDCl<sub>3</sub>):  $\delta$  /ppm = 165.6 (C=O), 156.4 (C-4), 149.9 (C-2), 147.8 (C-6), 145.3 (C-1'), 144.5 (C-4''), 137.8 (C-1''), 129.9 (2C, C-3'',5''), 128.8 (2C, C-3',5'), 127.5 (2C, C-2'',6''), 127.4 (C-4'), 126.7 (2C, C-6',2'), 126.0 (C-3), 124.2 (C-5), 65.8 (CH<sub>2</sub>), 53.1 (OCH<sub>3</sub>) 46.0 (C<sub>4</sub>), 27.2 (C<sub>4</sub>–CH<sub>3</sub>), 21.6 (CH<sub>3</sub>).

**MS** (ESI):  $m/z$  = 410.2 [M+H]<sup>+</sup>

**HRMS** (ESI-ToF)  $m/z$ : [M+H]<sup>+</sup> calcd for C<sub>15</sub>H<sub>18</sub>NO<sub>2</sub>S: 410.1421, found 410.1423.

## 5. References

- [1] A. Gilbert, *Nature* **1987**, 326, 215-215.
- [2] S. V. Gudkov, S. N. Andreev, E. V. Barmina, N. F. Bunkin, B. B. Kartabaeva, A. P. Nesvat, E. V. Stepanov, N. I. Taranda, R. N. Khramov A. P. Glinushkin, *Phys. Wave Phenom.* **2017**, 25, 207-213.
- [3] A. F. Bais, R. L. McKenzie, G. Bernhard, P. J. Aucamp, M. Ilyas, S. Madronich, K. Tourpali, *Photochem. Photobiol. Sci.* **2015**, 14, 19-52.
- [4] a) C. G. Bochet, *Synlett* **2004**, 2268-2274; b) S. E. Braslavsky, *Pure Appl. Chem.* **2007**, 79, 293-465.
- [5] K.-H. Pfoertner, T. Oppenländer in *Photochemistry*, **2012**, 1-28.
- [6] D. Frackowiak, *J. Photoch. Photobio. B* **1988**, 2, 399-408.
- [7] S. Protti, D. Dondi, M. Fagnonia, A. Albin, *Green Chem.* **2009**, 11, 239-249.
- [8] T. H. Rehm, *Chemphotochem* **2020**, 4, 234-234.
- [9] L. Buglioni, F. Raymenants, A. Slattery, S. D. A. Zondag, T. Noel, *Chem. Rev.* **2021**.
- [10] P. Klán, J. Wirz, *Photochemistry of organic compounds: from concepts to practice*, John Wiley & Sons, **2009**.
- [11] a) B. L. Diffey, *Methods* **2002**, 28, 4-13; b) B. Wardle, *Principles and Applications of Photochemistry*, Wiley, **2009**.
- [12] a) A. Einstein, *Ann. Phys.* **1905**, 322, 132-148; b) M. Plank, *Verhandl. Dtsch. Phys. Ges.* **1900**, 2, 237-245.
- [13] K. Fukui, T. Yonezawa and H. Shingu, *J. Chem. Phys.* **1952**, 20, 722-725.
- [14] V. Balzani, P. Ceroni, A. Juris, *Photochemistry and photophysics: concepts, research, applications*, John Wiley & Sons, **2014**.
- [15] a) C. K. Prier, D. A. Rankic and D. W. C. MacMillan, *Chem. Rev.* **2013**, 113, 5322-5363; b) N. A. Romero, D. A. Nicewicz, *Chem. Rev.* **2016**, 116, 10075-10166.
- [16] T. Forster, *Ann Phys-Berlin* **1948**, 2, 55-75.
- [17] D. L. Dexter, *J. Chem. Phys.* **1953**, 21, 836-850.
- [18] H. Sahoo, *J. Photochem. Photobiol. C: Photochem. Rev.* **2011**, 12, 20-30.
- [19] S. K. Sekatskii, *Philos T Roy Soc A* **2004**, 362, 901-919.
- [20] R. M. Clegg, *Curr. Opin. Biotechnol.* **1995**, 6, 103-110.
- [21] R. J. Forster, T. E. Keyes, J. G. Vos, *Interfacial Supramolecular Assemblies*, Wiley, **2003**, p. 35.
- [22] S. S. Skourtis, C. R. Liu, P. Antoniou, A. M. Virshup, D. N. Beratan, *P. Natl. Acad. Sci. U.S.A.* **2016**, 113, 8115-8120.
- [23] T. N. Singh-Rachford, F. N. Castellano, *Coord. Chem. Rev.* **2010**, 254, 2560-2573.
- [24] G. J. Kavarnos, *Top. Curr. Chem.* **1990**, 156, 21-58.
- [25] N. Hoffmann, *J. Photochem. Photobiol. C: Photochem. Rev.* **2008**, 9, 43-60.

- [26] a) G. L. Closs, J. R. Miller, *Science* **1988**, *240*, 440-447; b) R. A. Marcus, N. Sutin, *Biochim. Biophys. Acta* **1985**, *811*, 265-322.
- [27] D. Rehm, A. Weller, *Isr. J. Chem.* **1970**, *8*, 259-271.
- [28] L. Buzzetti, G. E. M. Crisenza, P. Melchiorre, *Angew Chem Int Edit* **2019**, *58*, 3730-3747.
- [29] N. J. Turro, V. Ramamurthy, V. Ramamurthy, J. C. Scaiano, *Principles of molecular photochemistry: an introduction*, University science books, **2009**.
- [30] S. E. Braslavsky, *Pure Appl. Chem.* **2007**, *79*, 293-465.
- [31] G. J. Kavarnos, N. J. Turro, *Chem. Rev.* **1986**, *86*, 401-449.
- [32] T. Förster, *Pure Appl. Chem.* **1970**, *24*, 443-450.
- [33] a) J. Cornelisse, *Chem. Rev.* **1993**, *93*, 615-669; b) D. De Keukeleire, S. L. He, *Chem. Rev.* **1993**, *93*, 359-380; c) F. Mueller, J. Mattay, *Chem. Rev.* **1993**, *93*, 99-117.
- [34] N. Hoffmann, *Synthesis* **2004**, *2004*, 481-495.
- [35] S. Clifford, M. J. Bearpark, F. Bernardi, M. Olivucci, M. A. Robb, B. R. Smith, *J. Am. Chem. Soc.* **1996**, *118*, 7353-7360.
- [36] R. S. Sheridan, *J. Am. Chem. Soc.* **1983**, *105*, 5140-5142.
- [37] K. N. Houk, *Pure Appl. Chem* **1982**, *54*, 1633-1650.
- [38] D. Chappell, A. T. Russell, *Org. Biomol. Chem.* **2006**, *4*, 4409-4430.
- [39] C. Baralotto, M. Chanon, M. Julliard, *J. Org. Chem.* **1996**, *61*, 3576-3577.
- [40] P. A. Wender, S. K. Singh, *Tetrahedron Lett.* **1985**, *26*, 5987.
- [41] a) I. V. Alexeeva, A. D. Shved, *Biopolym. Cell.* **2013**; b) B. A. Stankiewicz, P. F. van Bergen, *Acs Sym Ser* **1998**, *707*, 1-12.
- [42] R. J. Hoover, M. Kasha, *J. Am. Chem. Soc.* **1969**, *91*, 6508.
- [43] K. Jug, G. Hahn, *J. Comput. Chem.* **1983**, *4*, 410-418.
- [44] a) T. Nishio, Y. Omote, *J. Chem. Soc., Perkin Trans. 1* **1988**, 957-960; b) N. Takehiko, K. Katsuhiko, O. Yoshimori, *Chem. Lett.* **1982**, *11*, 1675-1678.
- [45] S. Prathapan, K. E. Robinson, W. C. Agosta, *J. Am. Chem. Soc.* **1992**, *114*, 1838-1843.
- [46] M. A. Brumfield, W. C. Agosta, *J. Am. Chem. Soc.* **1988**, *110*, 6790-6794.
- [47] C. J. Rao, W. C. Agosta, *J. Org. Chem.* **1994**, *59*, 2125-2131.
- [48] a) T. Gensch, M. Teders, F. Glorius, *J. Org. Chem.* **2017**, *82*, 9154-9159; b) T. P. Yoon, M. A. Ischay, J. N. Du, *Nat. Chem.* **2010**, *2*, 527-532.
- [49] a) A. M. de Almeida, M. V. de Almeida, G. W. Amarante, *Quim. Nova* **2015**, *38*, 1080-1092; b) J. M. R. Narayanam, C. R. J. Stephenson, *Chem. Soc. Rev.* **2011**, *40*, 102-113; c) J. W. Tucker, C. R. J. Stephenson, *J. Org. Chem.* **2012**, *77*, 1617-1622.
- [50] a) F. Strieth-Kalthoff, M. J. James, M. Teders, L. Pitzer, F. Glorius, *Chem. Soc. Rev.* **2018**, *47*, 7190-7202; b) N. J. Turro, *Modern molecular photochemistry*, University science books, **1991**.
- [51] S. P. Pitre, L. E. Overman, *Chem. Rev.* **2021**.

- [52] Q. Q. Zhou, Y. Q. Zou, L. Q. Lu, W. J. Xiao, *Angew. Chem. Int. Ed.* **2019**, *58*, 1586-1604.
- [53] a) T. Koike, M. Akita, *Org. Chem. Front.* **2016**, *3*, 1345-1349; b) X. W. Lan, N. X. Wang, Y. L. Xing, *Eur. J. Org. Chem.* **2017**, *2017*, 5821-5851.
- [54] a) T. Umemoto, *Chem. Rev.* **1996**, *96*, 1757-1777; b) T. Umemoto, S. Ishihara, *J. Am. Chem. Soc.* **1993**, *115*, 2156-2164.
- [55] a) J. Charpentier, N. Fruh, A. Togni, *Chem. Rev.* **2015**, *115*, 650-682; b) P. Eisenberger, S. Gischig, A. Togni, *Chem. Eur. J.* **2006**, *12*, 2579-2586.
- [56] T. Koike, M. Akita, *Acc. Chem. Res.* **2016**, *49*, 1937-1945.
- [57] R. Lin, H. N. Sun, C. Yang, W. B. Shen, W. J. Xia, *Chem. Commun.* **2015**, *51*, 399-401.
- [58] J. Cheng, Y. X. Cheng, J. Xie, C. J. Zhu, *Org. Lett.* **2017**, *19*, 6452-6455.
- [59] J. Hou, A. Ee, H. Cao, H. W. Ong, J. H. Xu, J. Wu, *Angew. Chem. Int. Ed.* **2018**, *57*, 17220-17224.
- [60] a) V. R. Yatham, Y. Y. Shen, R. Martin, *Angew. Chem. Int. Ed.* **2017**, *56*, 10915-10919; b) J. H. Ye, M. Miao, H. Huang, S. S. Yan, Z. B. Yin, W. J. Zhou, D. G. Yu, *Angew. Chem. Int. Ed.* **2017**, *56*, 15416-15420.
- [61] D. S. Yang, B. Huang, W. Wei, J. Li, G. Lin, Y. Liu, J. H. Ding, P. F. Sun, H. Wang, *Green Chem.* **2016**, *18*, 5630-5634.
- [62] H. Jiang, Y. Z. Cheng, Y. Zhang, S. Y. Yu, *Eur. J. Org. Chem.* **2013**, *2013*, 5485-5492.
- [63] T. F. Niu, J. Cheng, C. L. Zhuo, D. Y. Jiang, X. G. Shu, B. Q. Ni, *Tetrahedron Lett.* **2017**, *58*, 3667-3671.
- [64] Z. Lu, T. P. Yoon, *Angew. Chem. Int. Ed.* **2012**, *51*, 10329-10332.
- [65] T. R. Blum, Z. D. Miller, D. M. Bates, I. A. Guzei, T. P. Yoon, *Science* **2016**, *354*, 1391-1395.
- [66] R. Alonso, T. Bach, *Angew. Chem. Int. Ed.* **2014**, *53*, 4368-4371.
- [67] A. Troster, R. Alonso, A. Bauer, T. Bach, *J. Am. Chem. Soc.* **2016**, *138*, 7808-7811.
- [68] X. Li, C. Jandl, T. Bach, *Org. Lett.* **2020**, *22*, 3618-3622.
- [69] J. Zhao, J. L. Brosmer, Q. Tang, Z. Yang, K. N. Houk, P. L. Diaconescu, O. Kwon, *J. Am. Chem. Soc.* **2017**, *139*, 9807-9810.
- [70] H. U. Reissig, R. Zimmer, *Chem. Rev.* **2003**, *103*, 1151-1196.
- [71] a) A. Amador, E. Sherbrook, T. Yoon, *J. Am. Chem. Soc.* **2016**, *14*, 4722-4725; b) C. F. Wang, X. Ren, H. J. Xie, Z. Lu, *Chem. Eur. J.* **2015**, *21*, 9676-9680.
- [72] J. Luis-Barrera, V. Laina-Martin, T. Rigotti, F. Peccati, X. Solans-Monfort, M. Sodupe, R. Mas-Balleste, M. Liras, J. Aleman, *Angew. Chem. Int. Ed.* **2017**, *56*, 7826-7830.
- [73] A. Studer, D. P. Curran, *Angew. Chem. Int. Ed.* **2016**, *55*, 58-102.
- [74] T. Courant, G. Masson, *J. Org. Chem.* **2016**, *81*, 6945-6952.
- [75] P. Fodran, C. J. Wallentin, *Eur. J. Org. Chem.* **2020**, *2020*, 3213-3218.

- [76] A. Baeyer, *Ber. Dtsch. Chem. Ges.* **1885**, *18*, 2269-2281.
- [77] Z. Wang, U. Wille, E. Juaristi, *Encyclopedia of Physical Organic Chemistry*, **6**, Wiley, **2017**.
- [78] a) R. D. Bach, O. Dmitrenko, *J. Org. Chem.* **2002**, *67*, 2588-2599; b) T. Dudev, C. Lim, *J. Am. Chem. Soc.* **1998**, *120*, 4450-4458; c) P. R. Khoury, J. D. Goddard, W. Tam, *Tetrahedron* **2004**, *60*, 8103-8112.
- [79] W. T. G. Johnson, W. T. Borden, *J. Am. Chem. Soc.* **1997**, *119*, 5930-5933.
- [80] K. B. Wiberg, *Angew. Chem. Int. Ed.* **1986**, *25*, 312-322.
- [81] R. D. Bach, O. Dmitrenko, *J. Am. Chem. Soc.* **2004**, *126*, 4444-4452.
- [82] L. Souillart, N. Cramer, *Chem. Rev.* **2015**, *115*, 9410-9464.
- [83] T. Seiser, N. Cramer, *Org. Biomol. Chem.* **2009**, *7*, 2835-2840.
- [84] R. D. Bach, O. Dmitrenko, *J. Am. Chem. Soc.* **2004**, *126*, 4444-4452.
- [85] B. M. Trost, P. J. Morris, *Angew. Chem. Int. Ed.* **2011**, *50*, 6167-6170.
- [86] L. Y. Mei, Y. Wei, Q. Xu, M. Shi, *Organometallics* **2013**, *32*, 3544-3556.
- [87] L. Jiao, S. Ye, Z.-X. Yu, *J. Am. Chem. Soc.* **2008**, *130*, 7178-7179.
- [88] L. Jiao, M. Lin, Z. X. Yu, *Chem. Commun.* **2010**, *46*, 1059-1061.
- [89] R. K. Bowman, J. S. Johnson, *Org. Lett.* **2006**, *8*, 573-576.
- [90] R. Tombe, T. Kurahashi, S. Matsubara, *Org. Lett.* **2013**, *15*, 1791-1793.
- [91] a) T. R. McDonald, L. R. Mills, M. S. West, S. A. L. Rousseaux, *Chem. Rev.* **2021**, *121*, 3-79; b) A. Nikolaev, A. Orellana, *Synthesis* **2016**, *48*, 1741-1768.
- [92] S. B. Park, J. K. Cha, *Org. Lett.* **2000**, *2*, 147-149.
- [93] S. Cicchi, J. Revuelta, A. Zanobini, M. Betti, A. Brandi, *Synlett* **2003**, 2305-2308.
- [94] I. Novikau, A. Hurski, *Tetrahedron* **2018**, *74*, 1078-1084.
- [95] D. Rosa, A. Orellana, *Chem. Commun.* **2013**, *49*, 5420-5422.
- [96] J. F. Yang, Y. X. Shen, Y. J. Lim, N. Yoshikai, *Chem. Sci.* **2018**, *9*, 6928-6934.
- [97] X. K. Zhou, Z. S. Qi, S. J. Yu, L. H. Kong, Y. Li, W. F. Tian, X. W. Li, *Adv. Synth. Catal.* **2017**, *359*, 1620-1625.
- [98] Z. S. Ye, X. P. Cai, J. W. Li, M. J. Dai, *ACS Catalysis* **2018**, *8*, 5907-5914.
- [99] Y. H. Zhang, W. W. Zhang, Z. Y. Zhang, K. Zhao, T. P. Loh, *Org. Lett.* **2019**, *21*, 5101-5105.
- [100] A. Luque, J. Paternoga, T. Opatz, *Chem. Eur. J.* **2021**, *27*, 4500-4516.
- [101] a) G. Fumagalli, S. Stanton, J. F. Bower, *Chem. Rev.* **2017**, *117*, 9404-9432; b) T. A. Shah, P. B. De, S. Pradhan, S. Banerjee, T. Punniyamurthy, *Chem. Asian J.* **2019**, *14*, 4520-4533; c) F. Wang, S. J. Yu, X. W. Li, *Chem. Soc. Rev.* **2016**, *45*, 6462-6477.
- [102] J. Xuan, X. K. He, W. J. Xiao, *Chem. Soc. Rev.* **2020**, *49*, 2546-2556.
- [103] P. A. Wender, M. A. Delong, *Tetrahedron Lett.* **1990**, *31*, 5429-5432.
- [104] G. A. Fenton, A. Gilbert, *Tetrahedron* **1989**, *45*, 2979-2988.

- [105] C. S. Penkett, R. O. Sims, R. French, L. Dray, S. J. Roome, P. B. Hitchcock, *Chem Commun.* **2004**, 1932-1933.
- [106] C. S. Penkett, R. O. Sims, P. W. Byrne, S. Berritt, L. E. Pennicott, S. P. Rushton, A. G. Avent, P. B. Hitchcock, *Tetrahedron* **2006**, *62*, 9403-9409.
- [107] T. Bach, J. P. Hehn, *Angew. Chem. Int. Ed.* **2011**, *50*, 1000-1045.
- [108] J. A. Woolford, *The Double [3+ 2] Photocycloaddition Reaction*, Springer Science & Business Media, **2011**.
- [109] P. A. Wender, K. Fisher, *Tetrahedron Lett.* **1986**, *27*, 1857-1860.
- [110] P. A. Wender, J. J. Howbert, *J. Am. Chem. Soc.* **1981**, *103*, 688-690.
- [111] P. A. Wender, J. J. Howbert, *Tetrahedron Lett.* **1982**, *23*, 3983-3986.
- [112] P. A. Wender, R. J. Ternansky, *Tetrahedron Lett.* **1985**, *26*, 2625-2628.
- [113] a) V. Ganesh, S. Chandrasekaran, *Synthesis* **2016**, *48*, 4347-4380; b) M. Meazza, H. Guo, R. Rios, *Org. Biomol. Chem.* **2017**, *15*, 2479-2490; c) J. Wang, S. A. Blaszczyk, X. Li, W. Tang, *Chem. Rev.* **2021**, *121*, 110-139.
- [114] J. J. Cui, M. Tran-Dube, H. Shen, M. Nambu, P. P. Kung, M. Pairish, L. Jia, J. Meng, L. Funk, I. Botrous, M. McTigue, N. Grodsky, K. Ryan, E. Padrique, G. Alton, S. Timofeevski, S. Yamazaki, Q. H. Li, H. L. Zou, J. Christensen, B. Mroczkowski, S. Bender, R. S. Kania, M. P. Edwards, *J. Med. Chem.* **2011**, *54*, 6342-6363.
- [115] G. Bold, A. Fassler, H. G. Capraro, R. Cozens, T. Klimkait, J. Lazdins, J. Mestan, B. Poncioni, J. Rosel, D. Stover, M. Tintelnot-Blomley, F. Acemoglu, W. Beck, E. Boss, M. Eschbach, T. Hurlimann, E. Masso, S. Roussel, K. Ucci-Stoll, D. Wyss, R. Lang, *J. Med. Chem.* **1998**, *41*, 3387-3401.
- [116] T. D. Penning, J. J. Talley, S. R. Bertenshaw, J. S. Carter, P. W. Collins, S. Docter, M. J. Graneto, L. F. Lee, J. W. Malecha, J. M. Miyashiro, R. S. Rogers, D. J. Rogier, S. S. Yu, G. D. Anderson, E. G. Burton, J. N. Cogburn, S. A. Gregory, C. M. Koboldt, W. E. Perkins, K. Seibert, A. W. Veenhuizen, Y. Y. Zhang, P. C. Isakson, *J. Med. Chem.* **1997**, *40*, 1347-1365.
- [117] M. Koley, M. Schnürch, M. D. Mihovilovic, *Metal-Catalyzed Cross-Coupling Reactions in the Decoration of Pyridines*, Springer International Publishing, **2016**. 1-60.
- [118] E. A. Matiushenkov, N. A. Sokolov, O. G. Kulinkovich, *Synlett* **2004**, 77-80.
- [119] H. E. Simmons, R. D. Smith, *J. Am. Chem. Soc.* **1958**, *80*, 5323-5324.
- [120] a) D. C. Blakemore, A. Gilbert, *J. Chem. Soc. Perkin Trans. 1* **1992**, 2265-2270; b) D. C. Blakemore, A. Gilbert, *Tetrahedron Lett.* **1994**, *35*, 5267-5270.
- [121] a) J. Mattay, *Tetrahedron* **1985**, *41*, 2393-2404; b) J. Mattay, J. Runsink, H. Leismann, H.-D. J. T. L. Scharf, *Tetrahedron Lett.* **1982**, *23*, 4919-4922; c) D. E. Reedich, R. S. Sheridan, *J. Am. Chem. Soc.* **1985**, *107*, 3360-3361.
- [122] M. A. McCarrick, Y. D. Wu, K. N. Houk, *J. Am. Chem. Soc.* **1992**, *114*, 1499-1500.
- [123] H. Y. Tu, B. L. Hu, C. L. Deng, X. G. Zhang, *Chem. Commun.* **2015**, *51*, 15558-15561.
- [124] K. Sun, X. Wang, C. Li, H. Wang, L. Li, *Org. Chem. Front.* **2020**, *7*, 3100-3119.



- [125] P. A. Wender, G. G. Gamber, R. D. Hubbard, L. Zhang, *J. Am. Chem. Soc.* **2002**, *124*, 2876-2877.
- [126] M. C. Melcher, H. von Wachenfeldt, A. Sundin, D. Strand, *Chem. Eur. J.* **2015**, *21*, 531-535.
- [127] A. Luque, J. Gross, T. J. B. Zahringer, C. Kerzig, T. Opatz, *Chem. Eur. J.* **2022**, *28*, e2021043.
- [128] A. Gavezzotti in *The Chemistry of Sulphones and Sulphoxides* Eds.: S. Patai, Z. Rappoport, C. J. M. Stirling), Wiley, New York, **1988**. 1-32.
- [129] a) T. G. Back, *Tetrahedron* **2001**, *57*, 5263-5301; b) T. G. Back, K. N. Clary, D. Gao, *Chem. Rev.* **2010**, *110*, 4498-4553.
- [130] V. Nair, A. Augustine, T. D. Suja, *Synthesis* **2002**, *2002*, 2259-2265.
- [131] Y. Sun, A. Abdukader, D. Lu, H. Zhang, C. Liu, *Green Chem.* **2017**, *19*, 1255-1258.
- [132] a) G. J. Hoijtink, **1958**, *77*, 555-558; b) F. Wilkinson, A. Farmilo, *J. Chem. Soc., Faraday Trans. 2*, **1984**, *80*, 1117-1124.
- [133] T. Koike, M. Akita, *Inorg. Chem. Front* **2014**, *1*, 562-576.
- [134] a) M. S. Lowry, J. I. Goldsmith, J. D. Slinker, R. Rohl, R. A. Pascal, G. G. Malliaras, S. Bernhard, *Chem. Mater.* **2005**, *17*, 5712-5719; b) J. D. Slinker, A. A. Gorodetsky, M. S. Lowry, J. Wang, S. Parker, R. Rohl, S. Bernhard, G. G. Malliaras, *J. Am. Chem. Soc.* **2004**, *126*, 2763-2767.
- [135] C. R. Bock, J. A. Connor, A. R. Gutierrez, T. J. Meyer, D. G. Whitten, B. P. Sullivan, J. K. Nagle, *J. Am. Chem. Soc.* **1979**, *101*, 4815-4824.
- [136] M. J. James, J. L. Schwarz, F. Strieth-Kalthoff, B. Wibbeling, F. Glorius, *J. Am. Chem. Soc.* **2018**, *140*, 8624-8628.
- [137] a) C. Lee, W. Yang, R. G. Parr, *Phys. Rev. B* **1988**, *37*, 785-789; b) A. D. Becke, *J. Chem. Phys.* **1993**, *98*, 5648-5652; c) S. H. Vosko, L. Wilk, M. Nusair, *Can. J. Phys.* **1980**, *58*, 1200-1211.
- [138] T. Yanai, D. P. Tew, N. C. Handy, *Chem. Phys. Lett.* **2004**, *393*, 51-57.
- [139] Y. Zhao, D. G. Truhlar, *Theor. Chem. Acc.* **2008**, *120*, 215-241.
- [140] a) R. Krishnan, J. S. Binkley, R. Seeger, J. A. Pople, *J. Chem. Phys.* **1980**, *72*, 650-654; b) M. J. Frisch, J. A. Pople, J. S. Binkley, *J. Chem. Phys.* **1984**, *80*, 3265-3269.
- [141] J. Tomasi, B. Mennucci, E. Cancès, *J. Mol. Struct.* **1999**, *464*, 211-226.
- [142] C. S. Penkett, J. A. Woolford, I. J. Day, M. P. Coles, *J. Am. Chem. Soc.* **2010**, *132*, 4-5.
- [143] a) Y. Qin, R. Sun, N. P. Gianoulis, D. G. Nocera, *J. Am. Chem. Soc.* **2021**, *143*, 2005-2015; b) B. Xu, L. Troian-Gautier, R. Dykstra, R. T. Martin, O. Gutierrez, U. K. Tambar, *J. Am. Chem. Soc.* **2020**, *142*, 6206-6215.
- [144] a) M. S. Bertrams, C. Kerzig, *Chem. Commun.* **2021**, *57*, 6752-6755; b) T. J. B. Zahringer, M. S. Bertrams, C. Kerzig, *J. Mater Chem. C* **2021**.
- [145] F. M. Hormann, C. Kerzig, T. S. Chung, A. Bauer, O. S. Wenger, T. Bach, *Angew. Chem. Int. Ed.* **2020**, *59*, 9659-9668.
- [146] Y. Pellegrin, F. Odobel, *C. R. Chim.* **2017**, *20*, 283-295.

- [147] A. M. Halpern, D. A. Forsyth, M. Nosowitz, *J. Phys. Chem.* **1986**, *90*, 2677-2679.
- [148] M. Mitani, T. Kiriya, T. Kuratate, *J. Org. Chem.* **1994**, *59*, 1279-1282.
- [149] P. Herr, C. Kerzig, C. B. Larsen, D. Haussinger, O. S. Wenger, *Nat. Chem.* **2021**, *13*, 956-962.
- [150] C. J. Wallentin, J. D. Nguyen, P. Finkbeiner, C. R. J. Stephenson, *J. Am. Chem. Soc.* **2012**, *134*, 8875-8884.
- [151] L. J. Johnston, J. C. Scaiano, *Chem. Rev.* **1989**, *89*, 521-547.
- [152] D. Griller, K. U. Ingold, *Acc. Chem. Res.* **1980**, *13*, 317-323.
- [153] M. Newcomb, P. H. Toy, *Acc. Chem. Res.* **2000**, *33*, 449-455.
- [154] F. Strieth-Kalthoff, C. Henkel, M. Teders, A. Kahnt, W. Knolle, A. Gómez-Suárez, K. Dirian, W. Alex, K. Bergander, C. G. Daniliuc, B. Abel, D. M. Guldi, F. Glorius, *Chem.* **2019**, *5*, 2183-2194.
- [155] a) A. S. K. Hashmi, T. Wang, S. Shi, M. Rudolph, *J. Org. Chem.* **2012**, *77*, 7761-7767; b) J. P. Markham, S. T. Staben, F. D. Toste, *J. Am. Chem. Soc.* **2005**, *127*, 9708-9709; c) S. Mishra, P. Mondal, M. Ghosh, S. Mondal, A. Hajra, *Org. Biomol. Chem.* **2016**, *14*, 1432-1436; d) J. Sheng, J. D. Liu, L. Q. Chen, L. L. Zhang, L. Y. Zheng, X. C. Wei, *Org. Chem. Front.* **2019**, *6*, 1471-1475.
- [156] a) S. E. Kiruthika, R. Amritha, P. T. Perumal, *Tetrahedron Lett.* **2012**, *53*, 3268-3273; b) C. Q. Li, M. Shi, *Org. Lett.* **2003**, *5*, 4273-4276; c) L. Loots, D. A. Haynes, T. le Roex, *New J. Chem.* **2014**, *38*, 2778-2786.
- [157] a) Q. Y. Tan, Z. Yang, D. Jiang, Y. G. Cheng, J. Yang, S. Xi, M. Zhang, *Angew. Chem. Int. Ed.* **2019**, *58*, 6420-6424; b) Z. Yang, Q. Y. Tan, Y. Jiang, J. J. Yang, X. J. Su, Z. Qiao, W. Q. Zhou, L. He, H. Y. Qiu, M. Zhang, *Angew. Chem. Int. Ed.* **2021**, *60*, 13105-13111.
- [158] Y. A. Konik, G. Z. Elek, S. Kaabel, I. Jarving, M. Lopp, D. G. Kananovich, *Org. Biomol. Chem.* **2017**, *15*, 8334-8340.
- [159] G. W. Wang, T. Miao, *Chem. Eur. J.* **2011**, *17*, 5787-5790.
- [160] N. Nithiy, A. Orellana, *Org. Lett.* **2014**, *16*, 5854-5857.
- [161] a) X. F. Fan, H. J. Zhao, J. J. Yu, X. G. Bao, C. Zhu, *Org. Chem. Front.* **2016**, *3*, 227-232; b) K. F. Jia, F. Y. Zhang, H. C. Huang, Y. Y. Chen, *J. Am. Chem. Soc.* **2016**, *138*, 1514-1517; c) D. P. Wang, J. C. Mao, C. Zhu, *Chem. Sci.* **2018**, *9*, 5805-5809.
- [162] L. R. Mills, S. A. L. Rousseaux, *Eur. J. Org. Chem.* **2019**, *2019*, 8-26.
- [163] a) K. Cheng, P. J. Walsh, *Org. Lett.* **2013**, *15*, 2298-2301; b) D. Rosa, A. Orellana, *Org. Lett.* **2011**, *13*, 110-113.
- [164] T. Flessner, S. Doye, *J. Prakt. Chem.* **1999**, *341*, 186-190.
- [165] J. Sherwood, J. H. Clark, I. J. S. Fairlamb, J. M. Slattery, *Green Chem.* **2019**, *21*, 2164-2213.
- [166] J. A. M. de la Torre, P. Espinet, A. C. Albeniz, *Organometallics* **2013**, *32*, 5428-5434.
- [167] S. Wagschal, L. A. Perego, A. Simon, A. Franco-Espejo, C. Tocqueville, J. Albaneze-Walker, A. Jutand, L. Grimaud, *Chem. Eur. J.* **2019**, *25*, 6980-6987.

- [168] a) P. Z. Wang, Y. Gao, J. Chen, X. D. Huan, W. J. Xiao, J. R. Chen, *Nat. Commun.* **2021**, *12*; b) Y. Yasu, T. Koike, M. Akita, *Angew. Chem. Int. Ed.* **2012**, *51*, 9567-9571; c) Y. Yasu, T. Koike, M. Akita, *Org. Lett.* **2013**, *15*, 2136-2139.
- [169] R. J. Wiles, G. A. Molander, *Isr. J. Chem.* **2020**, *60*, 281-293.
- [170] B. Giese, *Angew. Chem. Int. Ed.* **1983**, *22*, 753-764.
- [171] F. J. R. Klauck, H. Yoon, M. J. James, M. Lautens, F. Glorius, *ACS Catal.* **2019**, *9*, 236-241.
- [172] a) L. M. Kammer, B. Lipp, T. Opatz, *J. Org. Chem.* **2019**, *84*, 2379-2392; b) J. Yang, J. Zhang, L. Qi, C. C. Hu, Y. Y. Chen, *Chem. Commun.* **2015**, *51*, 5275-5278.
- [173] L. Pantaine, C. Bour, G. Masson, *Photo-induced multi-component reactions, Vol. 46* The Royal Society of Chemistry, **2019**. 395-431.
- [174] D. J. Wilger, N. J. Gesmundo, D. A. Nicewicz, *Chem. Sci.* **2013**, *4*, 3160-3165.
- [175] L. Li, M. W. Huang, C. Liu, J. C. Xiao, Q. Y. Chen, Y. Guo, Z. G. Zhao, *Org. Lett.* **2015**, *17*, 4714-4717.
- [176] a) B. Lipp, A. Lipp, H. Detert, T. Opatz, *Org. Lett.* **2017**, *19*, 2054-2057; b) B. Lipp, A. M. Nauth, T. Opatz, *J. Org. Chem.* **2016**, *81*, 6875-6882.
- [177] a) D. Leifert, A. Studer, *Angew. Chem. Int. Ed.* **2020**, *59*, 74-108; b) A. Studer, *Chem. Eur. J.* **2001**, *7*, 1159-1164.
- [178] H. G. O. Alvim, E. N. da Silva, B. A. D. Neto, *RSC Adv.* **2014**, *4*, 54282-54299.
- [179] R. C. Cioc, E. Ruijter, R. V. A. Orru, *Green Chem.* **2014**, *16*, 2958-2975.
- [180] B. Lipp, L. M. Kammer, M. Kucukdisli, A. Luque, J. Kuhlborn, S. Pusch, G. Matuleviciute, D. Schollmeyer, A. Sackus, T. Opatz, *Chem. Eur. J.* **2019**, *25*, 8965-8969.
- [181] S. Q. Zhu, J. Qin, F. Wang, H. Li, L. L. Chu, *Nat. Commun.* **2019**, *10*.
- [182] F. Wang, J. Qin, S. Q. Zhu, L. L. Chu, *RSC Adv.* **2021**, *11*, 142-146.
- [183] K. Nakanishi, K. Mizuno, Y. Otsuji, *Bull. Chem. Soc. Jpn.* **1993**, *66*, 2371-2379.
- [184] J. Hoffmann, A. Belkasmoui, J. Simonet, *J. Electroanal. Chem.* **1991**, *307*, 155-168.
- [185] a) C. Punta, F. Minisci, *Trends Heterocycl. Chem.* **2008**, *13*, 1-68; b) J. Tauber, D. Imbri, T. Opatz, *Molecules* **2014**, *19*, 16190-16222.
- [186] K. Dedeian, P. I. Djurovich, F. O. Garces, G. Carlson, R. J. Watts, *Inorg. Chem.* **1991**, *30*, 1685-1687.
- [187] C. K. Prier, D. A. Rankic, D. W. C. MacMillan, *Chem. Rev.* **2013**, *113*, 5322-5363.
- [188] a) A. U. Meyer, K. Straková, T. Slanina, B. König, *Chem. Eur. J.* **2016**, *22*, 8694-8699; b) K. Qvortrup, D. A. Rankic, D. W. C. MacMillan, *J. Am. Chem. Soc.* **2014**, *136*, 626-629.
- [189] a) D. Cyr, P. Das, *Res. Chem. Intermed.* **2015**, *41*, 8603-8623; b) A. U. Meyer, K. Strakova, T. Slanina, B. König, *Chem. Eur. J.* **2016**, *22*, 8694-8699; c) H. G. Roth, N. A. Romero, D. A. Nicewicz, *Synlett* **2016**, *27*, 714-723; d) H. Wang, M. Y. Lin, H. J. Fang, T. T. Chen, J. X. Lu, *Chin. J. Chem.* **2007**, *25*, 913-916.
- [190] I. Ghosh, J. I. Bardagi, B. König, *Angew. Chem. Int. Ed.* **2017**, *56*, 12822-12824.

- [191] G. S. Hammond, *J. Am. Chem. Soc.* **1955**, *77*, 334-338.
- [192] J. I. Seeman, W. A. Farone, *J. Org. Chem.* **1978**, *43*, 1854-1864.
- [193] a) L. Capaldo, L. Buzzetti, D. Merli, M. Fagnoni, D. Ravelli, *J. Org. Chem.* **2016**, *81*, 7102-7109; b) D. Hager, D. W. C. MacMillan, *J. Am. Chem. Soc.* **2014**, *136*, 16986-16989; c) S. Montanaro, D. Ravelli, D. Merli, M. Fagnoni, A. Albini, *Org. Lett.* **2012**, *14*, 4218-4221.
- [194] J. Chen, S. Q. Zhu, J. Qin, L. L. Chu, *Chem. Commun.* **2019**, *55*, 2336-2339.
- [195] G. R. Fulmer, A. J. M. Miller, N. H. Sherden, H. E. Gottlieb, A. Nudelman, B. M. Stoltz, J. E. Bercaw, K. I. Goldberg, *Organometallics* **2010**, *29*, 2176-2179.
- [196] M. C. Burla, R. Caliendo, M. Camalli, B. Carrozzini, G. L. Cascarano, L. De Caro, C. Giacovazzo, G. Polidori, R. Spagna, *J. Appl. Crystallogr.* **2005**, *38*, 381-388.
- [197] G. M. Sheldrick, *Acta Cryst. A* **2015**, *71*, 3-8.
- [198] V. Nair, A. Augustine, T. D. Suja, *Synthesis* **2002**, 2259-2265.
- [199] L. L. Wang, W. Wei, D. S. Yang, H. H. Cui, H. L. Yue, H. Wang, *Tetrahedron Lett.* **2017**, *58*, 4799-4802.
- [200] Z. Y. Mo, Y. Z. Zhang, G. B. Huang, X. Y. Wang, Y. M. Pan, H. T. Tang, *Adv. Synth. Catal.* **2020**, *362*, 2160-2167.
- [201] Z. Wu, Y. H. Xu, H. H. Zhang, X. X. Wu, C. Zhu, *Chem. Commun.* **2021**, *57*, 6066-6069.
- [202] S. K. Kristensen, S. L. R. Laursen, E. Taarning, T. Skrydstrup, *Angew. Chem. Int. Ed.* **2018**, *57*, 13887-13891.
- [203] S. Doobary, A. T. Sedikides, H. P. Caldora, D. L. Poole, A. J. J. Lennox, *Angew. Chem. Int. Ed.* **2020**, *59*, 1155-1160.
- [204] N. Riddell, W. Tam, *J. Org. Chem.* **2006**, *71*, 1934-1937.
- [205] M. Uyanik, D. Suzuki, T. Yasui, K. Ishihara, *Angew. Chem. Int. Ed.* **2011**, *50*, 5331-5334.
- [206] S. Prathapan, K. E. Robinson, W. C. Agosta, *J. Am. Chem. Soc.* **1992**, *114*, 1838-1843.
- [207] R. I. Rodriguez, L. Mollari, J. Aleman, *Angew. Chem. Int. Ed. Engl.* **2021**, *60*, 4555-4560.
- [208] J. Paternoga, J. Kuhlborn, N. O. Rossdam, T. Opatz, *J. Org. Chem.* **2021**, *86*, 3232-3248.
- [209] M. Kaur, N. U. D. Reshi, K. Patra, A. Bhattacherya, S. Kunnikuruvan, J. K. Bera, *Chem. Eur. J.* **2021**, *27*, 10737-10748.
- [210] Y. Q. Yuan, S. R. Guo, *Synlett* **2011**, 2750-2756.

## 6. Appendix

### 6.1. Crystal structure analysis

#### Crystal data for compound 217c

formula	$C_{18}H_{17}F_3N_2O_4S$
molecular weight	414.39 $g\text{mol}^{-1}$
absorption	$\mu = 0.231\text{ mm}^{-1}$
transmission	$T_{\min} = 0.9321, T_{\max} = 0.9782$
crystal size	0.11 x 0.22 x 0.37 $\text{mm}^3$ colourless block
space group	P 2 <sub>1</sub> /c (monoclinic)
lattice parameters	a = 8.0831(6) Å
(calculate from	b = 17.1309(12) Å $\beta = 104.319(6)^\circ$
9176 reflections with	c = 13.8314(10) Å
2.6° < $\theta$ < 28.4°)	V = 1855.7(2) Å <sup>3</sup> z = 4      F(000) = 856
temperature	-80°C
density	$d_{\text{xray}} = 1.483\text{ gcm}^{-3}$

#### data collection

diffractometer	STOE IPDS 2T
radiation	Mo-K $\alpha$ Graphitmonochromator
Scan-type	$\omega$ scans
Scan – width	1°
scan range	2° ≤ $\theta$ < 28°
	-10 ≤ h ≤ 10   -19 ≤ k ≤ 22   -14 ≤ l ≤ 18
number of reflections:	
measured	9888
unique	4410 ( $R_{\text{int}} = 0.0296$ )
observed	2926 ( $ F /\sigma(F) > 4.0$ )

#### data correction, structure solution, and refinement

corrections	Lorentz and polarisation correction.
Structure solution	Program: SIR-2004 (Direct methods)
refinement	Program: SHELXL-2018 (full matrix). 253 refined parameters, weighting scheme: $w = 1/[\sigma^2(F_o^2) + (0.0633*P)^2 + 0.54*P]$ with $(\text{Max}(F_o^2, 0) + 2*F_c^2)/3$ . H-atoms at calculated positions and refined with isotropic displacement parameters, non H- atoms refined anisotropically.
R-values	wR2 = 0.1332 (R1 = 0.0483 for observed reflections, 0.0805 for all reflections)
goodness of fit	S = 1.026
maximum deviation	

## Appendix

of parameters 0.001 \* e.s.d  
 maximum peak height in  
 diff. Fourier synthesis 0.39, -0.40 eÅ<sup>-3</sup>

final coordinates and equivalent displacement parameters (Å<sup>2</sup>)

$$U_{\text{eq}} = (1/3) * \sum_{ij} a_i^* a_j^* a_i a_j$$

Atom	X	Y	Z	U <sub>eq</sub>
N1	-0.0254(2)	0.3795(1)	0.1609(1)	0.0403(6)
C2	0.1493(3)	0.3932(2)	0.1483(2)	0.0470(8)
C3	0.2532(3)	0.3327(1)	0.2183(2)	0.0402(7)
C4	0.4385(3)	0.3573(2)	0.2669(2)	0.0472(8)
C5	0.4422(3)	0.3770(1)	0.3763(2)	0.0374(7)
C6	0.4971(3)	0.3050(1)	0.4452(2)	0.0350(6)
C7	0.3574(3)	0.2447(1)	0.4269(2)	0.0381(7)
C8	0.2067(3)	0.2553(1)	0.3640(2)	0.0370(7)
C9	0.1631(2)	0.3301(1)	0.3054(1)	0.0328(6)
C10	-0.0260(3)	0.3415(1)	0.2576(1)	0.0380(7)
C11	0.2577(3)	0.3947(1)	0.3714(1)	0.0335(6)
C12	0.1952(3)	0.4528(1)	0.4132(2)	0.0453(8)
S13	-0.19409(7)	0.40721(3)	0.08475(4)	0.0421(2)
O14	-0.1627(2)	0.4213(1)	-0.0098(1)	0.0608(7)
O15	-0.3350(2)	0.3622(1)	0.0966(1)	0.0534(6)
C16	-0.2340(3)	0.5039(2)	0.1296(2)	0.0591(10)
F17	-0.1057(2)	0.5518(1)	0.1271(1)	0.0805(7)
F18	-0.3742(3)	0.5354(1)	0.0753(2)	0.1059(9)
F19	-0.2470(3)	0.5002(1)	0.2228(1)	0.0835(8)
C20	0.5490(3)	0.3290(1)	0.5541(2)	0.0328(6)
C21	0.7157(3)	0.3448(1)	0.6076(2)	0.0394(7)
C22	0.7562(3)	0.3658(1)	0.7076(2)	0.0527(9)
C23	0.6286(4)	0.3738(2)	0.7557(2)	0.0587(10)
C24	0.4623(4)	0.3594(2)	0.7054(2)	0.0520(9)
C25	0.4237(3)	0.3371(1)	0.6063(2)	0.0388(7)
N26	0.8587(3)	0.3403(1)	0.5608(2)	0.0545(8)
O27	0.8367(2)	0.3588(1)	0.4733(2)	0.0664(8)
O28	0.9973(2)	0.3191(2)	0.6131(2)	0.091(1)

anisotropic displacement parameters

Atom	U <sub>11</sub>	U <sub>22</sub>	U <sub>33</sub>	U <sub>12</sub>	U <sub>13</sub>	U <sub>23</sub>
N1	0.0370(10)	0.051(1)	0.0310(9)	0.0045(8)	0.0041(7)	0.0057(8)
C2	0.042(1)	0.066(2)	0.033(1)	0.002(1)	0.0091(9)	0.011(1)
C3	0.037(1)	0.051(1)	0.031(1)	0.0033(10)	0.0077(9)	0.0012(10)
C4	0.037(1)	0.068(2)	0.038(1)	-0.002(1)	0.0111(9)	0.008(1)
C5	0.035(1)	0.040(1)	0.035(1)	-0.0070(9)	0.0037(8)	0.0050(9)
C6	0.0320(10)	0.037(1)	0.034(1)	-0.0004(8)	0.0048(8)	-0.0012(9)
C7	0.044(1)	0.032(1)	0.035(1)	-0.0005(9)	0.0039(9)	-0.0007(9)
C8	0.039(1)	0.033(1)	0.036(1)	-0.0063(9)	0.0030(9)	-0.0016(9)
C9	0.0308(10)	0.037(1)	0.0288(9)	-0.0023(8)	0.0038(8)	0.0017(8)
C10	0.035(1)	0.048(1)	0.0285(10)	-0.0011(9)	0.0041(8)	0.0044(9)
C11	0.038(1)	0.031(1)	0.0300(9)	-0.0032(8)	0.0061(8)	0.0063(8)
C12	0.050(1)	0.036(1)	0.047(1)	0.001(1)	0.006(1)	0.001(1)
S13	0.0416(3)	0.0436(3)	0.0336(3)	-0.0025(2)	-0.0048(2)	0.0006(2)
O14	0.064(1)	0.079(1)	0.0309(8)	-0.0035(10)	-0.0036(8)	0.0072(9)
O15	0.0460(9)	0.050(1)	0.055(1)	-0.0110(8)	-0.0048(7)	0.0014(8)

Atom	U <sub>11</sub>	U <sub>22</sub>	U <sub>33</sub>	U <sub>12</sub>	U <sub>13</sub>	U <sub>23</sub>
C16	0.051(1)	0.044(1)	0.068(2)	0.003(1)	-0.011(1)	0.001(1)
F17	0.079(1)	0.0493(10)	0.104(1)	-0.0203(9)	0.006(1)	-0.0064(9)
F18	0.078(1)	0.063(1)	0.142(2)	0.0248(10)	-0.039(1)	-0.005(1)
F19	0.104(1)	0.068(1)	0.084(1)	0.019(1)	0.035(1)	-0.0126(10)
C20	0.0315(10)	0.0295(10)	0.0341(10)	-0.0021(8)	0.0016(8)	0.0038(8)
C21	0.034(1)	0.033(1)	0.045(1)	-0.0036(9)	-0.0019(9)	0.0066(9)
C22	0.054(1)	0.042(1)	0.047(1)	-0.009(1)	-0.016(1)	0.005(1)
C23	0.083(2)	0.050(2)	0.035(1)	-0.007(1)	-0.001(1)	-0.005(1)
C24	0.070(2)	0.048(1)	0.040(1)	-0.001(1)	0.017(1)	-0.001(1)
C25	0.042(1)	0.037(1)	0.035(1)	-0.0010(9)	0.0058(9)	0.0016(9)
N26	0.033(1)	0.056(1)	0.070(1)	-0.0039(9)	0.0041(9)	0.011(1)
O27	0.0432(10)	0.093(2)	0.065(1)	-0.0063(10)	0.0160(9)	0.013(1)
O28	0.0310(10)	0.125(2)	0.109(2)	0.012(1)	0.002(1)	0.043(2)

final coordinates and isotropic displacement parameters ( $\text{\AA}^2$ ) for H- atoms

Atom	X	Y	Z	U <sub>iso</sub>
H2A	0.18886	0.44686	0.16842	0.0564
H2B	0.15483	0.38425	0.07843	0.0564
H3	0.24897	0.28067	0.18496	0.0482
H4A	0.47072	0.40343	0.23252	0.0566
H4B	0.51851	0.31417	0.26366	0.0566
H5	0.51692	0.42306	0.40050	0.0449
H6	0.59892	0.28101	0.42794	0.0420
H7	0.37849	0.19672	0.46223	0.0457
H8	0.12389	0.21485	0.35551	0.0444
H10A	-0.08689	0.29082	0.24688	0.0456
H10B	-0.07988	0.37542	0.29899	0.0456
H12A	0.26990	0.49004	0.45236	0.0544
H12B	0.07528	0.45762	0.40434	0.0544
H22	0.87169	0.37463	0.74226	0.0633
H23	0.65467	0.38918	0.82377	0.0705
H24	0.37345	0.36475	0.73885	0.0624
H25	0.30809	0.32692	0.57299	0.0466

Crystal data for compound 219a

formula	C <sub>61</sub> H <sub>60</sub> F <sub>6</sub> N <sub>2</sub> O <sub>8</sub> S <sub>4</sub>	
moiety formula	2(C <sub>27</sub> H <sub>26</sub> F <sub>3</sub> NO <sub>4</sub> S <sub>2</sub> ), C <sub>7</sub> H <sub>8</sub>	
Formula weight	1191.35	
Temperature	120(2) K	
Wavelength, radiation type	0.71073 Å, MoKα	
Diffractionmeter	STOE IPDS 2T	
Crystal system	Monoclinic	
Space group name, number	P 21/c, (14)	
Unit cell dimensions	a = 13.4345(4) Å	α = 90°
	b = 18.1709(8) Å	β = 100.182(3)°
	c = 11.7583(4) Å	γ = 90°
Volume	2825.19(18) Å <sup>3</sup>	
Number of reflections	18469	
and range used for lattice parameters	2.72° ≤ θ ≤ 28.39°	
Z	2	
Density (calculated)	1.400 Mg/m <sup>3</sup>	
Absorption coefficient	0.246 mm <sup>-1</sup>	
Absorption correction	Integration	
Max. and min. transmission	0.9795 and 0.8638	
F(000)	1244	
Crystal size, colour and form	0.080 x 0.400 x 0.650 mm <sup>3</sup> , colourless	
plate		
Theta range for data collection	2.720 to 27.942°.	
Index ranges	-17 ≤ h ≤ 17, -23 ≤ k ≤ 22, -15 ≤ l ≤ 15	
Number of reflections:		
collected	13943	
independent	6713 [R(int) = 0.0211]	
observed [I > 2σ(I)]	5478	
Completeness to theta = 25.2°	99.9 %	
Refinement method	Full-matrix least-squares on F <sup>2</sup>	
Data / restraints / parameters	6713 / 0 / 373	
Goodness-of-fit on F <sup>2</sup>	1.037	
Final R indices [I > 2σ(I)]	R1 = 0.0416, wR2 = 0.0937	
R indices (all data)	R1 = 0.0554, wR2 = 0.1017	
Largest diff. peak and hole	0.432 and -0.353 eÅ <sup>-3</sup>	
remark	Toluene is located around a centre of inversion	

Atomic coordinates and equivalent isotropic displacement parameters (Å<sup>2</sup>)

for **219a**. U(eq) is defined as one-third of the trace of the orthogonalized U<sub>ij</sub> tensor.

Atom	x	y	z	U(eq)
N1	0.73294(10)	0.28175(8)	0.39428(12)	0.0178(3)
C2	0.62726(12)	0.26753(10)	0.41155(14)	0.0174(3)
C3	0.56351(12)	0.31345(9)	0.31572(14)	0.0151(3)
C4	0.45979(12)	0.28126(9)	0.27196(14)	0.0160(3)
C5	0.38243(12)	0.32359(9)	0.28941(14)	0.0163(3)
C6	0.42055(12)	0.39614(9)	0.34372(15)	0.0183(3)
C7	0.38632(14)	0.45961(10)	0.26362(17)	0.0234(4)
C8	0.46002(14)	0.48421(10)	0.21228(17)	0.0237(4)



C9	0.55821(13)	0.44398(10)	0.24904(15)	0.0196(3)
C10	0.58970(13)	0.39255(10)	0.15681(15)	0.0212(4)
C11	0.63062(12)	0.32368(10)	0.22270(14)	0.0168(3)
C12	0.73660(12)	0.33120(10)	0.29412(14)	0.0184(3)
C13	0.53734(12)	0.39368(9)	0.35029(15)	0.0168(3)
S14	0.82247(3)	0.22799(2)	0.44445(4)	0.01871(10)
O15	0.80439(10)	0.19759(8)	0.55034(11)	0.0266(3)
O16	0.91628(9)	0.26119(8)	0.43386(13)	0.0289(3)
C17	0.81463(16)	0.14811(12)	0.34757(18)	0.0307(4)
F18	0.73627(10)	0.10631(7)	0.35679(13)	0.0451(3)
F19	0.89762(10)	0.10745(8)	0.37477(13)	0.0463(4)
F20	0.80638(14)	0.16948(8)	0.23855(12)	0.0574(4)
S21	0.44630(3)	0.19816(2)	0.19290(4)	0.01735(10)
O22	0.54131(9)	0.15963(7)	0.22143(12)	0.0238(3)
O23	0.40980(10)	0.21479(7)	0.07302(11)	0.0239(3)
C24	0.35373(12)	0.14574(9)	0.24571(15)	0.0178(3)
C25	0.37405(14)	0.12178(10)	0.35963(16)	0.0220(4)
C26	0.30479(14)	0.07724(11)	0.40071(17)	0.0253(4)
C27	0.21490(14)	0.05641(11)	0.32977(18)	0.0275(4)
C28	0.19603(14)	0.08101(11)	0.21648(18)	0.0286(4)
C29	0.26495(13)	0.12588(10)	0.17335(16)	0.0231(4)
C30	0.13970(18)	0.00792(14)	0.3755(2)	0.0428(6)
C31	0.27253(12)	0.30823(10)	0.25913(15)	0.0182(3)
C32	0.22087(13)	0.28104(10)	0.34259(16)	0.0212(4)
C33	0.11760(13)	0.26751(12)	0.31542(17)	0.0272(4)
C34	0.06541(14)	0.28248(12)	0.20569(18)	0.0298(4)
C35	0.11639(14)	0.31021(12)	0.12284(18)	0.0304(4)
C36	0.21960(14)	0.32268(11)	0.14872(16)	0.0239(4)
C37	0.59316(13)	0.42240(11)	0.46627(15)	0.0223(4)
C1L	0.0656(2)	0.55647(15)	0.4844(3)	0.0574(8)
C2L	0.0681(2)	0.48997(15)	0.4273(3)	0.0553(7)
C3L	0.0023(2)	0.43374(15)	0.4439(3)	0.0571(8)
C4L	0.1376(3)	0.4787(3)	0.3605(4)	0.0356(10)

Anisotropic displacement parameters ( $\text{\AA}^2$ ) for **219a**. The anisotropic displacement factor exponent takes the form:  $-2\pi^2[h^2 a^{*2}U_{11} + \dots + 2 h k a^* b^* U_{12}]$

Atom	U11	U22	U33	U23	U13	U12
N1	0.0117(6)	0.0228(7)	0.0195(7)	0.0031(6)	0.0041(5)	0.0005(5)
C2	0.0112(7)	0.0226(9)	0.0191(8)	0.0031(7)	0.0042(6)	-0.0008(6)
C3	0.0121(7)	0.0167(8)	0.0165(7)	-0.0005(6)	0.0025(6)	-0.0005(6)
C4	0.0144(7)	0.0158(8)	0.0172(8)	0.0002(6)	0.0012(6)	-0.0018(6)
C5	0.0155(7)	0.0169(8)	0.0165(8)	0.0014(6)	0.0028(6)	-0.0008(6)
C6	0.0153(7)	0.0169(8)	0.0233(8)	-0.0029(7)	0.0045(6)	0.0004(6)
C7	0.0207(8)	0.0157(8)	0.0331(10)	-0.0015(7)	0.0026(7)	0.0013(7)
C8	0.0238(9)	0.0162(8)	0.0299(10)	0.0039(7)	0.0014(7)	0.0011(7)
C9	0.0177(8)	0.0170(8)	0.0243(9)	0.0016(7)	0.0039(6)	-0.0028(6)
C10	0.0215(8)	0.0232(9)	0.0192(8)	0.0037(7)	0.0048(7)	-0.0001(7)
C11	0.0148(7)	0.0199(8)	0.0163(8)	-0.0002(6)	0.0039(6)	-0.0006(6)
C12	0.0158(7)	0.0225(9)	0.0174(8)	0.0020(7)	0.0049(6)	-0.0020(6)
C13	0.0146(7)	0.0157(8)	0.0208(8)	-0.0025(6)	0.0047(6)	-0.0008(6)
S14	0.01281(18)	0.0235(2)	0.0196(2)	0.00068(16)	0.00226(14)	0.00115(16)
O15	0.0214(6)	0.0367(8)	0.0215(6)	0.0071(6)	0.0034(5)	0.0046(6)
O16	0.0125(6)	0.0345(8)	0.0397(8)	0.0054(6)	0.0045(5)	-0.0002(5)
C17	0.0335(10)	0.0267(10)	0.0314(11)	-0.0032(8)	0.0044(8)	0.0081(8)
F18	0.0360(7)	0.0284(7)	0.0668(9)	-0.0111(6)	-0.0025(6)	-0.0019(5)
F19	0.0375(7)	0.0368(8)	0.0655(9)	-0.0068(7)	0.0114(6)	0.0167(6)

## Appendix

F20	0.1035(13)	0.0442(9)	0.0259(7)	-0.0075(6)	0.0146(8)	0.0179(8)
S21	0.01530(19)	0.0168(2)	0.0198(2)	-0.00315(16)	0.00277(14)	-0.00066(15)
O22	0.0173(6)	0.0204(7)	0.0333(7)	-0.0052(5)	0.0036(5)	0.0027(5)
O23	0.0254(6)	0.0269(7)	0.0193(6)	-0.0030(5)	0.0040(5)	-0.0037(5)
C24	0.0163(7)	0.0141(8)	0.0231(8)	-0.0021(6)	0.0036(6)	-0.0001(6)
C25	0.0224(8)	0.0207(9)	0.0221(9)	-0.0030(7)	0.0018(7)	0.0033(7)
C26	0.0290(9)	0.0244(9)	0.0242(9)	0.0015(7)	0.0095(7)	0.0055(8)
C27	0.0251(9)	0.0208(9)	0.0390(11)	0.0013(8)	0.0123(8)	-0.0002(7)
C28	0.0204(9)	0.0268(10)	0.0374(11)	-0.0002(8)	0.0018(8)	-0.0060(7)
C29	0.0207(8)	0.0228(9)	0.0243(9)	-0.0003(7)	-0.0005(7)	-0.0029(7)
C30	0.0354(12)	0.0387(13)	0.0584(15)	0.0089(11)	0.0198(11)	-0.0059(10)
C31	0.0135(7)	0.0182(8)	0.0225(8)	-0.0013(7)	0.0021(6)	0.0014(6)
C32	0.0166(8)	0.0258(9)	0.0212(8)	-0.0004(7)	0.0032(6)	0.0010(7)
C33	0.0175(8)	0.0336(11)	0.0316(10)	-0.0006(8)	0.0077(7)	-0.0020(8)
C34	0.0127(8)	0.0399(12)	0.0356(11)	-0.0050(9)	0.0011(7)	-0.0018(8)
C35	0.0204(9)	0.0417(12)	0.0259(10)	0.0013(9)	-0.0044(7)	0.0020(8)
C36	0.0198(8)	0.0297(10)	0.0222(9)	0.0029(7)	0.0033(7)	-0.0002(7)
C37	0.0195(8)	0.0249(9)	0.0229(9)	-0.0069(7)	0.0043(7)	-0.0041(7)
C1L	0.0529(16)	0.0329(13)	0.074(2)	-0.0042(13)	-0.0221(15)	0.0005(12)
C2L	0.0501(15)	0.0392(14)	0.0662(18)	-0.0050(13)	-0.0179(13)	0.0082(12)
C3L	0.0536(16)	0.0325(13)	0.0726(19)	-0.0085(13)	-0.0230(14)	0.0041(12)
C4L	0.032(2)	0.032(2)	0.047(3)	0.0005(19)	0.0165(19)	0.0016(17)

Hydrogen coordinates and isotropic displacement parameters ( $\text{\AA}^2$ ) for **219a**.

Atom	x	y	z	U(eq)
H2A	0.617	0.284	0.489	0.021
H2B	0.610	0.215	0.402	0.021
H6	0.402	0.403	0.422	0.022
H7	0.320	0.480	0.251	0.028
H8	0.452	0.523	0.158	0.028
H9	0.614	0.480	0.278	0.024
H10A	0.531	0.380	0.096	0.025
H10B	0.642	0.416	0.120	0.025
H11	0.626	0.280	0.170	0.020
H12A	0.789	0.315	0.250	0.022
H12B	0.751	0.383	0.320	0.022
H25	0.435	0.136	0.409	0.026
H26	0.319	0.061	0.478	0.030
H28	0.135	0.067	0.167	0.034
H29	0.251	0.143	0.096	0.028
H30A	0.075	0.009	0.322	0.064
H30B	0.130	0.026	0.451	0.064
H30C	0.165	-0.043	0.383	0.064
H32	0.256	0.272	0.419	0.025
H33	0.083	0.248	0.372	0.033
H34	-0.005	0.274	0.187	0.036
H35	0.080	0.321	0.048	0.036
H36	0.254	0.341	0.091	0.029
H37A	0.666	0.417	0.470	0.034
H37B	0.572	0.394	0.529	0.034
H37C	0.577	0.475	0.474	0.034
H1L	0.111	0.595	0.473	0.069
H2L	0.115	0.483	0.377	0.066
H3L	0.005	0.388	0.405	0.068
H4LA	0.106	0.455	0.289	0.043
H4LB	0.192	0.447	0.401	0.043

H4LC	0.166	0.526	0.343	0.043
Bond lengths [Å] and angles [°] for <b>219a</b> .				
N1-C12	1.489(2)		C32-C33	1.389(2)
N1-C2	1.492(2)		C32-H32	0.9500
N1-S14	1.5807(15)		C33-C34	1.382(3)
C2-C3	1.536(2)		C33-H33	0.9500
C2-H2A	0.9900		C34-C35	1.381(3)
C2-H2B	0.9900		C34-H34	0.9500
C3-C4	1.515(2)		C35-C36	1.385(3)
C3-C11	1.547(2)		C35-H35	0.9500
C3-C13	1.570(2)		C36-H36	0.9500
C4-C5	1.338(2)		C37-H37A	0.9800
C4-S21	1.7657(17)		C37-H37B	0.9800
C5-C31	1.483(2)		C37-H37C	0.9800
C5-C6	1.514(2)		C1L-C3L#1	1.359(5)
C6-C7	1.509(2)		C1L-C2L	1.385(4)
C6-C13	1.558(2)		C1L-H1L	0.9500
C6-H6	1.0000		C2L-C4L	1.338(5)
C7-C8	1.325(3)		C2L-C3L	1.387(4)
C7-H7	0.9500		C2L-H2L	0.9500
C8-C9	1.503(2)		C3L-H3L	0.9500
C8-H8	0.9500		C4L-H4LA	0.9800
C9-C10	1.546(2)		C4L-H4LB	0.9800
C9-C13	1.565(2)		C4L-H4LC	0.9800
C9-H9	1.0000			
C10-C11	1.522(2)		C12-N1-C2	112.18(13)
C10-H10A	0.9900		C12-N1-S14	122.60(11)
C10-H10B	0.9900		C2-N1-S14	121.45(12)
C11-C12	1.526(2)		N1-C2-C3	103.10(13)
C11-H11	1.0000		N1-C2-H2A	111.1
C12-H12A	0.9900		C3-C2-H2A	111.1
C12-H12B	0.9900		N1-C2-H2B	111.1
C13-C37	1.527(2)		C3-C2-H2B	111.1
S14-O15	1.4217(14)		H2A-C2-H2B	109.1
S14-O16	1.4224(13)		C4-C3-C2	113.55(13)
S14-C17	1.837(2)		C4-C3-C11	114.99(14)
C17-F18	1.318(3)		C2-C3-C11	105.36(13)
C17-F20	1.325(3)		C4-C3-C13	102.23(12)
C17-F19	1.329(2)		C2-C3-C13	115.85(14)
S21-O23	1.4403(13)		C11-C3-C13	104.88(13)
S21-O22	1.4424(13)		C5-C4-C3	114.76(15)
S21-C24	1.7642(17)		C5-C4-S21	124.21(13)
C24-C29	1.385(2)		C3-C4-S21	120.78(12)
C24-C25	1.389(2)		C4-C5-C31	128.51(16)
C25-C26	1.383(3)		C4-C5-C6	110.57(14)
C25-H25	0.9500		C31-C5-C6	120.88(14)
C26-C27	1.393(3)		C7-C6-C5	111.06(14)
C26-H26	0.9500		C7-C6-C13	104.24(14)
C27-C28	1.385(3)		C5-C6-C13	104.98(13)
C27-C30	1.509(3)		C7-C6-H6	112.0
C28-C29	1.395(3)		C5-C6-H6	112.0
C28-H28	0.9500		C13-C6-H6	112.0
C29-H29	0.9500		C8-C7-C6	111.87(16)
C30-H30A	0.9800		C8-C7-H7	124.1
C30-H30B	0.9800		C6-C7-H7	124.1
C30-H30C	0.9800		C7-C8-C9	113.16(16)
C31-C32	1.389(2)		C7-C8-H8	123.4
C31-C36	1.391(2)		C9-C8-H8	123.4

## Appendix

---

C8-C9-C10	115.29(15)	C27-C28-C29	121.19(18)
C8-C9-C13	103.69(14)	C27-C28-H28	119.4
C10-C9-C13	106.77(14)	C29-C28-H28	119.4
C8-C9-H9	110.3	C24-C29-C28	118.95(17)
C10-C9-H9	110.3	C24-C29-H29	120.5
C13-C9-H9	110.3	C28-C29-H29	120.5
C11-C10-C9	105.00(14)	C27-C30-H30A	109.5
C11-C10-H10A	110.7	C27-C30-H30B	109.5
C9-C10-H10A	110.7	H30A-C30-H30B	109.5
C11-C10-H10B	110.7	C27-C30-H30C	109.5
C9-C10-H10B	110.7	H30A-C30-H30C	109.5
H10A-C10-H10B	108.8	H30B-C30-H30C	109.5
C10-C11-C12	115.11(14)	C32-C31-C36	119.33(16)
C10-C11-C3	104.80(13)	C32-C31-C5	119.87(15)
C12-C11-C3	103.03(13)	C36-C31-C5	120.78(16)
C10-C11-H11	111.1	C31-C32-C33	120.25(17)
C12-C11-H11	111.1	C31-C32-H32	119.9
C3-C11-H11	111.1	C33-C32-H32	119.9
N1-C12-C11	102.89(13)	C34-C33-C32	120.06(18)
N1-C12-H12A	111.2	C34-C33-H33	120.0
C11-C12-H12A	111.2	C32-C33-H33	120.0
N1-C12-H12B	111.2	C35-C34-C33	119.81(17)
C11-C12-H12B	111.2	C35-C34-H34	120.1
H12A-C12-H12B	109.1	C33-C34-H34	120.1
C37-C13-C6	111.45(14)	C34-C35-C36	120.45(18)
C37-C13-C9	110.73(14)	C34-C35-H35	119.8
C6-C13-C9	105.06(13)	C36-C35-H35	119.8
C37-C13-C3	116.83(14)	C35-C36-C31	120.08(17)
C6-C13-C3	106.47(13)	C35-C36-H36	120.0
C9-C13-C3	105.48(13)	C31-C36-H36	120.0
O15-S14-O16	122.19(8)	C13-C37-H37A	109.5
O15-S14-N1	109.30(8)	C13-C37-H37B	109.5
O16-S14-N1	109.43(8)	H37A-C37-H37B	109.5
O15-S14-C17	103.66(9)	C13-C37-H37C	109.5
O16-S14-C17	103.62(9)	H37A-C37-H37C	109.5
N1-S14-C17	107.49(9)	H37B-C37-H37C	109.5
F18-C17-F20	108.48(18)	C3L#1-C1L-C2L	119.4(3)
F18-C17-F19	107.95(17)	C3L#1-C1L-H1L	120.3
F20-C17-F19	108.60(18)	C2L-C1L-H1L	120.3
F18-C17-S14	111.31(14)	C4L-C2L-C1L	119.8(3)
F20-C17-S14	110.75(15)	C4L-C2L-C3L	119.9(3)
F19-C17-S14	109.66(14)	C1L-C2L-C3L	120.3(3)
O23-S21-O22	117.62(8)	C1L-C2L-H2L	119.9
O23-S21-C24	108.58(8)	C3L-C2L-H2L	119.9
O22-S21-C24	107.82(8)	C1L#1-C3L-C2L	120.3(3)
O23-S21-C4	108.74(8)	C1L#1-C3L-H3L	119.8
O22-S21-C4	106.76(8)	C2L-C3L-H3L	119.8
C24-S21-C4	106.83(8)	C2L-C4L-H4LA	109.5
C29-C24-C25	120.79(17)	C2L-C4L-H4LB	109.5
C29-C24-S21	120.57(14)	H4LA-C4L-H4LB	109.5
C25-C24-S21	118.56(13)	C2L-C4L-H4LC	109.5
C26-C25-C24	119.38(17)	H4LA-C4L-H4LC	109.5
C26-C25-H25	120.3	H4LB-C4L-H4LC	109.5
C24-C25-H25	120.3		
C25-C26-C27	121.02(18)		
C25-C26-H26	119.5		
C27-C26-H26	119.5		
C28-C27-C26	118.67(17)		
C28-C27-C30	120.73(19)		
C26-C27-C30	120.60(19)		

Symmetry transformations used to generate equivalent atoms: #1 -x,-y+1,-z+1  
Torsion angles [°] for **219a**.

C12-N1-C2-C3	-1.25(18)	C2-C3-C13-C9	134.46(14)
S14-N1-C2-C3	-159.92(12)	C11-C3-C13-C9	18.78(16)
N1-C2-C3-C4	149.64(14)	C12-N1-S14-O15	170.28(13)
N1-C2-C3-C11	22.94(17)	C2-N1-S14-O15	-33.29(16)
N1-C2-C3-C13	-92.46(16)	C12-N1-S14-O16	34.06(16)
C2-C3-C4-C5	117.18(17)	C2-N1-S14-O16	-169.51(13)
C11-C3-C4-C5	-121.36(17)	C12-N1-S14-C17	-77.84(15)
C13-C3-C4-C5	-8.35(19)	C2-N1-S14-C17	78.59(15)
C2-C3-C4-S21	-68.33(17)	O15-S14-C17-F18	44.62(16)
C11-C3-C4-S21	53.13(18)	O16-S14-C17-F18	173.15(14)
C13-C3-C4-S21	166.14(12)	N1-S14-C17-F18	-71.05(16)
C3-C4-C5-C31	-179.00(16)	O15-S14-C17-F20	165.39(15)
S21-C4-C5-C31	6.7(3)	O16-S14-C17-F20	-66.08(17)
C3-C4-C5-C6	3.3(2)	N1-S14-C17-F20	49.72(17)
S21-C4-C5-C6	-171.02(12)	O15-S14-C17-F19	-74.78(16)
C4-C5-C6-C7	115.56(16)	O16-S14-C17-F19	53.76(17)
C31-C5-C6-C7	-62.4(2)	N1-S14-C17-F19	169.56(14)
C4-C5-C6-C13	3.47(19)	C5-C4-S21-O23	68.22(17)
C31-C5-C6-C13	-174.48(15)	C3-C4-S21-O23	-105.72(14)
C5-C6-C7-C8	-102.81(18)	C5-C4-S21-O22	-163.94(15)
C13-C6-C7-C8	9.8(2)	C3-C4-S21-O22	22.12(15)
C6-C7-C8-C9	-1.3(2)	C5-C4-S21-C24	-48.79(17)
C7-C8-C9-C10	108.72(19)	C3-C4-S21-C24	137.27(13)
C7-C8-C9-C13	-7.6(2)	O23-S21-C24-C29	1.62(17)
C8-C9-C10-C11	-138.60(15)	O22-S21-C24-C29	-126.83(15)
C13-C9-C10-C11	-24.03(17)	C4-S21-C24-C29	118.73(15)
C9-C10-C11-C12	-76.40(17)	O23-S21-C24-C25	178.43(14)
C9-C10-C11-C3	36.01(17)	O22-S21-C24-C25	49.98(16)
C4-C3-C11-C10	77.41(17)	C4-S21-C24-C25	-64.46(15)
C2-C3-C11-C10	-156.77(13)	C29-C24-C25-C26	0.3(3)
C13-C3-C11-C10	-34.04(16)	S21-C24-C25-C26	-176.46(14)
C4-C3-C11-C12	-161.82(14)	C24-C25-C26-C27	-0.3(3)
C2-C3-C11-C12	-36.01(17)	C25-C26-C27-C28	0.2(3)
C13-C3-C11-C12	86.73(15)	C25-C26-C27-C30	-179.85(19)
C2-N1-C12-C11	-21.00(18)	C26-C27-C28-C29	-0.1(3)
S14-N1-C12-C11	137.38(13)	C30-C27-C28-C29	179.94(19)
C10-C11-C12-N1	147.49(14)	C25-C24-C29-C28	-0.3(3)
C3-C11-C12-N1	34.04(16)	S21-C24-C29-C28	176.48(15)
C7-C6-C13-C37	106.32(16)	C27-C28-C29-C24	0.1(3)
C5-C6-C13-C37	-136.82(15)	C4-C5-C31-C32	97.8(2)
C7-C6-C13-C9	-13.65(17)	C6-C5-C31-C32	-84.6(2)
C5-C6-C13-C9	103.21(15)	C4-C5-C31-C36	-84.0(2)
C7-C6-C13-C3	-125.22(14)	C6-C5-C31-C36	93.6(2)
C5-C6-C13-C3	-8.36(17)	C36-C31-C32-C33	0.9(3)
C8-C9-C13-C37	-107.56(16)	C5-C31-C32-C33	179.06(17)
C10-C9-C13-C37	130.25(15)	C31-C32-C33-C34	-1.3(3)
C8-C9-C13-C6	12.89(17)	C32-C33-C34-C35	0.7(3)
C10-C9-C13-C6	-109.30(15)	C33-C34-C35-C36	0.4(3)
C8-C9-C13-C3	125.17(14)	C34-C35-C36-C31	-0.9(3)
C10-C9-C13-C3	2.98(17)	C32-C31-C36-C35	0.2(3)
C4-C3-C13-C37	134.98(15)	C5-C31-C36-C35	-177.97(18)
C2-C3-C13-C37	11.0(2)	C3L#1-C1L-C2L-C4L	-177.1(3)
C11-C3-C13-C37	-104.70(16)	C3L#1-C1L-C2L-C3L	-0.4(4)
C4-C3-C13-C6	9.75(16)	C4L-C2L-C3L-C1L#1	177.1(3)
C2-C3-C13-C6	-114.26(15)	C1L-C2L-C3L-C1L#1	0.4(4)
C11-C3-C13-C6	130.07(13)		
C4-C3-C13-C9	-101.53(14)		

Symmetry transformations used to generate equivalent atoms:  
#1 -x,-y+1,-z+1

### Crystal data for compound 262t

formula	C <sub>21</sub> H <sub>19</sub> NO <sub>2</sub> S
molecular weight	349.43 gmol <sup>-1</sup>
space group	P 2 <sub>1</sub> /c (monoclinic)
absorption	$\mu = 0.202 \text{ mm}^{-1}$
crystal size	0.19 x 0.42 x 0.45 mm <sup>3</sup> colourless block
lattice parameters	a = 15.5300(10) Å
(calculate from	b = 13.5127(10) Å $\beta = 100.114(5)^\circ$
10546 reflections with	c = 8.3238(5) Å
2.6° < $\theta$ < 28.2°)	V = 1719.6(2) Å <sup>3</sup> z = 4 F(000) = 736
temperature	-80°C
density	$d_{\text{rön}} = 1.350 \text{ gcm}^{-3}$

### data collection

diffractometer	STOE IPDS 2T
radiation	Mo-K $\alpha$ Graphitmonochromator
Scan – Type	$\omega$ scans
Scan – width	1°
scan range	2° ≤ $\theta$ ≤ 28° -20 ≤ h ≤ 20 -15 ≤ k ≤ 17 -9 ≤ l ≤ 10
number of reflections:	
measured	9173
unique	4086 (R <sub>int</sub> = 0.0221)
observed	2918 ( F /σ(F) > 4.0)

### data correction, structure solution, and refinement

corrections	Lorentz and polarisation correction.
Structure solution	Program: SIR-2004 (Direct methods)
refinement	Program: SHELXL-2018 (full matrix). 275 refined parameters, weighting scheme: $w = 1/[\sigma^2(F_o^2) + (0.0563 * P)^2 + 0.51 * P]$ wobei $P = (\text{Max}(F_o^2, 0) + 2 * F_c^2) / 3$ . H-atoms at calculated positions and refined with isotropic displacement parameters, non H- atoms refined anisotropically.
R-values	wR2 = 0.1153 (R1 = 0.043 for observed reflections, 0.0712 for all reflections)
goodness of fit	S = 1.016
maximum deviation of parameters	0.001 * e.s.d
maximum peak height in diff. Fourier synthesis	0.46, -0.25 eÅ <sup>-3</sup>

final coordinates and equivalent displacement parameters ( $\text{\AA}^2$ )

$$U_{\text{eq}} = (1/3) * \sum_{ij} a_i^* a_j^* a_i a_j$$

Atom	X	Y	Z	$U_{\text{eq}}$
C1	0.0629(1)	0.4298(1)	0.6832(2)	0.0323(5)
C2	0.0105(1)	0.4855(2)	0.7673(2)	0.0392(6)
C3	-0.0672(1)	0.4444(2)	0.7987(3)	0.0454(7)
C4	-0.0915(1)	0.3501(2)	0.7439(3)	0.0477(7)
C5	-0.0396(1)	0.2953(2)	0.6579(3)	0.0452(7)
C6	0.0389(1)	0.3354(1)	0.6295(2)	0.0358(5)
C7	0.1075(1)	0.2896(2)	0.5459(3)	0.0411(6)
C8	0.1876(1)	0.3565(1)	0.6059(2)	0.0316(5)
C9	0.1498(1)	0.4595(1)	0.6374(2)	0.0300(5)
C10	0.2056(1)	0.5235(1)	0.7647(2)	0.0310(5)
C11	0.2240(1)	0.6206(2)	0.7320(3)	0.0462(7)
C12	0.2755(2)	0.6766(2)	0.8505(3)	0.0586(8)
N13	0.3082(1)	0.6446(2)	0.9991(2)	0.0548(6)
C14	0.2892(2)	0.5508(2)	1.0293(3)	0.0509(7)
C15	0.2391(1)	0.4886(2)	0.9193(2)	0.0423(6)
S16	0.26163(3)	0.35615(3)	0.46465(5)	0.0347(1)
O17	0.21850(9)	0.3969(1)	0.3121(2)	0.0481(5)
O18	0.29708(9)	0.2575(1)	0.4642(2)	0.0433(5)
C19	0.3452(1)	0.4378(1)	0.5517(2)	0.0347(5)
C20	0.3488(2)	0.5323(2)	0.4906(3)	0.0506(7)
C21	0.4115(2)	0.5974(2)	0.5670(3)	0.0591(9)
C22	0.4693(1)	0.5703(2)	0.7043(3)	0.0520(8)
C23	0.4652(1)	0.4752(2)	0.7623(3)	0.0560(8)
C24	0.4031(1)	0.4087(2)	0.6879(3)	0.0462(7)
C25	0.5344(2)	0.6443(2)	0.7904(4)	0.078(1)

anisotropic displacement parameters

Atom	$U_{11}$	$U_{22}$	$U_{33}$	$U_{12}$	$U_{13}$	$U_{23}$
C1	0.0310(8)	0.0339(9)	0.0286(8)	0.0006(7)	-0.0041(7)	0.0043(7)
C2	0.0355(9)	0.042(1)	0.0376(10)	0.0038(8)	0.0006(8)	0.0016(9)
C3	0.0335(9)	0.059(1)	0.042(1)	0.0066(9)	0.0036(8)	0.0076(10)
C4	0.0322(9)	0.058(1)	0.050(1)	-0.0040(9)	-0.0014(8)	0.014(1)
C5	0.039(1)	0.039(1)	0.052(1)	-0.0086(9)	-0.0067(9)	0.0078(10)
C6	0.0343(9)	0.0345(10)	0.0347(9)	-0.0012(7)	-0.0046(7)	0.0042(8)
C7	0.042(1)	0.033(1)	0.045(1)	-0.0038(8)	-0.0005(8)	-0.0061(9)
C8	0.0358(8)	0.0285(9)	0.0286(8)	0.0002(7)	0.0003(7)	-0.0006(7)
C9	0.0324(8)	0.0284(9)	0.0275(8)	0.0011(7)	-0.0001(6)	0.0012(7)
C10	0.0284(8)	0.0315(9)	0.0325(9)	0.0021(7)	0.0038(7)	-0.0044(7)
C11	0.052(1)	0.030(1)	0.051(1)	0.0019(9)	-0.0081(9)	0.0005(9)
C12	0.060(1)	0.031(1)	0.076(2)	-0.0024(10)	-0.012(1)	-0.010(1)
N13	0.0488(10)	0.050(1)	0.060(1)	-0.0013(9)	-0.0059(9)	-0.0207(10)
C14	0.053(1)	0.062(2)	0.034(1)	-0.004(1)	-0.0027(9)	-0.009(1)
C15	0.050(1)	0.043(1)	0.0328(9)	-0.0076(9)	0.0025(8)	0.0006(9)
S16	0.0390(2)	0.0332(2)	0.0306(2)	0.0035(2)	0.0030(2)	-0.0039(2)
O17	0.0558(8)	0.0580(10)	0.0288(6)	0.0083(7)	0.0023(6)	0.0014(6)
O18	0.0461(7)	0.0347(8)	0.0483(8)	0.0043(6)	0.0054(6)	-0.0111(6)

## Curriculum vitae

---

C19	0.0376(9)	0.0304(9)	0.0379(9)	0.0011(7)	0.0116(7)	-0.0024(8)
C20	0.070(1)	0.038(1)	0.043(1)	-0.002(1)	0.010(1)	0.0052(9)
C21	0.080(2)	0.034(1)	0.067(2)	-0.012(1)	0.024(1)	0.006(1)
C22	0.049(1)	0.043(1)	0.069(1)	-0.0127(10)	0.022(1)	-0.014(1)
C23	0.041(1)	0.050(1)	0.073(2)	-0.0062(10)	-0.003(1)	-0.001(1)
C24	0.041(1)	0.034(1)	0.059(1)	-0.0034(8)	-0.0013(9)	0.0058(10)
C25	0.069(2)	0.059(2)	0.109(2)	-0.029(1)	0.024(2)	-0.024(2)

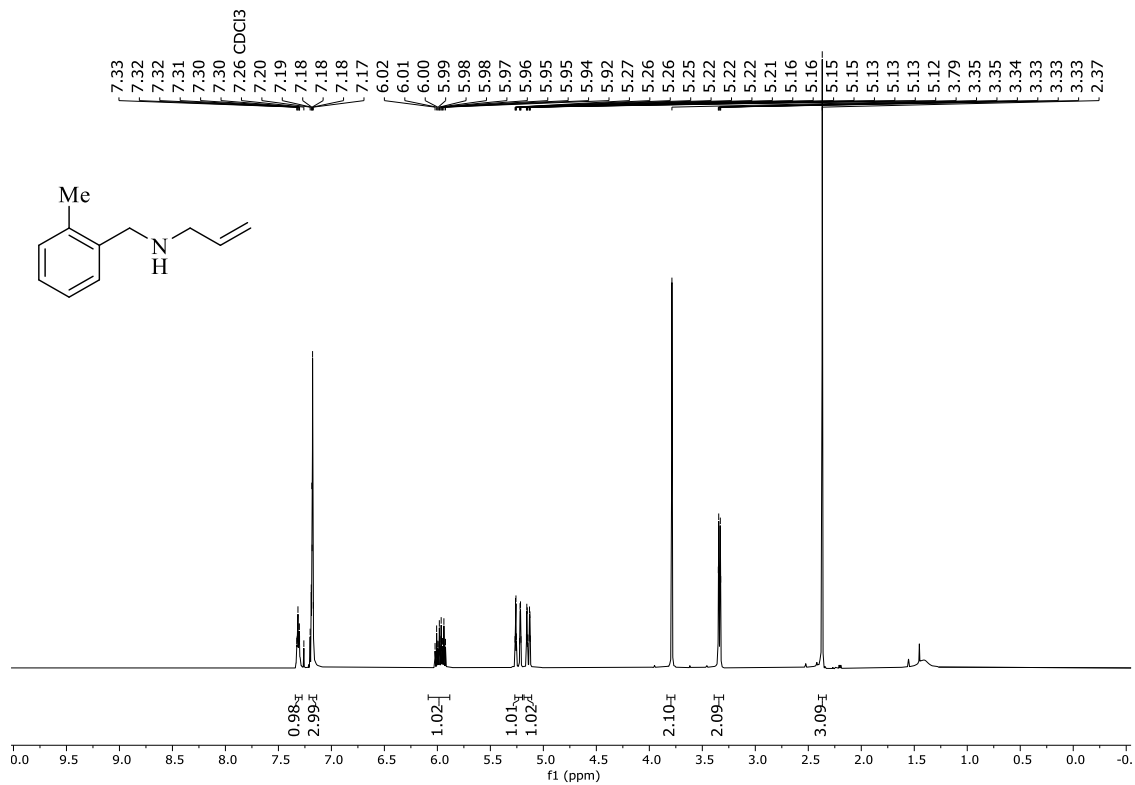
final coordinates and isotropic displacement parameters ( $\text{\AA}^2$ ) for H- atoms

Atom	X	Y	Z	$U_{\text{iso}}$
H2	0.029(1)	0.553(2)	0.805(3)	0.0470
H3	-0.103(1)	0.482(2)	0.861(3)	0.0545
H4	-0.145(2)	0.321(2)	0.772(3)	0.0573
H5	-0.056(1)	0.231(2)	0.617(3)	0.0543
H7A	0.118(1)	0.218(2)	0.579(3)	0.0493
H7B	0.091(1)	0.295(2)	0.427(3)	0.0493
H8	0.221(1)	0.330(1)	0.702(2)	0.0379
H9	0.139(1)	0.493(1)	0.534(2)	0.0361
H11	0.205(1)	0.647(2)	0.626(3)	0.0554
H12	0.293(2)	0.743(2)	0.826(3)	0.0704
H14	0.309(2)	0.530(2)	1.135(3)	0.0610
H15	0.231(1)	0.422(2)	0.951(3)	0.0508
H20	0.311(2)	0.549(2)	0.398(3)	0.0607
H21	0.411(2)	0.663(2)	0.520(3)	0.0709
H23	0.505(2)	0.456(2)	0.859(3)	0.0672
H24	0.397(1)	0.346(2)	0.726(3)	0.0554
H25A	0.50322	0.69630	0.83899	0.117
H25B	0.56689	0.67386	0.71165	0.117
H25C	0.57518	0.61071	0.87630	0.117

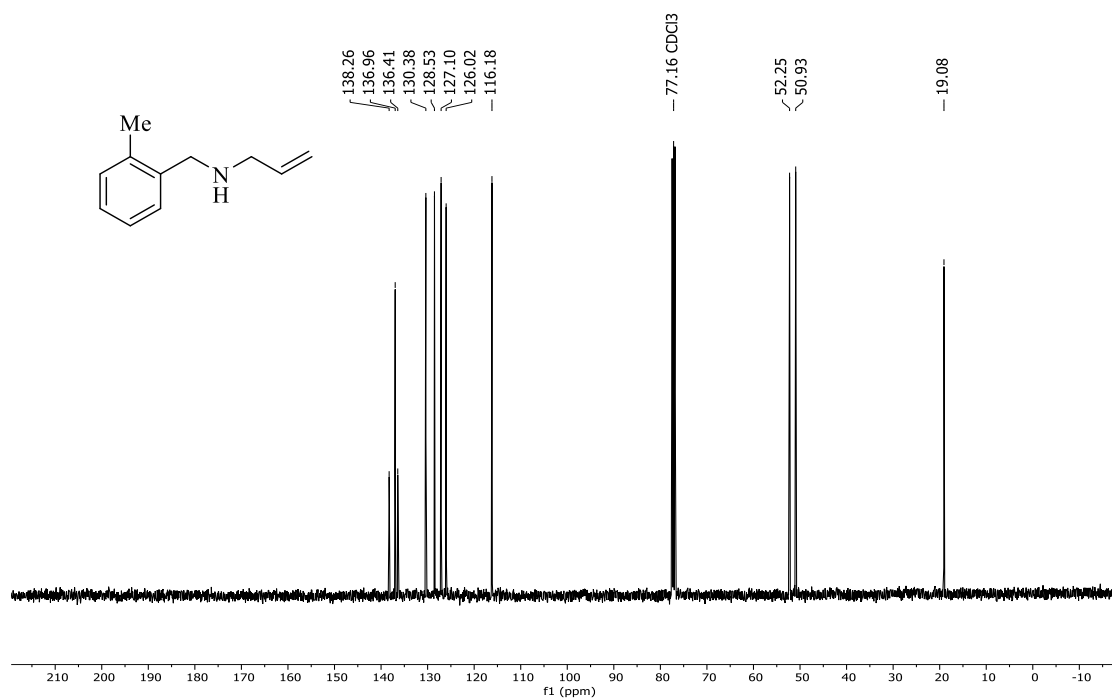


## 6.2. NMR Spectra

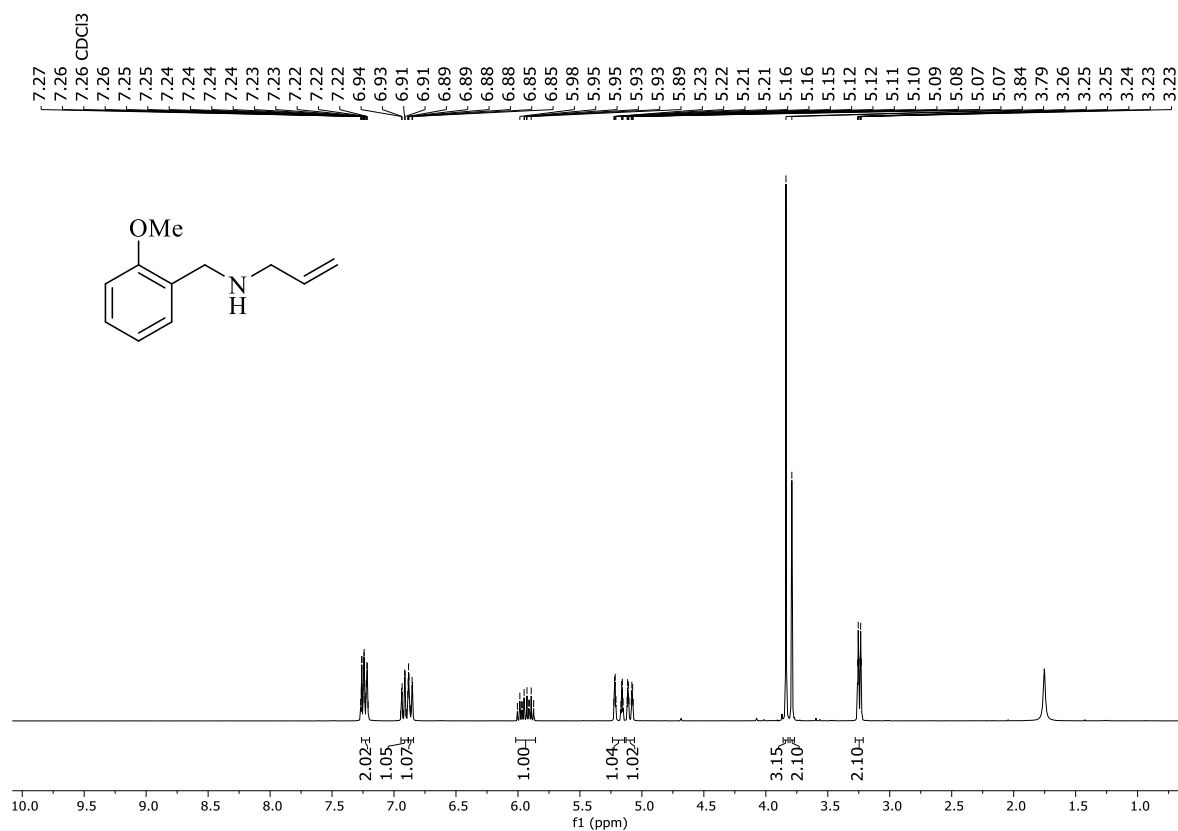
### 6.2.1. Spectra section 2.3.1



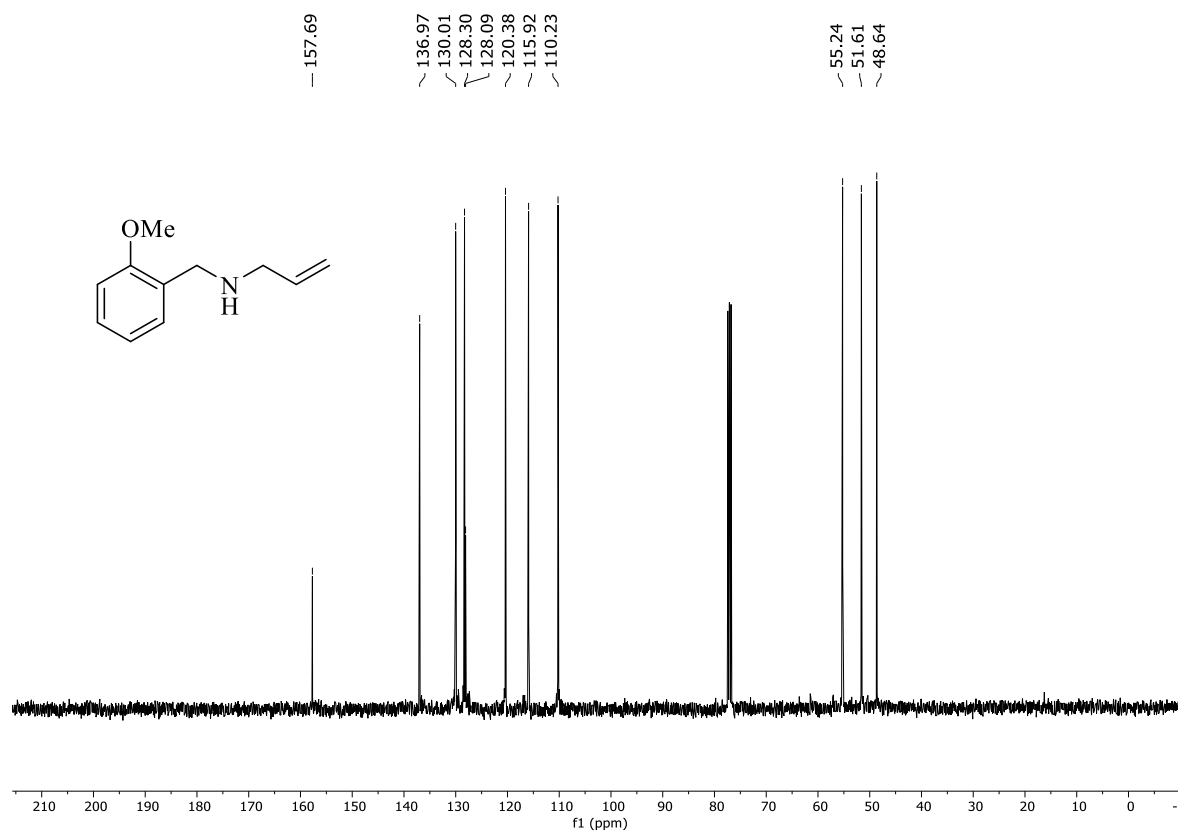
<sup>1</sup>H NMR (400 MHz, CDCl<sub>3</sub>) spectrum of **229a**



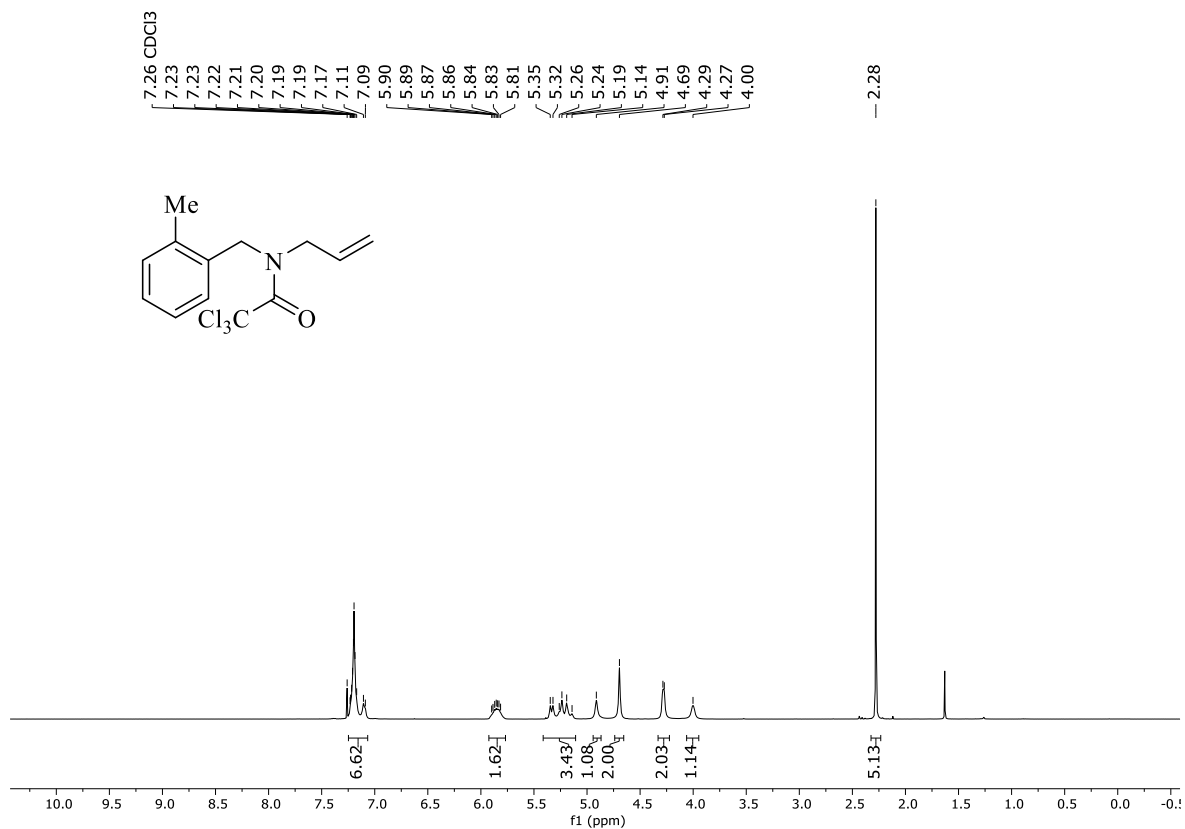
<sup>13</sup>C NMR (101 MHz, CDCl<sub>3</sub>) spectrum of **229a**



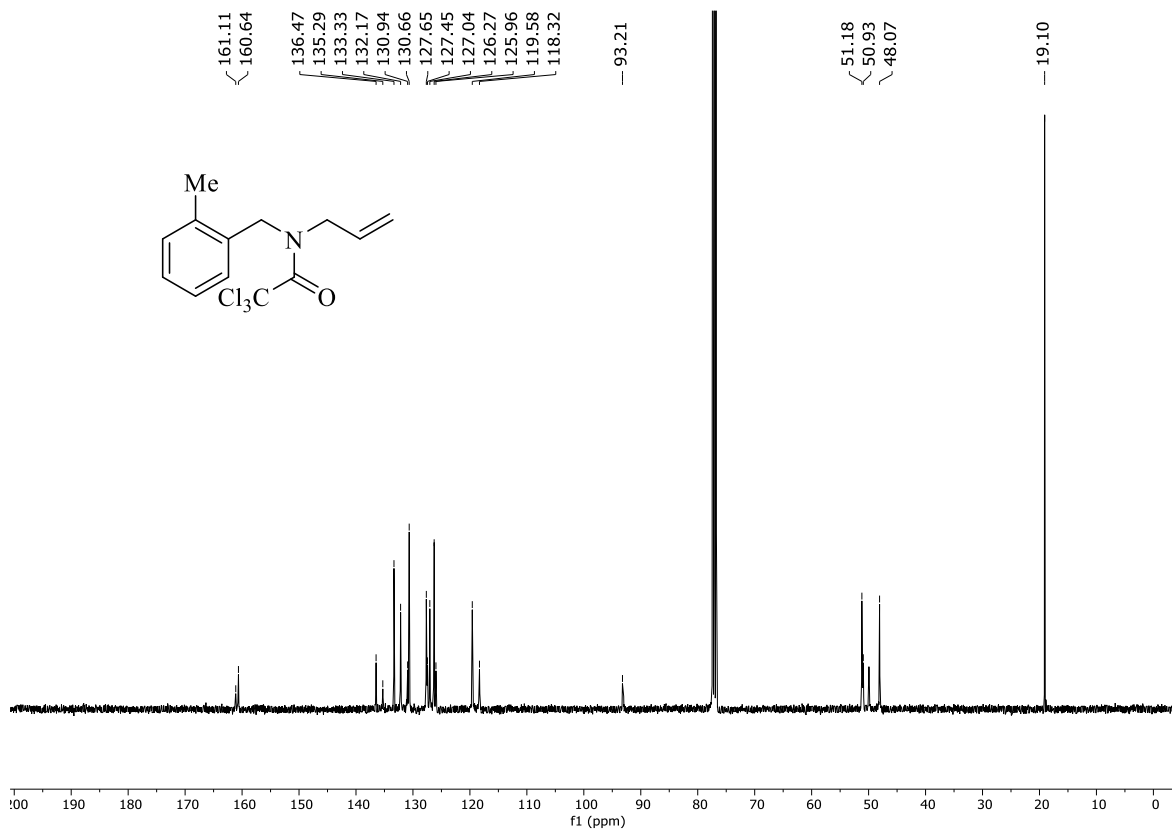
<sup>1</sup>H NMR (400 MHz, CDCl<sub>3</sub>) spectrum of **229b**



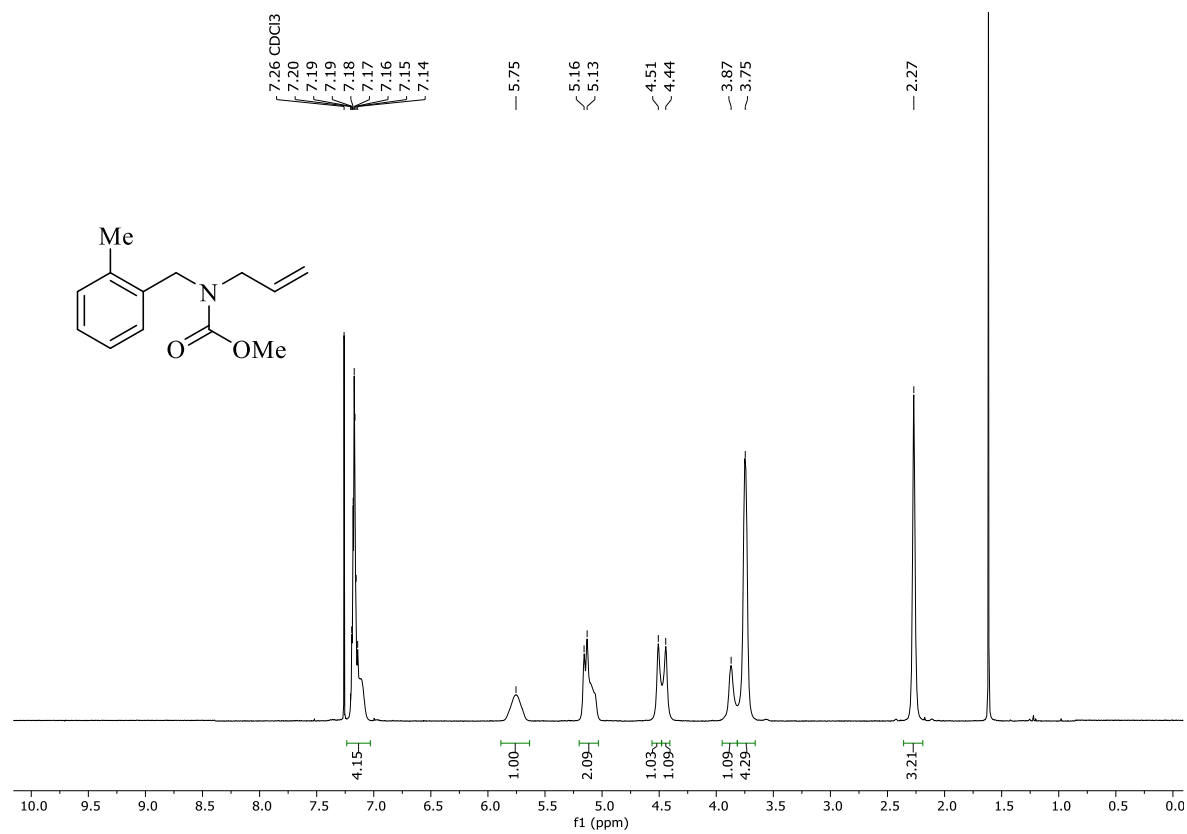
<sup>13</sup>C NMR (101 MHz, CDCl<sub>3</sub>) spectrum of **229b**



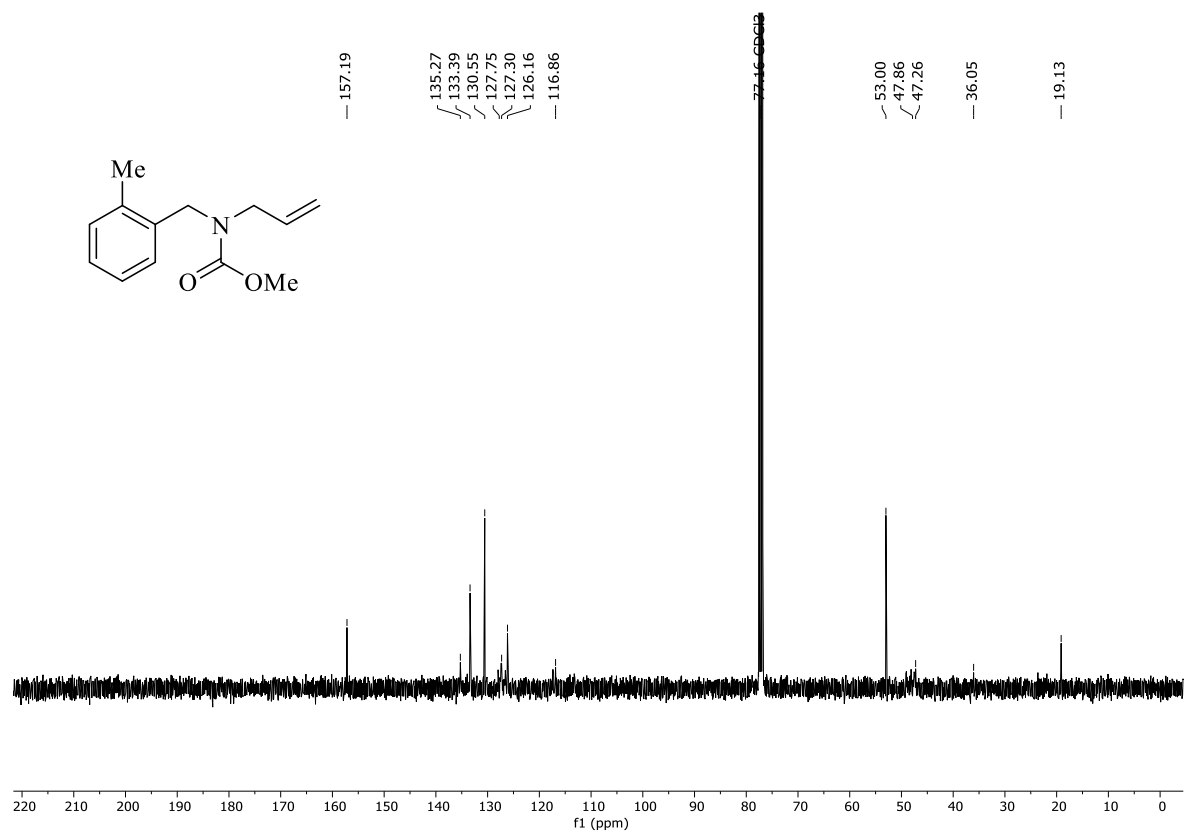
**<sup>1</sup>H NMR (400 MHz, CDCl<sub>3</sub>) spectrum of **213a****



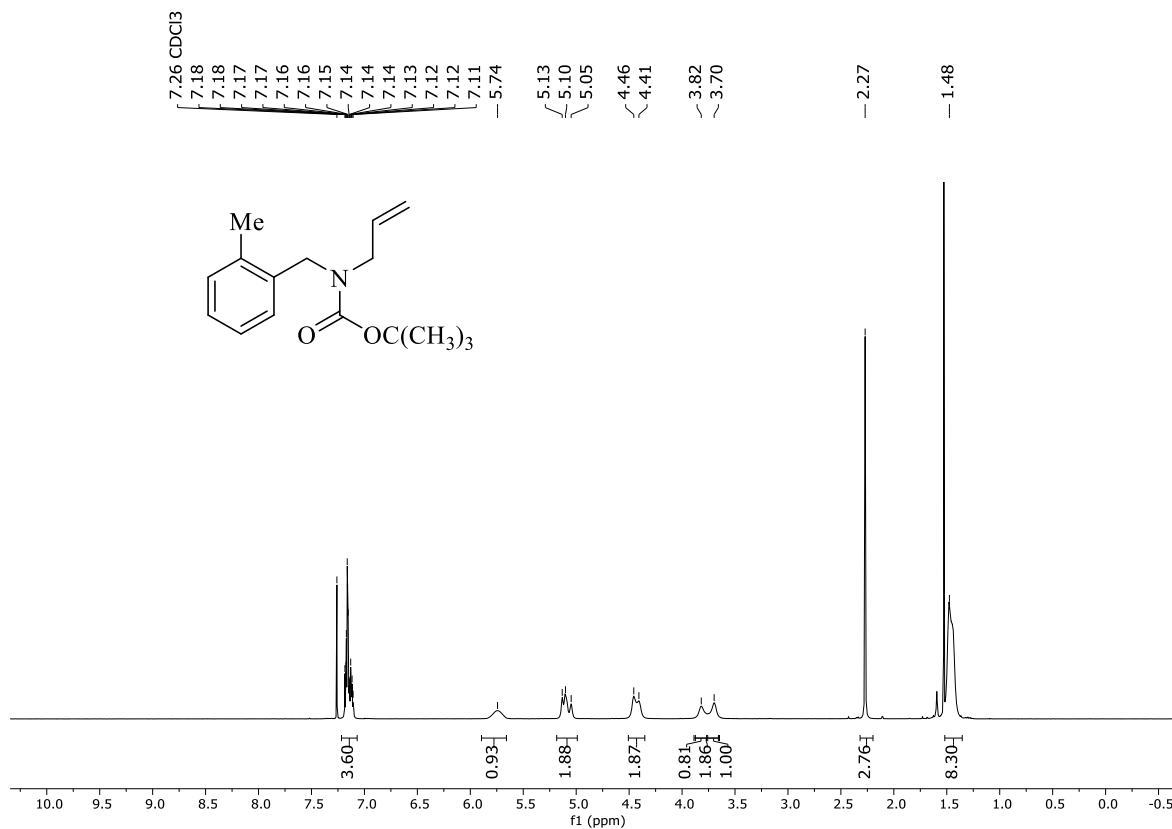
**<sup>13</sup>C NMR (101 MHz, CDCl<sub>3</sub>) spectrum of **213a****



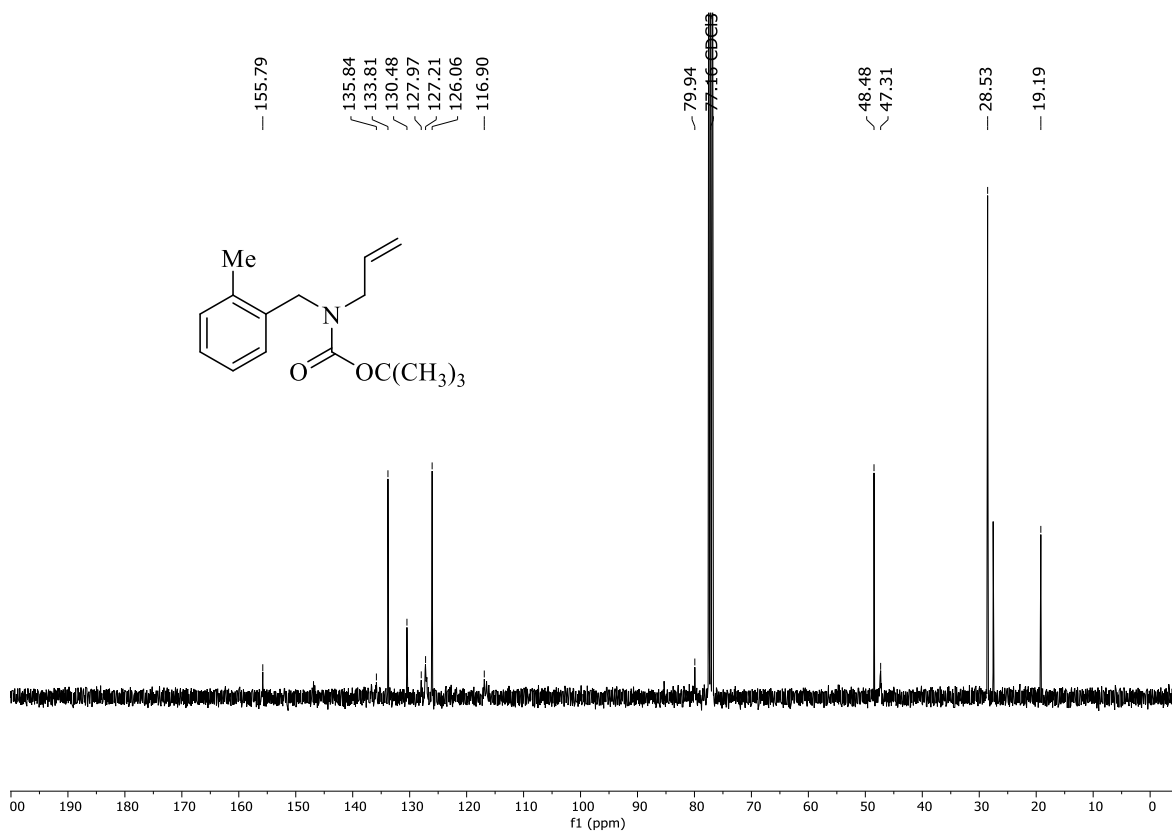
<sup>1</sup>H NMR (400 MHz, CDCl<sub>3</sub>) spectrum of **213b**



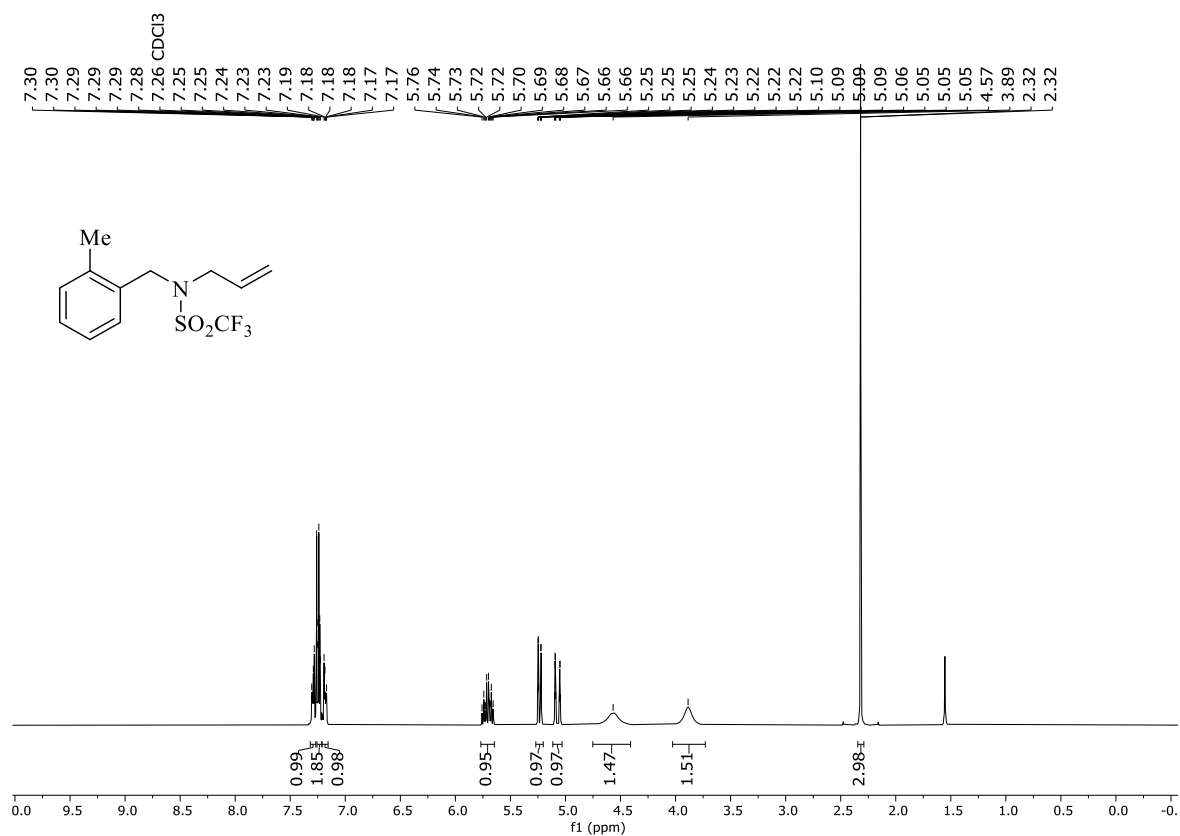
<sup>13</sup>C NMR (101 MHz, CDCl<sub>3</sub>) spectrum of **213b**



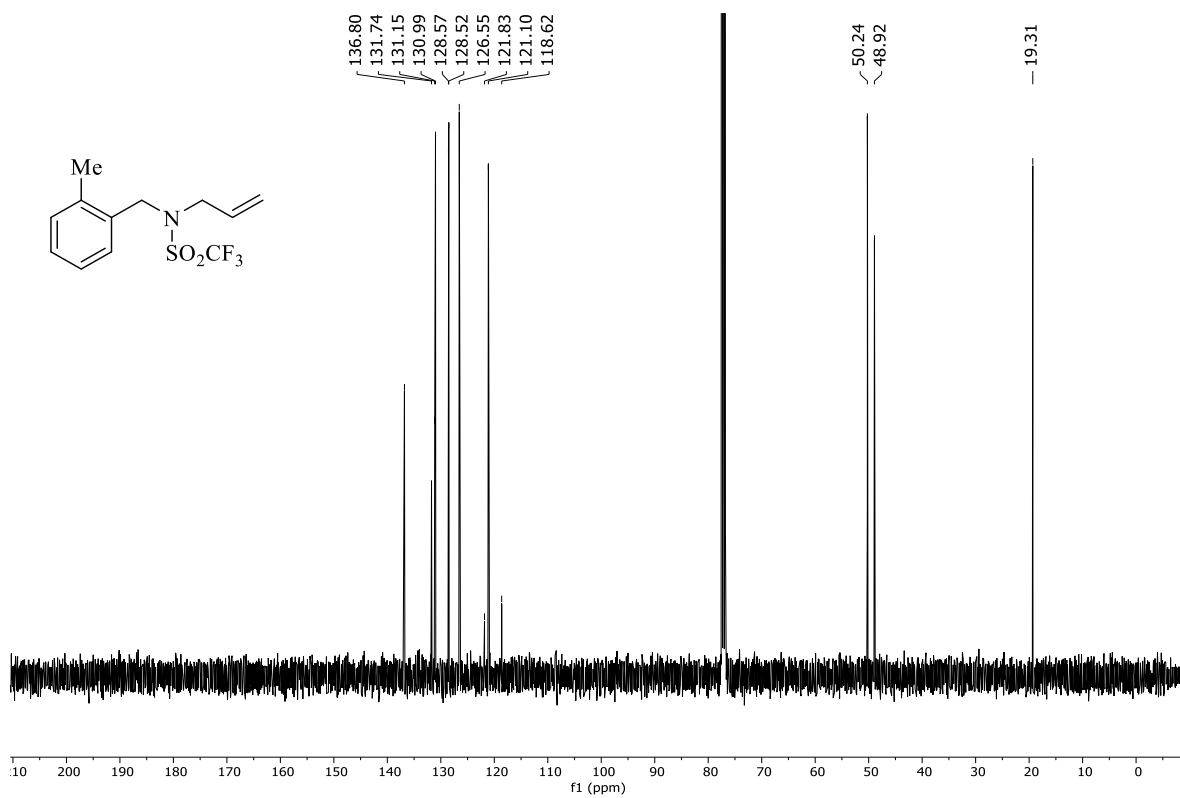
<sup>1</sup>H NMR (400 MHz, CDCl<sub>3</sub>) spectrum of **213c**



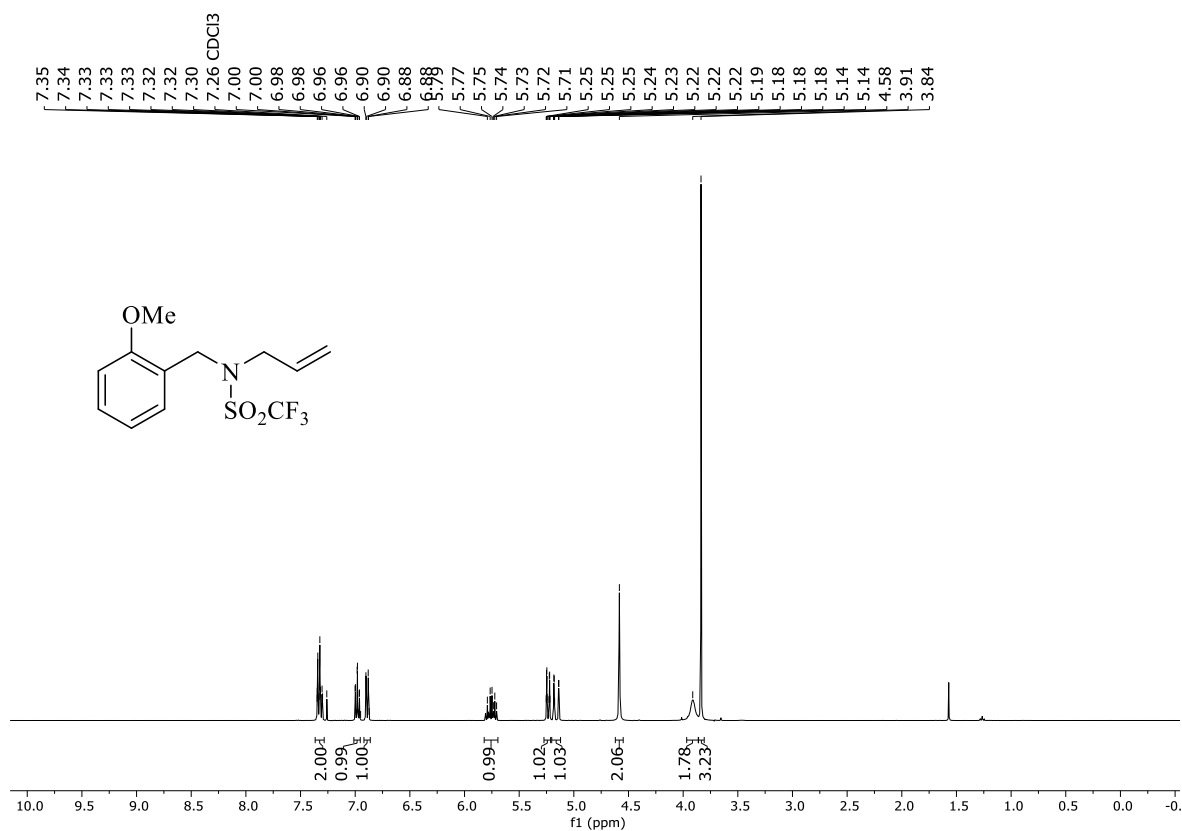
<sup>13</sup>C NMR (101 MHz, CDCl<sub>3</sub>) spectrum of **213c**



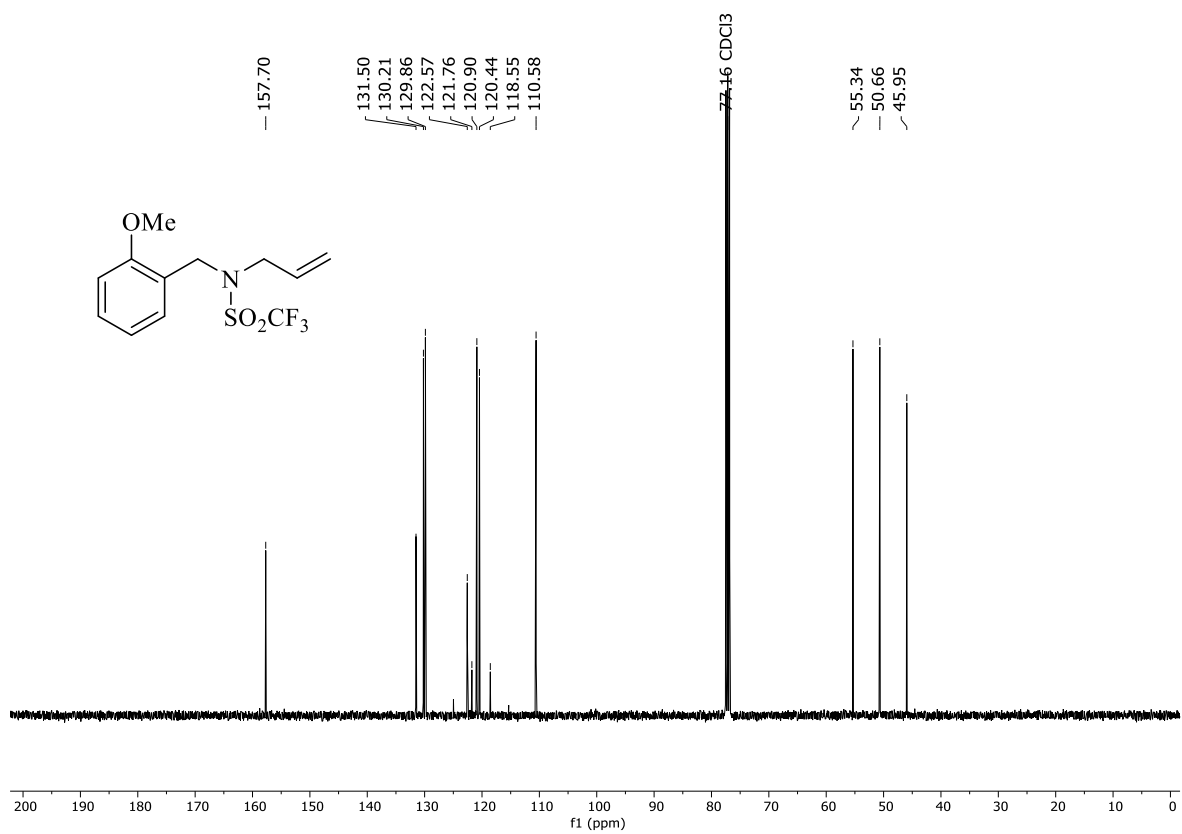
<sup>1</sup>H NMR (400 MHz, CDCl<sub>3</sub>) spectrum of **213e**



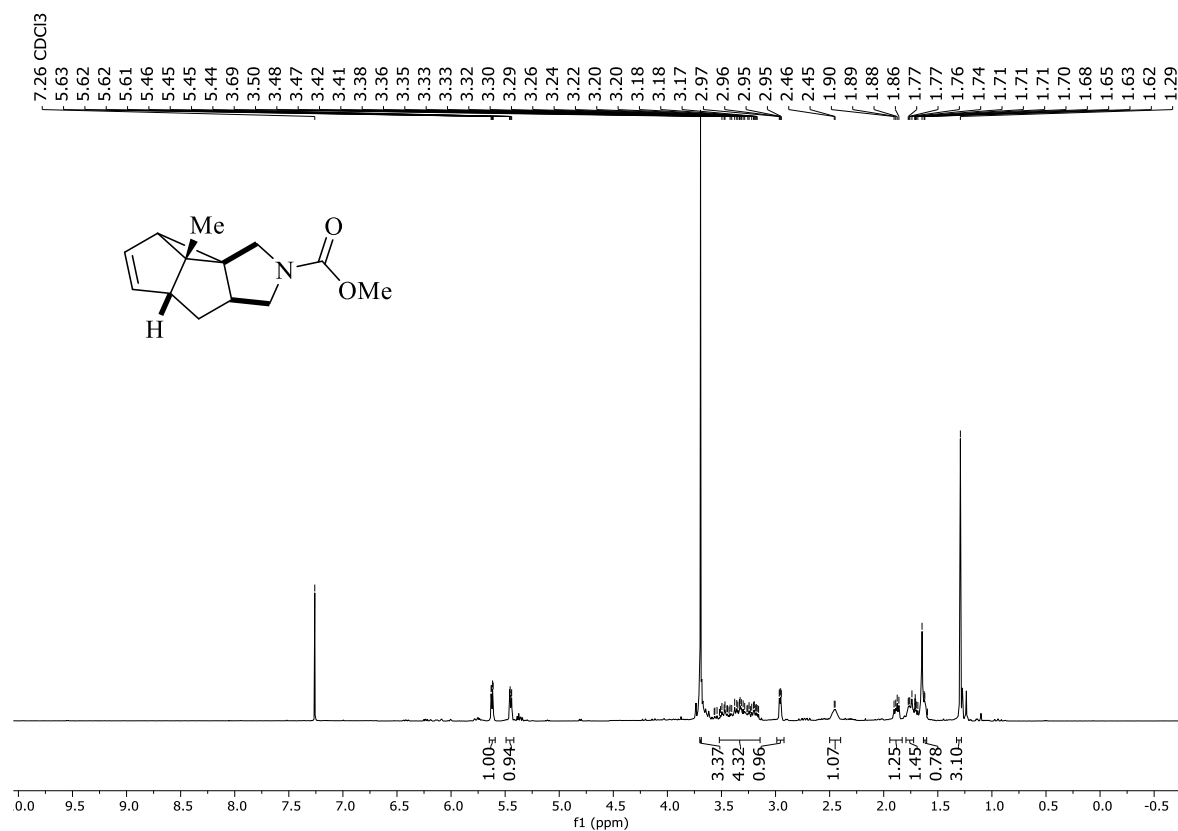
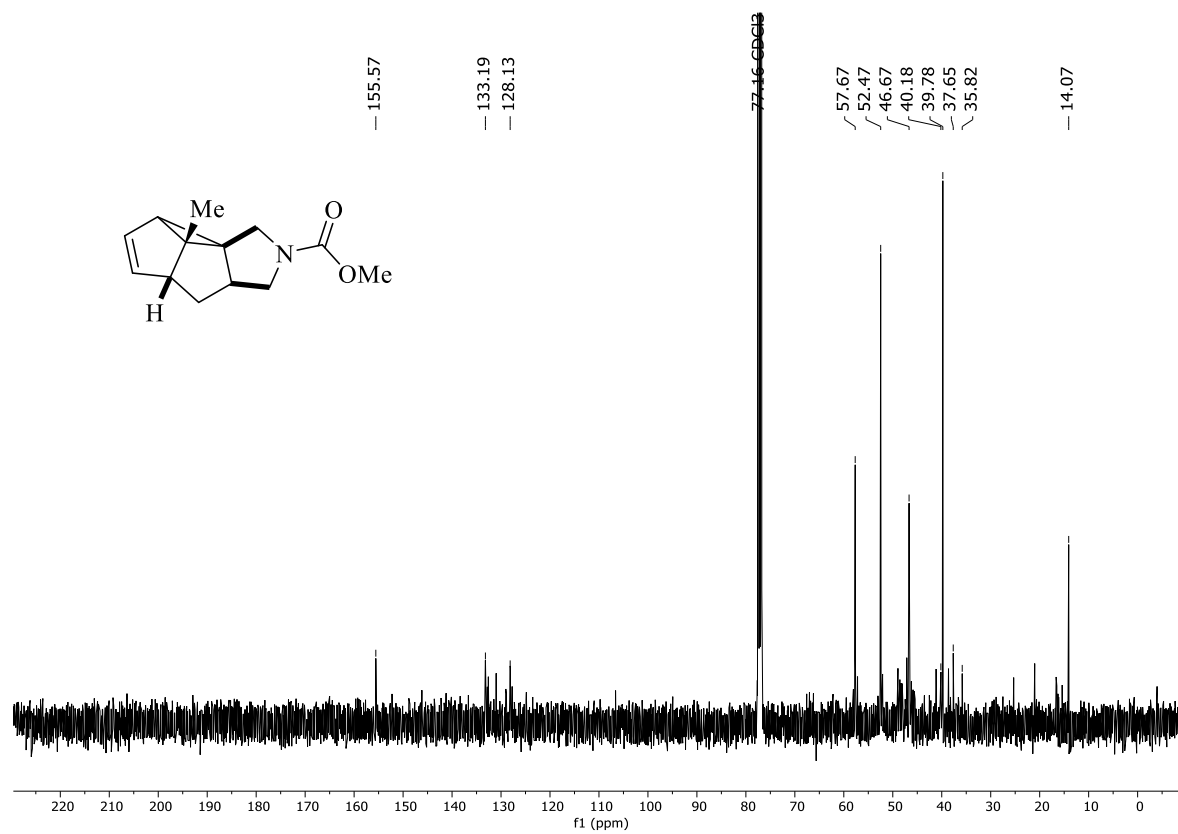
<sup>13</sup>C NMR (101 MHz, CDCl<sub>3</sub>) spectrum of **213e**



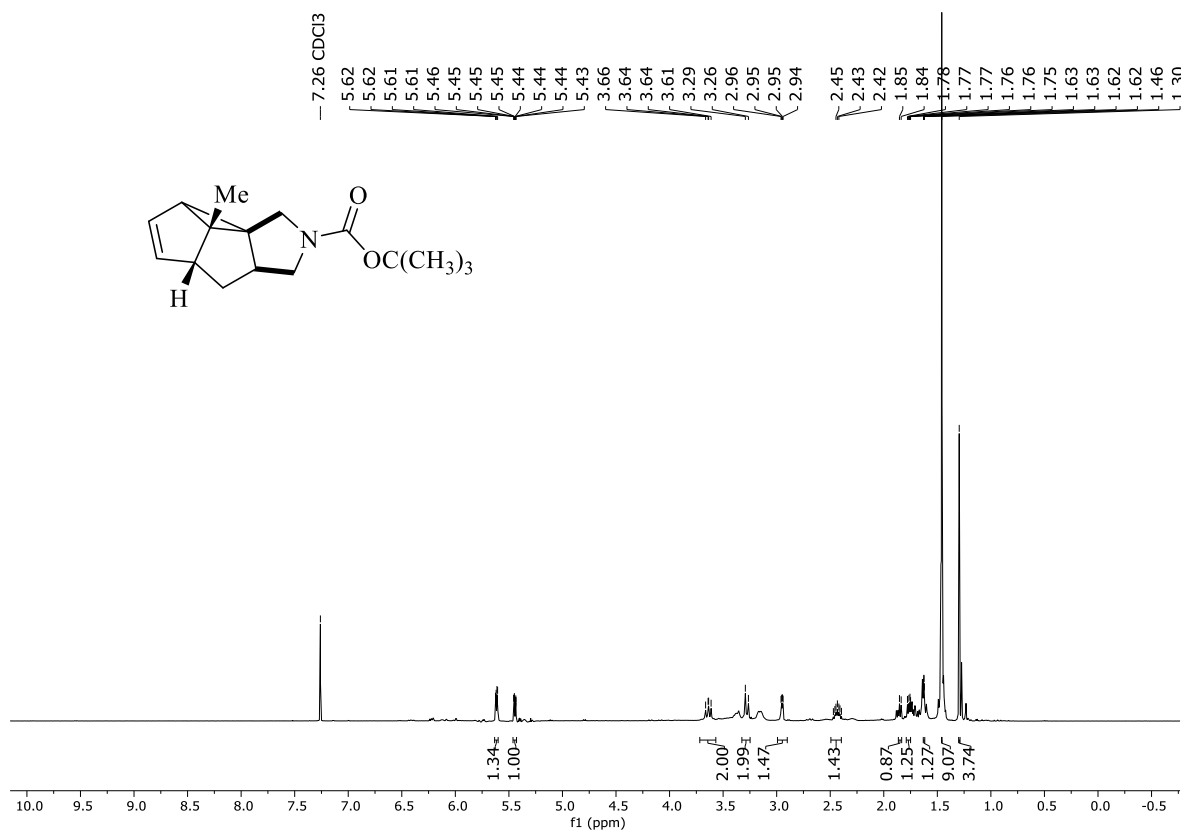
<sup>1</sup>H NMR (400 MHz, CDCl<sub>3</sub>) spectrum of **213f**



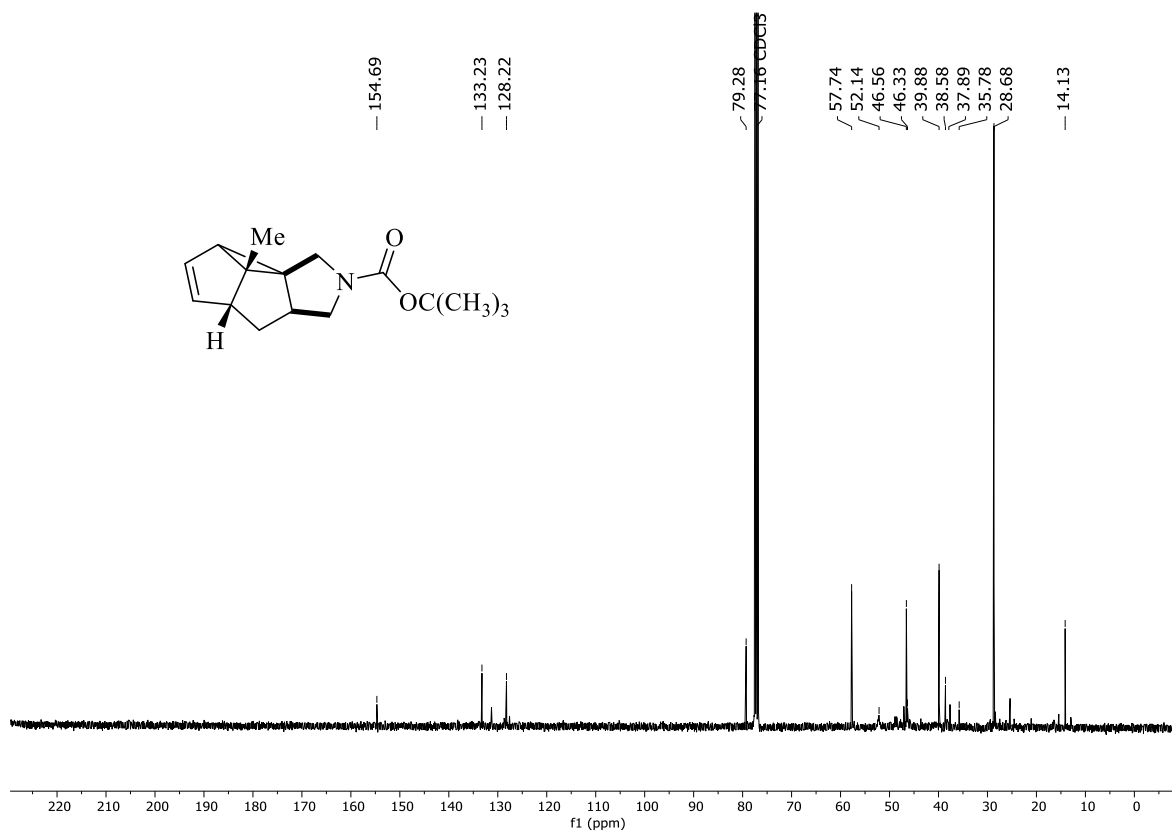
<sup>13</sup>C NMR (101 MHz, CDCl<sub>3</sub>) spectrum of **213f**

 $^1\text{H}$  NMR (400 MHz,  $\text{CDCl}_3$ ) spectrum of **214b** $^{13}\text{C}$  NMR (101 MHz,  $\text{CDCl}_3$ ) spectrum of **214b**

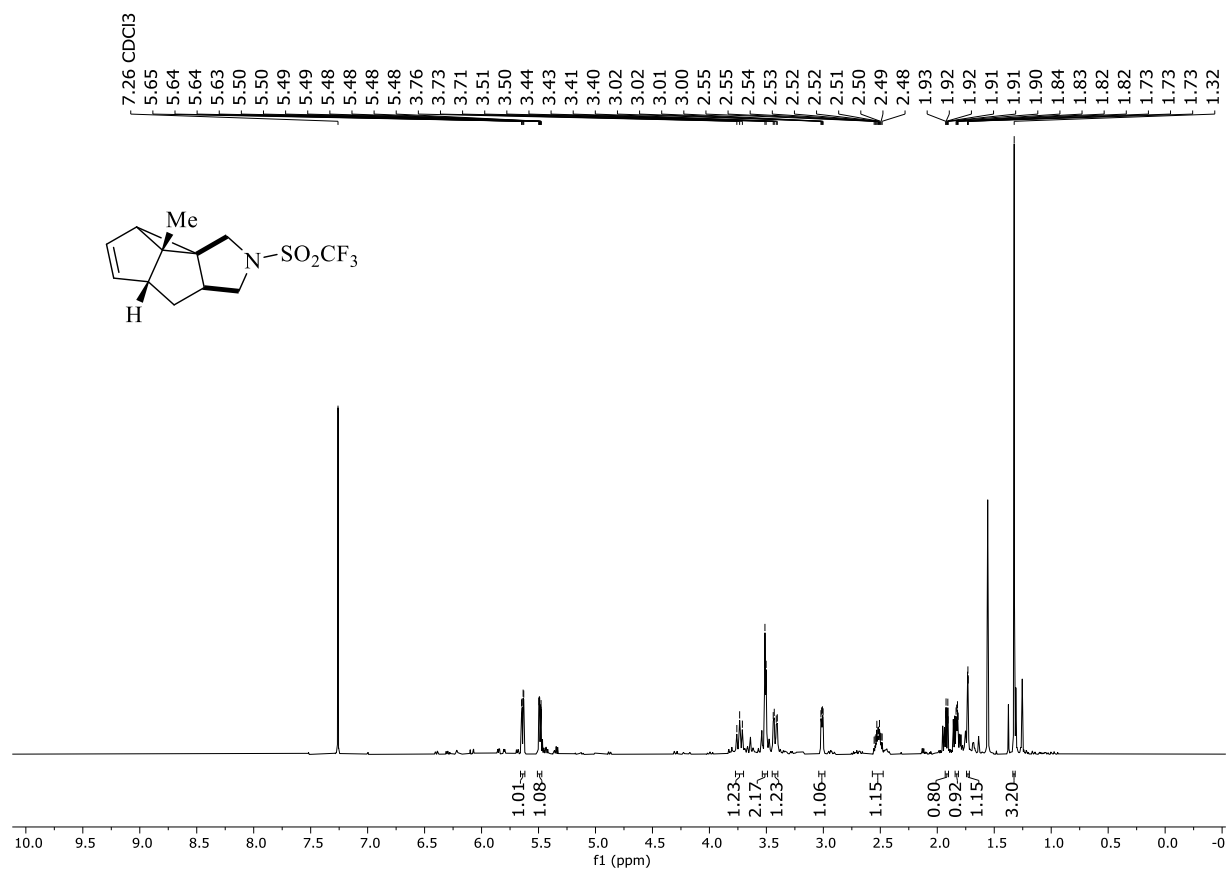




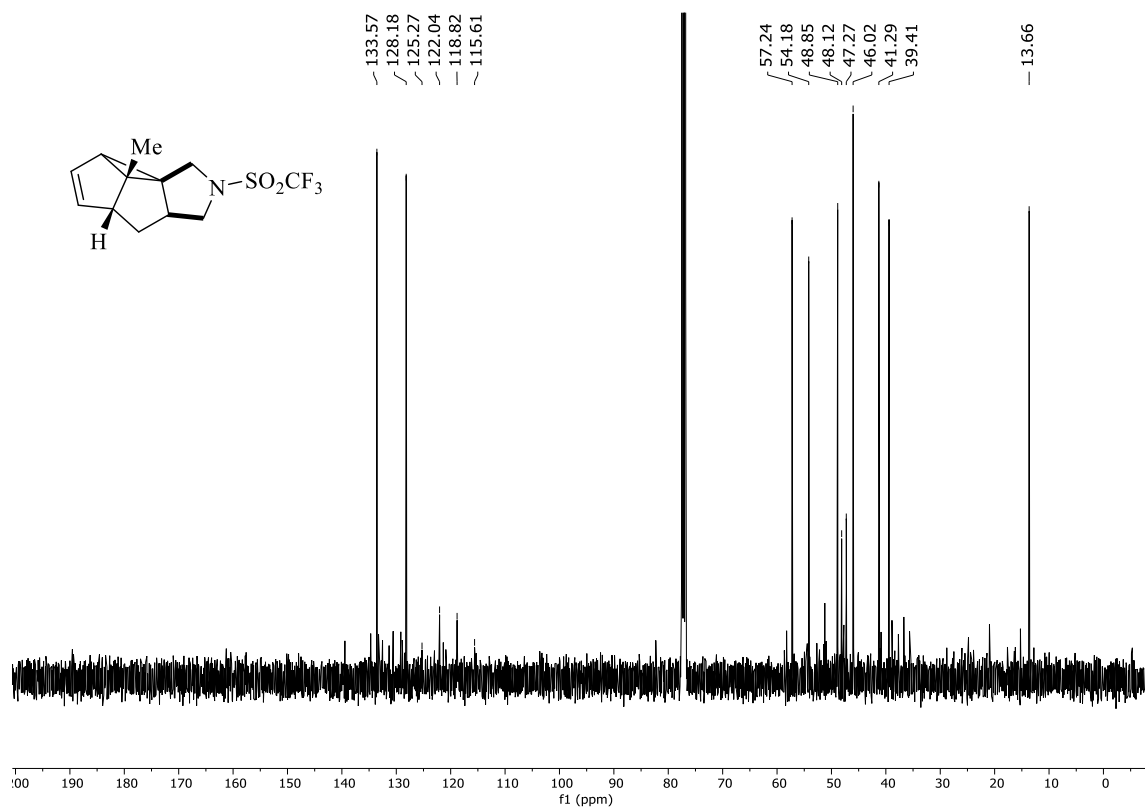
**<sup>1</sup>H NMR (400 MHz, CDCl<sub>3</sub>) spectrum of **214c****



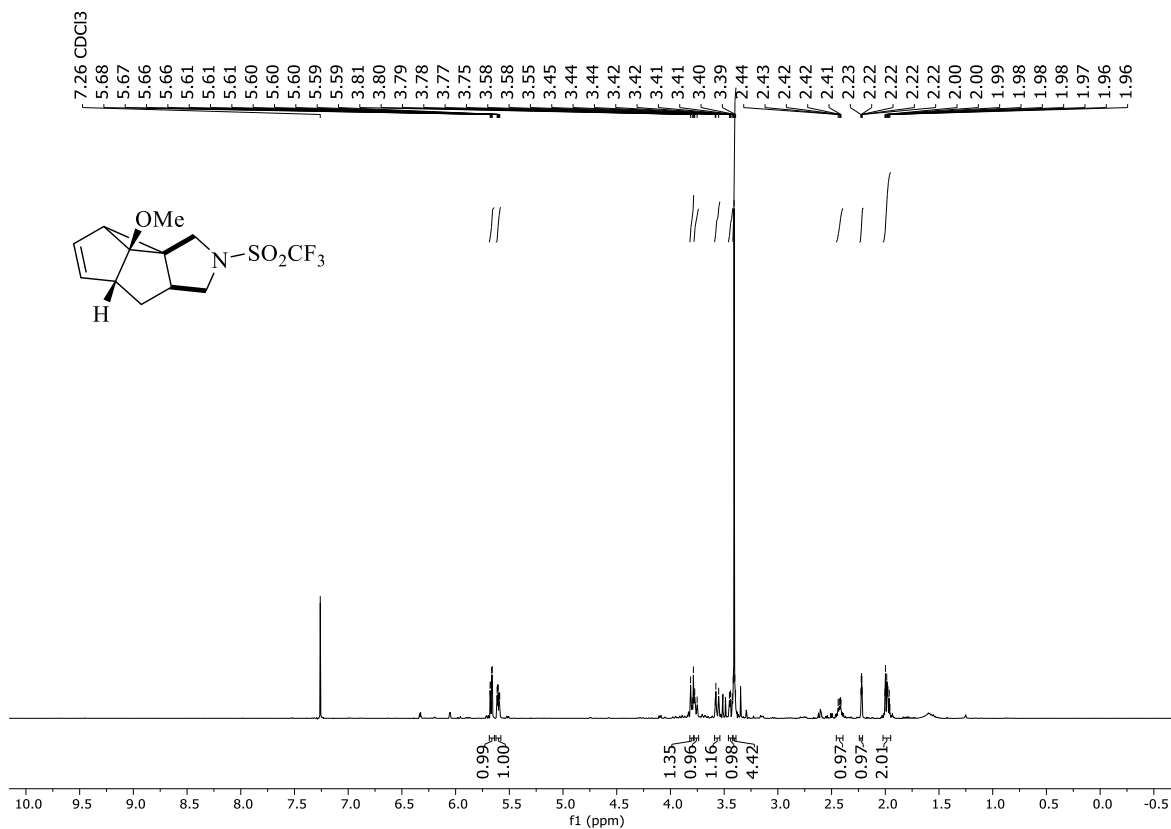
**<sup>13</sup>C NMR (101 MHz, CDCl<sub>3</sub>) spectrum of **214c****



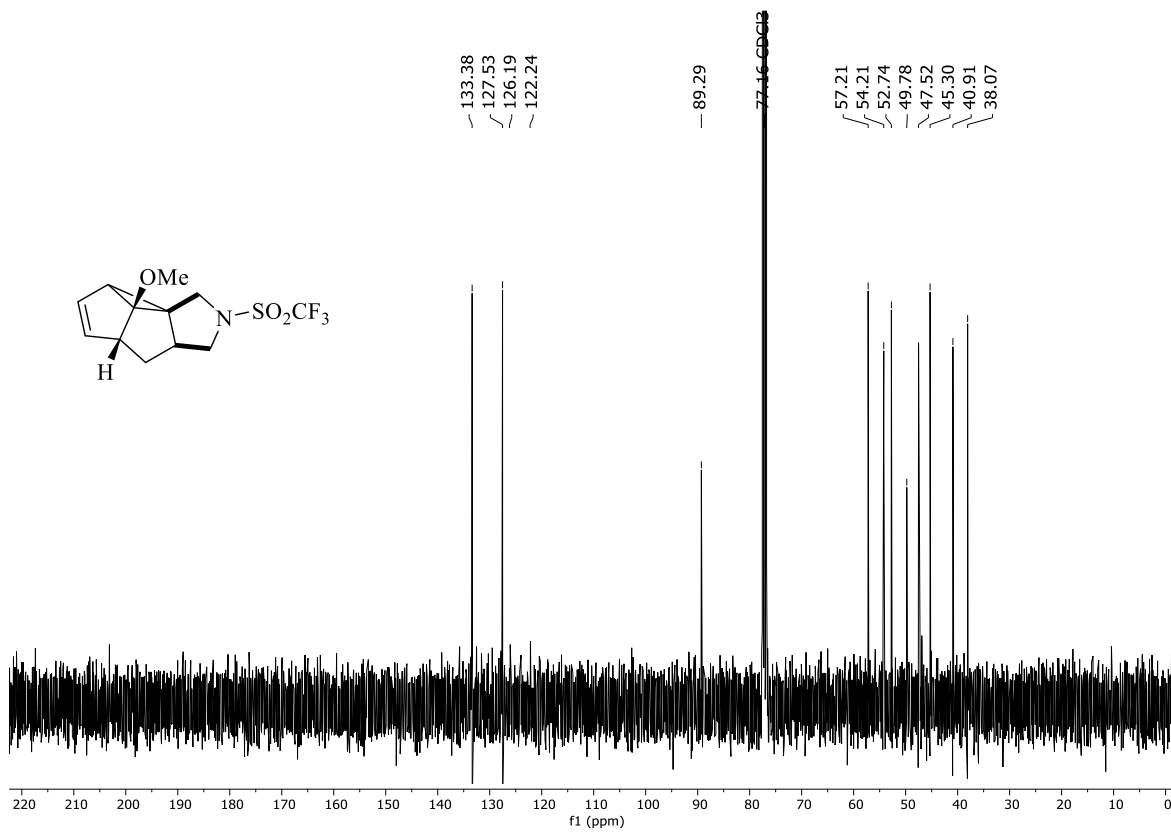
**<sup>1</sup>H NMR (400 MHz, CDCl<sub>3</sub>) spectrum of **214e****



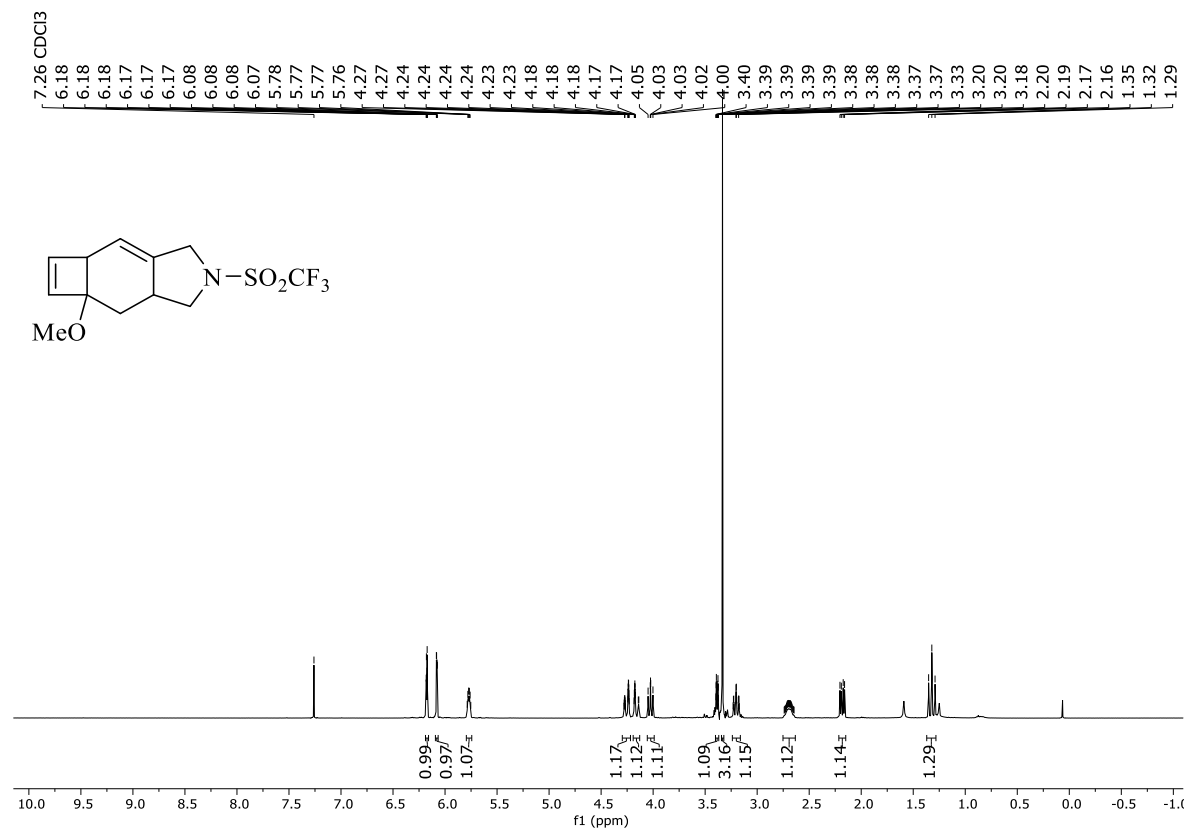
**<sup>13</sup>C NMR (101 MHz, CDCl<sub>3</sub>) spectrum of **214e****



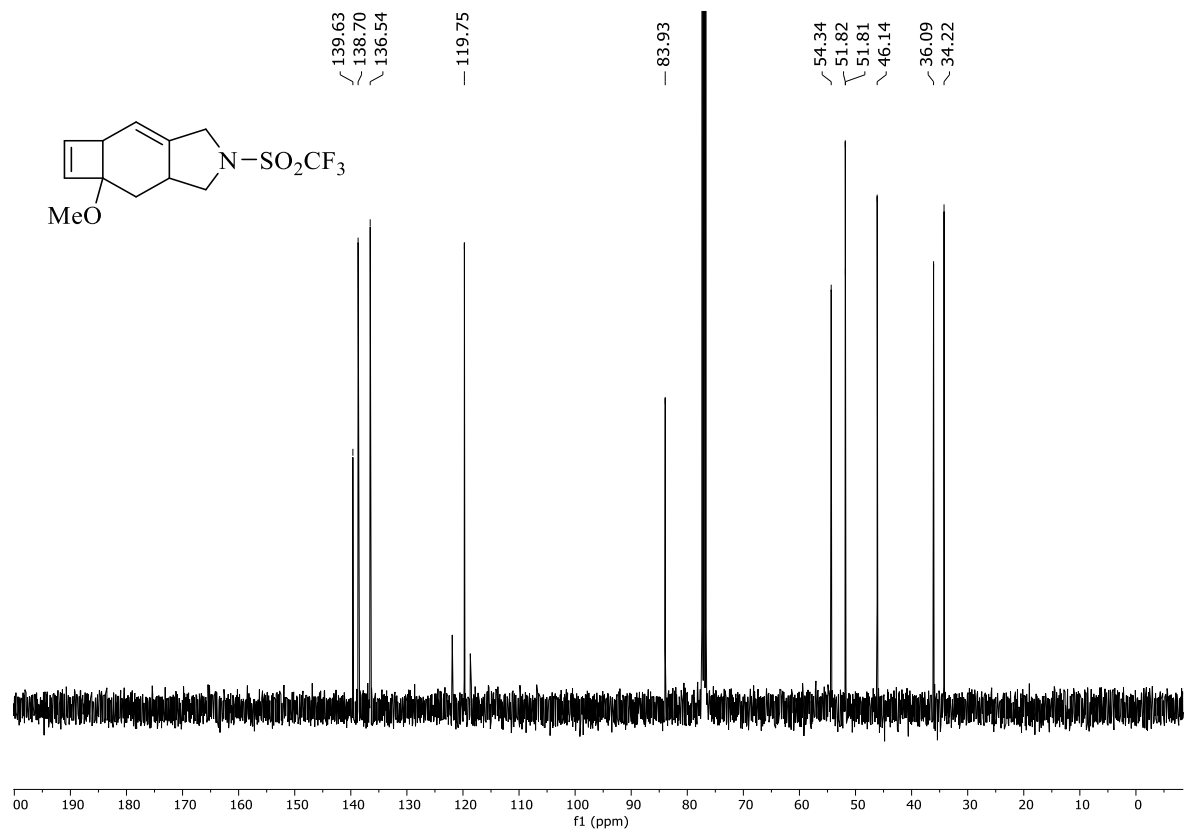
<sup>1</sup>H NMR (400 MHz, CDCl<sub>3</sub>) spectrum of **214f**



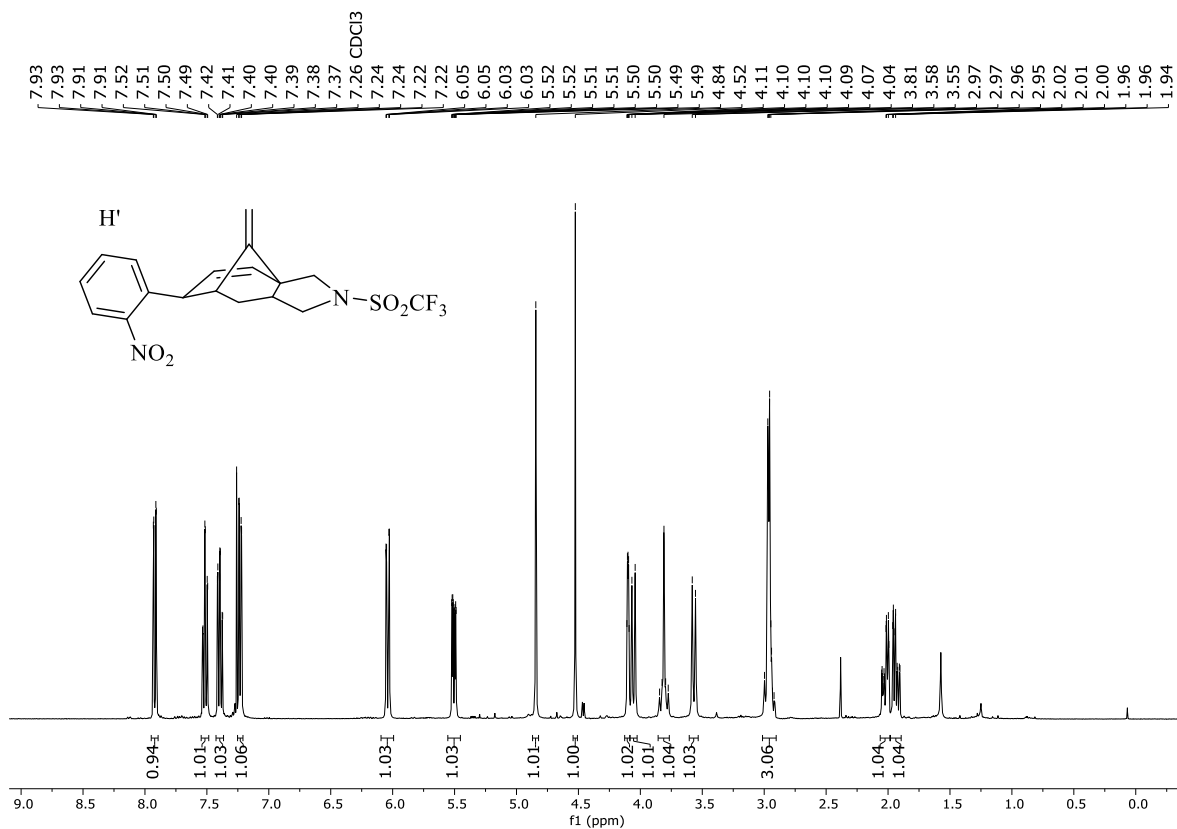
<sup>13</sup>C NMR (101 MHz, CDCl<sub>3</sub>) spectrum of **214f**



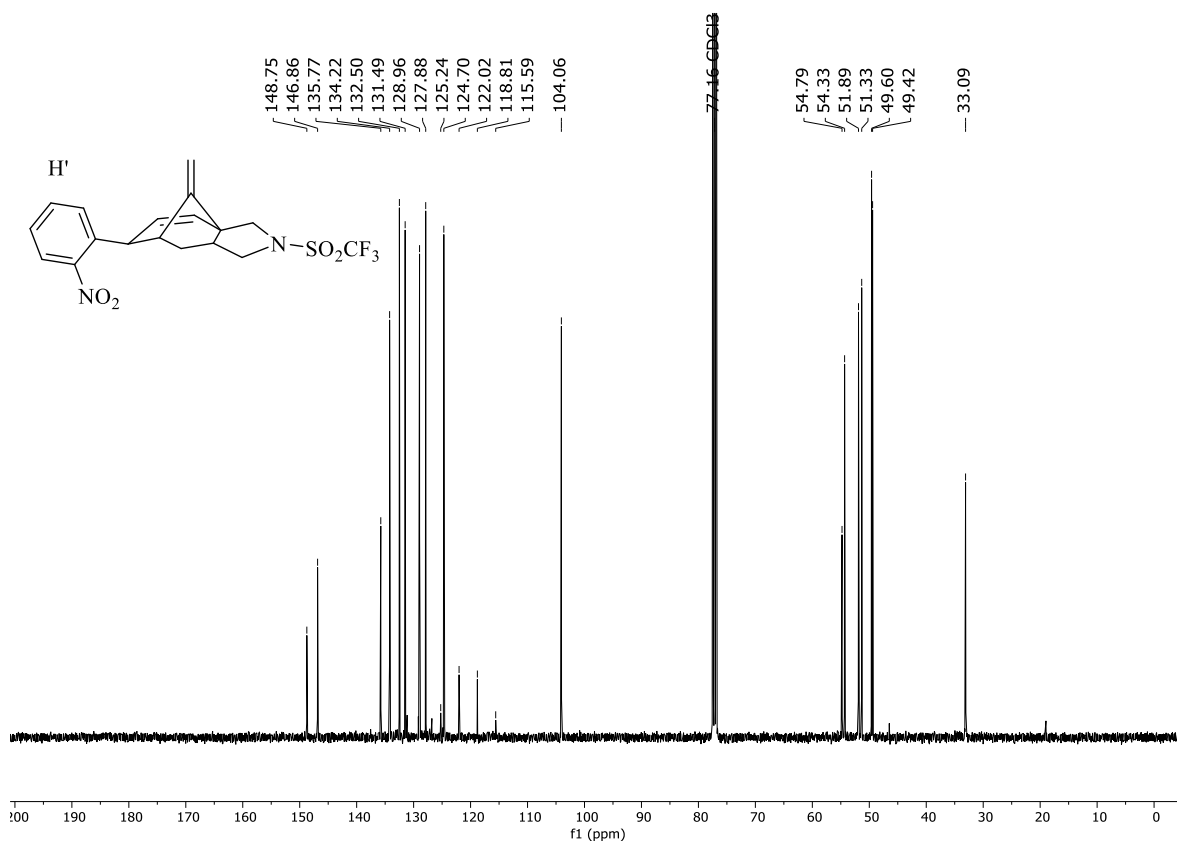
<sup>1</sup>H NMR (400 MHz, CDCl<sub>3</sub>) spectrum of **231**



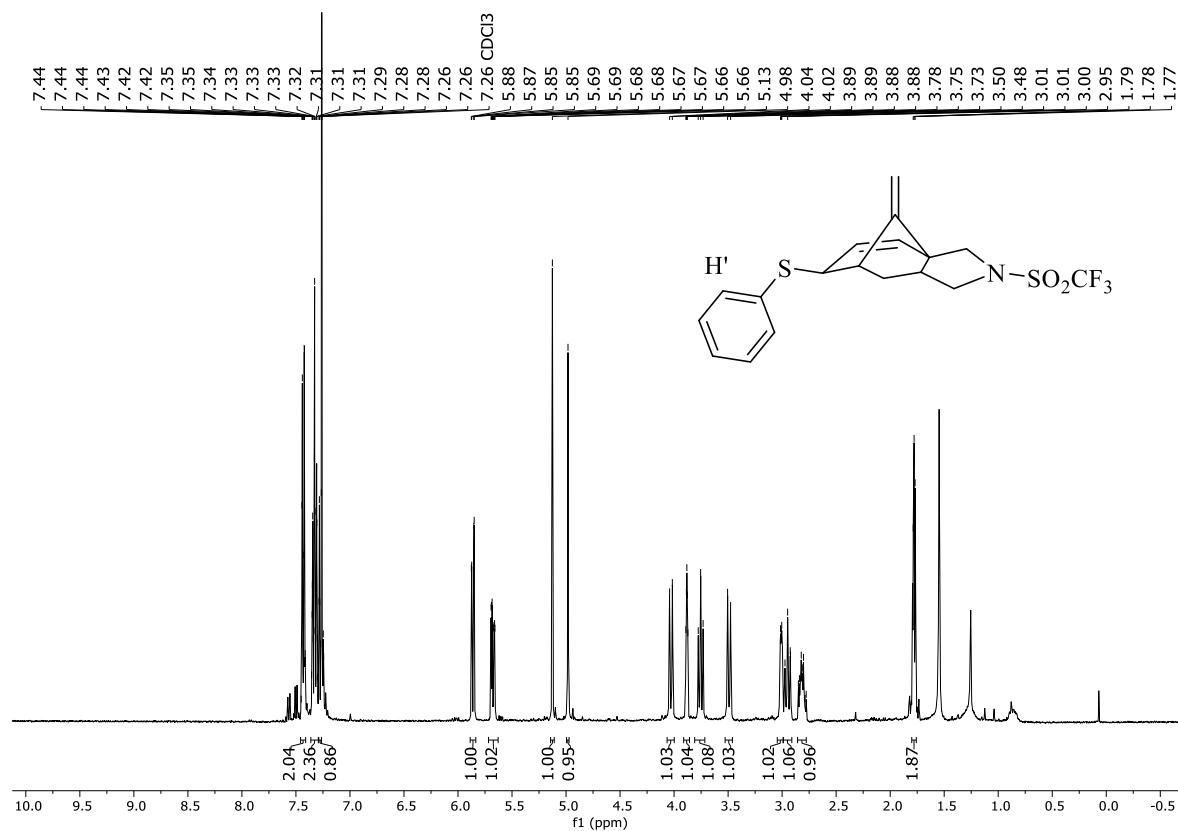
<sup>13</sup>C NMR (101 MHz, CDCl<sub>3</sub>) spectrum of **231**



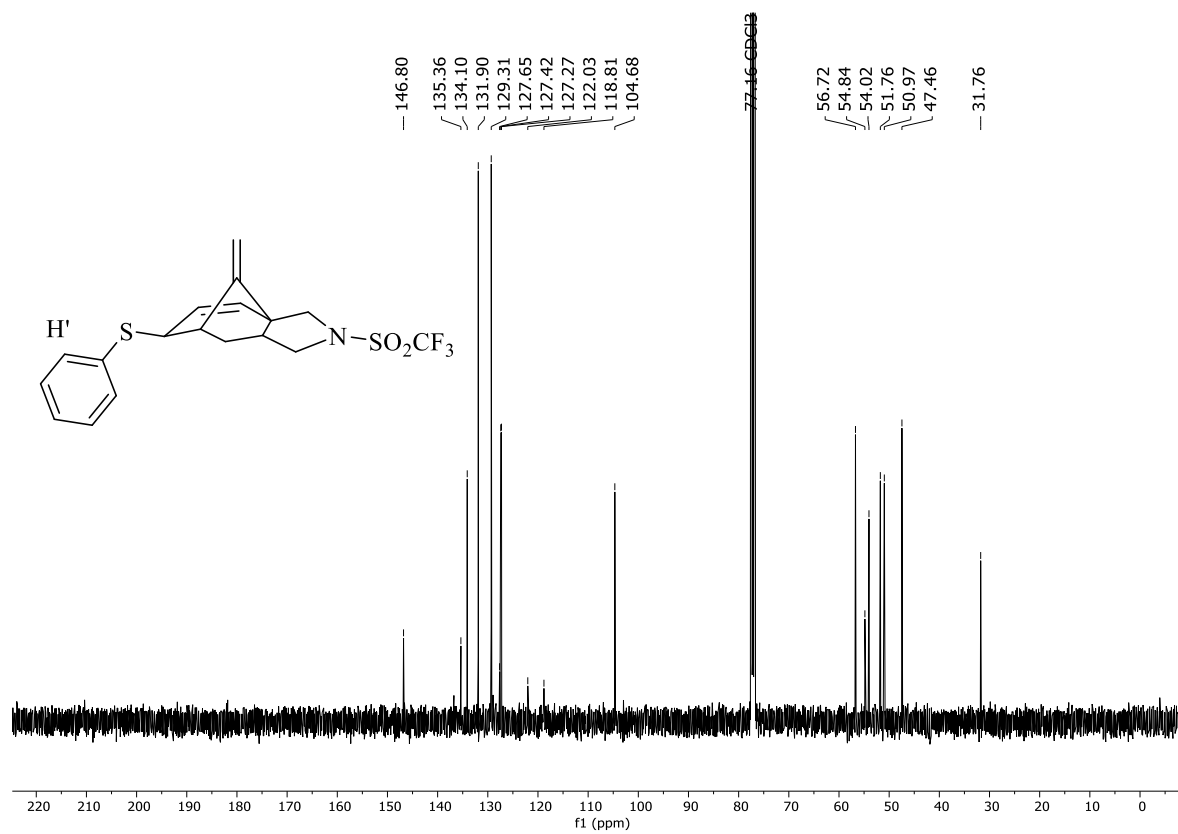
<sup>1</sup>H NMR (400 MHz, CDCl<sub>3</sub>) spectrum of **217c**



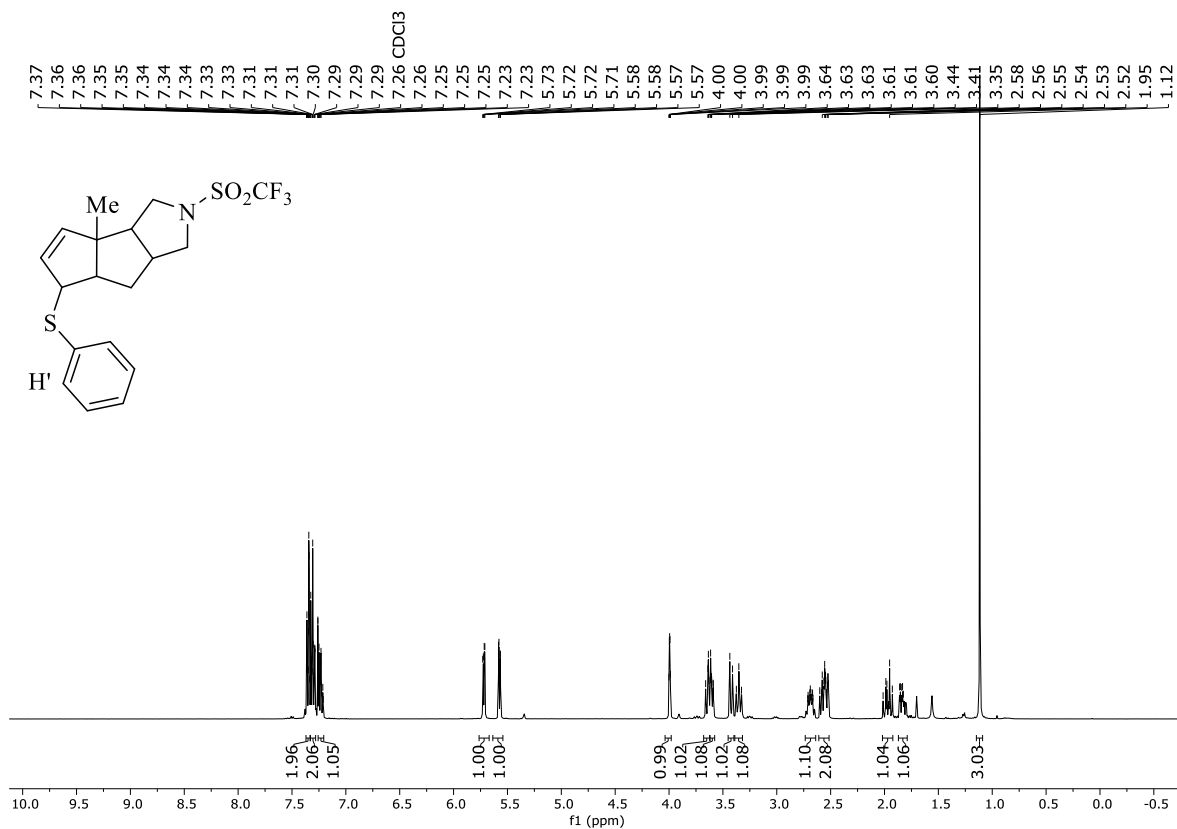
<sup>13</sup>C NMR (101 MHz, CDCl<sub>3</sub>) spectrum of **217c**



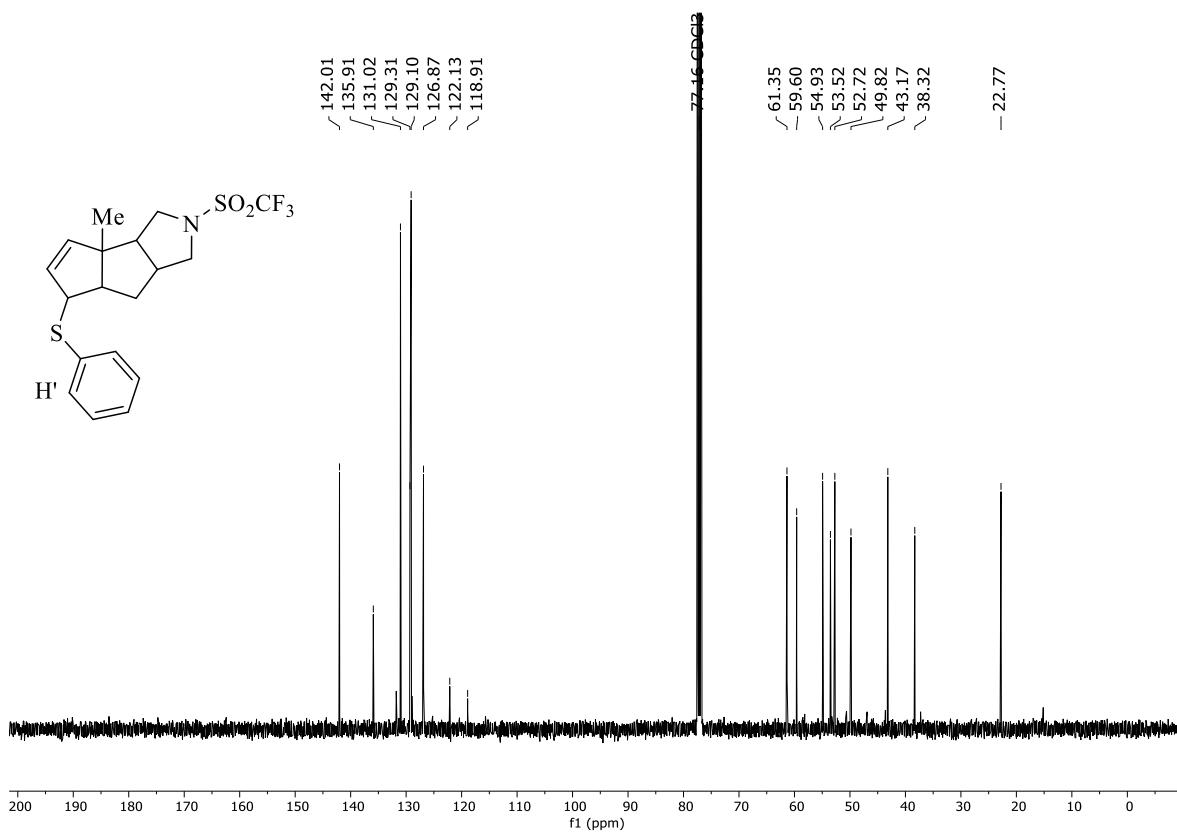
<sup>1</sup>H NMR (400 MHz, CDCl<sub>3</sub>) spectrum of **217k**



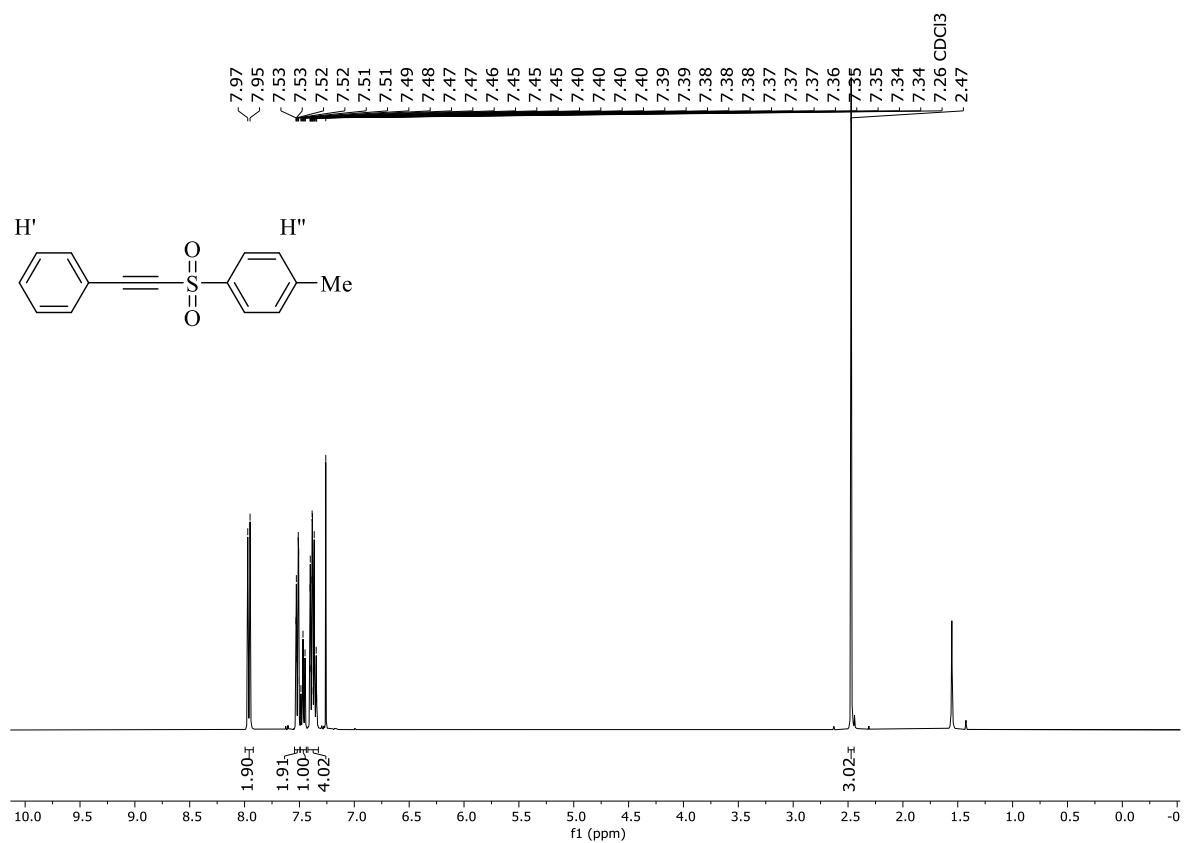
<sup>13</sup>C NMR (101 MHz, CDCl<sub>3</sub>) spectrum of **217k**



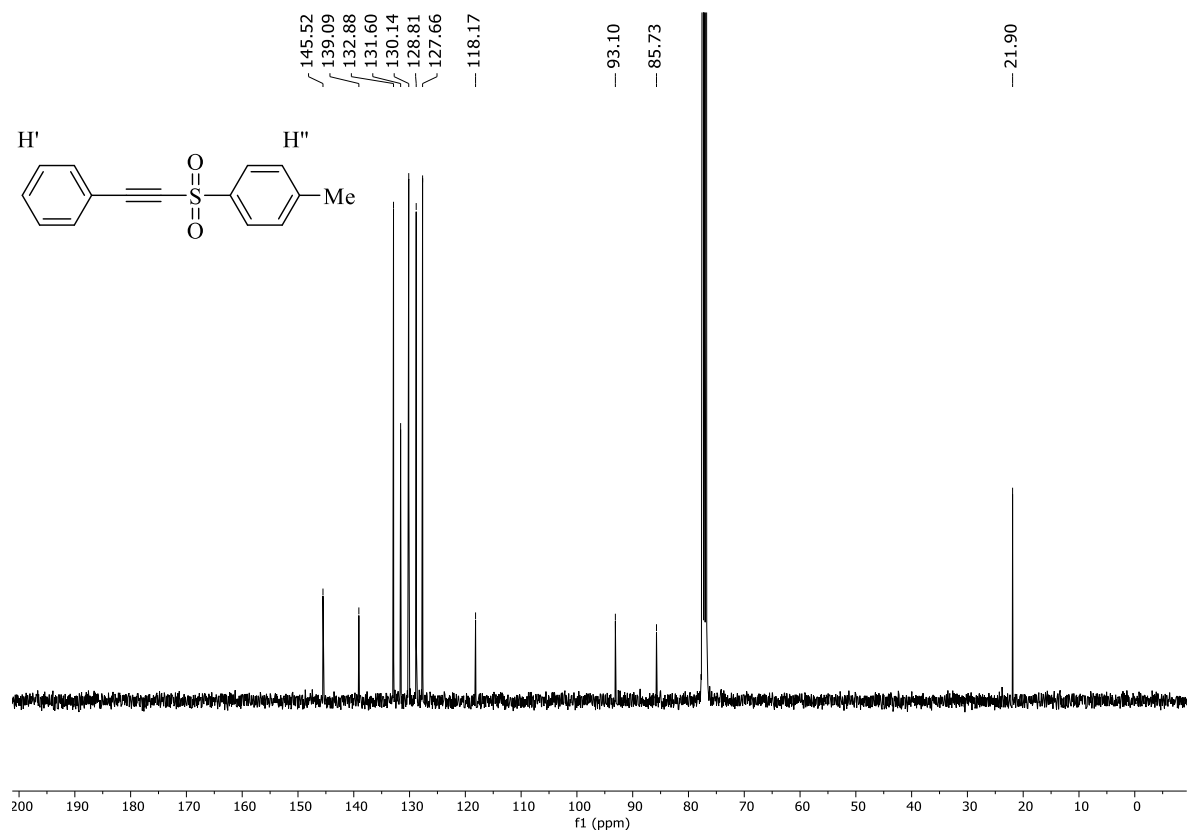
**<sup>1</sup>H NMR (400 MHz, CDCl<sub>3</sub>) spectrum of **216w****



**<sup>13</sup>C NMR (101 MHz, CDCl<sub>3</sub>) spectrum of **216w****

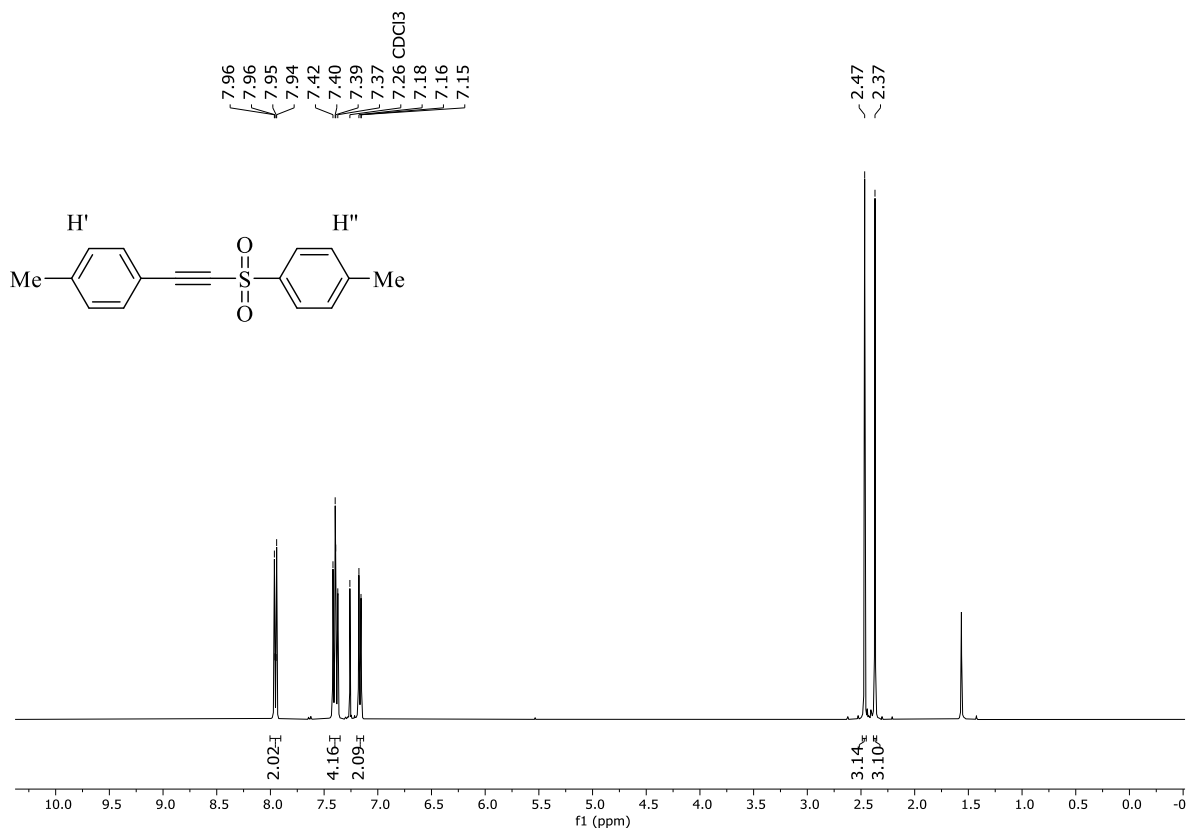


<sup>1</sup>H NMR (400 MHz, CDCl<sub>3</sub>) spectrum of **218a**

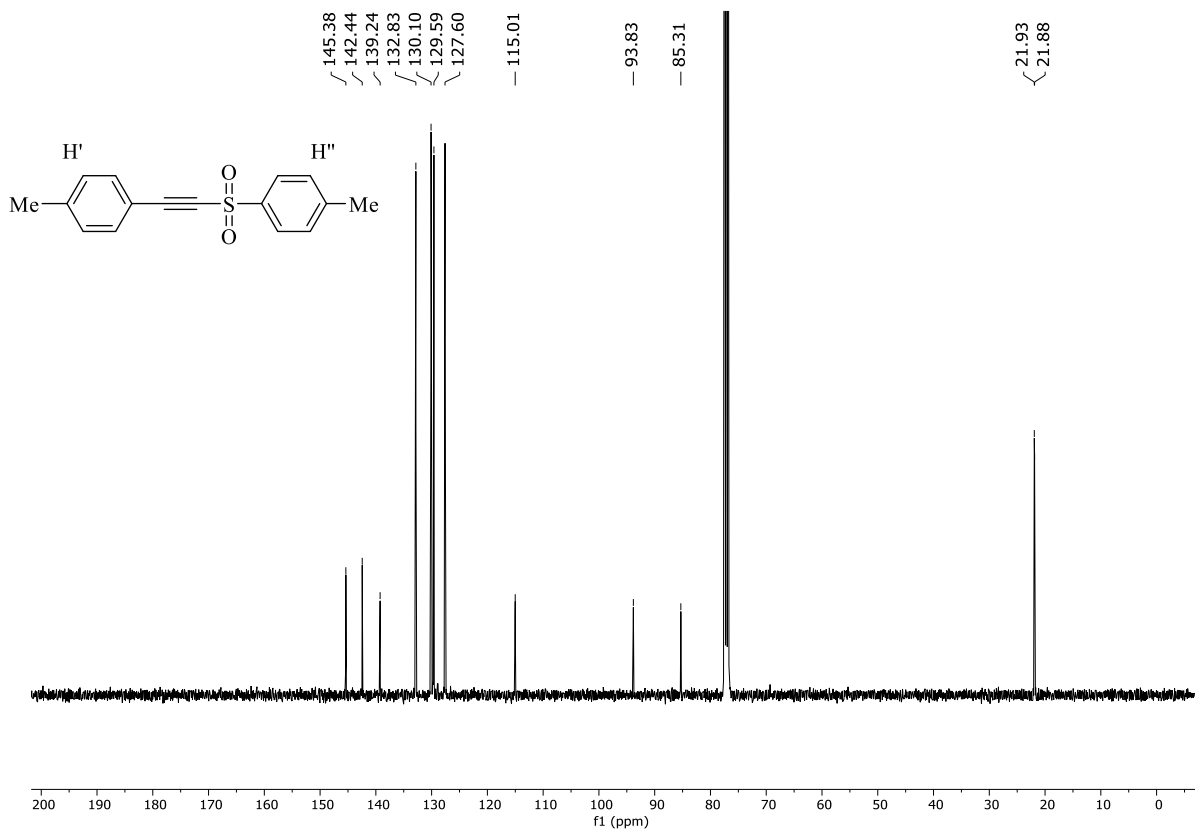


<sup>13</sup>C NMR (101 MHz, CDCl<sub>3</sub>) spectrum of **218a**

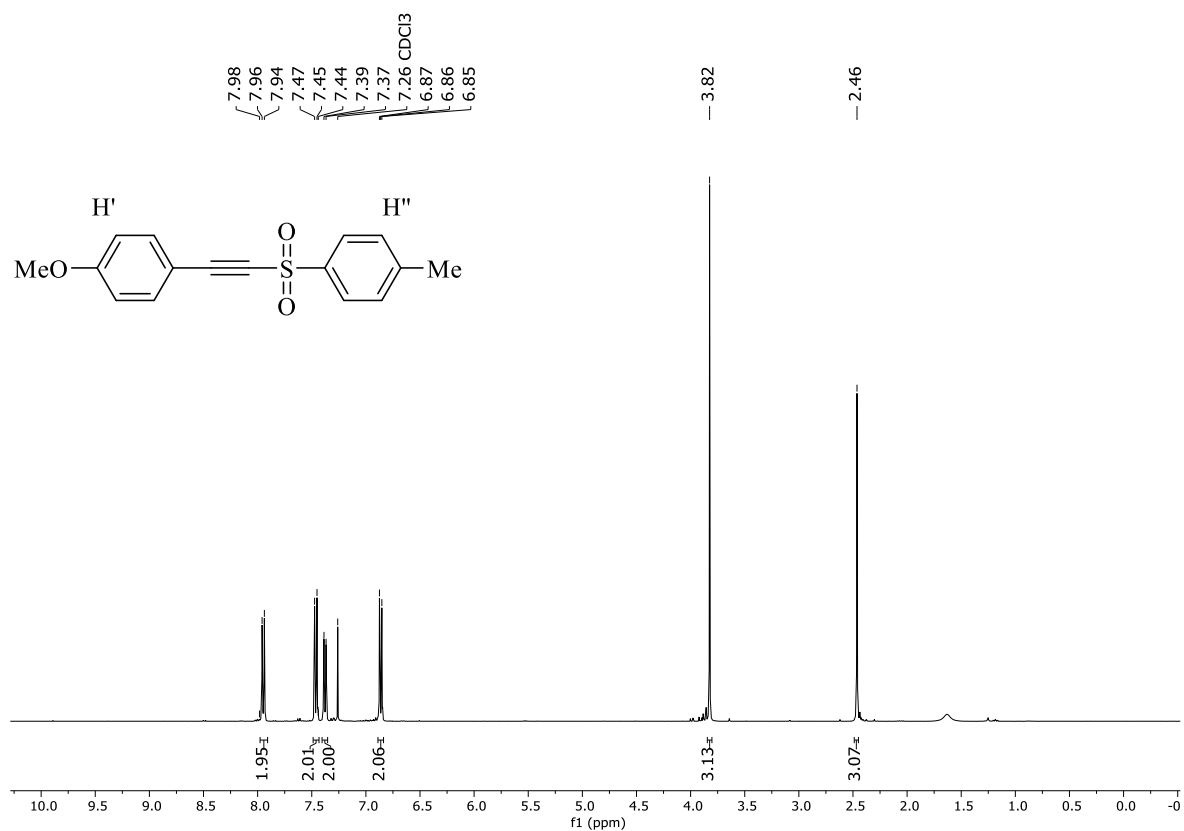




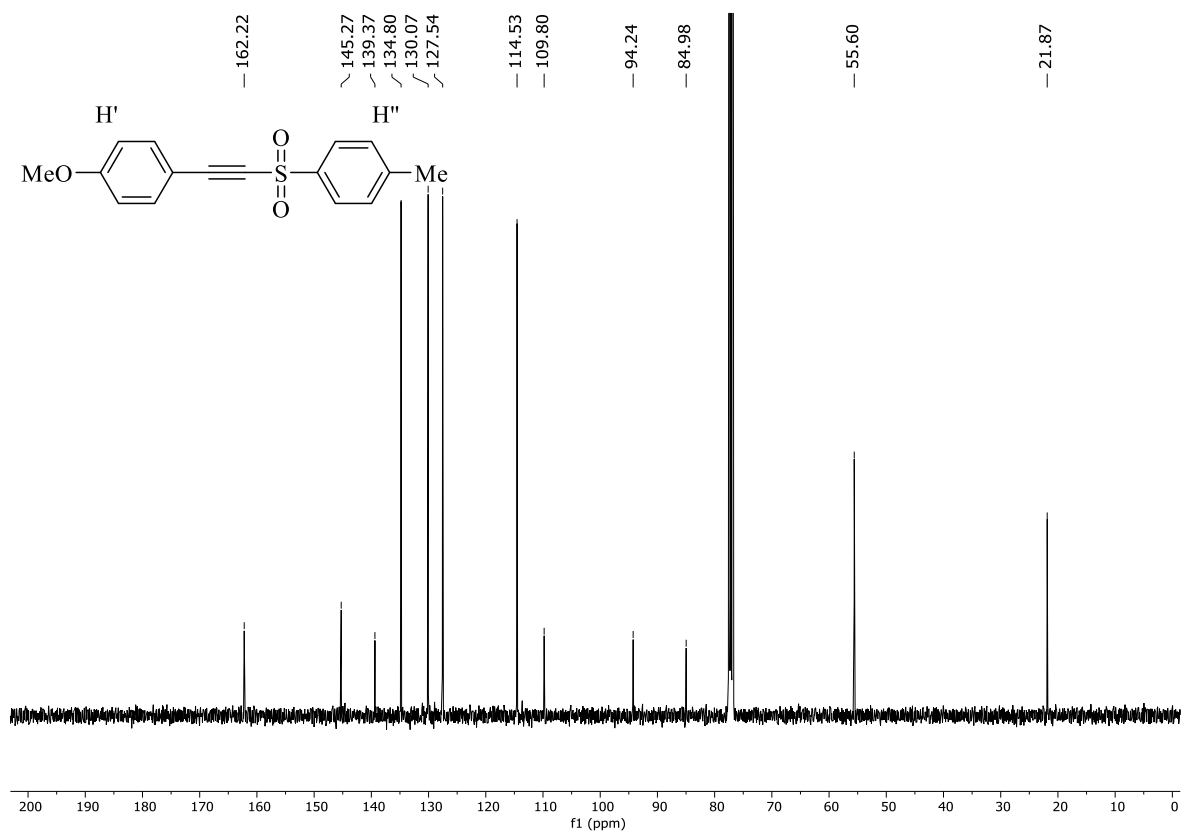
<sup>1</sup>H NMR (400 MHz, CDCl<sub>3</sub>) spectrum of **218b**



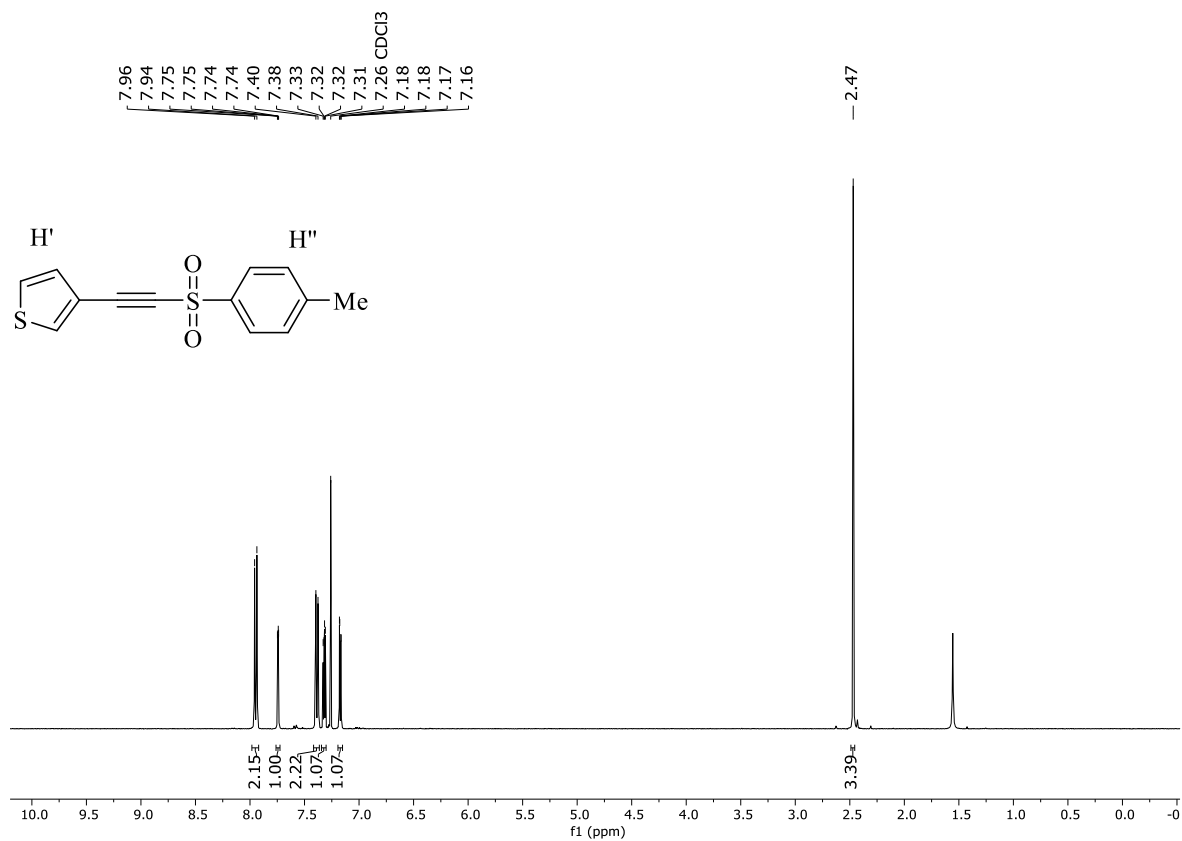
<sup>13</sup>C NMR (101 MHz, CDCl<sub>3</sub>) spectrum of **218b**



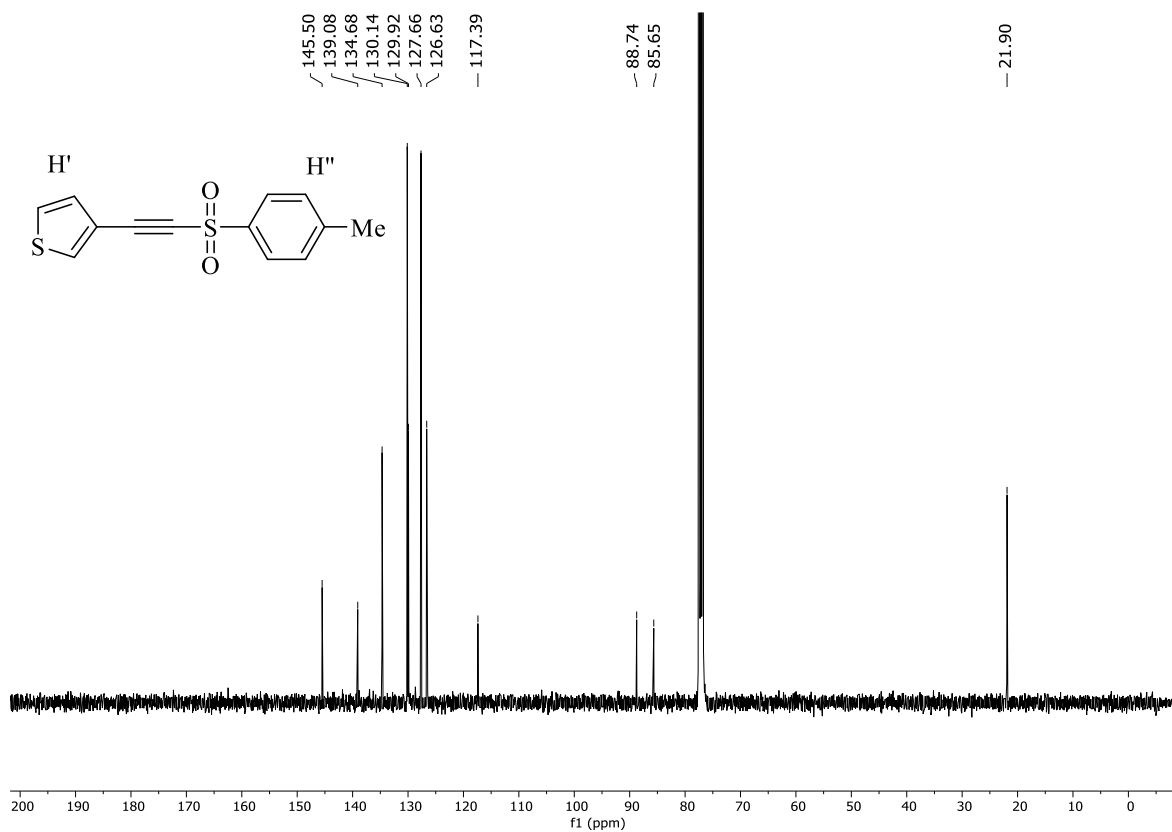
<sup>1</sup>H NMR (400 MHz, CDCl<sub>3</sub>) spectrum of **218c**



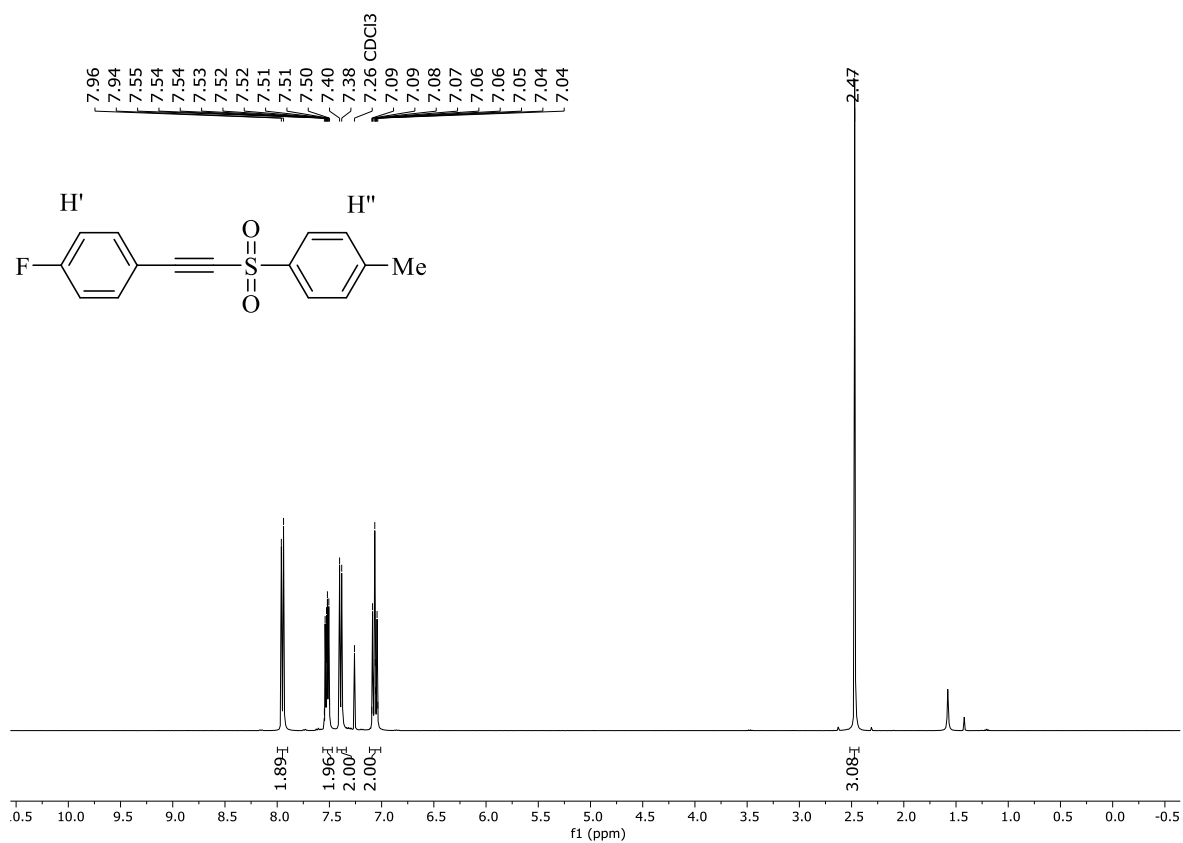
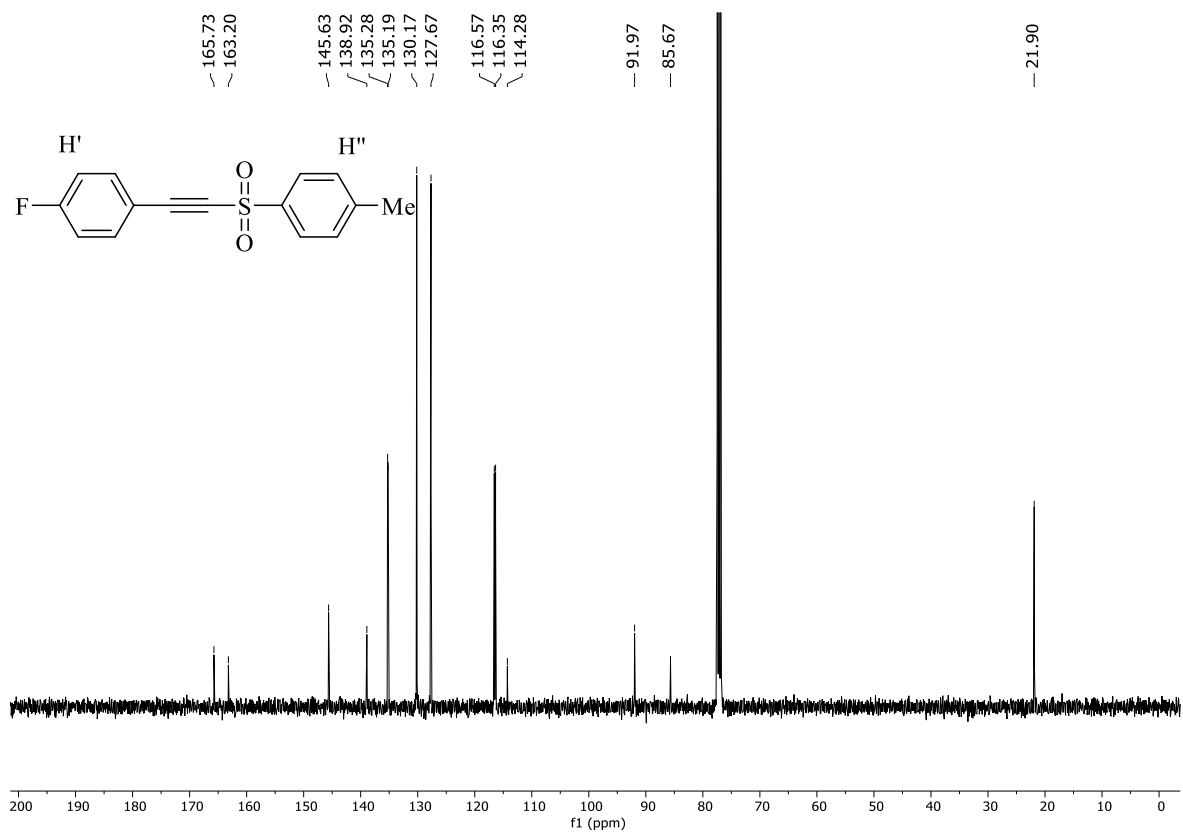
<sup>13</sup>C NMR (101 MHz, CDCl<sub>3</sub>) spectrum of **218c**

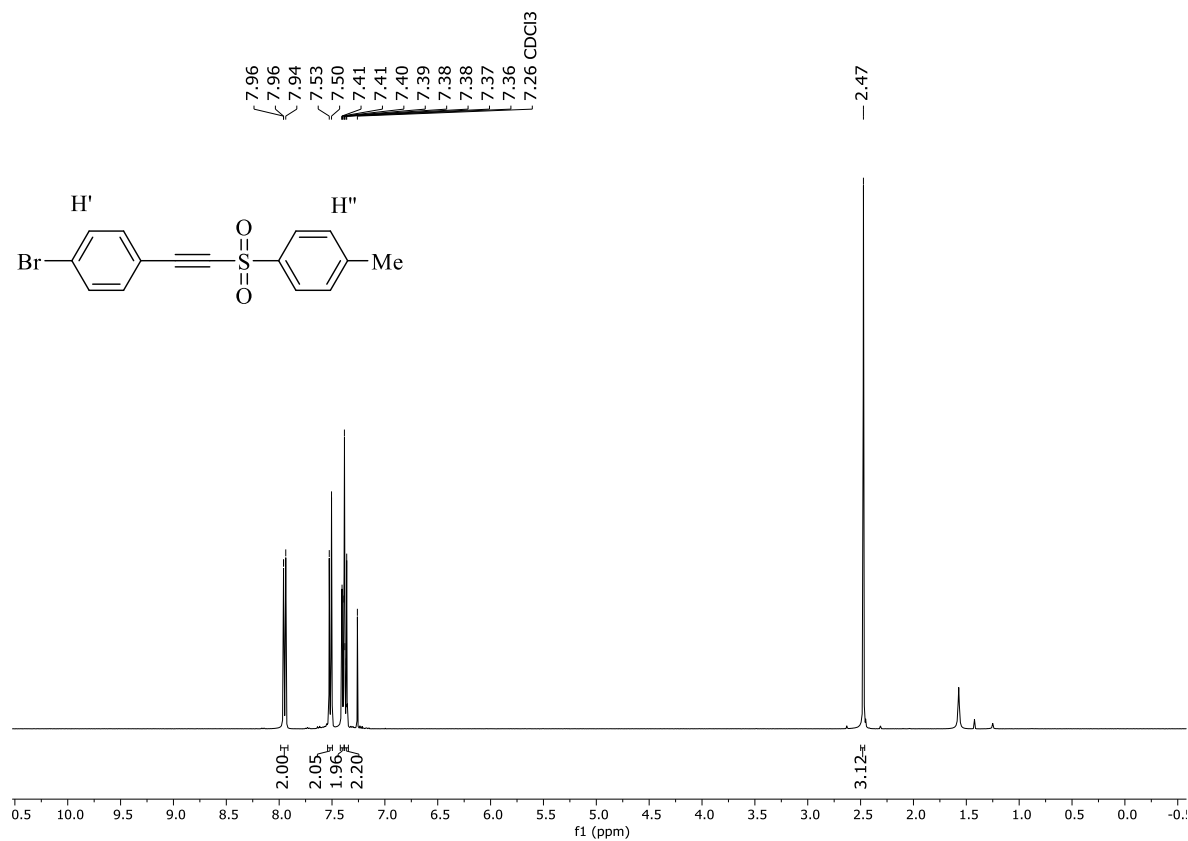


<sup>1</sup>H NMR (400 MHz, CDCl<sub>3</sub>) spectrum of **218d**

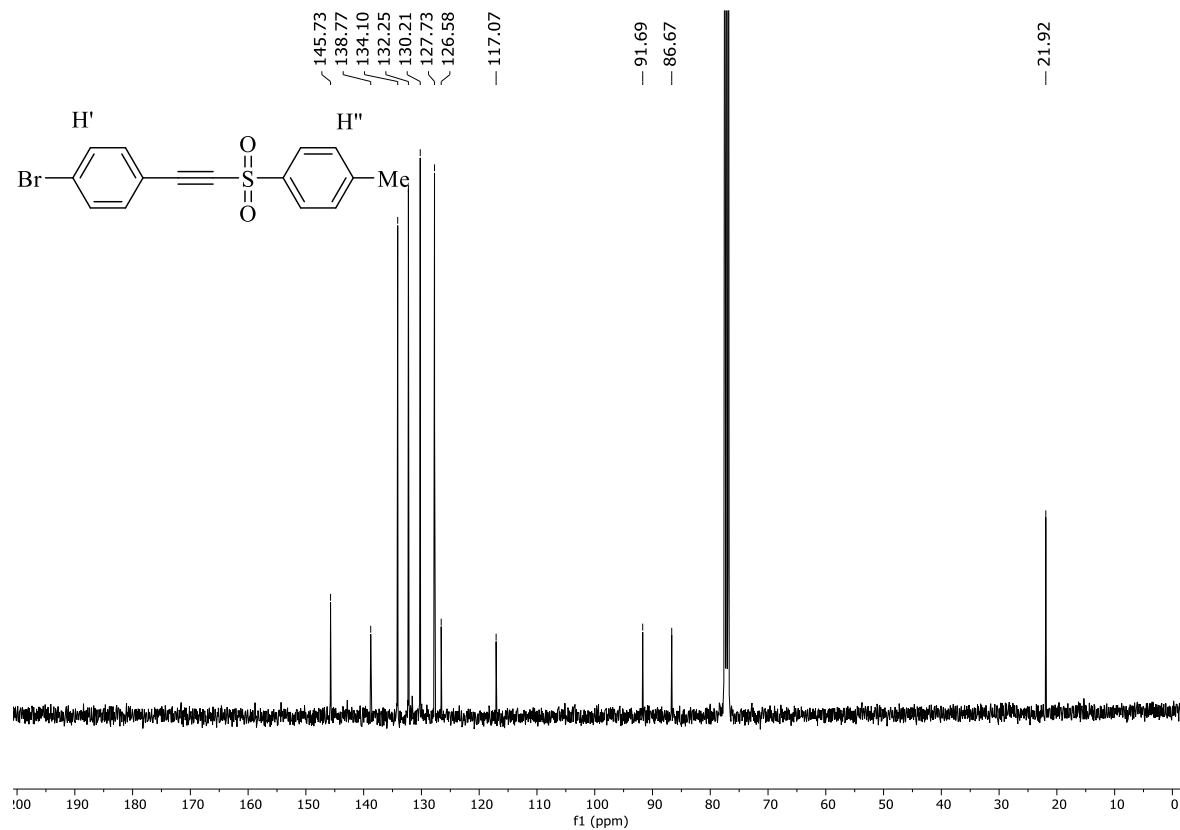


<sup>13</sup>C NMR (101 MHz, CDCl<sub>3</sub>) spectrum of **218d**

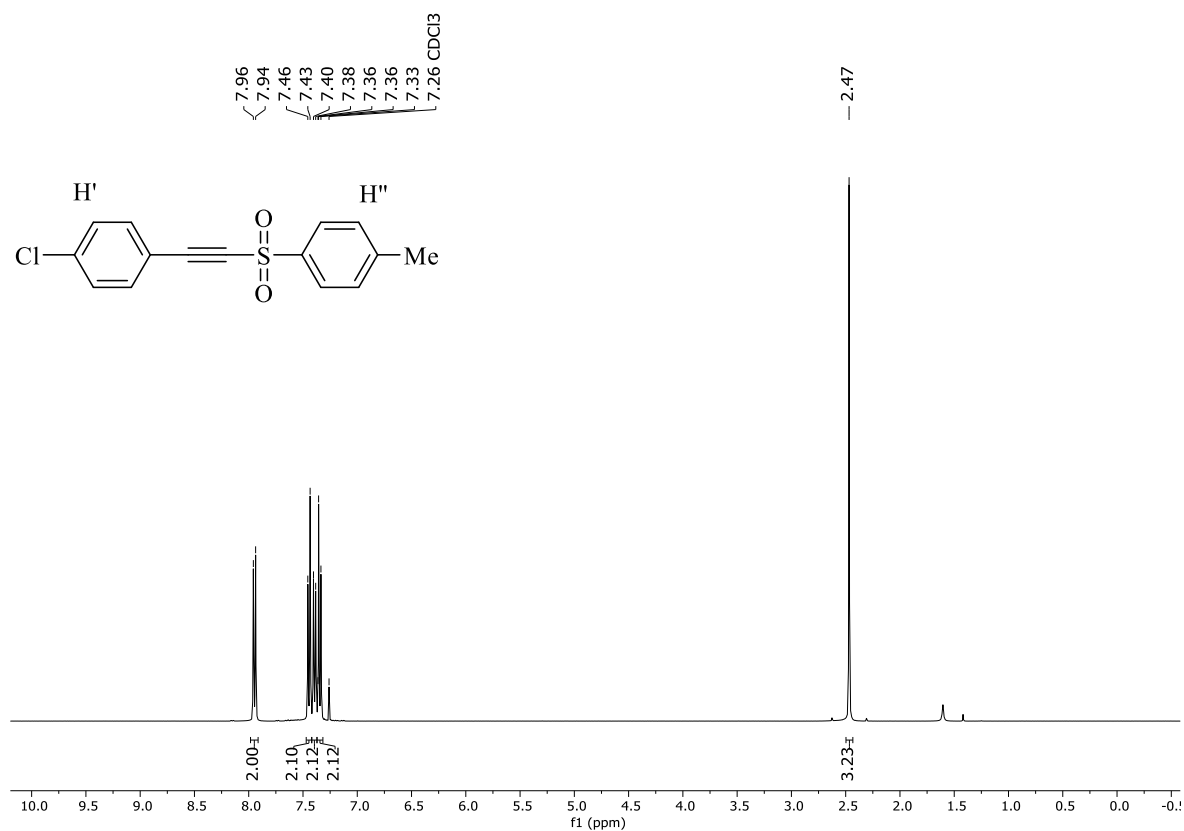
 $^1\text{H}$  NMR (400 MHz,  $\text{CDCl}_3$ ) spectrum of **218e** $^{13}\text{C}$  NMR (101 MHz,  $\text{CDCl}_3$ ) spectrum of **218e**



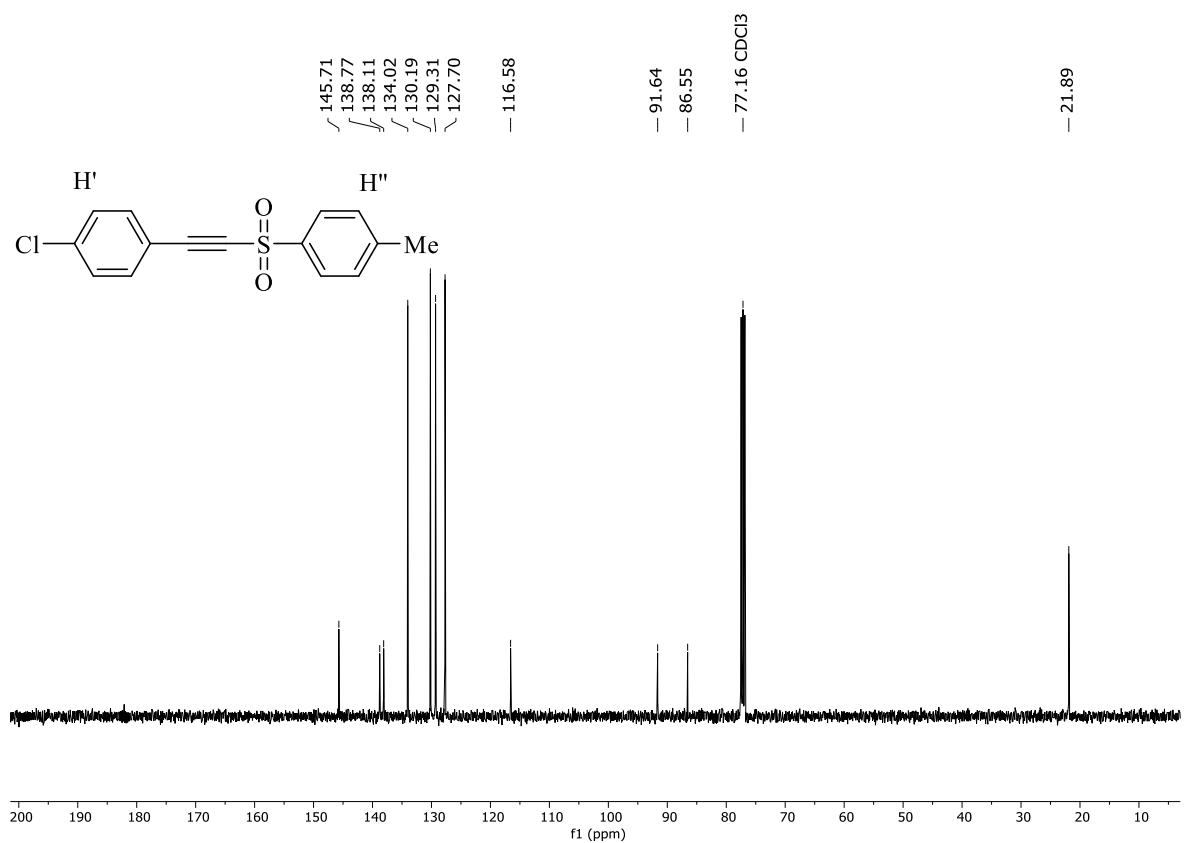
<sup>1</sup>H NMR (400 MHz, CDCl<sub>3</sub>) spectrum of **218f**



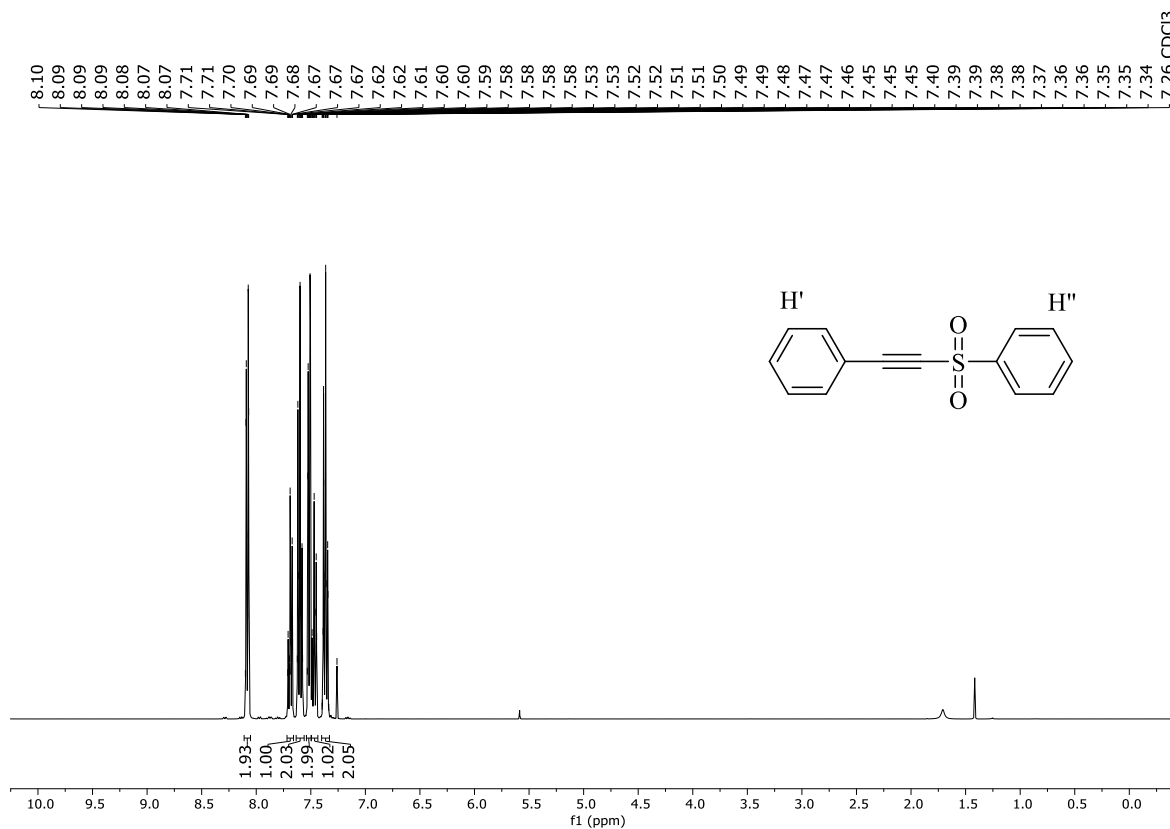
<sup>13</sup>C NMR (101 MHz, CDCl<sub>3</sub>) spectrum of **218f**



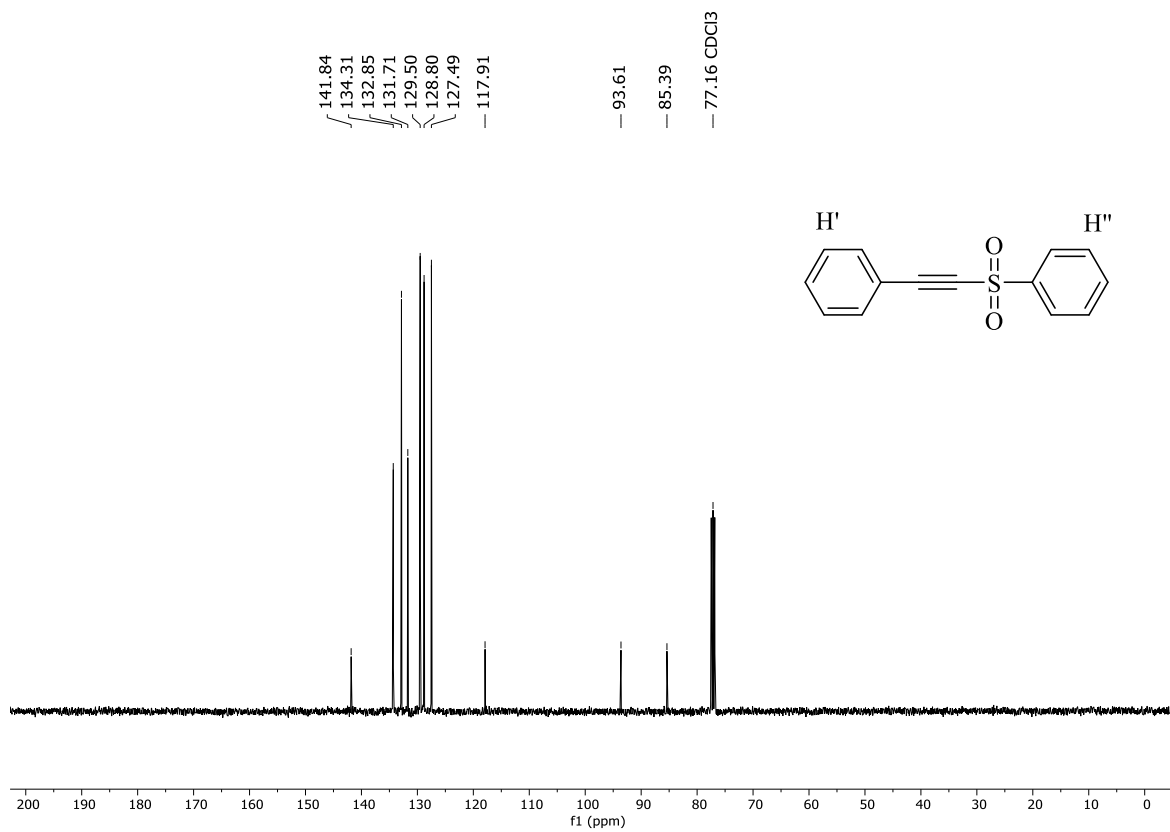
<sup>1</sup>H NMR (400 MHz, CDCl<sub>3</sub>) spectrum of **218g**



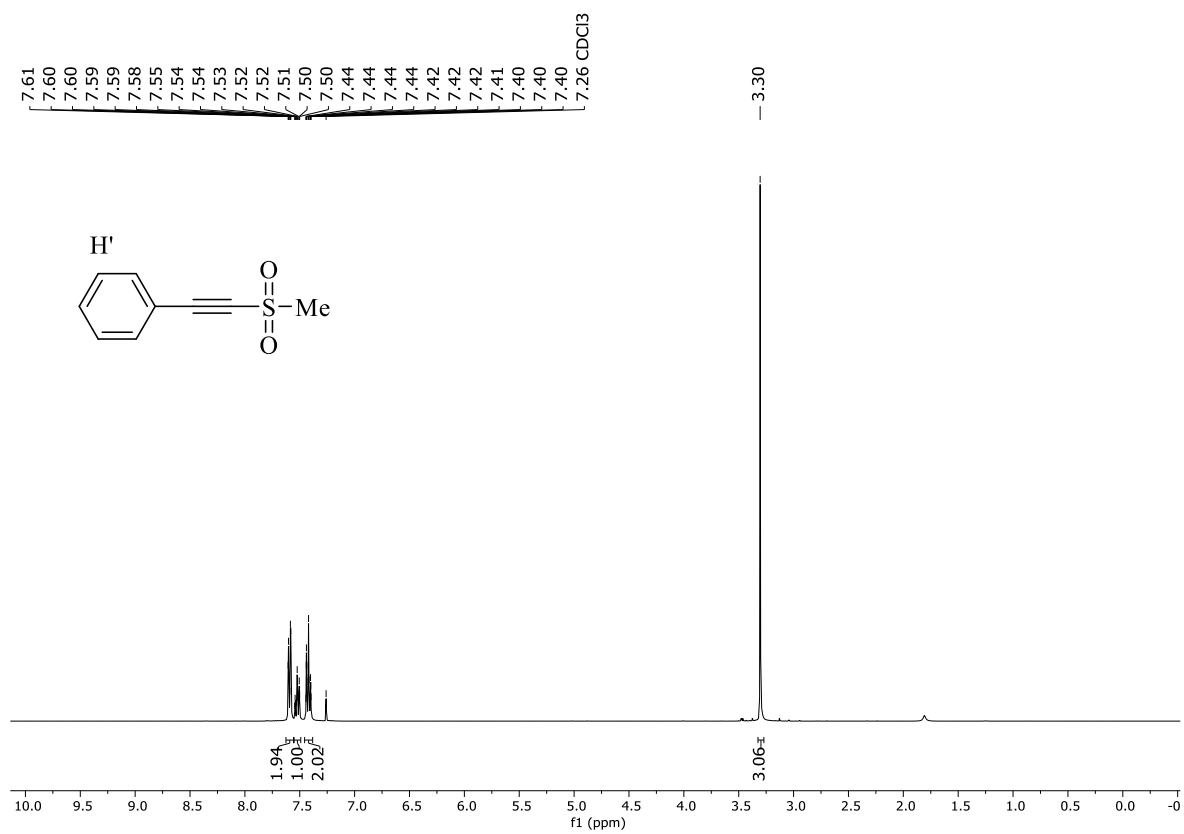
<sup>13</sup>C NMR (101 MHz, CDCl<sub>3</sub>) spectrum of **218g**



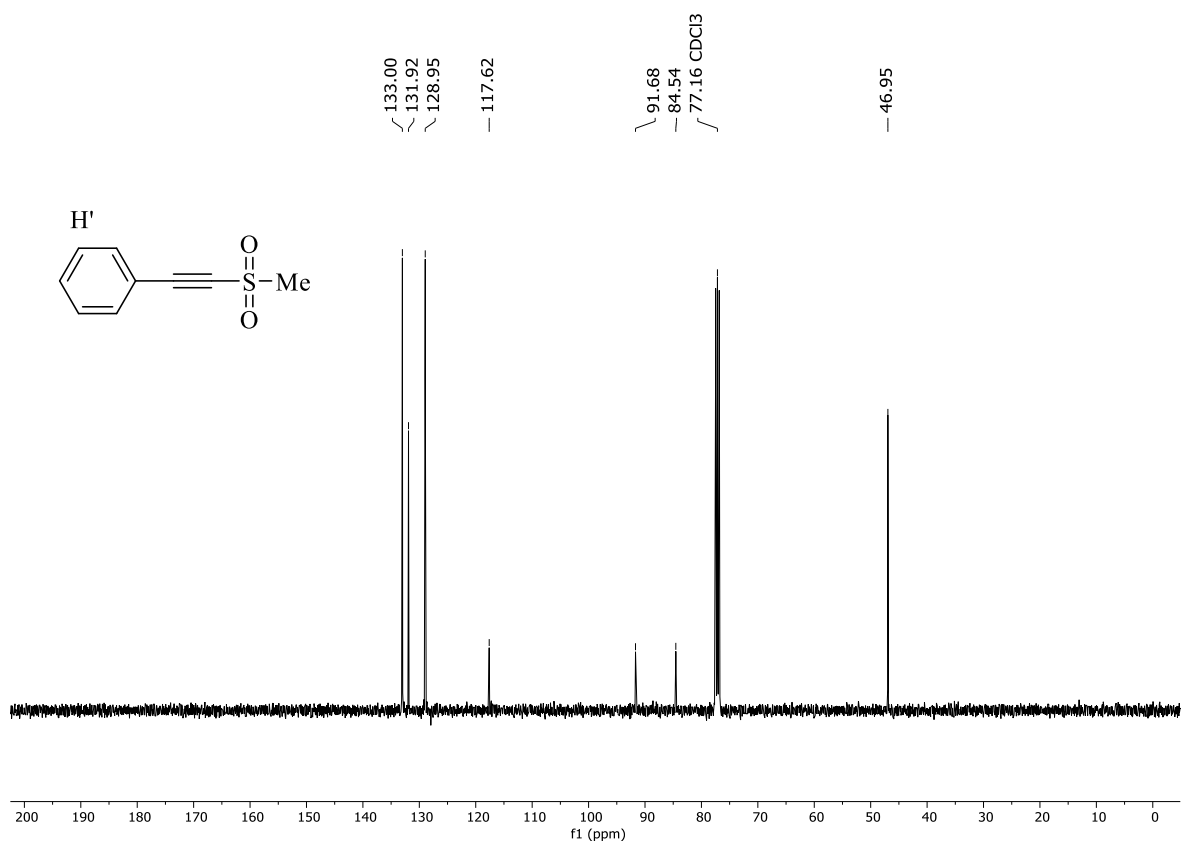
<sup>1</sup>H NMR (400 MHz, CDCl<sub>3</sub>) spectrum of **218h**



<sup>13</sup>C NMR (101 MHz, CDCl<sub>3</sub>) spectrum of **218h**

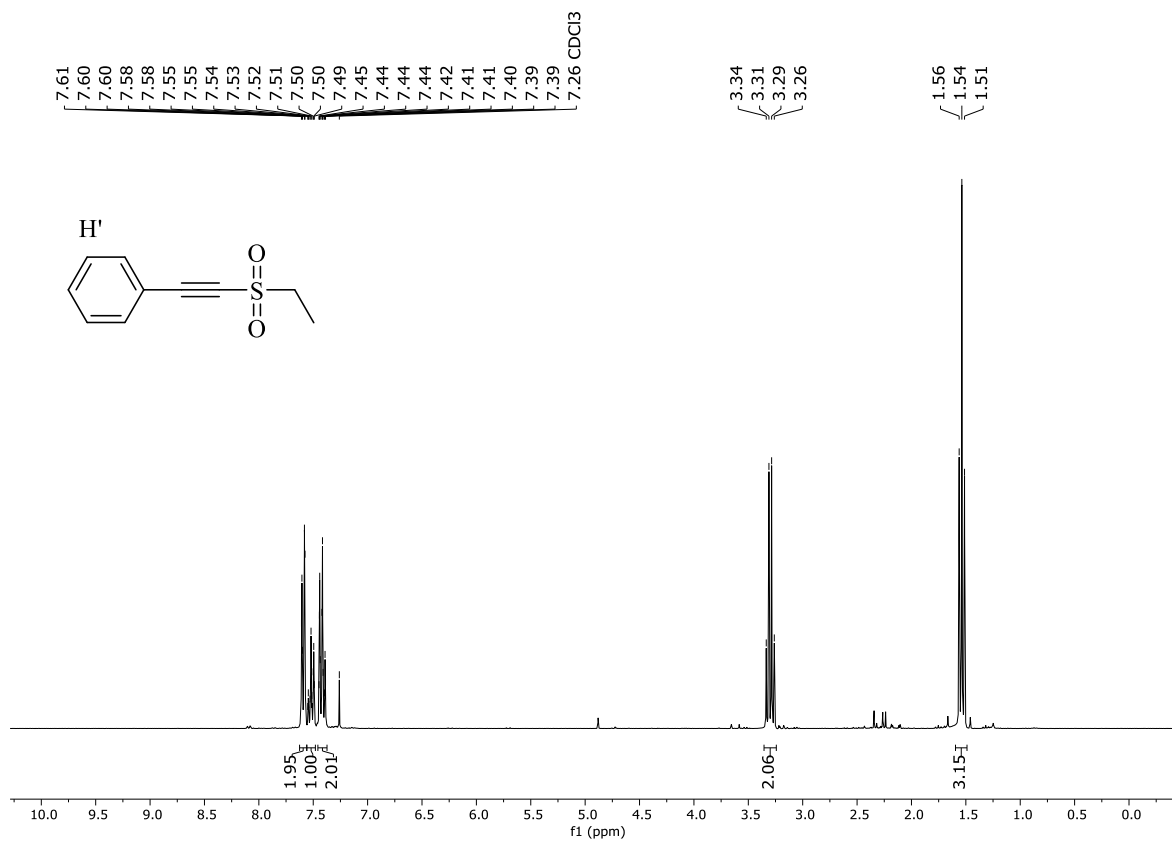
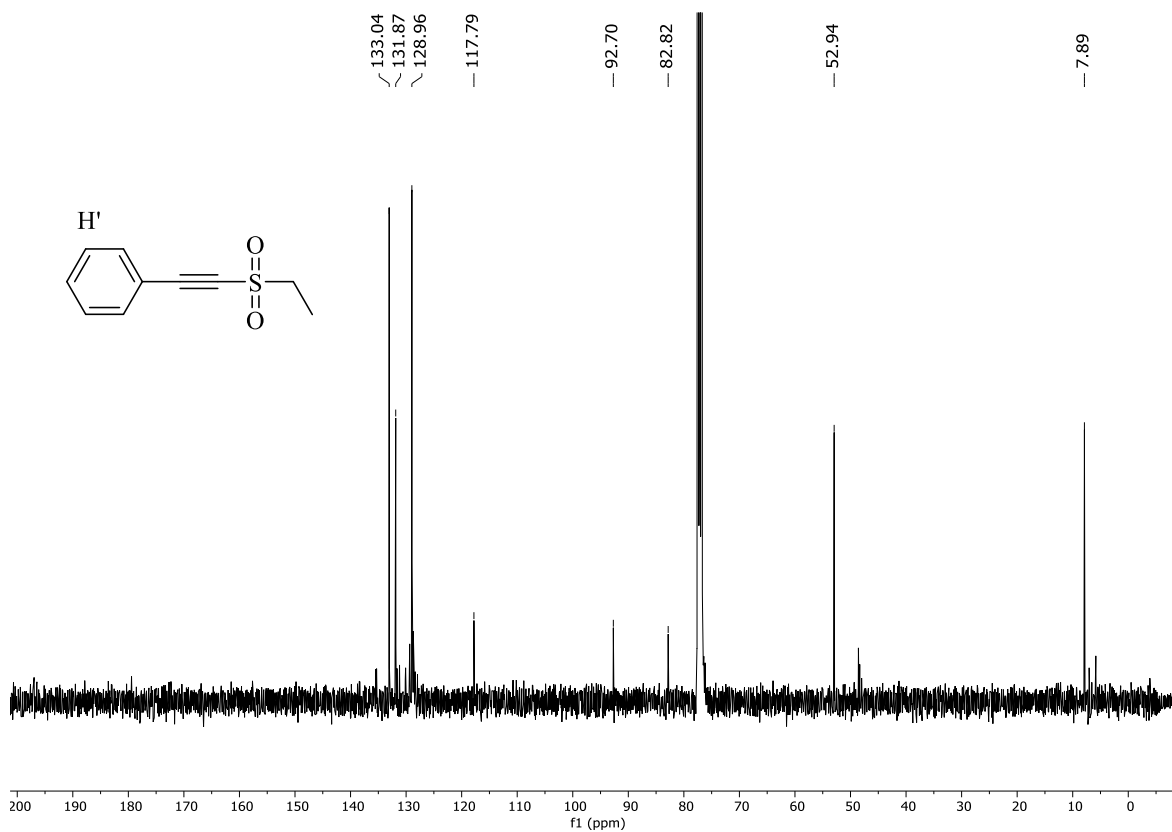


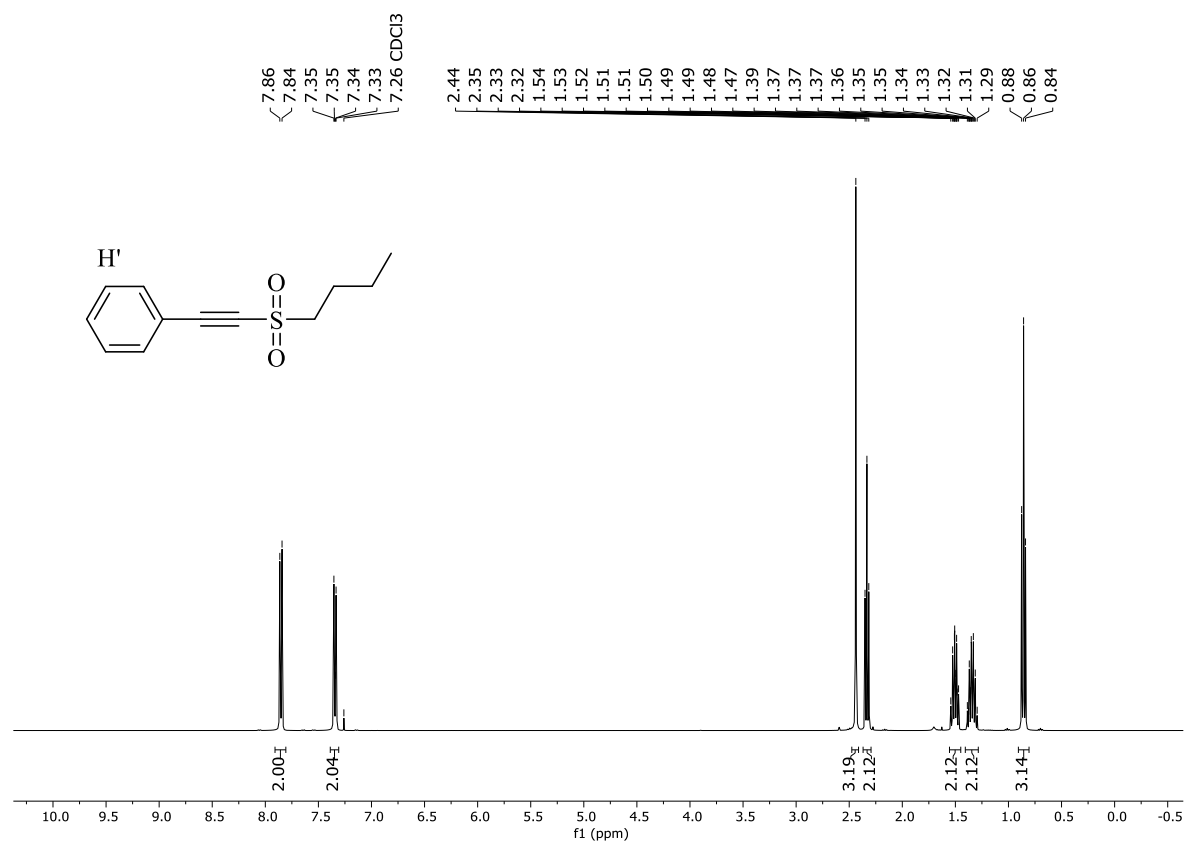
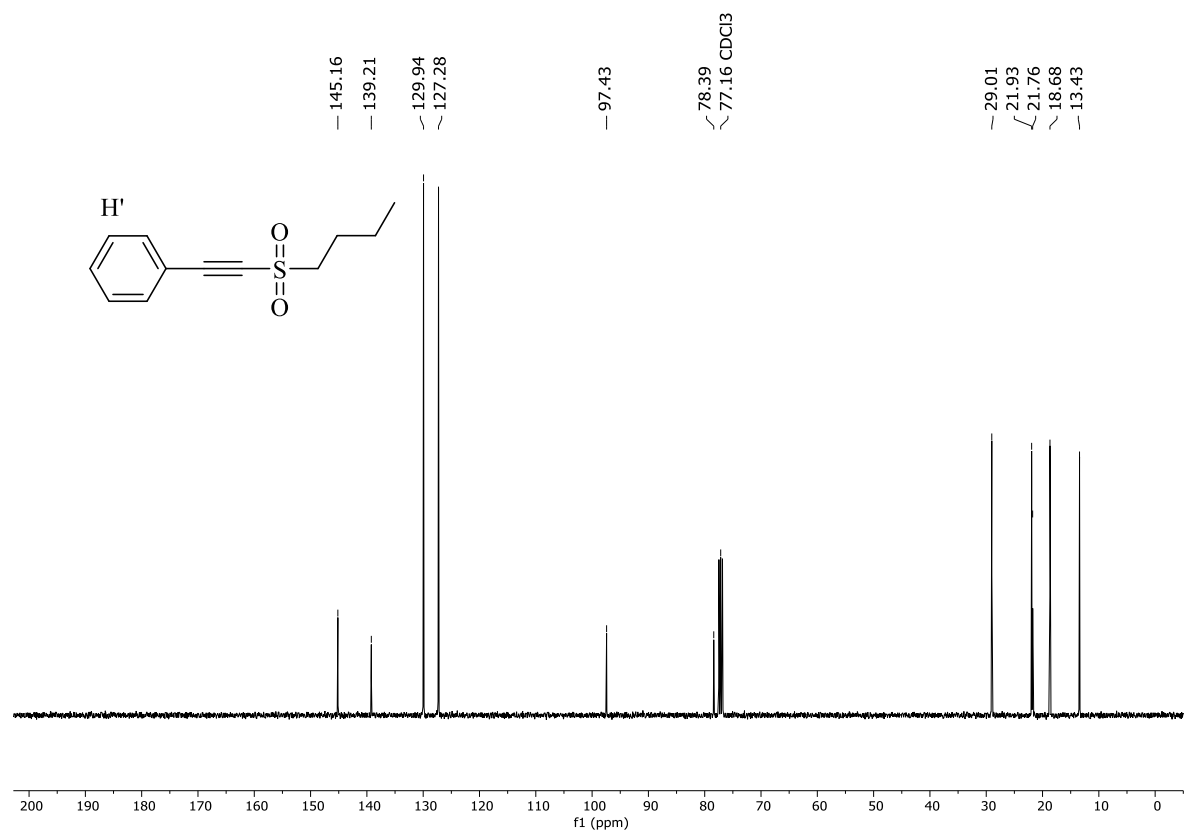
<sup>1</sup>H NMR (400 MHz, CDCl<sub>3</sub>) spectrum of **218i**

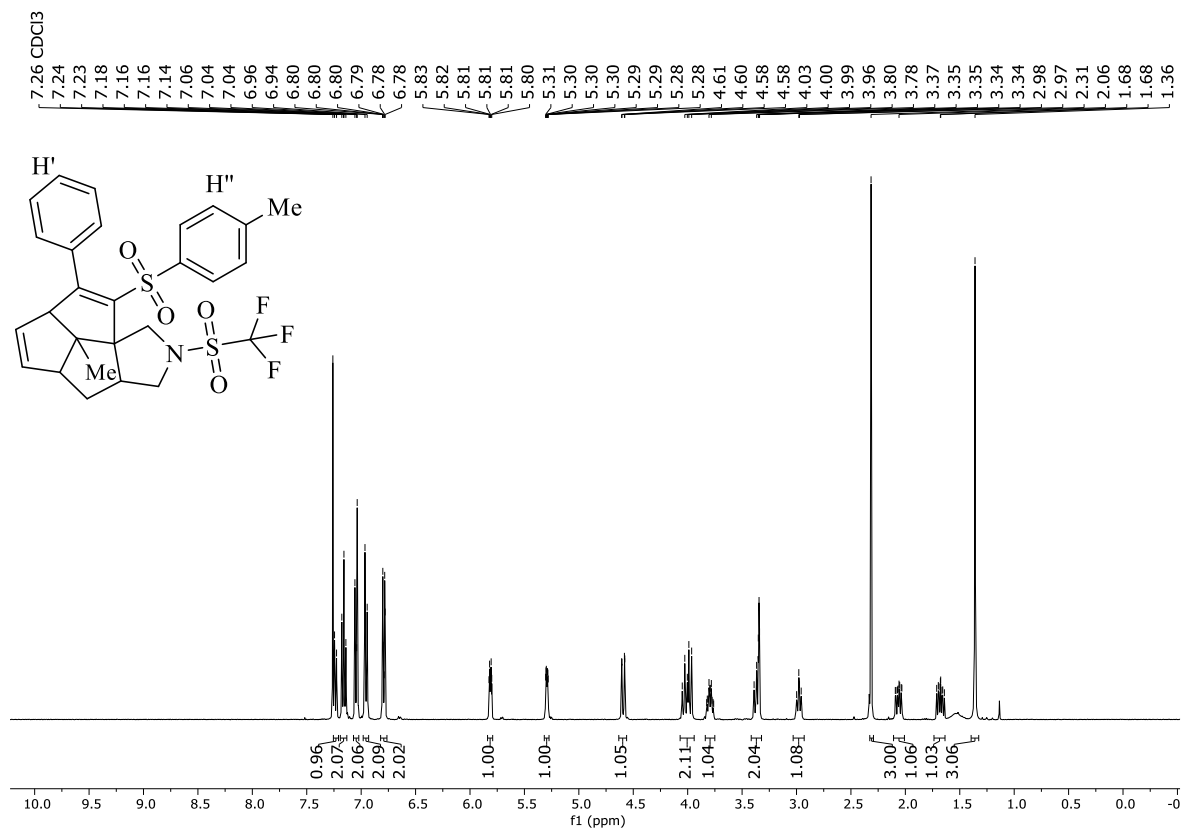
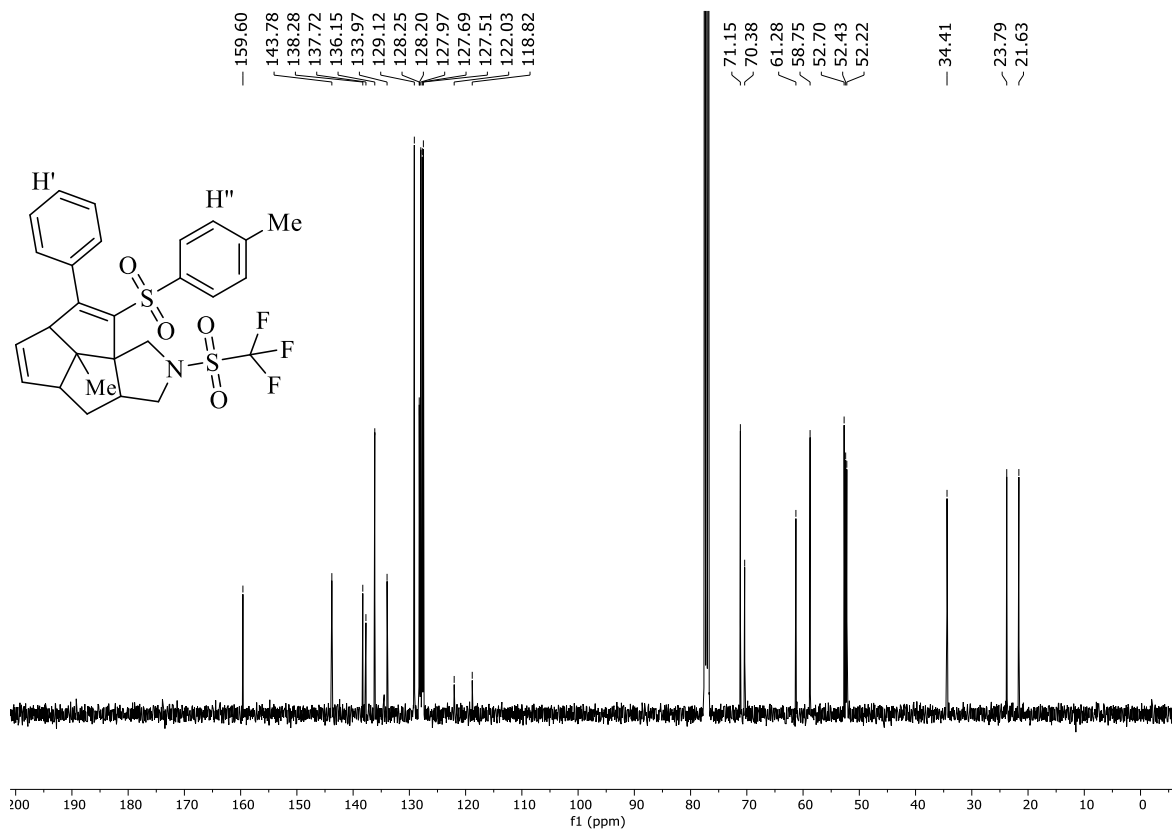


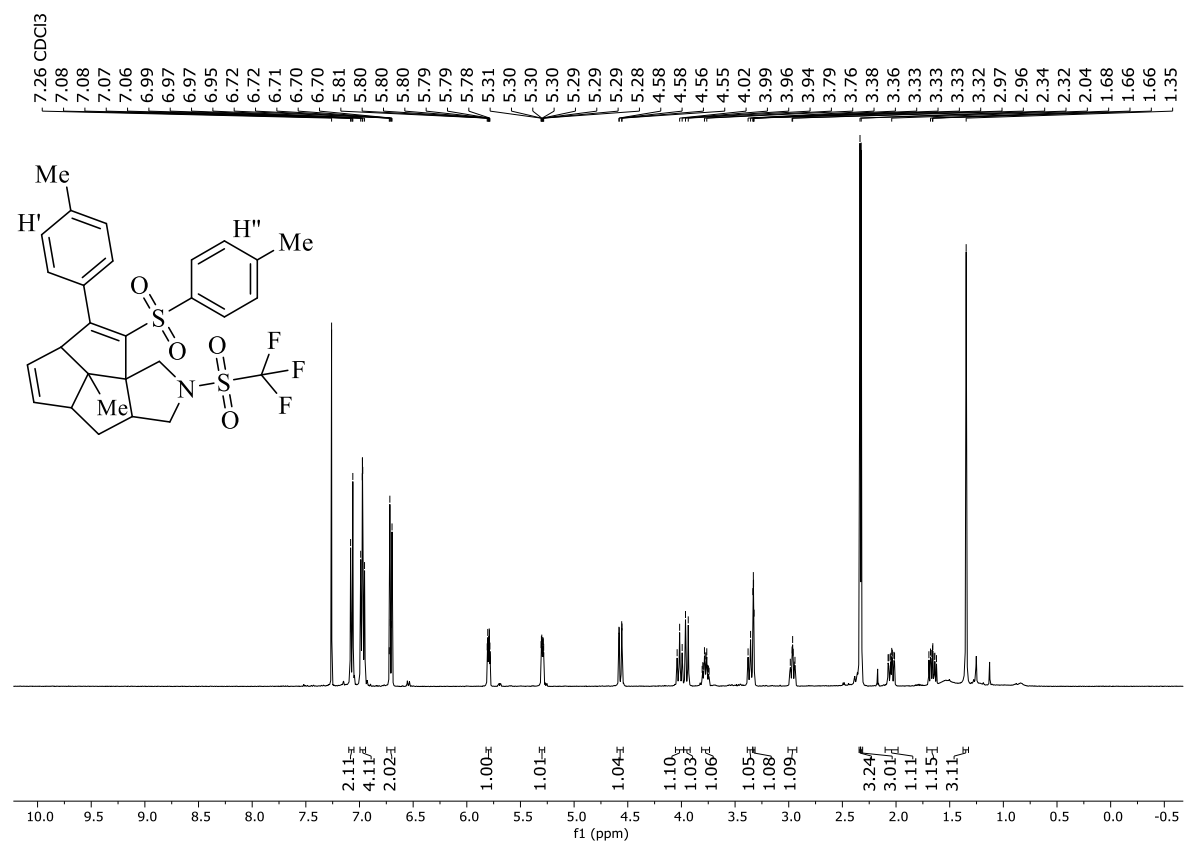
<sup>13</sup>C NMR (101 MHz, CDCl<sub>3</sub>) spectrum of **218i**



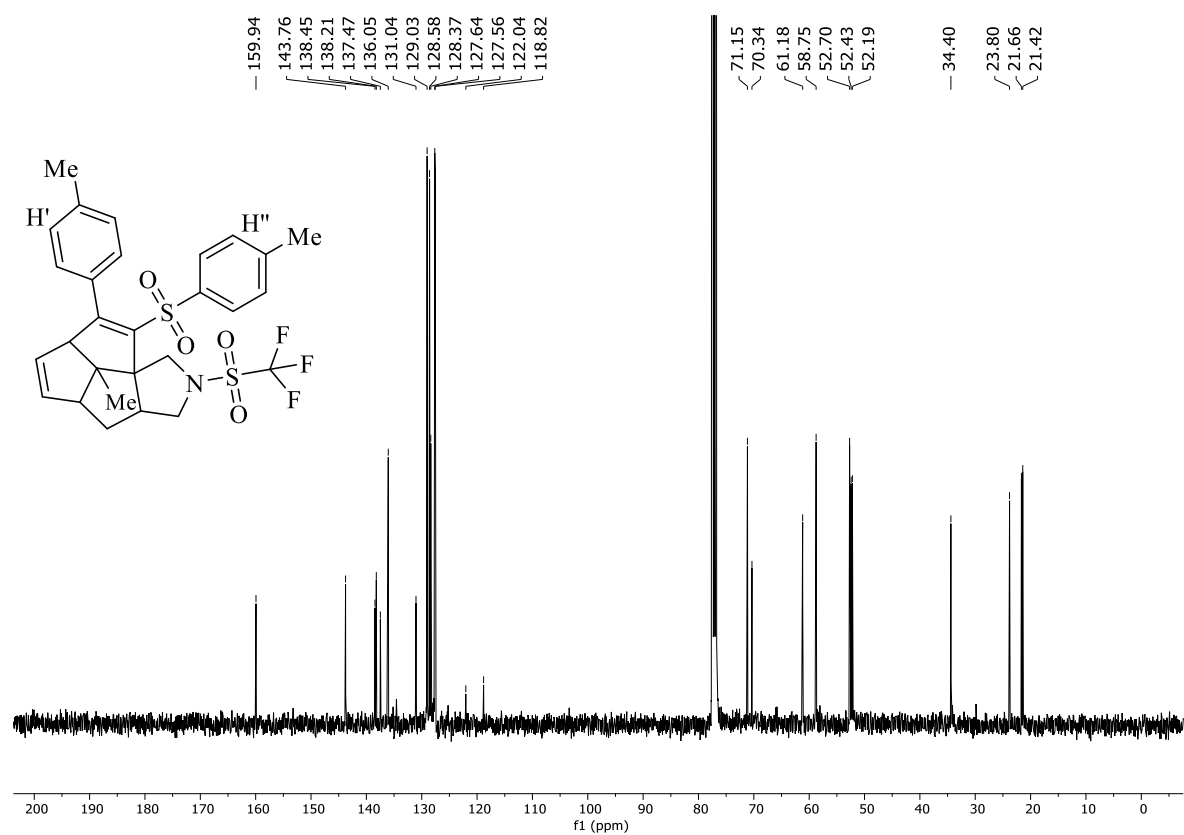
<sup>1</sup>H NMR (400 MHz, CDCl<sub>3</sub>) spectrum of **218j**<sup>13</sup>C NMR (101 MHz, CDCl<sub>3</sub>) spectrum of **218j**

<sup>1</sup>H NMR (400 MHz, CDCl<sub>3</sub>) spectrum of **218k**<sup>13</sup>C NMR (101 MHz, CDCl<sub>3</sub>) spectrum of **218k**

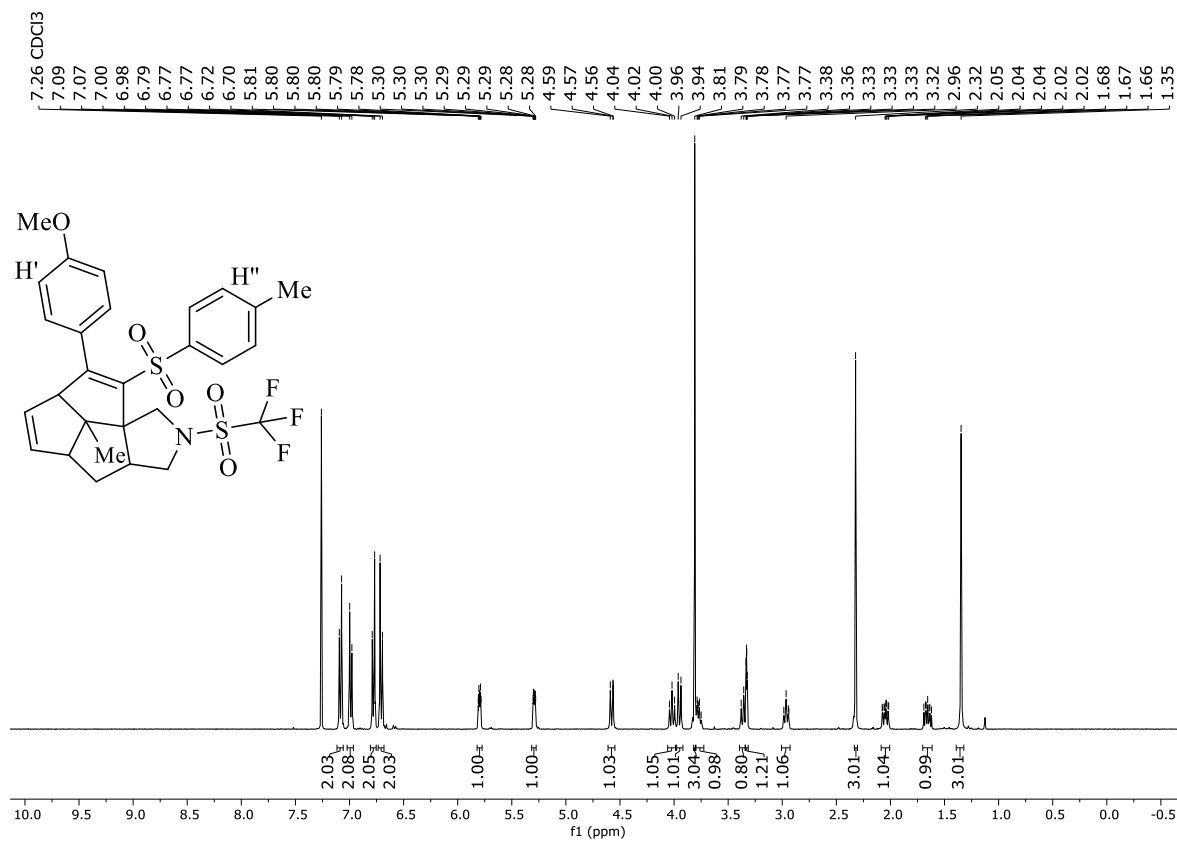
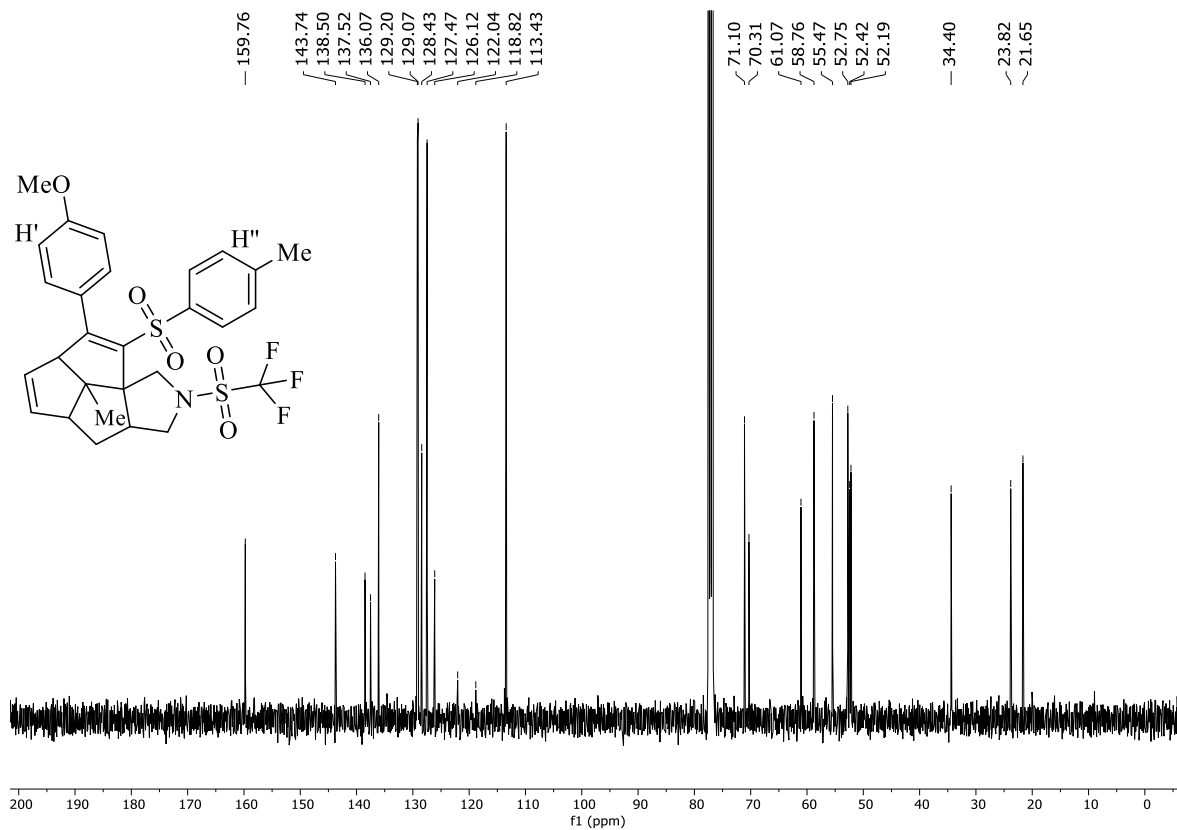
<sup>1</sup>H NMR (400 MHz, CDCl<sub>3</sub>) spectrum of **219a**<sup>13</sup>C NMR (101 MHz, CDCl<sub>3</sub>) spectrum of **219a**



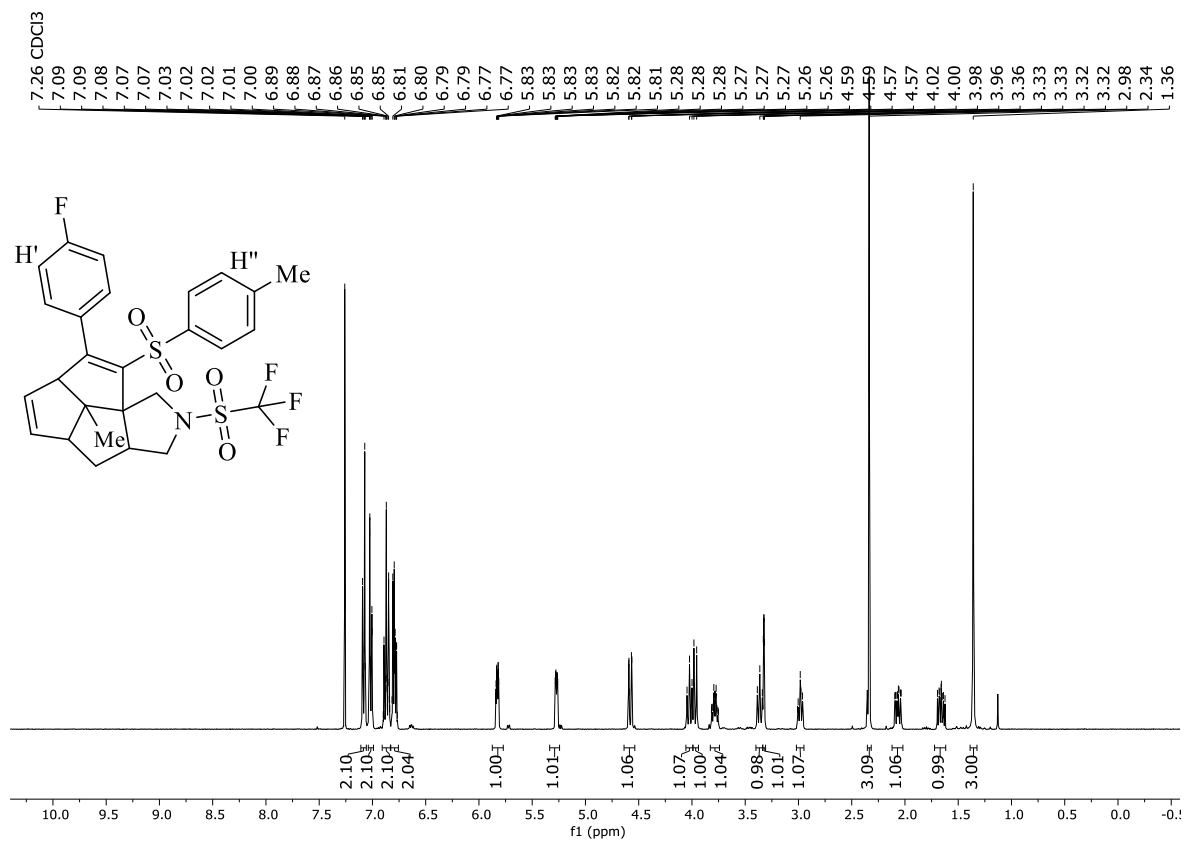
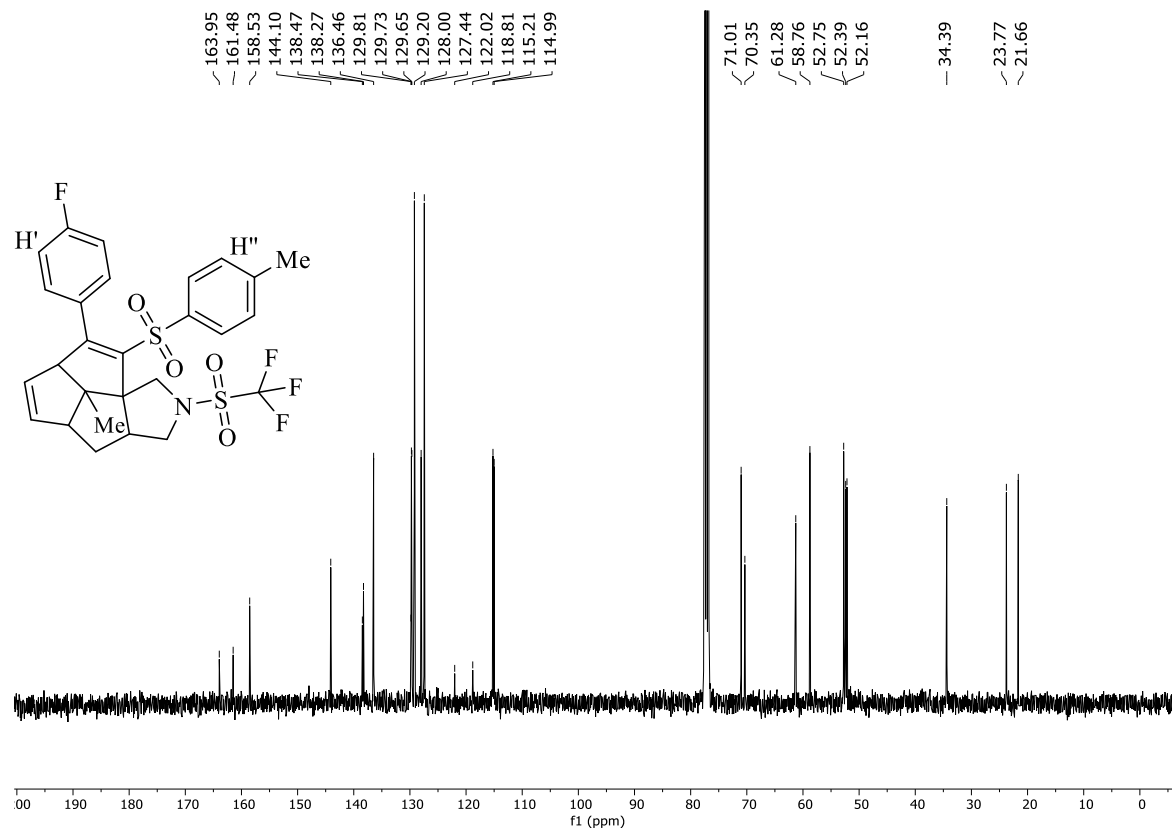
<sup>1</sup>H NMR (400 MHz, CDCl<sub>3</sub>) spectrum of **219b**

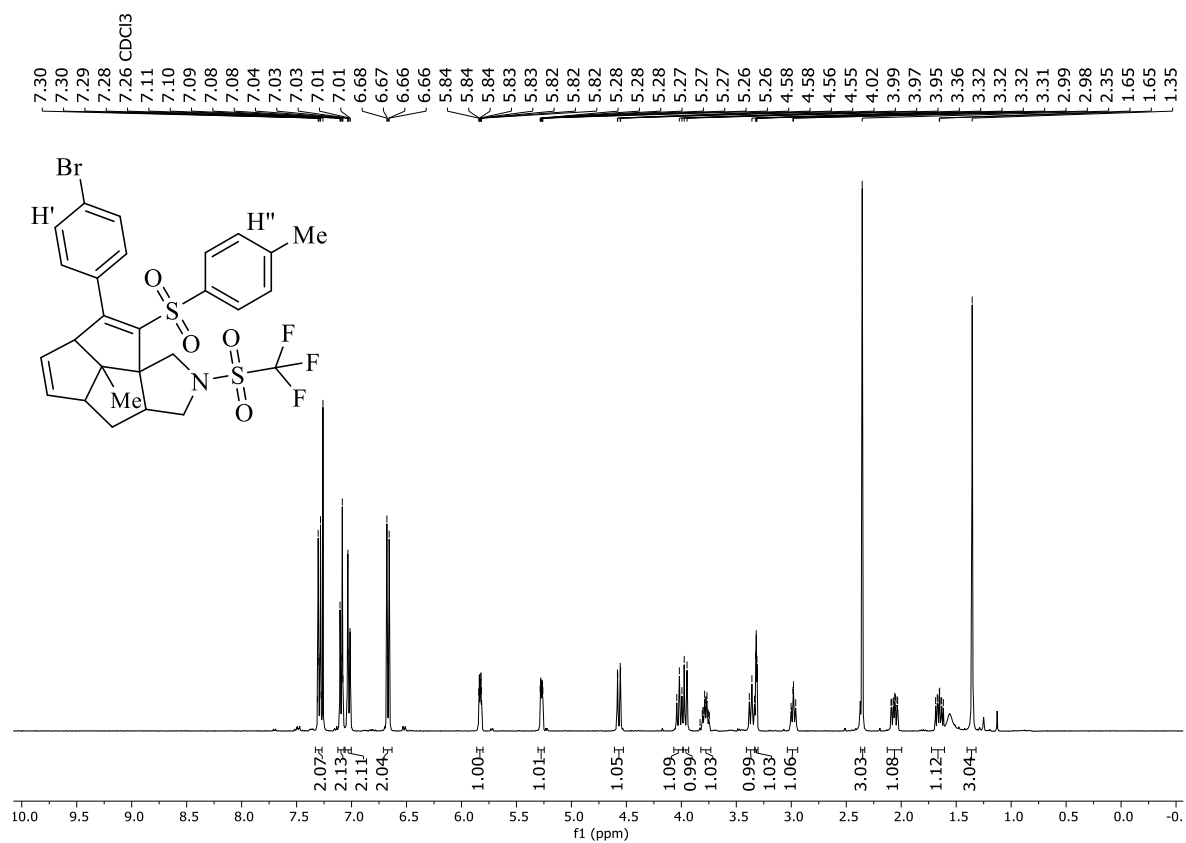


<sup>13</sup>C NMR (101 MHz, CDCl<sub>3</sub>) spectrum of **219b**

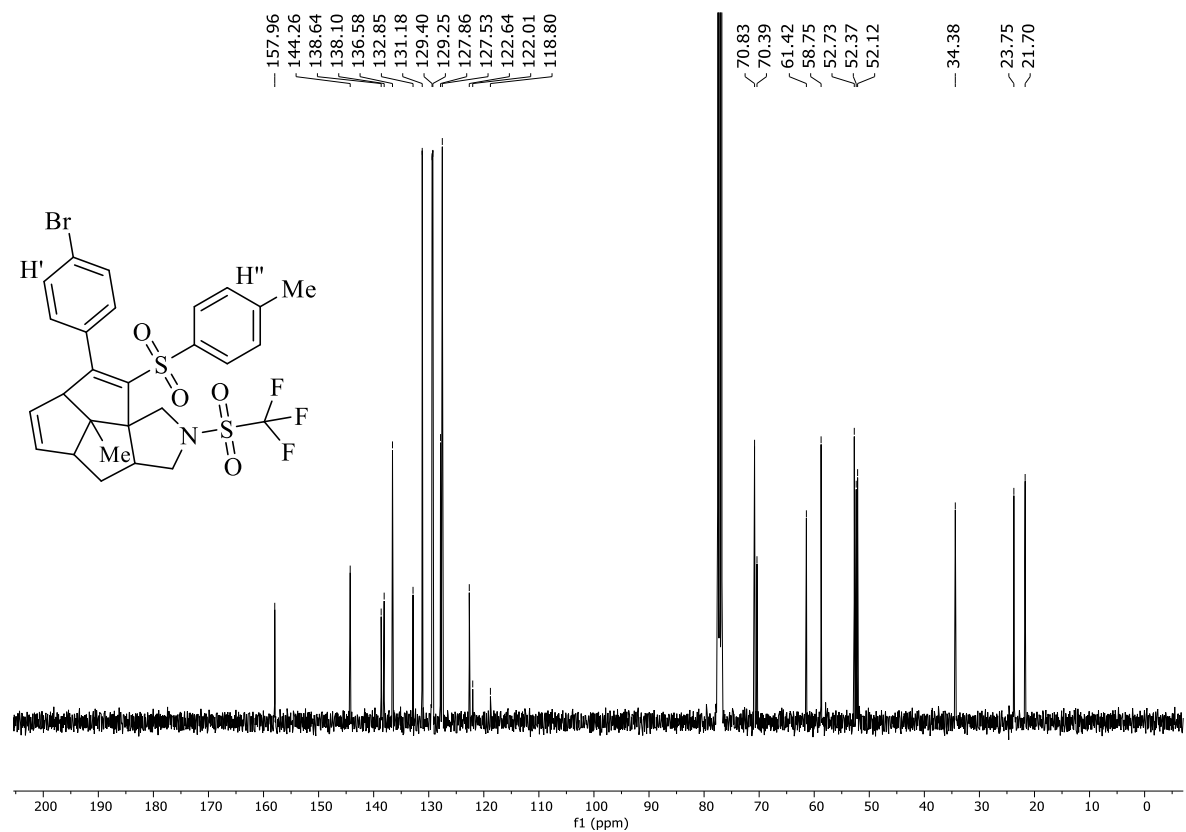
<sup>1</sup>H NMR (400 MHz, CDCl<sub>3</sub>) spectrum of **219c**<sup>13</sup>C NMR (101 MHz, CDCl<sub>3</sub>) spectrum of **219c**



<sup>1</sup>H NMR (400 MHz, CDCl<sub>3</sub>) spectrum of **219e**<sup>13</sup>C NMR (101 MHz, CDCl<sub>3</sub>) spectrum of **219e**

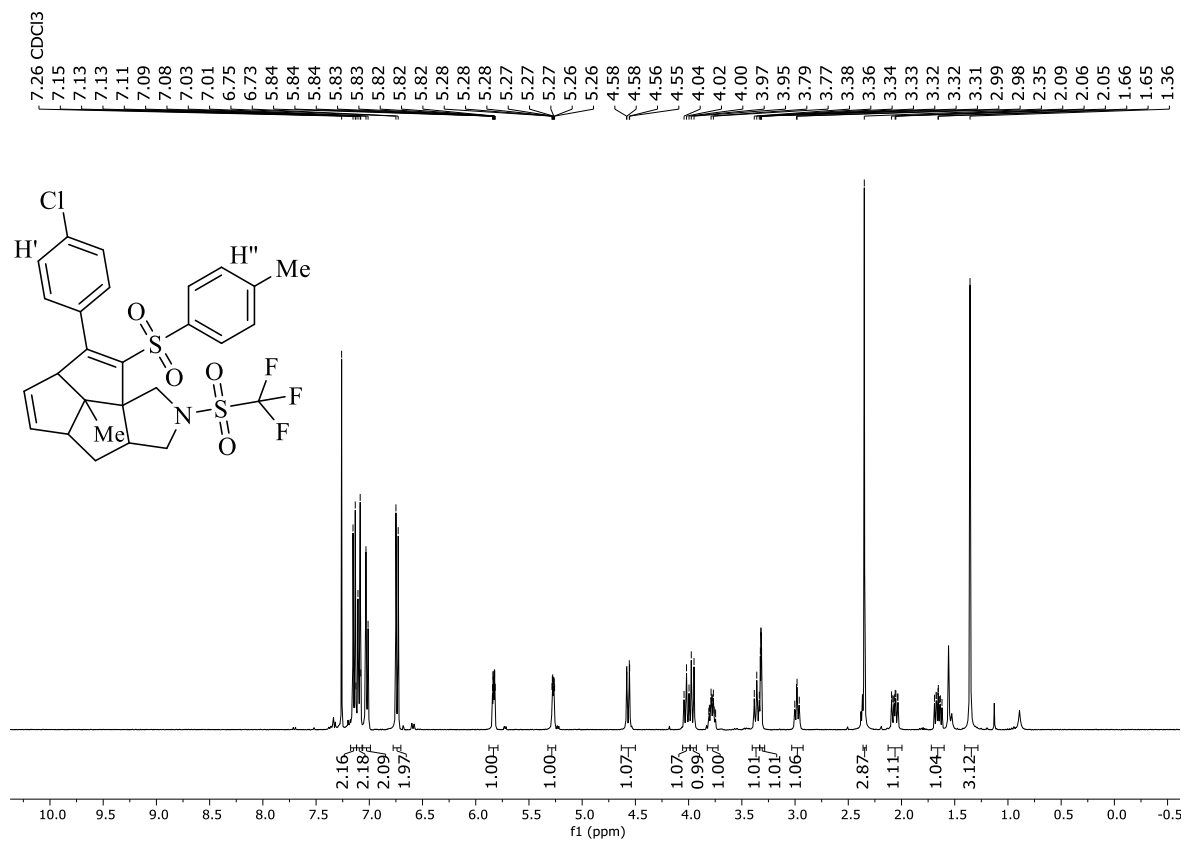
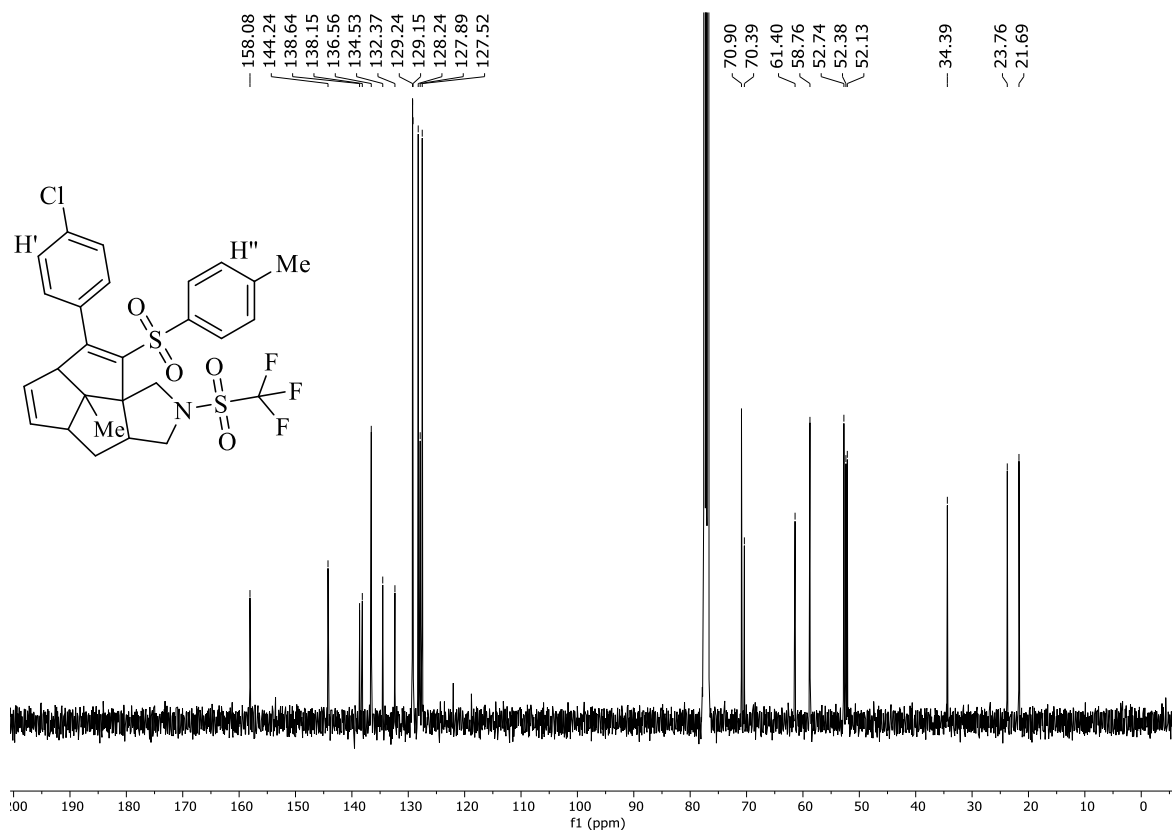


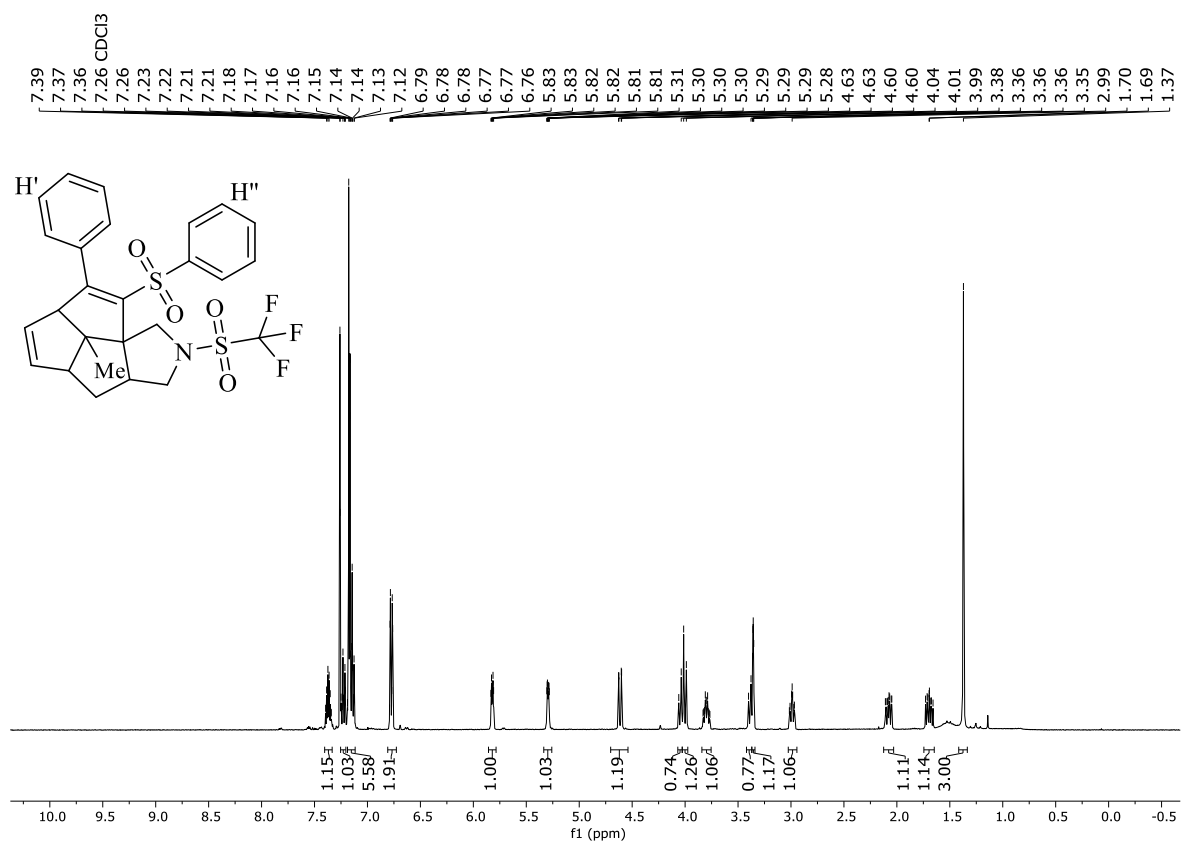
<sup>1</sup>H NMR (400 MHz, CDCl<sub>3</sub>) spectrum of **219f**



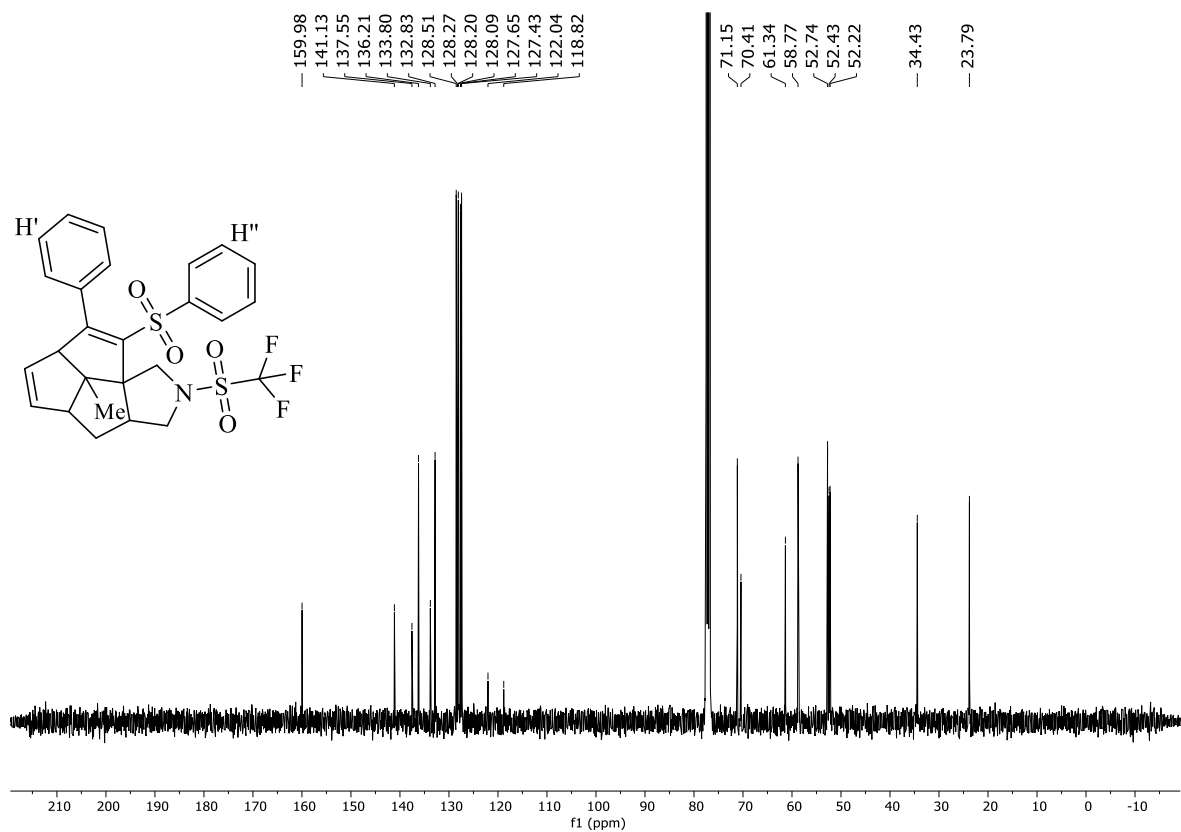
<sup>13</sup>C NMR (101 MHz, CDCl<sub>3</sub>) spectrum of **219f**



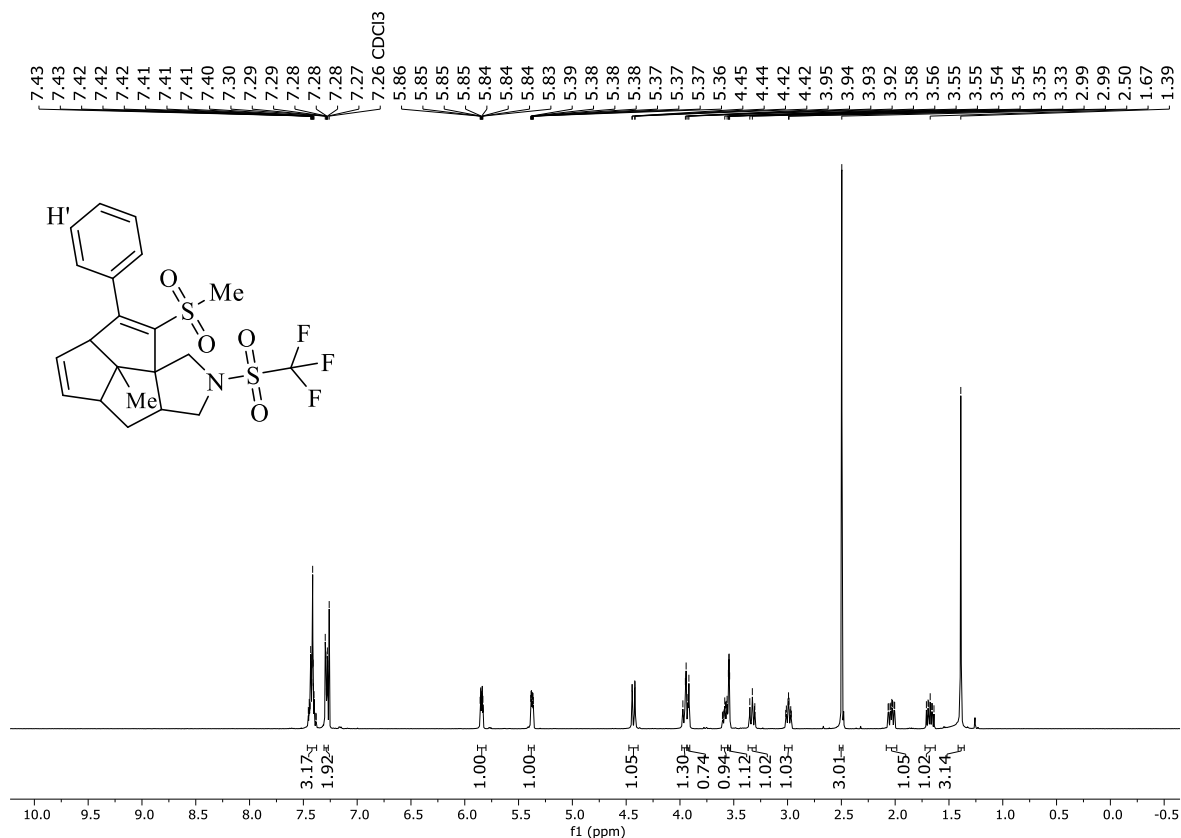
<sup>1</sup>H NMR (400 MHz, CDCl<sub>3</sub>) spectrum of **219g**<sup>13</sup>C NMR (101 MHz, CDCl<sub>3</sub>) spectrum of **219g**



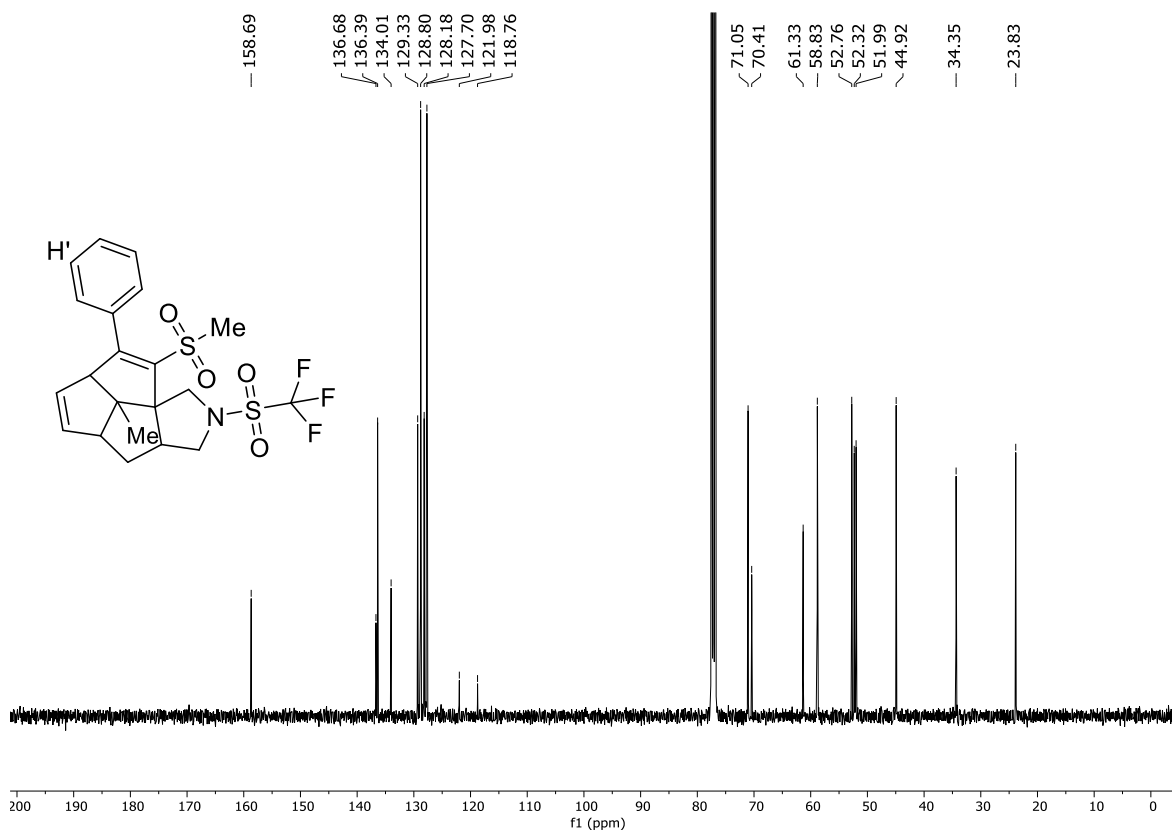
<sup>1</sup>H NMR (400 MHz, CDCl<sub>3</sub>) spectrum of **219h**



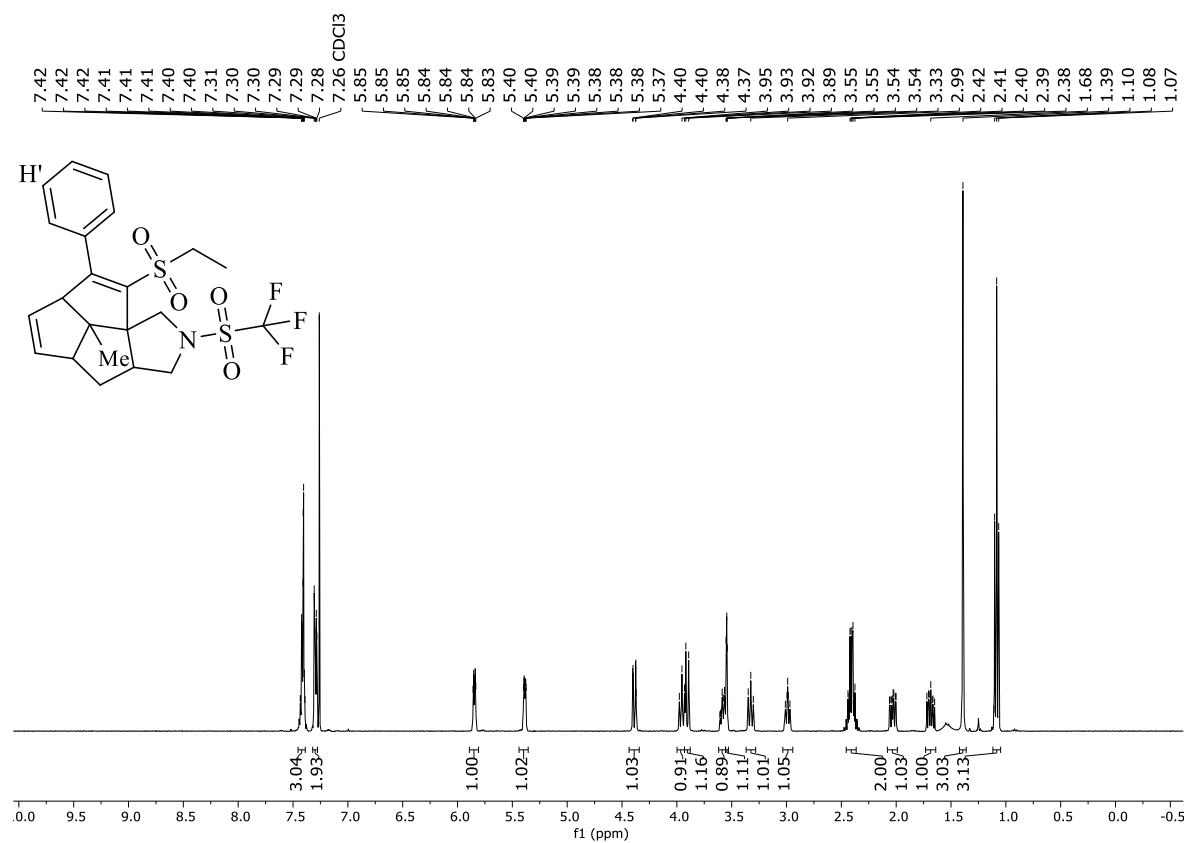
<sup>13</sup>C NMR (101 MHz, CDCl<sub>3</sub>) spectrum of **219h**



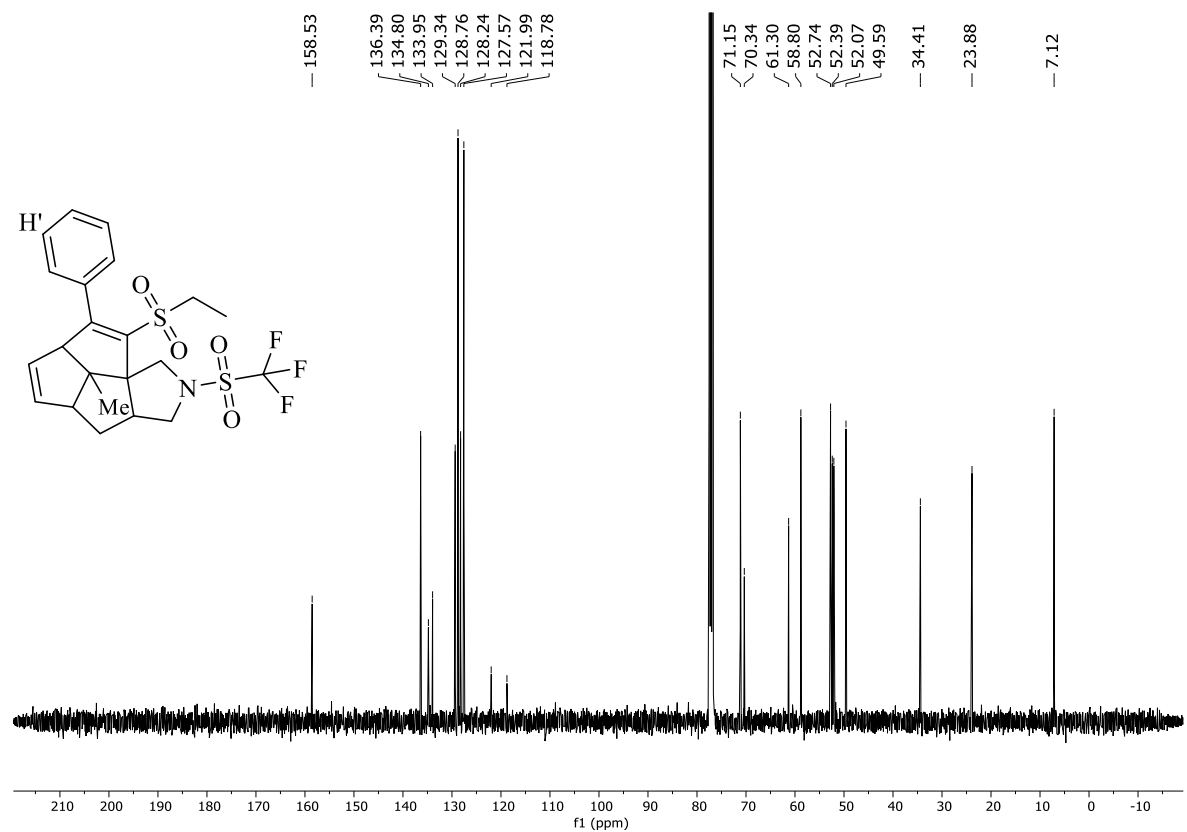
**<sup>1</sup>H NMR (400 MHz, CDCl<sub>3</sub>) spectrum of **219i****



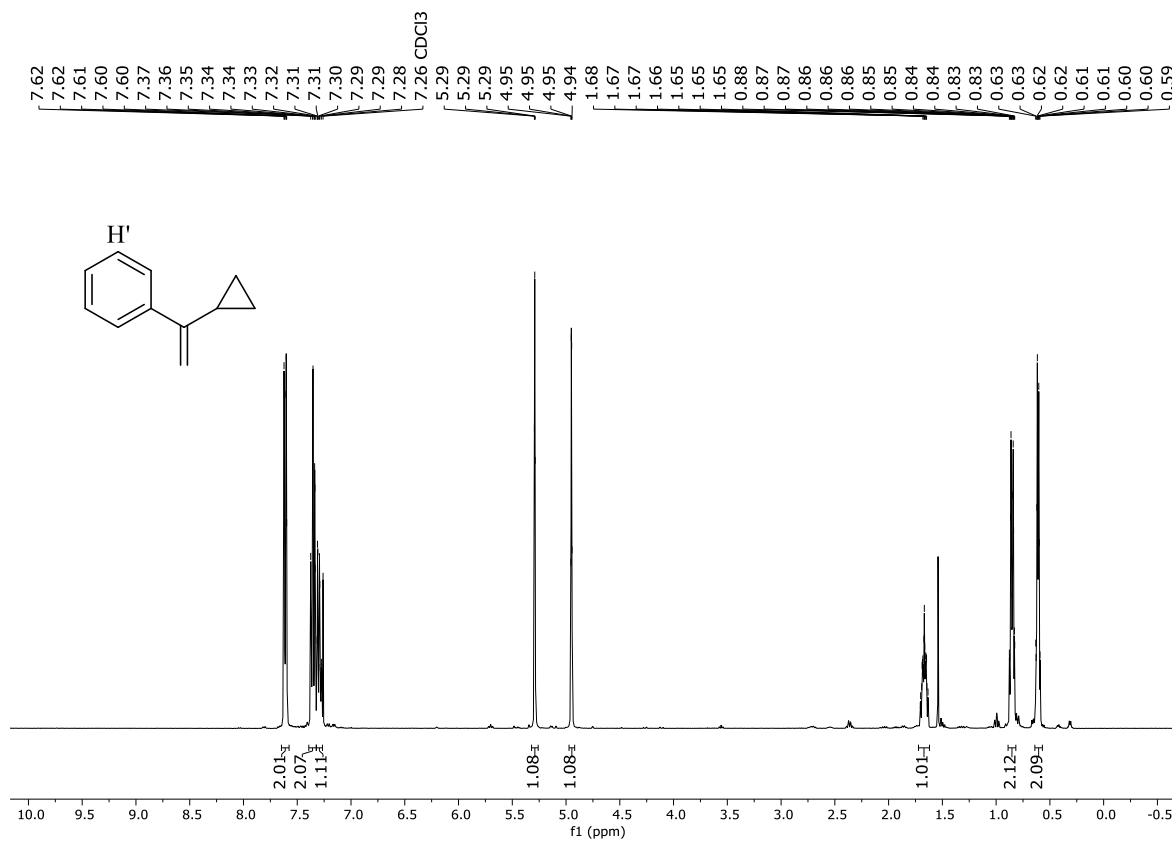
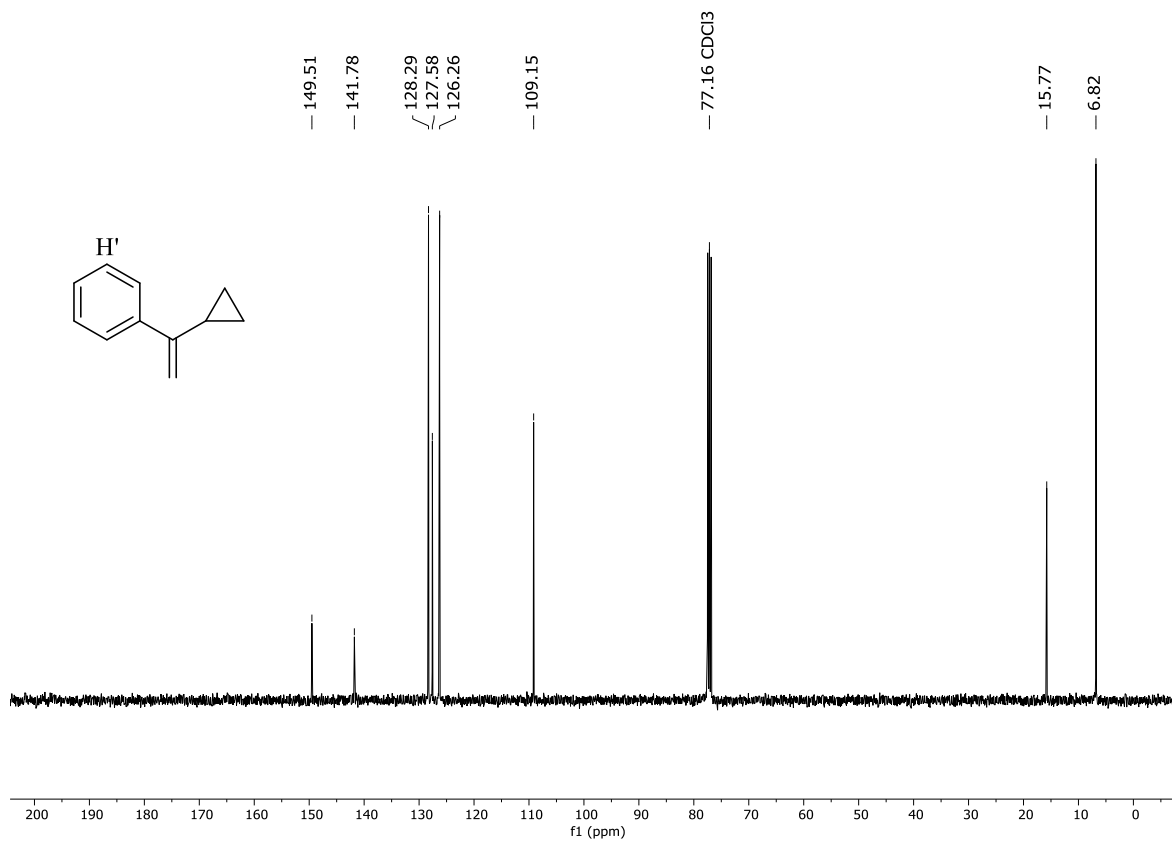
**<sup>13</sup>C NMR (101 MHz, CDCl<sub>3</sub>) spectrum of **219i****

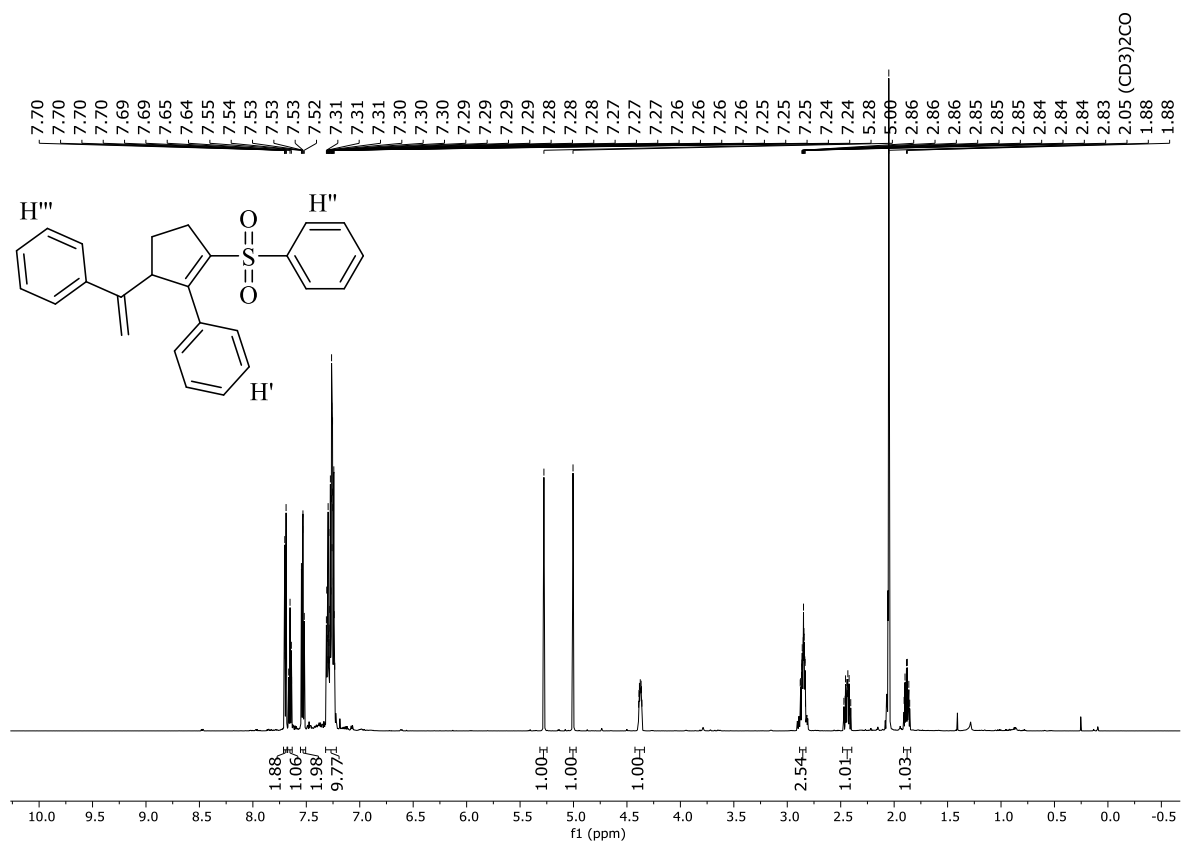


<sup>1</sup>H NMR (400 MHz, CDCl<sub>3</sub>) spectrum of **219j**

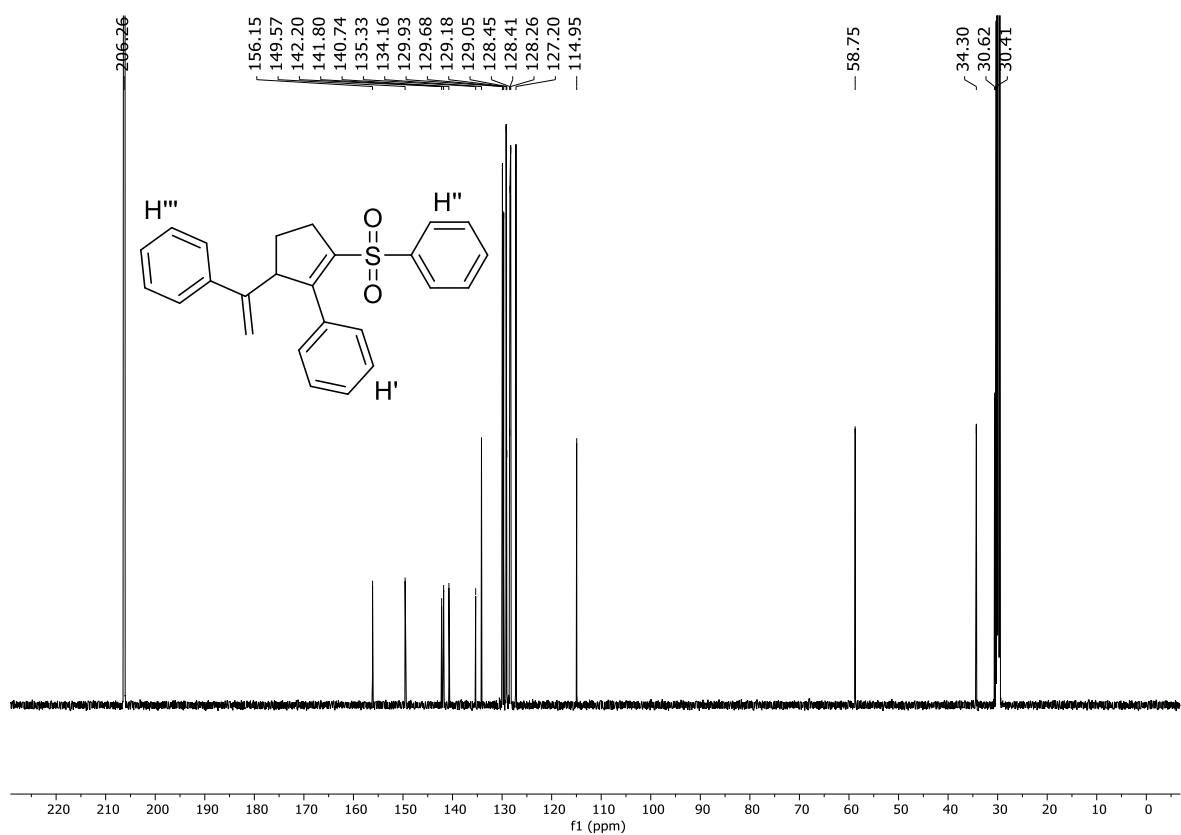


<sup>13</sup>C NMR (101 MHz, CDCl<sub>3</sub>) spectrum of **219j**

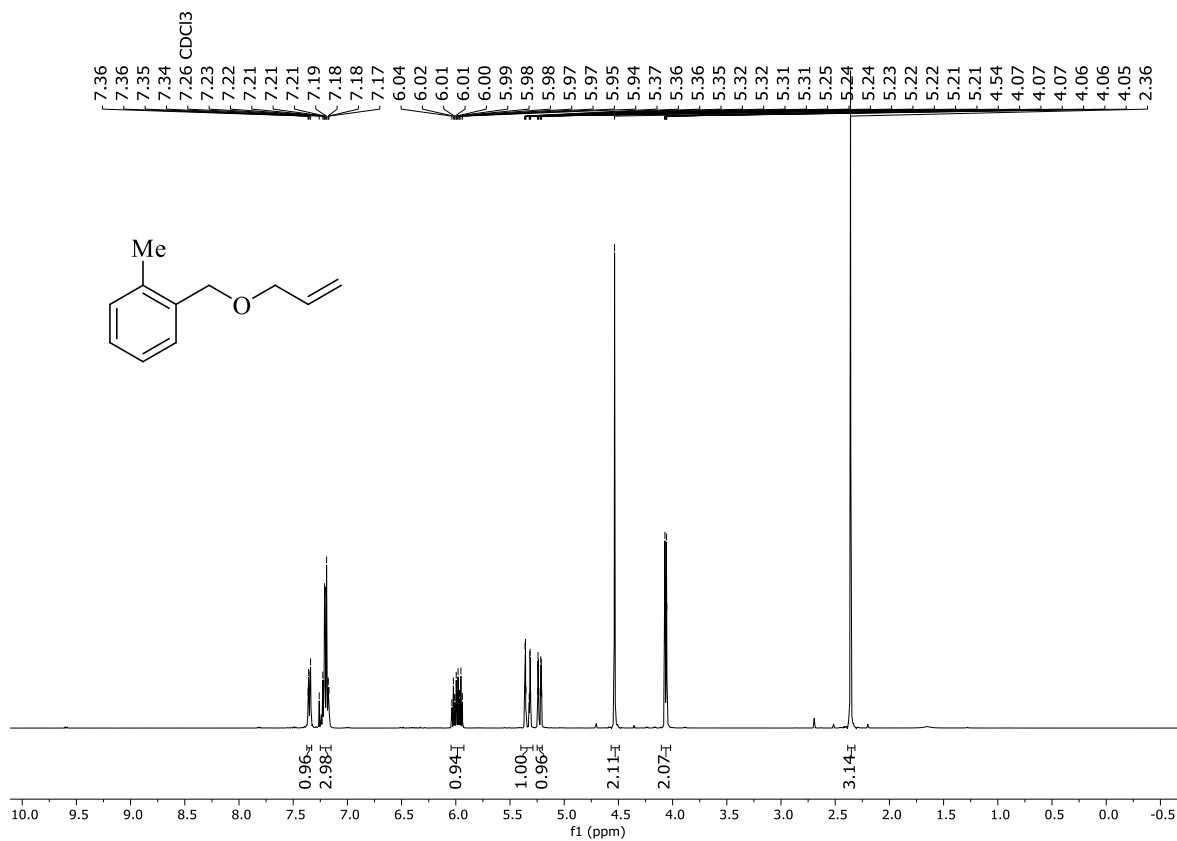
<sup>1</sup>H NMR (400 MHz, CDCl<sub>3</sub>) spectrum of **236**<sup>13</sup>C NMR (101 MHz, CDCl<sub>3</sub>) spectrum of **236**



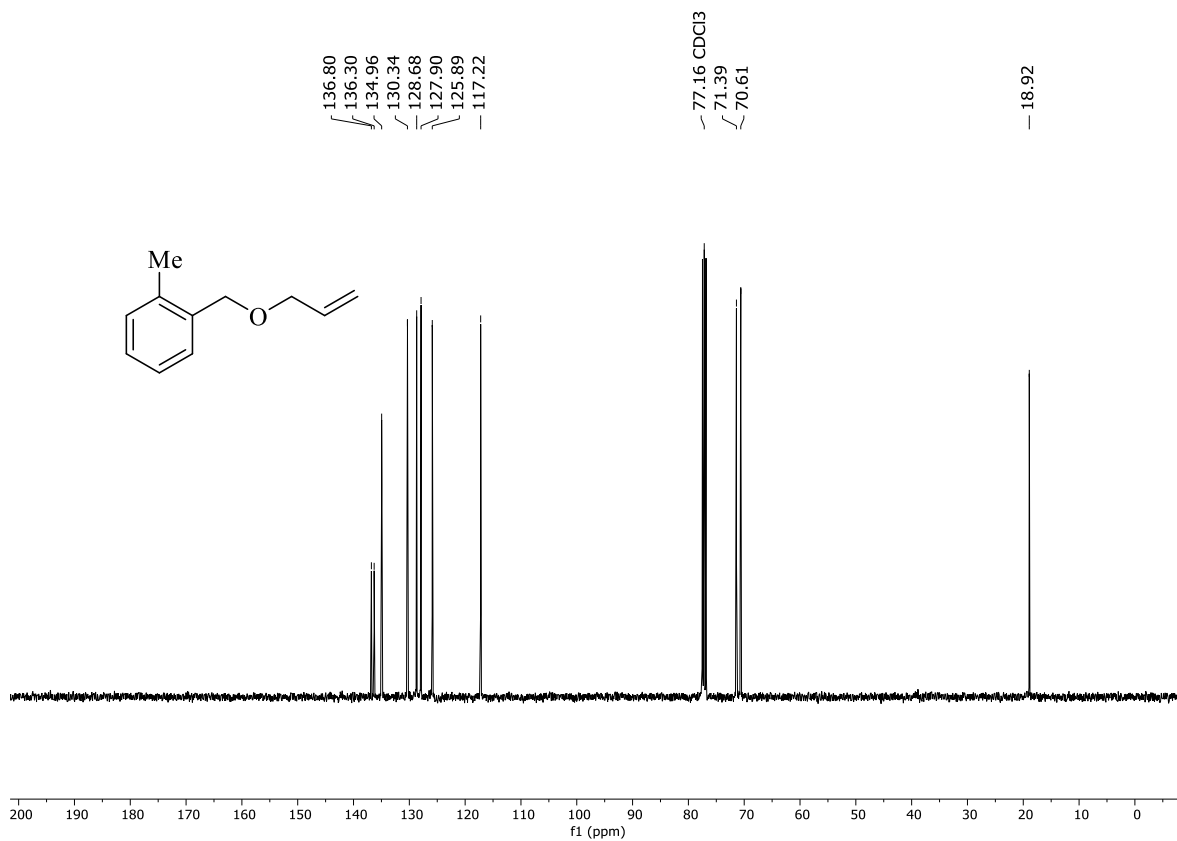
<sup>1</sup>H NMR (400 MHz, acetone-d<sub>6</sub>) spectrum of **237**



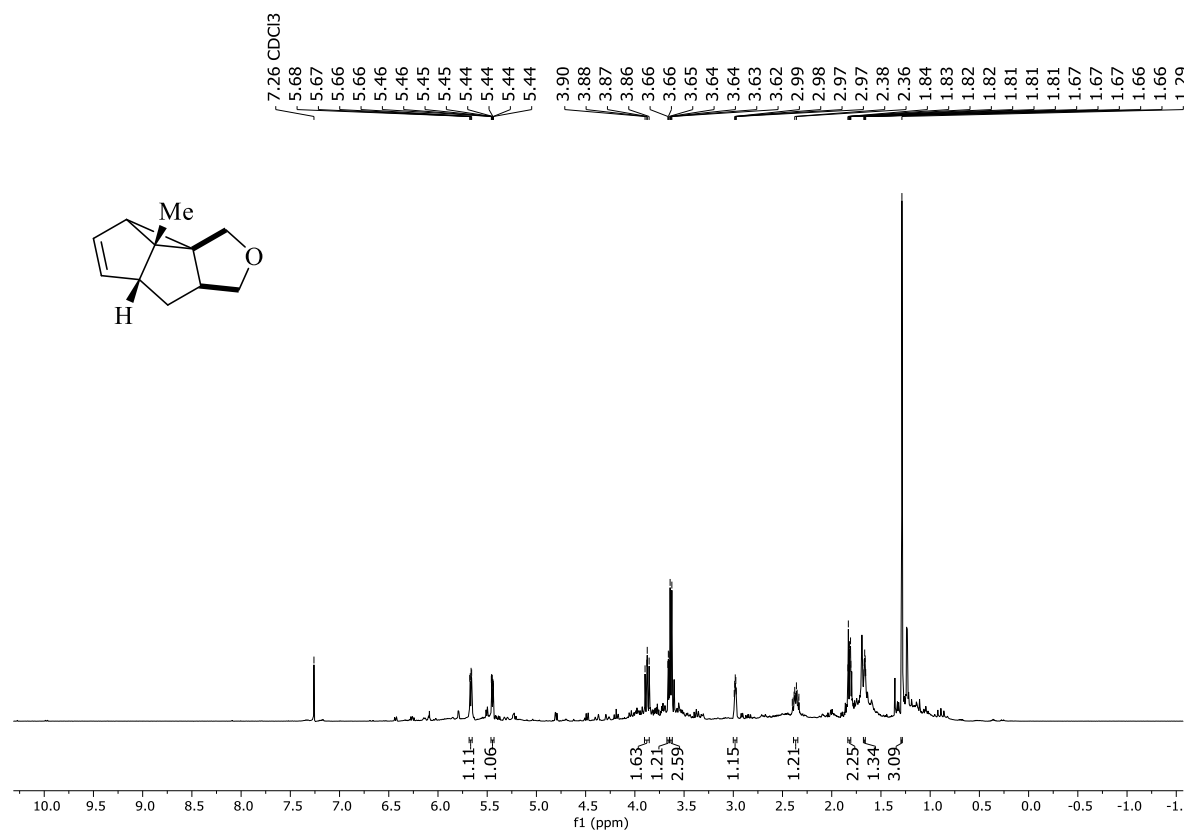
<sup>13</sup>C NMR (101 MHz, acetone-d<sub>6</sub>) spectrum of **237**



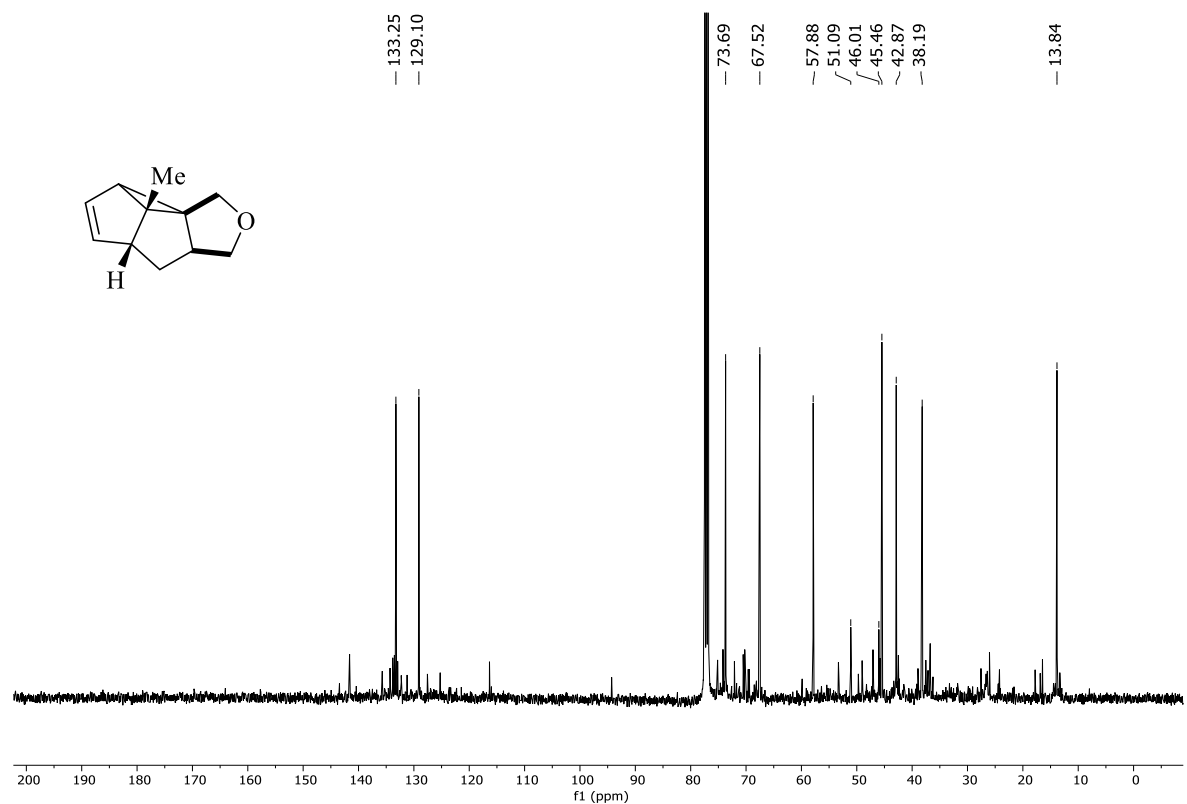
<sup>1</sup>H NMR (400 MHz, CDCl<sub>3</sub>) spectrum of **239**



<sup>13</sup>C NMR (101 MHz, CDCl<sub>3</sub>) spectrum of **239**

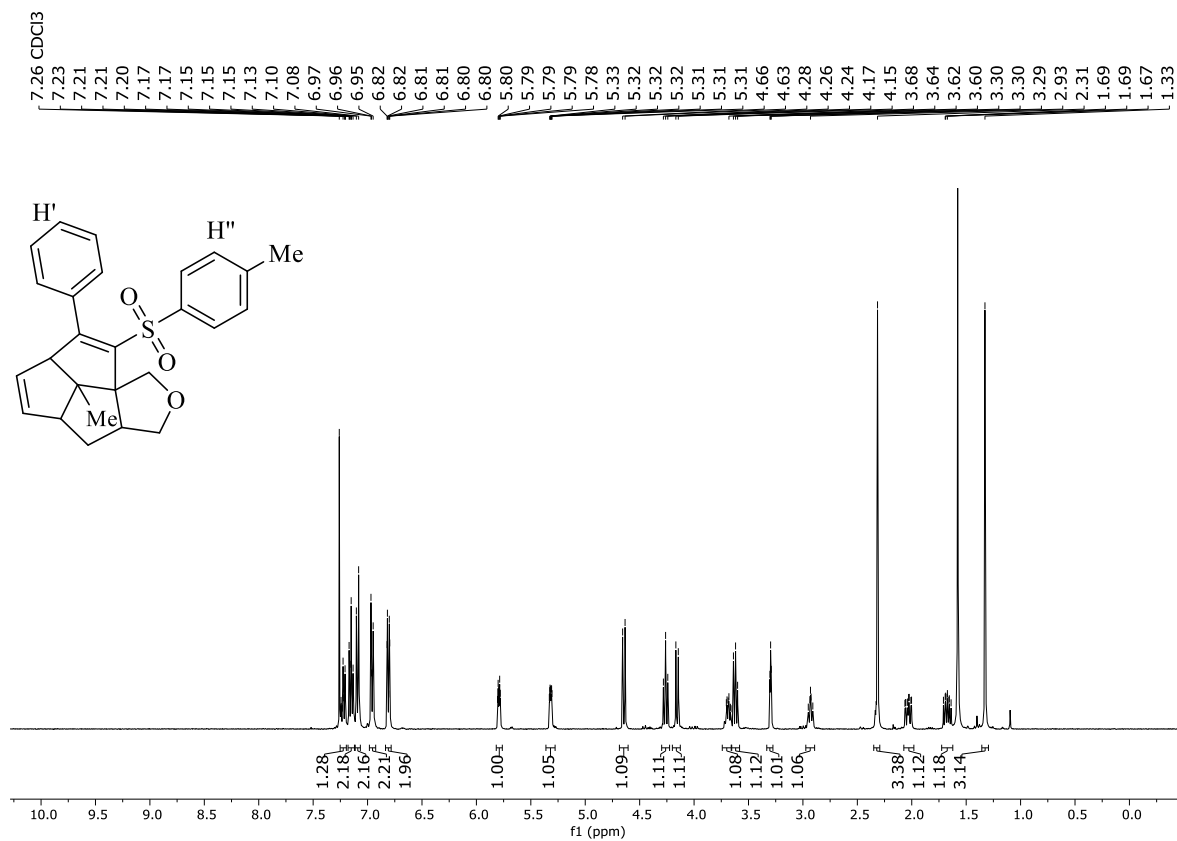
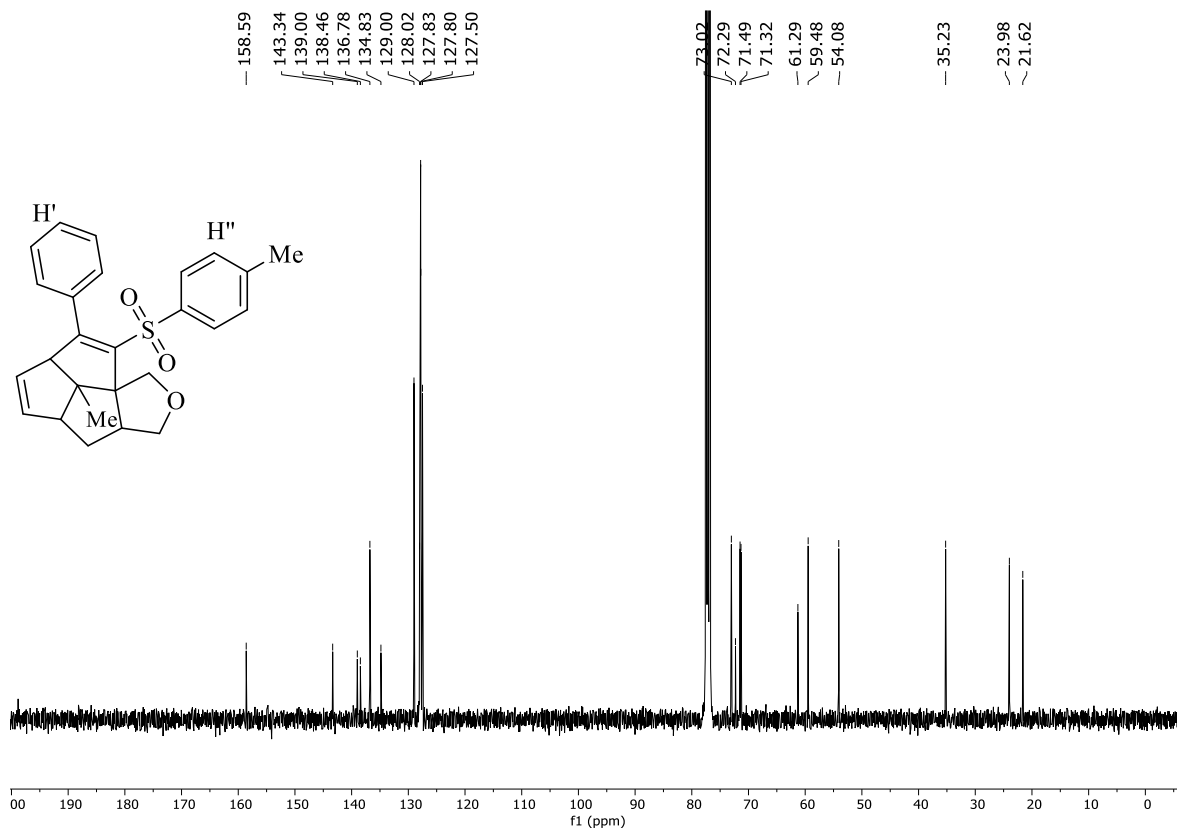


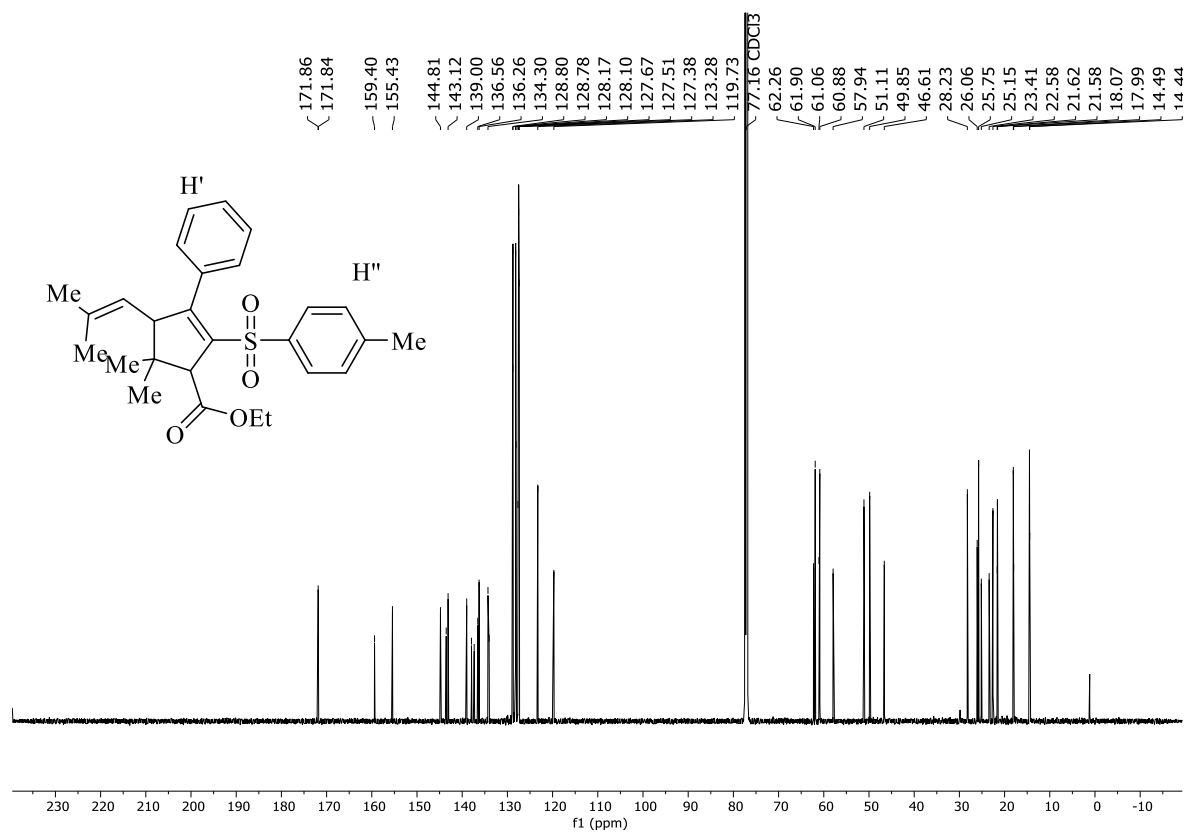
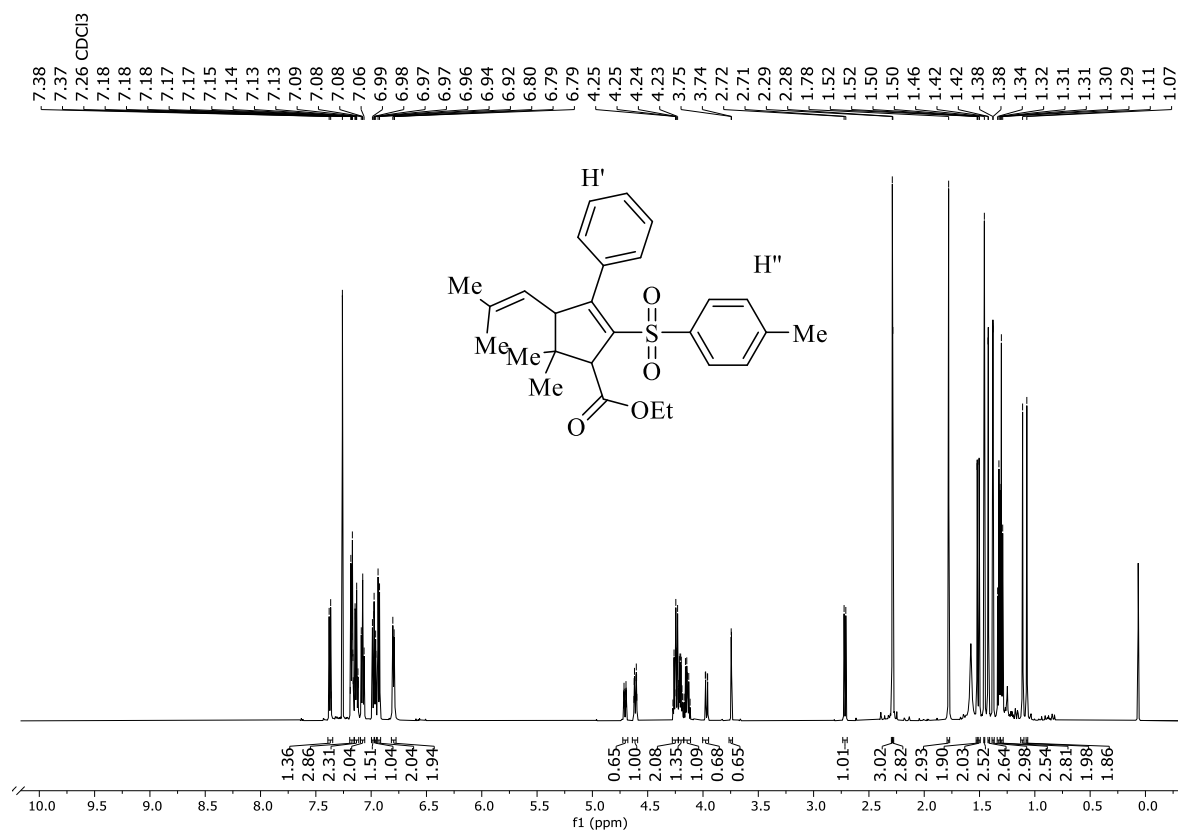
<sup>1</sup>H NMR (400 MHz, CDCl<sub>3</sub>) spectrum of **240**

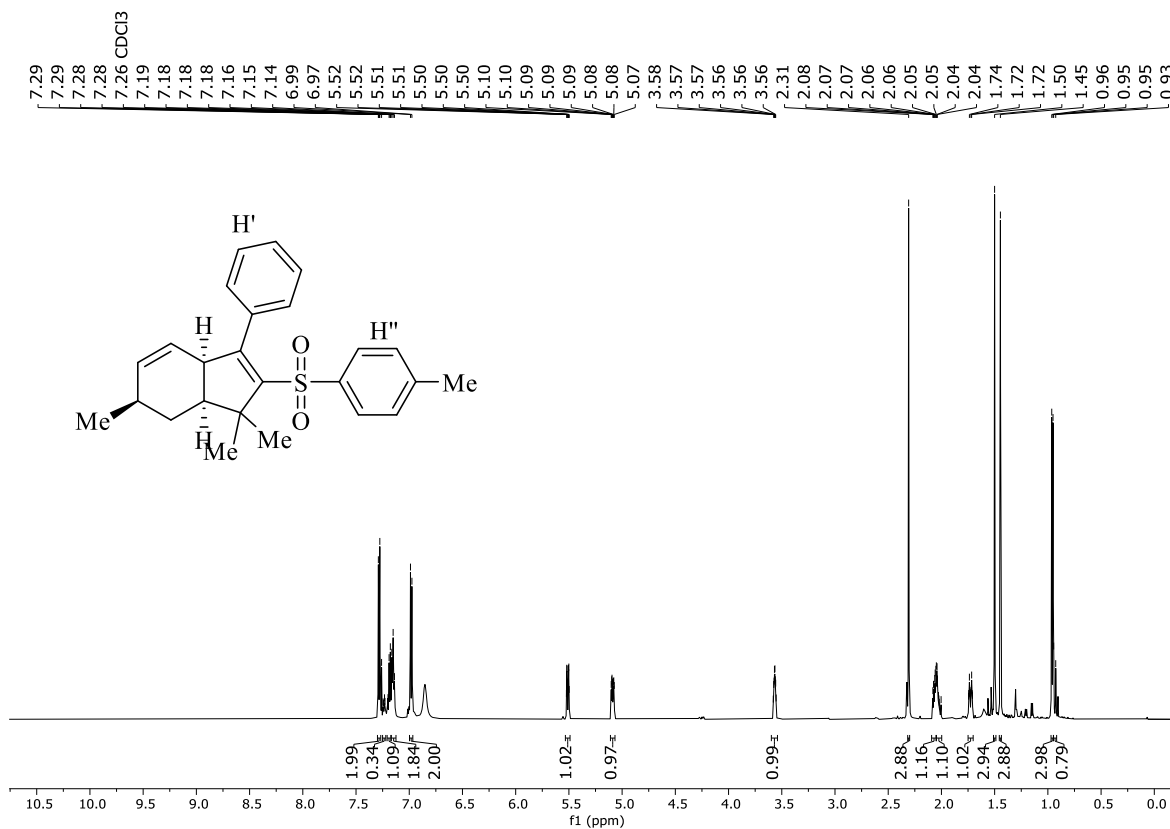
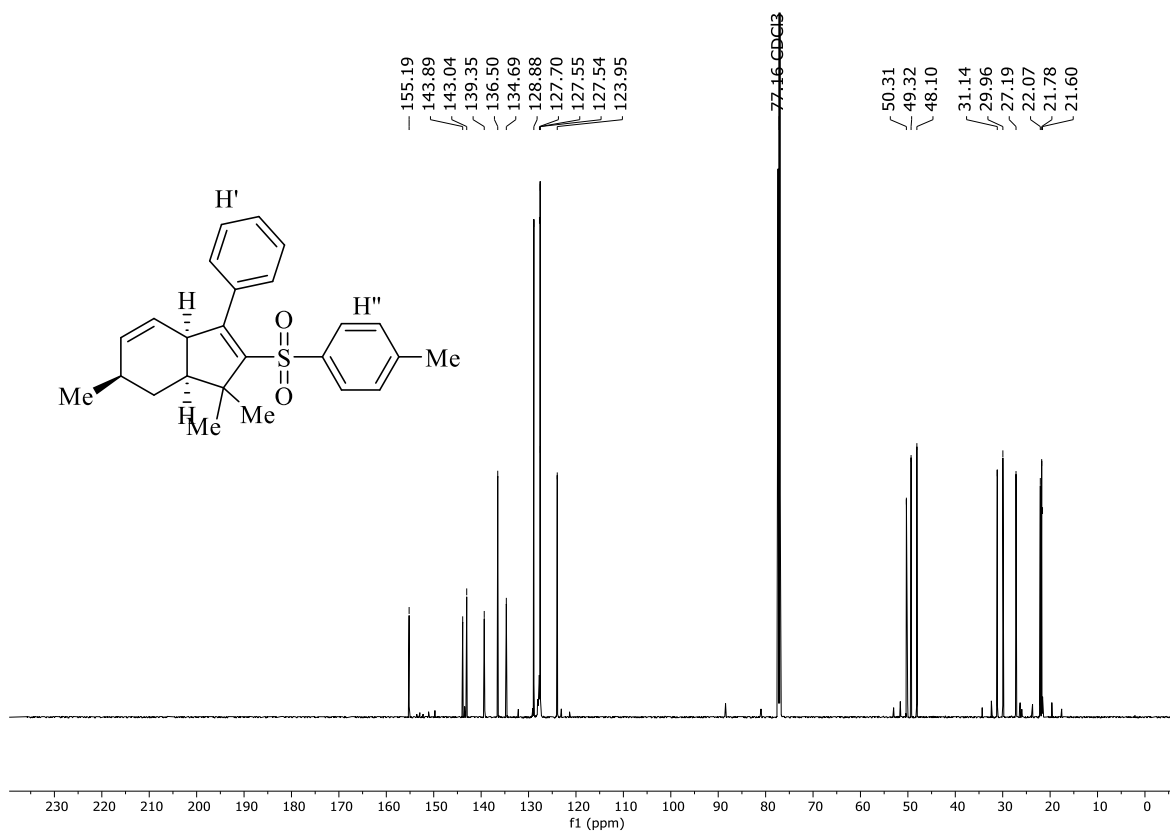


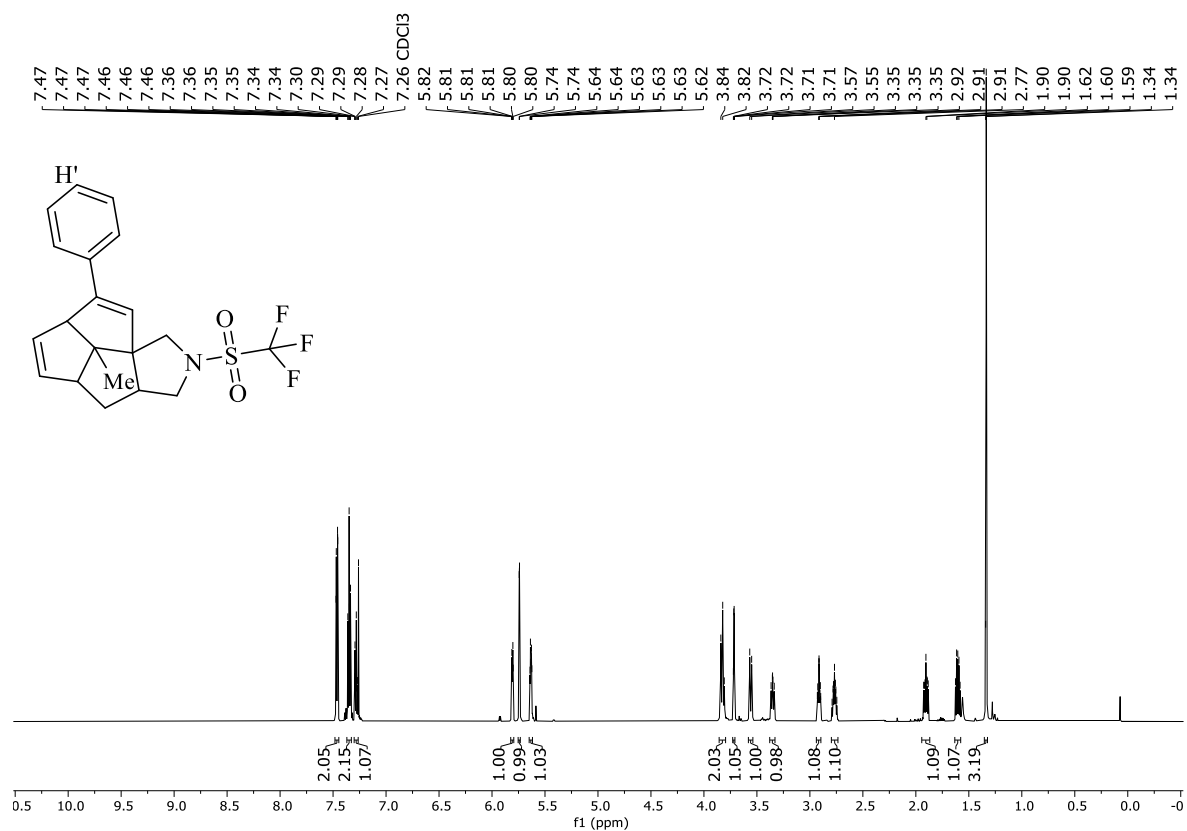
<sup>13</sup>C NMR (101 MHz, CDCl<sub>3</sub>) spectrum of **240**



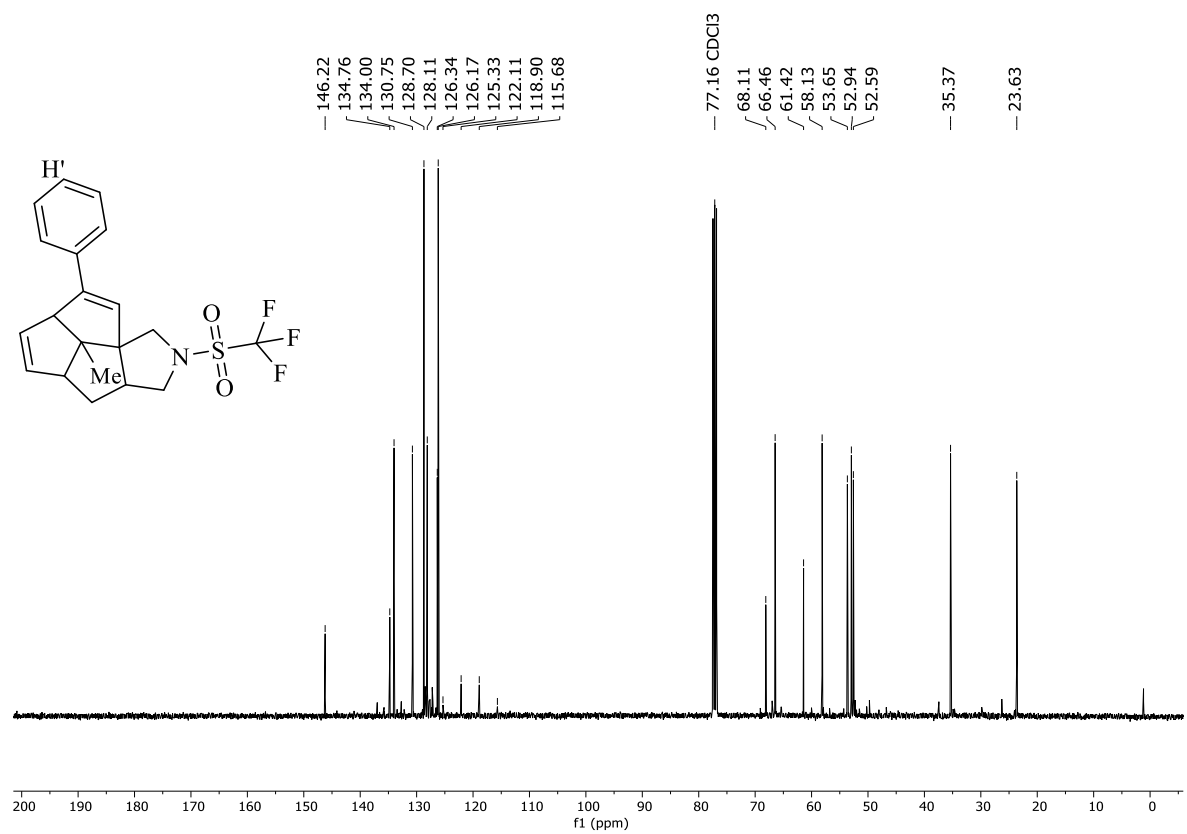
<sup>1</sup>H NMR (400 MHz, CDCl<sub>3</sub>) spectrum of **241**<sup>13</sup>C NMR (101 MHz, CDCl<sub>3</sub>) spectrum of **241**



<sup>1</sup>H NMR (600 MHz, CDCl<sub>3</sub>) spectrum of **243**<sup>13</sup>C NMR (151 MHz, CDCl<sub>3</sub>) spectrum of **243**

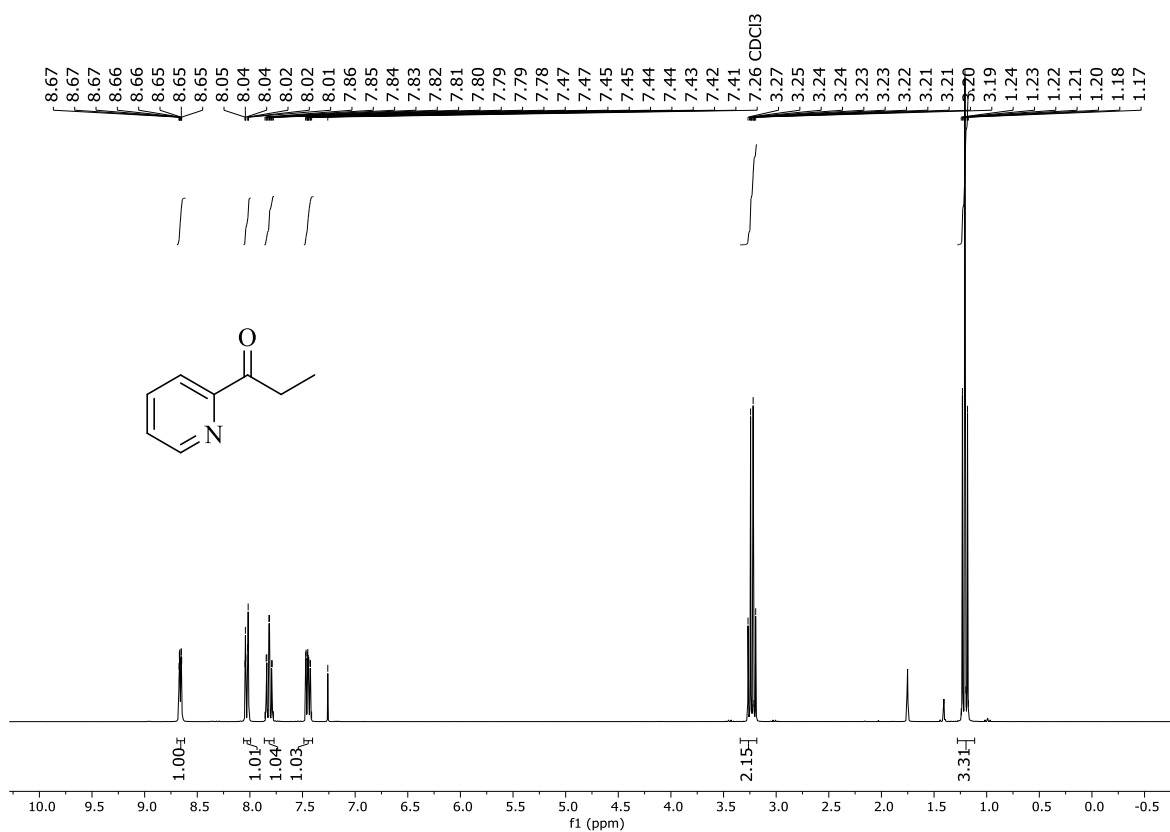
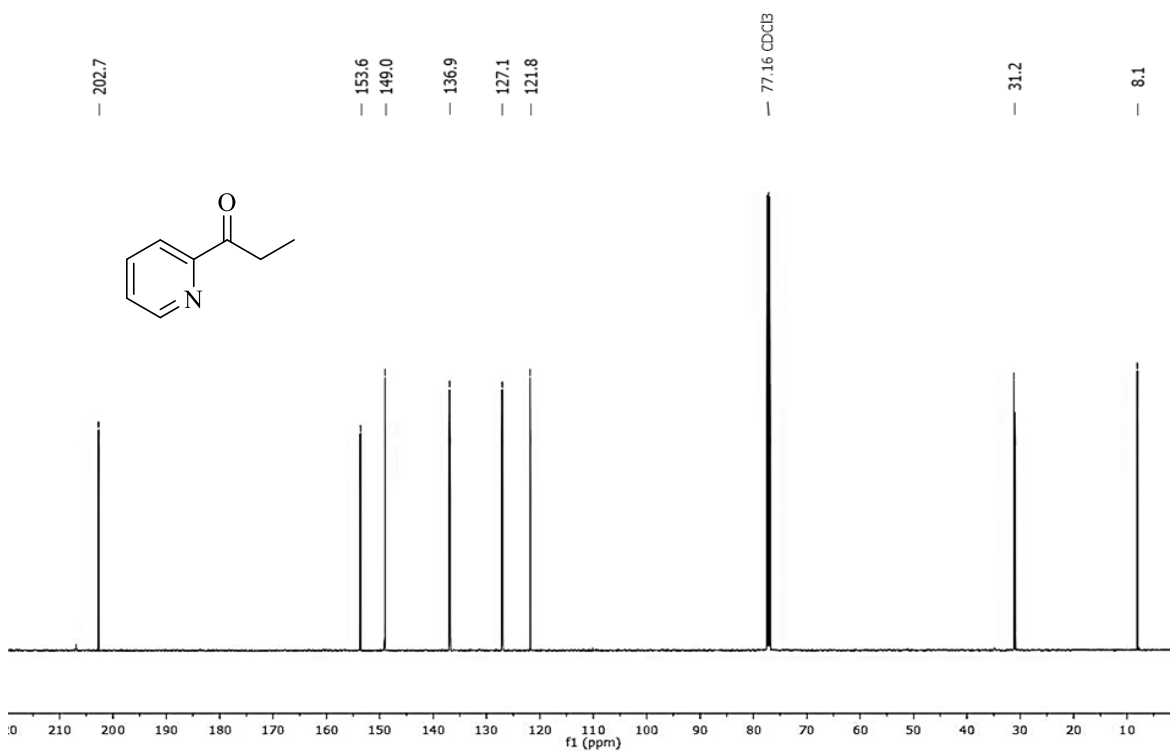


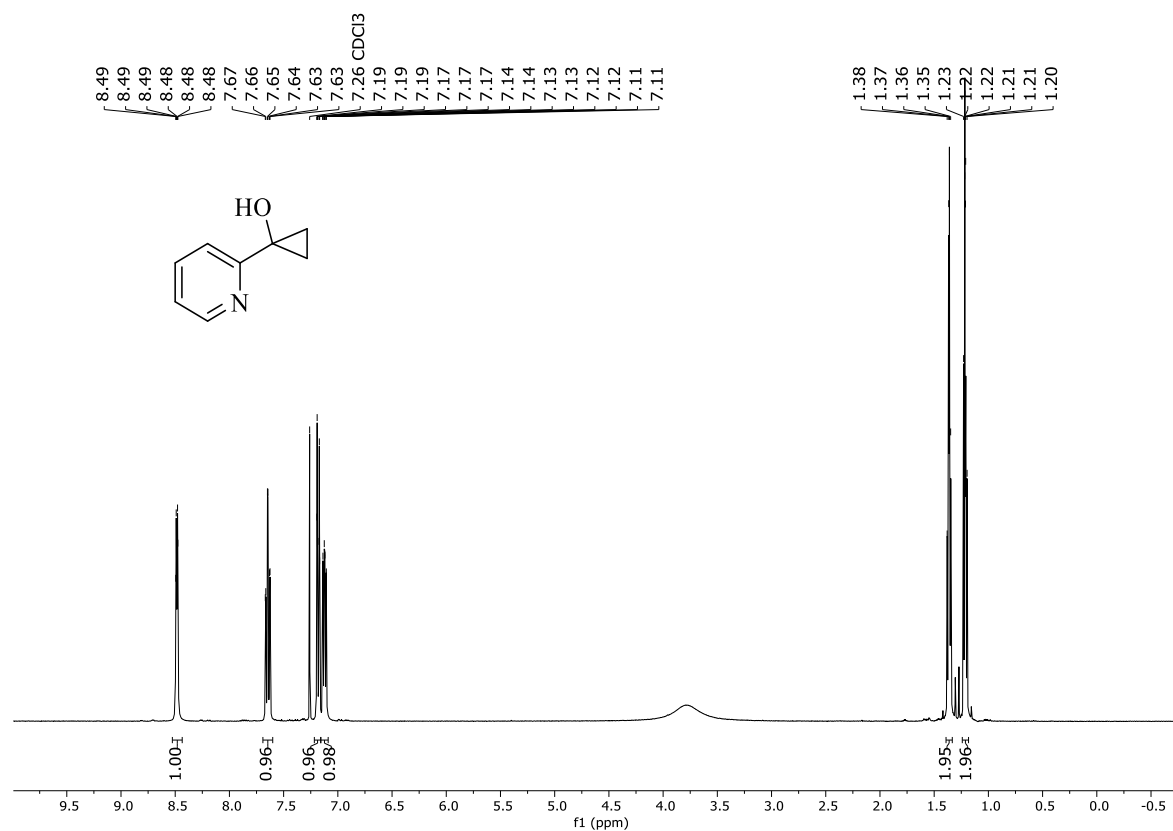
<sup>1</sup>H NMR (600 MHz, CDCl<sub>3</sub>) spectrum of **244**



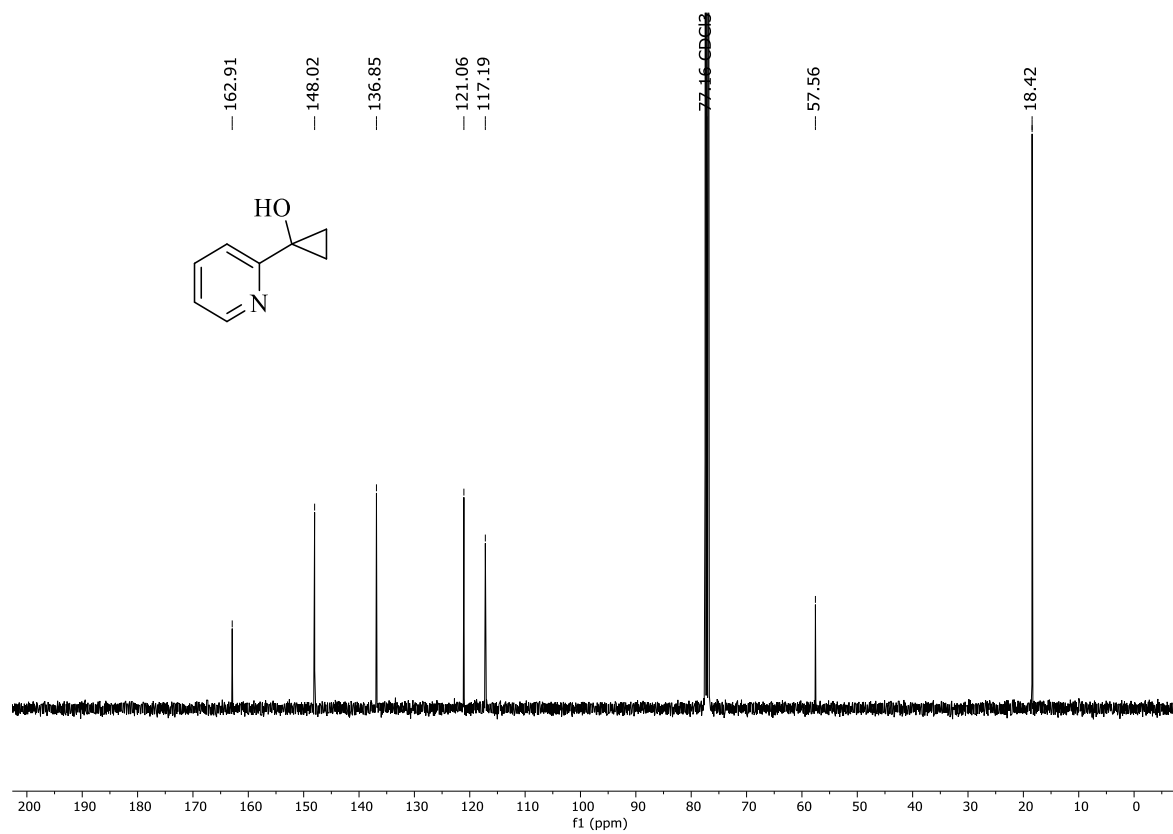
<sup>13</sup>C NMR (151 MHz, CDCl<sub>3</sub>) spectrum of **244**

## 6.2.2. Spectra section 2.3.2

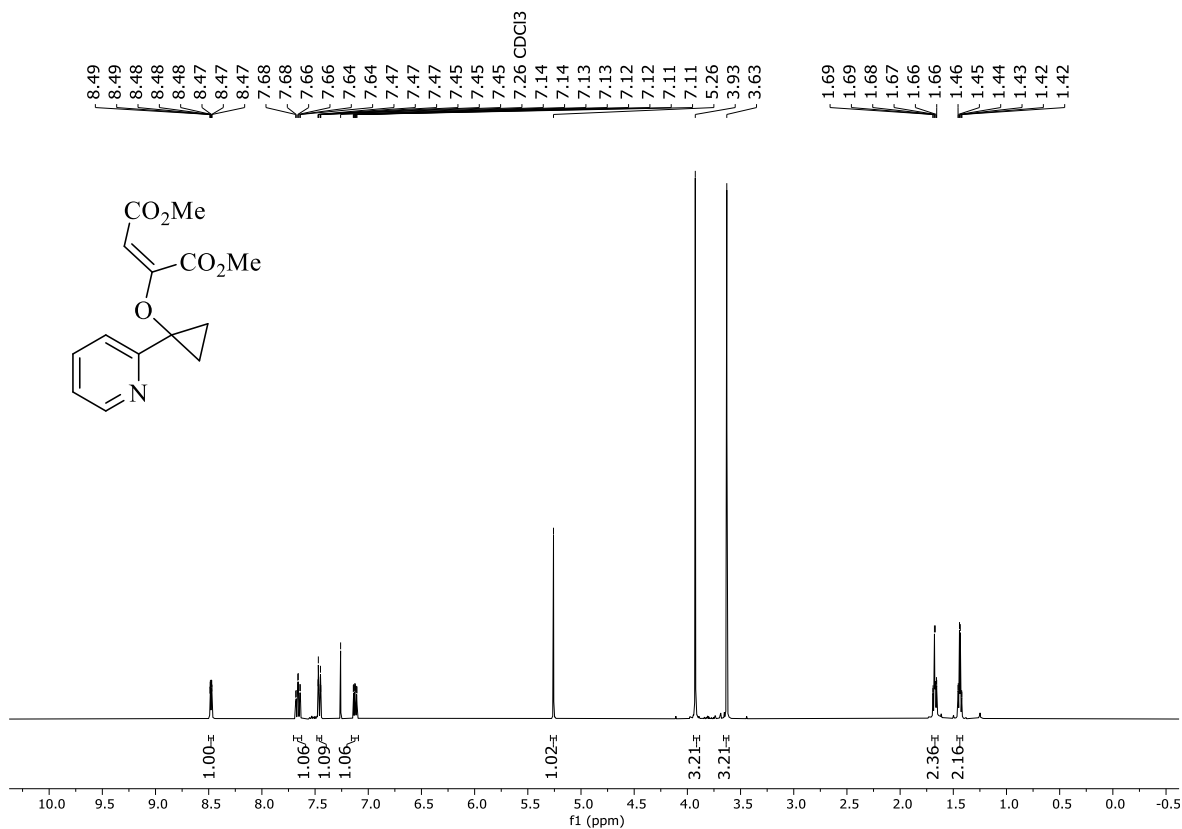
<sup>1</sup>H NMR (400 MHz, CDCl<sub>3</sub>) spectrum of **244**<sup>13</sup>C NMR (101 MHz, CDCl<sub>3</sub>) spectrum of **244**



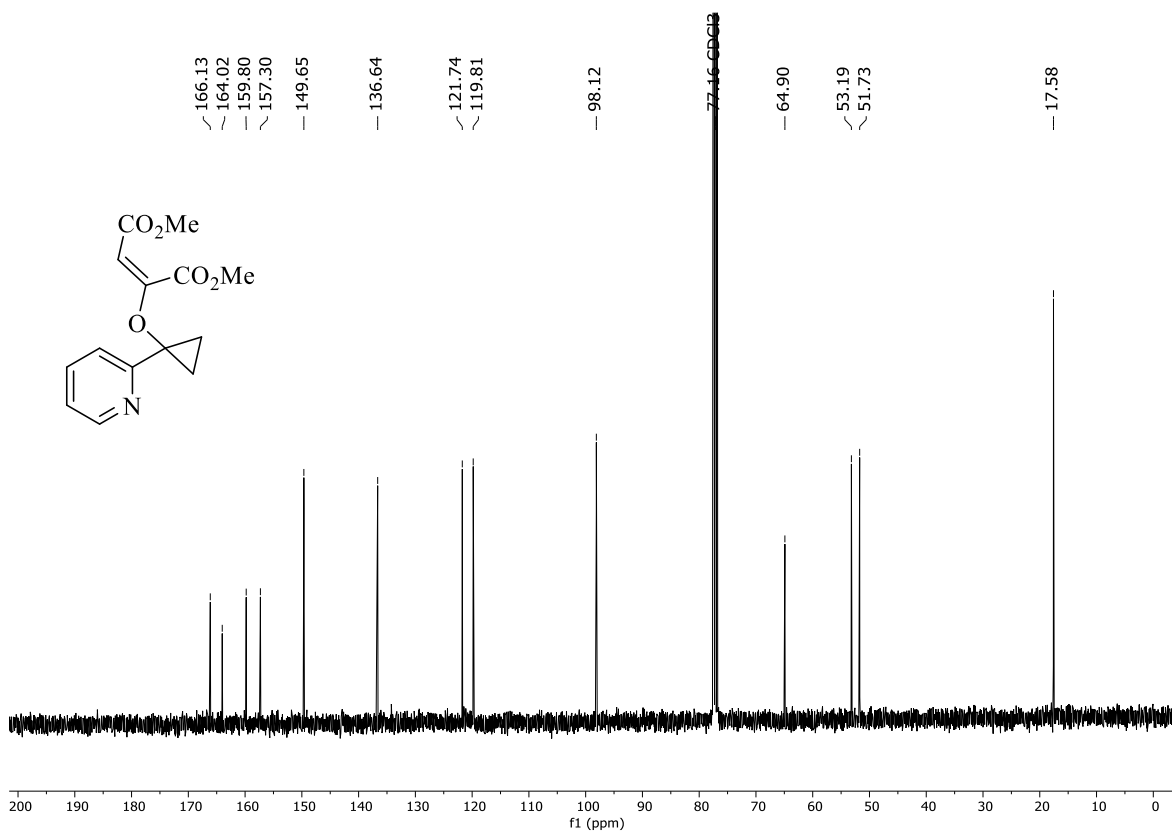
<sup>1</sup>H NMR (400 MHz, CDCl<sub>3</sub>) spectrum of **221**



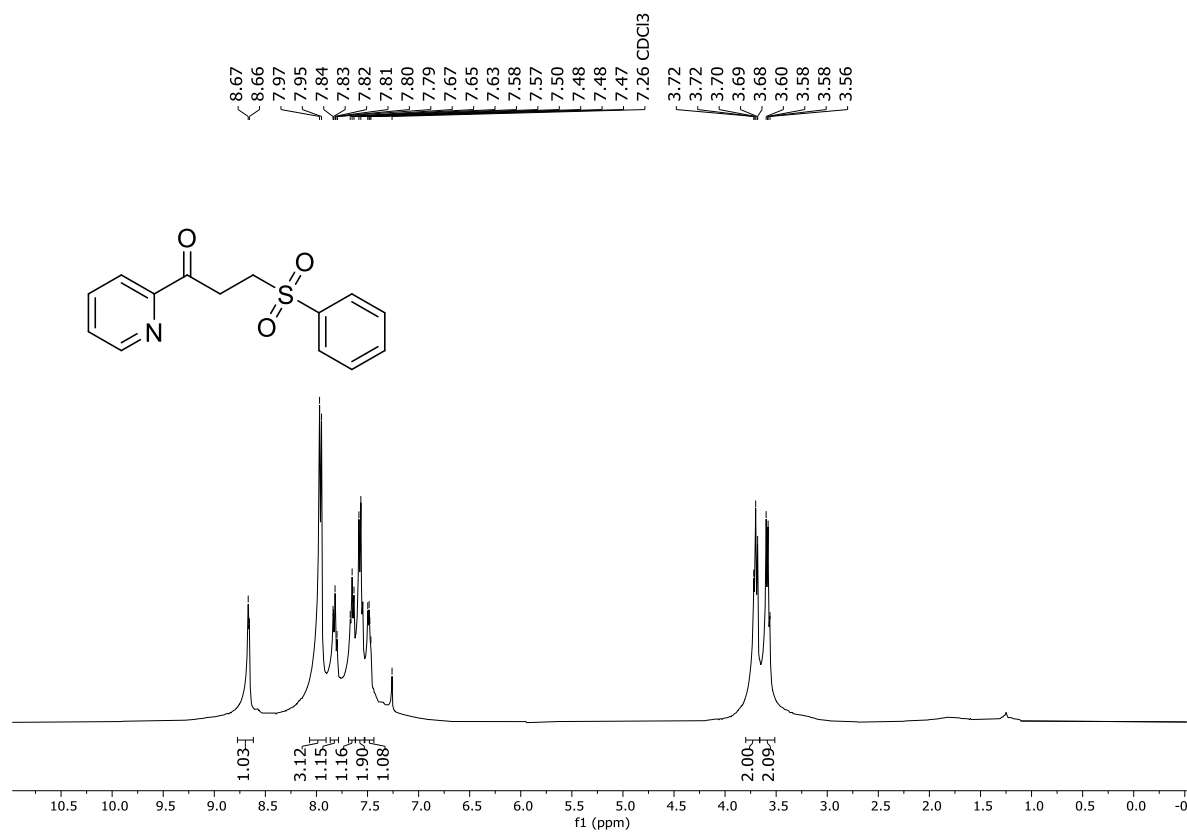
<sup>13</sup>C NMR (101 MHz, CDCl<sub>3</sub>) spectrum of **221**



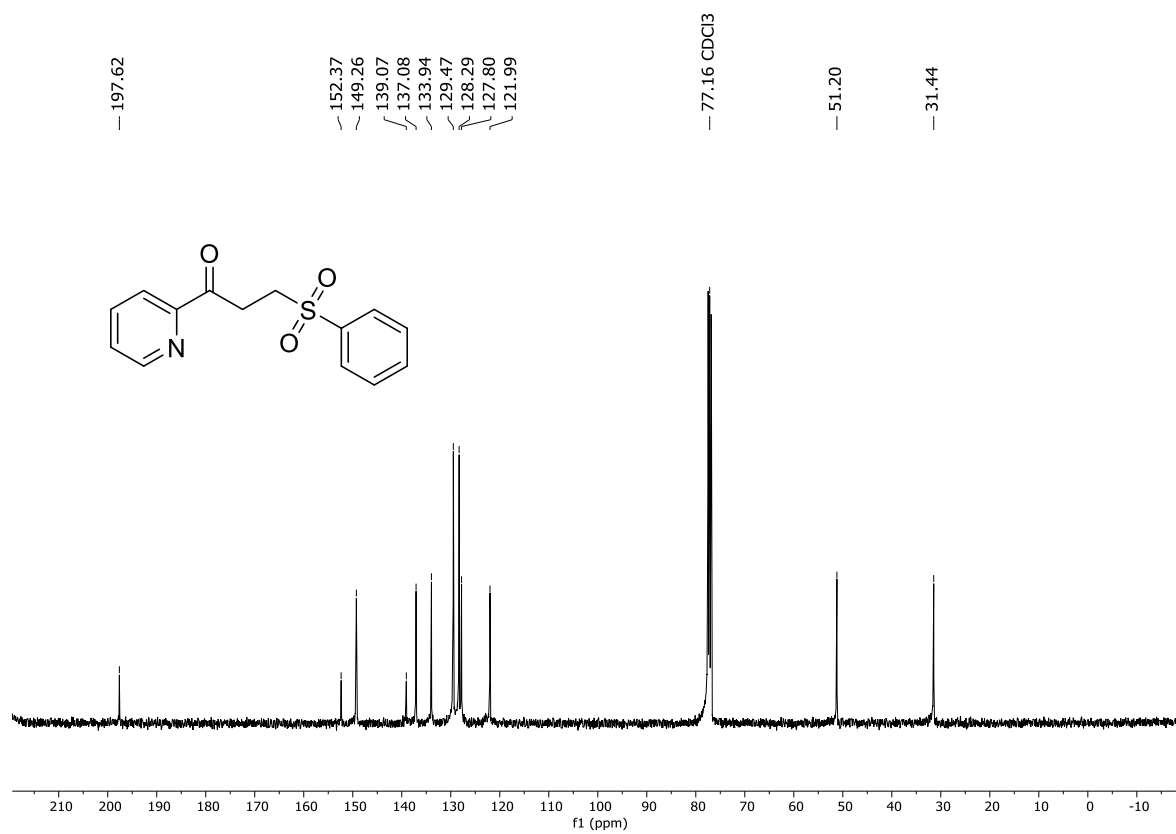
<sup>1</sup>H NMR (400 MHz, CDCl<sub>3</sub>) spectrum of **251**



<sup>13</sup>C NMR (101 MHz, CDCl<sub>3</sub>) spectrum of **251**

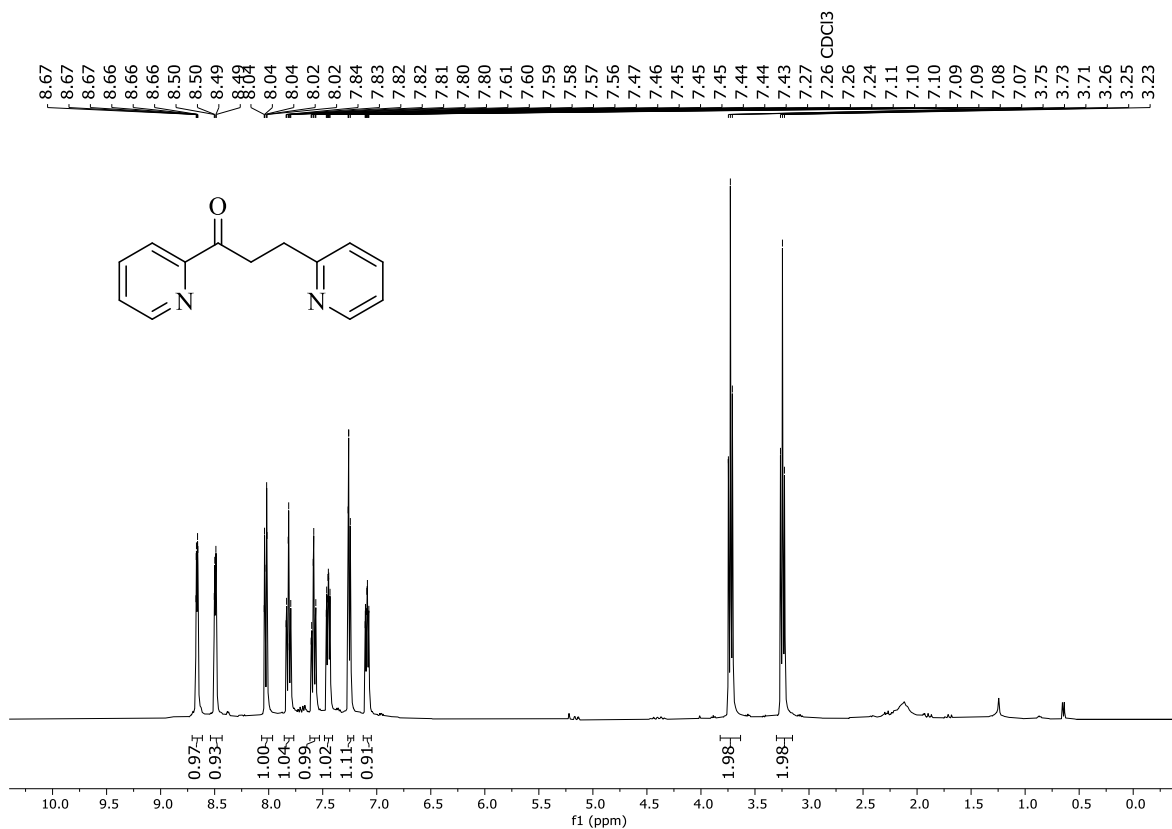


<sup>1</sup>H NMR (400 MHz, CDCl<sub>3</sub>) spectrum of **227d'**

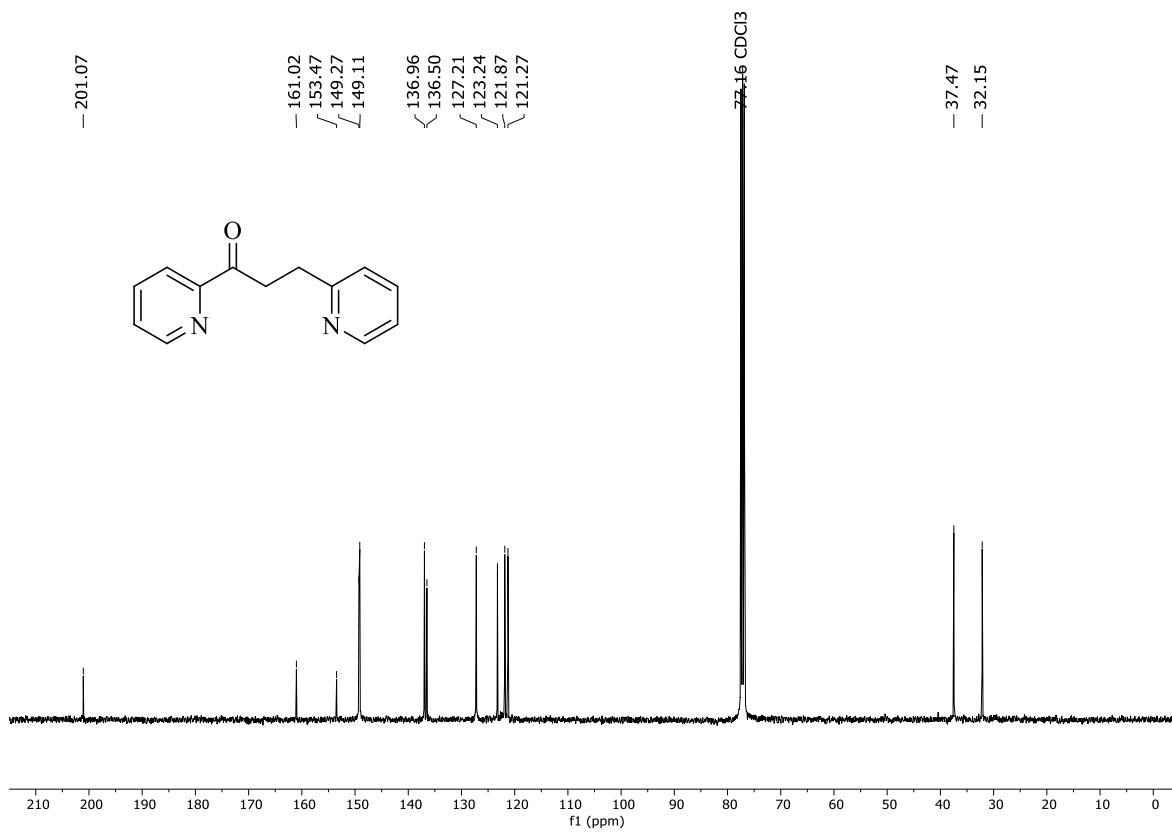


<sup>13</sup>C NMR (101 MHz, CDCl<sub>3</sub>) spectrum of **227d'**

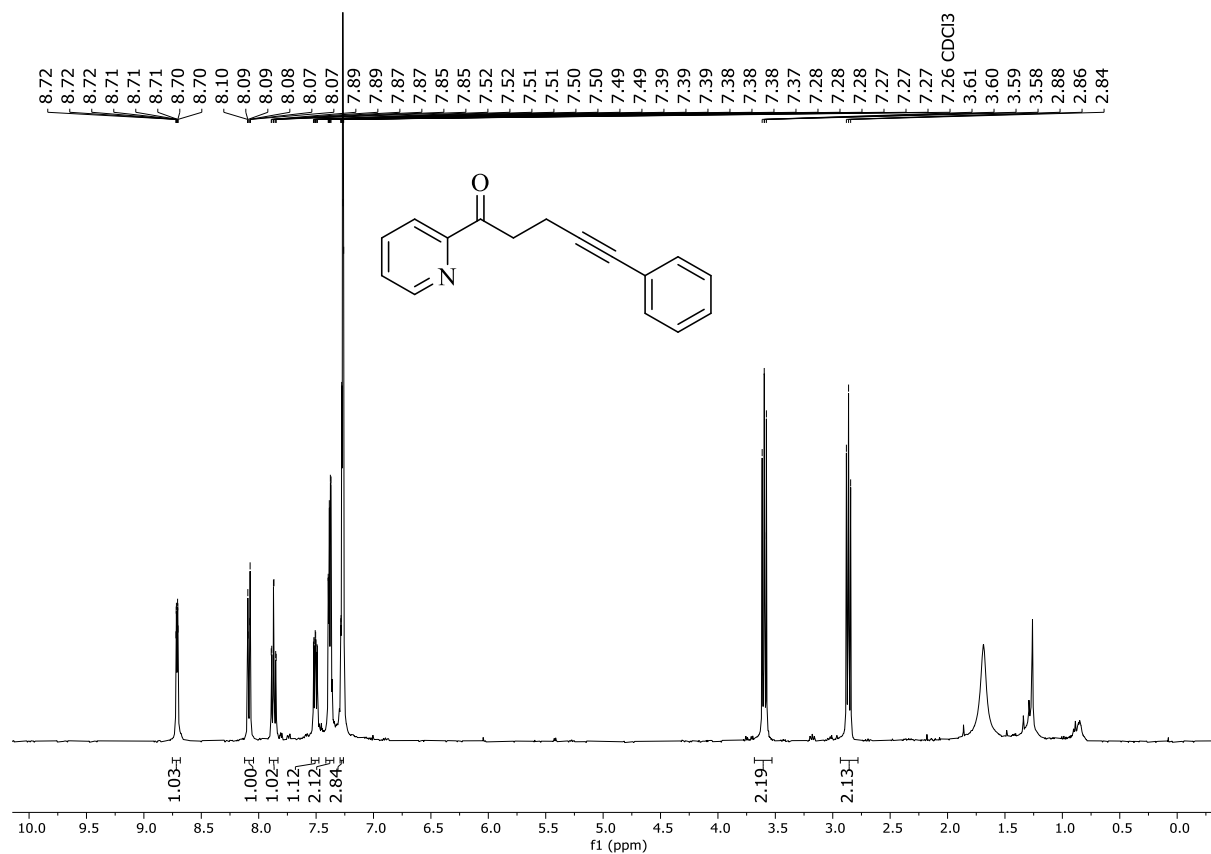




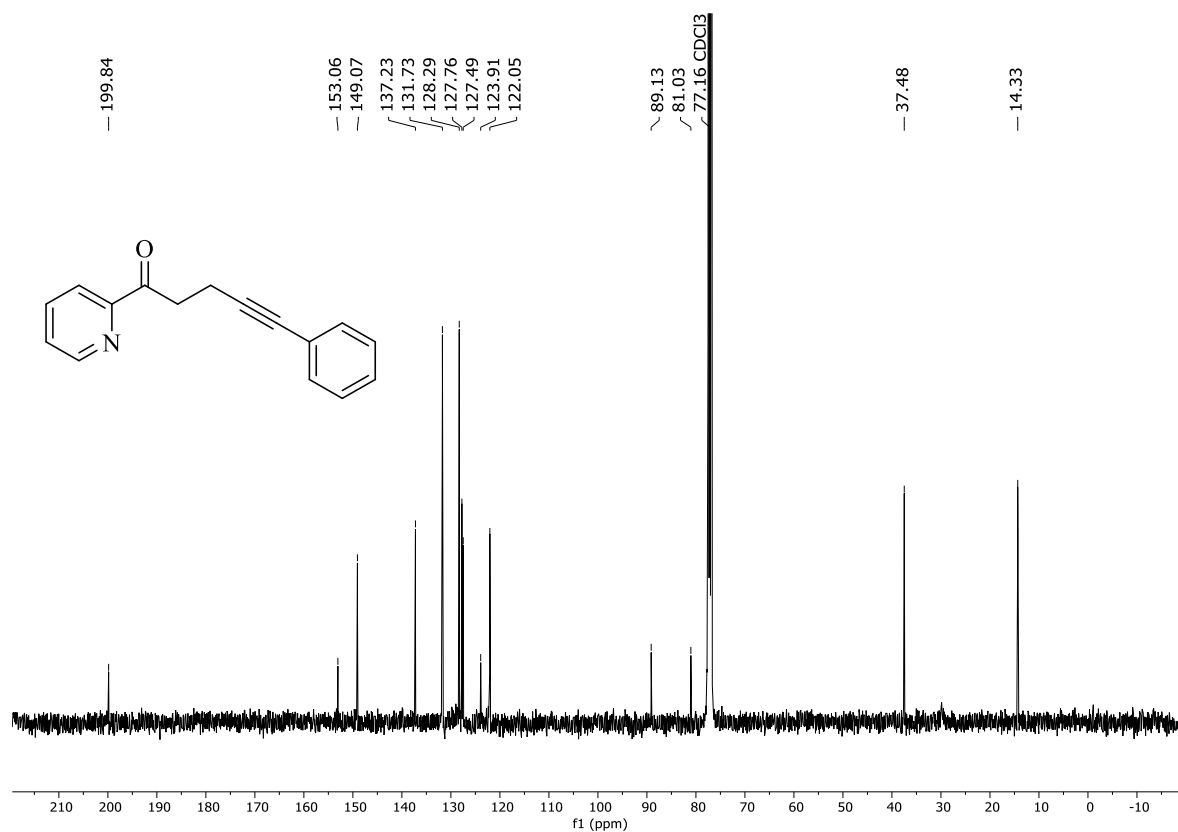
<sup>1</sup>H NMR (400 MHz, CDCl<sub>3</sub>) spectrum of **227g**'



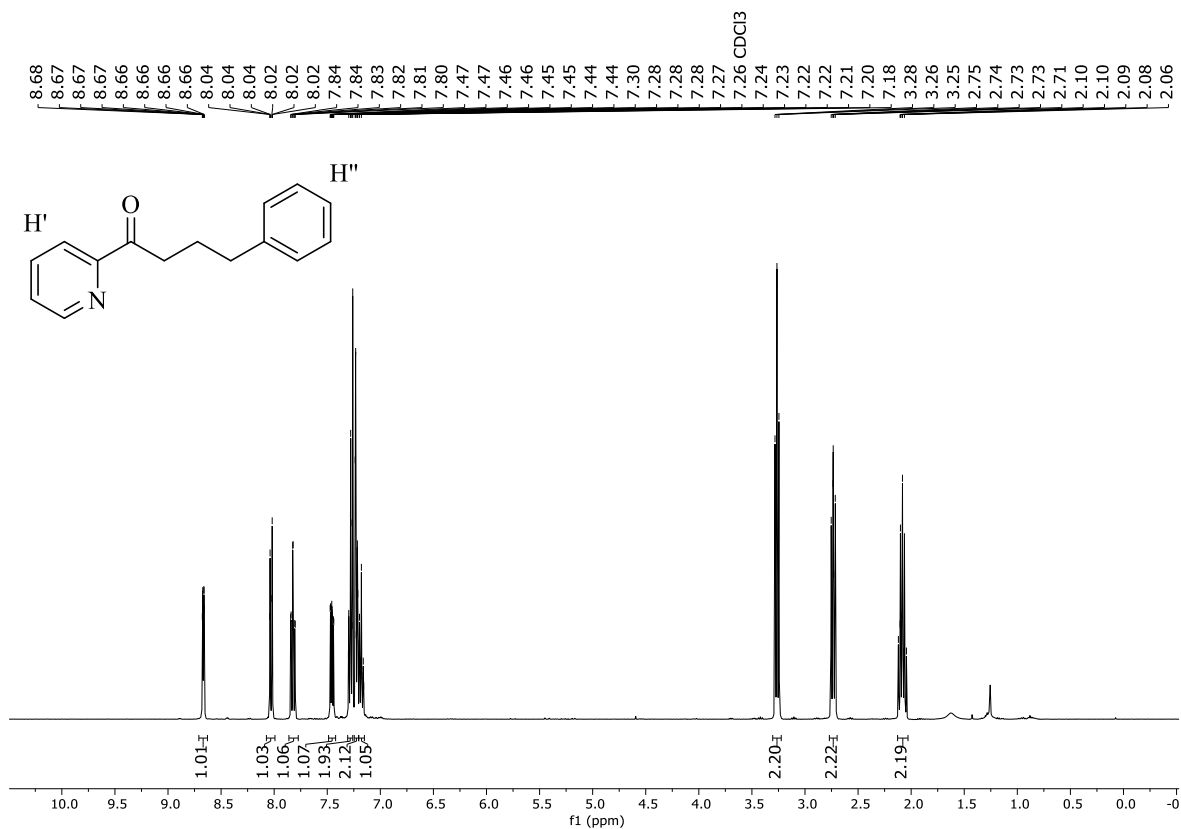
<sup>13</sup>C NMR (101 MHz, CDCl<sub>3</sub>) spectrum of **227g**'



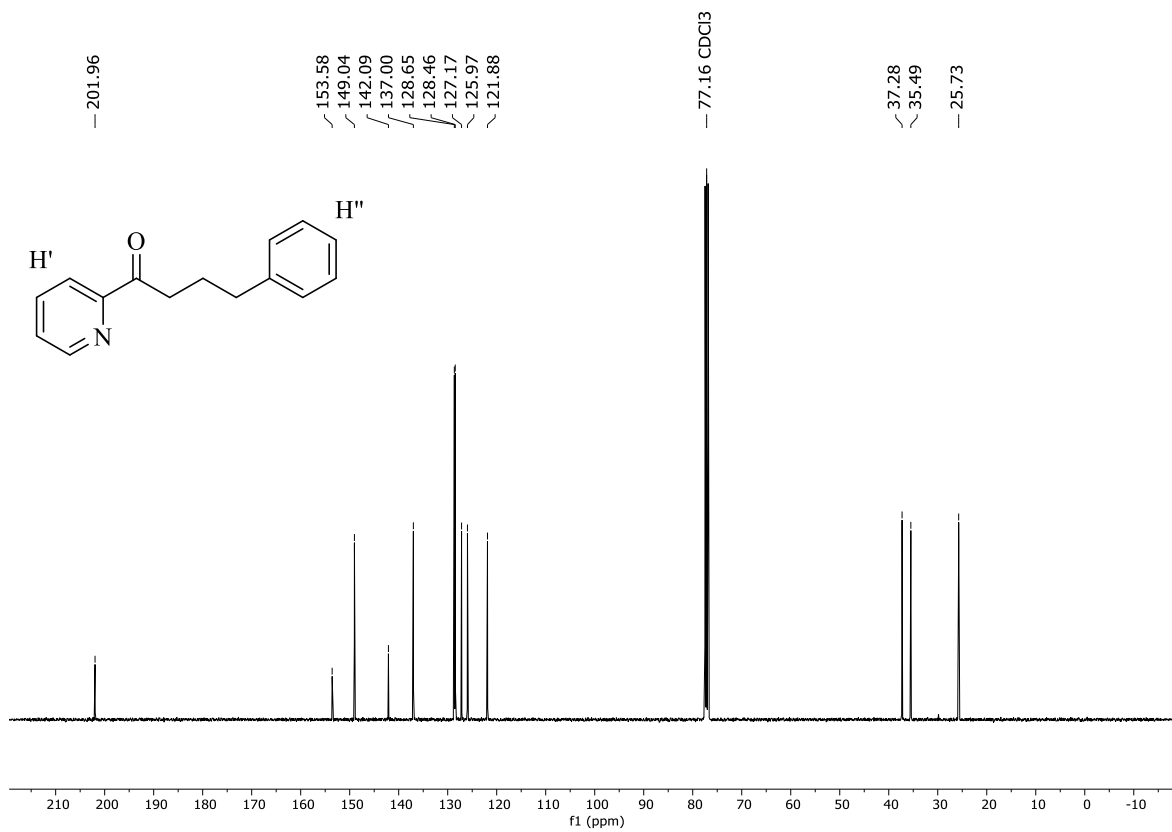
<sup>1</sup>H NMR (400 MHz, CDCl<sub>3</sub>) spectrum of **227j**



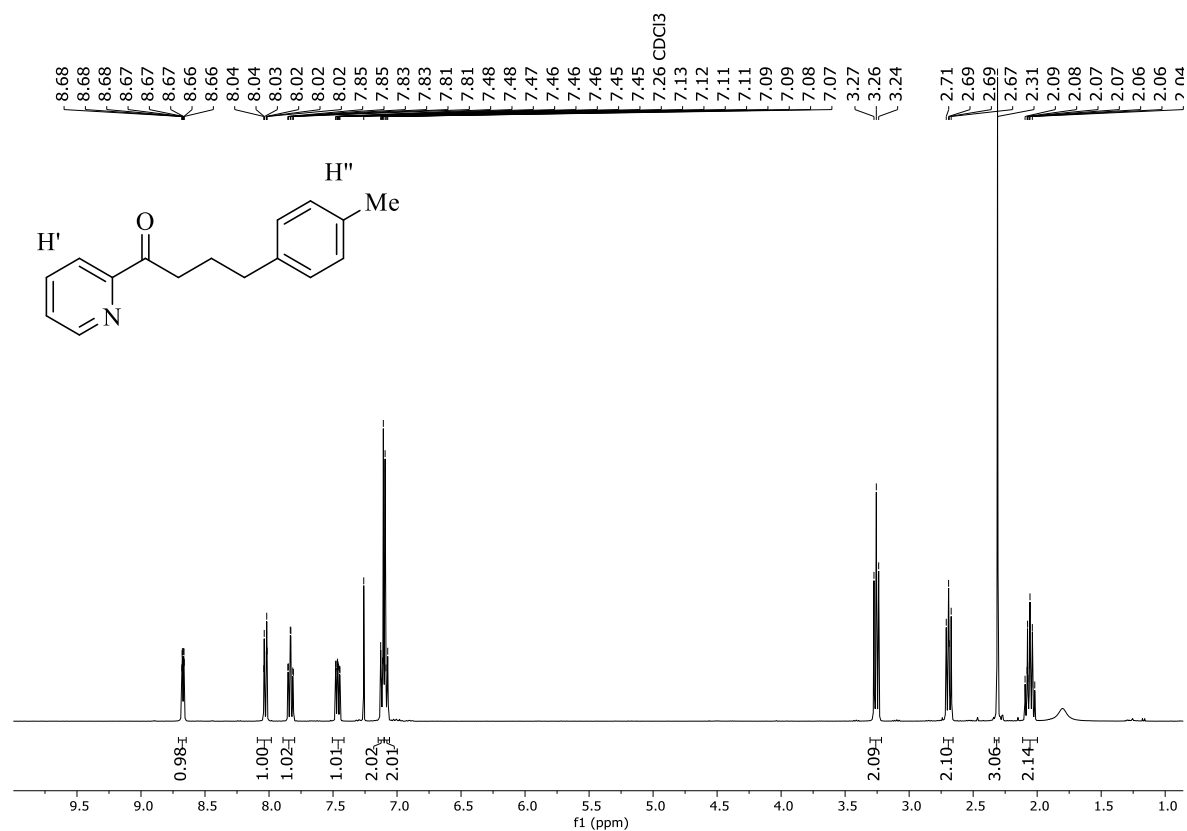
<sup>13</sup>C NMR (101 MHz, CDCl<sub>3</sub>) spectrum of **227j**



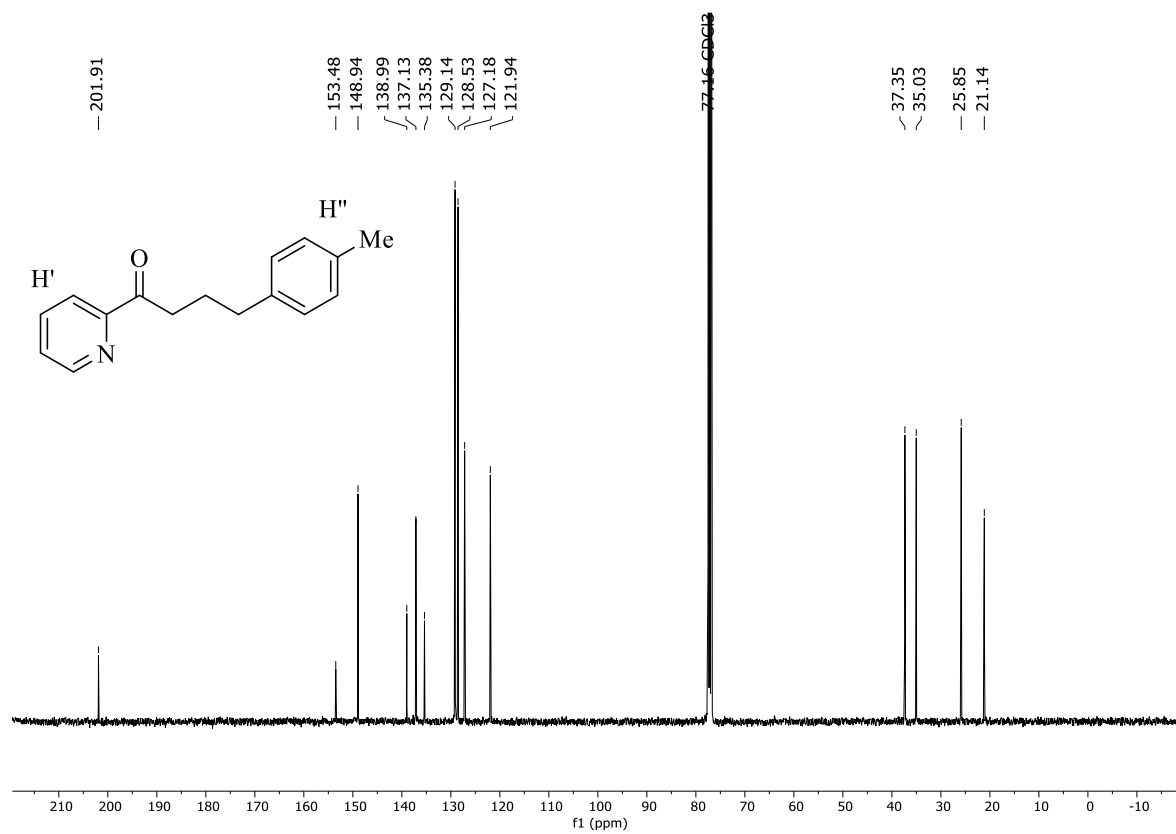
**<sup>1</sup>H NMR (400 MHz, CDCl<sub>3</sub>) spectrum of **227a****



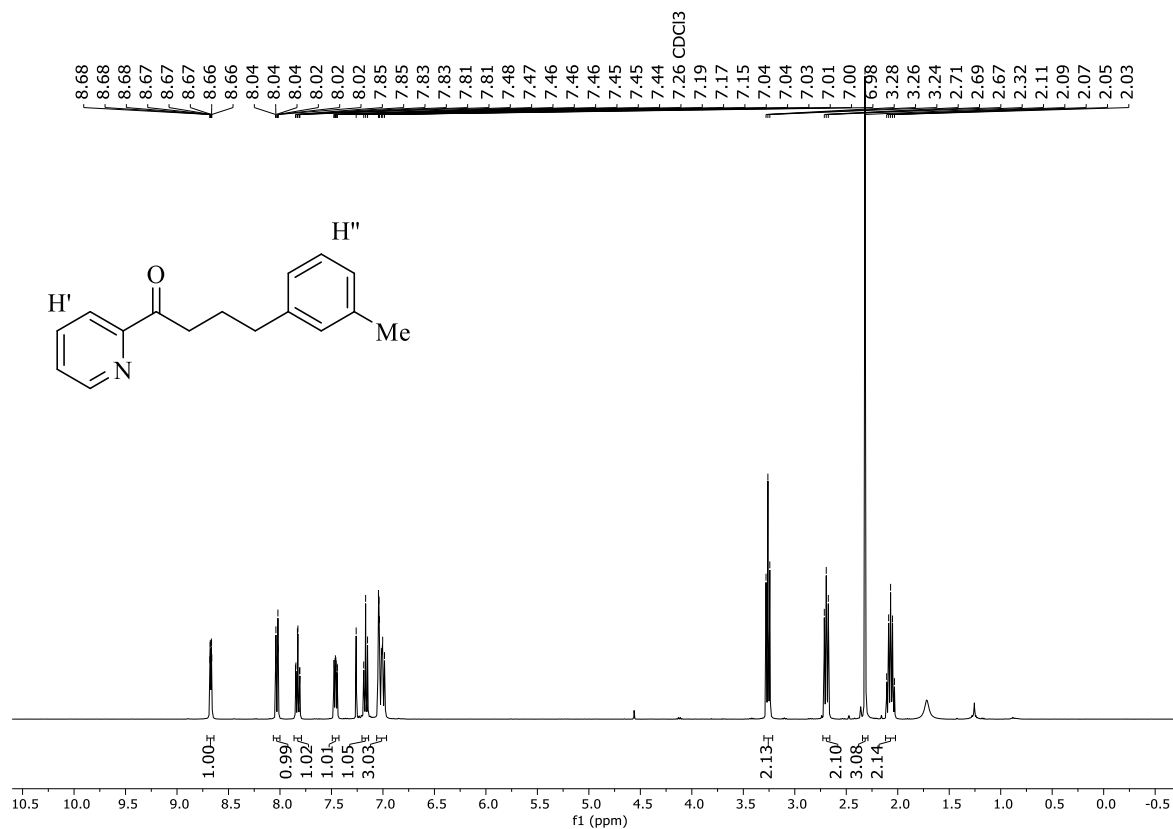
**<sup>13</sup>C NMR (101 MHz, CDCl<sub>3</sub>) spectrum of **227a****



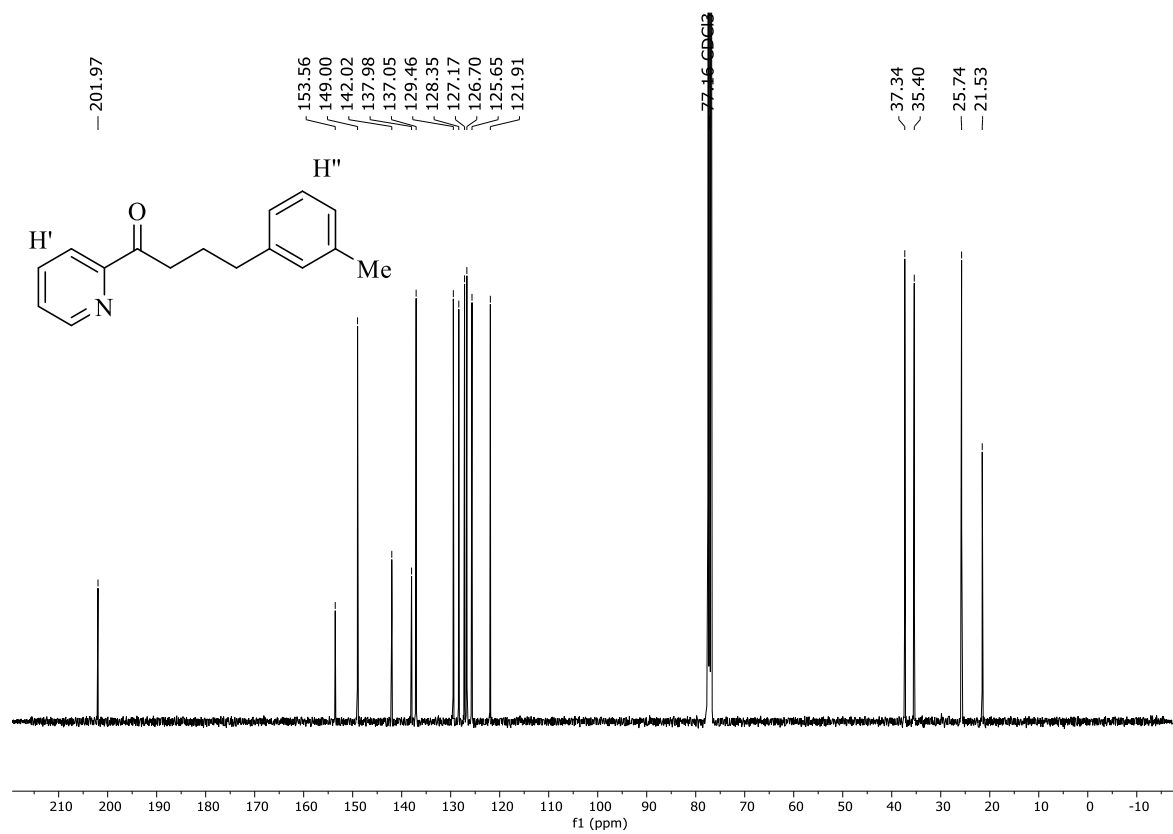
<sup>1</sup>H NMR (400 MHz, CDCl<sub>3</sub>) spectrum of **227b**



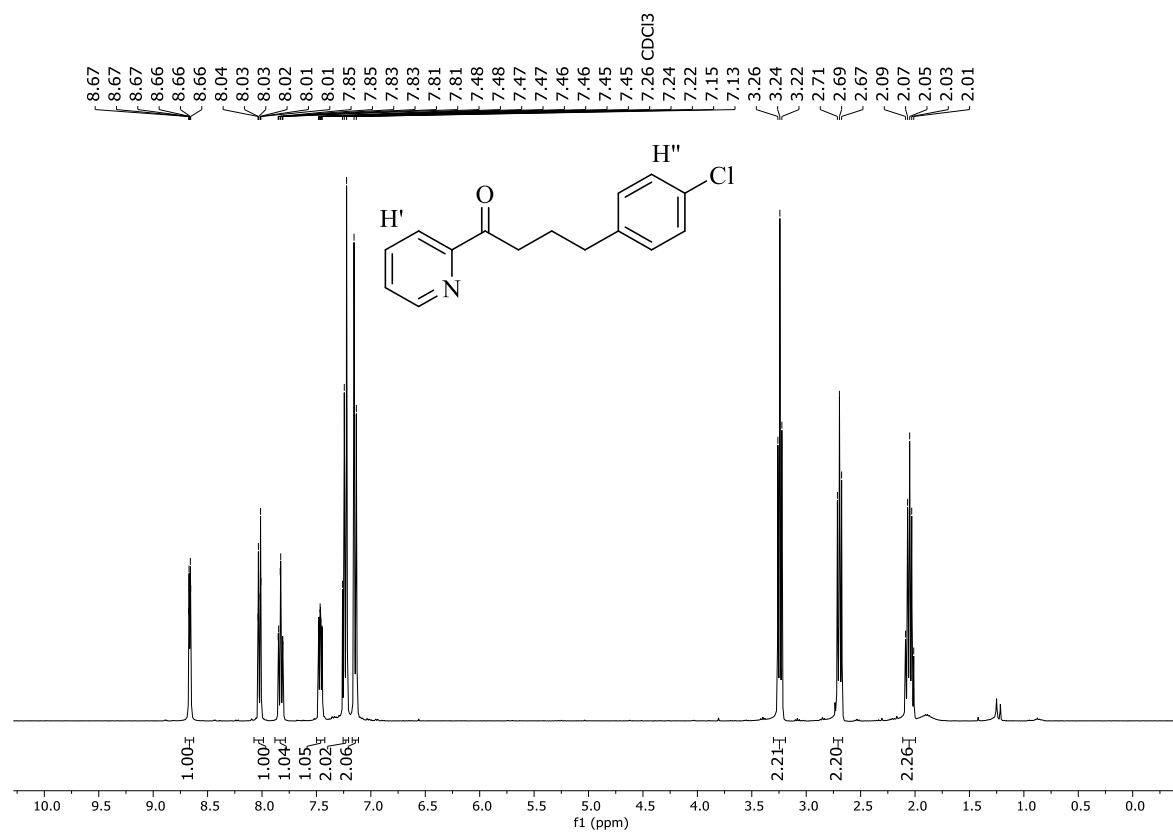
<sup>13</sup>C NMR (101 MHz, CDCl<sub>3</sub>) spectrum of **227b**



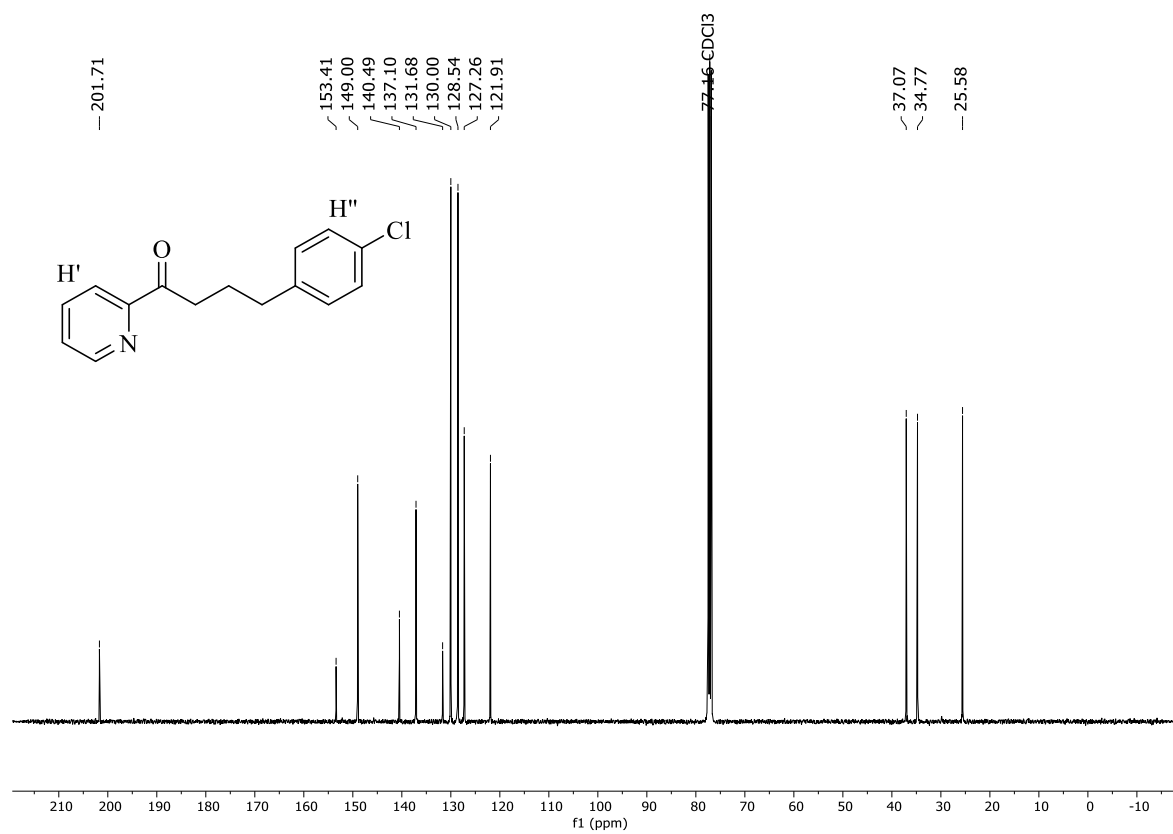
**<sup>1</sup>H NMR (400 MHz, CDCl<sub>3</sub>) spectrum of **227c****



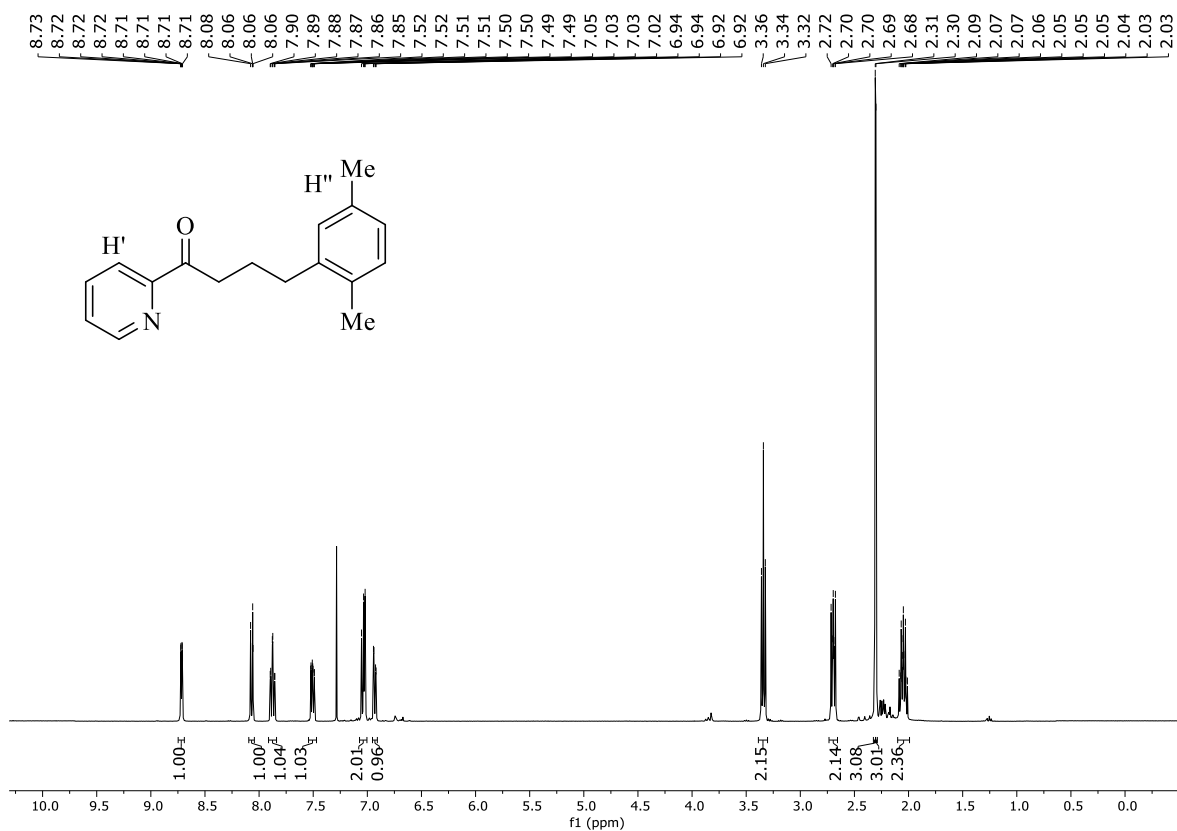
**<sup>13</sup>C NMR (101 MHz, CDCl<sub>3</sub>) spectrum of **227c****



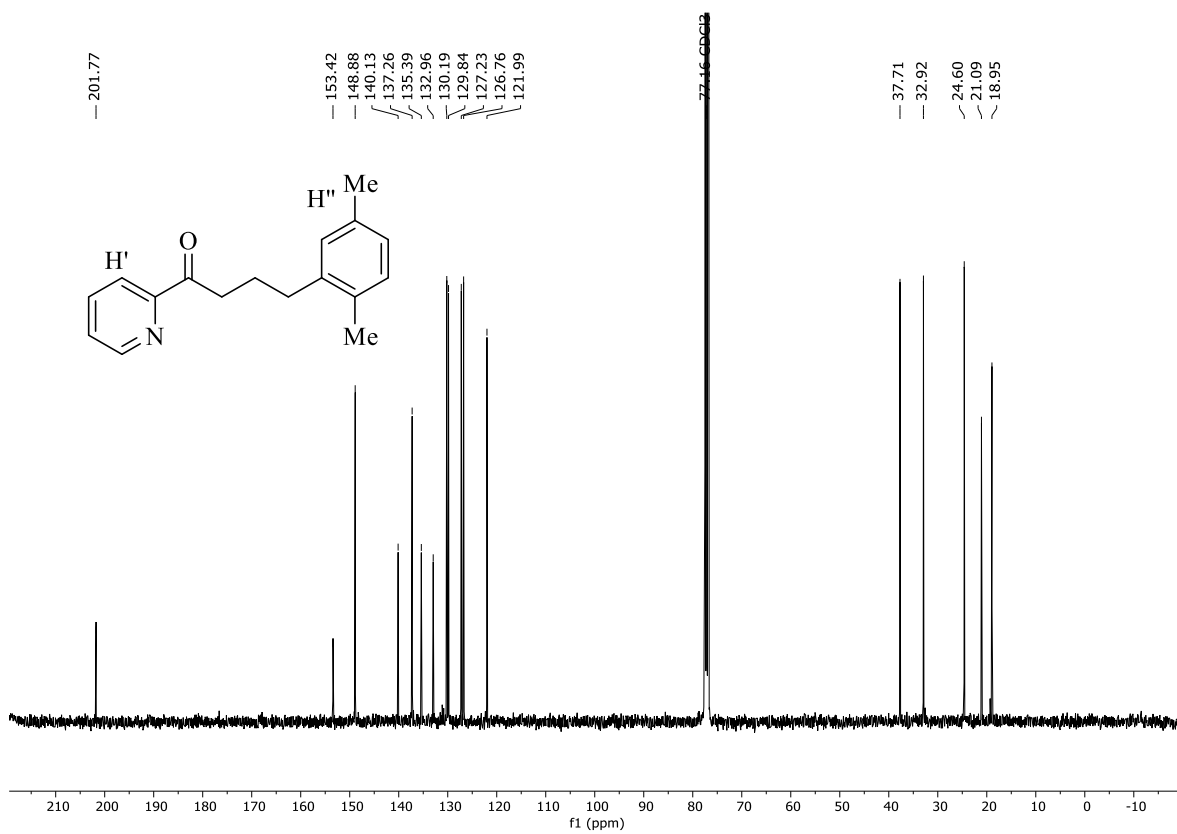
<sup>1</sup>H NMR (400 MHz, CDCl<sub>3</sub>) spectrum of **227d**



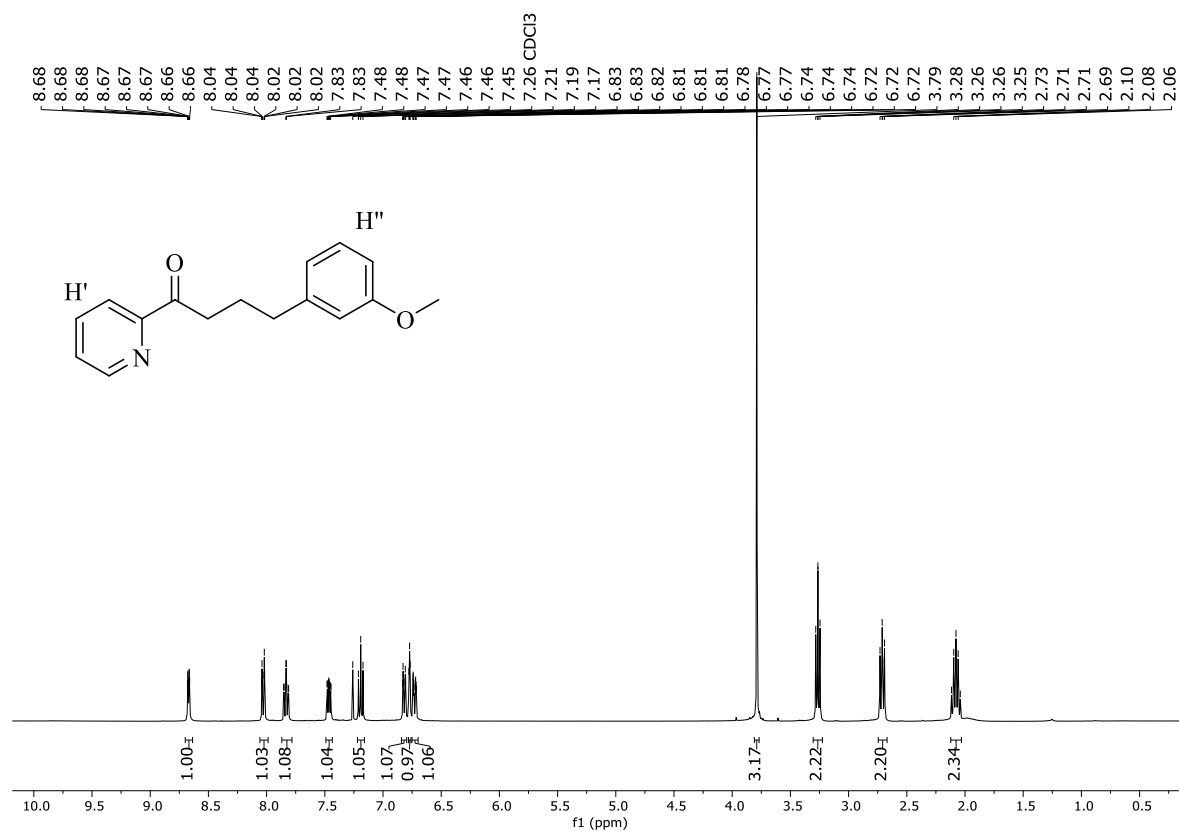
<sup>13</sup>C NMR (101 MHz, CDCl<sub>3</sub>) spectrum of **227d**



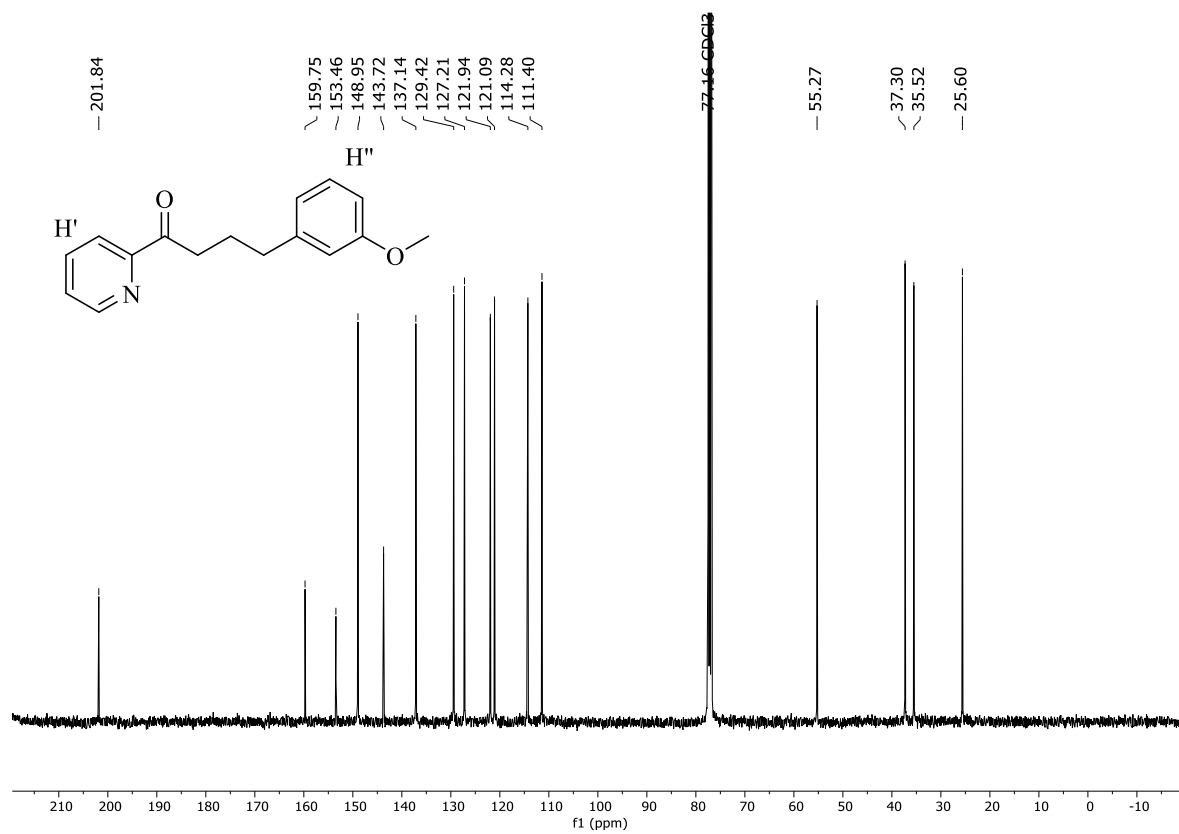
**<sup>1</sup>H NMR (400 MHz, CDCl<sub>3</sub>) spectrum of **227e****



**<sup>13</sup>C NMR (101 MHz, CDCl<sub>3</sub>) spectrum of **227e****

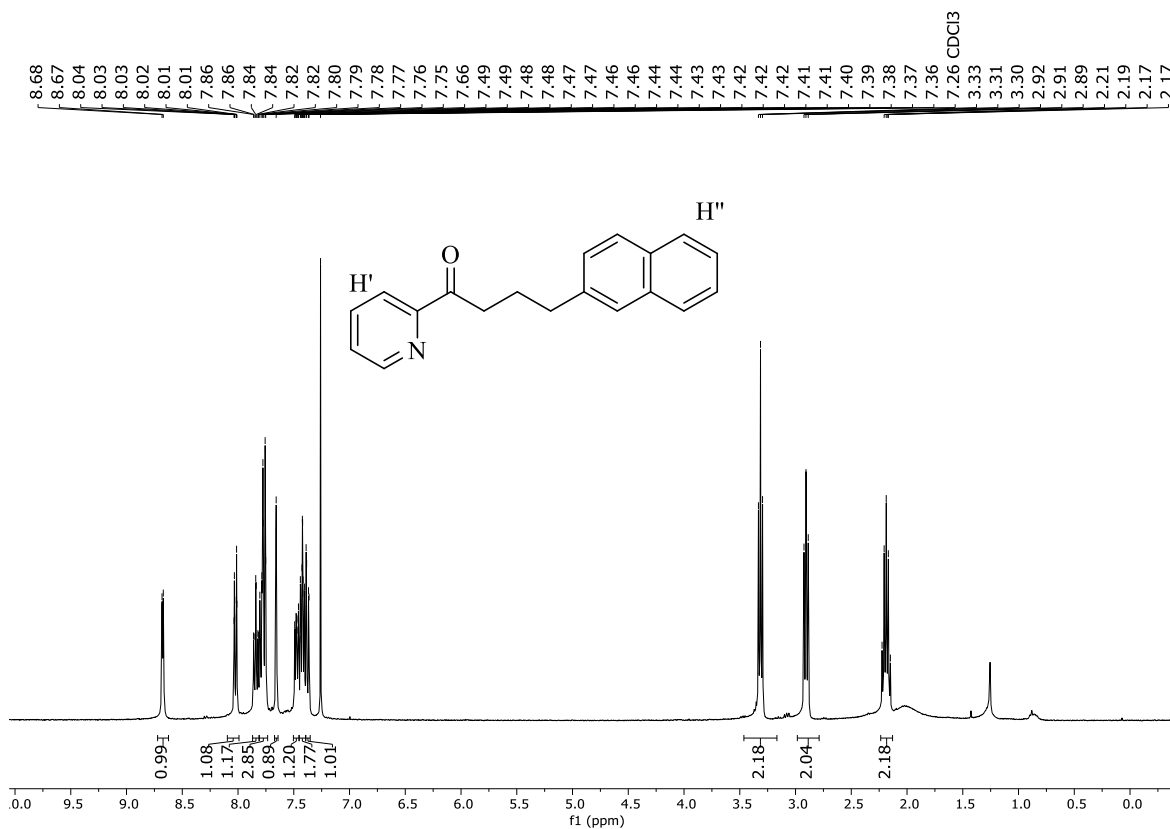


<sup>1</sup>H NMR (400 MHz, CDCl<sub>3</sub>) spectrum of **227f**

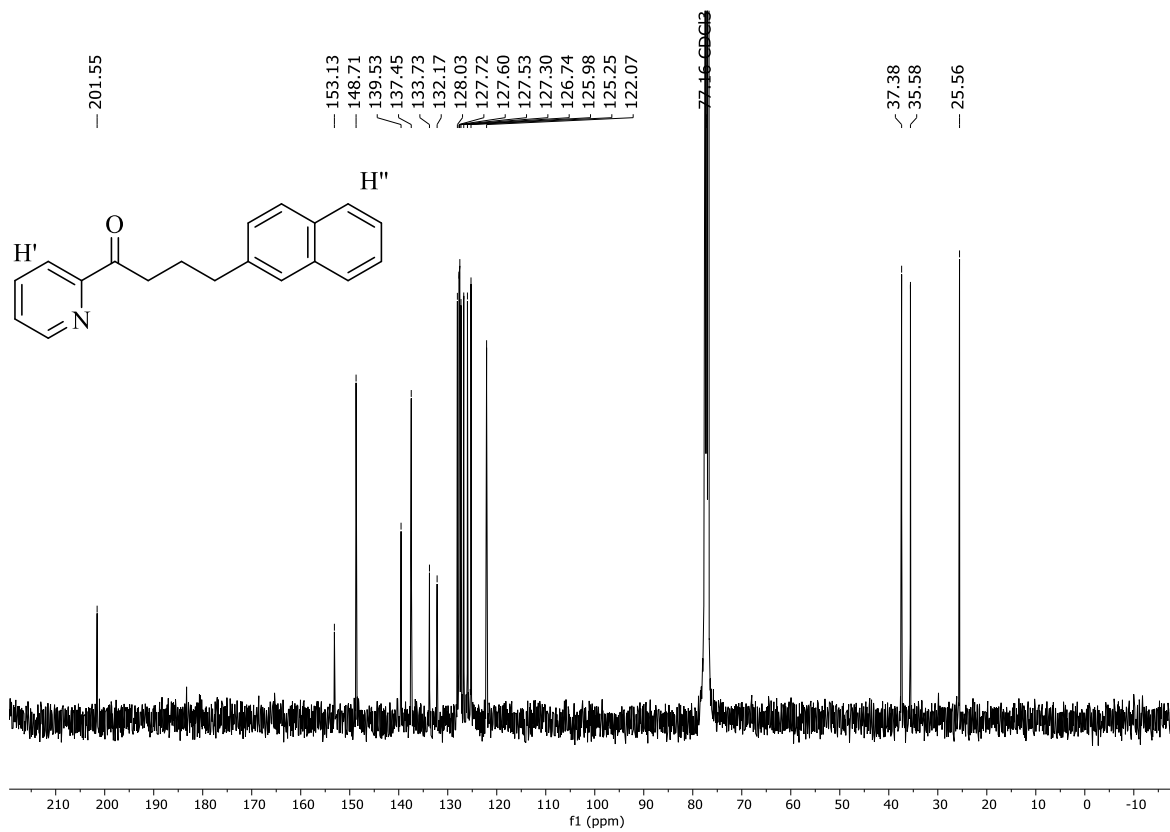


<sup>13</sup>C NMR (101 MHz, CDCl<sub>3</sub>) spectrum of **227f**

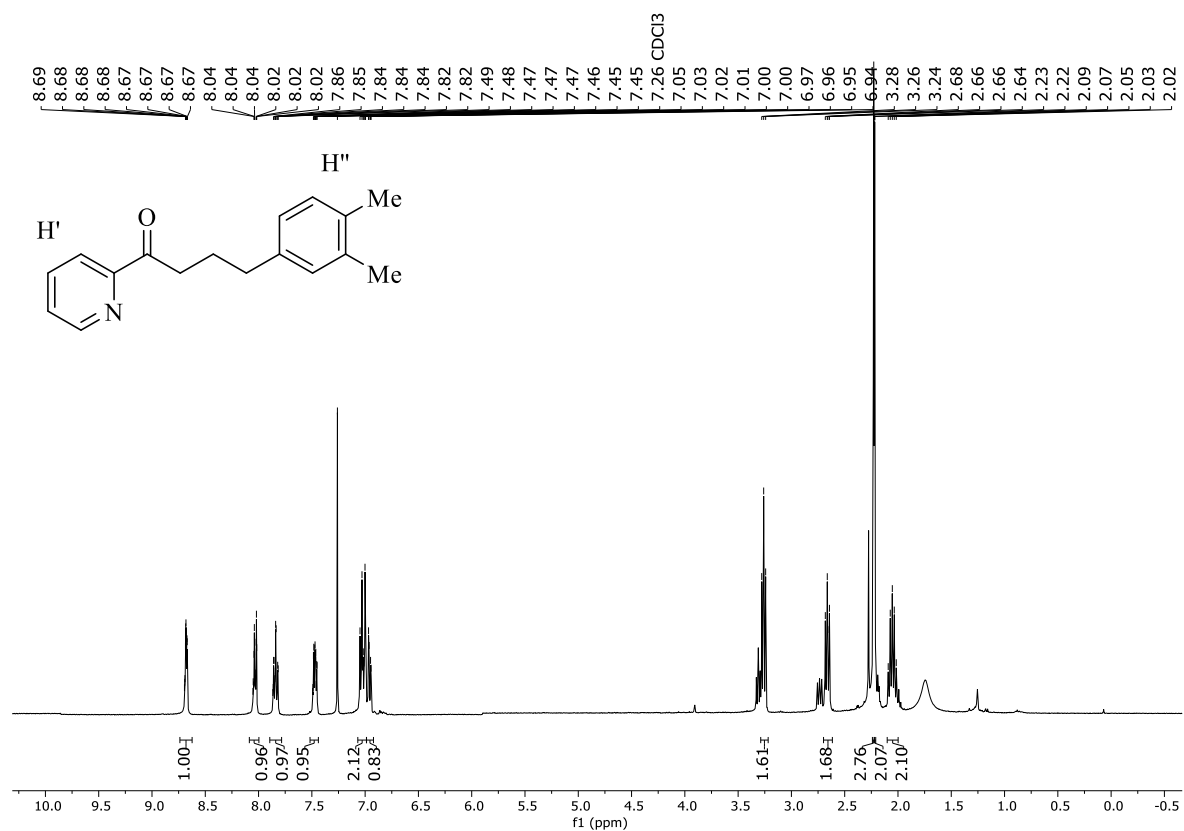




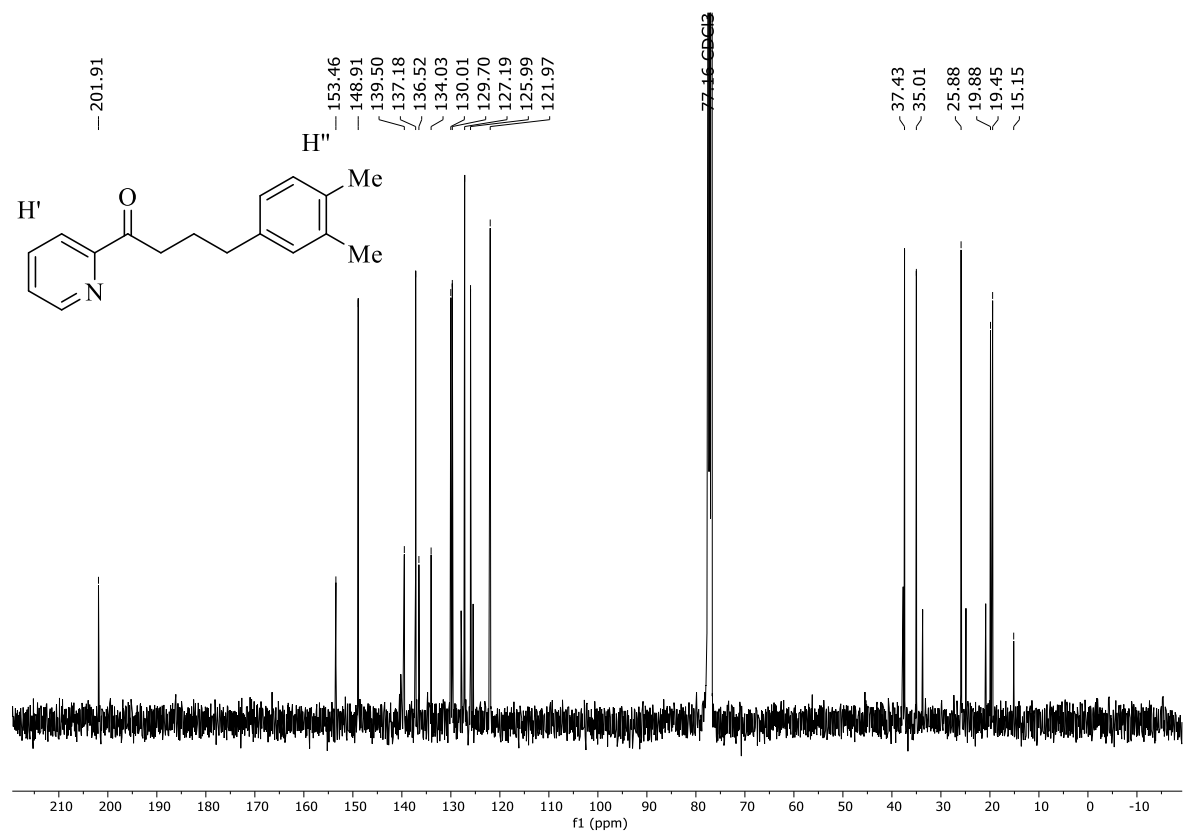
<sup>1</sup>H NMR (400 MHz, CDCl<sub>3</sub>) spectrum of **227g**



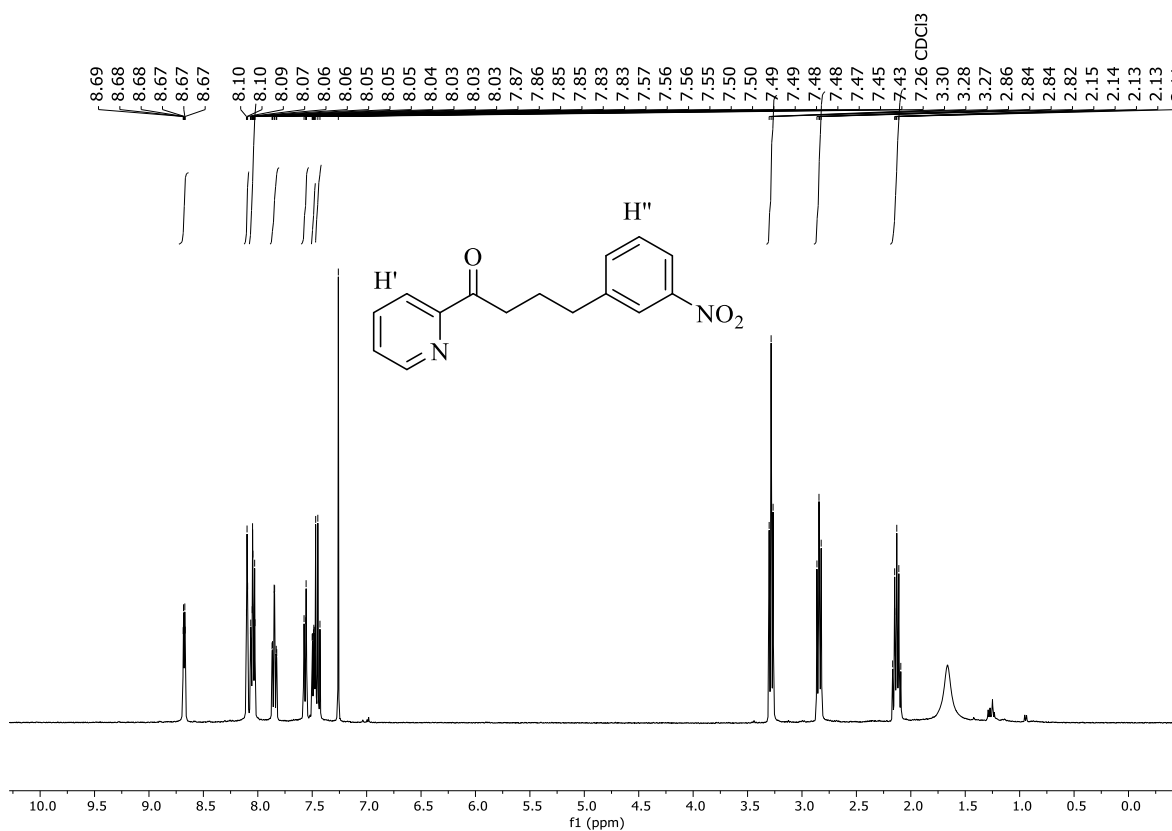
<sup>13</sup>C NMR (101 MHz, CDCl<sub>3</sub>) spectrum of **227g**



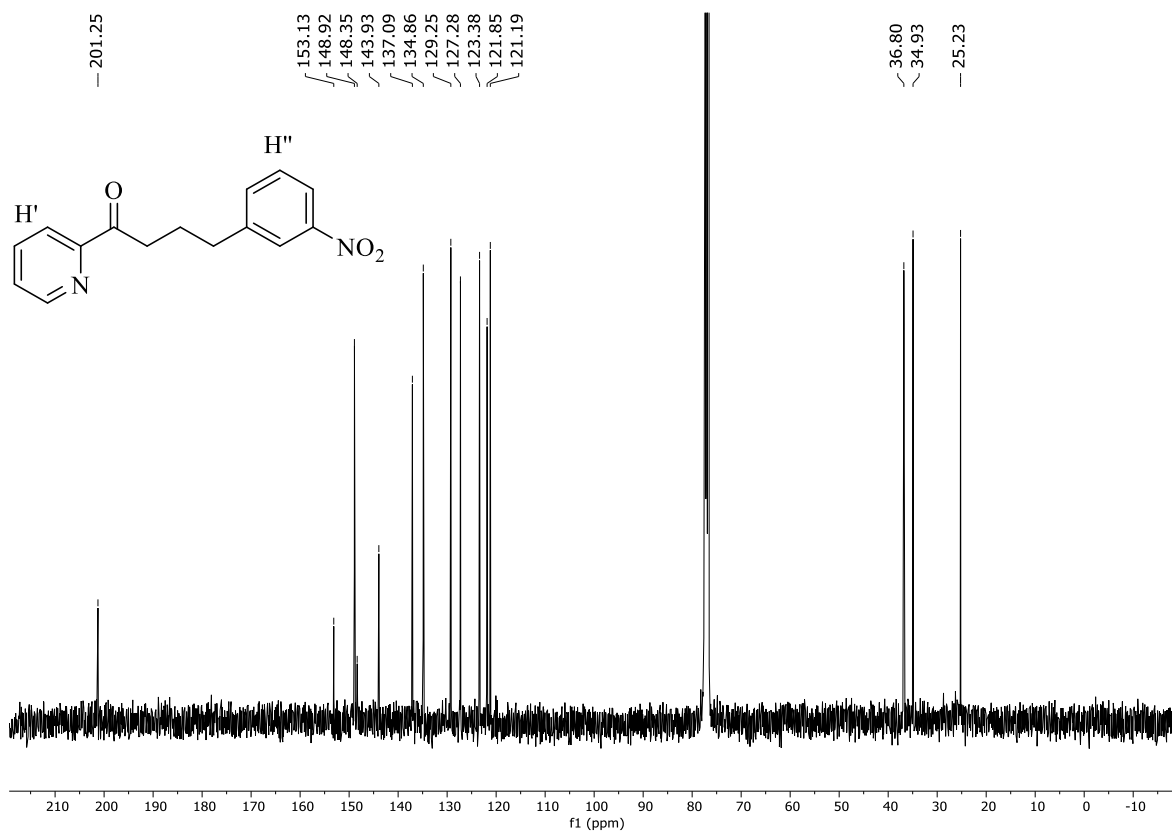
<sup>1</sup>H NMR (400 MHz, CDCl<sub>3</sub>) spectrum of **227h**



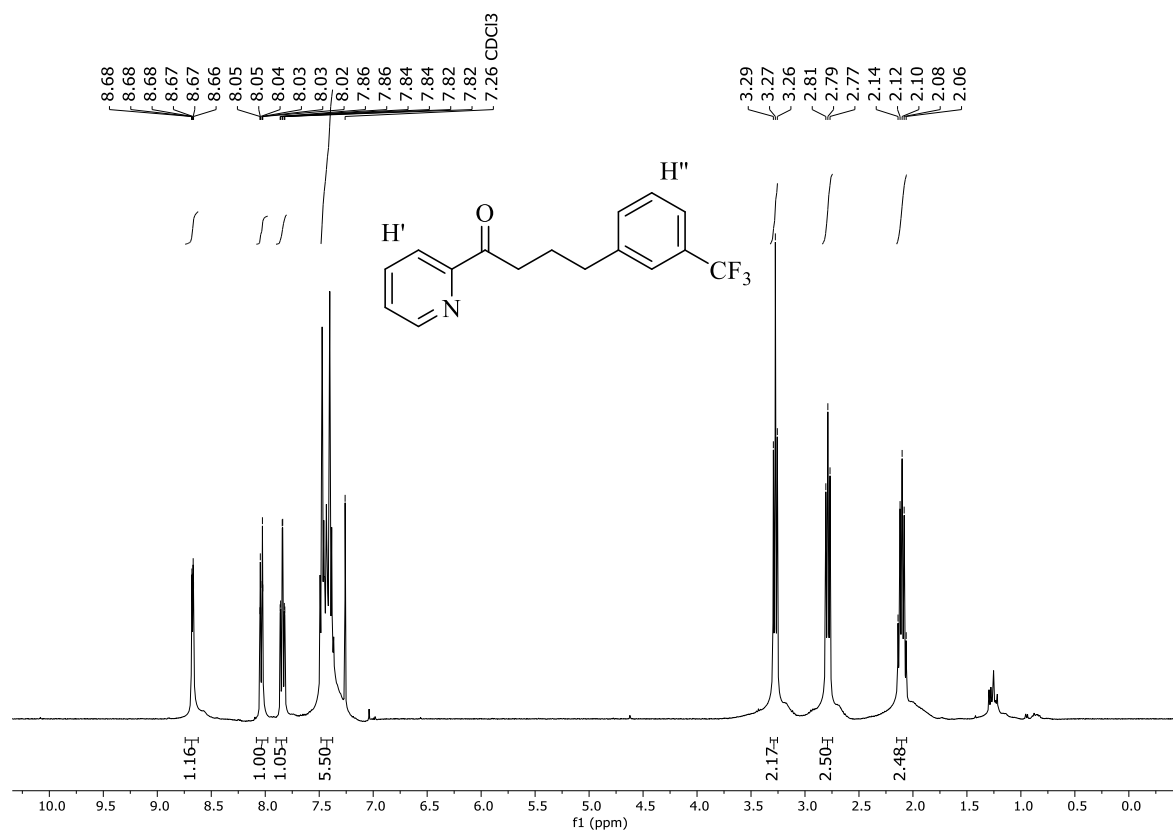
<sup>13</sup>C NMR (101 MHz, CDCl<sub>3</sub>) spectrum of **227h**



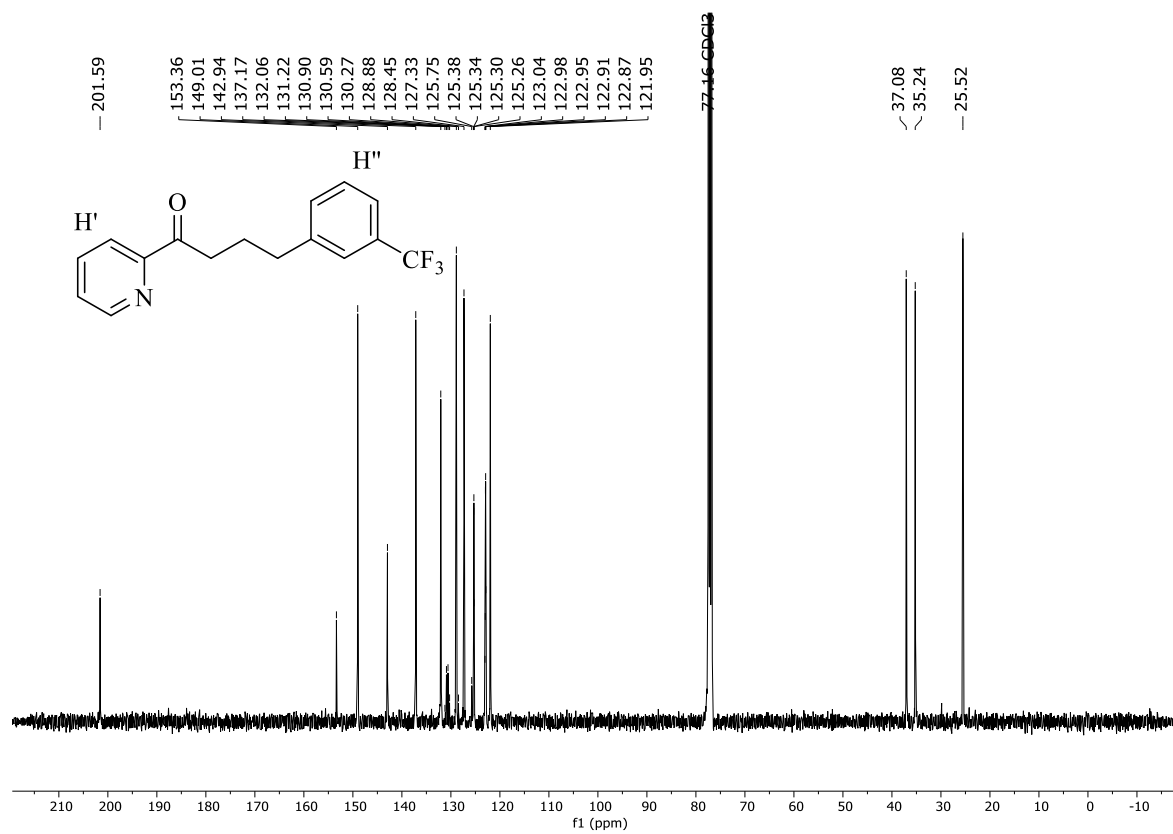
<sup>1</sup>H NMR (400 MHz, CDCl<sub>3</sub>) spectrum of **227i**



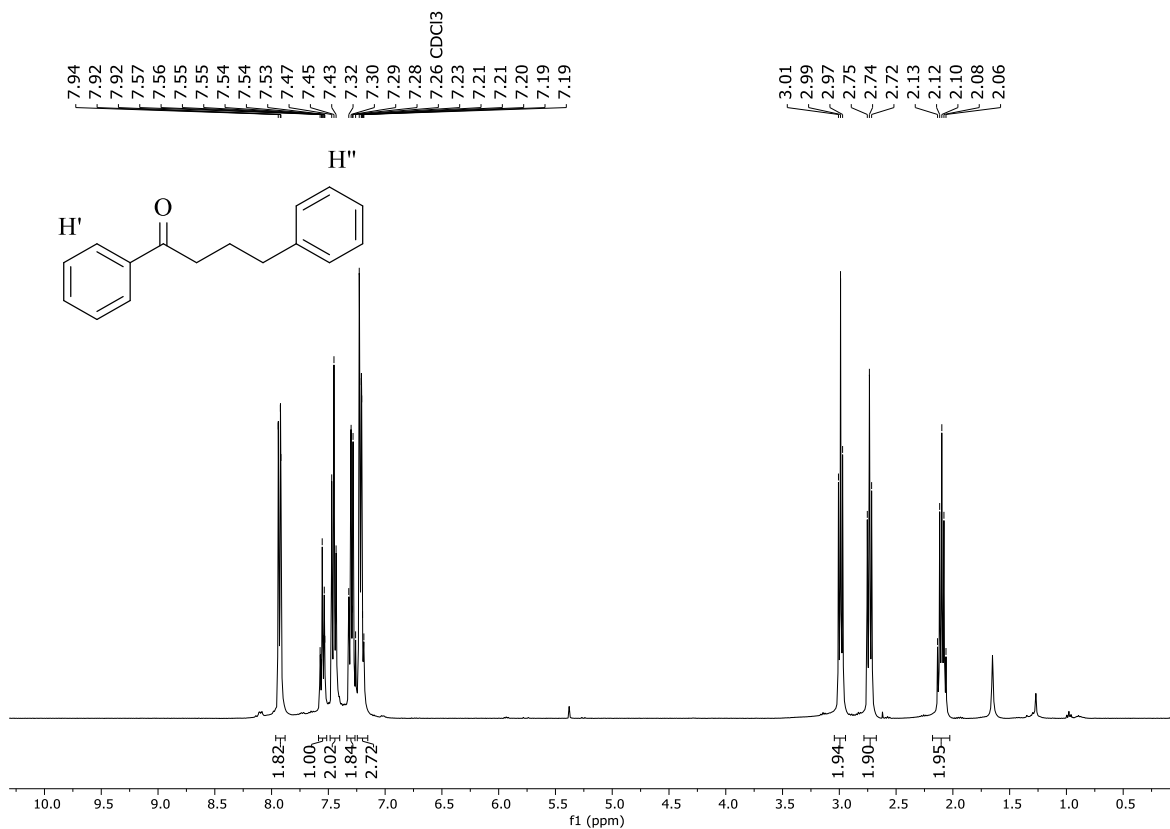
<sup>13</sup>C NMR (101 MHz, CDCl<sub>3</sub>) spectrum of **227i**



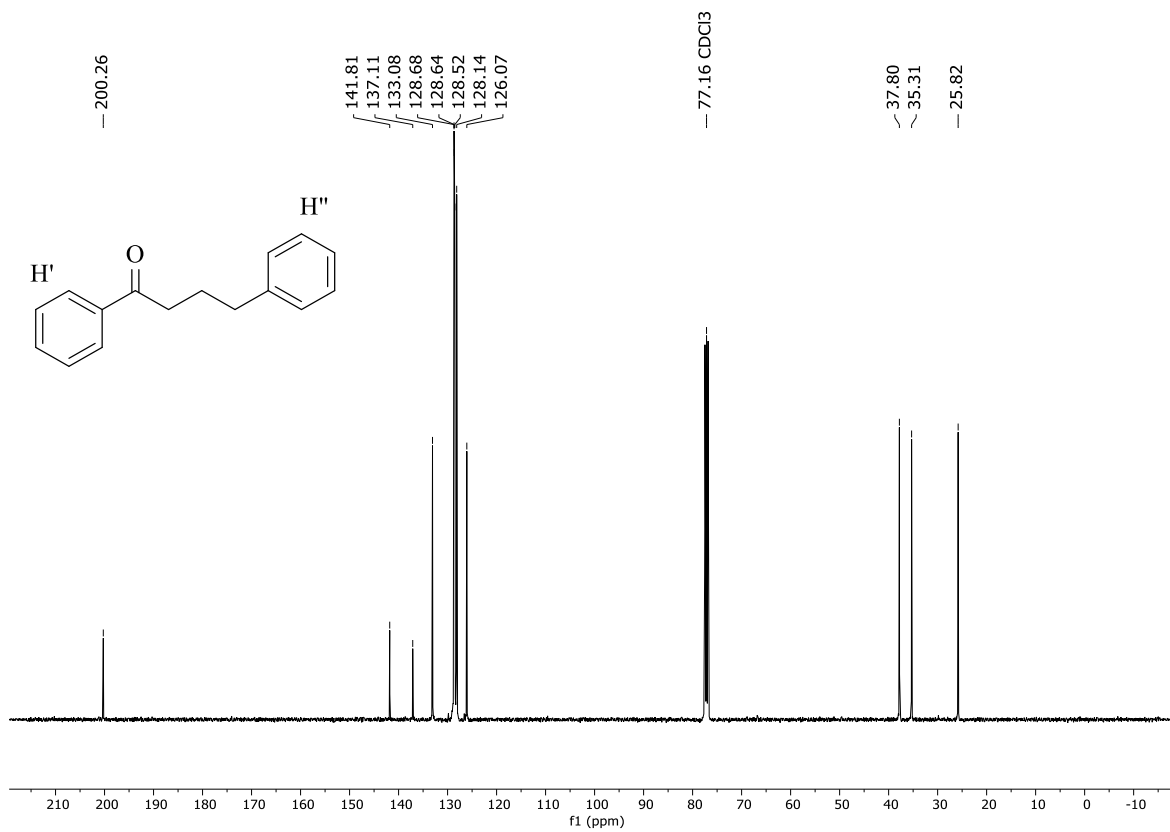
<sup>1</sup>H NMR (400 MHz, CDCl<sub>3</sub>) spectrum of **227j**



<sup>13</sup>C NMR (101 MHz, CDCl<sub>3</sub>) spectrum of **227j**

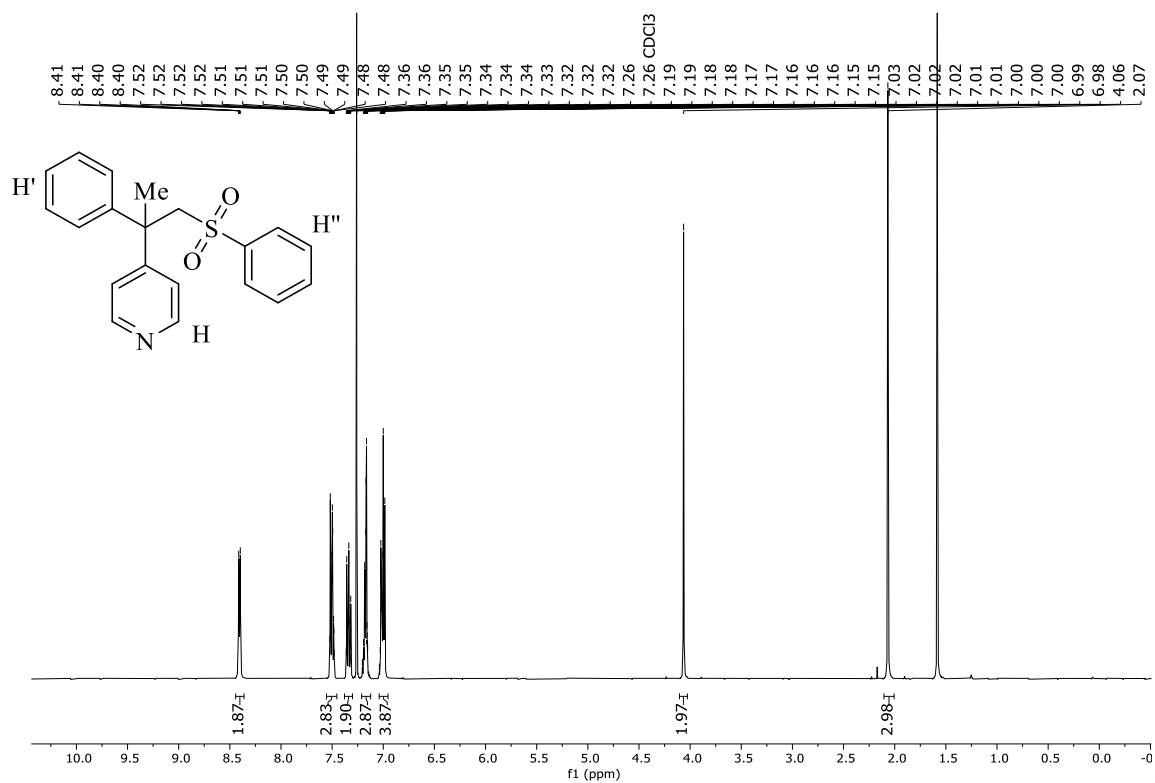
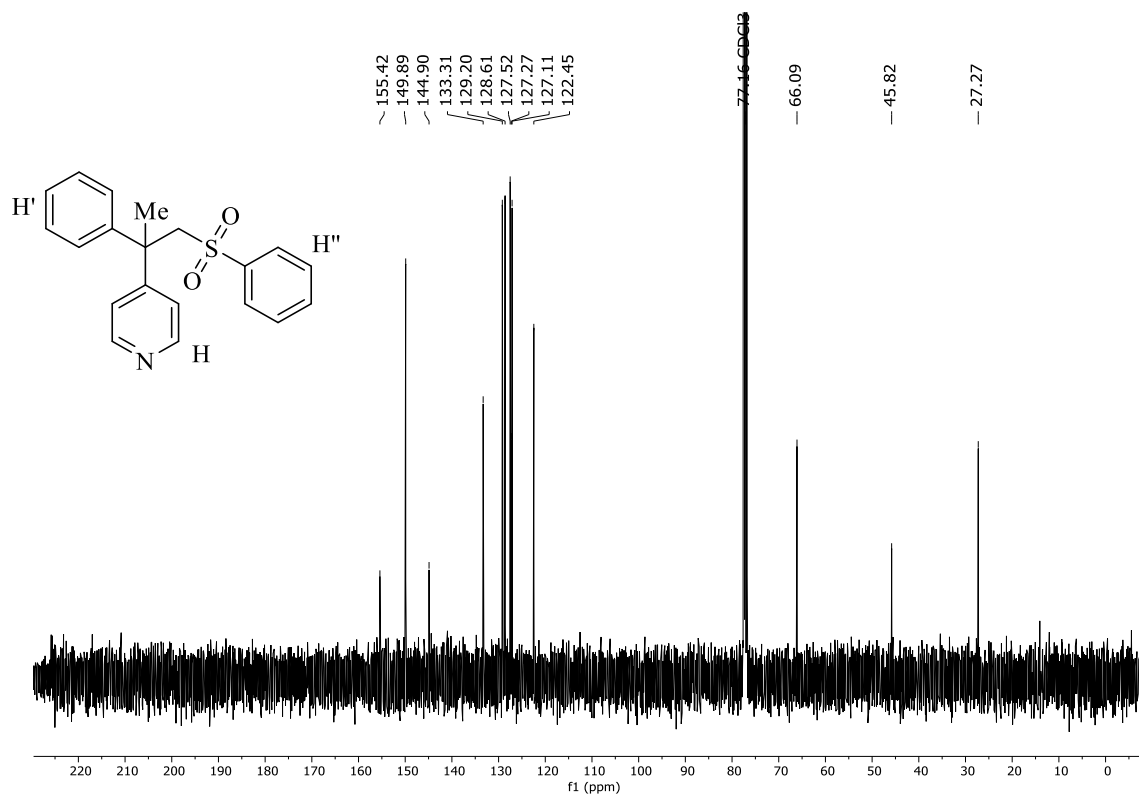


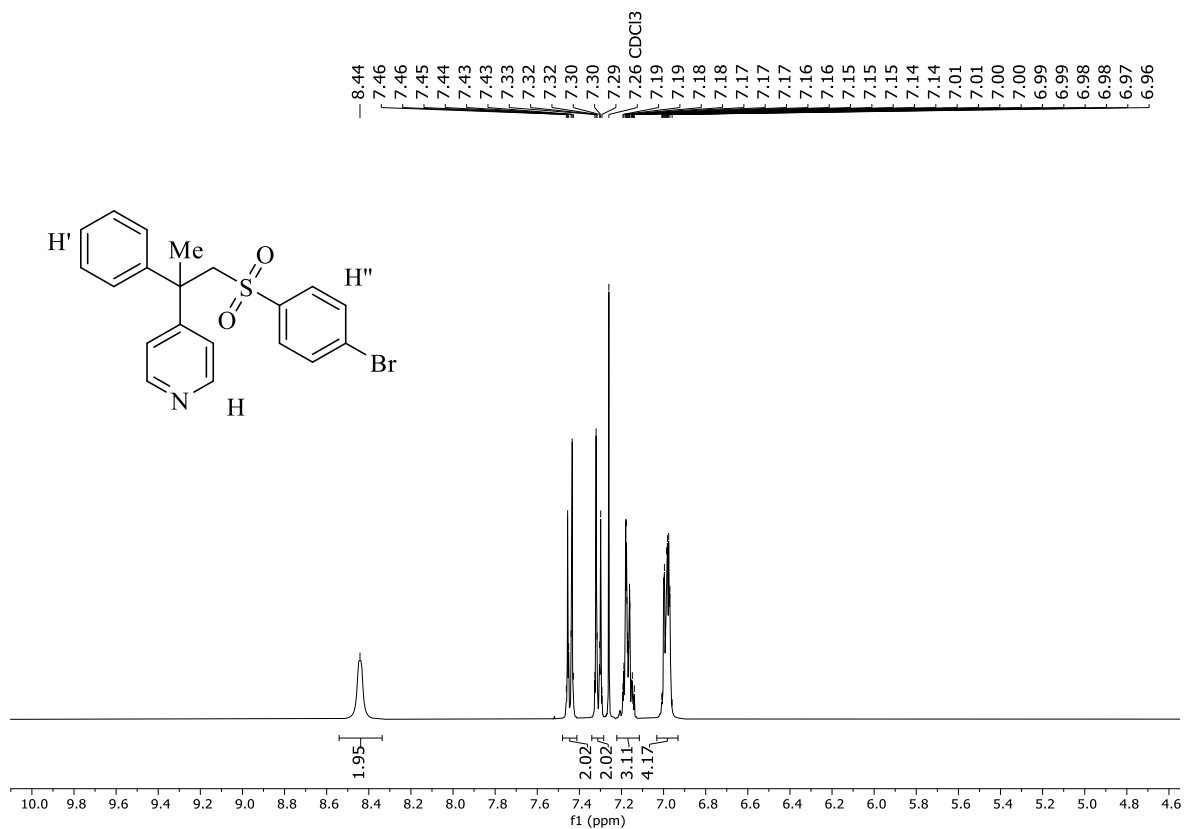
<sup>1</sup>H NMR (400 MHz, CDCl<sub>3</sub>) spectrum of **227k**



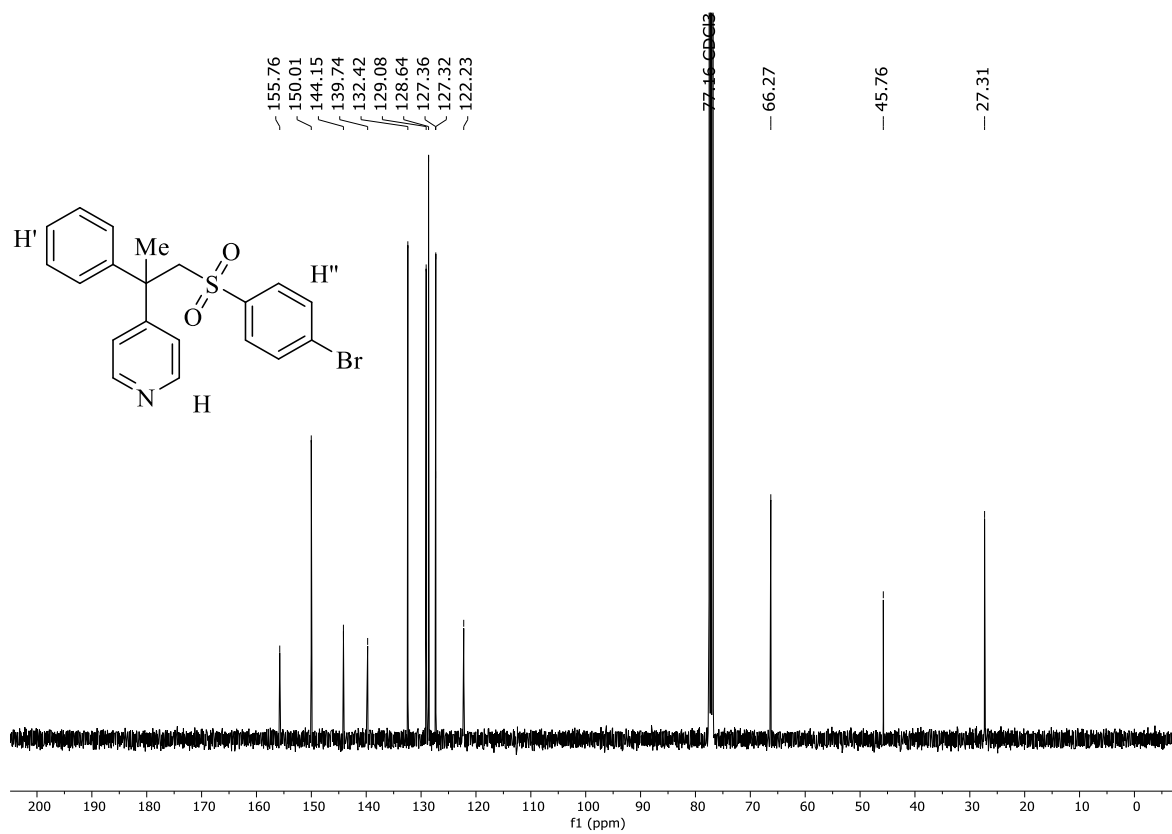
<sup>13</sup>C NMR (101 MHz, CDCl<sub>3</sub>) spectrum of **227k**

## 6.2.3. Spectra section 3.4.1

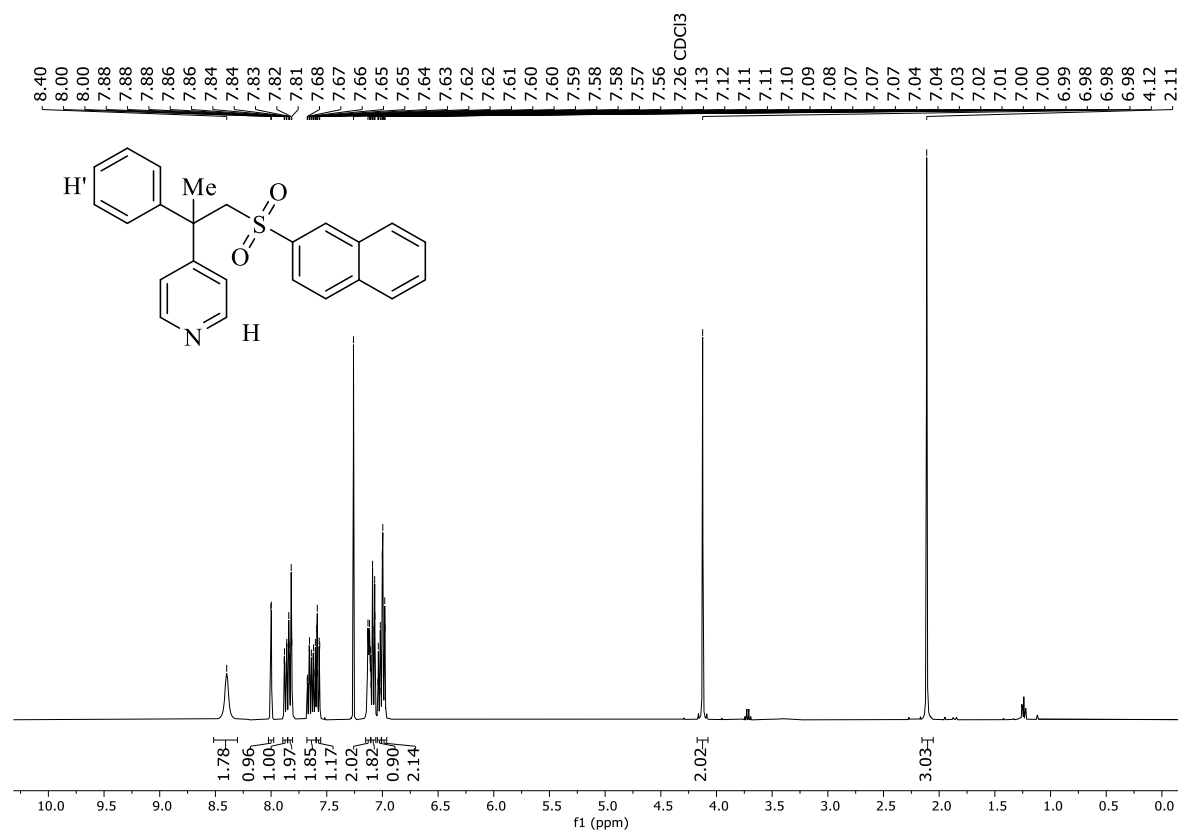
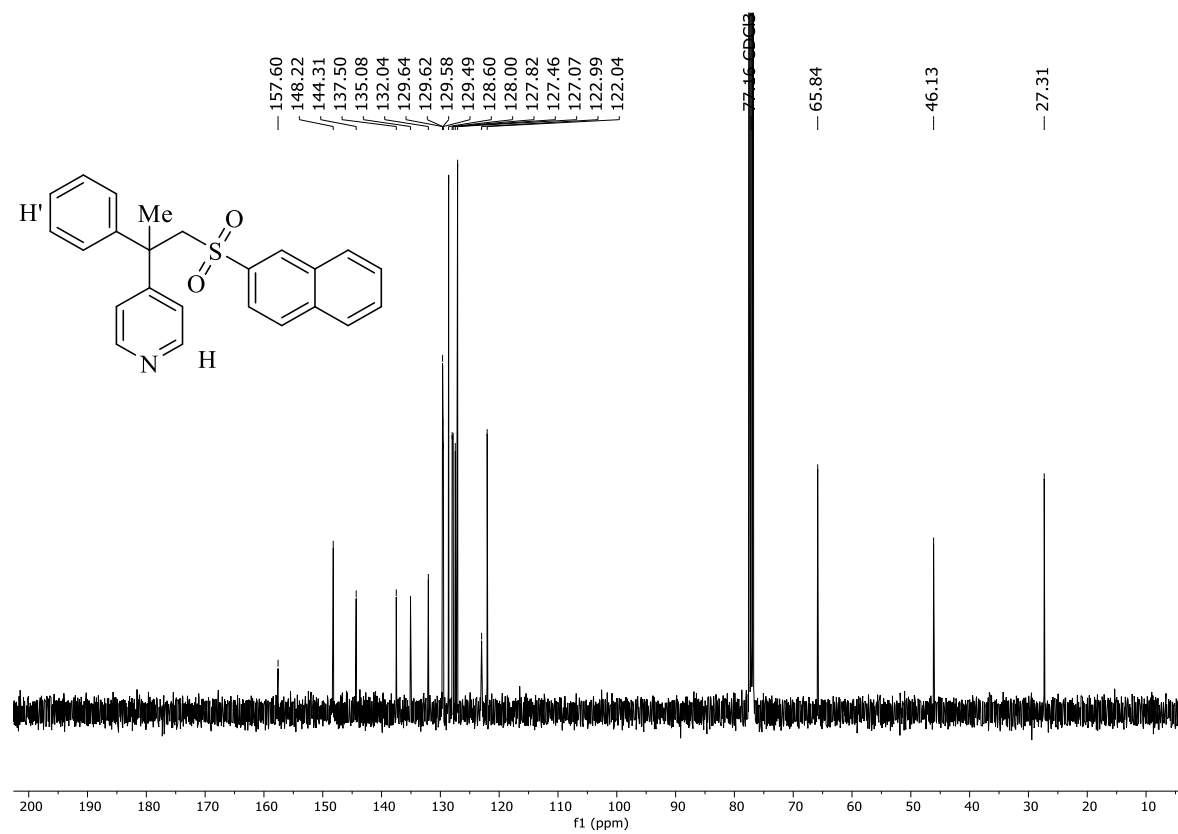
 $^1\text{H}$  NMR (400 MHz,  $\text{CDCl}_3$ ) spectrum of **262u** $^{13}\text{C}$  NMR (101 MHz,  $\text{CDCl}_3$ ) spectrum of **262u**



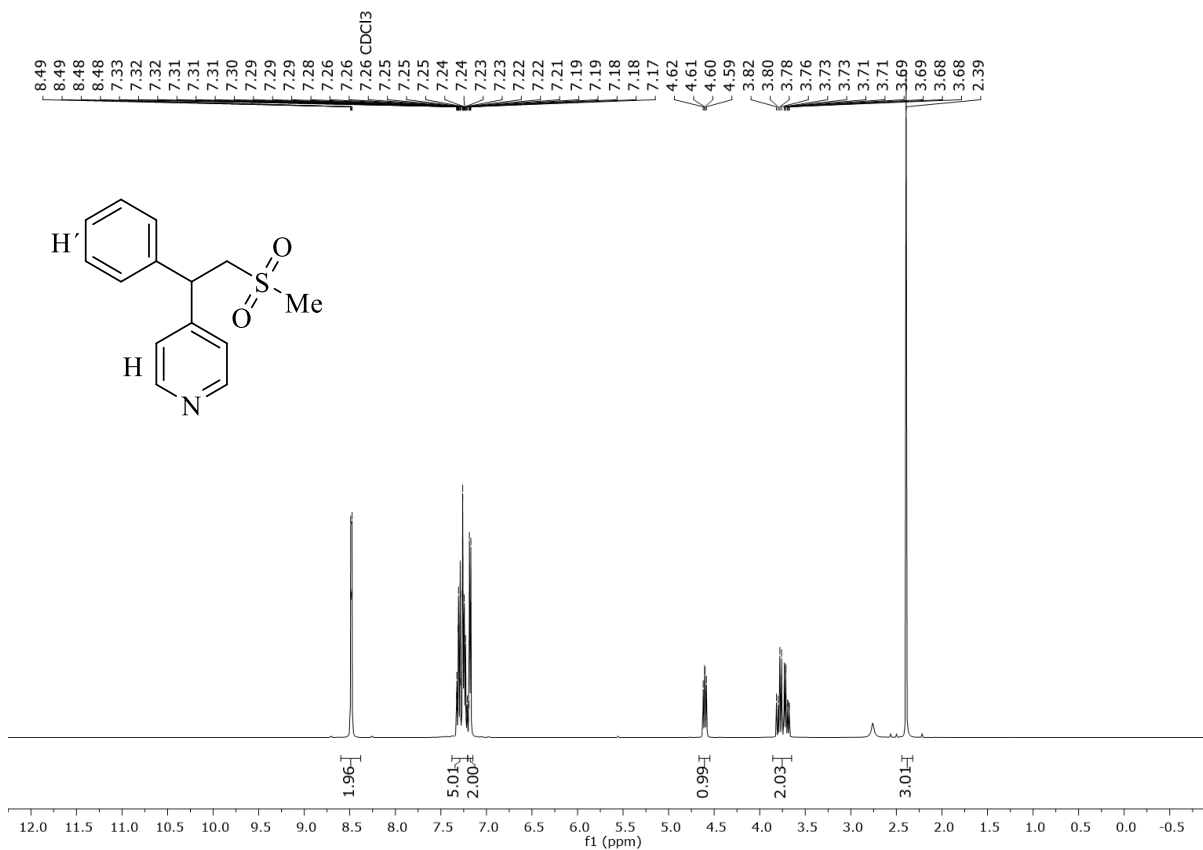
<sup>1</sup>H NMR (400 MHz, CDCl<sub>3</sub>) spectrum of **262v**



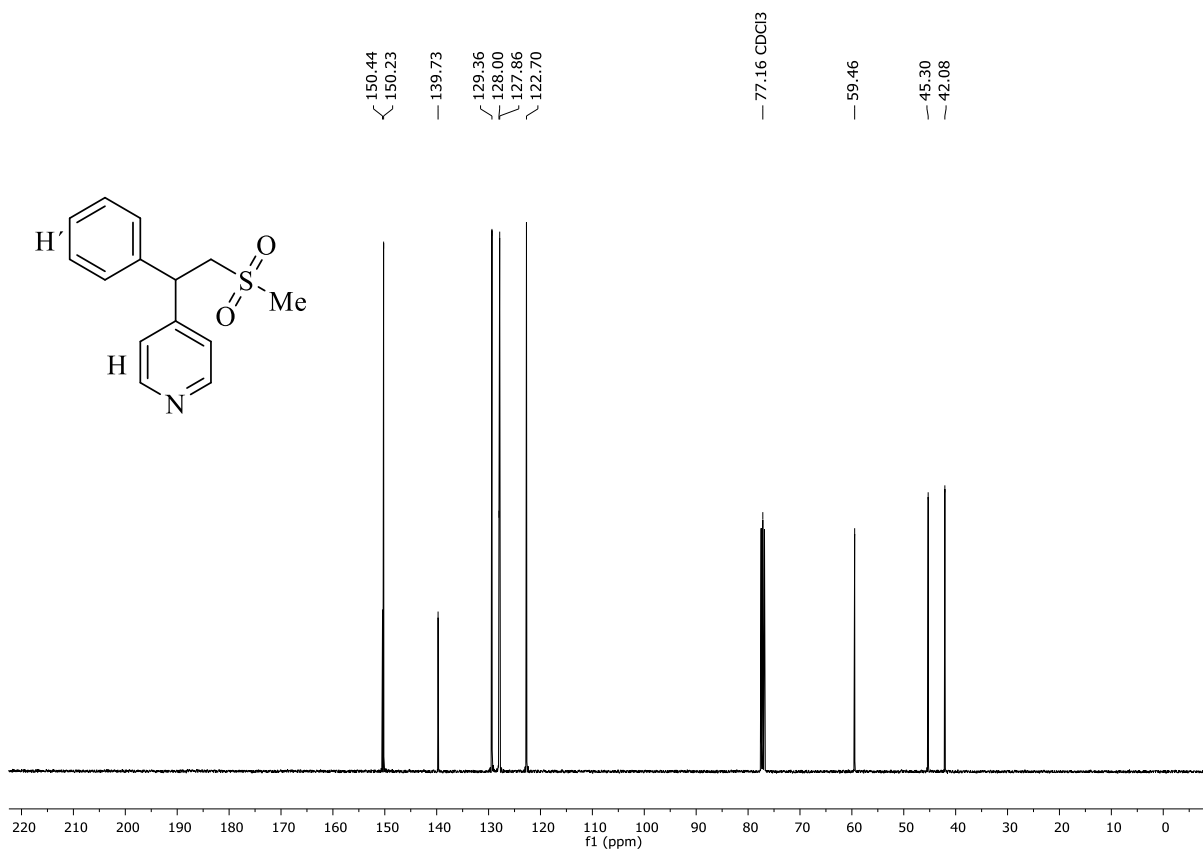
<sup>13</sup>C NMR (101 MHz, CDCl<sub>3</sub>) spectrum of **262v**

<sup>1</sup>H NMR (400 MHz, CDCl<sub>3</sub>) spectrum of **262w**<sup>13</sup>C NMR (101 MHz, CDCl<sub>3</sub>) spectrum of **262w**

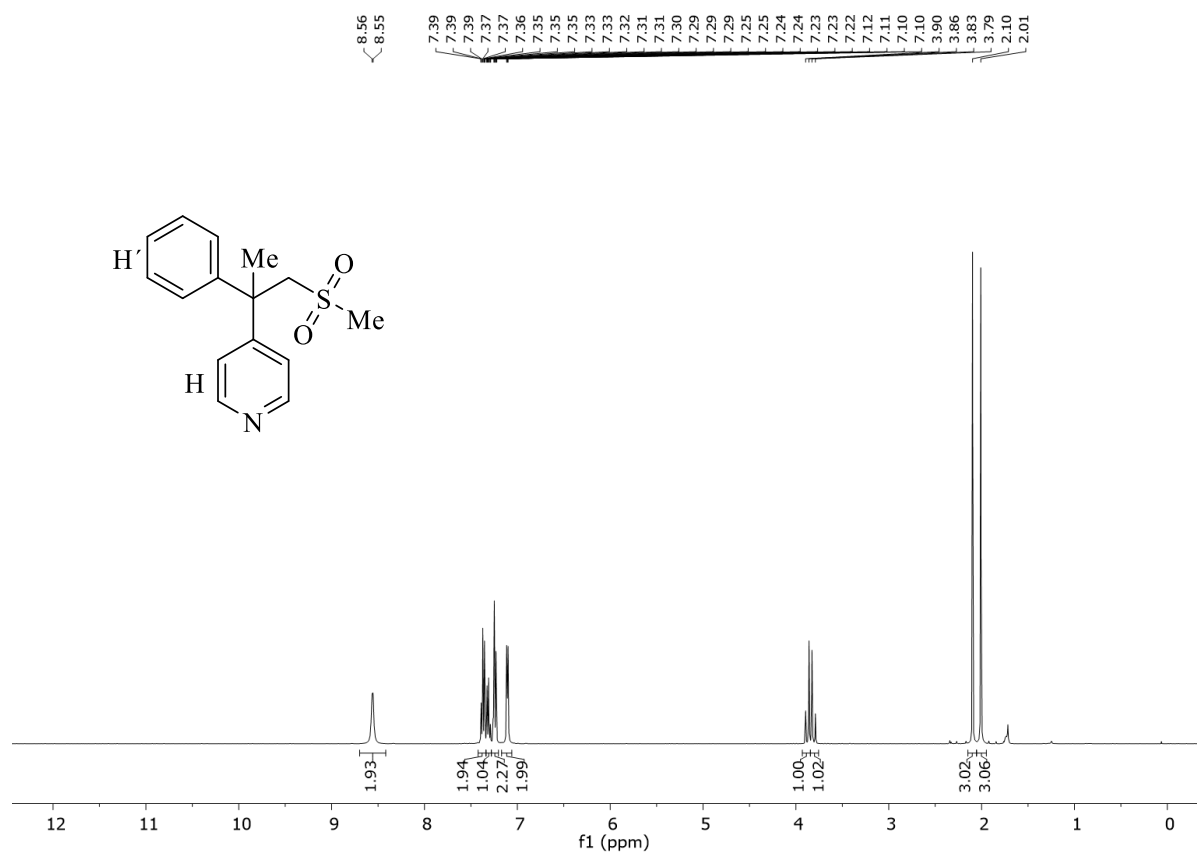
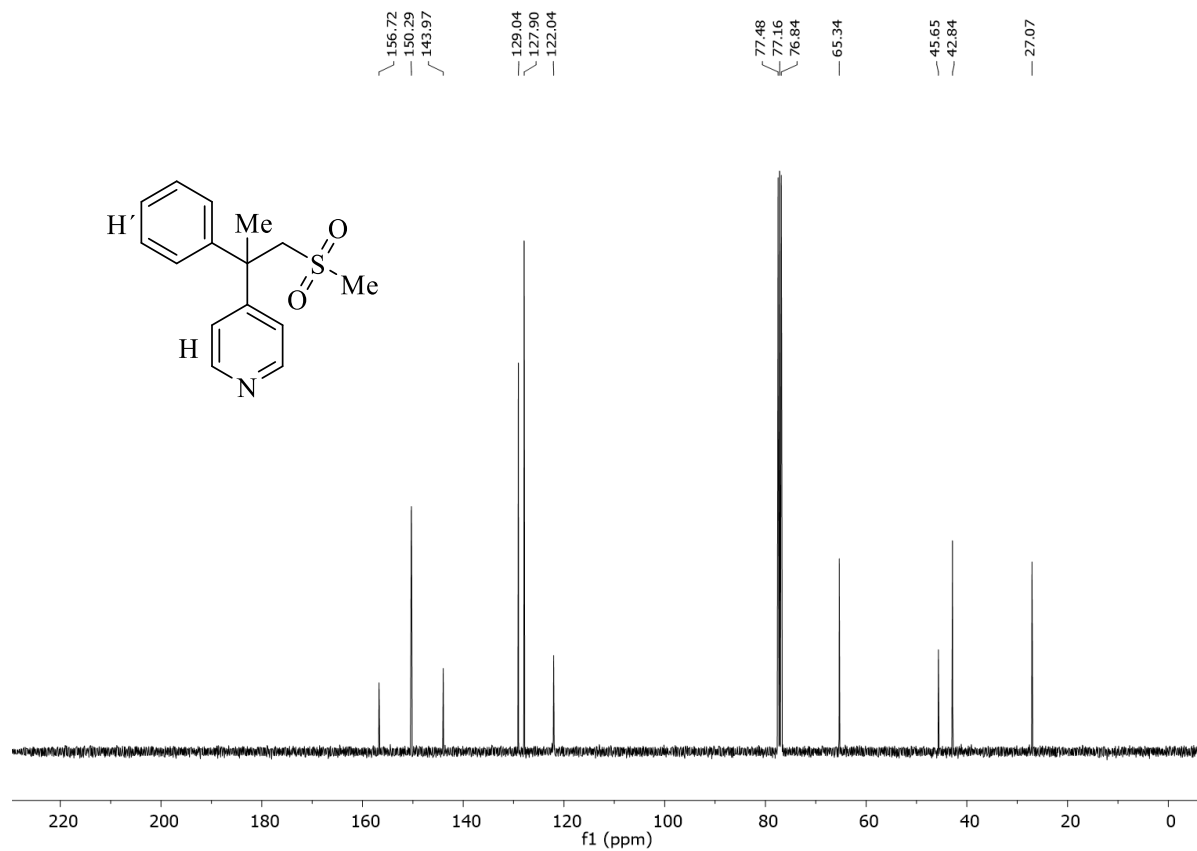


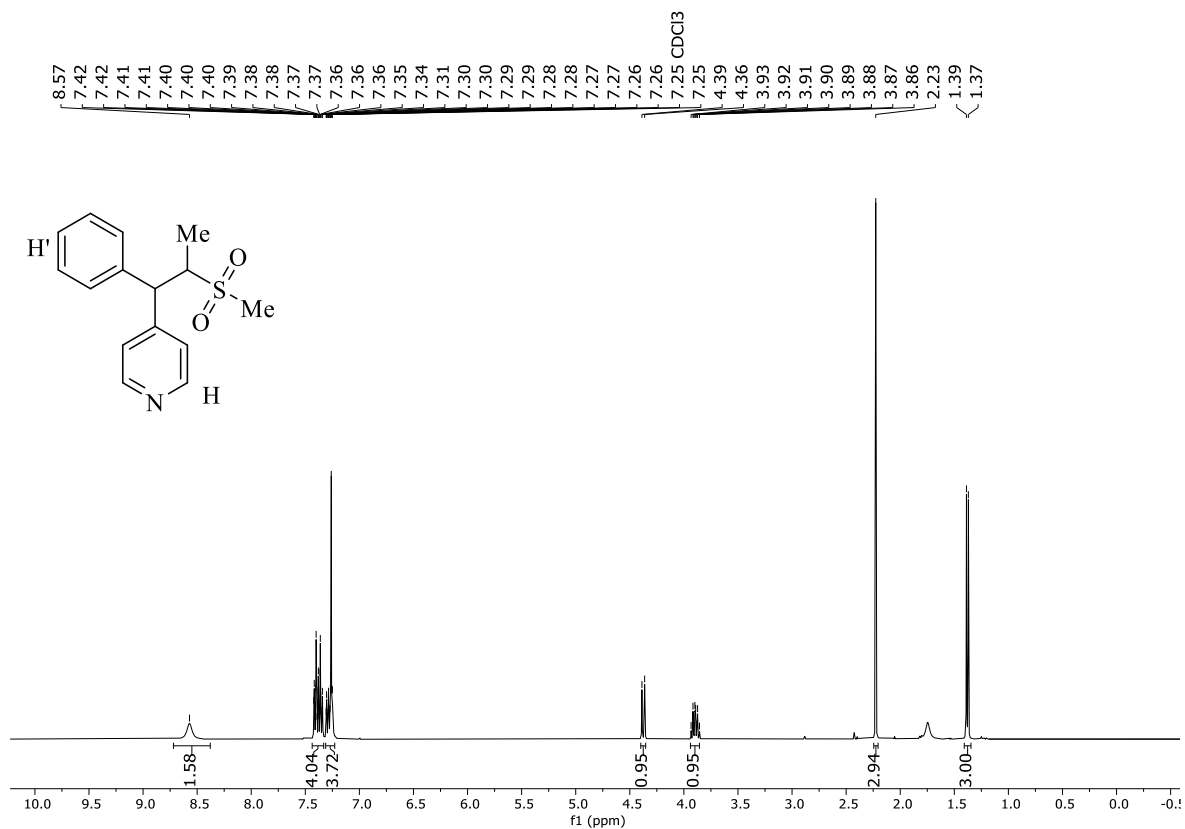


<sup>1</sup>H NMR (300 MHz, CDCl<sub>3</sub>) spectrum of **262x**

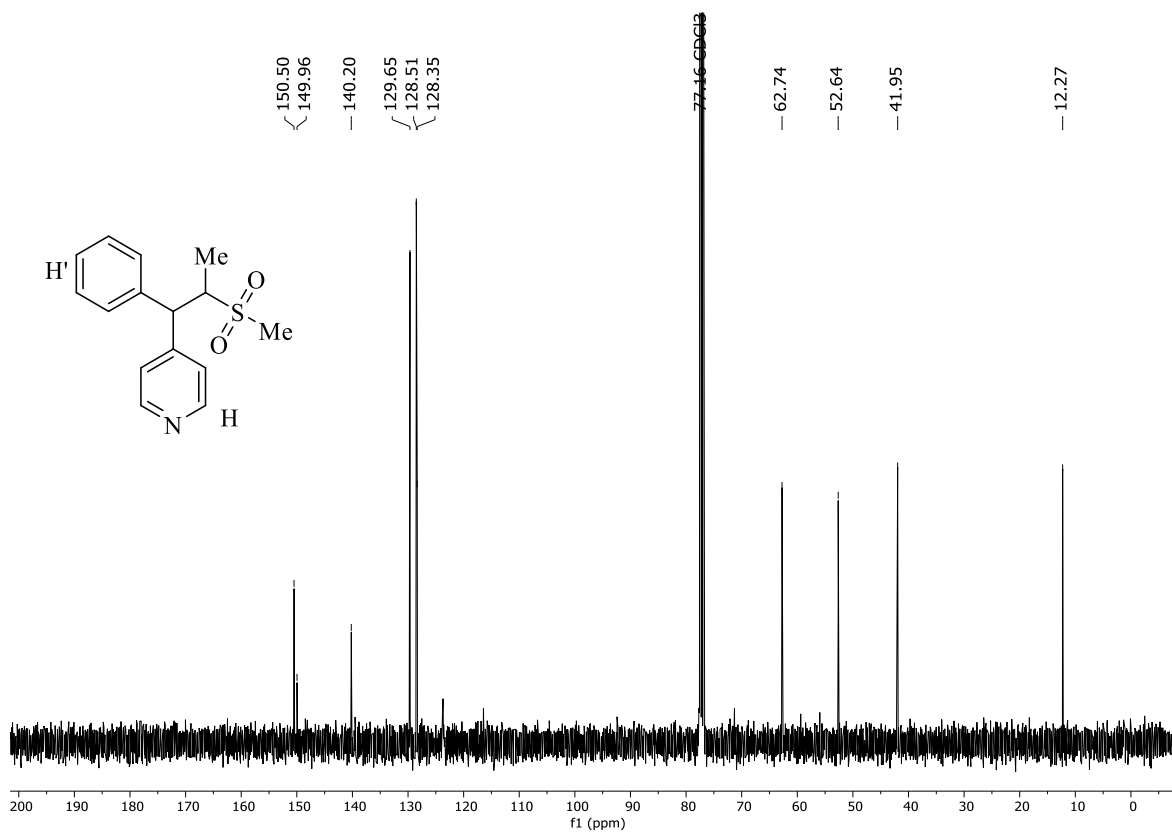


<sup>13</sup>C NMR (75 MHz, CDCl<sub>3</sub>) spectrum of **262x**

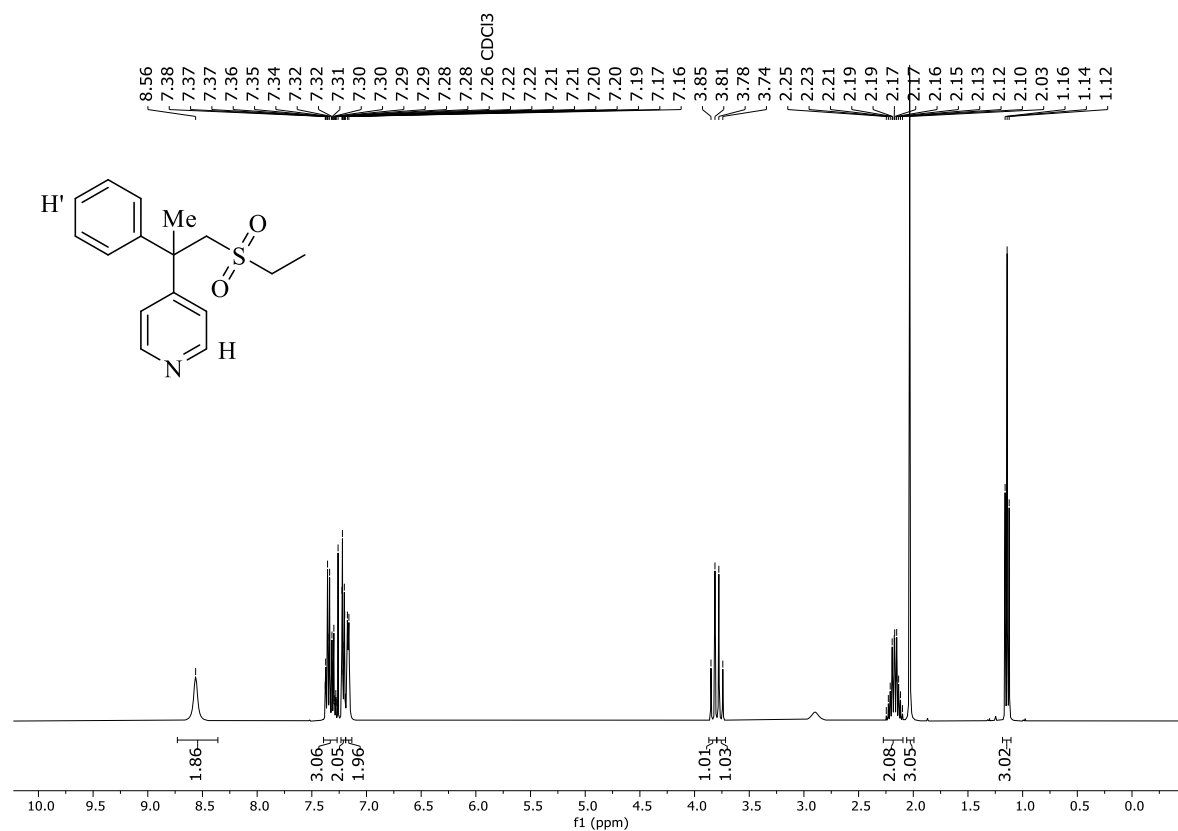
<sup>1</sup>H NMR (400 MHz, CDCl<sub>3</sub>) spectrum of **262y**<sup>13</sup>C NMR (101 MHz, CDCl<sub>3</sub>) spectrum of **262y**



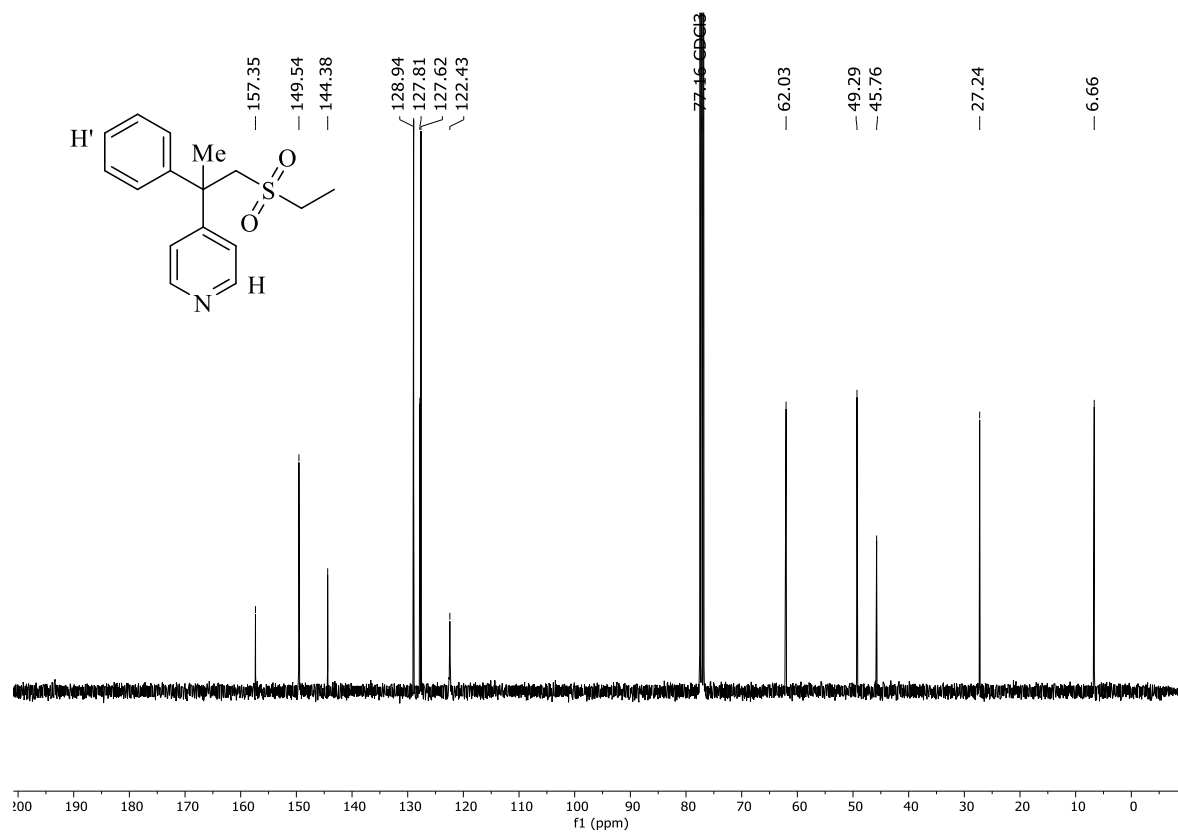
<sup>1</sup>H NMR (400 MHz, CDCl<sub>3</sub>) spectrum of **262y'**



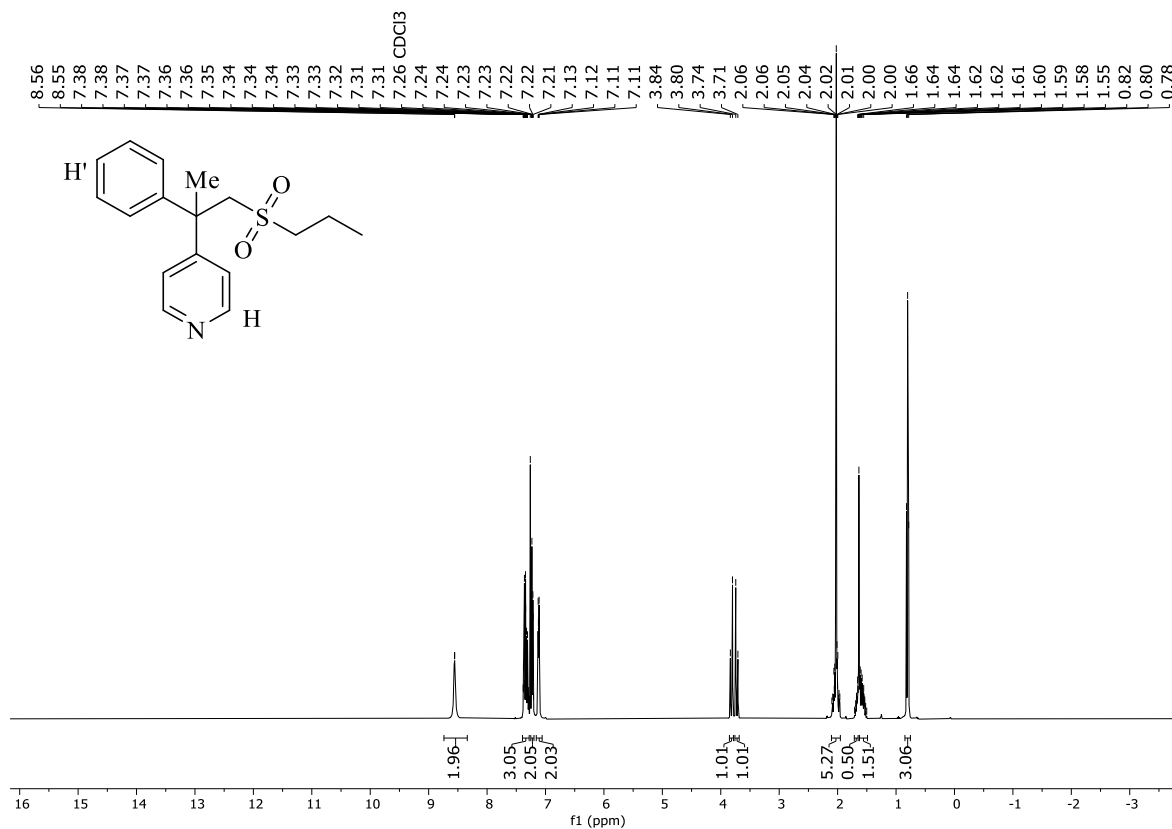
<sup>13</sup>C NMR (101 MHz, CDCl<sub>3</sub>) spectrum of **262y'**



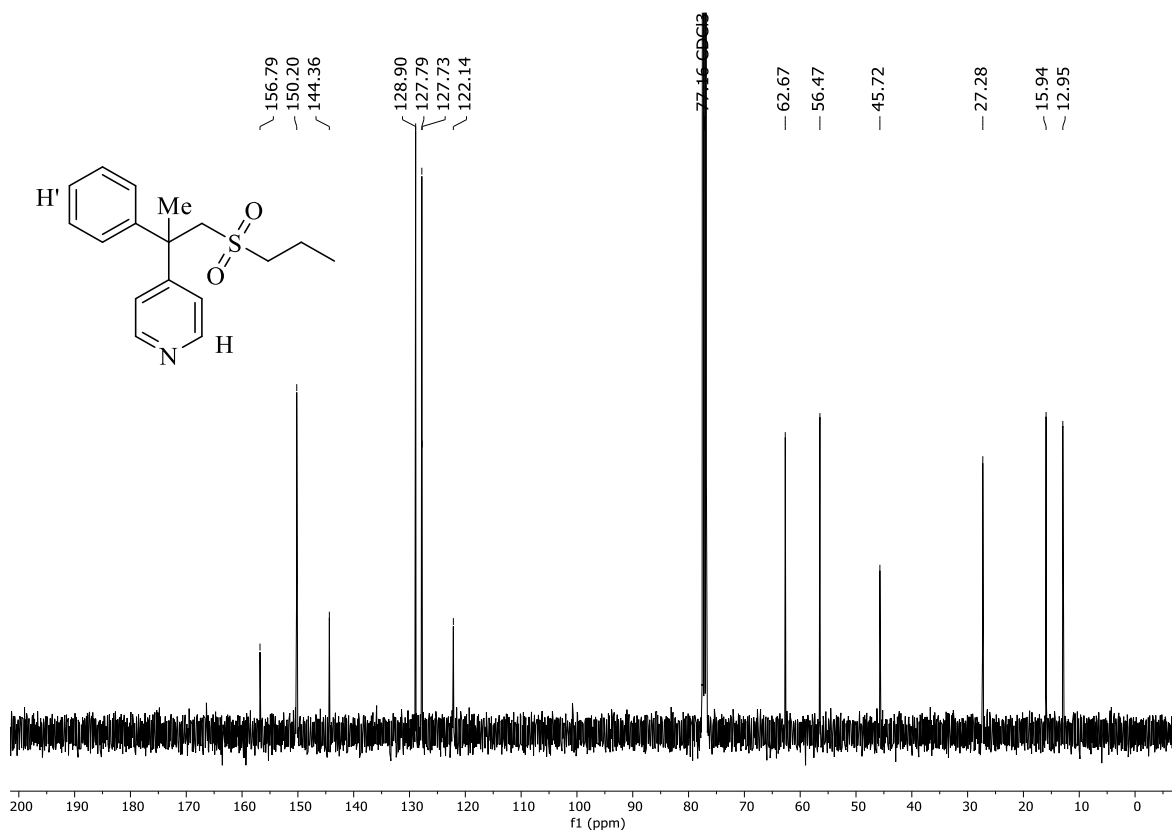
<sup>1</sup>H NMR (400 MHz, CDCl<sub>3</sub>) spectrum of **262z**



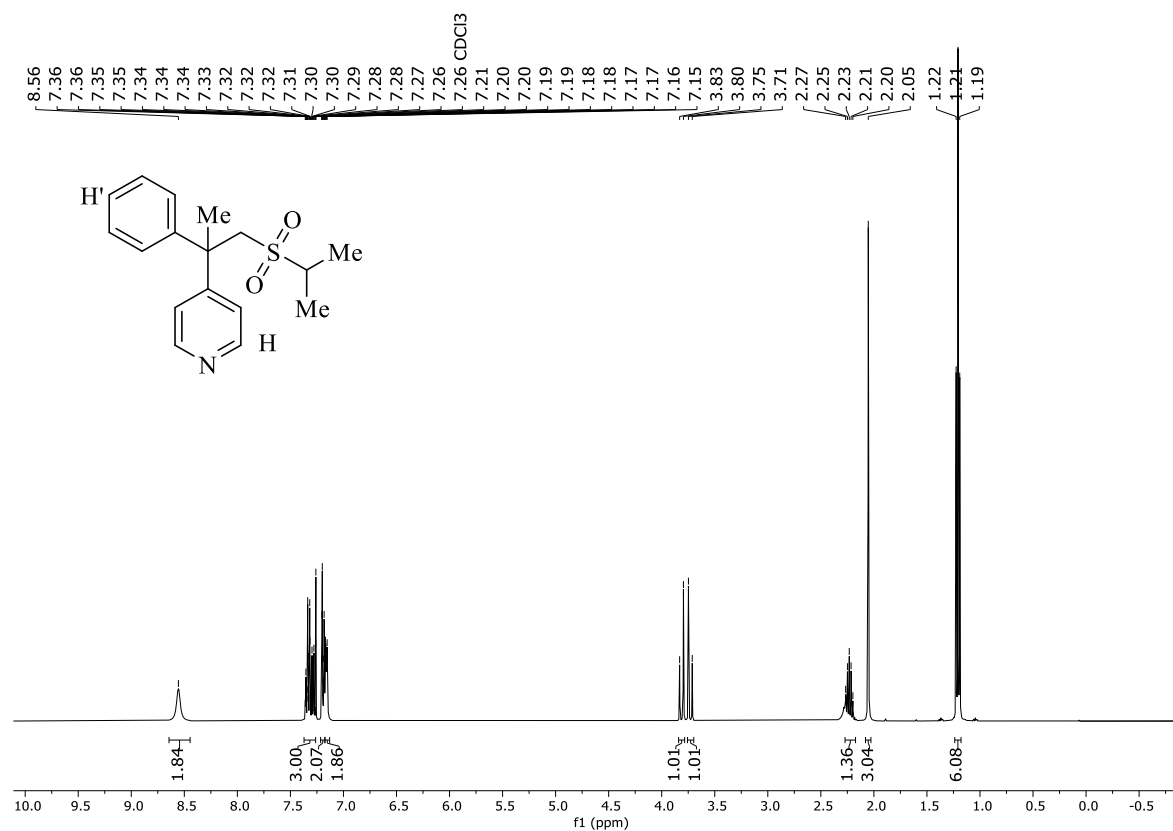
<sup>13</sup>C NMR (101 MHz, CDCl<sub>3</sub>) spectrum of **262z**



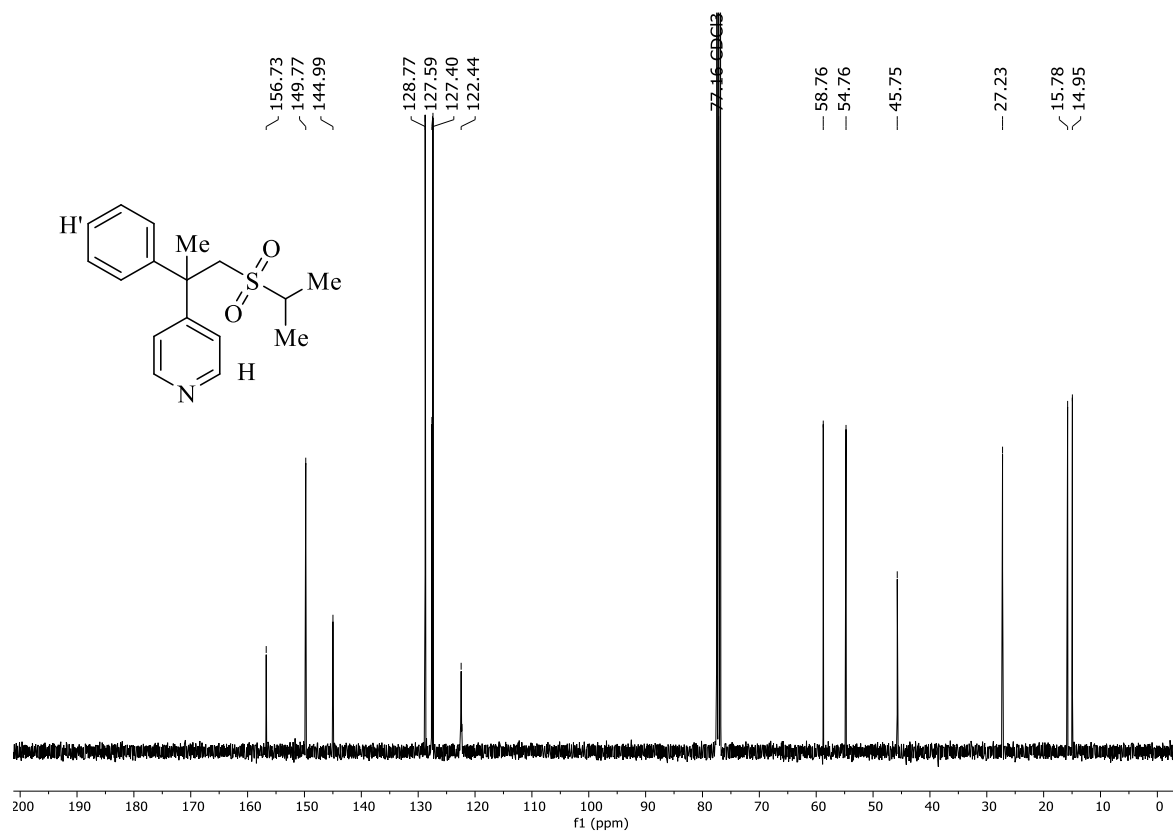
**<sup>1</sup>H NMR (400 MHz, CDCl<sub>3</sub>) spectrum of 262aa**



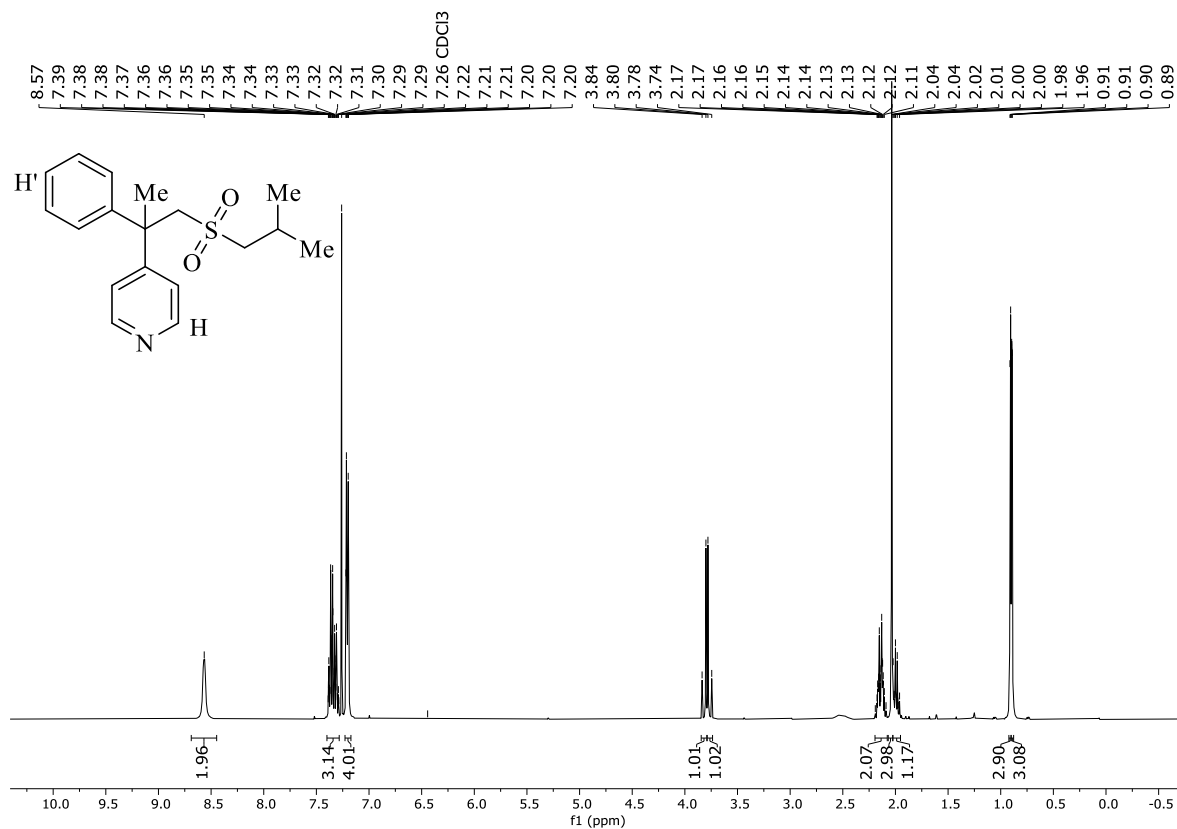
**<sup>13</sup>C NMR (101 MHz, CDCl<sub>3</sub>) spectrum of 262aa**



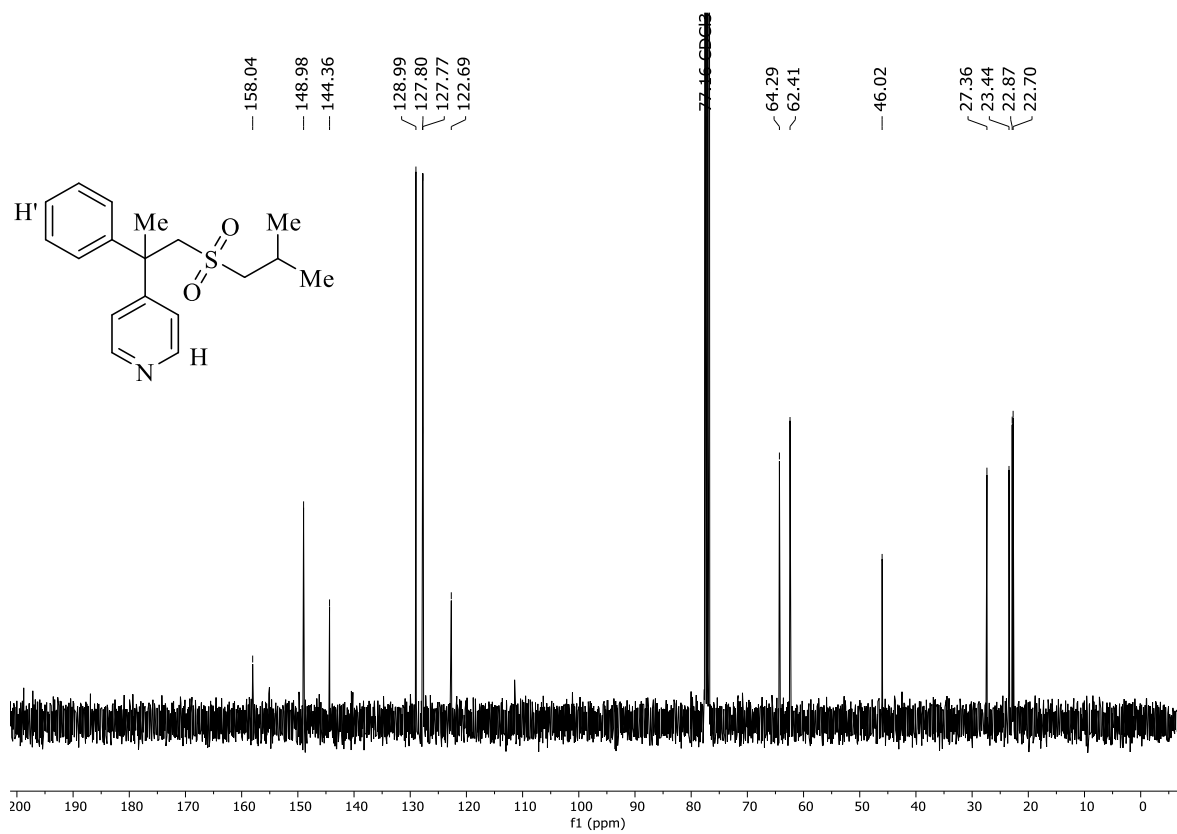
**<sup>1</sup>H NMR (400 MHz, CDCl<sub>3</sub>) spectrum of 262ac**



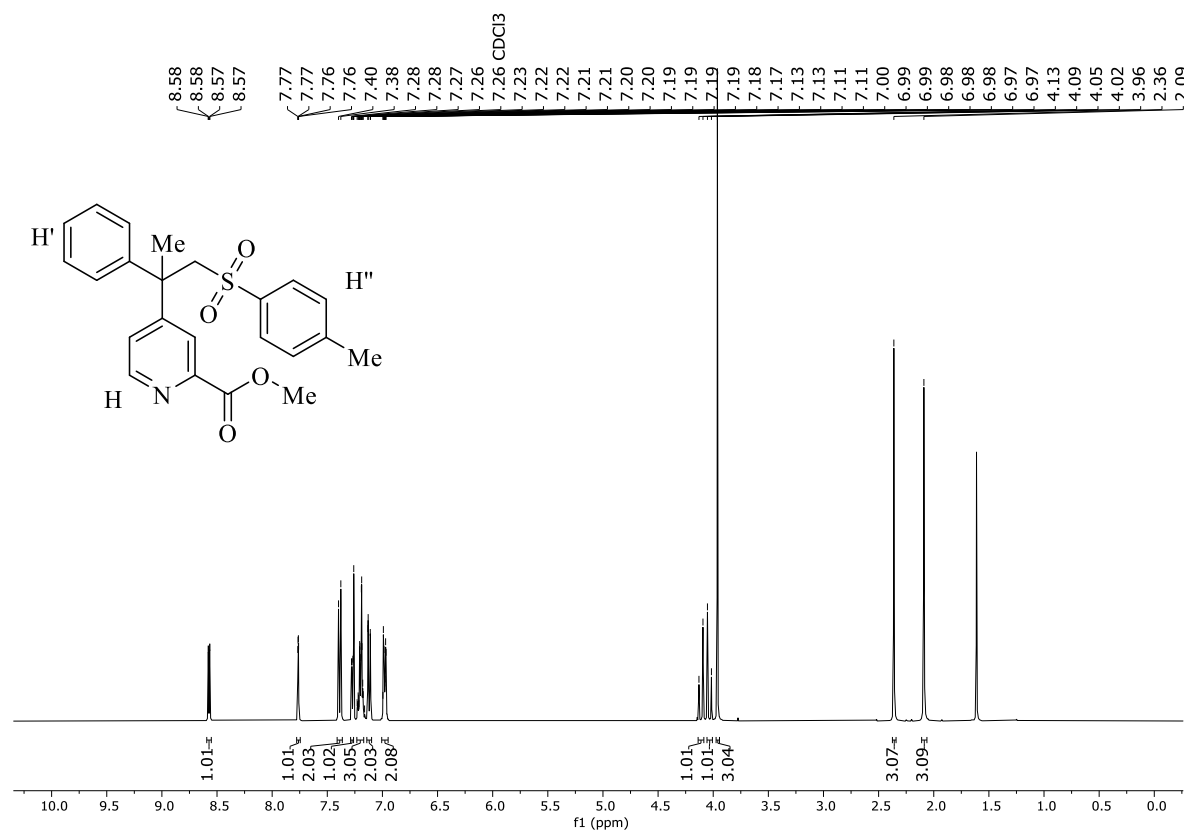
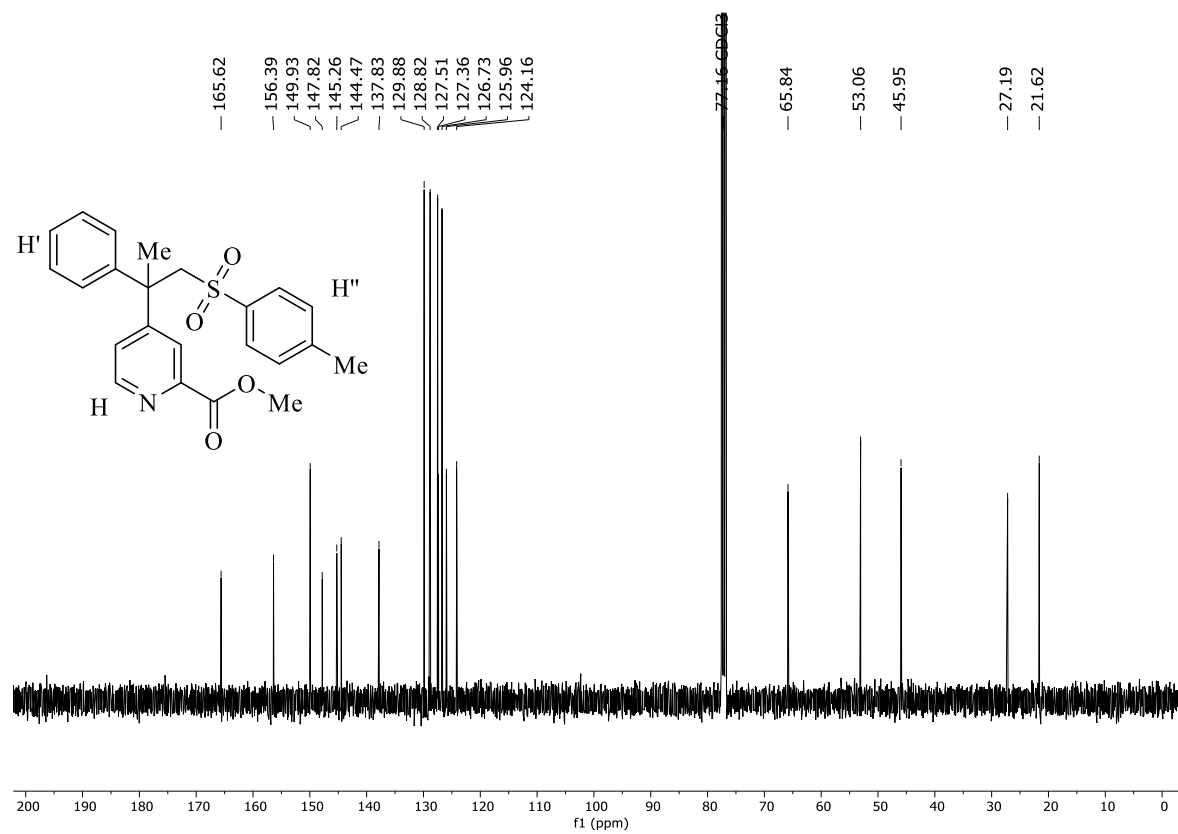
**<sup>13</sup>C NMR (101 MHz, CDCl<sub>3</sub>) spectrum of 262ac**



**<sup>1</sup>H NMR (400 MHz, CDCl<sub>3</sub>) spectrum of 262ad**



**<sup>13</sup>C NMR (101 MHz, CDCl<sub>3</sub>) spectrum of 262ad**

<sup>1</sup>H NMR (400 MHz, CDCl<sub>3</sub>) spectrum of **262av**<sup>13</sup>C NMR (101 MHz, CDCl<sub>3</sub>) spectrum of **262av**



# Acknowledgments

First, I would like to thank Prof. Dr. Till Opatz for including me in his working group and for providing an interesting research topic. I have always valued his trust, his support during the years in his working group, and the extensive freedom in project processing as important foundations for my personal and scientific development. Numerous discussions and suggestions as well as the provision of first-class laboratory equipment have made a significant contribution to the success of this work.

[Redacted]

[Redacted]

[Redacted]

[Redacted]

[Redacted]

[Redacted text block]